ALTERATION AS A VECTOR TO COPPER MINERALISATION IN THE ROYAL THARSIS DEPOSIT, MOUNT LYELL MINERAL FIELD

by

William J.D. Godsall

November 1997

A thesis submitted in partial fulfilment of the requirement for the degree of

Master of Economic Geology

Centre for Ore Deposit and Exploration Studies

University of Tasmania

Geology Department

CONFIDENTIALITY CLAUSE

The data and information contained in this thesis are to remain confidential for two years from the date of publication.

VERIFICATION

I declare that all inferences and conclusions drawn in this thesis are all my own work except where referenced and acknowledged. I further understand that to the best of my knowledge none of the contents contained herein have previously been submitted in any other degree or diploma except where due acknowledgment is given.

William J.D.Godsall
November 1997

Frontispiece

Royal Tharsis area dominated by Tharsis Ridge in the centre and Mount Lyell in the background

ABSTRACT

Royal Tharsis was mined as an underground operation and as part of the West Lyell Open Cut. The original orebody consisted of steep south-westerly dipping echelon lenses striking 315° and extending to a depth of some 600 metres. The topographical expression would have been steep slopes of CVC alteration assemblages dominated by the Tharsis Ridge, a buttress of Owen Group rock types that separates West Lyell from North Lyell.

Sulphide mineralisation is dominantly pyrite and for which at least one generation has been identified, with subordinate chalcopyrite. Bornite, chalcocite-digenite, covellite, molybdenite, sphalerite and galena have also been identified. Volcanic precursors include rhyolitic and dacitic volcanics, volcaniclastics (locally autobrecciated), brecciated lavas and minor porphyries. Intense and selective alteration has resulted in obliteration of primary textures. Feldspar destruction is almost ubiquitous. Rare albitised plagioclase occurs towards the periphery of the alteration system.

Broad correlation exists between sulphide mineralisation and alteration patterns. Ten main alteration assemblages have been identified: mixed mica, quartz-mixed mica, quartz-sericite, quartz-pyrite, quartz-chlorite±sericite, chlorite, meta-conglomerate, quartz-haematite, quartz-magnetite and magnetite-apatite. The most common alteration assemblages include: quartz-sericite; quartz-chlorite-sericite and/or quartz-sericite-chlorite; and chlorite or quartz-chlorite assemblages.

The Ishikawa alteration index increases up stratigraphy and shows a subtle change through the ore zone. The chlorite-pyrite-carbonate alteration index shows a change in gradient through the ore zone relative to hangingwall lithologies. The manganese-carbonate alteration index shows a relative drop at the stratigraphic footwall of copper mineralisation, but otherwise portrays a poorly defined response. The Ti/Zr value falls in the dacite - rhyolite range, with occasional andesite values.

Sulphide (pyrite) and carbonate show an almost inverse relationship, with a weak zonation evident between Fe-S-C-±O. Carbonate alteration through the mineralisation is muted and variable, and where distal is probably due to remobilisation rather than primary. K_2O shows a subtle response to mineralisation and thus may be a subtle vector to ore. Na_2O depletion occurs through the ore halo and into the hangingwall. Barium and Ba/Sr ratio show enrichment through the mineralised halo, identified by a Ba/Sr value that rises above 30. REE show uniform elevated responses through the mineralised halo.

Gold, silver, molybdenum, cobalt and ± nickel all correlate reasonably well with copper. Fe_2O_3 and P_2O_5 both correlate with copper, indicative of pyrite and apatite relationships respectively, the latter pointing to the influence of magmatic hydrothermal fluids. The abundance of illite is suggestive of the presence of weakly acidic (CO_2-rich) fluids.

CONTENTS

LIST OF TABLES

CONTENTS

LIST OF ILLUSTRATIONS

LIST OF ILLUSTRATIONS (Cont'd)

LIST OF APPENDICES

ACKNOWLEDGMENTS

Copper Mines of Tasmania are thanked for permission to use the data and information contained in this thesis. They are also thanked for time afforded to attend the short courses that constitute the Masters degree.

Staff at the CMT Geology Department are thanked for their assistance, advice and encouragement given throughout the duration of thesis. In particular Peter Benjamin for his constant encouragement and interest in the project; Keith Corbett, Ken Morrison and Paul Harbon for constructive comments and criticisms on the draft text, Jeremy Lawrence for his perusal of draft chapters and computing expertise; and Alistair Skey and Pat McDowell for their computing assistance, as well as other members who contributed in one or another. In addition Ashley Greenwood is acknowledged for highlighting the potential of the area as worthy of deeper investigation.

Ross Large, Bruce Gemmell and the staff at CODES provided valuable guidance and criticisms, as did Dave Huston during his work on site for the AMIRA P349 project.

Lastly (but not least) Helena for her patience, understanding and unstinting support.

ABBREVIATIONS

Common abbreviations used in this thesis:

Non Geological

CMT = Copper Mines of Tasmania

MLMRC = Mount Lyell Mining and Railway Company

WLOC = West Lyell Open Cut

Geological

GLF = Great Lyell fault

NLF = North Lyell fault

CVC = Central Volcanic Complex

MRV = Mount Read Volcanics

VHMS = volcanic hosted massive sulphides

VMS = volcanogenic massive sulphides

YRS = Yolande river sequence

EQS = eastern quartz phyric sequence

AI = Ishikawa alteration index

CI = chlorite alteration index

MI = manganese-carbonate alteration index

ppl = plane polarised light

cpl = crossed polarised light

BDL = below detection limit

CHAPTER 1
INTRODUCTION

1.1 PREVIOUS WORK

It has long been recognised that mineralisation within the Mount Lyell mineral field is associated with alteration (Thureau, 1886; Johnston, 1890; Gregory, 1905; Nye *et. al.*, 1934; Alexander, 1953; Wade and Solomon, 1958; Solomon, 1964 and 1967; McDonald, 1968; Reid, 1975; Walshe, 1977; Walshe and Solomon, 1981; Corbett, 1981; Sheppard, 1987; Hills, 1990; Berry, 1990; Raymond, 1996; Wills, 1996b). The importance of tectonics and later remobilisation has also been acknowledged (Loftus-Hills, 1927; Cox, 1979; Sillitoe, 1984; Solomon *et. al.*, 1987; Berry, 1990). Precise relationships between alteration and mineralisation have not been established, although hydrothermal alteration has been recognised by many of the workers in the field. Alteration associated with economic ore lenses exposed during mining operations has been identified (Walshe, 1977; Hendry, 1981; Raymond, 1992). Within a broader context distinction between the effects of different alteration modes on the primary volcanic facies has not been elucidated.

The Mount Lyell field has witnessed a plethora of learned papers and erudite publications. These have encompassed geochemistry, structure, tectonics and stratigraphy. Most of the geochemical work has been carried out on subsurface exposures (Edwards, 1939; Solomon, 1964; Solomon and Elms, 1965; Markham, 1968; Reid, 1975; Walshe, 1971 and 1977; Hendry, 1981; Walshe & Solomon 1981; Jones, 1985; Braithwaite, 1985; Eastoe *et. al.*, 1987; Solomon et. al., 1987; Flitcroft & McKeown, 1992; Raymond, 1992) although work by Sheppard (1987) also involved extensive surface geochemistry.

1.2 BACKGROUND

The Royal Tharsis deposit lying some 300 metres north of the Prince Lyell orebody was exposed during underground tunnel excavation in the late 1890s (Batchelor, 1901;

Cundy, 1901). The deposit has been mined as a separate orebody from underground and as part of a bigger operation in mining of the West Lyell Open Cut. Previous geological work on the Royal Tharsis as a separate deposit has been limited, primarily confined to diamond drilling and grade control measures employed during mining operations. Much of the early diamond drill core was not logged from an alteration perspective, but rather took the form of identifying volcanic precursors, sometimes with an emphasis on volcanic textures. Earlier work during mining operations has indicated that mineralisation in the Royal Tharsis is predominantly disseminated sulphides hosted by felsic volcanics. The deposit is conspicuous in that mafic to intermediate volcanics have a very restricted distribution. This is in direct contrast with other orebodies in the West Lyell group (notably the Prince Lyell deposit).

1.3 AIMS AND OBJECTIVES

The purpose of this study was to establish any relationships between copper mineralisation and alteration in the Royal Tharsis deposit with the aim of establishing vectors to economic mineralisation. The emphasis has been on the geochemistry of the deposit.

1.4 METHODOLOGY AND PRESENTATION

The study involved the following phases of investigation: review of old data, re-logging of historic core, delineation of alteration zoning, surface geochemistry, summary of thin section consultancy work commissioned by CMT and carried out by Barron (Barron, 1997), multi element analyses, whole rock geochemistry and interpretation.

The thesis is presented in several parts. The regional and local geological settings are described and a brief review of the history of the deposit is included. Surface geochemistry is investigated followed by alteration geology and alteration geochemistry. Data is presented as appendices and conclusions are drawn in the final chapter.

CHAPTER 2
REGIONAL GEOLOGY

2.1 REGIONAL SETTING

The Mount Lyell mineral field lies towards the southern end of the Mount Read Volcanic belt (MRV), (Figure 2.1) a Cambrian volcanic association of silicic lavas and volcaniclastics, abundant open-framework mass-flow breccias, minor intermediate volcaniclastics and intrusives, with scattered basic-intermediate dykes, and minor sedimentary lenses. The belt is some 10 - 20 km wide, extends over a strike length of about 230 km and is a major feature of the geology of Western Tasmania.

The belt occupies the eastern margin of the Lower Paleozoic Dundas trough, an elongate basin bounded unconformably by two blocks of Proterozoic metasediments - the Tyennan Region to the east and Rocky Cape Region to the north and west. The MRV are overlain by Late Cambrian to Early Ordovician siliciclastic Owen Conglomerate (Campana and King, 1963). The contact with the Tyennan is typically a depositional unconformity. The Dundas trough sequence can be considered in two parts, one related depositionally to the Rocky Cape and lacking felsic volcanics, and the other comprising the MRV and attached to the Tyennan region (Corbett and Lees, 1987).

The MRV comprises four major units or zones (Figure 2.2). The younger Tyndall Group overlies the three older units which are: a central volcanic complex (CVC), a western sequence (the Yolande River sequence (YRS) and equivalents) and an eastern sequence (Eastern Quartz Phyric sequence (EQS) and equivalents) (Corbett, 1992). The EQS has a basal unit of Precambrian-derived siliciclastics resting unconformably on Precambrian basement (Sticht Range Beds) and comprises quartz-feldspar-phyric lavas and volcaniclastic rocks, with intrusive porphyries and granitoids. The CVC comprises mainly felsic to andesitic lavas and interbedded pumice breccias. The YRS and equivalents contain Middle Cambrian fossils (Laurie *et al.*, 1995) and comprise

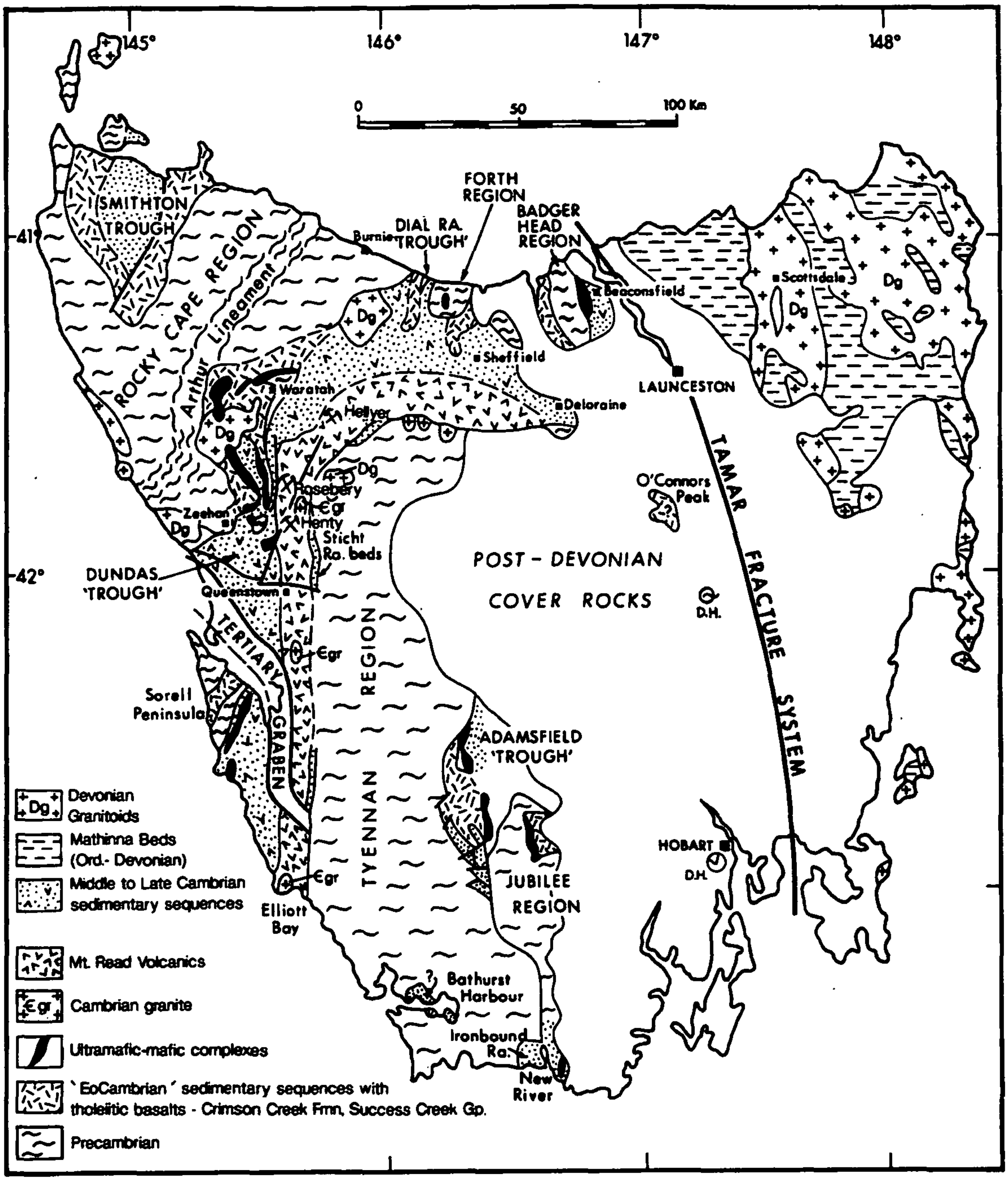

Figure 2.1 Simplified geological map of Tasmania showing the distribution of early Palaeozoic tectonic elements, emphasizing the MRV (after Corbett and Turner, 1989).

apron-like sequences of sandstone, shale and mass flow breccia, with bodies of intusive quartz-feldspar porphyry. The westerly limit of the YRS is in contact with the Crimson Creek Formation, a sequence of mafic greywacke, mudstone and basalt.

The MRV are predominantly Middle Cambrian with U-Pb zircon ages of around 502.6 ± 3.5 Ma; (Perkins and Walshe, 1993). The rocks have undergone locally intense hydrothermal alteration in the Cambrian and regional metamorphism to lower greenschist facies in the Devonian, giving quartz-sericite-chlorite-pumpellyite-epidote-actinolite bearing assemblages (Corbett and Lees, 1987). Most of the rocks appear to have been erupted in submarine environments, and include lavas, breccias, volcaniclastic rocks and subvolcanic intrusions. Non-welded submarine mass flow deposits are common within the host sequences of some of the VHMS polymetallic orebodies that characterise the MRV (McPhie and Allen, 1992; McPhie *et al.*, 1993). Geochemically, the MRV comprise medium to high K calc-alkaline andesites and more evolved lavas, with minor strongly LREE-enriched shoshonitic basalts (Crawford and Berry, 1991).

The MRV have undergone a complex tectonic history and show both textural and mineralogical modification. They are strongly cleaved and recrystalised, having been subjected to intense hydrothermal alteration during the Cambrian and to later local overprinting by the Devonian deformation. Berry and Kitto (1996) summarise ten major orogenic and depositional events of which the last five at least have impacted on MRV architecture.

Generally within the MRV the major fault trend is north - south. Of several dominant faults the Henty Fault (reverse extensional) divides the MRV into two distinct stratigraphic packages - an eastern and a western zone (Corbett and Solomon, 1989; Berry and Keele, 1993; Berry, 1994). North and west of the Henty Fault Zone the belt is divided into a Central Volcanic Complex and overlying correlates of the Dundas Group, large parts of which are of mainly andesitic composition. The massive sulphide deposits at Rosebery, Hercules, Que River and Hellyer are contained within this segment of the Mount Read Volcanic belt. South and east of the Henty Fault Zone,

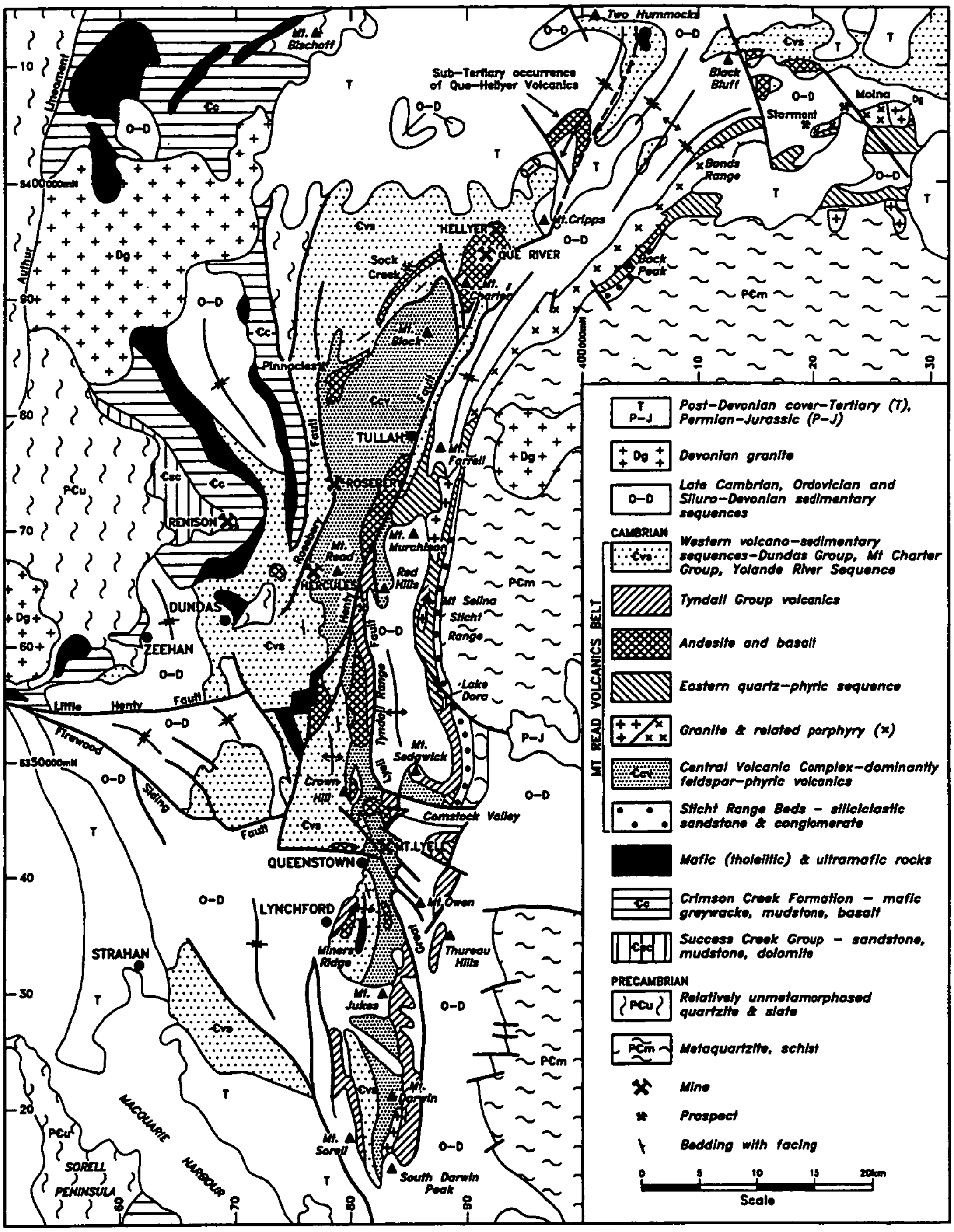

Figure 2.2 Simplified bedrock map of western Tasmania showing the linear extent of the CVC in the MRV with major Cambrian sequences and lithostratigraphic subdivisions (from Corbett, 1992).

the Mount Read Volcanics comprise a slightly younger Central Volcanic Complex of mainly feldspar-phyric rhyolitic volcanics, flanked by the volcano-sedimentary "western sequence". The Mount Lyell mineral field and the Henty gold deposit are located in this area. Both these packages are overlain by post-andesite Tyndall Group sequence of quartz - feldspar - phyric crystal - rich sandstones, mass-flow breccias and conglomerates with minor lavas and welded tuffs (White and McPhie, 1996). The Tyndall Group is in turn overlain by Owen Conglomerate.

The Owen Conglomerate comprises predominantly siliciclastic conglomerate and quartz sandstone being almost entirely derived from the Tyennan region to the east. Five formations have been recognised, attaining up to 2,000 metres total thickness, with each unit having a variable thickness and distribution (Solomon, 1964; Corbett, 1990). Exposure is broadly concentrated to the east of the CVC and west of the Tyennan block. Provenance is Precambrian, probably from rapidly uplifted Tyennan block metamorphics (Solomon, *op.cit.*; Corbett, *op.cit.*), with deposition taking place over a relatively short time span (Wills, 1996b). Clast size fines to the west while the dominant quartzite clasts are similar to basement lithologies. The depositional environment indicates a rapid transition from high energy subaqueous to alluvial to marine to intertidal (Laurie *et al.*, 1995) with a notable lack of haematite and chert clasts in the Lower Owen compared to the Middle and Upper Owen (Corbett, *op.cit.*). Minor volcanic detritus is common where the conglomerate is adjacent to or overlapping the MRV (Wade and Solomon, 1958; Solomon, 1969).

The Gordon Group comprises mainly limestones with some dolomites and minor sandstones overlying the Owen Group (Campana and King, 1963). The Gordon Group is in turn conformably overlain by the Siluro-Devonian Eldon Group sandstones and mudstones of shallow marine origin. Marine sedimentation continued through to the early Middle Devonian when onset of the Tabberabberan orogeny resulted in folding and faulting through most of Tasmania generally interrupting sedimentary processes (Banks and Baillie *in* Burrett and Martin, 1989, pp 182 - 237).

Numerous postkinematic granitoids were emplaced in Western Tasmania in the later stages of the Tabbberabberan (Solomon *et al.*, 1988), and significant mineral deposits are associated with some of these intrusions (e.g. Renison Bell, Mount Bischoff).

Deposition of marine sediments occurred through the Permo-Triassic period (Clarke and Forsyth *in* Burrett and Martin, 1989, pp 293 - 338), and these were subsequently intruded by Jurassic dolerite sills (Baillie *in op. cit.*, 1989, pp 339 - 409). Further faulting and folding occurred during the Mesozoic and Tertiary.

2.2 MOUNT LYELL MINERAL FIELD

2.2.1 Introduction

The Mount Lyell deposits are hosted in an extensive zone of intense hydrothermal alteration that extends six to eight kilometres of strike length (Figure 2.3). The mineral field covers approximately six km^2, comprises mainly CVC rocks bounded to the east by Denison, Gordon and Eldon Groups, and is characterised by prominent north-south and east-west trending faults. Tyndall Group rocks are present in the Comstock area (Corbett, 1989). Hydrothermal alteration (Wade and Solomon, 1958) has resulted in the almost complete destruction of feldspar with corresponding masking of the volcanic precursor. Direct evidence for the source of hydrothermal fluids is sparse. Granitic bodies have been postulated at depth (Large *et al.*, 1996), similar to the Darwin and Murchison granites and these represent potential heat sources. Over thirty mineralised deposits, containing copper, base metals and gold, have been recorded although not all of these have been mined. Several styles of mineralisation have been recognised (Wade and Solomon, 1958; Markham, 1968; McDonald, 1968; Bryant, 1975; Walshe and Solomon, 1981; Raymond, 1992; Wills, 1996b).

2.2.2 Stratigraphy

The stratigraphy of the Mount Lyell area is summarised in Table 2.1 (after Solomon and Carswell, 1989; Corbett and McPhie, 1993).

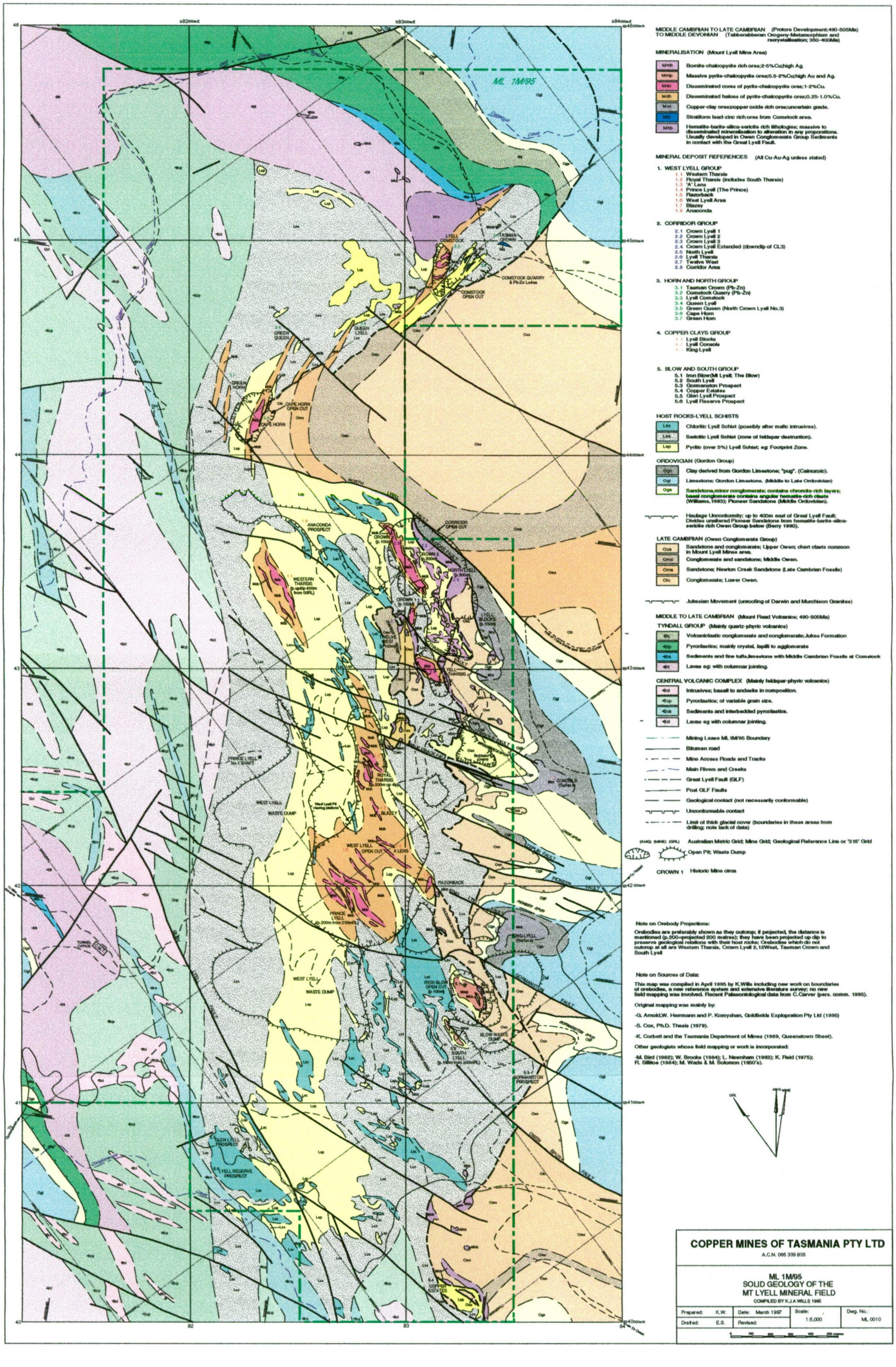

Figure 2.3 Mount Lyell mineral field solid geology interpretation (after Wills, 1995)

Table 2.1	**Mount Lyell Mineral Field** **Generalised Stratigraphic Succession**
Quaternary	Glacial till, alluvium, up to 100 metres thick.
Devonian	Lamprophyre dykes which post-date Devonian cleavage.
Ordovician	Grey limestone and dark grey shales of the Gordon Group, about 300 metres thick. Basal **Pioneer Beds** 10-30 metres thick overlying the Upper Owen with local discordance (Haulage Unconformity).
Upper Cambrian	**Owen Group**: siliciclastic conglomerates and sandstones, up to 1,000+ metres thick. Subdivided into: *Upper Owen sandstone* - mainly pink sandstone with minor conglomerates *Middle Owen conglomerate* - mainly pebble to cobble grade conglomerates and minor sandstones, locally with pebbles of haematite. *Middle Owen sandstone* - mainly red haematitic sandstone with interbedded chert-haematite clasts conglomerate. *Lower Owen conglomerate* - coase grained grey conglomerate, pebbles and boulders mainly of quartzite, quartz schist, and vein quartz ***Jukesian Unconformity***
Middle to Upper Cambrian	**Mt Read Volcanics**, at least 1,500 m thick, subdivided into: **Tyndall Group** - mainly volcaniclastic conglomerates in upper part, volcaniclastic sandstones in lower part with minor lavas, fossiliferous limestone and breccias. Subdivided into: *Upper Tyndall* (**Zig Zag Hill Formation**) *Middle Tyndall* (**Mount Julia Member**) *Lower Tyndall* (**Lynchford Member**) ***Unconformity*** ***"Central Volcanic Complex"*** (CVC) - consists of mixed felsic and andesitic volcanics and intrusives (lavas and pyroclastics of the "mine sequence" - Cox 1981) with andesites predominant in the upper part. ***"Western Sequence"***- consisting mainly of volcano-sedimentary rocks lying west of, and possibly of similar age to, the Central Volcanic Complex.

Central Volcanic Complex

The bulk of the Mount Lyell mineralisation is hosted by the CVC. Most of these rocks now consist of metamorphic assemblages of quartz, sericite, chlorite and sulphide in various proportions (Wade and Solomon, 1958). The felsic volcanics have podded and banded textures on weathered surfaces and tend to be siliceous and sericitic, whereas the more mafic volcanics tend to be more chloritic. Mineral assemblages are not diagnostic, as some of the intermediate- mafic volcanics have been converted to quartz-sericite schist in places, and some chloritic rocks have been derived from felsic protoliths. The highly variable assemblages demonstrate that alteration is not necessarily confined to lithofacies boundaries. The volcanics are mostly submarine erupted and deposited lavas, pyroclastics and epiclastics with minor interbedded sediments (Corbett, 1992). Facies within the Mount Lyell field include polygonal jointed massive lavas, fine grained intrusives, occasional pillow lavas, hyaloclastite breccias, as well as monomictic and polymictic debris flows (Perkins, 1996; Wills, 1996b).

Tyndall Group

Tyndall Group outcrops are present in the Comstock area at the northern end of the Mount Lyell mineral field, and also in the Queen river area to the west and south west (Corbett *et. al.*, 1989). The Group comprises variable lithologies (similar to the CVC) that tend to contain abundant, and hence diagnostic, quartz-phyric volcanics (Solomon, 1967; Arnold, 1985; Komyshan, 1985; Corbett, 1986). Tyndall Group rocks do not exhibit the same intense feldspar destruction as shown by the CVC altered volcanics, with regional metamorphism having converted remnant calcium to epidote resulting in a not uncommon pink and green appearance. Limestone, with late Middle Cambrian trilobites (Jago *et al.*, 1972) has been identified in the Tyndall rocks in the Comstock area and is indicative of shallow marine depositional conditions. The area is also characterised by mass-flow breccias and conglomerates containing polymict clasts of altered volcanics and andesites, and sulphide-bearing clasts (pyrite, galena, sphalerite and possibly chalcopyrite) (Green, 1971; Hall, 1975, Wills, 1996b). The welded tuff at Zig Zag hill has recently been reinterpreted by McPhie and White (1996) to represent a shallow marine depositional environment.

Owen Group (Owen Conglomerate)

In the Mount Lyell area hydrothermally altered MRV and siliciclastic Owen Conglomerate are juxtaposed along the Great Lyell Fault. The Owen Conglomerate consists of fine to very coarse siliciclastics of mixed fluvial and shallow marine facies, and in parts is coloured distinctively by fine haematite (Solomon, 1964). Near the Great Lyell Fault the Haulage unconformity separates the Owen Conglomerate from the overlying Pioneer Beds and Gordon Limestone (Corbett, 1990, 1996). The high energy sedimentary facies that are characteristic of the Owen Group would tend to indicate rapid deposition over a relatively short time span. Faunal evidence indicates this to be a time span of two to three million years (Laurie *et al.*, 1995; Wills, 1996b).

The **Lower Owen Conglomerate** is confined to limited outcrops at Cape Horn, Tharsis ridge and on Mount Lyell itself. The unit consists of a matrix-supported boulder conglomerate. Work by Solomon (1964) and Corbett (1990) suggests that the unit represents an emergent period for the underlying volcanics with a barrier to the west.

The **Middle Owen Sandstone** is a marine sequence of strongly haematitic quartz sandstone with thin bands of coarser sandstone and finer siltstone (Corbett, 1990). The **Middle Owen Conglomerate** is limited in outcrop occuring as a thin continuous band on Mount Owen that thickens rapidly towards Mount Tyndall (approximately 12 kilometres north of Mount Lyell). It is composed of bedded, pebble to boulder conglomerate and in which altered volcanic clasts tend to be less well rounded than Precambrian derived clasts (Corbett, 1990; Hart, 1993; Wills, 1996b).

The **Upper Owen Sandstone** is extensively exposed within the Mount Lyell field: on Mount Lyell itself; as a sedimentary contact over the CVC and as a fault bounded block juxtaposed against the Iron Blow; and to the south on Mount Owen. (Gregory, 1905; Solomon, 1964, Brophy, 1977; Corbett, 1990). It is a variable coarse to medium grained, haematitic sandstone with local shale and haematite-rich bands. Cross bedding, ripple marks and paleocurrent directions are all indicators of an intertidal environment (Solomon and Carswell, 1989; Corbett, 1992). Laurie *et al.*, (1995) have inferred an age of 493 Ma (Middle Late Cambrian or Payntonian).

Gordon Group

The middle Ordovician **Pioneer Beds** are considered to represent a semi continuous fine clastic to chemical sedimentary package (Seymour and Calver, 1995) and have been dated on marine gastropod and rhynchonellid brachipods as Middle Ordovician (possibly 458 - 400 Ma - Laurie *et al.*, 1995). In the Mount Lyell mineral field the Pioneer Beds are unconformable on the Upper Owen Sandstone, with an angular difference in places of 130° (Haulage Unconformity) (Wade, 1957; Solomon, 1964; Cox, 1981; Arnold, 1985; Berry, 1991; Williams, 1993). The unit is probably diachronous, generally being no more than 10 metres thick and comprises chromite-bearing sandstone, pebbly sandstone, and pelitic interbeds with a poorly preserved marine fauna. In the Comstock area and in several places around the Queen river the Pioneer Beds rest directly on Tyndall Group with no intervening Owen rocks. Chromite grains, with up to 3,000 ppm Cr, are diagnostic (Hart, 1993) and point to derivation by erosion of ultramafic rock(s)..

The **Gordon Limestone** comprises a sequence of basal interbedded limestone and sandstone followed by micritic impure limestone (Seymour and Calver, 1995) and is confined to the eastern edge of the Mount Lyell mineral field.

Lamprophyre Dykes

Intrusive lamprophyre dykes post date mineralisation within the Mount Lyell field and cut across cleavage and foliation. They have a variable composition ranging from coarsely porphyritic to fined grained, and are generally texturally well preserved with abundant magnetite and possibly titanomagnetite (Crawford, 1995a). The presence, in trace amounts, of sulphides are considered to be related to alteration and/or remobilisation rather than to primary, whilst small euhdral chromite inclusions have also been observed (Crawford, *op. cit*). The dykes are considered to be Devonian in age or possibly younger (Reid, 1975) and have been dated from 363 to 373 Ma (Baillie and Sutherland, 1992; McClenaghan *et al.*, 1994).

Glaciation and Paleogeomorphology

Glaciation in the Linda Valley occurred during the Pleistocene (Fitzsimons *et al.*, 1993) with a tongue of ice flowing up the valley away from the main glacier in the

King Valley. The Lyell Blocks area has glacited moraine overlying, and intermixed with, Pioneer/Gordon clays. Moraines at Gormanston and elsewhere in the Linda Valley are ascribed to the Pleistocene (Fitzsimons *et al.*, *op. cit.*)

2.2.3 Structure

The complex tectonic history interpreted generally for the MRV is clearly demonstrated in the Mount Lyell mineral field. Two major orogenies have been recognised; an earlier Cambrian (Delamerian or Tyennan) and a later Devonian (Tabberbberan) event. Both of these events probably occurred in several stages (Cox, 1979; Berry, 1991).

The overall structure of Mount Lyell (Figure 2.4) is that of a steeply dipping overturned limb of a large D1 anticline (Cox, 1981; Berry 1990). Different styles of deformation are seen in the volcanics and in the younger, sedimentary sequences. The geometry of the CVC is controlled largely by upright NNW trending D1 folds with wavelengths of 1.5km. Movement accommodated by tight upright folds in the Ordovician and Siluro-Devonian sediments is taken up by steep reverse faulting and cleavage-parallel shearing in the altered volcanics. Cleavage related to D1 is sporadically developed within the volcanics, probably due to low grade regional metamorphism associated with shallow depth of burial. A pervasive D2 cleavage/foliation tends to be the dominant structural feature, having a steep south - west dip (Berry, 1991). Rotation of the cleavage in the volcanics occurs adjacent to the more competent Owen Conglomerate. The D2 cleavage planes tend to preferentially accommodate stress arising from shears and faults and a strong down-dip elongation lineation (L2) is associated with D2 cleavage formation in the volcanics. Shortening of up to 60% perpendicular to the cleavage and elongation of up to 150% in the lineation direction are typical, and are responsible for the elongation of many of the sulphide mineral deposits down dip (Cox, 1979, 1981).

The Linda Disturbance is a west north west trending shear zone certainly activated during the Tabberabberan and probably formed during or before the earlier Cambrian

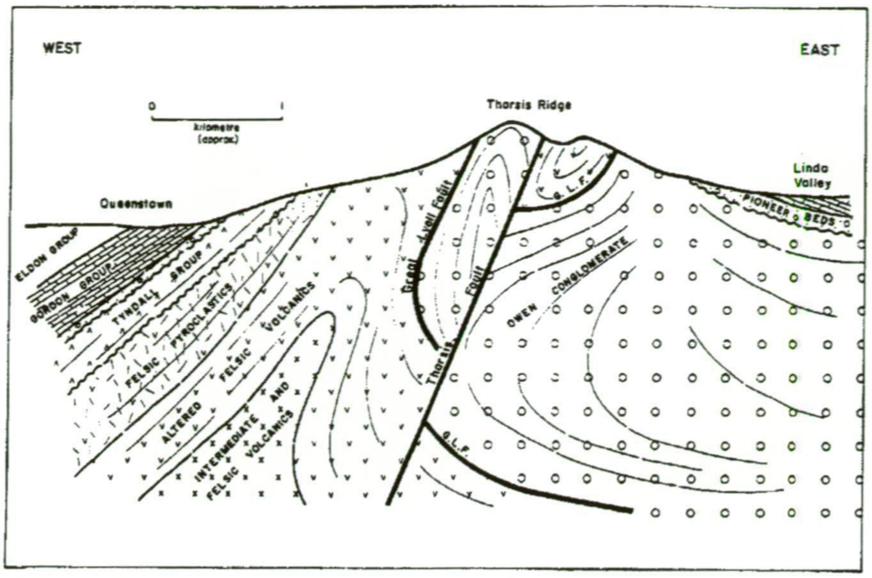

Figure 2.4 Schematic cross sections through Mount Lyell (looking north) showing broad structure (above) and representative attitude of ore deposits (below) (after Hills, 1990)

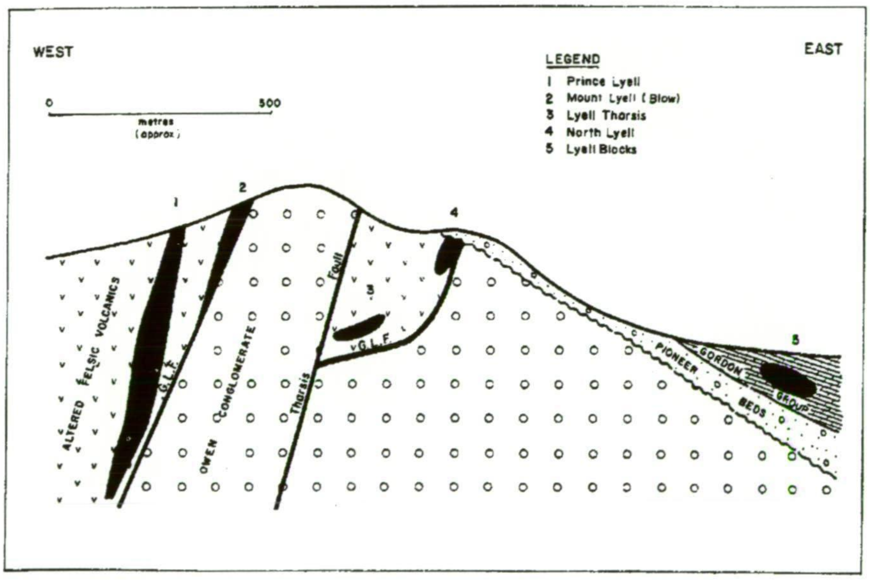

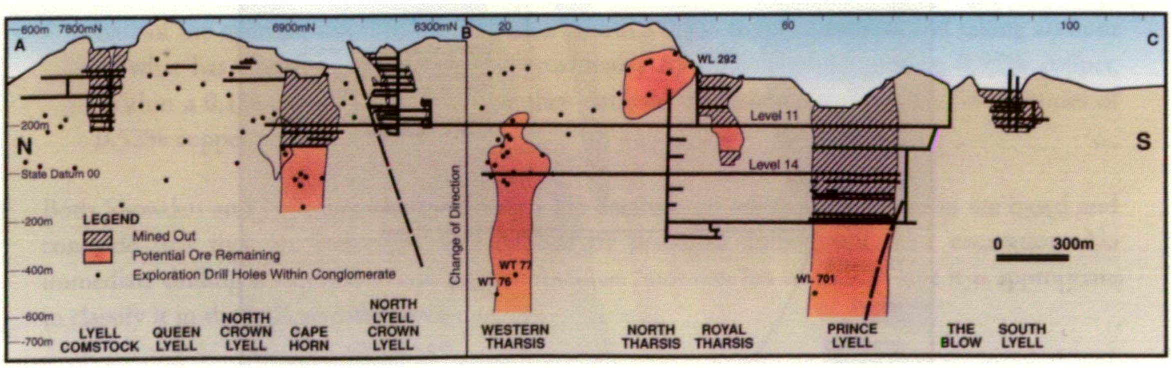

Figure 2.5 Longitudinal section (north - south) through Mount Lyell mineral field showing the position of some of the more important ore deposits

orogeny (Berry *in* Cooke and Kitto, 1994, p 9). Commensurate with the Linda Disturbance activation of the North Lyell Fault resulted in a significant westerly offset to the Great Lyell Fault as well as the development throughout the area of a regionally penetrative upright WNW - trending cleavage (Berry, 1990). Both the Great Lyell Fault and the North Lyell Fault exerted some control on the ultimate form of the Mount Lyell field, although exact relationships have not been established. Wills (1996b) has defined the Great Lyell Fault as an intermittent decollement structure that juxtaposes an upper rigid siliciclastic Owen Conglomerate and a lower ductile altered CVC sequence. Recognition by Corbett (1996) that the Great Lyell Fault is not present in the southern corridor area points to a pre-Devonian origin for this fault.

During the Cambrian orogeny Mount Lyell was tectonically very active. The Owen Group unconformities are the main evidence for Cambrian tectonism which appeared to occur over a very short time span of 510 to 495 Ma (Berry and Kitto, 1996). This correlates with the Delamerian orogeny of south eastern Australia (Williams, 1978). The Haulage Unconformity is explained as a product of more intense Cambrian deformation within a low strength hydrothermally altered area. The cause of the folding in the conglomerate beneath the Haulage Unconformity in a 400m wide zone adjacent to the Great Lyell Fault is contentious (Berry, 1990).

The Devonian orogeny has been dated at 390 to 380 Ma (Williams *et al.*, 1989; Seymour and Calver, 1995). Two major phases of deformation have been recognised, an earlier north - south event and a later WNW - ESE event, and during which temperature ranged from 275°C to 350°C under a confining pressure of about 2kb (Cox, 1981). Cleavage within the CVC is related to the hydrothermal alteration mineralogy. Cox (*op. cit.*) and Williams *et al.* (*op. cit*) recognise one Devonian cleavage while Arnold (1985) and Berry (1990) recognise two. Complex faulting has been recognised although evolution of knowledge has resulted in variations in the modus operandi of fault emplacement: Loftus-Hills (1927) proposed multiple complex phases; Cox (1979) suggested at least four stages of North Lyell faulting; while Berry (*op. cit*) recognised the Devonian tectonics as being a complex reactivation and extension of the early Cambrian structures. Berry (1991) further recognised the CVC sequence to be continually east facing with the Iron Blow deposit being overturned (Wills, 1996b).

Devonian veins tend to mimic local mineral assemblage (Green, 1971; Cox, 1981) and reflect proximity to the hydrothermal alteration system. Cox (*op.cit.*) has further inferred that vein assemblages are the product of fluid - wall rock interaction.

2.2.4 Ore Deposits

Several styles of mineralisation encompassing over twenty separate deposits have been recognised in the Mount Lyell field (Figure 2.5) as described by Wade and Solomon (1958), Markham (1968), Bryant (1975), Walshe and Solomon (1981). Wills (1996b) has extended this recognition by categorising the five groups and has further refined this classification by distinguishing massive and disseminated sulphides (Wills, *op.cit.*).

The massive sulphide deposits occur near the top of the mine sequence. Although largely recrystallised, these ores preserve some laminated textures, suggesting a sea-floor exhalative origin (Arnold and Carswell, 1990). The larger but lower grade pyrite-chalcopyrite deposits are found stratigraphically beneath the massive sulphide mineralisation and the bornite-chalcopyrite ores, whilst base metals (galena and sphalerite) occur at Comstock. The alteration zones are broadly coincident with the sulphide mineralisation which is confined to the altered CVC. The "copper clay" deposits occur within clay horizons of the Ordovician Gordon Limestone.

Table 2.2 Mount Lyell Ore Production, 1893 - 1997

Deposit	Tonnes	Cu %	Au g/t	Ag g/t
West Lyell Group	92,921,000	0.95	0.3	2.1
North Lyell Group	10,400,000	3.38	0.3	19.6
Horn Group	5,395,000	1.67	0.4	3.8
Copper clays	243,000	1.57	0	0
Blow Group	5,463,000	1.30	1.9	64.7
TOTAL	**114,422,000**	**1.22**	**0.4**	**6.7**

(West Lyell group = West Lyell open cut, Royal Tharsis, Prince Lyell (including A lens), Razorback;

North Lyell group = Crown Lyell 1, 2 and 3, Twelve West, North Lyell and Lyell Tharsis;
Horn group = Lyell Comstock, Cape Horn;
Copper clays = Lyell Blocks, Lyell Consuls, King Lyell;
Blow group = Iron Blow, South Lyell)

Production from the five main ore types is summarised in Table 2.2. Total contained metal yielded by the Mount Lyell mineral field amounts to some 1.41 million tonnes of copper, 773,000 kgs of silver and 1.46 million ounces of gold.

Styles

More recently Wills (1996b) has extended recognition of the main styles of mineralisation by categorising five main groups. His interpretation invokes an active hydrothermal field analogous to the TAG field along the Atlantic Ridge (Ronna *et al.*, 1993). The massive sulphides equate to the TAG mound while the disseminated sulphides represent stacked lenses in a very large hydrothermal field (also accounting for the relationship between alteration and sulphide mineralisation). A redox model has also been proposed by other workers (Solomon, 1969; Arnold, 1985; Sillitoe, 1985; Berry, 1990; Raymond, 1993; Large *et al.*, 1996). At the redox interface reducing hydrothermal fluids charged with base metals, sulphur and barite reacted with cooler connate water emanating from an eroding Owen Conglomerate. Bornite mineralisation is probably related to a separate thermal pulse(es) resulting in establishment of a redox interface at the altered CVC - Owen Conglomerate contact, and may be of a younger age than the more widespread disseminated and massive styles of mineralisation.

Disseminated pyrite-chalcopyrite

Disseminated pyrite-chalcopyrite mineralisation accounts for around 86% of the orebodies, and from which some 92 million tonnes with an average grade of 0.95% Cu, and 0.31g/t Au, and 2.10g/t Ag have been mined. Grades of deposits in this group range from 0.72% to 2.38% Cu and includes the following ore bodies; Prince Lyell, A lens, Blazey, Royal Tharsis, Western Tharsis, Crown Lyell 1 and 3, and Cape Horn.

Pyrite and chalcopyrite mineralisation is most abundant in the felsic volcanics, but is locally present in more mafic units. Chalcopyrite content is independent of pyrite abundance in detail, although on a broad scale copper mineralisation is invariably hosted by more pyritic zones within the volcanics. Minor amounts of galena and sphalerite are not uncommon. Magnetite bodies and apatite lenses have been exposed in the Prince Lyell orebody (Raymond, 1992). Gold occurs in the form of silver-rich electrum. Molybdenite is an accessory mineral in most deposits, occuring in trace amounts. (Crawford, 1995a, 1995b). Trace amounts of cobalt are associated with phase 3 of the pyrite mineralisation (Raymond, 1996).

In general the deposits are elongate, lensoid bodies with the longer axis parallel to local cleavage. Dip is steep and to the west (65° - 80°) and strike is to the north. The most obvious feature of this deposit style is extensive down dip continuity, unless truncated by the Great Lyell Fault, frequently being open both along strike and down dip. Both Prince Lyell and Western Tharsis orebodies extend 600 metres below sea level.

Generally the disseminated copper deposits comprise two distinct grade populations, namely high grade cores and low grade envelopes, resulting in high grade - low tonnage and low grade - high tonnage distributions. Production from these deposits, particularly from Prince Lyell has encompassed both distributions. Interpolation of these grade zones generally enables the deposits to be resolved into lenses of higher grade mineralisation that are concordant with the well developed foliation and broad stratification within the volcanics.

Massive pyrite-chalcopyrite

The largest bodies of this mineralisation style are the Iron Blow (the original Mount Lyell) and the adjacent sub-surface South Lyell deposit, and from which some 5.5 million tonnes at 1.30%Cu, 1.98g/t Au and 64.70g/t Ag were mined. Production grades were distorted by high grade gold and silver (stromeyerite) shoots of up to 15 g/t Au and 2,000 g/t Ag against the Great Lyell Fault (Blainey, 1954).

These deposits are the most convincingly volcanogenic mineralisation in the Mount Lyell field. Beds, boudins and large lenses of finely-laminated massive pyrite are accompanied by variable Cu, Pb and Zn sulphides (Sticht, 1905, 1906). Framboidal textures have been recognised (Markham, 1968). Mineralisation is hosted entirely by the silicic, rather than the more mafic volcanics, whilst the frequently fault bounded contact with the Owen Conglomerate is notable for haematite barite alteration. Significant tetrahedrite is also present at the Iron Blow (Gregory, 1905).

Bornite-chalcopyrite

Many of these orebodies are blind pods of mineralisation that do not outcrop. By comparison with the disseminated pyrite-chalcopyrite style orebodies they are small, ranging in size from 50m to 300m down dip, 30m to 150m along strike and 30m to 60m in width. They account for less than 10% of the gross resource, and from which some 10.4 million tonnes with average grades of 3.38% Cu, 0.38g/t Au and 19.57g/t Ag have been mined. Grades of deposits in this group range from 1.62% to 5.28% Cu with gades of up to 40% Cu reported locally. Ore bodies within this group include; North Lyell, Crown Lyell 2, Twelve West, Lyell Comstock and Lyell Tharsis.

These deposits are associated with intense haematite-barite or silica-hematite-barite alteration that occurs at the Owen Conglomerate contact. Primary textures are obliterated particularly in the most haematite-silica-barite altered zones. Sillitoe (1985) postulated bornite formation through the mixing of reduced hydrothermal fluid with cooler connate water. Anomalously steep to easterly dipping parts of the more prominent faults seem to be preferred sites for the remobilised alteration.

Base metals; pyrite-galena-sphalerite-chalcopyrite

Sub-economic amounts of galena and sphalerite occur in the Comstock area. Mineralisation is associated with both massive (e.g. Comstock quarry (Markham, 1968)) and disseminated (e.g. Cape Horn (Green,1971)) pyrite-chalcopyrite styles. Framboidal textures have been recognised (Green, *op. cit.*). Grades of 28% Pb, 20%

Zn and 0.5% Cu, associated with galena lodes, were recorded in Tasman Crown workings, but only in minor tonnages mined.

Some 5.4 million tonnes of ore at a grade of 1.67%Cu, 0.48g/t Au and 3.78g/t Ag have been mined from these deposits. The bulk of the tonnage has come from Cape Horn. Mineralisation occurs as brecciated chert bodies (Markham, 1968; Green, 1971) and is commonly associated with strong sericite-pyrite-quartz alteration. The lead - zinc rich sulphides are possibly representative of exhalative horizon(s) at the top of a large hydrothermal alteration zone that would be characteristic of a VHMS sytem.

Copper clays; native copper-cuprite

The Copper Clay style of deposit includes a small group of deposits along the eastern boundary of the mineral field. Deposits of this type include Lyell Blocks, Lyell Consuls and King Lyell. Production from these deposits was limited by ground conditions and water (Solomon, 1969).

Mineralisation occurs as native copper and copper oxides, including cuprite which gives way to chalcocite at depth, in weathered carbonaceous and ferruginous Gordon Limestone (Edwards, 1958; Markham, 1966; Reid, 1975). These deposits are in part associated with limonitic gossan (Solomon, *op. cit.*) and are thought to have been formed through fluvioglacial processes involving precipitation of copper in a clay residue after (Gordon) limestone (Wills, 1965). Mineralisation is considered to be geological young (Cainozoic) due to the incoherent nature of the host lithology within Gordon Group units that are above the Haulage unconformity (Wills, *op. cit.*).

Age of Mineralisation

The following evidence points to a Cambrian age for some of Mount Lyell mineralisation:

- radiometric zircon (U-Pb) dating of 502 ± 3.5 Ma (Perkins and Walshe, 1993; Perkins, 1996) on the host volcanics

- a biostratigraphic age of about 501 Ma through fossil identification (Jago *et al.*, 1972; Laurie *et al.*, 1995)
- framboidal and colloform textures suggestive of pre-metamorphic sulphides (Markham, 1968; Hall, 1975; Cox, 1981)
- lead isotope work pointing to a Cambrian age (Gulson and Porritt, 1987)
- sulphur and oxygen isotope work suggestive of derivation from Cambrian seawater (Raymond, 1992)
- similarity of the Iron Blow and Tasman Crown to the Rosebery (Braithwaite, 1974; Green *et al.*, 1981; Corbett, 1997) and Hellyer (Gemmell and Large, 1992; Allen *in* Cooke and Kitto, 1994, pp 107 - 108) systems which have been dated as Cambrian VHMS deposits
- mineralised clasts in the Tyndall Group suggestive that hydrothermal alteration and sulphide mineralisation are syn- or post-CVC and pre-Tyndall in age (Corbett, 1981)
- overlying Tyndall volcanics are significanlty less altered than CVC volcanics (i.e. main CVC alteration is pre-Tyndall) (Corbett, 1977)
- the abundance of haematite clasts after sulphides in the Owen suggests at least a pre-Owen age for some of the mineralisation
- sedimentological evidence (McPhie *et al.*, 1993) whereby sulphide clasts in volcanic units must be of at least the same age as the host rock
- similarity in haematitic clast chemistry with the chemistry of massive haematiic sulphide bodies (e.g. the Iron Blow and North Lyell) (Hart, 1993)

This evidence does not account for mineralised quartz veins that are common throughout the field. These are generally considered (Bird, 1984; Sillitoe, 1984, 1985; Arnold, 1985; Berry, 1990) to be Devonian remobilisation associated with the Tabberabberan Orogeny. These veins are thought to be post S2 development and pre-lamprophyre dyke emplacement (Cox, 1979), and have been assigned an age of 380 - 390 Ma. It should be noted that these veins alone do not carry significant economic mineralisation.

CHAPTER 3
ROYAL THARSIS - DISCOVERY, HISTORY AND GEOLOGY

3.1 HISTORICAL BACKGROUND

The actual discovery of the Royal Tharsis deposit is not fully recorded although the deposit was known at the turn of the century when South Tharsis and Royal Tharsis were separate mines purchased by MLMRC. At that time there was obviously some sub surface development as assessment reports (Batchelor, 1901; Cundy, 1901) refer to drive and tunnel excavations, rises and winze development, with some not insignificant copper grades. Prior to their purchase by MLMRC production from both mines was concentrated in a plant located on Glovers Creek (Nye *et al.*, 1934). Nye (*op. cit.*) describes Royal Tharsis surface outcrop located some 50 feet (approximately 15 metres) from the south west extremity of the Tharsis conglomerate with mineralisation occurring 6 inches (approximately 15 centimetres) below surface.

Lithologies were described as impregnated schists striking N65°W, dipping 72°W (Batchelor, 1901); and as schist and quartzites dipping 70°W with impregnated Fe and Cu pyrites (Cundy, 1901). Cundy distinguished two types of ore; one being quartzite with chalcopyrite and bornite mineralisation, and the other being schist with disseminated chalcopyrite. These are akin to North Lyell and West Lyell type mineralisation (Markham, 1968) and have implications for both geological settings and consequential exploration.

3.2 LOCATION

The Royal Tharsis deposit is located at the northern end of the former WLOC some 300 metres north of the Prince Lyell orebody. Any surface expression has long since been removed by mining. The mined deposit had a dip of between 60° and 80° to the west, a regional strike of 315°, approximate dimensions of 500 metres long by 30 metres wide and extended to a depth of 600 metres below surface. Depth extension is constrained by the Great Lyell Fault and westerly plunging Owen Conglomerate,

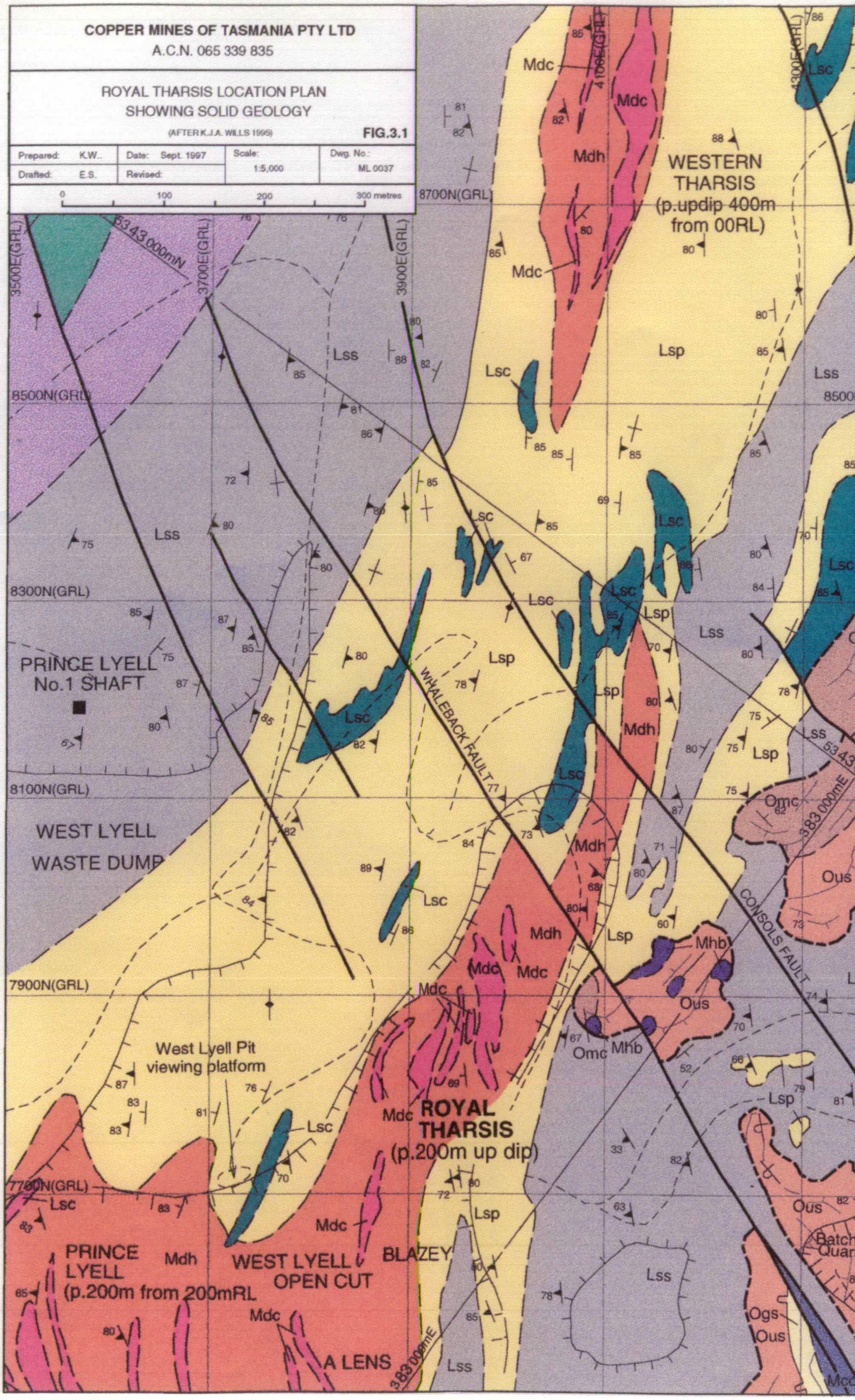
COPPER MINES OF TASMANIA PTY LTD
A.C.N. 065 339 835
ROYAL THARSIS LOCATION PLAN
SHOWING SOLID GEOLOGY
(AFTER K.J.A. WILLS 1995)
FIG.3.1
Prepared: K.W.
Drafted: E.S.
Date: Sept. 1997
Revised:
Scale: 1:5,000
Dwg. No.: ML 0037
0
100
200
300 metres
WESTERN THARSIS
(p.updip 400m from 00RL)
PRINCE LYELL No.1 SHAFT
WEST LYELL WASTE DUMP
WHALEBACK FAULT
CONSOLS FAULT
West Lyell Pit viewing platform
ROYAL THARSIS
(p.200m up dip)
PRINCE LYELL
(p.200m from 200mRL
WEST LYELL OPEN CUT
BLAZEY
A LENS
8700N(GRL)
8500N(GRL)
8300N(GRL)
8100N(GRL)
7900N(GRL)
7700N(GRL)
3500E(GRL)
3700E(GRL)
3900E(GRL)
4100E(GRL)
4300E(GRL)
5343 000mN
383 000mE
Lss
Lsp
Lsc
Mdc
Mdh
Mhb
Omc
Ous
Ogs

IDDLE CAMBRIAN TO LATE CAMBRIAN (Protore Development;490-505Ma)
O MIDDLE DEVONIAN (Tabberabberan Orogeny-Metamorphism and recrystallisation; 350-400Ma)

INERALISATION (Mount Lyell Mine Area)

Mmb Bornite-chalcopyrite rich ores;2-5%Cu;high Ag.

Mmp Massive pyrite-chalcopyrite ores;0.5-2%Cu;high Au and Ag.

Mdc Disseminated cores of pyrite-chalcopyrite ores;1-2%Cu.

Mdh Disseminated haloes of pyrite-chalcopyrite ores;0.25-1.0%Cu.

Mcr Copper-clay ores;copper oxide rich ores;uncertain grade.

Ms Stratiform lead-zinc rich ores from Comstock area.

Mhb Hematite-barite-silica-sericite rich lithologies; massive to disseminated mineralisation to alteration in any proporations. Usually developed in Owen Conglomerate Group Sediments in contact with the Great Lyell Fault.

Mine Access Roads and Tracks

Great Lyell Fault (GLF)

Post GLF Faults

Geological contact (not necessarily conformable)

Bedding trends in the Owen Conglomerate

20 60 S Bedding,strike and dip; vertical bedding; overturned

70 S Cleavage, strike and dip; vertical cleavage

(AMG) (MINE) (GRL) Australian Metric Grid; Mine Grid; Geological Reference Line or '315' Grid

Open Pit; Waste Dump

OST ROCKS-LYELL SCHISTS

Lsc Chloritic Lyell Schist (possibly after mafic intrusives).

Lss Sericitic Lyell Schist (zone of feldspar destruction).

Lsp Pyritic (over 5%) Lyell Schist; eg: Footprint Zone.

RDOVICIAN (Gordon Group)

Ogc Clay derived from Gordon Limestone; "pug". (Cainozoic).

Ogl Limestone; Gordon Limestone. (Middle to Late Ordovician)

Ogs Sandstone,minor conglomerate; contains chromite-rich layers; basal conglomerate contains angular hematite-rich clasts (Williams,1993); Pioneer Sandstone (Middle Ordovician).

Haulage Unconformity; up to 400m east of Great Lyell Fault; Divides unaltered Pioneer Sandstone from hematite-barite-silica-sericite rich Owen Group below (Berry 1990).

ATE CAMBRIAN (Owen Conglomerate Group)

Ous Sandstone and conglomerate; Upper Owen; chert clasts common in Mount Lyell Mines area.

Omc Conglomerate and sandstone; Middle Owen.

Oms Sandstone; Newton Creek Sandstone (Late Cambrian Fossils)

Olc Conglomerate; Lower Owen.

Jukesian Movement (unroofing of Darwin and Murchison Granites)

IDDLE TO LATE CAMBRIAN (Mount Read Volcanics; 490-505Ma)

YNDALL GROUP (Mainly quartz-phyric volcanics)

€tj Volcaniclastic conglomerate and conglomerate;Jukes Formation

€tp Pyroclastics; mainly crystal, lapilli to agglomerate

€ts Sediments and fine tuffs,limestone with Middle Cambrian Fossils at Comstock

€tl Lavas eg: with columnar jointing.

ENTRAL VOLCANIC COMPLEX (Mainly feldspar-phyric volcanics)

€ci Intrusives; basalt to andesite in composition.

€cp Pyroclastics; of variable grain size.

€cs Sediments and interbedded pyroclastics.

€cl Lavas eg with columnar jointing.

Note on Orebody Projections:

Orebodies are preferably shown as they outcrop; if projected, the distance is mentioned (p.200=projected 200 metres); they have been projected up dip to preserve geological relations with their host rocks; Orebodies which do not outcrop at all are Western Tharsis, Crown Lyell 2,12West, Tasman Crown and South Lyell

Note on Sources of Data:

This map was compiled in April 1995 by K.Wills including new work on boundaries of orebodies, a new reference system and extensive literature survey; no new field mapping was involved. Recent Palaeontological data from C.Carver (pers. comm. 1995).

Original mapping was mainly by:

-G. Arnold,W. Herrmann and P. Komyshan, Goldfields Explopration Pty Ltd (1995)

-S. Cox, Ph.D. Thesis (1979).

-K. Corbett and the Tasmania Department of Mines (1989, Queenstown Sheet).

Other geologists whose field mapping or work is incorporated:

-M. Bird (1982); W. Brooks (1984); L. Newnham (1993); K. Reid (1975); R. Sillitoe (1984); M. Wade & M. Solomon (1950's).

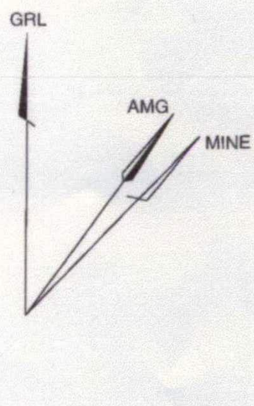

LEGEND FOR FIG 3.1
ROYAL THARSIS LOCATION PLAN

although the precise basal position has not been established and there is potential for the orebody being open at depth.

On plan (Figure 3.1) the deposit extends from an approximately southerly limit along 7700N to 8500N in the north, and from 3600E at its westerly limit to 4400E in the east (co-ordinates in 315GRL grid). The deposit can be split into two areas, one to the north (historically equivalent to the Royal Tharsis mine) and one to the south (historically equivalent to the South Tharsis mine). Mineralisation can be extrapolated along strike, to the north as the Western deposit, and to the south as A lens and the Prince Lyell deposits. The boundaries between the various orebodies are not precise, being more a function of gradually decreasing sulphide mineralisation and usually defined on a copper contour. To the north east the Tharsis Ridge (Figure 3.2) forms a potential topographic buttress between the West Lyell and North Lyell styles of mineralisation. To the west a subtle change to a gently sloping topography marks a rough correlation with the limit of the alteration system.

Figure 3.2
Photograph (looking north) of the Tharsis Ridge which marks the eastern limit of and dominates the northern boundary of the Royal Tharsis deposit. The ridge is composed of both middle and upper Owen Group and it is faulted across both north-south and east-west axes. The view is predominantly of middle Owen lithologies (to the west of the picture) that consist of sandstone and conglomerate. To the east of the picture the lithologies pass into upper Owen sandstone and conglomerate and in which chert clasts are common.

3.3 GEOLOGY

The geology and mineralisation of Royal Tharsis is similar to that of Prince Lyell. Little has been written about the Royal Tharsis deposit (Gregory, 1905; Nye *et. al.*, 1934), in contrast to a significant number of publications that describe the Prince orebody (Alexander (1953); Wade and Solomon, (1958); McDonald (1968); Reid (1978); Hendry (1981); Bird (1982); Arnold and Carswell (1990); Hills (1990); Flitcroft and McKeown (1992); Raymond (1992)).

3.3.1 Stratigraphy

The Royal Tharsis deposit occurs within steeply dipping overturned, altered rhyolitic volcanics. The local term of felsic has been used commonly in describing the main type of alteration lithology (Wade and Solomon, 1958). Relict igneous textures and trace element geochemistry indicate that a wide range of rhyolitic and dacitic lava breccias and volcaniclastic rock types may be the precursors to the alteration lithology described as felsic volcanics.

Copper mineralisation is almost entirely hosted within a sequence of intensely altered **felsic volcanics**. The structural footwall (stratigraphic hangingwall) rocks comprise altered felsic volcanics similar to the mineralised horizon, with enclaves of less altered volcanics, volcanic breccias and very occasional fine grained shale or ash units. The felsic volcanic sequence is up to 500 metres thick. A large proportion of the stratigraphic hangingwall sequence towards the south end of the ore zone is truncated by the Great Lyell Fault. Gregory (1905) refers to the faulted nature of the schist/conglomerate contact. As alteration and deformation become more intense an increasingly recrystallised siliceous groundmass is generated (see Appendix IV).

Within the ore horizon, the felsic volcanics are variably pink to grey, quartz chlorite-sericite rocks in hand specimen, often within medium to coarse phyllosilicate alteration domains. Pink colouration is caused by extremely fine grained disseminated haematite in the quartz rich domains. The haematite dusting is usually visible in the structural footwall rocks where the felsic volcanics may develop a very deep red colour. Highly altered dacitic volcanics are probably a minor component of the Royal Tharsis stratigraphy based on identification of similar lithologies in the Prince Lyell deposit as described by Raymond (1992) and where they probably represent altered lavas or shallow intrusives rather than bedded rocks.

In thin section the felsic volcanics consist predominantly of very fine grained mosaic-textured quartz (with minor disseminated sericite ± chlorite ± siderite) crossed by a network of anastomising wisps of sericite ± chlorite (Hendry, 1981; Braithwaite, 1985)(and Appendix IV). Accessory minerals such as pyrite, chalcopyrite, magnetite, monazite and apatite are concentrated in the phyllosilicate zones. The distribution of quartz-rich and phyllosilicate domains does not appear to be controlled by pre-existing compositional or textural heterogeneities in the original rock (Hendry, *op. cit.*). A nodular pseudofragmental texture results from the segregation of quartz and chlorite alteration. The pseudofragmental texture gives rise to the characteristic appearance on weathered surfaces that is common within the West Lyell area (Wade and Solomon, 1958; Walshe, 1971).

Small scale interfingering suggests that the majority of the felsic lavas and intrusives may be bedded with volcaniclastic rocks. This interfingering is sometimes seen on a much larger scale (see Figure 4.16 in chapter 4). Passively extruded lavas or shallow intrusives are indicated by the presence of rare euhedral and embayed quartz phenocrysts (Appendix V, Plate 1, Figure 4), which are the only definite primary igneous features identified in the felsic volcanics.

Intermediate - mafic volcanics that comprise the mining hangingwall of the Prince Lyell deposit (Walshe and Solomon, 1981; Hills, 1990) have not been identified at Royal Tharsis. These rocks are typically intercalated volcanics and are interpreted to be intensely altered andesitic to basaltic volcanics, mainly from their trace element geochemistry. The intense alteration and layer - parallel shearing almost completely masks original internal structures. They comprise a foliated groundmass of fine grained intergrown chlorite and sericite with disseminated quartz and accessory pyrite, magnetite, haematite, monazite and apatite (Raymond, 1992).

Very minor units of polymict **volcaniclastic breccias and conglomerates** are the only rocks in the Royal Tharsis area to preserve undoubted volcaniclastic textures (Walshe and Solomon, 1981; Raymond, 1992). These rocks occur throughout the Royal Tharsis sequence in horizons a few centimetres to a few metres thick, and can be clast or matrix supported. Clasts range in size from 1 to at least 50mm and are predominantly angular to sub-angular. The volcaniclastics are laterally impersistent and either wedge out or may be destroyed by alteration over less than 10 metres along strike. When intercalated with the felsic volcanics, the breccias occur as mildly altered enclaves which grade into more strongly foliated altered felsic volcanics.

Alteration of the breccias and conglomerates ranges from mild recrystallisation with clast textures largely intact, to more strongly altered rocks with only ghosts of the original clasts preserved. The progressive alteration of the breccias is completely destructive of the primary clastic texture. The matrix of the breccias is the most altered part, indicating high permeability, and giving rise to significant pyrite, chalcopyrite, magnetite and haematite mineralisation. Most common breccia clasts are fragments of felsic lavas and intrusives. Volcanic quartz phenocrysts and altered fragments of fine grained shale or siltstone also occur in the breccias. The origin of the breccias is unclear.

Rare, very thin altered **shale horizons** occur as intercalations in the volcanics. The lenses are up to ten centimetres thick and preserve no internal layering or sedimentary structures. They may extend laterally for at least several metres, but knowledge of their extent is limited. Contacts between the shales and surrounding altered volcanics varies from sharp to gradational. They commonly contain minor or accessory amounts of fine grained disseminated magnetite mineralisation. Finely disseminated or veinlet pyrite of similar grain size is developed to a lesser extent. Shale horizons towards the stratigraphic hangingwall contain disseminated haematite, commonly pseudomorphing euhedral embayed magnetite, imparting a purple-grey colour to the rocks. Strong pyrite and/or magnetite mineralisation at the margins of the shale units may suggest that fluids associated with deformation moved along lithological boundaries which dilated due to the ductility contrast between the shales and volcanics.

Lamprophyre dykes are similar to those in the Prince Lyell deposit where they behave as marker units in the structural hangingwall and where they sometimes branch dichotomously. The dykes are of Devonian age (McClenaghan *et. al.*, 1994), are locally strongly fractionated and cut across cleavage and foliation. They are fine grained biotitic microsyenitic rock types, with cognate inclusions of olivine and feldspar nepheline, frequently magnetic and sometimes containing sulphides (pyrite and ± chalcopyrite) probably associated with Devonian remobilisation (Berry, 1990). In thin section the rock shows serpentine-altered olivine and clusters of diopsidic clinopyroxene (Appendix IV, Plate 13, Figures 3 and 4).

Great Lyell Fault

The fault at Royal Tharsis varies in character from a sharply defined, narrow shear zone displaying a laminated, mylonitic texture, to a zone several metres wide of gradually increased shearing and frequently with prominent phyllosilicate gouge material. Conglomerate fragments and larger coherent fault slices of Owen Conglomerate may be included in the fault zone. Altered volcanics within the fault zone are commonly highly foliated, fine grained sericite-quartz schists with variable amounts of siderite and haematite alteration. Generally the fault zone is poorly demarcated, particularly at surface where expression is obscured by cross-cutting east-west trending faults.

Owen Conglomerate

In drill core conglomerate intersections consist of well-rounded metamorphic quartz clasts, up to several centimetres across in a sandy, siliceous, haematitic matrix, with lesser units of pink haematitic quartz sandstone. Silicification and minor sericite alteration is developed in places adjacent to the volcanics contact.

Figure 3.3
Drill core illustrating the contact between Owen Group lithologies and sheared CVC volcanics. The volcanics are heavily broken through the Great Lyell Fault resulting in incompetent ground conditions. Not clearly visible, but present in the core are both the haematitic dusting that is characteristic of the Owen and also distinctive sub-rounded fragments that readily identify the conglomerate.

3.3.2 Structure

The dominant structural feature of the Royal Tharsis volcanic sequence is the strong pervasive D2 foliation. Although D1 cleavage is developed in the Owen Conglomerate adjacent to the volcanics, it is rarely observed in the volcanic host rocks. The D2 foliation in Royal Tharsis area dips steeply to the south-west, parallel to the regional volcanic layering and to the orientation of the Royal Tharsis copper mineralisation (Cox, 1981).

Major discrete faults or shears with strong continuity through the Royal Tharsis sequence are rare as most of the strain has been accommodated by movement along D2 cleavage planes and along several less continuous cleavage-parallel shears. Discontinuous, post-cleavage, shallow-dipping reverse faults, locally referred to as "flat faults" (Cox, 1981; Berry, 1990; Raymond, 1992; Flitcroft and McKeown, 1992) are common in the Mount Lyell region. The faults occur as conjugate sets, dipping south-east and north-west and are generally no more than minor flexures and strongly developed joints as very little, if any, movement occurs along them. Quartz + siderite ± chlorite ± chalcopyrite ± fluorite ± haematite veins, which occur throughout the altered volcanics, are commonly associated with the "flat faults" an indication that the faults have acted as fluid conduits during late stages of Devonian deformation. The principal stress direction is subparallel to the strike of the orebody (Cox, *op. cit.*).

The position of the younger Owen lithologies relative to the CVC volcanics indicates that the sequence is overturned and thus the structural (or mining) footwall is the stratigraphic hangingwall. Sedimentary evidence for direction of younging is not recorded.

3.3.3 Orebody Description

The Royal Tharsis deposit is composed of a series of echelon lenses. The ore zone is the down dip extension of one of the major ore zones mined in WLOC. The wide ore zone represented by the 0.5% Cu envelope can be resolved into at least two higher grade ore lenses with high grade cores when a 1.5% Cu cutoff is applied (McDonald, 1968; Reid, 1978; Bird, 1982). Mineralisation occurs mainly in the form of disseminated pyrite - chalcopyrite with occasional trace bornite. Other minerals include sphalerite, galena, molybdenite, stromeyerite, mawsonite, tetrahedrite, tennanite, gold, magnetite and apatite (Markham, 1968; Reid, 1975).

Geological mapping has indicated stratiform control of the lenses (Arnold, 1985). In the main they are concordant with the dominant cleavage in the volcanics. The approximate dimensions of the lenses are up to 250 metres in strike length, 20 to 50 metres wide, and extend to a depth of 600 metres below surface. The ore zone strikes at 315° and has an average dip of 60° - 80° the southwest.

Wiggins and House (1991) determined the orebody as being petrologically distinct, characterised by a weak mining hangingwall that was prone to rapid deterioration on exposure. They recognised two principal rock types;

- a light grey structural hangingwall lithology: barren orange - sericite - pyrite - quartz and strongly foliated grey orange quartzite with light green sericite bands, typically angular in appearance.
- a fawn orebody lithology: muddy light silvery grey foliated schist with disseminations and veinlets of chalcopyrite, rounded and partly oxidised.

Harper (1992) described the host sequence as steeply dipping volcanics located in the immediate hangingwall of the Great Lyell fault. He recognised the orebody as being crudely stratabound in units of pink to grey locally fragmental felsic volcanics with the footwall demarcated by grey green foliated chlorite - sericite altered volcanics becoming mylonitic along the contact with the Great Lyell fault. The absence of intermediate to mafic volcanics was noted.

3.4 MINING HISTORY

Mining at the turn of the century was confined to flux for pyritic smelting (Sticht, 1905). The bulk of the operation was open pit although there was presumably some underground activity. Discrimination between ore source, whether from underground or from surface, is difficult to determine from existing records. Tonnages were not too large and dropped off as the century advanced, possibly commensurate with the transition away from surface operations. By 1909 mining of Royal Tharsis for flux had stopped.

It was not until the late 1920s that attention was again focussed on Royal Tharsis when the efficiency of the Mount Lyell mill and high grade ores from North Lyell enabled the lower grades of the Tharsis orebodies to be mined (Blainey, 1993). In 1931 - 1933 rising of the Royal Tharsis shaft (Jakins, 1931 and 1933) from underground (off the North Lyell tunnel) established an innovative precedent in Australian mining. At the same time use of waste from rising of the shaft as fill in underground stoping created another first in Australian mining. Shaft development was in lithologies described as "volcanic tuffs lying alongside Silurian conglomerate", striking to the NW and dipping 60° to the west (Jakins, 1933).

Underground mining initiated in the early 1930s continued virtually uninterrupted through to the middle of the 1950s when emphasis of the MLMRC operation shifted to surface with the developemnt of WLOC. Royal Tharsis was the last underground operation on the Mount Lyell field prior to commencement of underground mining of the Prince Lyell orebody (late 1960s to early 1970s) that has continued to date.

In the intervening decades occasional tonnages were mined sporadically from Royal Tharsis. The mid 1960s (McDonald, 1968) and early 1970s (Burgdorf, 1970) saw some mining but overall tonnages and copper grades were generally low. McDonald (*op. cit.*) reported a strike of 315° and a dip of 65° SW with the deposit having a vertical to northerly plunge. He determined the orebody to be pipelike, surrounded by a fringe of lower grade material and converging with the Owen Conglomerate at depth.

In the mid 1980s a more sustained period of operations ensued (Hills, 1985) during which vertical crater retreat mining was used. Bird (1982) recognised interconnected en echelon structures within the deposit and potential for extension at depth. Operations continued intermittently through to late 1991 when significant dilution caused by incompetent lithologies in the hangingwall reduced ore recoveries to unprofitable levels (Wiggins and House, 1991; Harper, 1992). Dilution was exacerbated by strike slip shears, which combined to preclude further underground mining. These adverse conditions were a repetition of the main period of underground mining (1930s to 1950s) when ground conditions were generally bad (Greenway, 1975).

3.4.1 Production Summary

Historical production from Royal Tharsis is summarised in Table 3.1 and depicted graphically in Figures 3.4, 3.5 and 3.6. It should be noted that some of the Royal Tharsis was mined as part of WLOC and tonnages involved were not discriminated from within the broader WLOC statistics.

Table 3.1	**Royal Tharsis Production Summary**	
Source of Ore	**Tonnes**	**% Cu**
Flux - surface operations	95,000	1.6
Underground mining	1,929,000	1.5
Total	2,024,000	1.5

Figure 3.4 illustrates production history from the Royal Tharsis deposit. The main period of mining was from the early 1930s through to the mid 1950s during which the copper grade remained remarkably consistent. A notable hiatus in production occurred at the onset of the second world war.

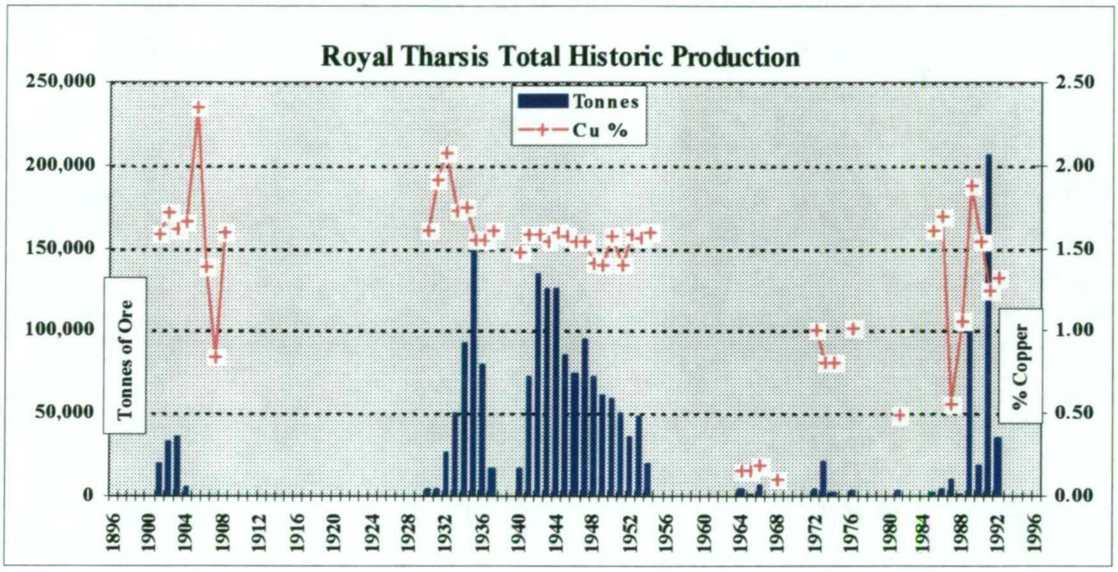

Figure 3.4
Total mine production from Royal Tharsis, 1900 - 1992

Flux was mined as a surface operation at the start of the century (Figure 3.5). Copper grades from this operation are similar to those from underground possibly indicating the absence of any surface enrichment around the Royal Tharsis deposit. Grades were estimated to be in the region of 2.25% Cu (Sticht, 1905). Sticht (*op. cit.*) considered this value to be optimistic primarily due to the "Fahlband" nature of the ore (Gregory, 1905), and in spite of an approximately 10 metre thick band of siliceous material with an average value of 1.65 % Cu.

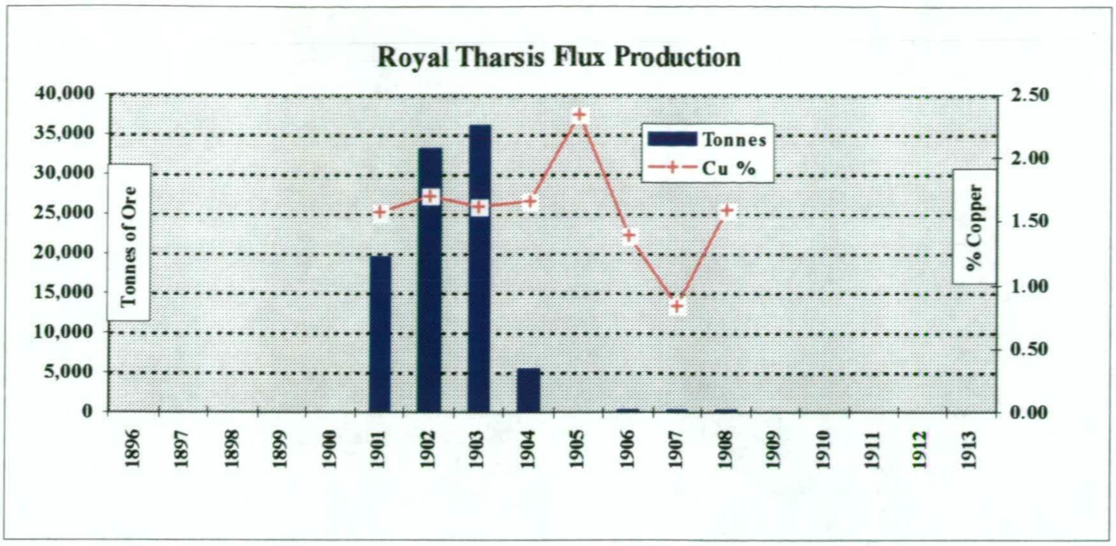

Figure 3.5
Total flux mined from Royal Tharsis, 1900 - 1908

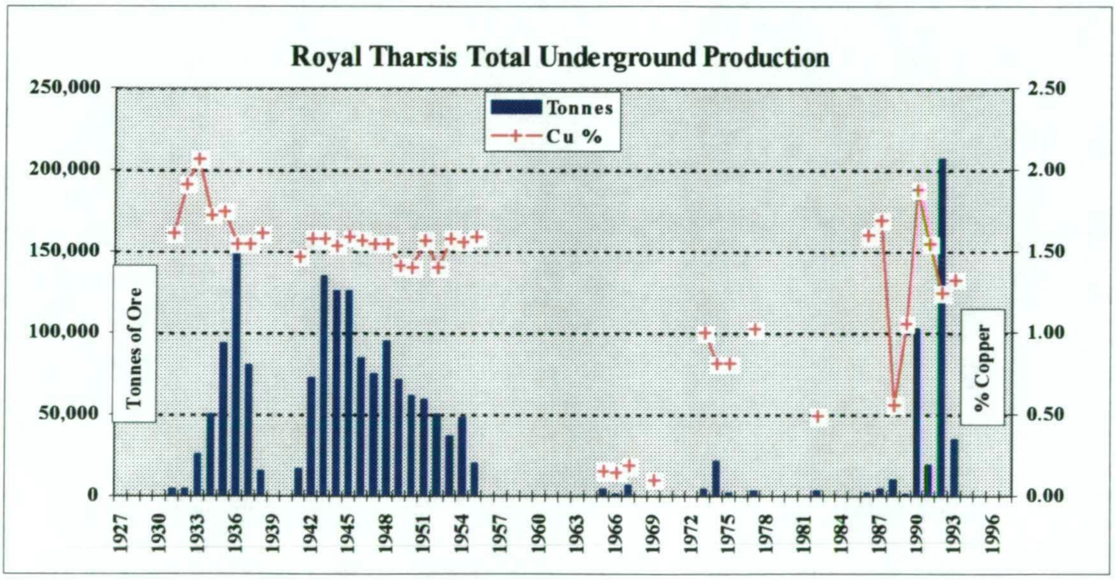

Figure 3.6
Total underground mine production from Royal Tharsis, 1930 - 1992

Most of the underground mining took place before commencement of mining from WLOC. After closure of WLOC additional underground mining of Royal Tharsis was used primarily to supplement mining of the Prince Lyell deposit. Figure 3.6 details total underground production from Royal Tharsis.

CHAPTER 4
SURFACE GEOCHEMISTRY

4.1 INTRODUCTION

An orientation rock chip survey was carried out to identify useful geochemical pathfinder elements, to determine possible inter-element relationships and as a tool in discriminating vectors to ore. Rock chip sampling of outcrops was carried out concurrent with the orientation survey. Orientation rock chip results are included as Appendix I. Assay profiles for rock chip traverses are included as Appendix II.

4.2 ORIENTATION ROCK CHIP GEOCHEMISTRY

4.2.1 Methodology

A grid based geochemical rock chip orientation survey was conducted across selected lines. The purpose was to identify useful geochemical pathfinder elements and potential inter-element relationships for use in areas of limited geological information. Selected lines were identified on aerial photographs and sample positions approximated by pacing out over 10 metre intervals. Sample sites were marked and later located with GPS or ETS. Geology, alteration and structural measurements were recorded at each sample site. Lines selected (i.e. 8130N from 3900E to 4115E, and 8010N from 3640E to 4275E) are shown in Figure 4.1. Previous mining activities precluded the taking of samples that would fall within the defined orebody, a constraint that has enforced investigation of primarily low grade copper material.

Results from the orientation geochemistry are included as Appendix I which contains;

- sample location coordinates (Appendix I, Table 1)
- sample assay results (Appendix I, Table 2)
- geology/alteration data (Appendix I, Table 3)
- descriptive statistics, correlation and covariance (Appendix I, Table 4)
- frequency distribution plots (Appendix I, Chart 1)

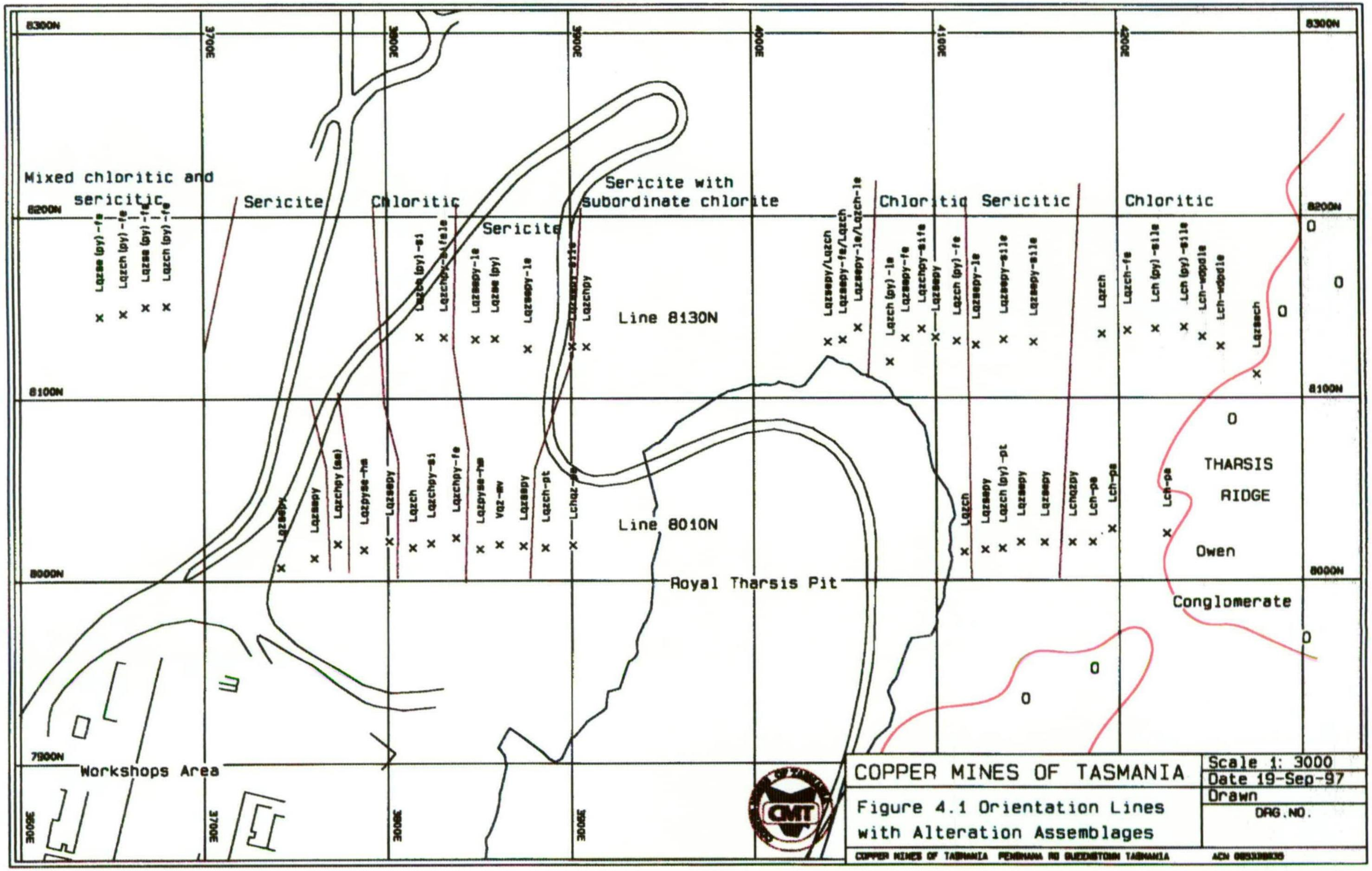

Figure 4.1 Orientation Lines with Alteration Assemblages

orientf.pf

K SSI - CMT Exploration.

- multi element charts for each element (Appendix. I, Chart 2)
- scatter plots for each element (Appendix I, Chart 3)

Additionally the profiles have been plotted for each element analysed for each individual line (lines 8130N and 8010N) (Appendix I, Charts 4 and 5 respectively).

4.2.2 Distribution Characteristics and Multi Element Plots

Results for each element are discussed. It should be noted that for plotting and statistical purposes assay results reported as below detection limits (BDL) have been assigned a value of half the lower detection limit (LDL). Both silver and nickel returned a significant proportion of results that were BDL. Analytical methods are outlined in Appendix I, Table 5.

Table 4.1 provides a statistical summary, full details of which are included as Table 4, Appendix I (tabulating descriptive statistics, correlation and covariance). Frequency distribution plots are included as Chart 1 in Appendix I. Correlation between elements is summarised in Table 4.2 and discussed below.

Table 4.1 Orientation Geochemistry Statistical Summary

Element	Count	Maximum	Minimum	Average	Std. Dev.
Cu	51	5790	10	235.5	830.7
Au	51	0.36	<0.001	0.03	0.06
Ag	51	8.3	<0.1	0.47	1.22
Mo	51	449	<1	21.4	68.7
Mn	51	653.3	2.6	115.6	157.8
Pb	51	426.4	1.5	46.2	70.1
Zn	51	699.7	1.9	99.6	154.6
Co	51	30	<3	9.4	6.9
Ni	51	36	<3	8.3	10.0
As	51	63.0	2.3	13.8	10.0
Ba	51	8030	30	1689	1639

Notes; all values in ppm

Table 4.2	Orientation Geochemistry Correlation Factors										
	Cu	Au	Ag	Mo	Mn	Pb	Zn	Ba	As	Ni	Co
Cu	1										
Au	0.37	1									
Ag	0.93	0.39	1								
Mo	0.14	0.09	0.19	1							
Mn	-0.07	-0.02	-0.10	-0.14	1						
Pb	0.01	0.03	0.12	0.06	0.04	1					
Zn	-0.08	-0.09	-0.10	-0.13	0.79	0.38	1				
Ba	-0.03	0.12	0.14	0.50	-0.14	0.00	-0.14	1			
As	-0.15	-0.04	-0.13	-0.08	0.12	0.32	0.14	-0.08	1		
Ni	0.02	0.18	-0.03	-0.13	0.52	-0.11	0.40	-0.17	-0.06	1	
Co	0.35	0.14	0.36	0.06	0.37	-0.08	0.34	0.19	-0.11	0.35	1

Copper

Copper grade ranges from a maximum of 5790 ppm to 10 ppm with an average of 235.5 ppm. Distribution shows some grouping of data. However separation of populations is difficult to justify on the small number of data points. The high value outliers may reflect higher grade ore lenses that constitute the orebodies which have sustained mining in the WLOC area for the last 70 years. The individual plots for both lines 8130N and 8010N (Appendix I, Chart 1) show similar distributions.

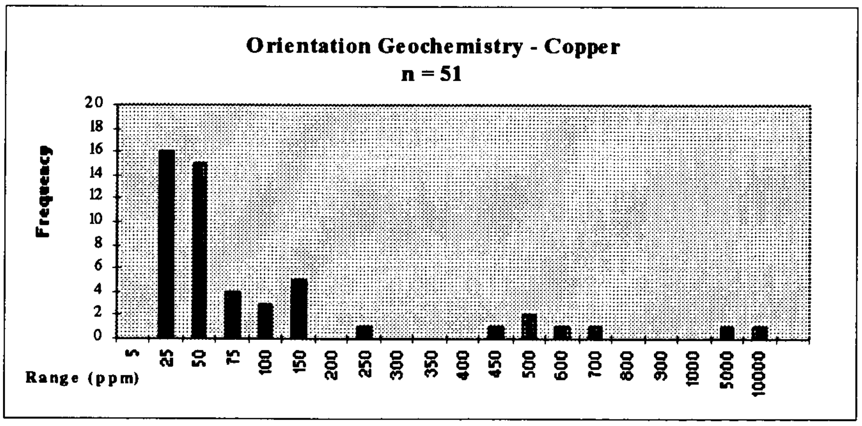

Figure 4.2
Royal Tharsis surface orientation geochemistry.
Copper distribution plot

Copper correlates (Appendix I, Chart 2) well with silver, more erratically with gold and moderately well with molybdenum, the latter tending to straddle copper. The correlation with silver is encouraging given the number of silver values that were BDL. Cobalt exhibits an erratic relationship with copper, whilst lead, zinc, manganese and barium all show a poor correlation. There would appear to be virtually no correlation with nickel although this could be function of nickel values being significantly BDL.

Gold

Definition of potential gold populations is a lot less distinct than those for copper. Gold grade ranges from a maximum of 0.36 ppm to a minimum of <0.001 ppm (i.e. below detection limit) with an average of 0.03 ppm. The distribution plot (Figure 4.3) shows a poorly defined population. The individual distribution plots for lines 8130N and 8010N (Appendix I, Chart 1) show a poor similarity.

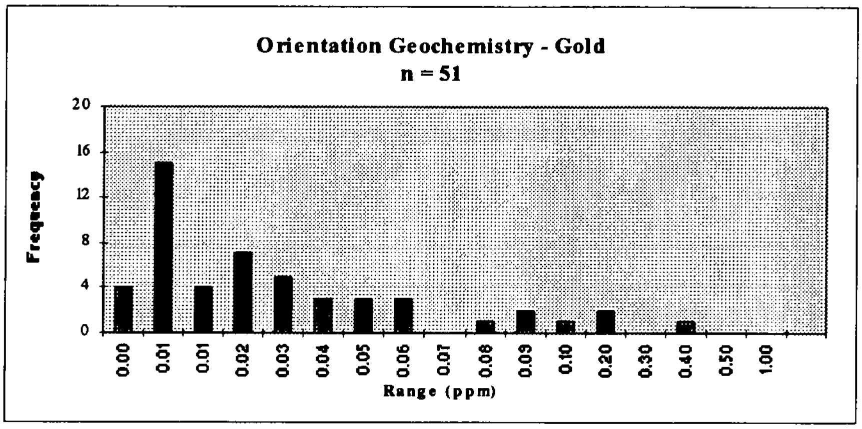

Figure 4.3
Royal Tharsis surface orientation geochemistry. Gold frequency distribution plot.

Commensurate with its distribution gold shows no strong correlation (Appendix I, Chart 2) with any of the elements analysed. Reasonable correlation is shown with both copper and silver, whilst that with molybdenum, manganese, nickel, cobalt and barium tends to be poor. No relationship is apparent with zinc and arsenic. In the case of zinc this is surprising, given the distribution of zinc (see below).

Silver

Silver grade averages 0.47 ppm, ranging from a maximum of 8.3 ppm to a minimum of < 0.1 ppm (i.e. below detection limit). 45% of assay results were BDL. Data distribution resolves into a single population with an outlier at 10 ppm being typical of anomalous silver evidenced through rock chip sampling.

Silver tends to show a broadly moderate to poor correlation (Appendix I, Chart 2) across the spectrum of elements analysed. Interpretation must be tentative given the significant proportion of results that were BDL. Specifically there would appear to be no relationship with zinc and arsenic, whilst correlation with copper is high.

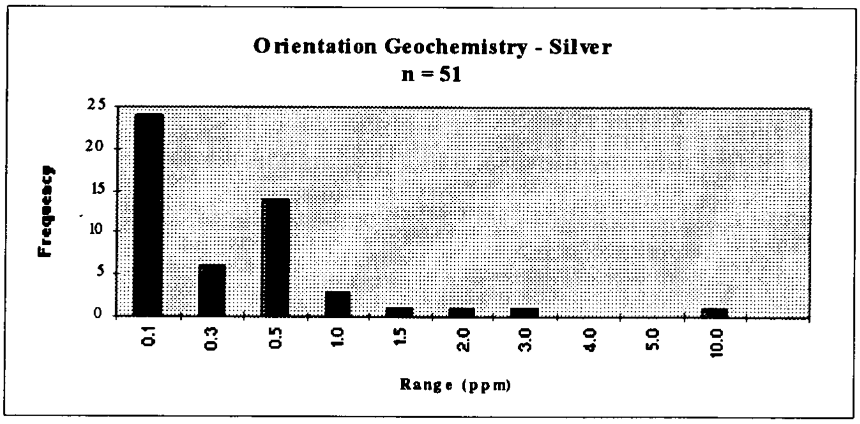

Figure 4.4
Royal Tharsis surface orientation geochemistry. Silver frequency distribution plot.

Molybdenum

Molybdenum resolves into a poorly defined single population (Figure 4.5) with an average of 21.4 ppm and ranging from a maximum of 449 ppm to a minimum of < 1 ppm (i.e. below detection limit). This distribution is reflected in the individual plots for lines 8130N and 8010N (Appendix I, Chart 1), with both showing an outlier above the 200 ppm boundary.

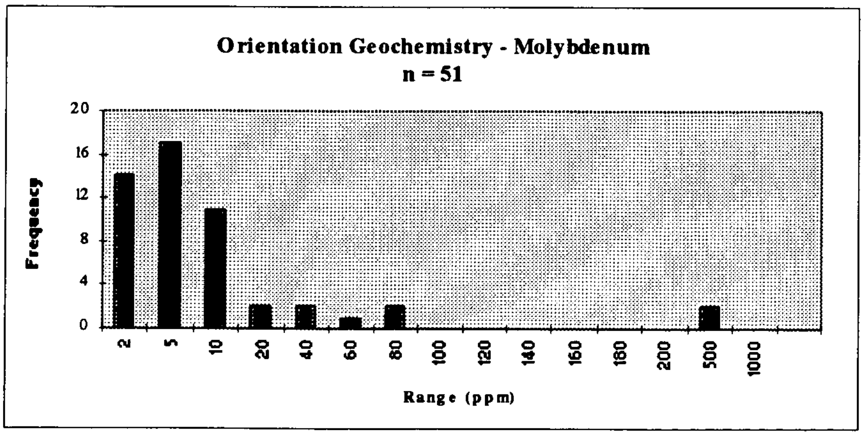

Figure 4.5
Royal Tharsis surface orientation geochemistry. Molybdenum frequency distribution plot.

Good correlation (Appendix I, Chart 2) is shown with barium where elevated values in both elements tend to coincide. This, together with a moderate correlation with copper, gold and silver, makes molybdenum a potential pathfinder element. Correlation with lead and cobalt tends to be weak with occasional coincidence between elevated values. Correlation with manganese, zinc, nickel and arsenic is markedly negative.

Manganese

Two reasonably distinct populations can be identified (Figure 4.6) with the upper being less well defined and falling in an approximate range of 200 ppm to 1000 ppm. Manganese averages 115.6 ppm with a maximum of 653.3 ppm and a minimum of 2.6 ppm. Distribution plots for individual lines similarly indicate two populations (Appendix I, Chart 1).

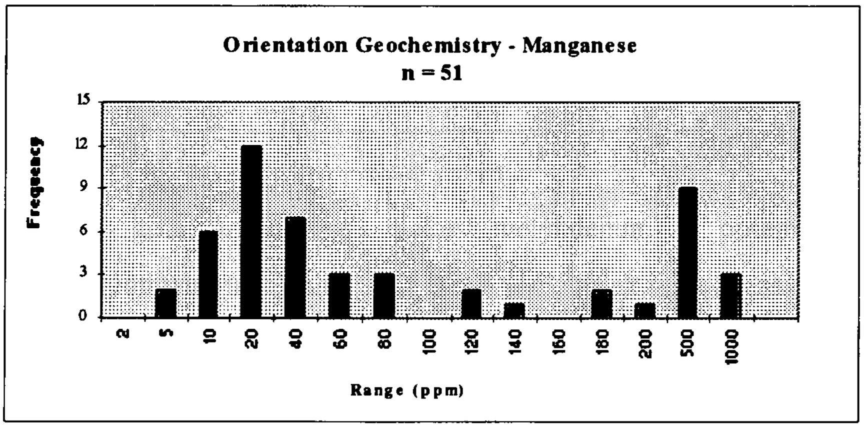

Figure 4.6
Royal Tharsis surface orientation geochemistry. Manganese frequency distribution plot.

Manganese shows good correlation (Appendix I, Chart 2) with zinc, nickel and to a lesser extent cobalt. A low negative correlation is shown generally with all the other elements analysed. Overall the element tends to exhibit erratic and variable elevated values and this correlates with a similar zinc distribution.

Lead

A single population between 5 ppm and 120 ppm with an apparent normal distribution (Figure 4.7). A basal outlier may represent background. An upper outlier at 500 ppm falls well beyond the normal distribution curve. Lead averages 46 ppm with a maximum of 426.4 ppm and a minimum of 2.6 ppm. The single population is shown in the distribution plots for each orientation line, that for 8010N being less well resolved. Both show an outlier above the 200 ppm boundary (Appendix I, Chart 1).

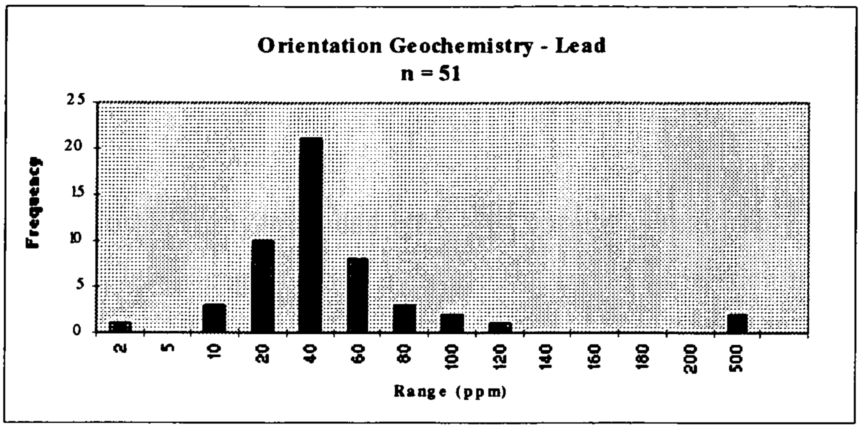

Figure 4.7 Royal Tharsis surface orientation geochemistry. Lead frequency distribution plot.

A moderate correlation (Appendix I, Chart 2) is shown with zinc and arsenic. Elevated lead values are coincident with zinc peaks whilst with arsenic there is slight offset between peak values. In the case of arsenic the two profiles tend to mimic each other. (Both lead and arsenic can be resolved into a single population with normal distributions). This is not as obvious with zinc which shows a significantly broader distribution. Correlation of lead with the other elements is extremely poor.

Zinc

Zinc averages 99.6 ppm with a maximum of 699.7 ppm, a minimum of 1.9 ppm and shows a wide single population (Figure 4.8) that contrasts with lead above. It also accounts for the reasonable correlation (Appendix I, Chart 2) that zinc is able to demonstrate with all other elements analysed. A zinc ratio (Huston and Large, 1987) of 48 does not however place the body within the range typical of MRV volcanogenic massive sulphide deposits. Similar distributions are shown in the individual plots for each line (Appendix I, Chart 1).

In addition to manganese and lead, zinc correlates reasonably well with nickel, cobalt and, to a lesser degree, with arsenic. This broad correlation is probably a function of the distribution characteristics of zinc. This is potentially similar to silver and in marked contrast to lead.

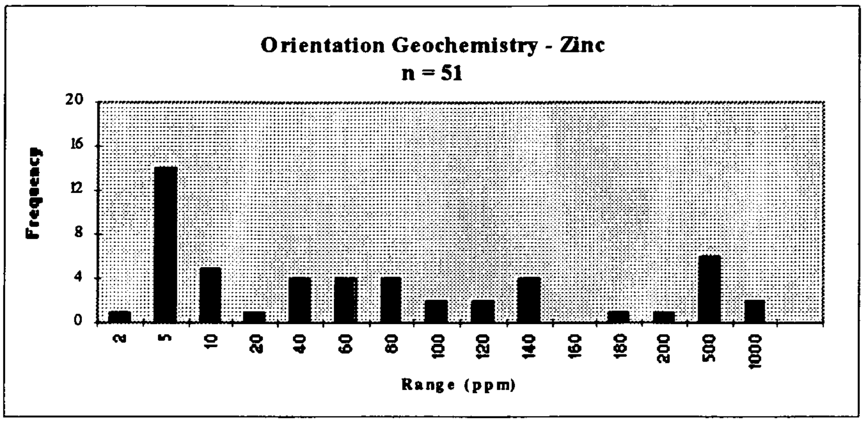

Figure 4.8
Royal Tharsis surface orientation geochemistry. Zinc frequency distribution plot.

Arsenic

Data resolves into a single population with an apparent normal distribution ranging up to 30 ppm. A solitary outlier occurs at 65 ppm (Figure 4.9). An average of 13.8 ppm ranges from a maximum of 63 ppm to a minimum of 2.3 ppm. This single population is shown by the distribution plots for each line (Appendix I, Chart 1). Arsenic shows a moderate to poor correlation (Appendix I, Chart 2) with lead (single population), zinc (multi population) and manganese (multi population). Correlation with all the other elements is negative (and low).

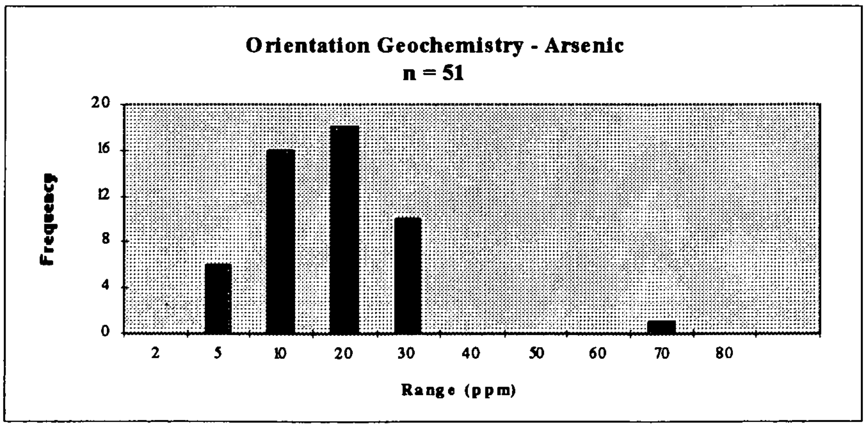

Figure 4.9
Royal Tharsis surface orientation geochemistry. Arsenic frequency distribution plot

Nickel

A significant proportion (45%) of nickel assays returned a value BDL. Of the remaining values an average 8.3 ppm has a maximum of 36 ppm i.e. nickel values tend to be very low (Figure 4.10). Plots for individual show a more erratic distribution (Appendix I, Chart 1).

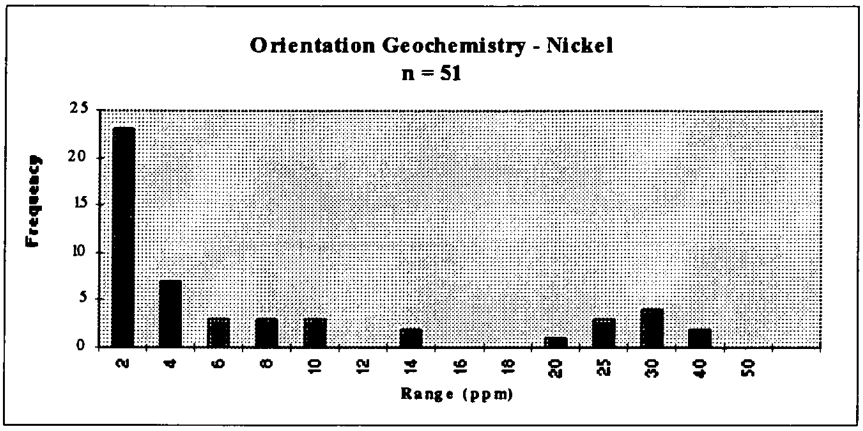

Figure 4.10 Royal Tharsis surface orientation geochemistry. Nickel frequency distribution plot.

Nickel correlates (Appendix I, Chart 2) well with manganese and zinc, and less so with gold. Correlation with other elements is generally poor to negative, although the significant proportion of BDL nickel results mitigates against an interpretation that can be made with any high degree of confidence.

Cobalt

Cobalt results all returned low values, with an average of 9.4 ppm, a maximum of 30 ppm and a minimum of < 3 ppm (i.e. below detection limit). The poor resolution of data (Figure 4.11) is also shown by the distribution plots for each line (Appendix I, Chart 1). Cobalt values are all generally low (?background) and these show a moderate correlation (Appendix I, Chart 2) with copper, silver, manganese, zinc and nickel, partially a reflection on the distribution pattern shown by cobalt. Correlation with gold, molybdenum and barium is broad but low. A low negative correlation is shown with arsenic and lead.

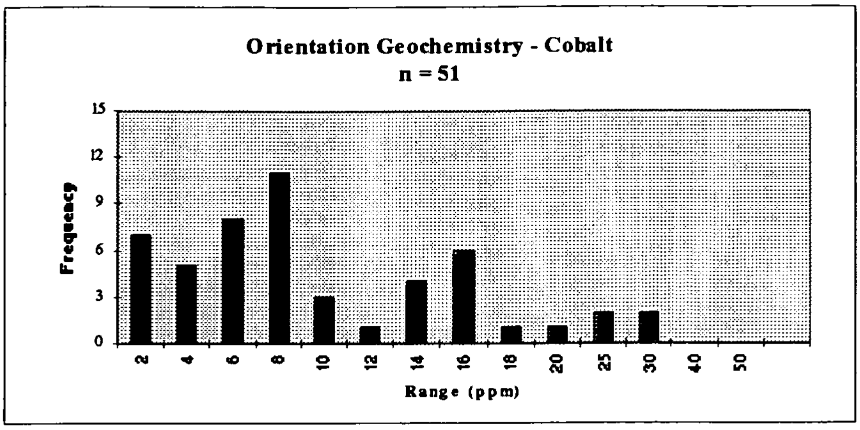

Figure 4.11
Royal Tharsis surface orientation geochemistry. Cobalt frequency distribution plot.

Barium

Barium averages 1,689 ppm with a maximum of 8,030 ppm and a minimum of 30 ppm. Minimal barite has been identified in the Royal Tharsis area (although Nye *et. al.* (1934) recorded barite being present in small quantities on dumps from adits) (Figure 4.12). The good correlation (Appendix I, Chart 2) shown with molybdenum has already been commented on. Poor correlation with barium tends to occur with all other elements, that with copper, manganese, zinc, arsenic and nickel being negative (and generally low).

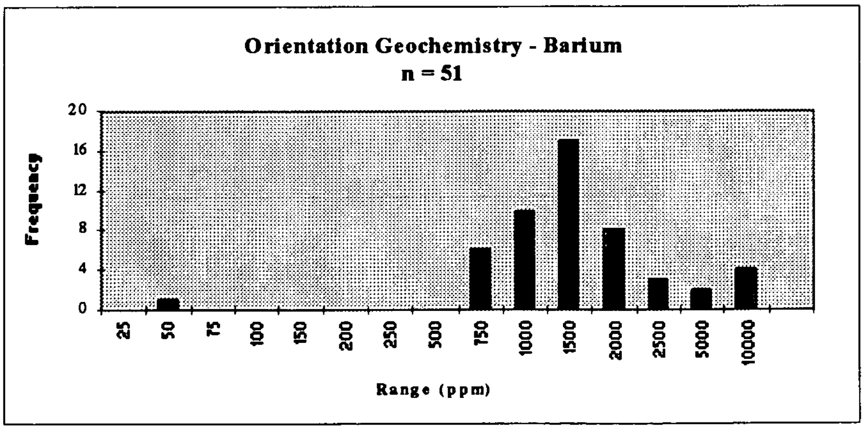

Figure 4.12
Royal Tharsis surface orientation geochemistry. Barium frequency distribution plot.

4.2.3 Discussion and Conclusions

The most prominent copper anomaly occurs around 4100E over an area of intercalated quartz chlorite and quartz sericite pyrite schists that equate to the north Royal Tharsis prospect as described by Flitcroft & McKeown (1992). At 4250E a 500 ppm copper anomaly occurs in sheared chlorite schists adjacent to the Tharsis ridge inlier.

Overall silver distribution follows copper very strongly, in spite of a significant proportion of assays being BDL, especially on line 8130N. Gold also correlates reasonably well but tends to be more erratic, probably a reflection of nuggety distribution. Molybdenum shows subtle but significant enhancement over elevated copper with occasional anomalous values. Barium shows a strong relation to molybdenum and is elevated over a broad range of copper values but does not resolve into individual zones. Manganese shows a broad correlation that is particularly good with zinc, but which does not correlate with copper. Lead, zinc and nickel distributions do not seem to be related to copper, whilst cobalt which tends to occur in low ranges shows a poor and erratic relationship with copper. These elemental associations can be summarised:

- Cu, Au, Ag, (Mo), (Co)
- Mo, Ba
- Mn, Zn

From the multi element plots and based on individual element distributions the elements that appear to show the best correlation are copper, gold, silver and molybdenum. Anomalous pathfinder values for these elements are tentatively assigned as follows:

- copper > 450 ppm
- gold > 0.08 ppm
- silver > 2.5 ppm
- molybdenum > 70 ppm

Composite plots reflecting similar profiles are shown in Figures 4.13 and 4.14 (Greenwood, 1996). Gold and molybdenum values have been multiplied by factors of 10 to emphasise relational trends.

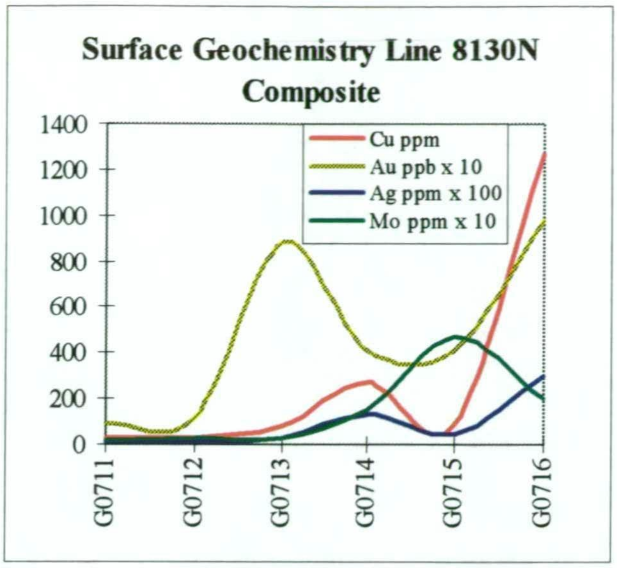

Figure 4.13
Correlation fit between copper, gold, silver and molybdenum. Gold and molybdenum multiplied by a factor of 10 to emphasis anomalous trends. Direction of profile 045° looking north west.

Line 8130N is located to the north of the Royal Tharsis open pit (Figure 4.1). Elevated copper is reflected in the profiles of each of gold, silver and molybdenum although the peaks tend to be offset. Troughs are all common except of that for molybdenum. The two peaks shown by copper, gold and silver can be considered indicators of potential extension to known mineralisation northwards from Royal Tharsis. Any such trend towards the east would be approaching the Tharsis ridge and would possibly be cut off by the GLF (which has not been identified at surface) and or possibly displaced by east-west trending faults that cut the Tharsis ridge (see Figure 3.1 in chapter 3).

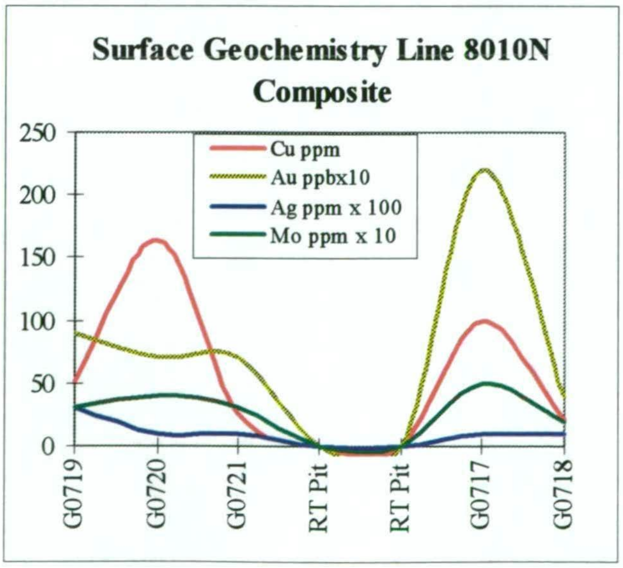

Figure 4.14
Correlation fit between copper, gold, silver and molybdenum. Gold and molybdenum multiplied by a factor of 10 to emphasis anomalous trends. Direction of profile 045° looking north west.

Line 8010N passes across the Royal Tharsis open pit (Figure 4.1). To the north east (i.e. up the stratigraphy) elevated peaks are coincident. To the south west (structural hangingwall) peaks are noticeably more obtuse, with silver showing an anomalous shape that contrasts with the overall trend.

4.3 ROCK CHIP SAMPLING AND GEOCHEMISTRY

4.3.1 Methodology

Outcrops were chip sampled at approximately 10 metre spaced intervals. Samples were taken in situ by chipping away the weathered superficial veneer and sampling fresh rock. Samples were routinely analysed for copper, gold, silver, molybdenum, cobalt, lead and zinc. The nature of surface exposure dictated traverse direction/location and hence the ideal of sampling perpendicular to strike was frequently not possible. Similarly contamination was avoided by locating traverses away from historic dumps. A total of 20 traverses were sampled (Figure 4.15). Coordinates for each sample site were located with GPS or theodolite. Results are detailed in Appendix II which contains for each traverse:

- assay profiles for each element
- multi element profiles for each element against copper

Details on sample locations and assay results are available. It should be noted that plotted assay profiles (Appendix II, Charts 1 - 20) are not topographical but simply a straight line representation of sample positions - thus interpretation has needed to take into consideration the topographic profile and underlying geology. The findings in each traverse are discussed below.

4.3.2 Rock Chip Traverse Results

Traverses 7 and 27 (Appendix II, Charts 1 and 19)

Located towards the northern limit of and close to the demarcation between Royal Tharsis and Western Tharsis areas. Traverse 7 is along strike where lithology is

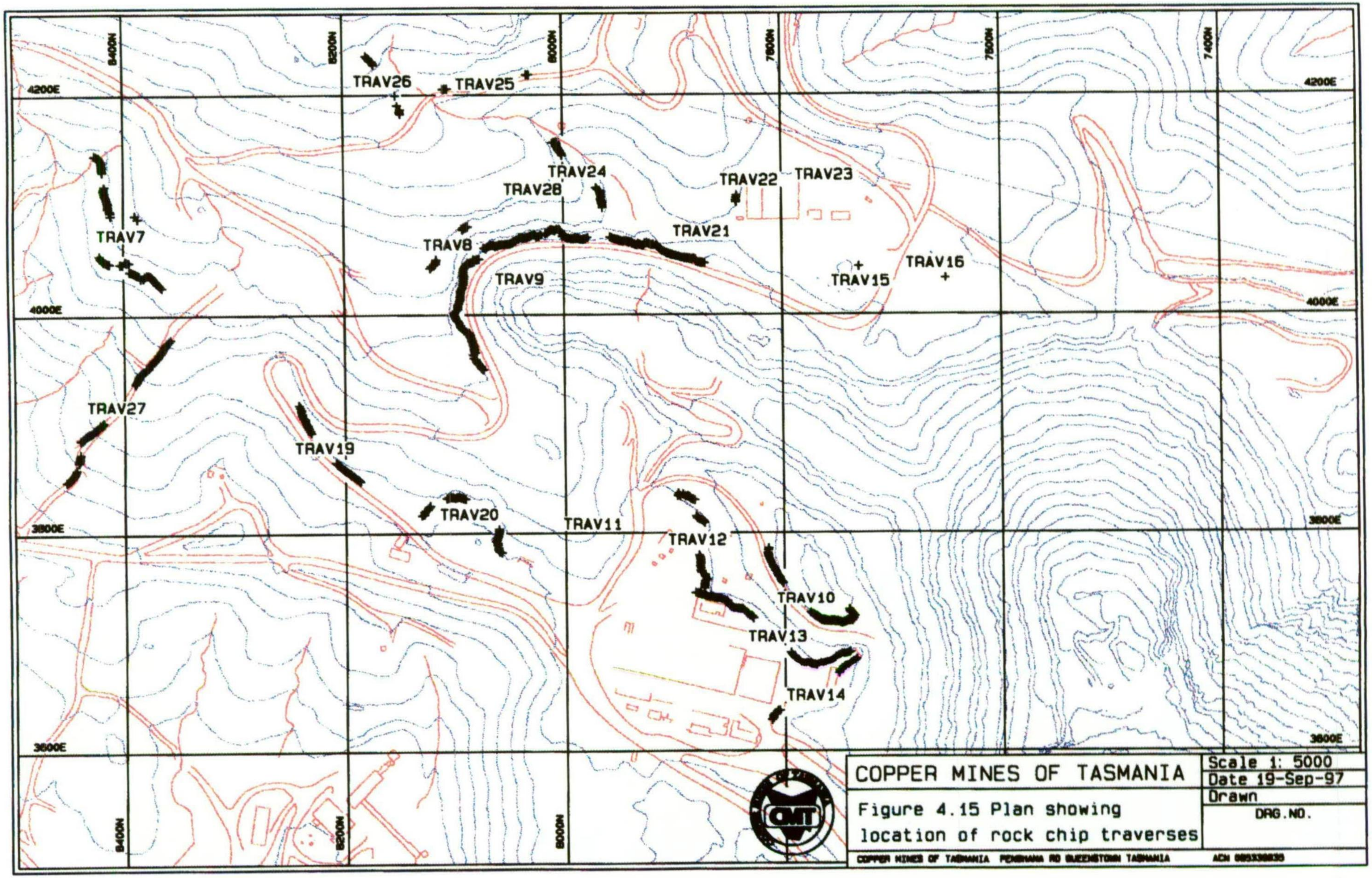

Figure 4.15 Plan showing location of rock chip traverses

allrockc.pf

SSI - CMT Exoloration.

broadly a quartz mica schist that exhibits predominant sericite alteration. Assay results were all low except for an anomalous zone of silver mineralisation (approximately 25 metres @ 15 ppm Ag) that shows no obvious correlation with any other feature. Correlation of silver with other elements is poor.

Figure 4.16

Photograph (facing east) of alternating chlorite (grey colouration) and sericite alteration (yellow-red-brown colouration) that is south and east of, but contrasts with, lithologies sampled by traverses 7 and 27. Geological hammer for scale.

Traverse 27 was sampled across strike (in contrast to traverse 7). Subtle differences are shown by individual assay profiles and this is considered to reflect some form of boundary - possibly lithological, alteration or mineralogical. Copper shows a marked change in profile shape, evidenced by both cobalt and, to a lesser degree, by silver. Conversely gold shows a gradual more diffuse change in profile up the traverse. Anomalous silver values confirm those highlighted in traverse 7.

Traverses 8 and 9 (Appendix II, Charts 2 and 3)

Traverse 8 was located close to the pit wall of the Royal Tharsis open pit. Multi element values were all generally low with the exception of an anomalous peak that is reflected in copper, gold, silver and molybdenum values. The gold anomaly is encouragingly high. This anomaly is not shown by lead zinc, nickel and cobalt which all exhibit much more uneven profiles.

Traverse 9 marks the northern edge of the Royal Tharsis open pit and represents the orebody boundary of previous mining operations. As expected anomalous copper assays above 5000 ppm Cu were returned. Gold values tend to be of global background value with a notable anomalous peak that is almost coincident with a molybdenum high but not with any copper or silver values. Silver highs broadly straddle the 1000 ppm Cu zone. Cobalt values are erratic. An elevated lead and zinc anomaly are coincident and are located in the stratigraphic hangingwall (i.e. towards the GLF) of the main copper - gold - silver mineralisation.

Traverses 10, 11, 12, 13 and 14 (Appendix II, Charts 4 - 8)
These traverses are located around the former WLOC workshops area - i.e. towards the structural hangingwall of Royal Tharsis.

Traverse 10 shows intense pyrite alteration, is predominantly sericitic with multi element assay values that all tend to be low. Traverse 11 is a mixture of sericite and chlorite altered schists and returned an elevated value (reflected in the profiles of virtually all elements with the exception of lead) that can not be related directly to any obvious geological feature. Traverse 12 returned variable low value results, isolated highs for both gold and silver and almost no molybdenum. Both traverses 13 and 14 show predominant sericite alteration. Elevated copper was returned from traverse 14, the copper showing moderate correlation with gold and molybdenum, variable cobalt and elevated lead coincident with elevated copper. An anomalous silver value is similarly coincident with elevated gold and copper values. Traverse 13 returned lower overall values with similar trends in element relationships.

Traverses 15 and 16 (Appendix II, Charts 9 and 10)
These traverses are located in the structural footwall towards the south end of the Royal Tharsis area, in the vicinity of the GLF. Lithologies are mixed chlorite sericite schists, locally sheared with striation movements along joint or shear planes. The

surface outcrops overlie relatively shallow Owen Conglomerate that is a function of the southerly plunging Tharsis Ridge which encloses the corridor to the east.

Figure 4.17

Photograph (looking north east) of traverse 16 outcrop, showing mixed sericite (brown-red colouration) and chlorite (grey colouration) alteration with shearing/striations (not visible in photograph) along joint surfaces. Scale is two metres long.

Traverse 15 was assayed for copper, gold and sulphur only. Pyrite values are all below 5%, copper shows some elevations while gold shows an extremely even distribution. Results from traverse 16 (Figure 4.16) show similar copper values with a greater number of elevated highs. Elevated values are shown by molybdenum, lead and zinc, whilst profiles for copper, silver and cobalt are broadly similar.

Traverses 19 and 20 (Appendix II, Charts 11 and 12)

The lithology in both these traverses is typically Lyell schists with minor inter fingering chlorite bands. All assay values tend to be low with individual profiles showing local elevations. Molybdenum shows a distinctly erratic distribution along both traverses, whilst cobalt distribution in traverse 20 is similarly erratic. Similarities in local highs can be identified between profiles but establishment of any direct relationship is difficult.

Traverse 21, 22, 23 and 24 (Appendix II, Charts 13 - 16)

Three traverses were located in the structural footwall area towards the Tharsis ridge. Traverse 21 returned very low assay values with a broad elevation being common to individual profiles. Values from traverse 22 (close to the conglomerate contact) were similarly very low. A common elevated value is shown on all profiles (albeit somewhat obscured in the molybdenum profile) and it is possible that this demarcates a geological contact/boundary. Profiles for traverse 23 are a lot less uniform, values tend to be higher and correlation not as obvious. Results would tend to confirm the relative position of each line and proximity to the Tharsis ridge. Proximity to unexposed GLF may be a factor in the low assay returns. The profiles in traverse 24 do not really reflect direction to/from known mineralisation. All values are low with those for silver being BDL. Localised elevated peaks may reflect a splay off the GLF which is not exposed at surface. Comparison with results from traverse 28 is instructive (vis-a-vis relative proximity and overall assay results).

Traverses 25 and 26 (Appendix II, Charts 17 and 18)

Both of these traverses were located close to the Tharsis ridge. Results from traverse 25 are all generally low. Reasonable correlation is evidenced between copper, gold and silver, whilst that of copper with molybdenum and cobalt is not quite as good. A single elevated high is common to all profiles becoming multi peaked in molybdenum, zinc and cobalt, and much less identifiable in the lead profile. It is possible that this peak represents the northerly extension of mineralisation trends that have been identified in the Prince Lyell orebody. Profiles from traverse 26 are significantly more variable than those for traverse 25. However peaks in the copper profile are generally coincident with those for gold, silver, molybdenum and cobalt, and to a lesser extent in those for lead and zinc. Traverse 26 is also of interest for the anomalous silver band that would appear to tail off towards the Tharsis ridge.

Traverse 28 (Appendix II, Chart 20)

Traverse 28 is an old trench cut across strike close to the limit of Royal Tharsis open pit (Figure 4.18). Historic data has not been identified. Results returned elevated copper (as expected as the trench is well inside the mineralised copper envelope) and anomalous silver values. The gold profile is remarkably uniform. Away from the orebody (i.e. in the direction of the Tharsis Ridge) both molybdenum and cobalt assays show an increasing value, whilst those for lead and zinc mimic each other along a descending gradient.

Figure 4.18

Photograph (looking east) of trench that was sampled (yellow lines) as traverse 28. Lithology is typical Lyell schist assemblage showing distinctive pyrite-sericite alteration (yellow-red-brown colouration). Scale is two metres long.

4.3.3 Discussion and Conclusions

results from rock chip sampling all returned low values as expected by visual inspection of traverse locations. Local anomalies were identified from several of the sample sites. These anomalies can sometimes be related to lithological alteration, but not on a regular basis. Pathfinder elements show a generally viable correlation across traverse areas, necessitating treatment of each area as a separate target for alteration related mineralisation. Conclusions are as follows:

- anomalous silver mineralisation appears to correlate with the northern boundary of the Royal Tharsis deposit and this is associated with sericitic alteration.

- extension of the copper envelope is indicated to the north and east of the former Royal Tharsis pit with potential for anomalous gold, associated with major sericite and minor chlorite alteration (Flitcroft & McKeown, 1992).
- to the south of the Royal Tharsis area potential exists for possible limited extension of the copper envelope into or towards the corridor area (Corbett, 1997), associated with intercalated sericite and chlorite alteration and with some possible fault control.
- to the south in the structural hangingwall of Royal Tharsis elevated copper correlates with elevated gold and local anomalous silver is associated with chlorite and sericite alteration; alternatives include possible cross-cutting fault controls as well as possible strike extension to the Prince Lyell mineralisation.

4.4 GENERAL CONCLUSIONS FROM SURFACE GEOCHEMISTRY

- Copper correlates with gold, silver and molybdenum. Anomalous threshold values for pathfinder elements are: Cu 450ppm, Au 0.08ppm, Ag 2.5 ppm, Mo 70 ppm.
- The copper envelope is associated with intercalated sericite and chlorite alteration.
- Anomalous silver responses are frequently not related directly to other element(s) and this may be due to silver occurring in the form of tetrahedrite.
- Elevated responses in copper, gold and silver in the stratigraphic hangingwall are associated with chlorite and sericite alteration.
- Manganese correlates with zinc, nickel and ± cobalt; arsenic correlates with zinc and lead; barium correlates with molybdenum.
- The zinc ratio (Huston and Large, 1987) of 48 returned from the orientation work is well outside the range typical of MRV VHMS deposits. As zinc is typically scavenged by Mn/Fe oxides the high zinc to manganese ratio suggests that much of the zinc is remobilised in surface environments. The zinc ratio in this context as an indicator of depositional environment is probably not valid, particularly as minimal visible sphalerite and galena have been recorded.

CHAPTER 5
ALTERATION GEOLOGY

5.1 SUMMARY

Broad based alteration patterns have been established through the Royal Tharsis deposit. This has been done by identifying the dominant alteration mineral, usually in the form of sericite or chlorite. These patterns show a broad correlation to copper mineralisation and sulphide/pyrite distribution. The method of pattern delineation was kept deliberately simple for interpretation purposes although complex alteration assemblages are evidenced within the overall alteration halo. In addition to sericite and chlorite, alteration assemblages include quartz, haematite, magnetite, carbonate, siderite and pyrite. The method of work entailed core logging and sectional interpretation accompanied by petrological and mineragraphic work (this chapter) and followed up by whole rock geochemistry with multi element scans (Chapter 6).

5.2 DRILL HOLE SELECTIONS

5.2.1 Methodology and Drill Core Availability

As a study criteria it was necessary to review and re-log all drill holes with the emphasis being on alteration mineralogy. A standard logging system was employed, whereby descriptors have all been coded in a standard format. This coding system is as used by CMT, details of which are included in Appendix III. The system is broken down into three tiers of lithological descriptors that are further expanded on by alteration coding and alteration description, sulphide mineralisation and structural information.

The optimum of selecting drill holes uniformly across the study area was not possible due to the practical constraints of drill hole locations and extant core. Ideally information from outside the orebody environs would be necessary in order to establish alteration assemblages away from the zone of economic mineralisation, both into the hangingwall and footwall. Drill hole density is greatest within the orebody (as expected) and falls off towards the orebody periphery. Limitations on data availability (i.e. low drill hole density) in the hangingwall and footwall lithologies have resulted in low confidence levels on interpretation in these areas.

Table 5.1	**Drill Hole Statistics**	
	Metres	**Number of drill holes**
Drill Holes Logged	1,670.21	9
Drill Holes Summarised	9,048.40	45
Totals	10,0718.61	54

Drill hole selection was based on availability of core, and distribution of data both along strike and down dip. Core availability resulted in drill holes selected for re-logging being constrained to the central and southern part of the deposit with holes being restricted from section 7770N through to 8070N. North of section 8370N drill hole density drops off rapidly. Drill hole statistics are detailed in Table 5.1.

5.2.2 Drill holes logged

Table 5.2 lists holes logged and for which logs are included as Appendix III. For each drill hole there is a summary cover sheet, assay data in the form of down hole profiles and a more detailed log sheet that contains coded descriptors, major and minor lithologies, alteration codes and description, details on mineralisation and structural data. Collar coordinates are in 315GRL grid, which is the current grid as used by CMT. The relationship between the 315GRL grid and AMG is depicted schematically in Figure 1, Appendix I. The relative positions of the drill holes are depicted in Figure 5.1.

From the available core nine drill holes were selected to allow an even coverage across strike and down dip. Some of the drill holes selected are offset from section and have been projected onto section for diagrammatic representation. Two holes WL0530A and WL0531 provide an extended intersection down dip of the orebody through the structural hangingwall and into footwall lithologies, although ore mineralisation is not

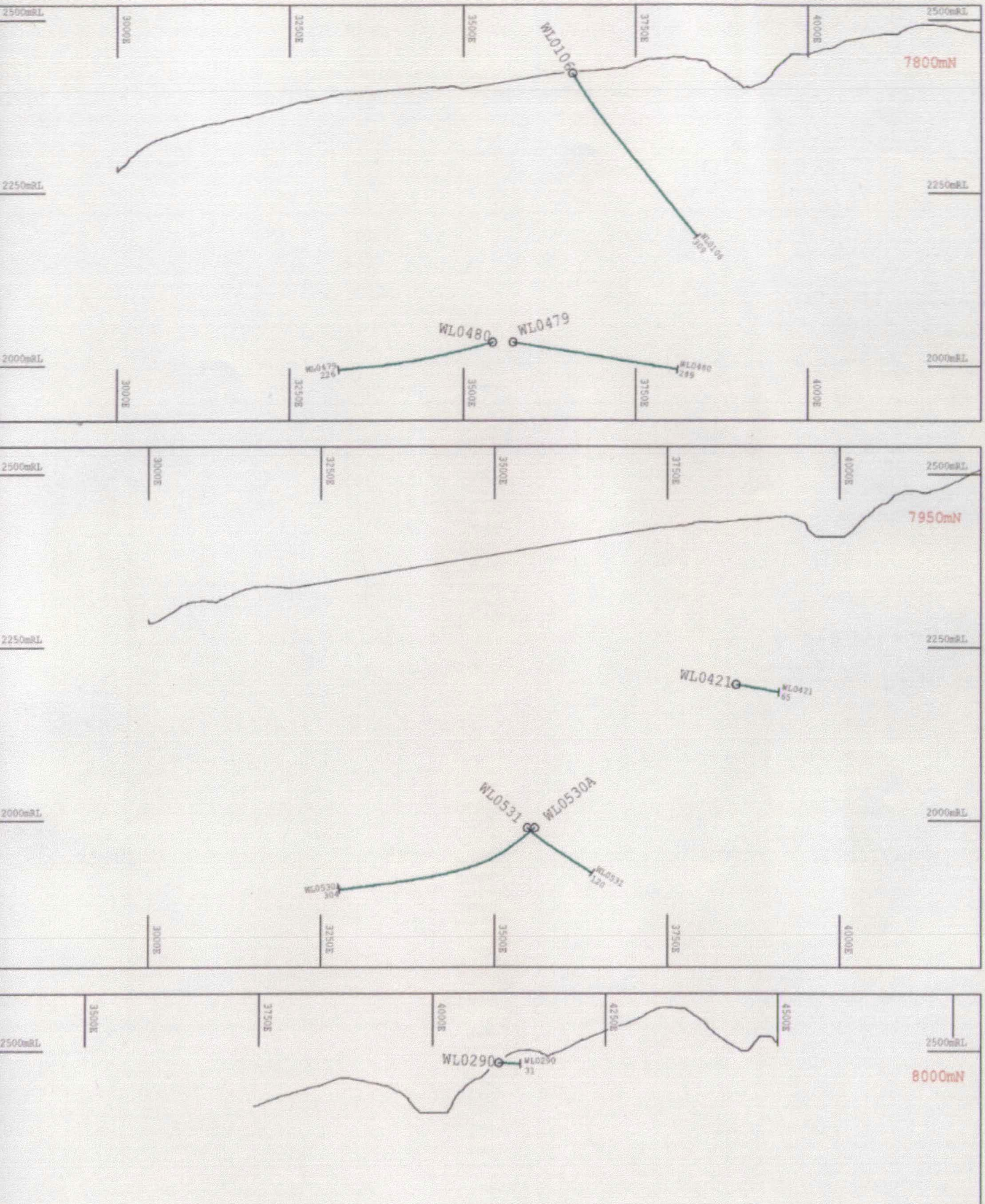

COPPER MINES OF TASMANIA	Scale 1: 7500
	Date 29-Sep-97
Directional Traces and Position of Drill Holes	Drawn AJS
	DRG.NO. Figure 5.1
COPPER MINES OF TASMANIA PENGHANA RD QUEENSTOWN TASMANIA	ACN 065339835

intersected. Holes WL0479 and WL0480 provide a similar intersection but are located further south and intersect low grade halo mineralisation. Drill hole WL0106 passes through a significant mineralised halo towards the southerly limit of Royal Tharsis. Hole WL0421 is a good typical orebody intersection. Similarly drill holes WL0348 and WL0609 both returned reasonable to good ore intersections. The northerly limit to the mineralised ore zone is partly exposed by drill hole WL0290 which intersects sub-economic pyritic volcanics in the structural footwall. No core was available from the northern end of the deposit where in any case drill hole density drops off significantly.

Table 5.2 Logged Drill Holes

Drill Hole Number	Section	Depth (metres)
WL0479	7770N	226.15
WL0480	7770N	249.10
WL0106	7770N - 7830N	308.46 *
WL0421	7950N	65.20
WL0530A	7950N	303.90
WL0531	7950N	119.90
WL0348	8010N	159.72 *
WL0609	8010N	207.00
WL0290	8070N	30.78 *
Totals	***9 holes***	***1,670.21***

* = original log in imperial units

5.2.3 Drill holes summarised

Drill holes that have been summarised from the original log are listed in Table 5.3. The listing encompasses the majority of holes that have been drilled in the Royal Tharsis area. The summary logs are available for inspection. Each summary contains a coded descriptor that may or may not be further described, information on chalcopyrite and pyrite mineralisation, and basic structural data. The coded descriptor incorporates alteration assemblage and texture, whilst not all (historical) logs contain mineralisation and structural data. Where assay data are available significant grade intersections have also been determined (mainly copper, usually pyrite and occasionally gold and silver).

Table 5.3 Drill Holes Summarised

Drill Hole Number	Northing (GRL)	Easting (GRL)	RL (GRL)	Azimuth (°)	Dip (°)	Depth - metres	(feet)
RT0013	8017	3970	2415	000	-90	191.77	(629.17 ft)
RT0028	8046	4045	2468	065	-10	128.02	(420 ft)
WT0001 (WL0079)	8527	3889	2383	065	-45	380.09	(1247 ft)
WL0022	7790	3835	2456	102	-66	133.50	(438 ft)
WL0045	8529	3259	2396	057	-15	91.44	(300 ft)
WL0054	7676	4064	2476	057	-65	163.98	(538 ft)
WL0056	7959	3919	2439	057	-30	123.14	(404 ft)
WL0057	8025	3917	2451	102	-41	112.78	(370 ft)
WL0075	7909	3805	2422	045	-90	872.64	(2863 ft)
WL0076	8151	3900	2445	057	-50	129.54	(425 ft)
WL0077	8268	3933	2425	057	-60	132.59	(435 ft)
WL0078	8396	3917	2431	057	-45	142.04	(466 ft)
WL0082	7892	3797	2422	105	-27	198.12	(650 ft)
WL0137	7944	3649	2195	105	-50	268.07	(879.5 ft)
WL0138	7903	3652	2195	063	-52	260.91	(856 ft)
WL0139	7904	3651	2195	030	-87	418.64	(1373.5 ft)
WL0163	7872	3892	2201	266	33	103.02	(338 ft)
WL0154	7985	3877	2200	272	0	59.28	(194.5 ft)
WL0190	7859	3723	2422	045	-30	269.60	(8445 ft)
WL0198	7742	3640	2196	046	-76	262.51	(861.25 ft)
WL0211	7986	3756	2196	091	-9	165.51	(543 ft)
WL0213	7955	3759	2196	090	-16	150.57	(494 ft)
WL0215	7929	3755	2422	045	-46	206.65	(678 ft)
WL0223	7955	3757	2195	090	-68	189.28	(621 ft)
WL0246	7864	3744	2196	045	-25	162.53	(533.25 ft)
WL0258	8172	4025	2480	042	-21	200.86	(659 ft)
WL0261	8152	4174	2523	090	-21	96.93	(318 ft)
WL0263	8259	4159	2509	046	-26	152.10	(499 ft)
WL0264	8351	4128	2492	045	-24	185.01	(607 ft)
WL0266	8353	4031	2467	047	-50	256.64	(842 ft)
WL0267	8261	4089	2486	087	-66	209.09	(686 ft)
WL0276	7944	3647	2195	108	-69	334.67	(1098 ft)
WL0278	8072	4060	2457	091	-30	103.63	(340 ft)
WL0283	8020	4045	2443	089	-5	144.17	(473 ft)
WL0284	7981	4043	2442	090	-5	103.33	(339 ft)
WL0285	8016	4016	2406	089	0	77.72	(255 ft)
WL0288	7982	3644	2195	045	-90	60.66	(199 ft)
WL0289	7988	3607	2421	045	-90	73.30	(240.5 ft)
WL0292	8078	4048	2483	089	-5	52.64	(176 ft)
WL0297	8187	3647	2195	087	-68	57.61	(189 ft)
WL0298	8206	3550	2345	045	-90	726.96	(2385 ft)
WL0332	8513	3705	2197	074	-50	413.61	(1357 ft)
WL0578	7729	3444	1911	060	6	38.00	
WL0608	7995	3662	2070	119	30	272.50	
NL0818	7827	4145	2488	088	-19	172.75	(566.75 ft)
Totals	***45 holes***					***9,048.40 metres***	

(datum RL = 2000 RL GRL)

Note: most of the summarised drill holes originally drilled in imperial units

5.3 ALTERATION ASSEMBLAGES

5.3.1 Interpretation

Interpretation was made on sections spaced at 60 metre intervals along strike and down to a depth of some 400 metres below surface. This interval is the same as that used routinely in adjacent orebodies (i.e. Western Tharsis and Prince Lyell). The elevation is the approximate known depth of the Royal Tharsis deposit.

5.3.2 Lyell schists

Logging has enabled recognition of some ten principle alteration assemblages. These are listed below. Some of these assemblages are fairly common whilst others are restricted to occasional occurrences. Gradations within assemblages is the norm rather than the exception. These principle assemblages are here restricted to the volcanic Lyell schists, although haematitic alteration at the contact with the Owen Group is almost ubiquitous. The term Lyell schist is of historic significance and a result of schistosity being readily recognisable in surface outcrop. However in drill core and subsurface exposures schistosity is frequently difficult to identify and the consequential classification as schist sometimes dubious. The Lyell schists are here defined as feldspar replaced, hydrothermally altered and regionally metamorphosed volcanics, shallow intrusives and epiclastics, and in which relict primary textures are not common.

- Lmx - mixed mica alteration assemblage

  Lyell schist with mixed micas occurring in the form of sericite and/or chlorite and/or hydromicas as the dominant alteration mineral(s). The micas generally occur in equal proportions but with significant local variations between members. Primary texture(s) is usually not identifiable in hand specimen. The rock has a variable pyrite content, that is usually less than 5 % by weight.
- Lqzmx - quartz mixed mica alteration assemblage

  Similar to Lmx but with a significant amount of quartz, often in the form of silicification, and frequently with significant (> 5 %) pyrite content. Usually has a well developed uniform foliation (that is not as well developed as in Lmx assemblages).

- Lqzse - quartz sericite alteration assemblage

  Comprises the major proportion of the sericite alteration zone, sometimes carrying relict K-feldspar and albite, particularly towards the distal regions, and which are not readily identifiable in hand specimen. The assemblage can often be further classified on sulphide and pyrite content, and also often carries economic mineralisation. Classification based on pyrite entails a visual estimate of content within arbitrarily defined boundaries (0 - 5%; 5 - 10%; and > 10% by weight of pyrite) and which correspond to peripheral, halo and core mineralisation respectively. The unit is frequently siliceous and/or silicified and characteristically grades into distinctive chert-like units. Commonly "hosts" the carbonate alteration that occurs distal to the economic halo (and which is sometimes associated with veining that characterises Devonian remobilisation).

- Lqzpy - quartz pyrite alteration assemblage

  Typical schist lithology that characterises the alteration halo and which may or may not be siliceous/silicified. Pyrite content is equal to or greater than 10% by weight. The assemblage can be identified by a nodular pseudofragmental/segregation texture that gives rise to a characteristic appearance on weathered surfaces.

- Lqzch - quartz chlorite alteration assemblage

  Volcanics dominantly altered to quartz and chlorite, sometimes with variable subordinate sericite. Relict primary textures are sometimes evident, notably as segregated clots of dark green chlorite (also sometimes described as pseudofragmental) and in which sericite is usually absent. Pyrite content is variable, generally less than 5 % (estimated), and the assemblage is sometimes copper (chalcopyrite) mineralised.

- Lch - chlorite alteration assemblage

  Diagnostic green and textureless chloritic unit that may or may not have discernible foliation, and which generally represents an incompetent and poorly mineralised lithology. The assemblage is distinctive but not common, having a variable and unpredictable distribution. Volcanic texture is usually completely destroyed often giving rise to a weathered regolith profile at surface. Alteration may possibly be after mafic-intermediate and/or mafic intrusives.

- Lct - meta conglomerate alteration assemblage

  Volcaniclastic unit with a variable poorly to well developed foliation, sometimes heavily silicified/siliceous and frequently brecciated (possible locally autobrecciated). The unit is not strictly an alteration assemblage in its own right, but more of a segregation texture, and frequently is associated with haematitic and/or chloritic assemblages.

- Lqzhm - quartz haematite alteration assemblage

  Variable red haematitic dusting that often imparts a diagnostic red colouration to the lithology, which can also sometimes be grey in colour similar to Lqzch. The unit is frequently brecciated and becomes more common towards the contact with the Owen Conglomerate where occasional trace barite may be observed. The assemblage often contains notable sulphide content that may be of economic value, particularly distal to the Owen rock types.

- Lqzmt - quartz magnetite alteration assemblage

  Similar to Lqzhm but with blebs of magnetite and subordinate rare haematite. Generally not well mineralised, but may be adjacent to or enclosed by economic mineralisation. The assemblage is not common and is not diagnostic to any particular lithology.

- Lmtai - magnetite apatite alteration assemblage

  Apatite bearing horizon that is diagnostic of but not confined to the higher grades of the mineralised halo (chalcopyrite, ± sphalerite, ± galena, ± bornite, and ± molybdenite (microscopic)). The magnetite content tends to be variable and may occur as an irregular enclosing rim, coarse disseminated blebs or fine grained disseminations. Distal to the mineralised halo the magnetite content of the assemblage becomes negligible to non-existent.

Distribution af alteration assemblages

No obvious distribution pattern of these assemblages has been identified, although simplification to an assemblage dominated by either sericite or chlorite has enabled broad or common alteration zones to be identified. These are described below. Sectional interpretations are included as Figures 5.2 to 5.12. The zones are generally concordant to dip, are often laterally impersistent and are characterised by rapid and gradational boundaries. Through the central portion of the deposit sericite tends to be dominant, while into the stratigraphic footwall chlorite banding (or lenses) becomes more dominant, frequently with diagnostic carbonate alteration. This latter interpretive chlorite feature is partly a function of sparse drill hole data. Sericite alteration is broadly contiguous with pyrite mineralisation that has been contoured at 5% intervals. Frequent silicification tends to mask primary textures, particularly in the sericitic and pyritic assemblages. The stratigraphic hangingwall is in part demarcated by the contact with the Owen Conglomerate and GLF and along which alteration characteristics tend to be obscured by later pervasive dusty haematite.

5.3.3 Common assemblages

Within the ten principle assemblages described above three can be recognised as being common throughout the Royal Tharsis deposit:

- Quartz-sericite bearing assemblages that are fairly ubiquitous in the felsic rock types, are sulphide (pyrite) bearing, and which generally contain copper mineralisation that may or may not be of economic value. Foliation tends to be well developed, particularly where exposed near surface, but is frequently hidden (or overprinted) where silicification is high. This implies that silicification is post-foliation and further complicates interpretation of alteration which is pre-foliation. The lithology encompasses volcaniclastics, lavas and probable rhyolitic-dacitic precursors.
- Quartz-chlorite-sericite and/or quartz-sericite-chlorite assemblages that tend to be associated with the ore mineralisation and which are frequently haematitic, occasionally magnetic, and in which chlorite development tends to be extremely variable. Foliation is moderately well developed and interfingering of chlorite and sericite is common. The magnetite apatite assemblage described above can often be

identified within this broader alteration assemblage. The presence of ubiquitous green hydromicas frequently make distinction between chlorite and sericite difficult.

- Chlorite or quartz-chlorite bearing assemblages that are often associated with barren or sub economic mineralisation and which are synonymous with the Lch and Lqzch alteration assemblages described above. Broadly textureless (i.e. primary textures completely masked or obliterated) with a variable foliation that is generally poorly developed. Chlorite clots impart a segregated texture that is frequently diagnostic and which may be associated with mineralisation that is anomalous for the assemblage.

Distribution of these silicate assemblages is difficult to relate to orebody boundaries that are defined primarily by economic parameters. However there would certainly appear to be some relationship between these alteration silicates and the distribution of sulphide and copper mineralisation. Distribution of Fe-S-C-O would also appear to take on some form of symmetry although the paucity of analytical data particularly in the distal regions of the deposit tends to preclude quantification.

5.3.4 Feldspar and carbonate alteration

Intense feldspar destruction characterises the alteration assemblages described above. The intensity of feldspar alteration appears to have a broad, and possibly indirect, relationship to copper mineralisation; remnant feldspars tend to be identifiable towards the boundary of the alteration system whilst within the main portion of the alteration system identification of feldspars has been restricted to relict crystal form that is usually completely altered to a xenolithic quartz mosaic. Towards the stratigraphic footwall at the periphery of the alteration system relict albite and albitised plagioclase have been recorded at depth (drill hole WL0530A). In the deposit K feldspar has not been recorded.

Carbonate alteration (recognisable as siderite, but also present as ankerite) is probably late (either veins and/or shears) and is usually identified towards the edge of the footwall alteration zone. Carbonate is usually subordinate in the presence of pyrite and is generally absent when the latter approaches 2%. Veins are commonly up to 50 cm thick, frequently occurring as irregular cross-cutting veinlets and stringers and, more rarely, may attain a distribution over 3 metres. Carbonate alteration is frequently accompanied by chlorite alteration and, where veined (i.e quartz carbonate veins) the chlorite is often diagnostically lath-shaped, with lathes up to 5mm long, and very dark green to almost black in colour.

5.3.5 Sectional interpretation

Common alteration assemblages have been identified and interpretation showing the dominant assemblage depicted in Figures 5.2 through 5.12 which are included at the end of the chapter. A broad description from south to north through the deposit is outlined below.

Section 7770N (Figure 5.2) is characterised by discrete bands of chlorite alteration that extend across the deposit. The alteration has a uniform appearance that may allow prediction of ore vectors by relating copper mineralisation to the alteration pattern. The bands are generally concordant and sub-parallel to dip, while in the structural hangingwall isolated bands occur towards the limit of the sulphide halo. On section 7830N (Figure 5.3) the ratio of chlorite alteration decreases with interfingering contacts between sericite and chlorite alteration becoming clearly evident. Pods of sericite alteration enclosed by chlorite alteration are not uncommon. Interfingering continues through to section 7950N (Figure 5.5) at the same time grading locally (section 7890N - Figure 5.4) into a crudely laminated sericite - chlorite alteration pattern. The chlorite content swells locally. North through to section 8070N (Figure 5.7) chlorite alteration bands become less voluminous with one significant swollen patch (from approximately 3650E to 3780E) interfingering with and enclosing pods of sericite alteration. By 8370N (Figure 5.12) the alteration patterns have become more uniform partly as a result of decreasing drill data, with chlorite showing a notable increase near surface northwards from section 8250N (Figure 5.10). This tends to agree with findings from surface rock chip work (see Figure 4.16 showing alternating or coarsely banded sericite-chlorite assemblages). The increasing dominance of the chlorite assemblage is particularly noticeably in the structural hangingwall where decreasing drill hole data is commensurate with minimal mineralisation. Lack of information beyond section 8370N makes confidence in further interpretation low. Broadly, chlorite alteration appears to increase with an apparent decrease in near surface mineralisation

5.4 PETROLOGY AND MINERAGRAPHY

5.4.1 Acknowledgment

Thin section and petrological work was commissioned by CMT and carried out by Consultant Petrologist Dr. J. Barron. This section summarises Barron's report in the context of known geology and alteration.

5.4.2 Overview

A total of 30 samples were thin sectioned and examined petrologically (Barron, 1997). Sample details and photographs are included as Plates 1 to 16 in Appendix IV. The EXPA numbers referred to in the text below are samples that are listed in Table 1, Appendix IV. Findings broadly confirm observations from logging. i.e. the protolith is poorly preserved, having undergone both selective and intense alteration, and having been subjected to strong and variable tectonic deformation with development of characteristic foliation. The presence of local shallow intrusive(s) complicate a cupriferous hydrothermal alteration system, of possible porphyry provenance, that is strongly pyrite mineralised and which contains subordinate molybdenum (Barron, 1997). Minor gold and silver returned by assay results were not identified in the petrological work.

5.4.3 Alteration and deformation

Alteration is both intense and selective resulting in assemblages that are predominantly illite/sericite with lesser chlorite and minor carbonate (Plate 13, Figure 2). Other assemblages include sericite-quartz-rutile, quartz - sericite ± chlorite ± carbonate (Plate 12, Figure 4) and predominant chlorite assemblages. Primary textures have been almost completely destroyed although occasional relict forms can be discriminated. Phenocrysts are usually relict being poorly recognised and frequently either destroyed, replaced or altered. Occasional traces of tourmaline (EXPA3208 - WL0106) indicate the presence of boron and halogens in the hydrothermal fluid. Carbonate is mostly siderite and ankerite with lesser (?late) amounts of calcite (plate 4, Figure 2). Glass shards (Plate 6, Figure 2) attest to volcanic source(s). (EXPA3215 - WL0106, EXPA3217 & EXPA3220 - WL0530A) Minor but not insignificant amounts of albite (Plate 10, Figure 2) (EXPA3219, EXPA3223 & EXPA3224 - WL0530A) have been recorded towards edges of the alteration system.

Intense deformation is almost ubiquitous frequently being typified by an S1 foliation (i.e. slaty cleavage) of illite-sericite wavy tails that wrap around more competent lensed domains of granular quartz. This wrap around feature is common on a mesoscopic scale (Berry, 1990 and 1991). Microfractures are approximately normal to S1. Later kink or strain-slip folding has produced a second penetrative foliation - S2. (i.e. deforms the slaty cleavage) (Cox, 1979; Wills, 1996b). Ptygmatic forms are common. Early quartz veins are commonly fractured and deformed. Carbonate veins terminate against late microfractures that are associated with S2. (EXPA3216 & EXPA3222 - WL0530A)

Down dip of the orebody volcaniclastics with compositions suggestive of trachyandesite (EXPA3224 - WL0530) to trachybasalt (EXPA3225 - WL0531) characterise the footwall (Plate 11). Lithologies are intensely and selectively altered with significant carbonate veining identified towards the limit of the alteration system (drill holes WL0530A and WL0531). Vitric tuffs and lithic fragmentals (Plate 2, Figures 1 and 2) are common with lesser amounts of volcaniclastics. Relict textures incorporate glass shards (Plate 9, Figure 4) and possible evidence for feldspathic precursors. Rare relict albitised plagioclase (EXPA3221 - WL0530A) is evidence of the distal parts of an alteration system that is sparsely sulphide mineralised. Distally the system is characterised by an altered amphibole-plagioclase intermediate volcanic rock of possible trachyandesite composition with abundant dusty haematite (Plate 2, Figure 4) and anomalously abundant apatite (Plate 4, Figure 1) (EXPA3224 - WL0530A).

Lithologies grade into selectively altered fragmentals (± lithics) and/or volcaniclastics (EXPA3223 & EXPA3222 - WL0530A) in which carbonate veining is prominent. The intersection of S1 and S2 foliation with quartz-rich domains resembles autobrecciation. Locally strong feldspathic alteration can be identified (Plate 10, Figure 3) (EXPA3221 - WL0530A) (possibly shallow intrusive source(s)). The alteration assemblages are frequently different either side of the veining suggestive of post-vein emplacement alteration (EXPA3220 - WL0530A). Two possible phases of carbonate alteration/generation can be distinguished, one vein-hosted and the other alteration-assemblage hosted. Haematitic dusting (EXPA3219 - WL0530A) is suggestive of a strongly feldspathic precursor. Carbonate veined lithic fragmentals (EXPA3217 - WL0530A) (? acidic volcanic source) are characteristically microporphyritic with traces of pyrite, zircon, leucoxene and haematitic dust. Carbonaceous dust and appressed rootless fold hinges associated with lensed layering are evident in some of the volcaniclastics (EXPA3216 - WL0530A).

5.4.4 Southern limit

Towards the southern end of the deposit an intensely and selectively altered shallow feldspar porphyry (EXPA3230 & EXPA3229 - WL0480) (Plate 12, Figure 4) that is sulphide mineralised is a potential heat source (or associated heat source) that could have been influential in the alteration phase(s) (Plate 11, Figure 4). Subordinate carbonate is contained within the alteration assemblage as is patchy chlorite. Alteration is both intense and patchy with development of quartz-illite/sericite-chlorite-(carbonate) and quartz-illite/sericite-(carbonate-chlorite) assemblages with minor/trace zircon, sphene, apatite and leucoxene (EXPA3229 & EXPA3230 - WL0480). Relict feldspars are locally abundant frequently giving rise to a "crowded" porphyritic texture (EXPA3229 - WL0480) that is difficult to classify (Plate 1, Figure 1). Sulphides are significant (chalcopyrite and pyrite) with one generation of pyrite recognised.

Along strike autobrecciated volcanics (EXPA3209 - WL0106; EXPA3219 & EXPA3224 - WL0530A; EXPA3225 - WL0531) (Plate 6, Figure 4) and volcaniclastics (EXPA3209 - WL0106) (Plate 7, Figure 2) contain disseminated sulphide mineralisation associated with the economic copper halo. The rocks are typically haematitic and are characterised by pyrite and chalcopyrite with minor amounts of molybdenite (EXPA3207 - WL0421) (Plate 15, Figure 1) and trace bornite-chalcocite-digenite (EXPA3210 - WL0106)(Plate 15, Figures 3 and 4).

At the base of the sequence carbonate-rich fragmentals (EXPA3220 - WL0530A) from a clastic parent are deformed and possibly boudinaged (EXPA3212 - WL0106) (Plate 8, Figure 2) with interstitial chlorite-illite/sericite assemblages. Cuspate volcanic glass shards (Plate 9, Figure 4) are evidence for spherulitic devitrification. Overlying fragmental/volcaniclastics have a weakly preserved porphyritic texture that contains evidence for sub-parallel alignment of feldspathic prisms during magmatic flow (EXPA3213 - WL0106). Tuffaceous rocks (EXPA3215 - WL0106) that have been intensely altered to quartz-sericite assemblages contain magmatically embayed quartz (Plate 1, Figure 4), possible glass shards, altered feldspars, rutile/titanium oxides and accessory zircon and apatite. Possible cordierite (Plate 9, Figure 1) is suggestive of post-alteration metamorphism of hydrothermslly altered rocks that have undergone strong Mg-Fe enrichment and Na-Ca-K depletion (Thompson and Thompson, 1996). Altered lithic breccias and autobrecciated flows (EXPA3208 - WL0106) show evidence of selective alteration and intense silicification. Towards the hangingwall a microporphyritic texture is preserved in a mineralised pumiceous fragmental host (EXPA3210 - WL0106). Hydrothermally brecciated tuffs that are intensely altered and silicified occur towards the footwall. Quartz-chlorite stringers are common and vein quartz contains trails of fluid inclusions.

5.4.5 Mineralisation and mineralised lithologies

Relict textures through the mineralised halo are poorly preserved (if at all), the orebody itself being selectively and intensely altered, recrystallised and foliated (drill hole WL0421). The structural hangingwall (i.e. stratigraphic footwall) is characterised by glomeroporphyritic mafic phenocrysts (Plate 11, Figure 2) with some poor subhedral shapes suggestive of amphibole and/or pyroxene. The absence of epidote tends to corroborate a lack of mafic and mafic - intermediate rock types. Possible rare plagioclase laths have been completely clay altered to a granular groundmass that is composed of quartz-rich domains which impart an almost lens-like appearance. Hydrothermal and metamorphic alteration is evident with the development of schist assemblages that contain rutile, carbonate and apatite (plate 3, Figure 3). Trace minerals include sphene and zircon. Sphene is commonly replaced by leucoxene. Microscopic molybdenite cannot be identified in hand specimen whilst two possible phases of monomineralic pyrite mineralisation can be distinguished (EXPA3207 - WL0421). Anhedral chalcopyrite occurs as blebs and disseminations, is frequently interstitial and often encloses spongy clusters of pyrite.

Sulphides are dominated by pyrite, frequently containing chalcopyrite inclusions (Plate 14, Figure 3). Rare inclusion of bornite-(chalcocite-digenite) have also been identified (EXPA3210 - WL0106)(Plate 15, Figures 3 and 4). Trace anhydrite and barite (EXPA3201 - WL0290) (towards the stratigraphic footwall) and secondary covellite (EXPA3201 - WL0290) have been identified towards the stratigraphic footwall. Traces of molybdenite are fairly common particularly through the orebody environs (EXPA3207 - WL0421; EXPA3213 - WL0106)(Plate 16, Figure 1). Traces of sphalerite (EXPA3211 - WL0106; EXPA3226 and EXPA3228 - WL0531) and galena (rare EXPA3226 and EXPA3228 - WL0531) have also been identified (Plate 16, Figures 3 and 4), the former being characterised by a pale colour (i.e. iron poor) that tends to suggest oxidisng fluids or lower temperatures. Trace pyrrhotite is occasionally observed in the mineralised halo (EXPA3209 - WL0106; EXPA3229 - WL0480). Selectively altered ?plagioclase pyroxene porphyritic vesicular volcanics of possible trachybasaltic composition contain abundant dusty haematite and abundant accessory apatite (EXPA3225 - WL0530A). Angular fragments with a jig saw texture suggest some autobrecciation. Lithic fragmentals (EXP3226 - WL0530A) and volcaniclastics that are intensely altered and recrystallised, foliated and carbonate veined contain disseminated monomineralic pyrite and vein-located galena and sphalerite, the latter being near colourless and suggestive of a fairly distant heat source. Minute trails of dusty rutile, clusters of intergrown apatite and rare traces of chalcopyrite demarcate the mineralised halo (EXPA3228 - WL0531).

5.4.6 Northern end

In the hangingwall (drill hole WL0290) intense alteration continues to be a diagnostic feature, possibly becoming more pervasive and less selective. Brecciated fragmentals (EXPA3201 - WL0290) (Plate 1, Figure 1) are characterised by quartz-illite/sericite assemblages with ± chlorite and ± carbonate. The carbonate is possibly not typical of the hangingwall whilst significant sulphide mineralisation is primarily pyrite (monomineralic) (Plate 14, Figure 1) of which two possible generations can be identified (EXPA3202 - WL0290). Traces of covellite, anhydrite, barite, magnetite and haematite may reflect proximity to the Owen sediments with commensurate changes in redox conditions and pH during alteration.

5.5 CONCLUSIONS

- Broad correlation exists between sulphide mineralisation (principally pyrite) and alteration patterns.
- Some ten main alteration assemblages have been identified: mixed mica, quartz-mixed mica, quartz-sericite, quartz-pyrite, quartz-chlorite±sericite, chlorite, meta-conglomerate, quartz-haematite, quartz-magnetite and magnetite-apatite.
- The most common alteration assemblages include: quartz-sericite; quartz-chlorite-sericite and/or quartz-sericite-chlorite; and chlorite or quartz-chlorite assemblages.
- Weak zonation is evident between Fe-S-C-±O, although quantification has not been established.
- Carbonate alteration that is distal tends to be associated with Devonian vein emplacement and may be due more to remobilisation rather than primary alteration.
- Intense and selective alteration has resulted in obliteration of primary textures.
- Feldspar destruction is almost ubiquitous. Rare albitised plagioclase occurs towards the periphery of the alteration system.

- Volcanic precursors included rhyolitic and dacitic (i.e. felsic) volcanics, volcaniclastics (locally autobrecciated), brecciated lavas and minor porphyries.
- Sulphide mineralisation is dominantly pyrite and for which at least one generation has been identified, and which contains subordinate chalcopyrite. Other sulphides that occur in trace amounts include bornite, chalcocite-digenite, covellite, molybdenite, sphalerite and galena.
- The abundance of illite (Barron, 1997) is suggestive of the presence of weakly acidic (CO_2-rich) fluids (Thompson and Thompson, 1996).
- S1 foliation wraps around lensoidal domains of granular and mosaic quartz. S2 penetrative foliation is a result of later strain slip folding. Carbonate veins terminate against late S2 microfractures.

Notes to accompany Figures 5.2 to 5.12

- Alteration patterns have been identified through logging of drill core and interpretation of drill hole logs. Patterns represent assemblages simplified to show dominant sericite or chlorite alteration.

- Sections are spaced at 60 metre intervals from 7770N (Figure 5.2) to 8370N (Figure 5.12). North of 8370N there is insufficient data for meaningful interpretation.

- Sericite and/or chlorite alteration does not generally extend into the Owen Conglomerate.

- Quartz-sericite assemblages are usually associated with felsic rocks, generally have a well developed foliation and are often highly siliceous.

- Quartz-chlorite-sericite assemblages contain a highly variable chlorite content and are frequently characterised by interfingering of chlorite and sericite.

- Quartz-chlorite or chlorite assemblages may have a diagnostic clotted texture (pseudofragmental) or may be textureless with no obvious foliation (not discernible at 1:5000 scale).

- Drill hole traces show copper assays (where assays are available). Darker hatches represent low copper values. Orange hatches represent >1% Cu contour.

- Most drill holes have been drilled up stratigraphy i.e. collared in the footwall (west or left side of diagram) and drilled through to the hangingwall/Owen Conglomerate. Obvious exceptions are WL0479 (Figure 5.2 - section 7770N) and WL0530A (Figure 5.4 - section 7950N) which have been drilled into the structural hangingwall.

- Great Lyell Fault - within the interpreted alteration zone the GLF is along or close to the Owen Conglomerate contact.

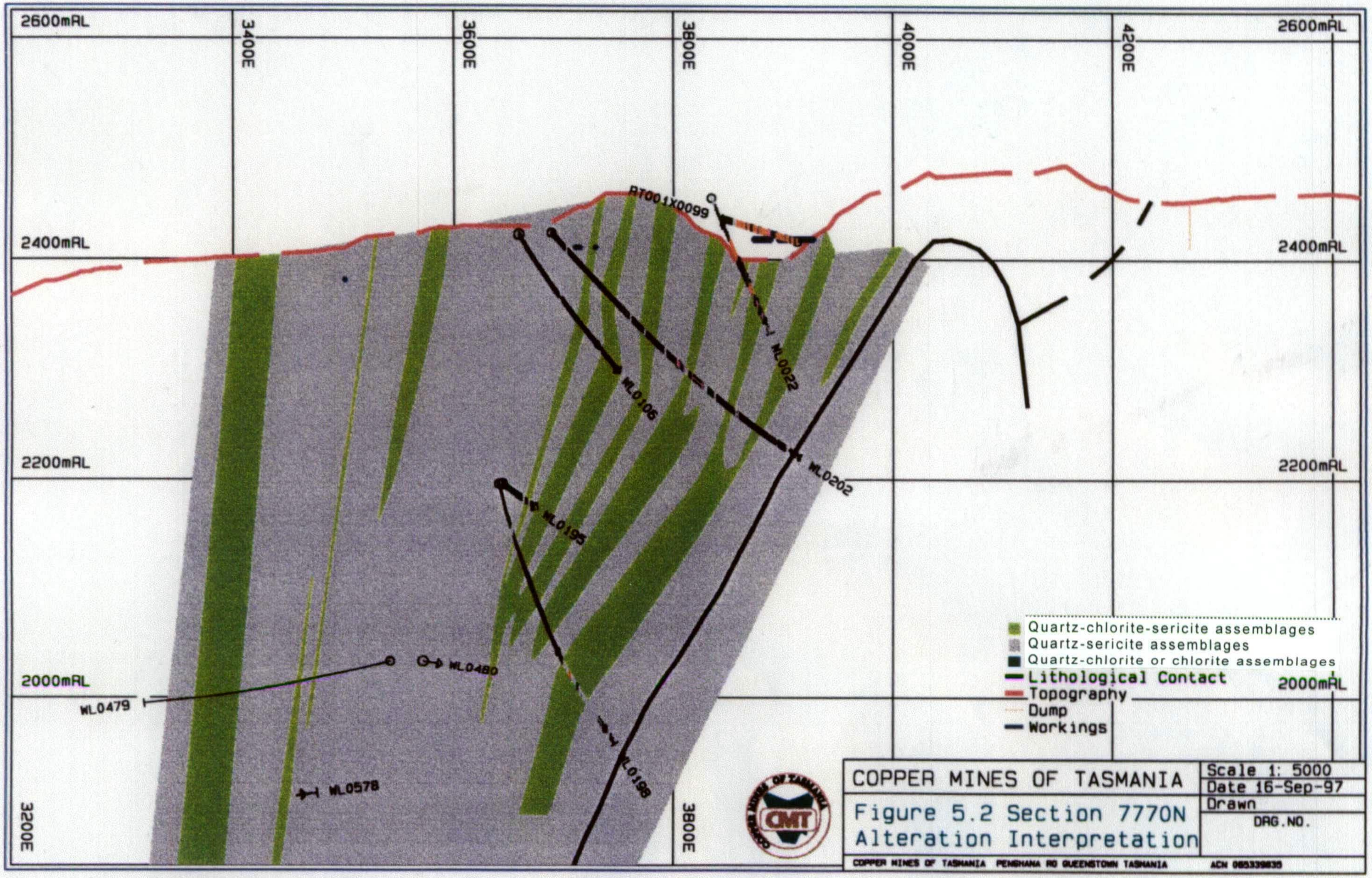

Figure 5.2 Section 7770N Alteration Interpretation

K SSI - CMT Exploration.

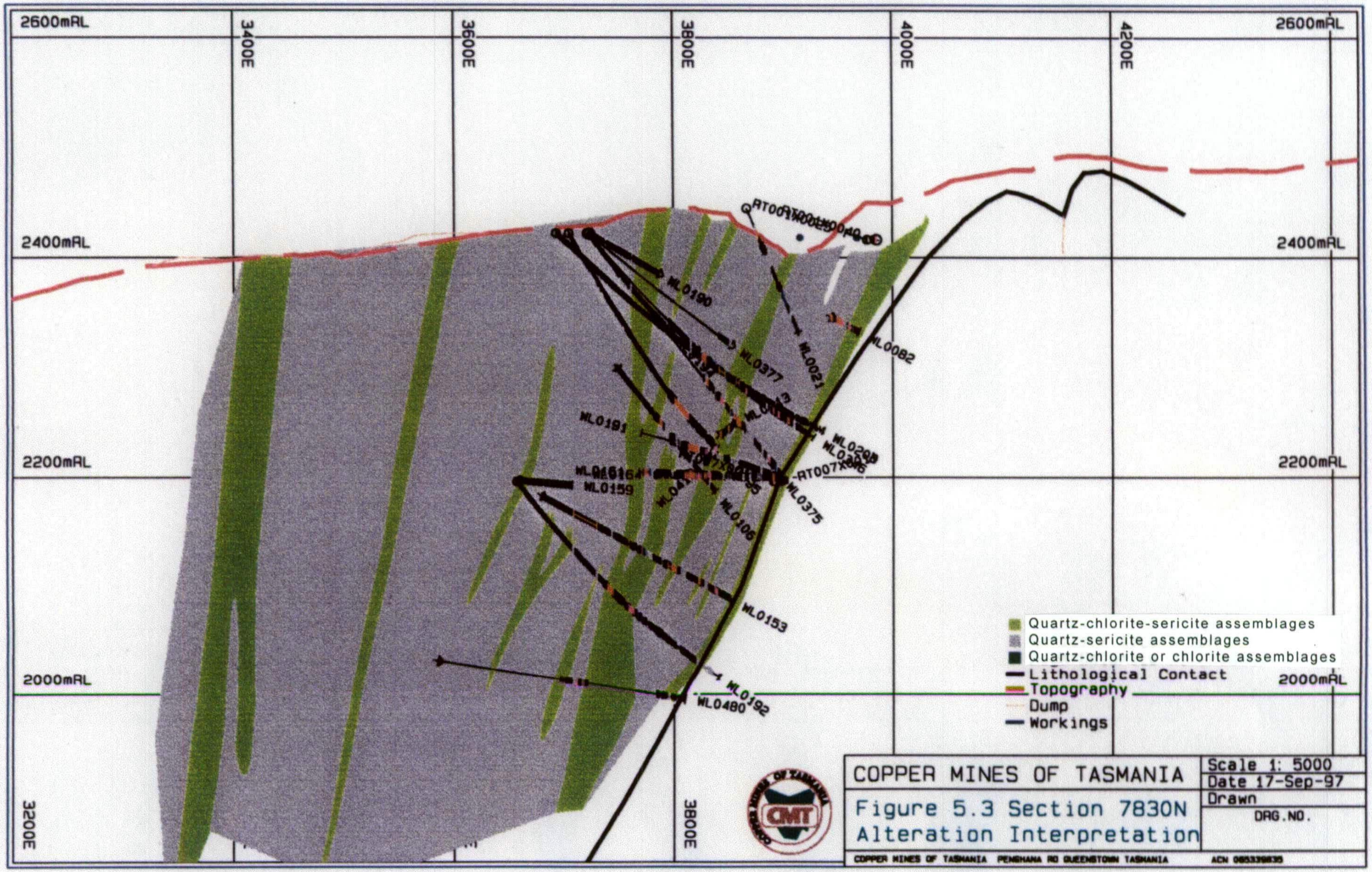

Figure 5.3 Section 7830N Alteration Interpretation

altnwl1c.pf

K SSI - CMT Exploration.

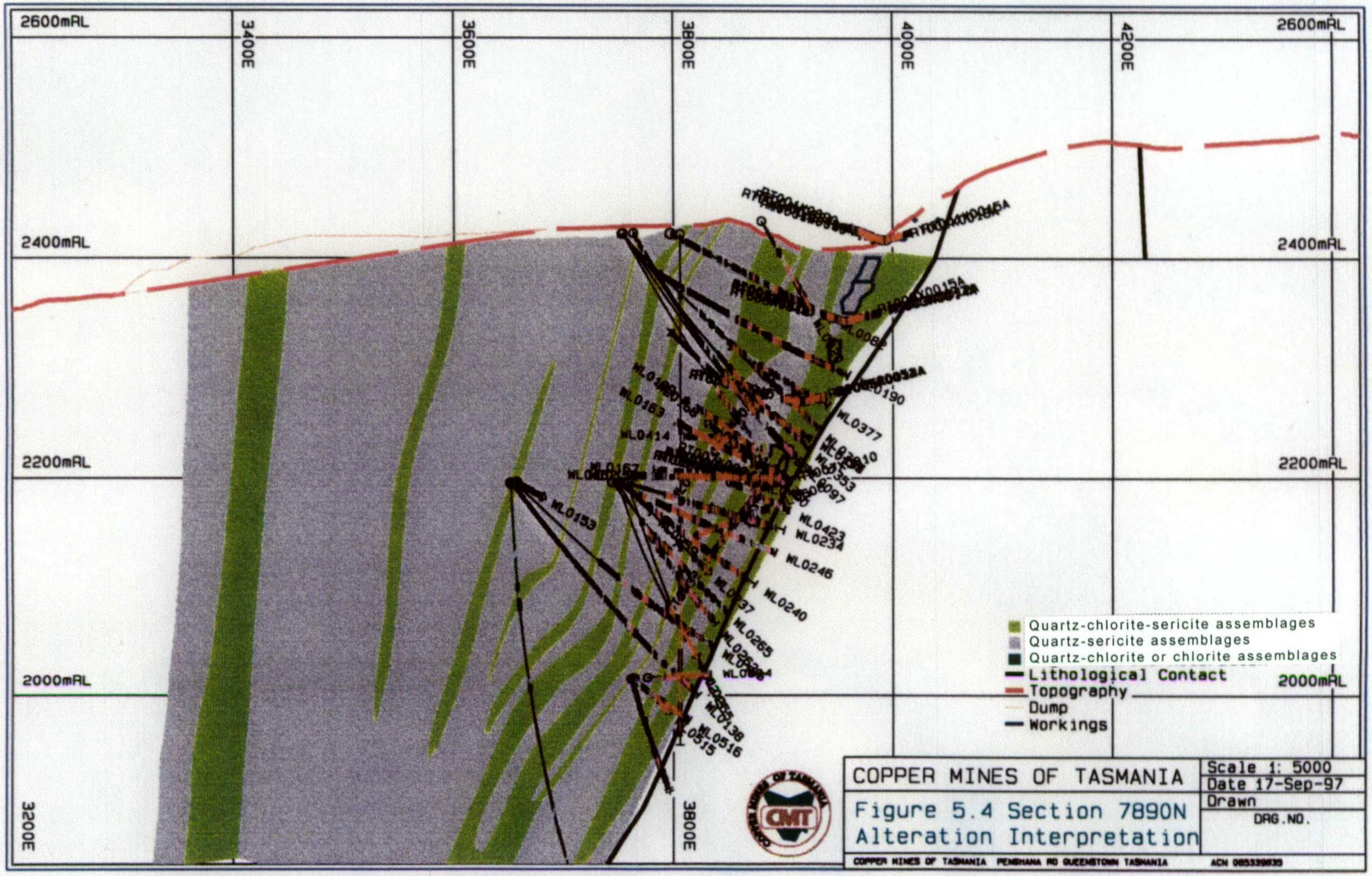

altnwl1d.pf

K SSI - CMT Exploration.

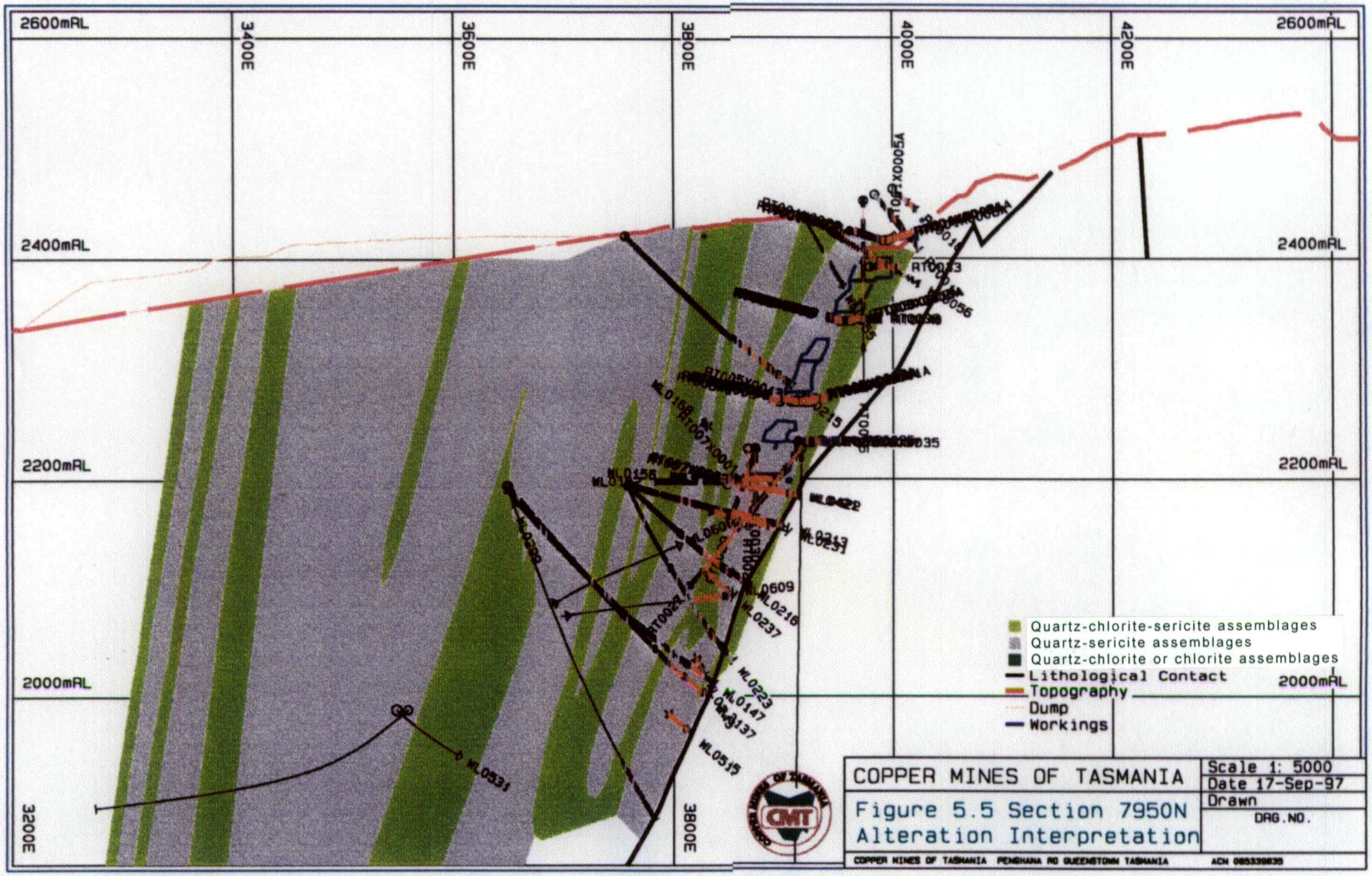

altnwl1e.pf

SSI - CMT Exploration.

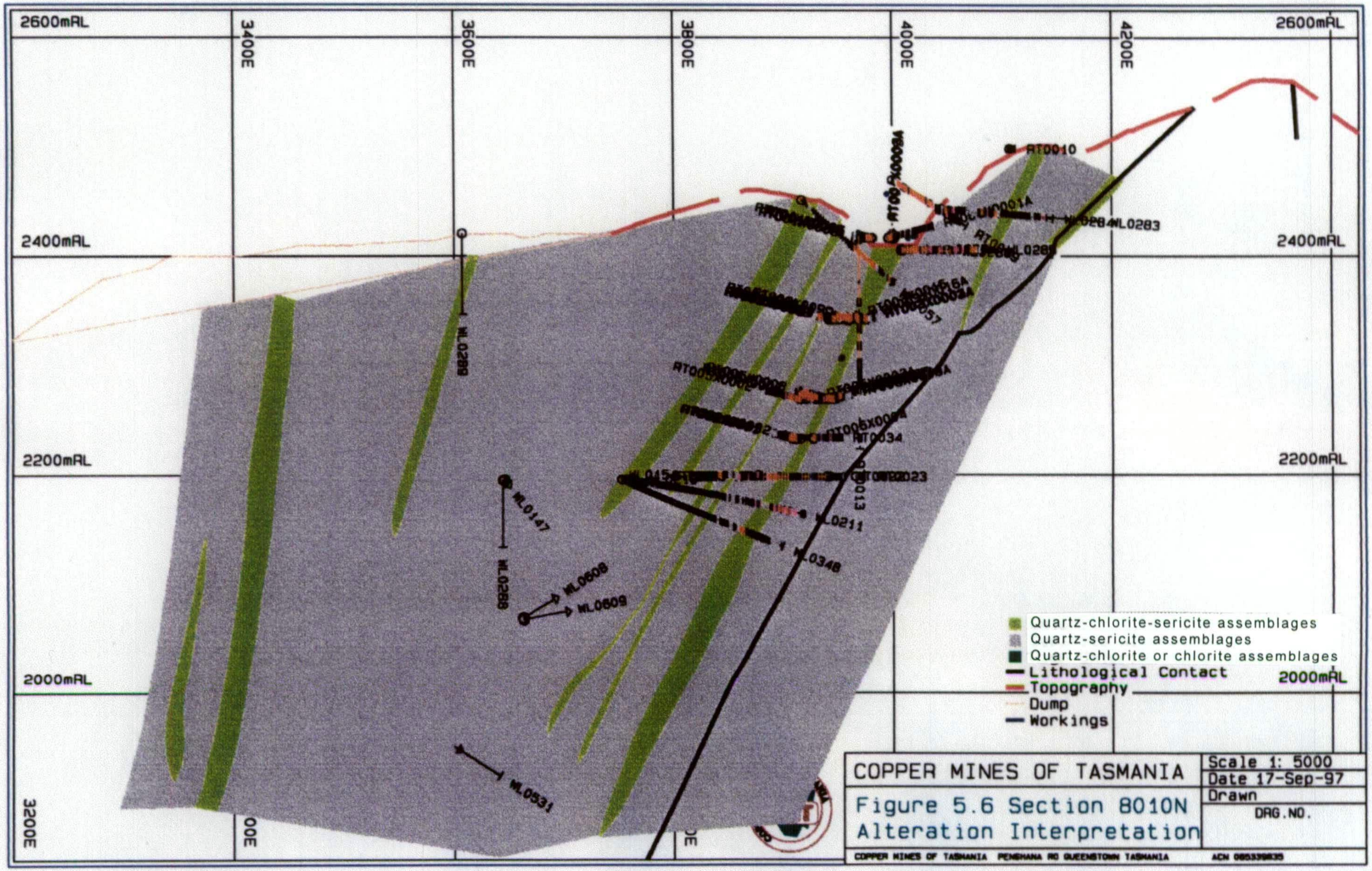

altnwl1f.pf

SSI - CMT Exploration.

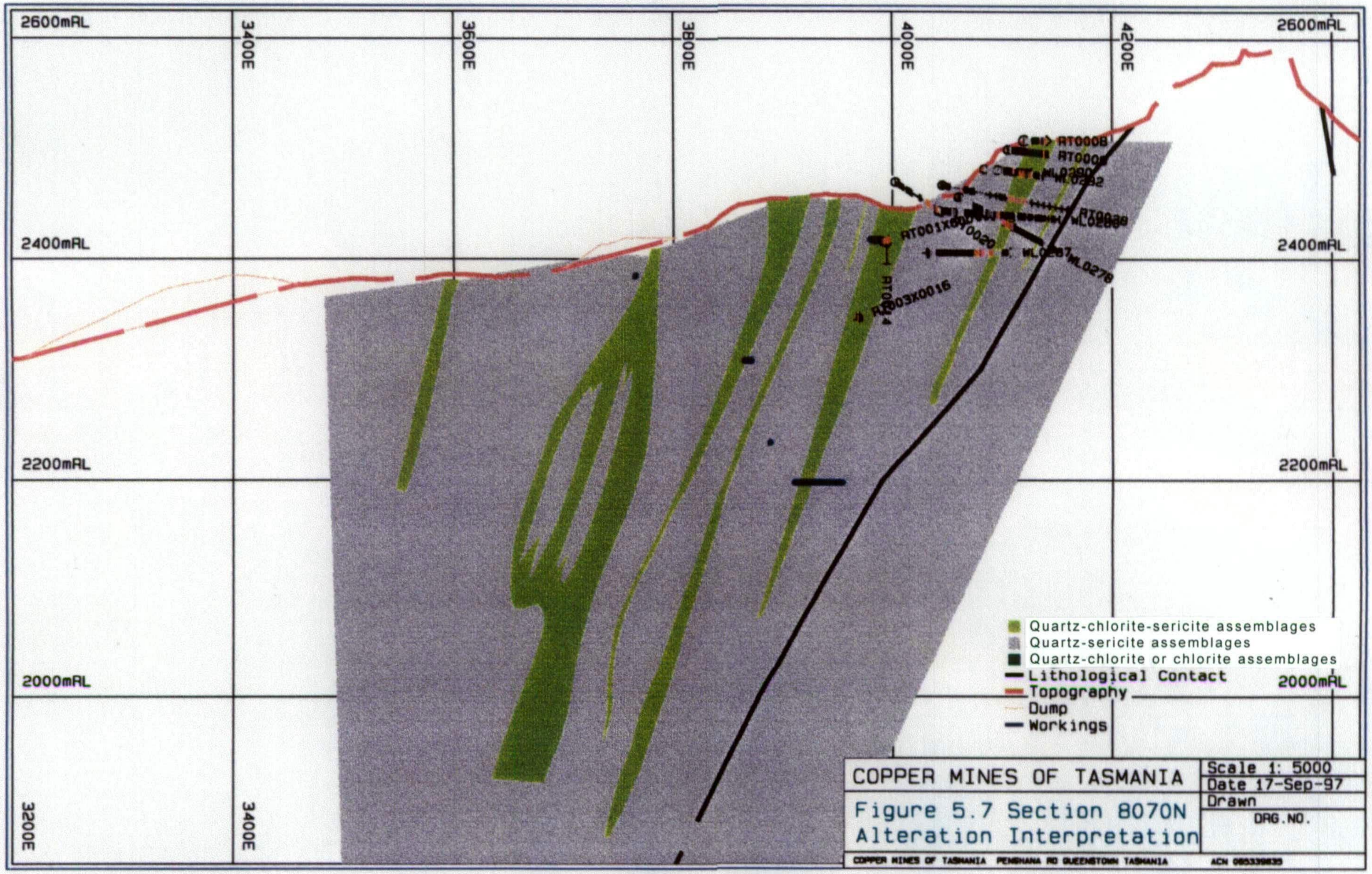

Figure 5.7 Section 8070N Alteration Interpretation

K SSI - CMT Exploration.

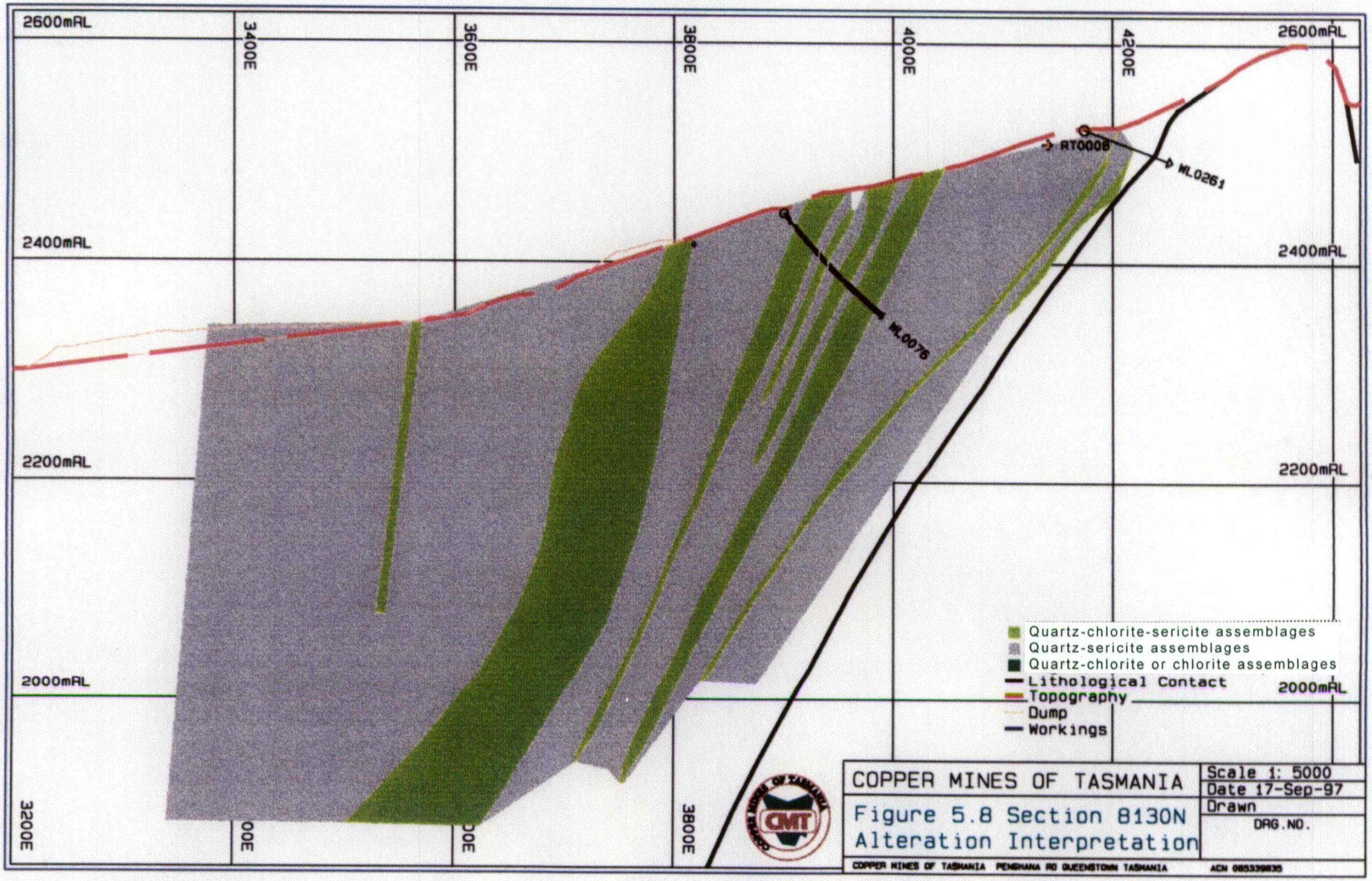

altnwl1h.pf

SSI - CMT Exoloration.

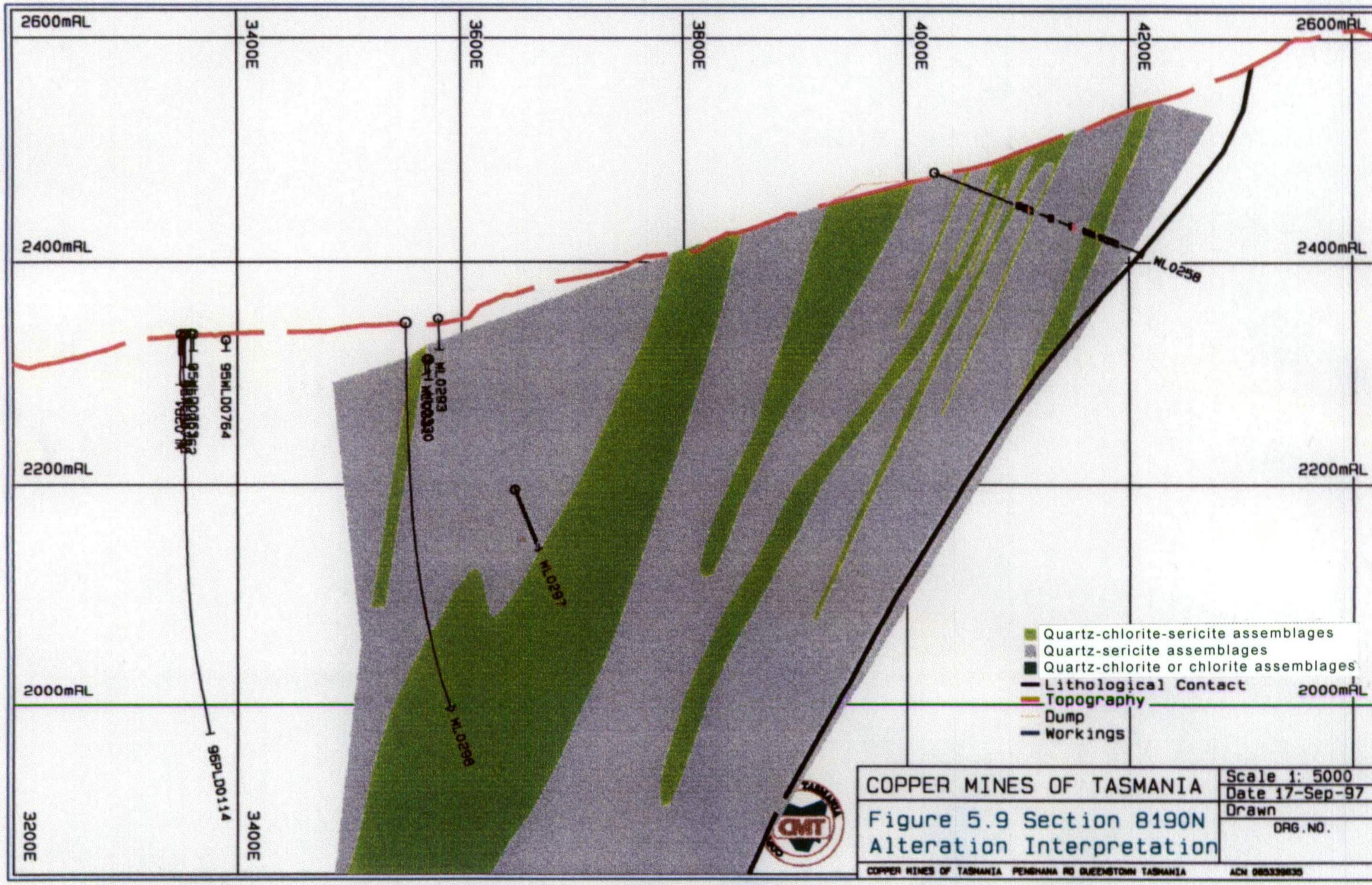

Figure 5.9 Section 8190N Alteration Interpretation

altnwl1i.pf

SSI - CMT Exploration.

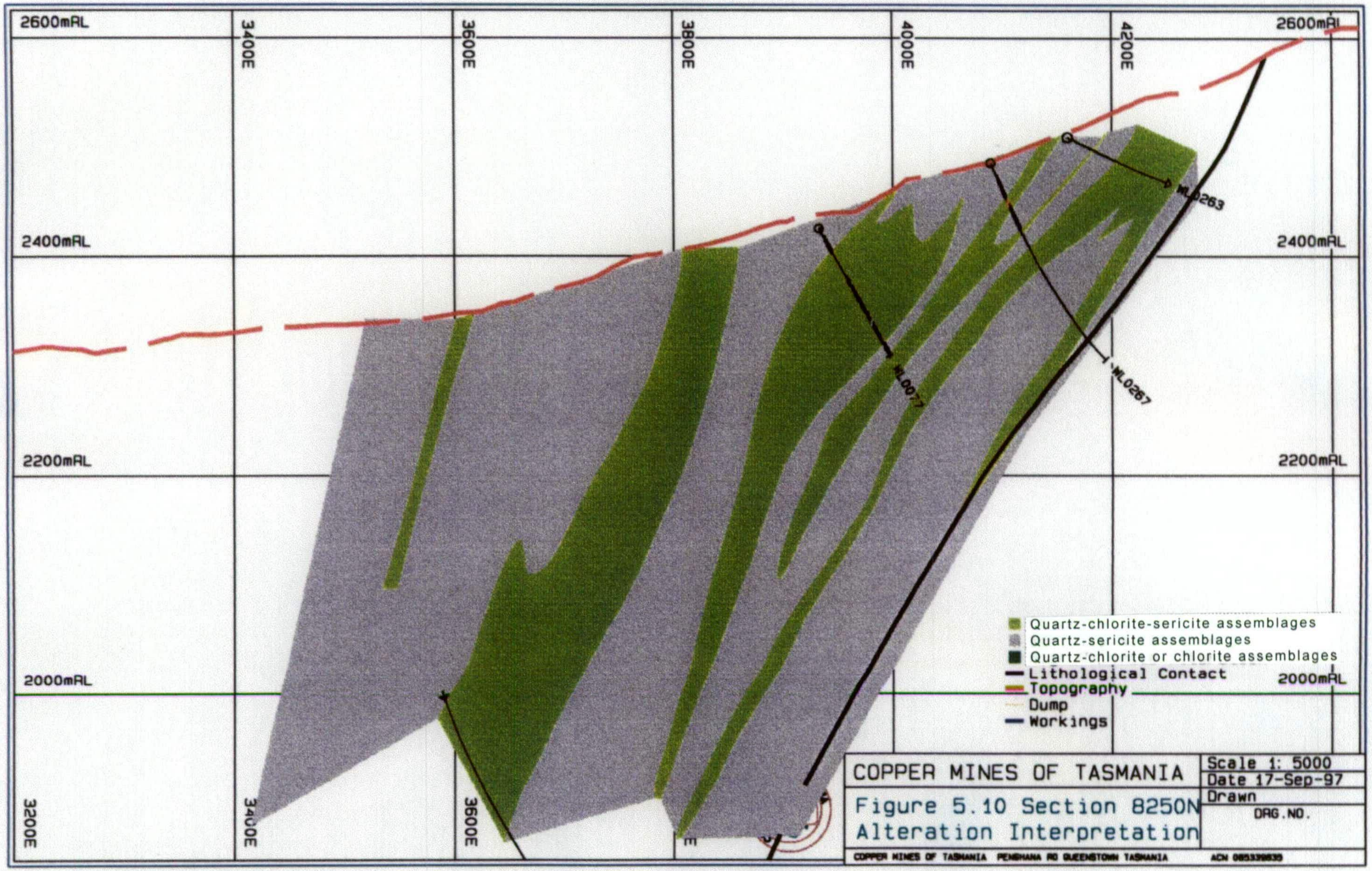

Figure 5.10 Section 8250N Alteration Interpretation

altnwl1j.pf

K SSI - CMT Exploration.

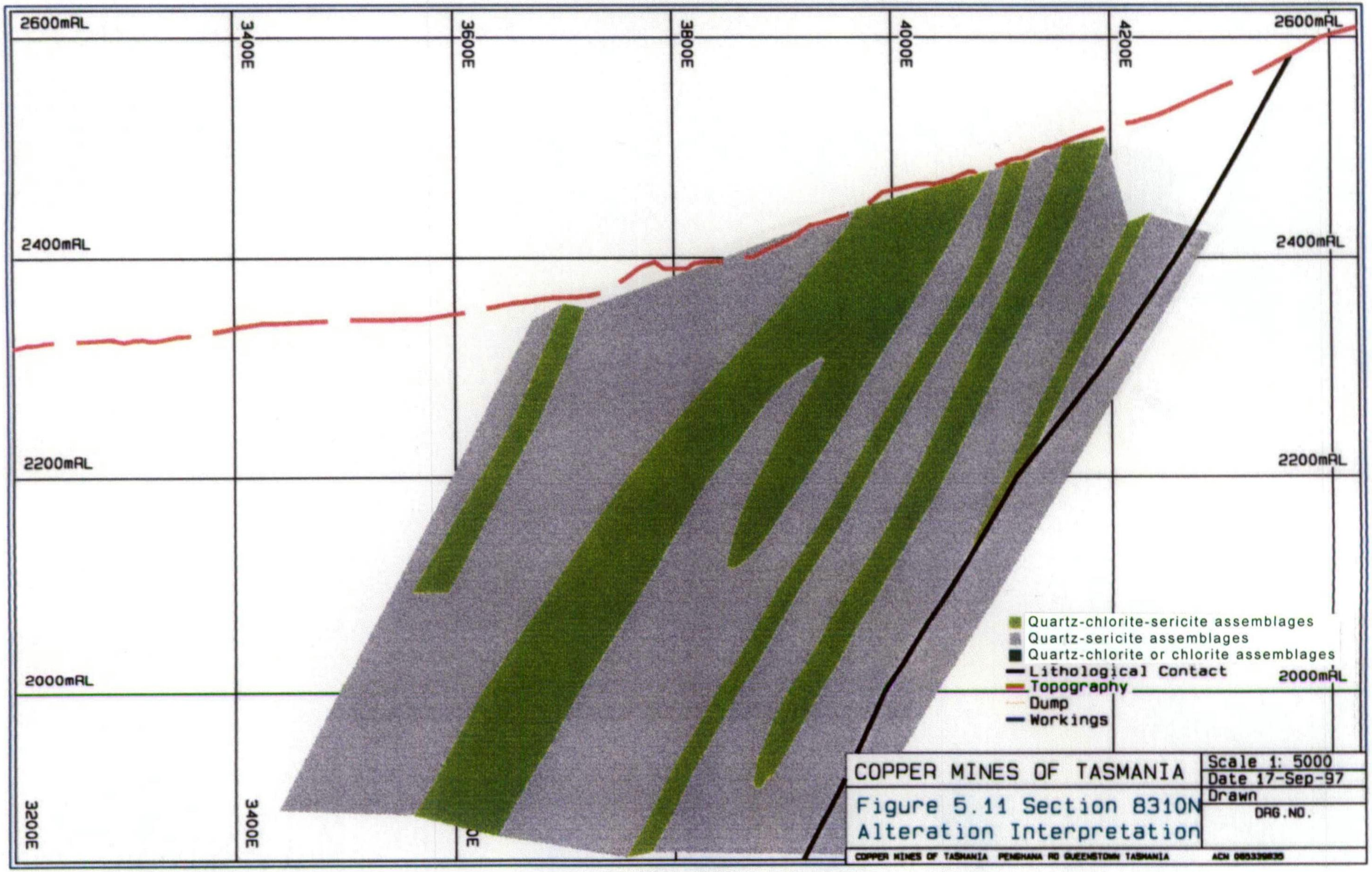

altnwl1k.pf

SSI - CMT Exploration.

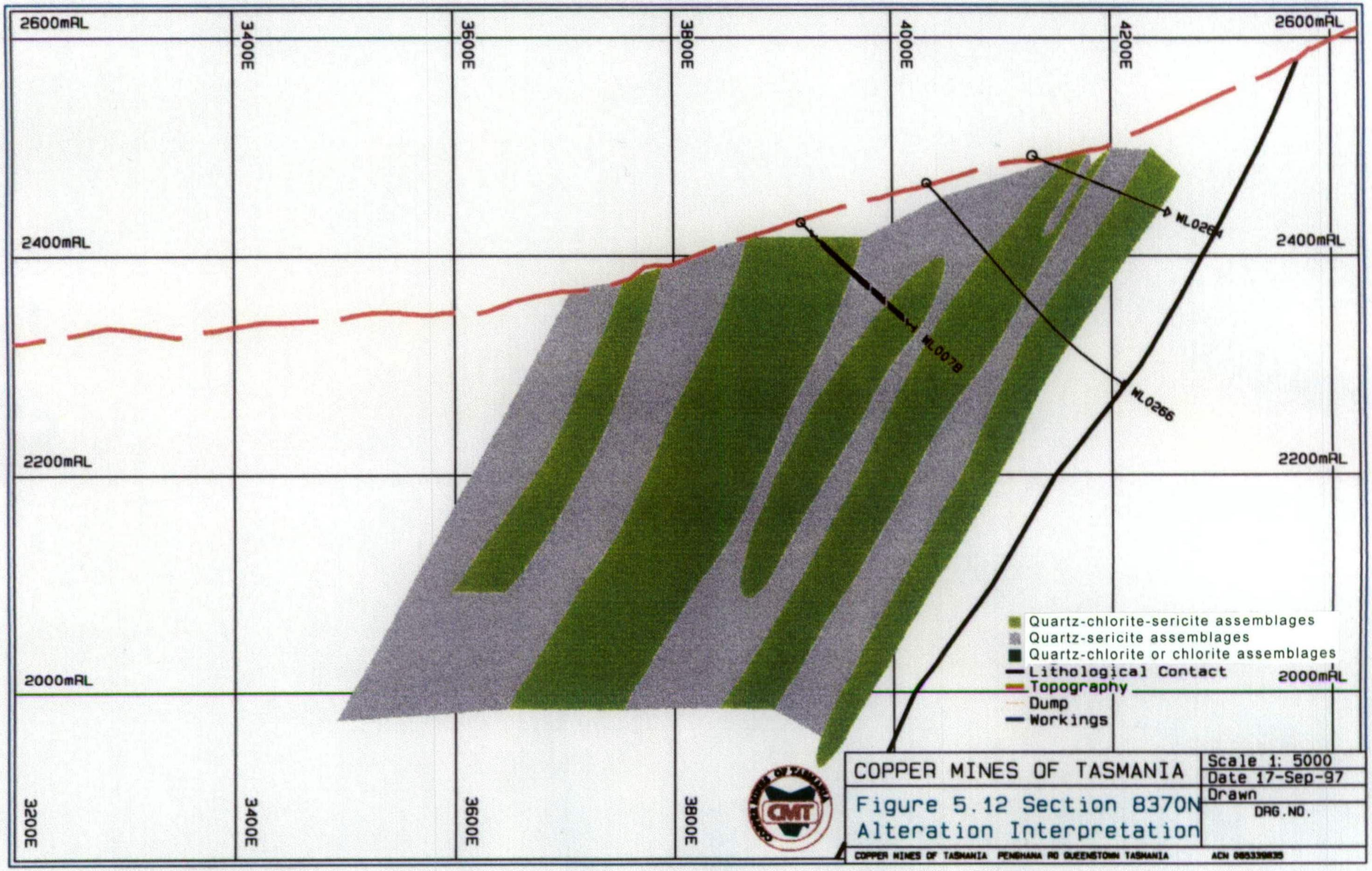

altnwl1l.pf

K SSI - CMT Exploration.

CHAPTER 6
ALTERATION GEOCHEMISTRY

6.1 METHODOLOGY

6.1.1 General

Samples were taken from selected drill holes to investigate alteration geochemistry. The relative position of the drill holes is shown in Figure 5.1. Results are included as Appendix V which contains:

- plots for majors and trace elements (Chart 1 and Chart 2)
- sample analyses results (Table 1)
- sample locations (Table 2)
- analytical methods (Table 3)
- dataset statistics (Table 4)

6.1.2 Analytical Techniques

Samples were analysed by total fusion followed by ICP analyses - both MS and OES - on majors and trace elements. Copper, silver and base metals were assayed by aqua regia digest followed by ICP-OES finish. Gold was determined by fire assay. Determination of total sulphur was carried out volumetrically and total carbon gravimetrically, both using Leco analysis (IR spectrophotometry). Analtyical methods are detailed in Table 3, Appendix V.

6.1.3 Representation

Geochemical plots of major and trace elements are shown in Appendix V as Charts 1 and 2. Also included in Appendix V as Table 2 are whole rock and multi element data for each sample. The plots have been arranged in approximate stratigraphic order from footwall in the west (left hand side of plots) through to the hangingwall in the east (right hand side of the plots). It should be noted that the sequence is overturned and hence the stratigraphic hangingwall acts locally as the structural (or mining) footwall.

Plots have been drawn along two "composite" lines that represent a transect across stratigraphy. One line encompasses sections 7950N to 8070N and results are shown in Chart 1, Appendix V. The other line encompasses sections 7770N to 7830N, with results shown as Chart 2, Appendix V. Projection has been both along strike and dip. The orebody has been intercepted in drill hole WL0421 (see also Appendix III) and this can be seen on the plots representing sections 7950N to 8070N. The plots representing sections 7770N to 7830N do not intersect an economic orebody although copper mineralisation was intersected in drill hole WL0106 (see also Appendix III). This line represents the mineralised halo surrounding the orebody (that has subsequently been mined) and does not transect the stratigraphy as comprehensively as line 7950N-8070N.

6.2 DISCUSSION AND INTERPRETATION OF RESULTS

6.2.1 Metals

Generally gold and silver correlate well with copper, the gold responses peaking almost exactly with copper. Silver responses tend to be a bit more erratic particularly in the stratigraphic footwall. Molybdenum, cobalt and, to a lesser extent nickel, show a similarly good correlation with copper. The nickel correlation contrasts with the surface rock chip results. Molybdenum tends to mimic copper very closely while cobalt has a more erratic relationship through the stratigraphic hangingwall. Base metals show a relatively weakened response through the orebody halo and generally across the complete stratigraphic sequence a variable response that does not enable obvious identification of any potential ore vectors/discriminants.

Table 6.1 lists copper correlation factors. In addition to the metals decribed above the high correlation with P_2O_5 is anomalous and is probably a reflection of apatite mineralisation that has been recorded in the deposit and which is known to occur in the Prince Lyell deposit (Hendry, 1982; Raymond, 1992).

Table 6.1 Copper Correlation Factors

Metals	**Au**	**Ag**	**Mo**	**Co**	**Ni**	**Ba**	**Bi**
Cu:	0.92	0.77	0.74	0.83	0.38	0.49	0.70
Metals	**S**	**Nb**	**La**	**Ce**	**Nd**	**Pb**	**Zn**
Cu:	0.22	0.71	0.57	0.55	0.49	-0.10	0.10
Majors	**Al_2O_3**	**Fe_2O_3**	**SiO_2**	**K_2O**	**Na_2O**	**CaO**	**TiO_2**
Cu:	-0.17	0.45	-0.31	0.07	-0.21	-0.22	0.02
Majors	**MgO**	**MnO**	**P_2O_5**				
Cu:	0.00	0.18	0.67				
Elements	**Cs**	**Rb**	**Sr**	**Ga**	**Sb**	**As**	**Hf**
Cu:	-0.32	-0.04	-0.15	0.27	-0.11	0.04	-0.11
Elements	**Y**	**Zr**	**V**	**W**	**Cr**	**Th**	**U**
Cu:	-0.30	-0.12	0.27	0.22	-0.06	0.21	0.16

Apart from Fe_2O_3 and P_2O_5 copper correlation with the other majors is low to negative. The poor correlation with the immobile elements is possibly a reflection on alteration processes and contrasts with the high correlation shown with niobium. Similarly the high correlation with bismuth is anomalous. The good correlation of copper with niobium and the REE is probably due to these elements being present in apatite and is discussed further under section 6.2.9.

Zinc and lead show a reasonable correlation. The zinc ratio (Huston and Large, 1987) (Figure 6.1) returns an average that is a characteristic of MRV VHMS deposits and is in fact not dissimilar to the average for the Prince Lyell deposit (67.1 - Raymond, 1992). Interestingly there is a notable proportion of values that fall within the lower end of the scale (i.e. 30-40) and these may represent higher temperatures with corresponding increases in lead and zinc solubilities (Huston and Large, *op. cit.*)

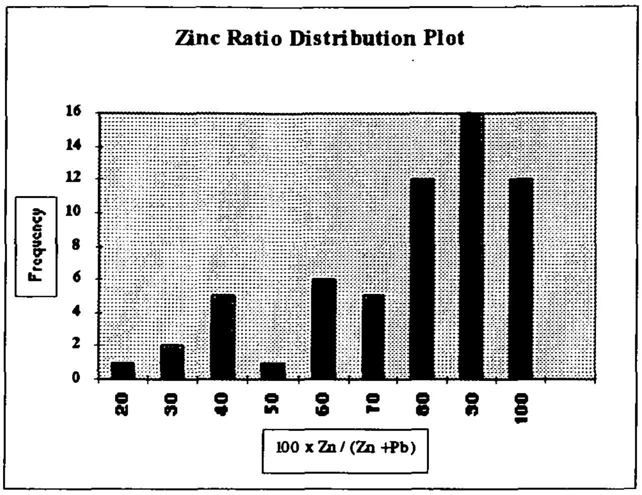

Figure 6.1
Zinc ratio distribution plot.
Count = 60
Average = 72.3
SD = 21.0

6.2.2 Sulphur and Carbon

Sulphide and carbonate show an almost inverse relationship. Sulphide has been determined from total sulphur and assumes all sulphur occurs as either chalcopyrite or pyrite. Trace amounts of other sulphides (e.g. bornite, galena, sphalerite etc.) occur but have been ignored for determination of pyrite content. Similarly all carbon is assumed to be carbonate in origin (usually siderite, sometimes ankerite (i.e. Fe-rich carbonate) and/or dolomite (which may or may not be Mn-rich) and more commonly as calcite) and thus CO_2 and hence carbonate content has been determined from total carbon analyses. A plot of CO_2 against CaO (Figure 6.2) indicates that most of the carbonate occurs as calcite with a broad trend towards siderite. This would need to be confirmed by XRD and/or probe analysis.

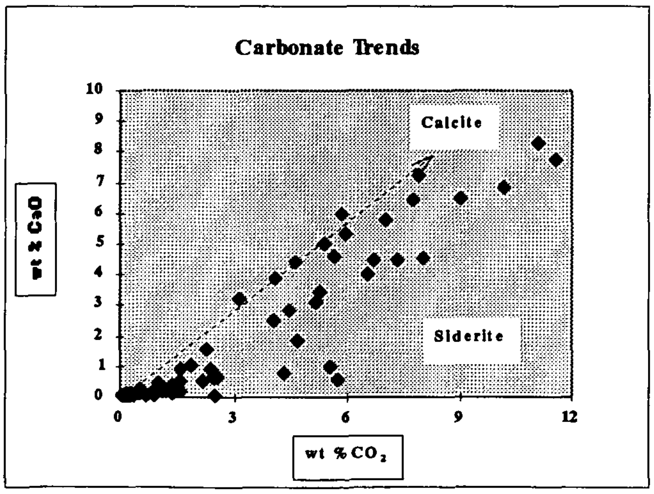

Figure 6.2
Carbonate form through the Royal Tharsis deposit based on ICP analyses. Dashed line represents approximate calcite position.

Further examination of siderite distribution shows that as much FeO occurs in chlorite and/or magnetite as in carbonate (Figure 6.3).

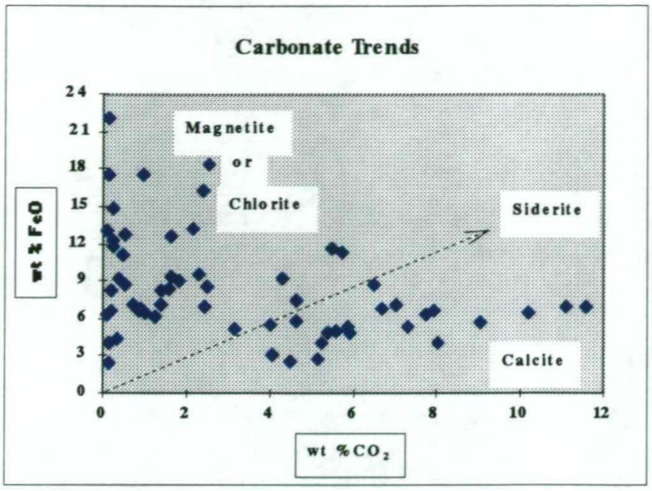

Figure 6.3
$FeO-CO_2$ distribution in the Royal Tharsis deposit. The dashed line represents approximate position of siderite. Calcite as the main form of carbonate would result in minimal CO_2 being available for siderite formation.

The inverse sulphide - carbonate relationship is clearly demonstrated along 7950N-8070N (Figure 6.4) where low pyrite (< 2% by weight) in the stratigraphic footwall increases dramatically through the copper halo (> 15% by weight) and then drops off erratically into the footwall (between 5% and 10% by weight). A similar pattern can be identified along line 7770N-7830N (Figure 6.5) although the profile displays isolated anomalies well into the stratigraphic footwall (up to 30% by weight as massive pyrite) and through which ubiquitous pyrite mineralisation has been recorded (drill hole log WL0106).

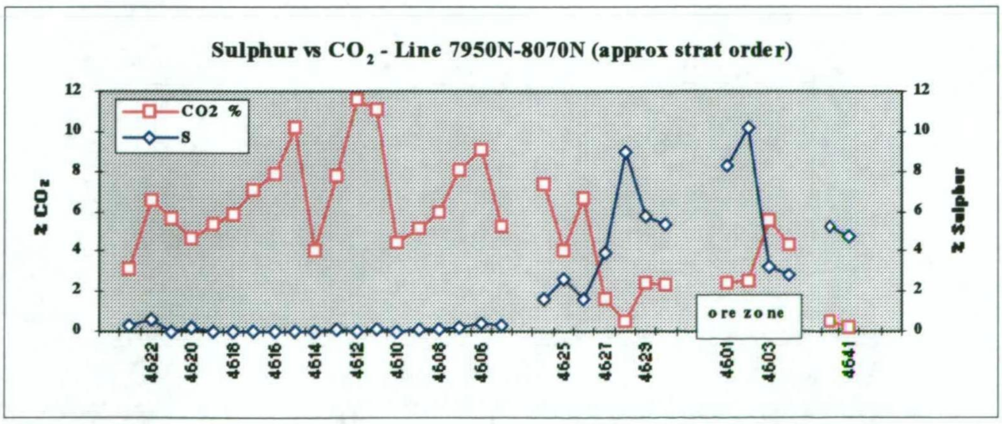

Figure 6.4 Sulphur-CO_2 profile along line 7950N-8070N (drill holes WL0530A, WL0531, WL0421 and WL0290) as a representation of carbonate-pyrite distribution, and which shows reversal through the ore zone.

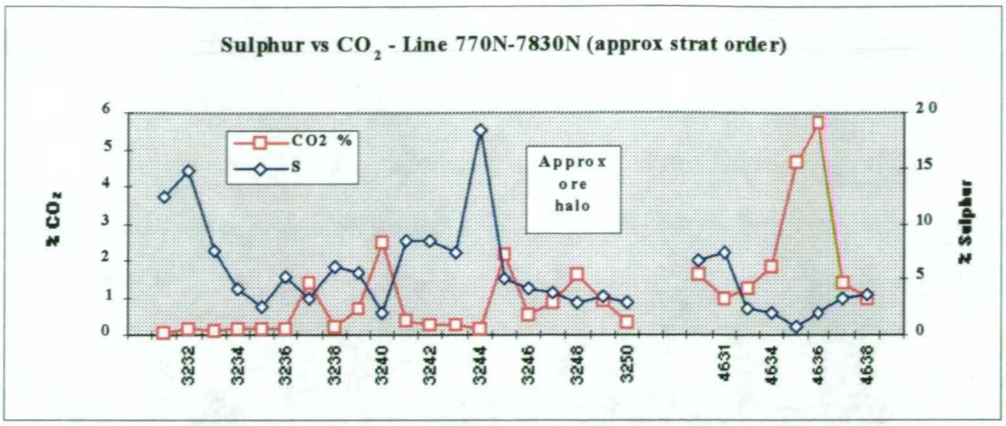

Figure 6.5 Sulphur-CO_2 profile along line 7770N-7830N (drill holes WL0106 and WL0480) as representation of carbonate and pyrite distribution.

The carbonate profile tends to show a sharp relative drop in the immediate stratigraphic hangingwall of the orebody and this gradient change could be a potential (but coarse) ore vector. Elevated carbonate values (up to 15% by weight $FeCO_3$) through the orebody agrees with observations made during logging (drill hole WL0421). In the stratigraphic footwall the carbonate profile is generally smooth with localised variations that can be correlated with carbonate recorded in drill hole logs (drill hole WL0530A).

6.2.3 Trace Elements

Element mobilities and alteration trends are demonstrated by zirconium plots. The plot against Al_2O_3 (Figure 6.6) shows a relatively steady slope whilst the plot against titanium indicates precursors to be mainly rhyolitic and dacitic (Figure 6.7) (Barret and MacLean, 1994b).

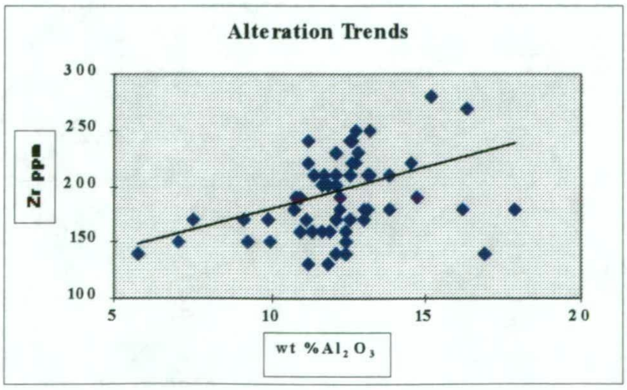

Figure 6.6
Zr - Al_2O_3 scatter plot showing relative consistency of immobile elements. Straight line represents linear trend.

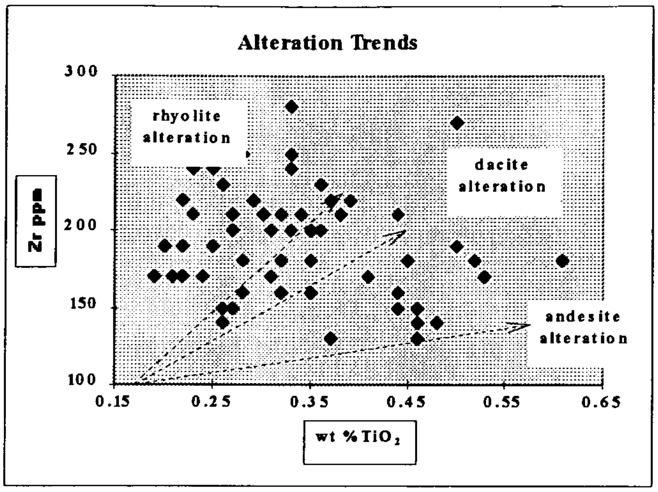

Figure 6.7
Zr - TiO_2 scatter plot showing alteration trends and volcanic precursors.

The Ti/Zr value (Figures 6.8 and 6.9) generally falls within the rhyolite - dacite zone (i.e. a Ti/Zr ratio of between 4 and 20) (Large *et. al.*, 1989) with occasional andesitic values occurring well into the stratigraphic hangingwall. Along line 7770N-7830N the Ti/Zr ratio from drill hole WL0106 is confined to the rhyolitic range. Along line 7950N-8070N the ratio extends over a significantly broader range as would be expected.

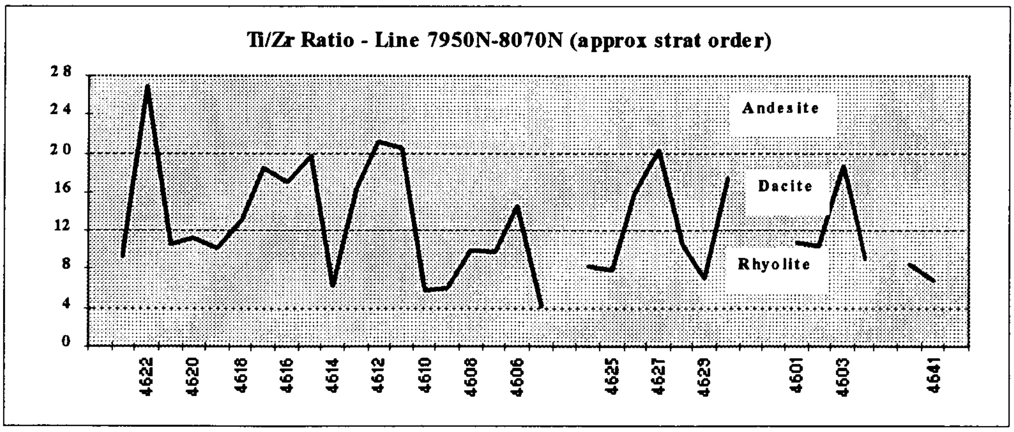

Figure 6.8 Ti/Zr ratio along line 7950N-8070N (drill holes WL0530A, WL0531, WL0421 and WL0290). (Classification of rock types after Large *et. al.*, 1989)

Andesites returned by T/Zr values are not readily identifiable in hand specimen or thin section. This is mainly due to intense alteration that overprints and obscures primary textures, and strong deformation with accompanying foliation.

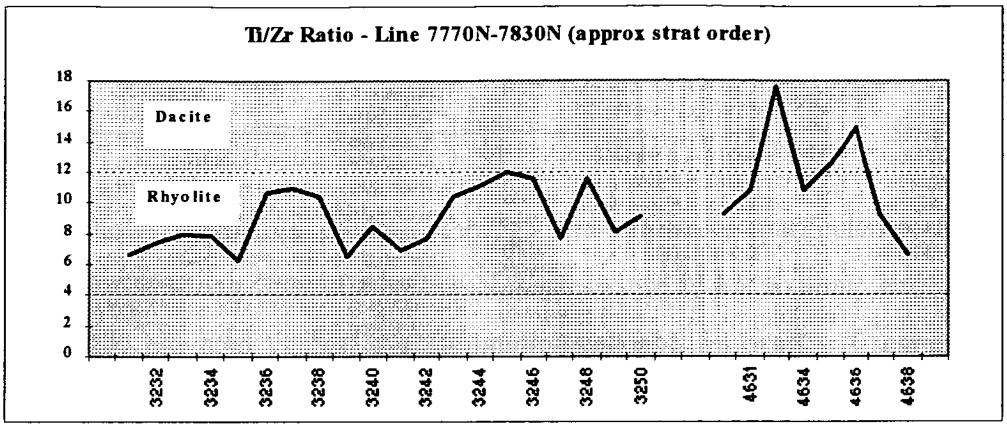

Figure 6.9 Ti/Zr ratio along line 7770N-7830N (drill holes WL0106 and WL0480). (Classification of rock types after Large *et. al.*, 1989)

Of other immobile element ratios the Y/Zr ratio is not diagnostic showing variable trends along both lines. However along line 7950N-8070N a weak distinction between a uniform footwall and a variable hangingwall ratio is indicated by a drop in the Y/Zr ratio through the ore zone. This is similarly shown in line 7770N-8030N, albeit weakly, and may in fact be a weak and subtle vector of mineralisation.

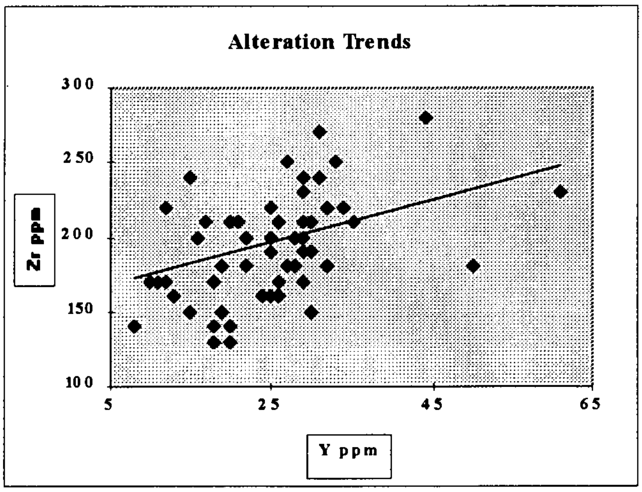

Figure 6.10
Scatter plot of Zr against Y through the Royal Tharsis deposit. Straight line represents linear trend.

Niobium shows a notable increase through the ore zone, particularly along line 7950N-8070N. Along line 7770N-7830N the response is not so sharp and is further obfuscated by elevated values in both hangingwall and footwall. A scatter plot of niobium and zirconium does not show any relationship between the two elements while the Nb/Zr ratio profile mimics that of niobium showing anomalous responses through the mineralised zones.

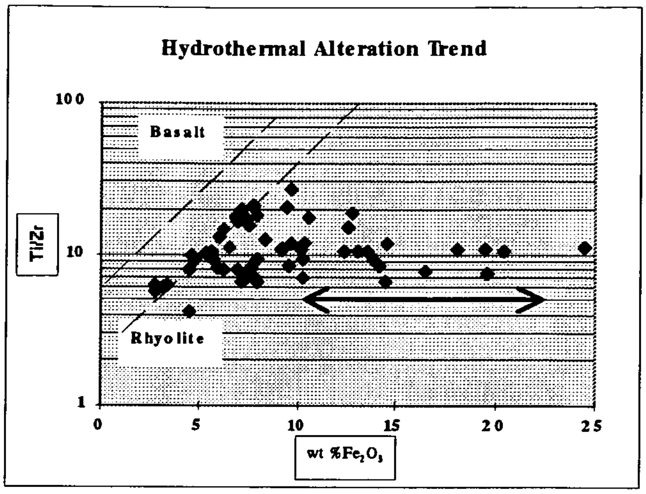

Figure 6.11
Hydrothermal alteration trend (bold arrow) at the Royal Tharsis showing enrichment in Fe_2O_3 at constant Ti/Zr and contrasting with magmatic differentiation trend (dashed lines) of rhyolite-dacite-andesite-basalt in the MRV (after Large *et. al*, 1989).

General conclusions concerning the immobile elements need to be treated with caution. In a system of such intense alteration that is evidenced at Royal Tharsis the potential for these element showing some mobility should not be ruled out. However Large *et. al.*, (1989) have demonstrated the resistance of the Ti/Zr ratio to hydrothermal alteration within the broader MRV, notably determining magmatic differentiation trends for rhyolite-dacite from the Rosebery deposit. Figure 6.11 contrasts broad MRV magmatic differentiation trends against potential hydrothermal alteration trend of Royal Tharsis showing Fe_2O_3 enrichment at constant Ti/Zr ratio.

Of the transition elements analysed (i.e. vanadium, chromium and tungsten) chromium shows a relative depletion in the stratigraphic hangingwall. The opposite is the case with tungsten which exhibits enrichment in the stratigraphic hangingwall. The apparent change in tungsten would serve as a more reliable ore vector than chromium which tends to exhibit a more erratic profile, particularly through the footwall.

6.2.4 Major Elements

K_2O does not show any obvious trend that has immediate implications vis-a-vis sericite alteration with respect to the orebody position. This is broadly confirmed by the geology. However subtle indicators point to an indirect relationship. On both sample lines there is a weak positive gradient into the stratigraphic hangingwall. In the stratigraphic footwall the profile shows an overall drop away from the ore halo. This could be used as a diagnostic feature to distinguish the relative position of mineralisation i.e. a potential but subtle ore vector.

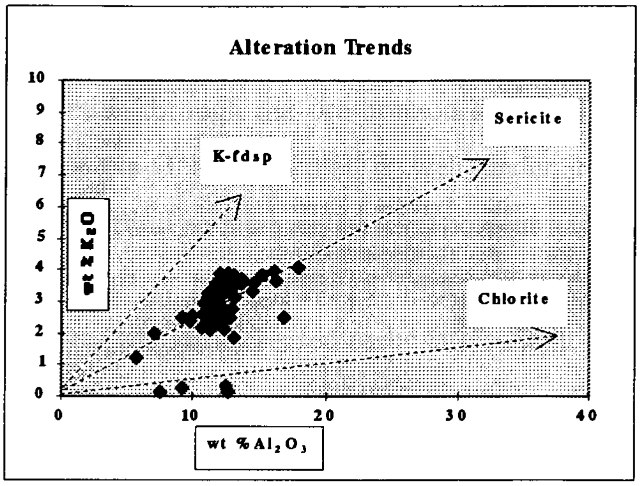

Figure 6.12
Plot of wt % K_2O vs wt % Al_2O_3 showing alteration trends through the Royal Tharsis deposit

The dominant sericite alteration is confirmed by a significant increase in K_2O content through the distal parts of the mineralisation halo (drill hole WL0106). A plot of K_2O against Al_2O_3 (Figure 6.12) shows a dominant alteration trend to be sericitic, with minor chlorite alteration and minimal K-feldspar alteration.

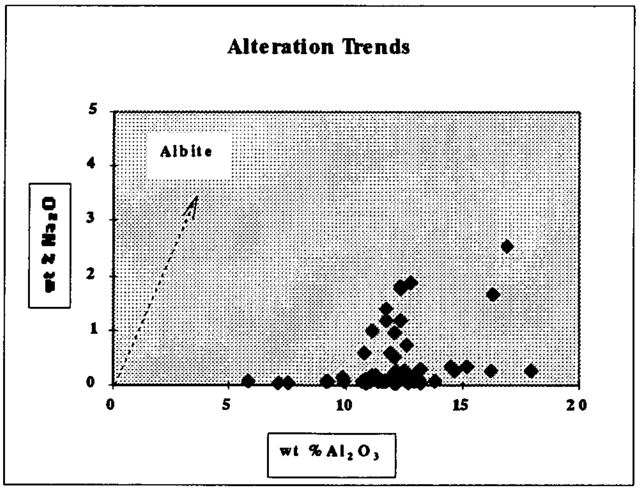

Figure 6.13
Plot of wt % Na_2O vs wt % Al_2O_3 showing alteration trends and relative Na depletion through the Royal Tharsis deposit.

Sodium depletion through the ore horizon and into the stratigraphic hangingwall is reflected in a Na_2O content that is well under 1 wt % (Figure 6.13). In the stratigraphic footwall an increase in Na_2O content has no obvious relationship to either alteration patterns or to the position of ore mineralisation, although the increase in Na_2O correlates with an increased carbonate content and by occasional occurrences of albite. The increase in Na_2O reaches a maximum of just under 3% by weight, which alone is not high. Albite identified toward the periphery of the deposit in the stratigraphic hangingwall (drill hole WL0290) is not confirmed by the low Na_2O content.

CaO content tends to be uniform through the ore halo showing a relatively weak decrease into the stratigraphic hangingwall. Into the footwall the profile fluctuates locally along line 7950N-8070N, whilst along line 7770N-7830N the profile remains flat (generally less than 0.6 wt % CaO) possibly representing the immediate edge of the ore zone.

MgO and MnO content show contrasting trends and hence interpretation is not conclusive. Along line 7770N-7830N MgO shows a gradual increase from footwall through to hangingwall. In contrast, along line 7950N-8070N the profile is significantly more erratic with no diagnostic features identifiable through the ore zone. The variable MgO content possibly reflects variations in Fe-Mg rich chlorites (Hendry, 1981; Braithwaite, 1985), although MgO depletion is indicated by a value that is less than 1 wt %. MnO shows a similar pattern to MgO, i.e. an erratic profile, but differing in that an anomalous MnO peak in the vicinity of the stratigraphic footwall of the orebody may be diagnostic. The MnO value does not exceed 1% by weight, averaging less than 0.2% by weight.

P_2O_5 content is less than 1 wt %. The relative amount increases through the ore zone halo and in which apatite has been identified (drill holes WL0421 and WL0106). This elevated P_2O_5-Cu association is in agreement with findings on the Prince Lyell orebody subsurface (Hendry, 1981; Raymond, 1992) and would tend to corroborate the influence of magmatic hydrothermal fluids (Large *et. al.*, 1996a). An alternative source of the elevated P_2O_5 is the Suite II andesites (Crawford *et. al.*, 1992) that are known to occur elsewhere in the Mount Lyell field. The P_2O_5 content is not as high as that recorded in the Prince Lyell deposit (0.8 Wt % - Raymond, *op. cit*) whilst the apatite-magnetite relationship would appear to have a more restricted distribution as can be seen in the plot of P_2O_5 against FeO (Figure 6.14).

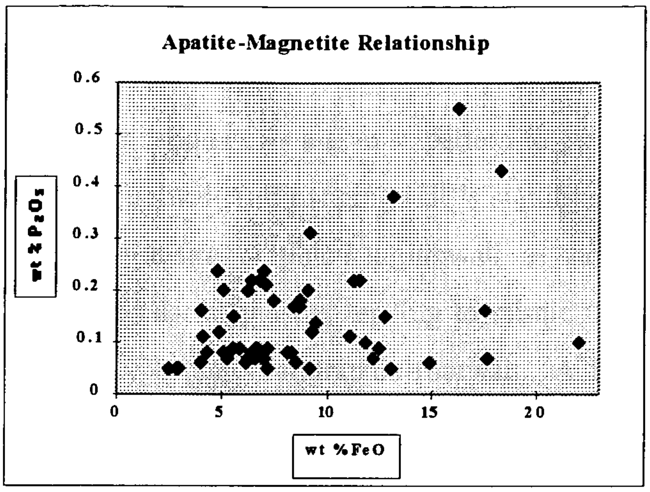

Figure 6.14
Apatite-magnetite representation through the Royal Tharsis deposit.

P_2O_5 content in either hangingwall or footwall is not sufficiently contrasting to be immediately diagnostic. Away from the influence of the mineralisation halo P_2O_5 shows a variable distribution in the stratigraphic footwall (drill holes WL0530A and WL0531) varying from a low of 0.05 wt % up to a high of approximately 0.3 wt %.

6.2.5 Barium

Barium shows enrichment in both the mineralised/sulphide halo and through the orebody. This is clearly demonstrated along line 7950N-8070N. Values in the stratigraphic hangingwall tend to be higher than those in the footwall, the relative hangingwall enrichment being associated with proximity to the Owen Group lithologies. Elsewhere haematite-barite along the contact with the Owen conglomerate is distinctive (Hart, 1993), although such alteration has not been observed in Royal Tharsis.

The Ba/Sr ratio shows a similar pattern to the barium profile. However the contrast between footwall and hangingwall is significantly more distinctive with ratios being higher in the stratigraphic hangingwall, as shown on line 7950N-8070N. The Ba/Rb ratio is not as diagnostic, tending to mimic the barium profile and showing greater irregularity in the stratigraphic footwall. A Ba/Sr value of 30 tends to identify the mineralised halo and ore zone along both sample lines and this may be a good vector to mineralisation (Figure 6.15). Both barium and rubidium substitute for potassium in sericite (Barrett and MacLean, 1994b) during hydrothermal alteration and this may account for the distinctive Ba/Sr ratio.

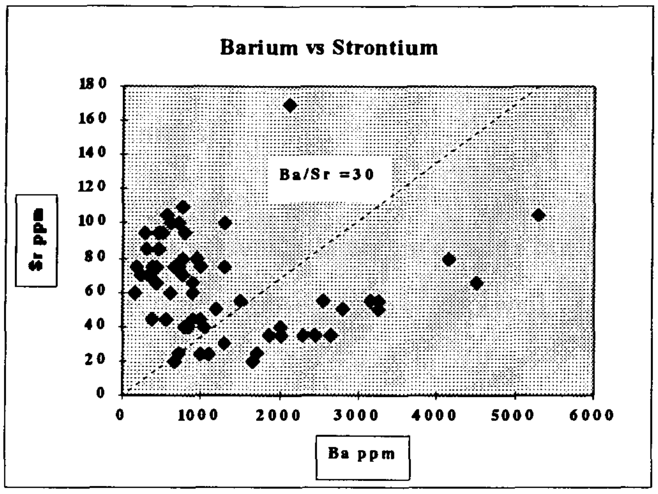

Figure 6.15
Scatter plot through Royal Tharsis of strontium against barium. A Ba/Sr ratio of 30 is a potential vector to ore mineralisation. The dashed line represents a Ba/Sr ratio of 30. Samples below this line (i.e.Ba/Sr > 30) are generally from within the orebody or mineralised halo.

6.2.6 Bismuth, Antimony and Arsenic

Bismuth portrays a distinctive increase through the mineralised zone contrasting with a "background" value that falls within a range of 0 to 10 ppm in both hangingwall and footwall (line 7950N-8070N). This elevated bismuth is a potential ore vector, and also explains the good correlation (correlation factor 0.70 - see Table 6.1) with copper. Antimony and arsenic do not show any obvious or diagnostic patterns.

6.2.7 Radiogenic Elements

Ceasium does not show any diagnostic features. Rubidium shows some relative differences between hangingwall and footwall values, although profiles tend to be variable and conflicting. Strontium values tend to be similarly variable, giving rise to a Rb/Sr ratio that is not immediately diagnostic with respect to potential ore vectors.

6.2.8 Actinides

Thorium values are variable within a range but show no distinctive differences between hangingwall - mineralised halo - footwall. However uranium shows an elevated response of up to 20 ppm that coincides with ore mineralisation. Within the stratigraphic footwall uranium values range from 0 to 6 ppm whilst in the hangingwall there would appear to be an increase in value from between 5 to 145 ppm. This gives rise to a Th/U ratio that shows a relative drop in the stratigraphic hangingwall.

6.2.9 Rare Earth Elements

Lanthanum, cerium and neodymium all show elevated responses through the mineralised halo. Along both lines a marked increase in values (by a factor of between three and four) occurs coincident with increasing copper content. In the stratigraphic footwall values tend to be fairly constant and low (50 to 100 ppm for lanthanum and cerium, and 20 to 50 ppm for neodymium). In the hangingwall results are more conflicting, showing an upward trend along line 7950N-8070N and a very slightly decreasing trend along line 7770N-7830N.

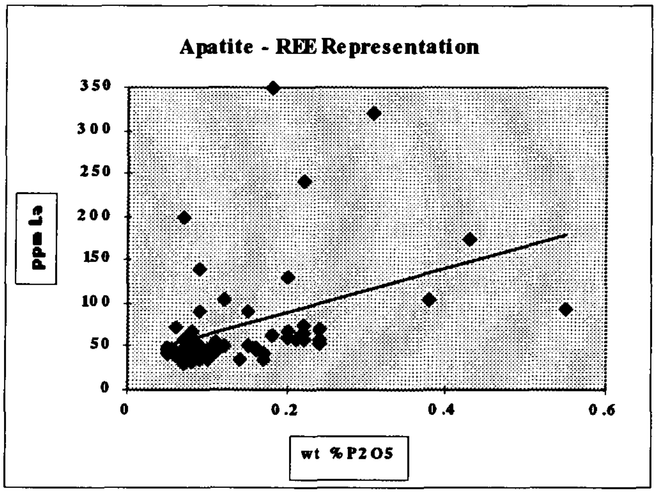

Figure 6.16
Scatter plot representing REE content in apatite. Plots for Ce and Nd show a similar distribution. Straight line is a linear trend.

The elevated responses of the these REE is probably due to the presence of apatite in the mineralised halo. The elements all show reasonable correlation with P_2O_5 (Table 6.2 and Figure 6.16).

Table 6.2	**P_2O_5 - REE Correlation Factors**		
	La	**Ce**	**Nd**
P_2O_5	0.40	0.39	0.41

6.2.10 Alteration Indices

Traditionally the Ishikawa (Ishikawa *et. al.*, 1976) alteration index (AI) has proven to be a useful indicator of VHMS mineralisation. The AI quantifies the intensity of sericite/chlorite alteration that occurs immediately adjacent to VHMS deposits. In this work two other alteration indices have been determined, each being an additional instrument that could be applied in identifiying vectors to ore. (Large *et al.*, 1996b):

- the Ishikawa alteration index
- chlorite pyrite alteration index
- manganese - carbonate alteration index

Ishikawa alteration index

The Ishikawa alteration index is based on the geochemical destruction of feldspars and their replacement by sericite and chlorite. In such hydrothermal systems alteration results in a loss of Na_2O and CaO and an enrichment in K_2O, MgO and FeO. The essential chemical changes can be represented through the following reactions:

$NaAlSi_3O_8$ (albite) → → $KAl_3Si_3O_{10}(OH)_4$ (sericite)

$CaAl_2Si_2O_8$ (anorthite) → → $KAl_3Si_3O_{10}(OH)_4$ (sericite)

$NaAlSi_3O_8$ (plagioclase) → → $(Fe,Mg)_5Si_3Al_2O_{10}(OH)_8$ (chlorite)

$CaAl_2Si_2O_8$ (anorthite) → → $(Fe,Mg)_5Si_3Al_2O_{10}(OH)_8$ (chlorite)

The Na_2O content is a key factor in determining the alteration status of a particular sample or litho type. Highly altered volcanic rocks are diagnostically defficient in Na_2O, with generally less than 0.5 wt % Na_2O, whilst unaltered rocks will have an Na_2O content that is equal to or greater than 4 wt %. In situations where complete feldspar replacement/destruction has occurred the resultant AI is in the region of 100. As a general guide, altered rocks will have an AI in the range of 50 to 100, and unaltered rocks an AI value that falls in the range of 20 to 50. In spite of being a good indicator of alteration the AI does not distinguish between chlorite and sericite alteration while the presence of carbonate alteration will result in an overall lowering of the AI value (Large *et al*, *op.cit.*). Generally a high K_2O value with a high AI is an indicator of sericite alteration, while chloritic alteration is generally associated with low K_2O.

The alteration index (Ishikawa *et.al.*, 1976) has been determined from the following formula:

$$AI = \frac{100 \times (K_2O + MgO)}{(K_2O + MgO + Na_2O + CaO)}$$

At Royal Tharsis the AI shows a notable rise in value up stratigraphy (i.e. from the stratigraphic footwall through to the hangingwall) the footwall value falling in the range 40 to 90 and the hangingwall being more constrained between 65 to 100. The AI values through the mineralised halo/zone do not appear to be uniquely diagnostic although there is a weak reversal in the overall trend. The higher values are consistent with intense hydrothermal alteration while the intermediate AI values are possibly associated with feldspar alteration that occurs towards the periphery of the system.

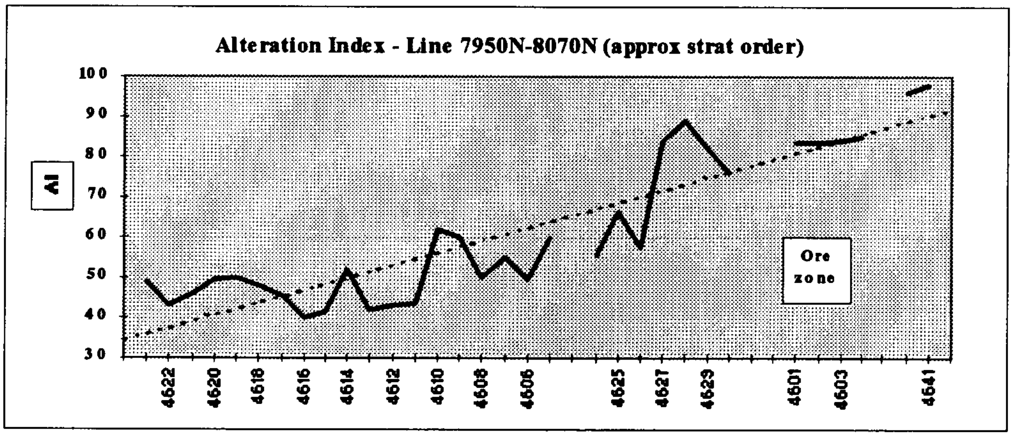

Figure 6.17 Ishikawa alteration index along line 7950N-8070N (drill holes WL0530A, WL0531, WL0421 and WL0290). Dashed line is a linear trend line.

Along line 7950N-8070N (Figure 6.17) a strong hangingwall alteration halo compares with a significantly weaker alteration index in the footwall. Along line 7770N-7830N (Figure 6.18) the contrast in the alteration index between footwall and hangingwall is less marked and this is probably due to the line being within the influence of the mineralisation halo.

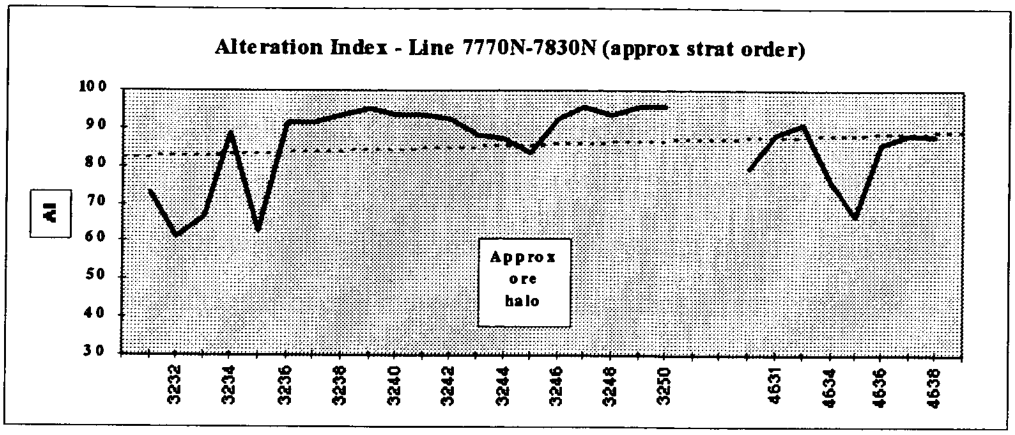

Figure 6.18 Ishikawa alteration index along line 7770N-7830N (drill holes WL0106 and WL0480). Dashed line is a linear trend line.

Chlorite alteration index

Chlorite alteration is common close to VHMS deposits and identification of zones with an elevated chlorite content is important. The chlorite index is an attempt to delineate such zones (Large *et. al.*, 1996b). Samples containing pyrite, haematite and/or magnetite will return relatively higher CI values due to their FeO content and would need to be identified and possibly filtered. The chlorite index (CI) measures the amount of chlorite - carbonate and/or pyrite alteration and has been determined from the following formula:

$$CI = \frac{100 \times (MgO + FeO)}{(MgO + FeO + Na_2O + K_2O)}$$

In the case of the Royal Tharsis deposit the CI is probably the least informative of the three indices. The overall trend through the stratigraphic sequence is a weak increase as shown along line 7950N-8070N (Figure 6.19). This contrasts with line 7770N-7830N (Figure 6.20) which shows a moderate decreasing trend. This latter can be attributed to the influence of the mineralisation halo and in fact within the actual ore zone/halo along both lines there is a sharp drop in gradient from footwall to hangingwall, a fact which may warrant further investigation. Outside the orebody the profile gradient is notably steeper particularly in the hangingwall and this may be an ore vector.

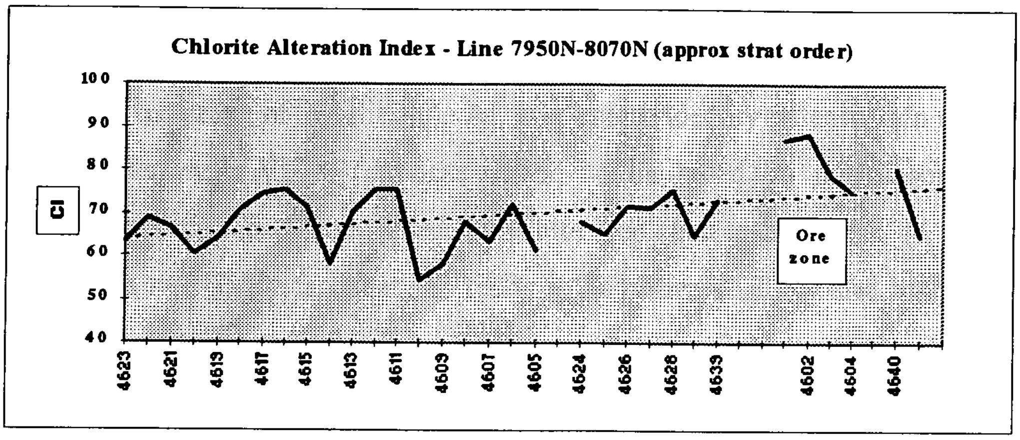

Figure 6.19 Chlorite-carbonate-pyrite alteration index along line 7950N-8070N (drill holes WL0530A, WL0531, WL0421 and WL0106). Dashed line is a linear trend line.

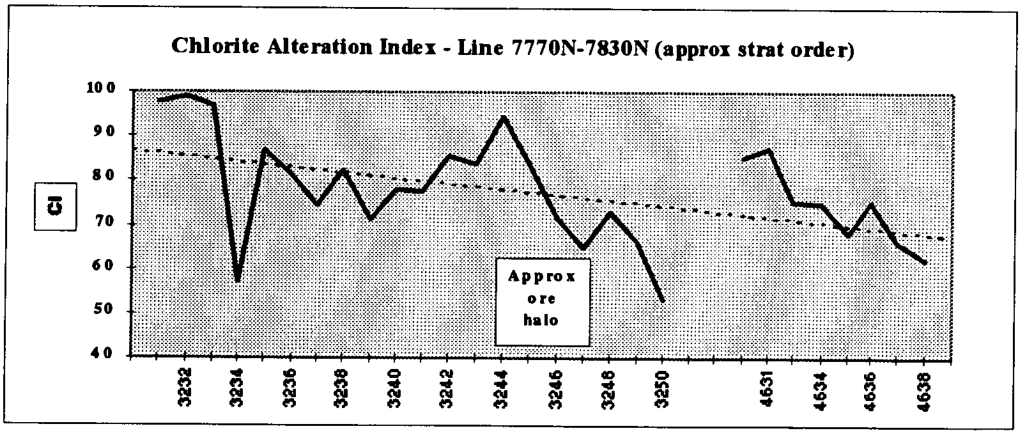

Figure 6.20 Chlorite-carbonate-pyrite alteration index along line 7770N-7830N (drill holes WL0106 and WL0480). Dashed line is a linear trend line.

Mn-carbonate alteration index

The Mn-carbonate index is an attempt to both allow for carbonate alteration which otherwise has the affect of lowering the AI, and also to identify potential Mn alteration halos associated with VHMS deposits. The MI is based on the reasoning that plagioclase alteration is accompanied by albite depletion and sericite (± chlorite) enrichment, as well as the fact that Mn tends to be preferentially hosted by carbonate minerals (such as dolomite, siderite, ankerite, calcite) (Large *et. al.*, 1996b). The manganese - carbonate index has been determined from the following formula:

$$MI = \frac{100 \times (CaO + 10MnO)}{(CaO + 10MnO + Na_2O + K_2O)}$$

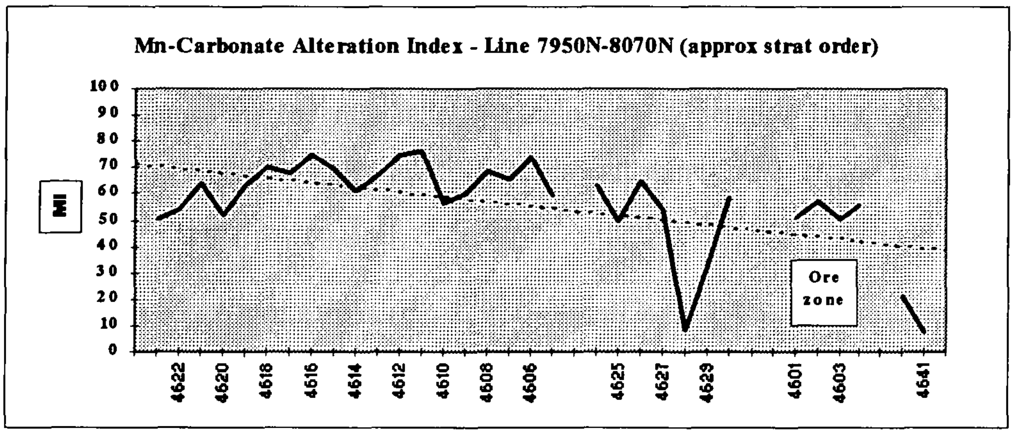

Figure 6.21 Mn-carbonate alteration index along line 7950N-8070N (drill holes WL0530A, WL0531, WL0421 and WL0106). Note trend reversal of MI through the ore zone. Dashed line is a linear trend line.

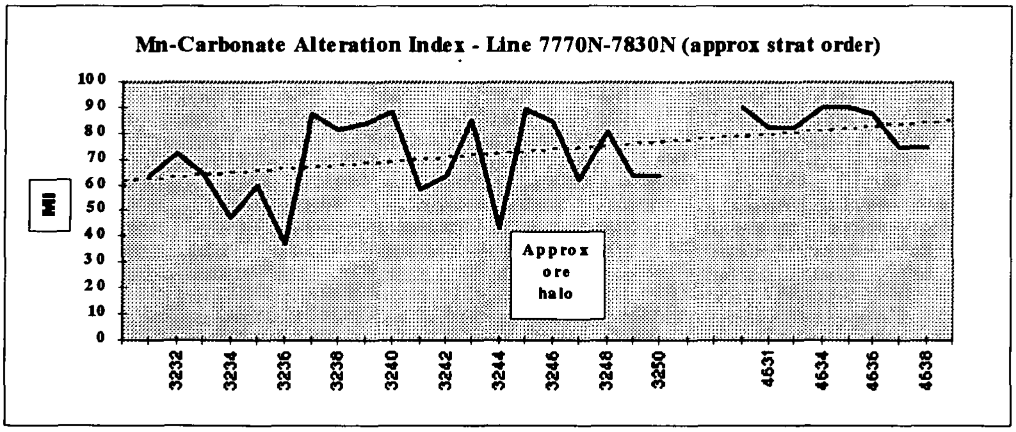

Figure 6.22 Mn-carbonate alteration index along line 7770N-7830N (drill holes WL0106 and WL0480). Note trend reversal of MI through the ore/mineralised halo. Dashed line is a linear trend line.

As with the chlorite index the MI shows contrasting tends along lines 7950N-8070N (Figure 6.21) and 7770N-7830N (Figure 6.22). Again this can be attributed the influence and nature of the mineralisation halo. The detailed trend through the orebody (WL0421, line 7950N-8070N) tends to mimic the trend through the mineralised halo (WL0106, line 7770N-7830N) and this trend reversal may be a vector to mineralisation/ore.

Another notable feature is a sharp and possibly diagnostic drop in value along the stratigraphic footwall of the copper mineralisation. This feature can be seen in the profiles of both lines. The drop is relatively high (from approximately 50 to 80 down to approximately 5 to 40) and may herald the introduction of sulphides as shown by a corresponding increase in pyrite content.

6.2.11 Results below detection limit

Several elements in the whole rock analyses returned results that were below detection limits. These are listed in Table 6.3.

Table 6.3	**Results Below Detection**	
Element	**Lower Detection Limit**	**% of results BDL**
Cd	3 ppm	100
In	0.5 ppm	87
Ta	2 ppm	100
Te	5 ppm	100
Tl	3 ppm	100

Cadmium, which is a recognised pathfinder for base metals, shows responses that tend to be similar to those for the Prince Lyell deposit (Davis *et.al.*, 1995). Tantalum is sometimes used in mobility ratios, sometimes with niobium which has shown some response through the mineralised zone, and thus the potential usefulness of tantalum should not be discounted.

Both indium and thallium fall in group 5 of the periodic table and similar responses could be expected as with other elements in the same group. Thus gallium in the same group showed conflicting differences (along both lines) between hangingwall and footwall lithologies and thus the potential usefulness of either indium or thallium at lower limits of detection would be questionable. Tellurium would not be expected to show any responses.

6.3 CONCLUSIONS

- Comparison across stratigraphy has been shown by plotting profiles along two lines composited both along strike and up/down dip. The first line, 7770N - 7830N, is representative of the mineralised halo. The second line, 7950N - 8070N, transects stratigraphy.
- Copper correlates reasonably well with gold, silver, molybdenum, cobalt and ± nickel. Fe_2O_3 and P_2O_5 both correlate with copper, indicative of pyrite and apatite relationships respectively, the latter pointing to the influence of magmatic hydrothermal fluids.
- The AI shows an increasing trend up stratigraphy and a subtle change through the ore zone. The CI (chlorite-pyrite-carbonate alteration index) shows a change in gradient through the ore zone relative to hangingwall lithologies. The MI (manganese carbonate alteration index) shows a relative drop at the stratigraphic footwall of copper mineralisation, but otherwise portrays a poorly defined response.
- The Zn ratio of 72 (Huston and Large, 1989) can be considered typical for MRV VHMS deposits. This contrasts with results from surface geochemistry.
- Sulphide (pyrite) and carbonate show an almost inverse relationship, with carbonate alteration through the mineralisation being subtle and variable. Carbonate alteration is further masked by overprinting associated with later Devonian remobilisation.
- K_2O (and hence sericite) shows a subtle response to mineralisation and thus may be a subtle vector to ore. Na_2O depletion occurs through the ore halo and into the hangingwall. A variable MgO content possibly reflects Fe-Mg rich chlorites.
- The Ti/Zr value falls within the dacite - rhyolite range, with occasional andesite values.
- Barium and Ba/Sr ratio show enrichment through the mineralised halo. The halo tends to be identified by a Ba/Sr value that rises above 30.
- Uranium shows an elevated response that coincides with the footwall of the ore mineralisation.
- Rare earths (lanthanum, cerium and neodymium) show uniform elevated responses through the mineralised halo.

CHAPTER 7
SUMMARY AND CONCLUSIONS

7.1 SURFACE GEOCHEMISTRY

- Surface orientation work has indicated that mineralisation is associated with intercalated sericite and chlorite alteration in lithologies broadly classified as Lyell schists. Sulphide mineralisation is dominantly pyritic with subordinate chalcopyrite in the ore halo. The Lyell schists have volcanic precursors in the form of dacites - rhyolites - andesites and volcaniclastics.
- Copper correlates with gold, silver and molybdenum. Copper distribution shows three populations that can be resolved into lens occurrence that is typical of the West Lyell group of deposits and which includes Royal Tharsis. The nuggety effect of gold is demonstrated by several poorly defined populations. Anomalous outcrop values (Greenwood, 1996) for pathfinder elements are; Cu 450 ppm, Au 0.08 ppm, Ag 2.5 ppm and Mo 70 ppm.
- Anomalous silver responses are frequently not related directly to other element(s) and this may be due to silver occurring in the form of tetrahedrite. The fact that within the orebody silver usually shows some correlation with copper would indicate that silver alone can be considered as a vector to mineralisation. Historically the Iron Blow returned high silver values and thus anomalous silver should be considered as both a vector on its own as well as for copper.
- Of other potential pathfinder elements manganese correlates with zinc, nickel and ± cobalt; arsenic correlates with zinc and lead; and barium correlates with molybdenum. Some of these elements (e.g. zinc and manganese) show a distribution that can be resolved into several populations. These patterns are possibly associated with mobility during metamorphic and tectonic events and hence metal introduction during different mineralising pulses or phases.
- The zinc ratio (Huston and Large, 1989) of 48 returned from the orientation work places the orebody well outside the range typical of MRV VHMS deposits. Minimal sphalerite and galena were recorded in surface exposures. As zinc is

typically scavenged by Mn/Fe oxides the high zinc to managanese ratio suggests that much of the zinc is remobilised in surface environments. The zinc ratio is thus probably not a true indicator of the depositional environment in this context.

7.2 ALTERATION GEOLOGY AND GEOCHEMISTRY

- As with surface geochemistry, sulphide mineralisation is dominantly pyrite. Copper mineralisation occurs chiefly as chalcopyrite and is subordinate to pyrite. At least one generation of pyrite has been identified. Other sulphides of economic interest and which occur in trace amounts include bornite, chalcocite-digenite, covellite, molybdenite, sphalerite and galena.
- Broad correlation exists between sulphide mineralisation and alteration patterns. Sulphide distribution is typified by a central copper - gold bearing core that falls away in grade towards the periphery of the deposit commensurate with decreasing intensity of alteration. Alteration has been both intense and selective. Intensity is evidenced by almost ubiquitous feldspar destruction and accompanying obliteration of primary volcanic textures. Rare albitised plagioclase occurs towards the periphery of the alteration system.
- Some ten main alteration assemblages have been identified although their distribution has not been established. As vectors to ore mineralisation the most common alteration assemblages include: quartz-sericite; quartz-chlorite-sericite and/or quartz-chlorite-sericite; and chlorite or quartz-chlorite assemblages. Those assemblages in which chlorite is dominant are frequently barren or carry low grade sulphide mineralisation.
- Weak zonation is evident between Fe-S-C-±O, although quantification has not been proven. Carbonate alteration tends to be distal and there would appear to be an almost inverse carbonate - sulphide relationship as demonstrated through alteration geochemistry.
- Volcanic precursors included rhyolitic and dacitic (i.e. felsic) volcanics, volcaniclastics (locally autobrecciated), lavas and volcaniclastics and minor porphyries. The Ti/Zr value falls within the dacite - rhyolite range, with occasional andesite values.

- S1 foliation wraps around lensoidal domains of granular and mosaic quartz. S2 penetrative foliation is a result of later strain slip folding. Carbonate veins terminate against late S2 microfractures.
- Across stratigraphy copper correlates reasonably well with gold, silver, molybdenum, cobalt and ± nickel. Fe_2O_3 and P_2O_5 both correlate with copper, indicative of pyrite and apatite relationships respectively, the latter pointing to the influence of magmatic hydrothermal fluids. Alteration fluids of slightly acidic pH 5-6 and temperatures in the region of 200°C to 250°C are indicated, with fluid being weakly enriched in boron and halogens, and a fairly distant heat source. Temperature ranges are further confirmed by the abundance of illite as evidenced in thin sections (Barron, 1997) and the fine grained form of sericite (Thompson and Thompson, 1996).
- The AI (Ishikawa alteration index) shows an increasing trend up stratigraphy and a subtle change through the ore zone. The relative difference in values between footwall and hangingwall is thus a potential vector to ore. The CI (chlorite pyrite alteration index) shows a change in gradient through the ore zone relative to hangingwall lithologies. As an ore vector this is a subtle change that would need to be considered in with other evidence for ore mineralisation. The MI (manganese carbonate alteration index) shows a relative drop at the stratigraphic footwall of copper mineralisation, but otherwise the response is not diagnostic as a vector to ore..
- The zinc ratio (Huston and Large, 1989) of 72 can be considered typical for MRV VHMS deposits. This contrasts markedly with results from surface geochemistry. The latter covered a less constrained sampling spectrum whilst the former was more closely confined to the orebody environs.
- K_2O shows a subtle response with mineralisation and thus may be a subtle vector to ore. However as a stand alone factor the content is not an obvious ore vector. The response is seen as a gradual increase through the footwall as the orebody is approached followed by a sharp (and positive) change in gradient that smooths out into the hangingwall. Na_2O depletion occurs through the ore halo and into the hangingwall where the content remains well below 1 wt %. Distally into the footwall Na_2O this rises to a maximum of just under 4 wt %. A variable MgO

content possibly reflects Fe-Mg rich chlorites. A high Al and high K_2O content are indicative of strong sericite alteration, with low K_2O content being indicative of chlorite alteration.

- Barium and Ba/Sr ratio show enrichment through the mineralised halo with the hangingwall showing higher values than the footwall.
- Of the trace elements uranium shows an elevated response that coincides with the footwall of the ore mineralisation and the rare earths (lanthanum, cerium and neodymium) show uniform elevated responses through the mineralised halo.

REFERENCES

ADAMS, C.J., BLACK, L.P., CORBETT, K.D., and GREEN, G.R., 1985, Reconnaissance isotopic studies bearing on the tectonothermal history of Early Paleozoic and Late Proterozoic sequences in western Tasmania. *Aust. Jnl. of Earth Sci.,* 32: pp 7-36

ALEXANDER, 1953, Geology of the Mount Lyell field. In: Geology of Australian ore deposits, *5th Empire Min and Metal. Congress,* vol 1, pp 1129-1144

ARNOLD, G.O., 1985, Mount Lyell 1985: an exploration perspective. *Unpubl. Report*, Gold Fields Exploration Pty. Ltd., Queenstown, Tasmania

ARNOLD, G.O., and CARSWELL, J.T., 1990, The Mount Lyell deposits. In: Hughes, F. (ed), Economic Geology of Australia and Papua New Guinea., *Aust Inst. Of Min and Metall.*, Melbourne

ARNOLD, G.O., and FITZGERALD, F.C., 1986, Mount Lyell: an exploration perspective. In: Large, R.R. (ed), *The Mount Read Volcanics and Associated Ore Deposits*. Geol Soc Aust., Tasm. Div., Hobart, pp 21-23

BAILLIE and SUTHERLAND, 1992, Devonian lamprophyres from Mount Lyell, Western Tasmania. *Pap. & Proc. Royal Soc. Of Tasmania*, 126, pp 19-22

BARRETT, T.J., and MacLEAN, W.H., 1994a, Mass changes in hydrothermal alteration zones associted with VMS deposits of the Noranda area. *Can. Inst. Min. Metall. and Petroleum*, Explor. Min. Geol. vol 3, no 2 pp 131-130

BARRETT, T.J., and MacLEAN, W.H., 1994b, Chemostratigraphy and hydrothermal alteration in exploration for VHMS deposits in greenstones and younger volcanic rocks. *In* Lentz, D.R., ed., Alteration and alteration processes associated with ore-forming systems. *Geological Society of Canada*, short course notes 11: pp 433-467

BARRON, B.J., 1995, Petrological and Mineragraphic examination of forty six drill core samples from the Western Tharsis orebody and surrounding areas at Mt Lyell. *Unpubl. Report*, Copper Mines of Tasmania Pty. Ltd., Queenstown, Tasmania

BARRON, B.J. 1997, Petrological and mineragraphic examination of thirty drill core samples from Royal Tharsis deposit, Mount Lyell mineral field, Tasmania. *Unpubl. Report*, Copper Mines of Tasmania Pty. Ltd., Queenstown, Tasmania

BARTON, P.B., jnr, 1970, Sulphide petrology. *Min. Soc. Amer. Spec. Pap., 3*, pp 187-198

BATCHELOR, W.T., 1901, Report on the Royal Tharsis property. *Unpubl. Report*, Mount Lyell Mining and Railway Co. Ltd., Queenstown, Tasmania

BERRY, R.F., 1989a, The history of movement on the Henty fault zone, western Tasmania: an analysis of fault striations. *Aust. Jnl. of Earth Sci.,* 36: pp 189-206

BERRY, R.F., 1989b, Microstructural evidence for a westward transport direction during Middle Cambrian obduction in Tasmania. *Geol. Soc. of Aust., abstracts* 24, pp 8-9

BERRY, R.F., 1990, Structure of the Queenstown area and its relation to mineralisation. In: Structure and mineralisation of western Tasmania. *Unpubl. AMIRA project P291*, *Report 1,* pp 17-26

BERRY, R.F., 1991, An excursion guide for the Mount Lyell Mining Lease with emphasis on the Great Lyell fault, Haulage unconformity and North Lyell alteration. *Unpublished AMIRA project P291, Report* 2, pp 1-22

BERRY, R.F., 1991,Mt Lyell Mine Leases. In: Structure and mineralisation of western Tasmania. *Unpubl. AMIRA project P291*, *Report 3,* pp 31-39

BERRY, R.F., 1992, Mt Lyell Mine Leases: Summary. In: Structure and mineralisation of western Tasmania. *Unpubl. AMIRA project P291*, *Report 4,* pp 67-75

BERRY, R.F., 1994, Tectonics of western Tasmania: late Precambrian-Devonian, *Geol. Soc. of Aust., abstracts 35*, pp 5-7

BERRY,R.F., and ARNOLD, G.A., 1990, *Unpubl.* Correspondence on faulting along the Great Lyell fault, Mount Lyell. R.G.C. Exploration Ltd.

BERRY, R.F., and CRAWFRORD, A.J, 1988, The tectonic significance of Cambrain allochthonous mafic-ultramafic complexes in Tasmania. *Aust. Jrnl. of earth Sciences*, v, 35, pp 523-533

BERRY, R.F., and KEELE, R.A., 1993 Cambrian structures in western Tasmania. *Unpubl. AMIRA project report,* P291 (in CODES course work manual 6 (fourth edition), Tectonics Structure and Ore Deposits, part 3, 1996)

BERRY, R.F., and KITTO, P.A., 1996, Structural studies in mineralised areas. *CODES course work manual 6 (fourth edition*), Tectonics Structure and Ore Deposits, part 3

BIRD, M., 1982, An assessment of the economic geology of Mt Lyell. *Unpubl. Report*, Mount Lyell Mining and Railway Co. Ltd., Queenstown, Tasmania

BIRD, M., 1984, A progress report on the economic potential of Mt Lyell. *Unpubl. Report*, Mount Lyell Mining and Railway Co. Ltd., Queenstown, Tasmania

BISHOP, J.R., 1983, Geophysics of the Mount Lyell mining field. *Proc. 3rd biennial conf.,* Brisbane 1983, pp 107-109

BLAINEY, G., 1954, The peaks of Lyell (1993 edition), ISBN 0 7246 2265 9 , 361p

BOTTRILL, R.S., 1992, The mineralogy of gold in the Mount Lyell orebodies. *Tasmanian Dept. Of Mines*, report 1992/28

BRADLEY, J., 1956, The Geology of the West Coast Range of Tasmania, Part II - Structure and ore deposits. *Pap. Proc. R. Soc. Tasm.*, 90, pp 65-130

BRAITHWAITE, R.L., 1974, The geology and origin of the Rosebery ore deposit, Tasmania. *Econ. Geol.*, v 69, no 7, pp 1086-1101

BRAITHWAITE, C.J., 1985, Chlorite geochemistry and its relationship to aspects of lithology and mineralisation in the south-eastern margin of the Prince Lyell copper deposit, Tasmania. *Unpubl. B.Sc. (Hons.) thesis*, University of Sydney

BROOK, W.A., 1984a, Mineralisation at Mount Lyell and exploration of the buffer zone, mine lease and EL 9/66. *Unpubl. Report*, Gold Fields Exploration Pty. Ltd., Queenstown, Tasmania

BROOK, W.A., 1984b, Exploration for gold deposits at Mount Lyell within the mine lease and buffer zone: regional and general aspects. *Unpubl. Report*, Gold Fields Exploration Pty. Ltd., Queenstown, Tasmania

BROPHY, P.,1977, Geology and mineralisation of the Great Lyell area, Tasmania and problems in the application of various exploration techniques. *Unpubl. M.Sc. thesis*. James Cook University

BRYANT, C.J., 1975, The geology and mineralisation of the corridor area, Mount Lyell, Tasmania. *Unpubl. BSc (Hons) thesis*, University of Tasmania

BURGDORF, P.G., 1970, Royal Tharsis resource file, *Unpubl. Report*, Mount Lyell Mining and Railway Co. Ltd., Queenstown, Tasmania

BURRETT, C.F., and MARTIN, E.L., (eds.), 1989, Geology and mineral resources of Tasmania. *Geol. Soc. of Aust., spec pub.,* ISBN 0 909869 69 3, 15: 574 p

CAMPANA, B, and KING, D., 1963, Palaeozoic tectonism, sedimentation and mineralisation in western Tasmania. *Geol. Soc. of Aust.,* 10: 1-54

CAREY, S.W., 1953, Geological, structure of Tasmania in relation to mineralisation. *5th Emp. Min, Metall. Congr.*, 1, pp 1108-1128

CARR, G.R., and DEAN, J.A., 1992, Lead Isotope study of galena samples from Prince Lyell and North Lyell, western Tasmania. *Unpubl. report by CSIRO Div of Expl. Geoscience* for RGC Exploration Pty. Ltd.

CAS, R.A.F., and WRIGHT, J.V., 1987, *Volcanic successions: Modern and ancient.* Allen and Unwin, London, 528p

CAS, R.A.F. 1992, Submarine volcanism: eruption styles, products and relevance to understanding the host-rock successions to volcanic-hosted massive sulphide deposits. *Econ. Geol.*, v 87, no 3, pp 511-541

COLHOUN, A., 1989a, Cainozoic geomorphology. In Burrett, C.F. and Martin, E.L., (eds), Geology and mineral resources of Tasmania, *Geol. Soc. Of Aust., special publ.*, no 15, pp 403-409

COLHOUN, E.A., 1989b, Quaternary. In Burrett, C.F. and Martin, E.L., (eds), Geology and mineral resources of Tasmania, *Geol. Soc. Of Aust., special publ.*, no 15, pp 410-418

CONNOLLY, H.J.C., 1947, Geology in exploration: Mount Lyell example. *Proc. Aust. Inst. Min. Metall.*, 147, pp 1-122

CONNOLLY, H.J.C., 1949, Mount Lyell exploration. *Unpubl. report.* Mount Lyell Mining and Railway Co. Ltd.

COOKE, D.R., and KITTO, P.A., 1994, Contentious issues in Tasmanian geology. *Geol. Soc. Aust. Abstract series No 3. A symposium, Hobart, 3 - 4 November 1994.* 136 p

CORBETT, K.D., 1979, Stratigraphy, correlation and evolution of the Mount Read Volcanics in the Queenstown-Jukes-Darwin and Mount Sedgewick areas: *Tas. Geol. Surv. Bull.* 58, 75p

CORBETT, K.D., 1981, Stratigraphy and mineralisation in the Mount Read Volcanics, western Tasmania. *Econ. Geol.* v 76, no 2, pp 209-230

CORBETT, K.D., 1986, Geological setting of mineralisation in the Mount Read Volcanics. In: Large, R.R. (ed), The Mount Read Volcanics and associated ore deposits. *Geol. Soc. Of Aust., Tasmanain Div., Hobart*, pp 1-10

CORBETT, K.D., 1989, Stratigraphy, paleogeography and geochemistry of the Mount Read Volcanics: *Geol. Soc. Aust. Spec. Pub.* 15, pp 86-116

CORBETT, K.D., 1990, Cambro - Ordovician stratigraphy, West Coast range to Black Buff. *Geology in Tasmania* - A Generalist's Influence, M.R.Banks symposium, 14 December 1990, pp 8-13

CORBETT, K.D., 1992, Stratigraphic - volcanic setting of massive sulfide deposits in the Cambrian Mount Read Volanics, Tasmania. *Econ. Geol.*, Spec issue, v. 87, no 3, pp 564-586

CORBETT, K.D., 1996, The geology and copper potential of the Harbacks quarry area and the southern corridor schist belt, Mount Lyell mine lease. *Unpubl. Report*, Copper Mines of Tasmania Pty. Ltd., Queenstown, Tasmania

CORBETT, K.D., CALVER, C.R., EVERARD, J.L. and SEYMOUR, D.B., 1989, Queenstown 1:25,000 sheet. *Geological Survey of Tasmania*, Hobart

CORBETT, K.D., and LEES, T.C., 1987, Stratigraphic and structural relationships and evidence for Cambrian deformation at the western margin of the Mount Read Volcanics, Tasmania. *Aust. Jrnl. Earth Sc.*, v. 34, pp 45-67

CORBETT, K.C., and McPHIE,J., 1993, Mount Read Volcanics and associated ore deposits. IAVCEI, Canberra 1993, Ancient volcanism and modern analogues, excursion guide C3. *AGSO record 1993/63* ISBN 0 642 19664 8

CORBETT, K.D., REID, K.O., CORBETT, E.B., GREEN, G.R., WELLS, K., and SHEPPARD, N.W., 1974, The Mount Read Volcanics and Cambro-Ordovician relationships at Queenstown, Tasmania. *J. Geol. Soc. Aust.*, 21, pp 173-186

CORBETT, K.D., and SOLOMON, M., 1989, Cambrian Mount Read volcanics and associated mineral deposits. In: Burrett, C.F. and Martin, E.L., (eds), Geology and mineral resources of Tasmania. *Geol Soc of Aust., spec. Publ.,* 15: pp 84-153

CORDERY,G., and GREENWOOD,A.J., 1995, Western Tharsis geological and resource report. *Unpubl. report.* Vol 1 - 9. Copper Mines of Tasmania Pty. Ltd. Queenstown, Tasmania

COX, S.F., 1979, Deformation of the Mt. Read volcanics and associated sulphide deposits, Mt. Lyell. *Unpubl. PhD thesis*, Monash University. 271 p

COX. S.F., 1981, The stratigraphy and structural setting of the Mount Lyell volcanic-hosted sulphide deposits. *Econ. Geol.*, v 76, no 2, pp 231-245

CRAWFORD, A.J., 1987, Geochemistry of the Mount Read Volcanics: internal correlations and tectonic implications. In: Controls on gold and silver grades in volcanogenic sulphide deposits. *Unpubl. AMIRA report*, 84/P210, pp 79-108

CRAWFORD, A.J., 1995a, Petrography and mineragraphy of a suite of samples from Mount Lyell plus a discussion of their significance. *Unpubl. report* for Copper Mines of Tasmania Pty. Ltd., Queenstown, Tasmania

CRAWFORD, A.J., 1995b, Petrography and mineragraphy of a suite of rocks from West Tharsis, Mount Lyell field, west Tasmania. *Unpubl. report* for Copper Mines of Tasmania Pty. Ltd., Queenstown, Tasmania

CRAWFORD, A.J., and BERRY, R.F., 1992, Implications of late Proterozoic - early Palaeozoic igneous rock associations for the tectonic evolution of Tasmania. *Tectonophysics* 214, pp 37-56

CRAWFORD, A.J., CORBETT, K.D. and EVERARD, J.L., 1992, Geochemistry of the Cambrian volcanic - hosted massive sulphide - rich Mount Read volcanics, Tasmania, and some tectonic implications. *Econ. Geol.*, Spec issue, v 87, no 3, pp 597-619

CUNDY, W.H., 1901, Royal Tharsis. *Unpubl. Report*, Mount Lyell Mining and Railway Co. Ltd., Queenstown, Tasmania

DAVIS, J, GODSALL, W.J.D., and GREENWOOD, A.J, 1995, Prince Lyell deeps geological and resources report. *Unpubl. report*, Vol 1 - 9. Copper Mines of Tasmania Pty Ltd. Queenstown, Tasmania

DEER,W.A., HOWIE R.A., and ZUSSMANN, J.,1966, An introduction to the rock forming minerals. Longman, ISBN 0 582 44210 9, 528pp

DOYLE, M.G., 1990, The geology of the Jukes Propriety prospect. *Unpubl. BSc thesis* (Hons) Univ. of Tasmania

DAVIDSON, G.J., 1992, Hydrothermal geochemistry and ore genesis of sea - floor volcanogenic copper - bearing oxide ores. *Econ. Geol.*, Spec issue, v 87, no 3, pp 889-912

DUFTY, M.J., FLITCROFT, M.J., and McKEOWN, M.V., 1991, Progress report on the assessment of the ore potential of the Mt Lyell copper field. *Unpubl. Report*, Mount Lyell Mining and Railway Co. Ltd., Queenstown, Tasmania

EASTOE, C.J., SOLOMON, M., and WALSHE, J.L., 1987, District scale alteration associated with massive sulphide deposits in the Mount Read Volcanics, western Tasmania. *Econ. Geol.* v 82, no 5, pp 1239-1258

EDWARDS, A.B., 1939, Some observations on the mineral composition of the Mount Lyell copper ores, Tasmania, and the modes of occurrence. *Proc. Aust. Inst. Min. Metall.*, 114, pp 67-109

EDWARDS, A.B., 1958, Cuprite and native copper in the Mount Lyell Copper Clay deposits. CSIRO, *Mineragraphic Investigations*, report no. 752

FINLOW-BATES, T., and STUMPFL, E.F., 1981, The behaviour of so-called immobile elements in hydrothermally altered rocks associated with volcanogenic submarine-exhalative ore deposits. *Min. Deposita.*, 16, pp 319-328

FLITCROFT, M.J., and McKEOWN, M.V., 1992, Old mines - new vision, *Unpubl. report*, Mount Lyell Mining and Railway Company, Queenstown, Tasmania

FITZSIMONS, S.J., CALHOUN, E.A., VAN DE GREER, G., and POLLINGTON, M., 1993, The Quaternary geology and glaciation of the King Valley. *Geol. Surv. Bulletin 68*, Tasm. Dept. of Mines

GEMMELL, J.B., and LARGE, R.R., 1992 Stringer system and alteration zones underlying the Hellyer volcanogenic massive sulphide deposit, Tasmania. *Econ. Geol.*, Spec issue, v 87, no 3, pp 620-649

GREEN, G.R., 1971, Geology and mineralisation of the Cape Horn - Lyell Comstock area, Mount Lyell. *Unpubl. BSc (Hons) thesis*, University of Tasmania

GREEN, G.R., 1990, Rock alteration, mineral and isotope zonation in the Rosebery district, Tasmania. *10th Aust. Geol. Conv. Abstracts*, Hobart, pp 15-16

GREEN, G.R., SOLOMON, M., and WALSHE, L.L., 1981, The formation of the volcanic - hosted massive sulphide ore deposit at Rosebery, Tasmania. *Econ. Geol.*, v 76, no 2, pp 304-338

GREENWAY, D.C., 1975, West Lyell cave study. *Unpubl. Report*, Mount Lyell Mining and Railway Co. Ltd., Queenstown, Tasmania

GREENWOOD, A.J., 1996, Orientation outcrop rock sampling, West Lyell area. *Unpubl. memorandum*, Copper Mines of Tasmania Pty Ltd., Queenstown, Tasmania

GREGORY, J.W., 1905, The Mount Lyell mining field, Tasmania. *Trans. Aust. Inst. Min. Eng.*, 10, pp 26-196

GULSON, B.L., and PORRITT, P.M., 1987, Base metal exploration of the Mount Read Volcanics, western Tasmania: Part II. Lead isotope signatures and genetic implications. *Econ. Geol.*, v 82, no 2, pp 291-307

HALL, C.R.J., 1975, The geology of the Cape Horn orebody. *Unpubl. M.Sc. thesis*, University of Leicester, England

HALL, G., and SOLOMON, M., 1962, Metallic mineral deposits in geology of Tasmania. *Jrnl. of Geol. Soc. of Aust.*, 9: pp 285-309

HARPER, P., 1992, Sensitivity analysis on the Royal Tharsis. *Unpubl. Report*, Mount Lyell Mining and Railway Co. Ltd., Queenstown, Tasmania

HART, I., 1993, Hematite - barite alteration in the Owen Conglomerate, North Lyell. *Unpubl. M.Sc. thesis*. University of Tasmania

HENDRY, D.A.F., 1972, The geochemistry of the Mount Lyell copper ores, Tasmania. *Unpubl. Ph.D. thesis*, University of Cambridge, 105p

HENDRY, D.A.F., 1981, Chlorites, phengites and siderites from the Prince Lyell ore deposit, Tasmania, and the origin of the deposit. *Econ. Geol.*, v 76, no 2, pp 285-303

HILLS, C.L., 1927, A synopsis of the geology of the Lyell district of Tasmania. *Proc. Aust. Inst. Min. Metall.*, 66, pp 129-148

HILLS, P.B., 1985, Revised preliminary ore reserves Royal Tharsis, *Unpubl. Report*, Mount Lyell Mining and Railway Co. Ltd., Queenstown, Tasmania

HILLS, P.B., 1990, The Mount Lyell copper-gold deposits. In: Hughes, F. (ed), Economic geology of Australia and Papua New Guinea. *Aust. Inst. Min. Metall., Melbourne*, pp 1257-1266

HOUSE, M.J., 1991, Royal Tharsis grade control. *Unpubl. report*, Mount Lyell Mining and Railway Co. Ltd., Queenstown, Tasmania

HOUSTON, M.L., 1968, Planning of the Royal Tharsis tunnel level development. *Unpubl. Report*, Mount Lyell Mining and Railway Co. Ltd., Queenstown, Tasmania

HUSTON, D.L., 1997, Research program and preliminary results of alteration studies at Western Tharsis deposit, Mt Lyell field. *Unpubl. AMIRA/ARC Project P439*, report 4, May 1997, pp 331-341

HUSTON, D.L., 1997a, Geochemical variations in the alteration zone surrounding the Western Tharsis deposit and their utility in exploration. *Unpubl. AMIRA/ARC Project P439*, report 5, October 1997, pp 1-33

HUSTON, D.L., and LARGE, R.R., 1987, Genetic and exploration significance of the zinc ratio [100 Zn/(Zn+Pb)] in massive sulphide systems. *Econ. Geol.*, v 82, no 6, pp 1521-1539

HUSTON, D.L., and LARGE, R.R., 1989, A chemical model for the concentration of gold in massive sulphide deposits. *Ore Geol. Rev.*, 4, pp 171-200

ISHIHARA, S., 1981, The granitoid series and mineralisation. *Econ. Geol.*, Seventy fifth anniversary volume, v 76, pp 458-484

ISHIKAWA,Y., SAWAGUCHI, T., IWAYA, S. and HORIACHI, M., 1976, Delineation of prospecting targets for Kuroko deposits based on modes of volcanism of underlying dacite and alteration halos. *Mining Geology* 26: pp 105-117

JAGO, J.B., REID, K.O., QUILTY, P.G., GREEN, G.R., and DALY, B., 1972, Fossiliferous Cambrian limestone from within the Mount Read Volcanics, Mount Lyell mine area, Tasmania. *Geol. Soc. of Aust.* 19: pp 379-382

JAKINS, G.F., 1930, Royal Tharsis mine, *Unpubl. Report*, Mount Lyell Mining and Railway Co. Ltd., Queenstown, Tasmania

JAKINS, G.F., 1933, Raising the Royal Tharsis shaft at Mt Lyell, *Unpubl. Report*, Mount Lyell Mining and Railway Co. Ltd., Queenstown, Tasmania

JOHNSTON, 1890, The "Iron Blow" at the Linda Goldfield. *Proc. of Royal Soc. of Tas.* (1889 meeting), pp 21-26

JONES, M., 1985, Gold targets in the Mount Lyell area and results. *Unpubl. report*, Gold Fields Exploration Pty. Ltd., Queenstown, Tasmania

KOMYSHAN, P., 1985, Geological investigations in the Cape Horn - Lyell Comstock - West Sedgewick area. *Unpubl. report*, Gold Fields Exploration Pty. Ltd., Queenstown, Tasmania

LARGE, R.R., 1992, Australian volcanic-hosted massive sulphide deposits: features, styles, and genetic models. *Econ. Geol.*, Spec issue, v 87, no 3, pp 471-510

LARGE, R.R., 1992, Submarine volcanism: eruption styles, products, and relevance to understanding the host successions to volcanic-hosted massive sulphide deposits. *Econ. Geol.*, Spec issue, v 87, no 3, pp 511-541

LARGE, R.R., 1996, The Hercules-Mt Read traverse: Relationships between volcanic mineralogy, alteration and geochemistry. *Unpubl. AMIRA/ARC Project P439*, report 3, October 1996, pp 153-233

LARGE, R.R., and BLAKE, D., 1997, Surface lithogeochemical responses of known VHMS deposits based on the MRV geochemical database. *Unpubl. AMIRA Project P439*, report 4, May 1997, pp 93-95

LARGE, R.R., CRAWFORD, A.J., and ADRICHEM, S., 1989, Primary and alteration geochemistry of the Mount Read volcanics. In: Controls on gold and silver grades in volcanogenic massive sulphide deposits. *Unpubl. AMIRA report*, 86/P210, November 1986, pp 38-45

LARGE, R.R., DOYLE, M., RAYMOND, O.L., COOKE, D., JONES, A., and HEASMAN, L., 1996a, Evaluation of the role of Cambrian granites in the genesis of world class VHMS deposits in Tasmania. *Unpubl. AMIRA Project P439*, report 1, May 1996, pp 39-56; and also *Ore Geology Reviews*, Spec issue, v 10, nos 3 - 6, pp 215-230

LARGE, R.R., HERRMANN, W., and CORBETT, K.D., 1987, Base metal exploration of the Mount Read Volcanics, western Tasmania: Part I, Geology and exploration, Elliott Bay: *Econ. Geol.,* v 82, no 2, pp 267-290

LARGE, R.R., STOLZ, A.J. and DUHIG , N., 1996b, Preliminary assessment of MRV geochemical database in terms of possible vectors to ore. *Unpubl. AMIRA Project P439,* May 1996, pp 197-209

LAURIE, J.R., JAGO, J.B., and BAO JIN-SONG, 1995, Review of Tasmania Cambrian biostratigraphy. *AGSO Record 1995/69.* ISBN: 0 642 22373 4

LOFTUS-HILLS, C.L., 1927, A synopsis of the geology of the Lyell district of Tasmania, *Proc. Aust. Inst. of Min. and Metall.*, no. 66: pp 129 -148

LOFTUS-HILLS, G., and SOLOMON, M., 1987, Cobalt, nickel and selenium in sulphides as indicators of ore gensis. *Min. Deposita*, 2, pp 228-242

MARKHAM, N.L., 1963, An interpretation of the Mount Lyell copper ore paragenesis, *Proc. Aust. Inst. of Min. and Metall.,* no. 206: pp 123-141

MARKHAM, N.L., 1966, Notes on the mineralogy of the copper clay deposits, Mt. Lyell. *Unpubl. Private Report* to Mount Lyell Mining and Railway Co. Ltd, Queenstown, Tasmania.

MARKHAM, N.L., 1968, Some genetic aspects of the Mount Lyell mineralisation, *Min. Deposita.*, 3, pp 199-221

McCLENAGHAN, SEYMOUR and VILLA, 1994, Lamprophyre dyke suites from western Tasmania, their radiometric dating and the age of thrust faulting in the Point Hibbs area. *Aust. Jnl. Of Earth Sci.,* 41: pp 47-54

McDONALD, M.J., 1968, Progress report on the geology of the West Lyell orebodies at Mount Lyell, Queenstown, Tasmania. *Unpubl. Report*, Mount Lyell Mining and Railway Co. Ltd, Queenstown, Tasmania. 47p

McPHIE, J., and ALLEN, R.L., 1992, Facies architecture of mineralised submarine volcanic sequences, Cambrian Mount Read Volcanics, western Tasmania: *Econ. Geol.*, Spec issue, v. 87, pp 587-596

McPHIE, J., DOYLE, M., and ALLEN, R.L., 1993, Volcanic Textures, CODES, University of Tasmania, ISBN 0 85901 522 X, 198p

NYE, P.B., BLAKE, F., and HENDERSON, Q.J., 1934, Report on the geology of the Mount Lyell mining field. *Unpubl. Report*, Tasmanian Deptartment of Mines

PERKINS, C., 1996, 40Ar/39Ar age constraints on deformation and mineralisation, Rosebery Zn-Pb-Cu and Mount Lyell Cu deposits, Tasmania, Australia. *Intern. Jrnl. For Geology, Mineralogy and Geochemistry of Mineral Deposits*, v 31, no 1/2, pp 60-71

PERKINS, C., and WALSHE, J.L., 1992, Geochronology of the Mount Read Volcanics, Tasmania. *Econ. Geol.*, v 88, pp 1176-1197

RANKINE, G.M., 1993, Magnetic susceptibility project 60 series, *Unpubl. report*, Mount Lyell Mining and Railway Co. Ltd. Queenstown, Tasmania

RAYMOND, O.L., 1992, Geology and mineralisation of the southern Prince Lyell deeps, Queenstown, Tasmania. *Unpubl. MSc thesis*, University of Tasmania, 161 p

RAYMOND, O.L., 1996, Pyrite composition and ore genesis in the Prince Lyell copper deposit, Mount Lyell mineral field, western Tasmania, Australia. *Ore Geology Reviews*, Spec issue, vol 10, nos 3 - 6, pp 231-250

REID, K.O., 1975, Mt Lyell copper deposits. In: Knight, C.L (ed), Economic geology of Australia and Papua New Guinea, *Aust. Inst of Min and Metall.*, Mon.5, pp 604-619

REID, K.O., and MEARES, R.M.D., 1981, Exploration for volcanogenic massive sulphides deposits in western Tasmania. *Econ. Geol.* v 76, no 2, pp 350-364

ROLLINSON, H., 1993, Using geochemical data: evaluation, presentation, interpretation, Longman, ISBN 0 582 06701 4, 343 pp

RONNA, P.A., HANNINGTON, M.D., RAMAN C.V., THOMPSON, G., TIVEY, M.K., HUMPHRIS, S.E., LALOU, C., and PETERSEN, S., 1993, Active and relict sea-floor hydrothermal mineralisation at the TAG hydrothermal field, mid - Atlantic ridge. *Econ. Geol.* v 88, no 8, pp 1989-2017

SEYMOUR, D.B., and CALVER, C.R., 1995, Explanatory notes for the time-space diagram and stratotectonic elements map of Tasmania. Tasgo NGMA Project, Sub-Project 1: geological synthesis. *Tasmanian Geological Survey*, Record 1995/01

SHEPPARD, N.W., 1987, Exploration and rock geochemistry at Mount Lyell, Tasmania. *Unpubl. PhD thesis*, University of N.S.W., 348 p

SILLITOE, R.H., 1984, A reappraisal of the Mount Lyell copper deposits, Tasmania: Implications for exploration. *Unpubl. report*, Gold Fields Exploration Pty. Ltd, Queenstown, Tasmania

SILLITOE, R.H., 1985, Further comments on geology and exploration at Mount Lyell, Tasmania. *Unpubl. report*, Gold Fields Exploration Pty. Ltd, Queenstown, Tasmania

SOLOMON, M., 1964, The spillite-keratophyre association of west Tasmania and the ore deposits at Mount Lyell, Rosebery and Hercules. *Unpubl. PhD thesis*, University of Tasmania, 419p

SOLOMON, M., 1967, Fossil gossans at Mount Lyell, Tasmania. *Econ. Geol.*, v 62, pp 757-772

SOLOMON, M., 1969, The copper-clay deposits at Mount Lyell, Tasmania. *Proc. Aust. Inst of Min. and Metall.*, 230, pp 39-47

SOLOMON, M., 1976, "Volcanic" massive sulphide deposits and their host rocks - a review and explanation. In: Wolf, K. (ed), *Handbook of Stratabound and Stratiform Ore Deposits*. Elsevier, Amsterdam, pp 21-54

SOLOMON, M., 1981, An introduction to the geology of metallic ore deposits of Tasmania. *Econ. Geol.*, v 76, no 2, pp 194-208

SOLOMON. M., 1984, The dissolution of sulphides in Tasmanian massive sulphide deposits - two contrasting examples. In: The mechanical and chemical remobilisation of metaliferous mineralisation. *7th Aust. Geol. Convention, Short course notes*, Sydney, pp 99-102

SOLOMON, M., and CARSWELL, J.T., 1989, Mount Lyell. In: Burnett, C.F. and Martin, E.L. (eds), Geology and Mineral Resource of Tasmania, *Geol. Soc. of Aust., spec. publ.*, 15: pp 125-132

SOLOMON, M., EASTOE, C.J., WALSHE, J.L., and GREEN, G.R., 1988, Mineral deposits and sulphur isotope abundances in the Mount Read Volcanics between Que River and Mount Darwin, Tasmania. *Econ. Geol.*, v 83, no 7, pp 1307-1328

SOLOMON, M., and ELMS, R.G., 1965, Copper and ore deposits of Mount Lyell. *8th Comm. Min. and Metall. Congr. (1965)*, Publ., 1, pp 478-484

SOLOMON, M., and GRIFFITHS, J.R., 1972, Tectonic evolution of the Tasman orogenic zone, eastern Australia: *Nature*, v. 237, pp 3-6

SOLOMON, M. AND GROVES, D.I., 1994, The Geology and origin of Australia's mineral deposits. *Oxford Monographs on Geology and Geophysics*, 24, 951p

SOLOMON, M., VOLKES, F.M., and WALSHE, J.L., 1987, Chemical remobilisation of volcanic-hosted sulphide deposits at Rosebery and Mount Lyell, Tasmania. *Ore Geol. Rev.*, 2, pp 173-190

STANTON, R.L., 1972, Ore petrology. New York, McGraw-Hill Book Co., 713 p

STICHT, C., 1905, Metal bearing fluxes, *Unpubl. Report*, Mount Lyell Mining and Railway Co. Ltd., Queenstown, Tasmania

STICHT, C., 1906, The development of pyritic smelting: an outline of its history, Presidential address to AusIMM, *Trans. Of Australasian Institute of Mining Engineers*

TAYLOR, H.P., 1979, Geochemistry of hydrothermal ore deposits, John Wiley & Sons, New York, pp 236-277

TAYLOR, R.G., 1992, Ore textures, recognition and interpretation: volume 2, Alteration textures. Key Centre in Economic Geology - Economic Geology Research/Resource Unit, James Cook University, North Queensland

THOMPSON, A.J.B., and THOMPSON, J.F.H., 1996, Atlas of alteration. A field and petrographic guide to hydrothermal alteration minerals. *Geol. Soc. of Canada*, Mineral Deposits Division, ISBN 0-919216-5-5, 119p

THUREAU, G., 1886, The Linda Goldfield: its auriferous and other mineral deposits. *Report by the Government Geologist*, no. 146, Government Printer, Hobart, 8p

THUREAU, G., 1889, The "Iron Blow" at Linda Goldfield. *Proc. of Royal Soc. of Tas.* (1889 meeting), pp 1-7

TITLEY, S.R., 1982, The style and progress of mineralisation and alteration in porphyry copper systems: American southwest. In Titley, S.R. (ed.), Advances in Geology of the porphyry copper deposits: Southwestern North America. Arizona Press

VARNE, R., and FODEN, J.D., 1987, Tectonic setting of Cambrian rifting, volcanism and ophiolite formation in western Tasmania: *Tectonophysics*, v 140, pp 275-295

VEEVERS, J.J., 1984, The Phanerozoic earth history of Australia, *Oxford University Press*: 418p

WADE, M.L., 1957, Structural and stratigraphical control of copper mineralisation at Mount Lyell. *Unpubl. M.Sc. thesis*. University of Tasmania. 52p

WADE, M.L., 1958, A history of geological thought at Mount Lyell. *Unpubl. report*. Mount Lyell Mining and Railway Co. Ltd.

WADE, M.L., and SOLOMON, M., 1958, Geology of the Mount Lyell Mines, Tasmania. *Econ. Geol.*, v 53, pp 367-416

WALSHE, J.L., 1971, Geology of the southern Mount Lyell field and trace element studies of the pyrite mineralisation. *Unpubl. BSc (hons) thesis*, University of Tasmania

WALSHE, J.L., 1977, The geochemistry of the Mount Lyell copper deposits. *Unpubl. PhD thesis*, University of Tasmania, 174p

WALSHE, J.L., and SOLOMON, M., 1981, An investigation into the environment of formation of the volcanic-hosted Mount Lyell copper deposits using geology, mineralogy, stable isotopes and a six-component chlorite solid solution model. *Econ. Geol.*, v 76, no 2, pp 246-284

WHITE, N.C., 1975, Cambrian volcanism and mineralisation in south-west Tasmania. *Unpubl. PhD thesis*, University of Tasmania. 339 p

WHITE, N.C., and McPHIE, J., 1996, Stratigraphy and paleovolcanology on the Cambrian Tyndall Group, Mount Read Volcanics, western Tasmania. *Aust. Jnl. Of Earth Sci.,* April 1996, v 43, no 2, pp 147-159

WIGGINS, T.R., and HOUSE, M.J., 1991, Review of Royal Tharsis grade performance, *Unpubl. Report*, Mount Lyell Mining and Railway Co. Ltd., Queenstown, Tasmania

WILLIAMS, E., 1978, Tasman fold belt system in Tasmania. *Tectonophysics*, v. 48, pp 159-205

WILLIAMS, E., 1993, Notes on the geology of the Lyell quadrangle between the East Queen river and Linda creek. *Mineral Resources Tasmania.* Report 1993/10.

WILLIAMS, E., McCLENAGHAN, M.P., and COLLINS, P.L.F., 1989, Mid-palaeozoic deformation, granitoids and ore deposits. In Burrett, C.F. and Martin, E.L., (eds), Geology and mineral resources of Tasmania, *Geol. Soc. Of Aust., special publ.*, no 15, pp 238-291

WILLS, K.J.A., 1995, Solid geology interpretation map (1:5000). *Unpubl. propriety map*, Copper Mines of Tasmania Pty. Ltd.

WILLS, K.J.A., 1996a, Lyell super pit scoping study. *Unpubl. report*, Copper Mines of Tasmania Pty Ltd.

WILLS, K.J.A., 1996b, A synthesis of Mount Lyell geology and exploration. *Unpubl. report*, Copper Mines of Tasmania Pty Ltd., 74p

WILSON, M., 1996, Igneous petrogenesis, Chapman and Hall, ISBN 0 412 53310 3, 456 p

WYMAN, W., 1996, Road log of the Jukes road and the Jukes Cu-Au Prospect with emphasis on petrography, alteration assemblages and preliminary geochemistry. *Unpubl. report,* CODES AMIRA Project P439, report 3, pp 235-290

WYMAN, W., ALLEN, R., and DUHIG, N., 1995, Jukes road: Preliminary volcanic facies analysis and alteration petrography. *Unpubl. report,* CODES AMIRA Project P439, report 2, May 1996, pp 29-54

Appendix I

Royal Tharsis

Surface Orientation Rock Chip Geochemistry

APPENDIX I - CONTENTS

Copper Mines of Tasmania Pty Ltd
Grid Transformation Relationships

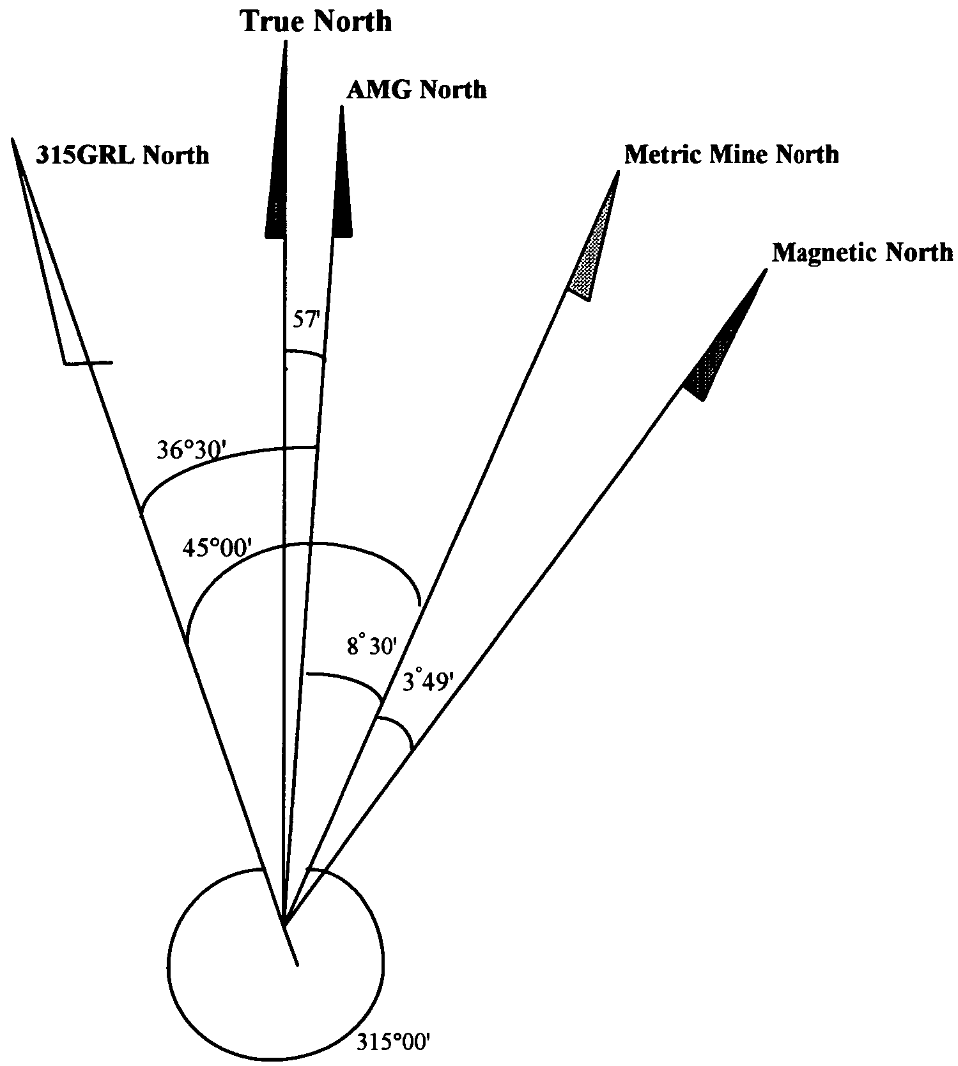

(After Flitcroft & McKeowen, 1992)
(Magnetic north as at 1997)

AMG - 315GRL Grid Transformation			
315GRL:	2000 RL	7500.00N	3500.00E
AMG:	0 RL	5 341 998.02N	382 689.92N
AMG	0 RL	5 340 000.00N	380 000.00E
315GRL	2000 RL	7494.077N	148.272E
Metric Mine:	0 RL	4750.00N	5550.00E
315GRL:	2000 RL	7500.00N	3500.00E
Rotation:	315 degrees (clockwise)		

Current working grid is 315GRL
AMG bearings converted to 315GRL by +036°30'11"
Previous mine grid bearings converted to 315GRL by +045°.

SAMPLE LOCATIONS

Sample No	Line	AMG North	AMG East	AMG RL	GRL North	GRL East	GRL RL	Survey Method
	Line 8130N							
G5342	8130N	5342601.688	382421.640	367.677	8145.014	3643.495	2367.677	GPS
G5343	8130N	5342610.747	382430.982	373.874	8146.739	3656.397	2373.874	GPS
G5344	8130N	5342620.955	382438.492	378.276	8150.478	3668.509	2378.276	GPS
G5345	8130N	5342628.014	382447.455	378.787	8150.821	3679.916	2378.787	GPS
G5346	8130N	5342696.088	382567.981	421.907	8133.839	3817.332	2421.907	GPS
G5347	8130N	5342703.907	382578.861	427.719	8133.651	3830.733	2427.719	GPS
G5348	8130N	5342713.182	382593.365	434.410	8132.479	3847.914	2434.410	GPS
G5349	8130N	5342719.744	382601.734	438.127	8132.775	3858.547	2438.127	GPS
G5350	8130N	5342725.741	382619.302	443.605	8127.143	3876.241	2443.605	GPS
G5351	8130N	5342741.348	382638.036	448.330	8128.545	3900.591	2448.330	GPS
G5352	8130N	5342745.748	382644.415	450.200	8128.287	3908.338	2450.200	GPS
G5353	8130N	5342826.841	382749.556	483.362	8130.928	4041.131	2483.362	GPS
G5354	8130N	5342832.637	382755.490	485.702	8132.057	4049.351	2485.702	GPS
G5356	8130N	5342842.945	382758.220	487.877	8138.721	4057.679	2487.877	GPS
G5357	8130N	5342838.243	382783.355	494.018	8119.984	4075.091	2494.018	GPS
G5358	8130N	5342853.535	382782.425	497.026	8132.833	4083.443	2497.026	GPS
G5359	8130N	5342863.152	382786.673	499.888	8138.038	4092.581	2499.888	GPS
G5360	8130N	5342863.796	382795.439	502.993	8133.339	4100.012	2502.993	GPS
G5361	8130N	5342869.053	382805.844	507.120	8131.375	4111.507	2507.120	GPS
G5362	8130N	5342873.446	382815.570	511.586	8129.120	4121.941	2511.586	GPS
G5363	8130N	5342884.889	382826.072	516.360	8132.072	4137.194	2516.360	GPS
G5364	8130N	5342893.555	382839.957	521.004	8130.777	4153.515	2521.004	GPS
G5365	8130N	5342919.395	382867.457	524.607	8135.191	4191.002	2524.607	GPS
G5366	8130N	5342929.334	382877.531	528.037	8137.188	4205.016	2528.037	GPS
G5367	8130N	5342939.138	382889.258	530.096	8138.093	4220.279	2530.096	GPS
G5368	8130N	5342949.169	382901.345	536.340	8138.966	4235.966	2536.340	GPS
G5369	8130N	5342950.875	382912.447	540.837	8133.732	4245.908	2540.837	GPS
G5370	8130N	5342952.447	382923.492	545.564	8128.424	4255.724	2545.564	GPS
G5371	8130N	5342951.870	382948.439	556.008	8113.115	4275.440	2556.008	GPS

See Figure 1, Appendix I, for relationship between AMG and GRL

SAMPLE LOCATIONS

Sample No	Line	AMG North	AMG East	AMG RL	GRL North	GRL East	GRL RL	Survey Method
	Line 8010N							
G5376	8010N	5342778.189	382877.804	498.786	8015.497	4115.299	2498.786	GPS
G5377	8010N	5342785.990	382886.073	501.383	8016.849	4126.590	2501.383	GPS
G5378	8010N	5342792.202	382893.334	504.144	8017.523	4136.124	2504.144	GPS
G5379	8010N	5342801.018	382899.334	507.358	8021.041	4146.195	2507.358	GPS
G5380	8010N	5342808.666	382909.817	504.489	8020.953	4159.174	2504.489	GPS
G5381	8010N	5342817.566	382921.912	498.118	8020.912	4174.195	2498.118	GPS
G5382	8010N	5342824.391	382930.894	499.195	8021.055	4185.478	2499.195	GPS
G5383	8010N	5342836.610	382935.104	504.387	8028.375	4196.134	2504.387	GPS
G5384	8010N	5342852.407	382960.492	519.113	8025.970	4225.947	2519.113	GPS
G5385	8010N	5342549.489	382582.595	420.601	8007.269	3741.851	2420.601	GPS
G5386	8010N	5342564.391	382593.939	423.859	8012.501	3759.839	2423.859	GPS
G5387	8010N	5342578.239	382599.433	428.016	8020.367	3772.497	2428.016	GPS
G5388	8010N	5342584.168	382613.007	433.505	8017.057	3786.939	2433.505	GPS
G5389	8010N	5342596.079	382621.194	437.727	8021.762	3800.609	2437.727	GPS
G5390	8010N	5342600.798	382633.617	443.222	8018.165	3813.406	2443.222	GPS
G5391	8010N	5342608.664	382640.230	445.430	8020.554	3823.404	2445.430	GPS
G5392	8010N	5342619.265	382649.313	449.604	8023.673	3837.015	2449.604	GPS
G5393	8010N	5342621.895	382663.659	455.810	8017.252	3850.115	2455.810	GPS
G5395	8010N	5342630.142	382670.578	457.607	8019.766	3860.585	2457.607	GPS
G5396	8010N	5342637.325	382681.454	459.512	8019.070	3873.604	2459.512	GPS
G5397	8010N	5342643.696	382691.769	460.824	8018.054	3885.689	2460.824	GPS
G5398	8010N	5342653.671	382702.950	455.479	8019.422	3900.615	2455.479	GPS

See Figure 1, Appendix I, for relationship between AMG and GRL

ASSAY RESULTS

Sample No	Cu ppm (GA115)	Au ppm (GG334)	Au (R) (GG334)	Ag ppm (GA115)	Mo ppm (GA115)	Mn ppm (GA115)	Pb ppm (GA115)	Zn ppm (GA115)	Ba ppm (GX401)	As ppm (GA140)	As ppm (HA140)	Ni ppm (GA140)	Co ppm (GA140)
Line 8130N													
G5342	35.1	0.007		<0.1	1	2.6	1.5	2.4	1030		9.8	<3	<3
G5343	10.5	0.011	0.010	<0.1	<1	22.4	49.3	44.4	1305		3.4	21	<3
G5344	19.9	0.001		<0.1	3	12.8	12.8	6.7	2330		8.7	<3	5
G5345	21.7	0.003	0.002	<0.1	<1	24.9	9.4	47.8	952		6.4	10	7
G5346	79.3	0.004		<0.1	4	39.6	28.2	61.9	792		26.4	<3	7
G5347	33.4	0.005		<0.1	2	29.1	39.1	55.6	703		26.3	<3	5
G5348	42.3	0.031		<0.1	5	13.1	21.3	4.7	533		16.1	<3	3
G5349	17.2	0.004		<0.1	1	5.4	13.4	2.1	545		6.1	<3	5
G5350	20.3	0.021		0.3	9	13.7	50.1	3.5	811		14.6	<3	<3
G5351	57.8	0.102		0.3	1	5.0	18.6	1.9	1735		9.8	9	13
G5352	137.4	0.359		0.3	7	262.5	20.8	127.1	928		15.9	22	7
G5353	125.5	0.086		0.2	2	67.9	13.6	61.9	1575		7.5	25	7
G5354	39.8	0.011		0.2	4	138.2	8.3	84.8	1345		7.6	32	16
G5355	7.7	0.002		<0.1	3	23.4	2.5	1.9	<10		2.0	7	<3
G5356	43.6	0.041		0.3	6	48.5	40.2	51.0	1405		9.8	20	8
G5357	12.5	0.043		<0.1	9	105.0	9.8	164.8	1595		13.8	14	21
G5358	22.0	0.022		0.2	13	14.7	20.2	8.1	2070		7.9	3	14
G5359	476.1	0.037		0.5	28	71.3	67.6	66.6	513		26.4	<3	16
G5360	625.7	0.060		2.9	62	18.4	43.0	3.3	8030		8.8	4	29
G5361	126.9	0.016		0.3	4	189.3	31.9	88.0	5250		15	<3	5
G5362	99.5	0.100		0.5	11	15.8	77.9	5.2	6500		25.2	<3	8
G5363	209.4	0.054		0.6	449	9.0	35.1	2.4	7630		9.1	<3	7
G5364	22.6	0.005		0.2	6	14.8	89.4	3.5	966		23.6	<3	4
G5365	38.0	0.023		0.7	7	37.9	15.0	28.2	1410		9.0	<3	10
G5366	49.8	0.001		<0.1	3	254.2	29.8	123.0	1270		6.5	<3	7
G5367	45.1	0.002		0.5	2	271.1	21.5	113.5	1515		11.5	<3	8
G5368	131.5	0.042		0.5	6	176.4	37.0	127.5	1475		10.8	<3	14
G5369	57.1	0.055		1.1	3	7.9	64.2	6.2	2240		3.0	<3	3
G5370	5790.0	0.160		8.3	76	59.6	41.4	30.1	695		3.9	10	21
G5371	403.1	0.086		1.8	22	59.5	306.3	65.6	1670		21.7	8	6

ASSAY RESULTS

Sample No	Cu ppm (GA115)	Au ppm (GG334)	Au (R) (GG334)	Ag ppm (GA115)	Mo ppm (GA115)	Mn ppm (GA115)	Pb ppm (GA115)	Zn ppm (GA115)	Ba ppm (GX401)	As ppm (GA140)	As ppm (HA140)	Ni ppm (GA140)	Co ppm (GA140)
Line 8010N													
G5376	451.0	0.024		0.4	59	232.6	32.3	130.9	1705		8.1	14	30
G5377	1520.0	0.076		0.6	10	12.5	22.4	4.3	979		7.9	<3	14
G5378	106.1	0.020		0.3	6	335.4	33.3	192.9	1005		17.6	30	16
G5379	26.3	0.003		<0.1	3	7.1	29.0	4.6	1150		14.5	<3	6
G5380	39.1	0.003		<0.1	5	10.6	27.1	5.6	1145		23.0	<3	3
G5381	16.9	0.001		0.1	3	338.7	18.3	208.0	1215		12.8	4	17
G5382	25.4	0.007		0.2	3	61.9	46.2	33.2	862		14.9	5	12
G5383	20.9	0.004		<0.1	1	7.8	10.8	4.7	1070		4.2	3	9
G5384	15.6	0.001		<0.1	3	10.2	44.3	10.3	2760		2.3	3	<3
G5385	28.3	0.005		0.4	208	29.3	108.5	25.5	1155		13.0	3	6
G5386	80.8	0.014		0.4	7	272.3	426.4	699.7	881		26.0	5	9
G5387	21.5	0.005		0.1	1	614.3	23.2	617.4	1400		5.4	6	15
G5388	64.5	0.009		0.3	7	108.0	87.3	108.0	1440	63	>50.0	<3	6
G5389	33.9	0.036		<0.1	4	9.8	20.8	4.5	1530		12.6	<3	3
G5390	22.2	0.004		<0.1	4	165.3	28.5	211.5	2620		12.8	7	8
G5391	575.0	0.012		0.1	2	203.2	15.6	249.0	1665		12.6	27	16
G5392	51.7	0.012		0.2	2	539.7	27.9	470.3	886		18.1	26	20
G5393	43.7	0.006		<0.1	3	13.3	54.3	4.8	1085		2.5	<3	<3
G5394	6.2	0.001		<0.1	11	36.2	3.6	6.2	20		16.2	3	8
G5395	10.0	0.002		<0.1	4	23.7	10.9	2.9	30		10.6	8	<3
G5396	15.4	0.002		<0.1	5	14.2	10.5	3.1	677		21.6	3	<3
G5397	29.4	0.003		<0.1	1	653.3	32.4	255.3	761		26.5	36	8
G5398	20.6	0.021	0.023	<0.1	2	243.3	28.2	442.7	1315		10.2	30	15

Assay Data for 10 metre Spaced Sample Sites

GEOLOGICAL DESCRIPTION

Sample No	Geology/Alteration	Contact strike	Contact dip	Contact dip dir'n	Foliation strike	Foliation dip	Foliation dip dir'n	Lineation dip	Lineation dir'n	Comments
	Line 8130N									
G5342	fe qz-se-(py) schist				150	70	SW			
G5343	fe qz-ch-(py) schist				nm					
G5344	fe qz-se-(py) schist				120	81	SW			
G5345	fe qz-ch-(py) schist				nm					
G5346	si qz-ch-py schist				333	68	NE			
G5347	si qz-ch-py schist				350	65	NE			leached & locally fe
G5348	qz-se-py schist				334	66	NE			leached
G5349	qz-se-(py) schist				nm					
G5350	qz-se-py schist				118	76	SW			leached & locally fe
G5351	si qz-se-py schist				330	78	NE			leached & locally fe
G5352	qz-ch-py schist				nm					
G5353	qz-se-py & qz-ch schist	150	73	SW	130	70	SW			intrusive andesite(?) contact
G5354	fe qz-se-py & qz-ch schist				118	76	SW			
G5355	qz				nm					blank sample
G5356	qz-se-py & qz-ch schist				132	82	SW			leached
G5357	qz-ch-(py) schist				130	74	SW			leached
G5357	qz-ch-(py) schist				134	72	SW			leached
G5358	fe qz-se-py schist				119	82	SW			
G5359	fe qz-ch-py schist				124	76	SW			silicified zone/head
G5359	qz-ch-py schist				135	65	SW			
G5360	qz-se-py schist				130	83	SW			
G5361	fe qz-ch-(py) schist				123	83	SW			
G5362	qz-se-py schist				132	76	SW			leached
G5363	si qz-se-py schist				128	63	SW			
G5364	si qz-se-py schist				128	75	SW			leached
G5365	qz-ch schist				120	88	SW			
G5365	qz-ch schist				133	78	SW			
G5366	fe qz-ch schist				140	81	SW			mod-weakly fe
G5367	si ch-(py) schist				138	73	SW			leached with cubic voids post py
G5368	si ch-(py) schist				146	58	SW			leached with cubic voids post py
G5369	wd ch schist				145	80	SW			pallid & leached
G5370	wd ch schist				210	50	W			pallid & leached
G5371	qz-se-ch schist				165	90				
G5371	qz-se-ch schist				315	88	E			local fracturing
G5371	glf	179	79	W						
G5371	glf	185	63	W						

GEOLOGICAL DESCRIPTION

Sample No	Geology/Alteration	Contact strike	Contact dip	Contact dip dir'n	Foliation strike	Foliation dip	Foliation dip dir'n	Lineation dip	Lineation dir'n	Comments
	Line 8010N									
G5376	qz-ch schist				130	69	SW			
G5377	qz-se-py schist				138	72	SW	68	170	
G5378	qz-ch-(py) schist				120	70	SW			pitted, local hm alt'n
G5379	qz-se-py schist				125	77	SW	78	185	
G5380	qz-se-py schist				128	80	SW			
G5381	ch-qz-py schist				130	76	SW			
G5382	ch schist				138	66	SW			pallid
G5383	ch schist				nm					pallid
G5384	ch schist				nm					pallid
G5385	qz-se-py schist				142	81	SW			
G5386	qz-se-py schist				134	83				
G5387	qz-ch-py+se schist				112	76				
G5388	hm qz-py-se schist				128	76				
G5389	qz-se-py schist				nm					
G5390	ch schist				103	76	SW			
G5391	si qz-ch-py schist				155	70	SW			
G5392	fe qz-ch-py schist				121	74	SW			
G5393	hm qz-py-se schist				121	81	SW			
G5394	qz				nm					blank sample
G5395	qz vein				130	86	SW			massive vein
G5396	qz-se-py schist				nm					
G5397	qz-ch schist				144	68	SW			pitted
G5398	ch-qz schist				nm					pallid

nm = no measurement

Geological Data for 10 metre Spaced Sample Sites

STATISTICS

Lines 8130N & 8010N

Descriptive Statistics	*Cu ppm (GA115)*	*Au ppm (GA334)*	*Au (R) (GA334)*	*Ag ppm (GA115)*	*Mo ppm (GA115)*	*Mn ppm (GA115)*	*Pb ppm (GA115)*	*Zn ppm (GA115)*	*Ba ppm (GX401)*	*As ppm (HA140)*	*Ni ppm (GA140)*	*Co ppm (GA140)*
Mean	235.518	0.033	0.012	0.468	21.373	115.629	46.175	99.627	1689.294	13.820	8.284	9.402
Standard Error	116.327	0.008	0.006	0.171	9.643	22.093	9.816	21.655	229.487	1.395	1.406	0.963
Median	39.800	0.012	0.010	0.200	4.000	37.900	28.500	44.400	1270.000	11.500	3.000	7.000
Mode	-	0.003	-	0.050	3.000	-	28.200	2.400	-	9.800	1.500	1.500
Standard Deviation	830.738	0.057	0.011	1.219	68.863	157.776	70.102	154.644	1638.865	9.965	10.040	6.880
Sample Variance	690125.2	0.003	0.000	1.485	4742.068	24893.30	4914.259	23914.8	2685878	99.300	100.793	47.330
Kurtosis	42.015	21.313	#DIV/0!	35.706	31.580	3.654	20.648	6.180	8.009	10.798	0.777	1.119
Skewness	6.292	4.131	0.690	5.703	5.402	1.947	4.367	2.460	2.856	2.567	1.447	1.126
Range	5780.000	0.359	0.021	8.250	448.500	650.700	424.900	697.800	8000.000	60.700	34.500	28.500
Minimum	10.000	0.001	0.002	0.050	0.500	2.600	1.500	1.900	30.000	2.300	1.500	1.500
Maximum	5790.000	0.359	0.023	8.300	449.000	653.300	426.400	699.700	8030.000	63.000	36.000	30.000
Sum	12011.4	1.662	0.035	23.850	1090.000	5897.100	2354.900	5081.000	86154.0	704.800	422.500	479.500
Count	51	51	3	51	51	51	51	51	51	51	51	51
Confidence Level (95.000%)	227.996	0.016	0.012	0.334	18.899	43.302	19.239	42.442	449.786	2.735	2.755	1.888

Correlation	*Cu ppm (GA115)*	*Au ppm (GA334)*	*Au (R) (GA334)*	*Ag ppm (GA115)*	*Mo ppm (GA115)*	*Mn ppm (GA115)*	*Pb ppm (GA115)*	*Zn ppm (GA115)*	*Ba ppm (GX401)*	*As ppm (HA140)*	*Ni ppm (GA140)*	*Co ppm (GA140)*
Cu ppm (GA115)	1											
Au ppm (GA334)	0.366	1										
Au (R) (GA334)	0.047	0.997	1									
Ag ppm (GA115)	0.929	0.388	0.000	1								
Mo ppm (GA115)	0.139	0.088	0.926	0.186	1							
Mn ppm (GA115)	-0.069	-0.021	0.922	-0.096	-0.138	1						
Pb ppm (GA115)	0.011	0.034	0.346	0.122	0.056	0.043	1					
Zn ppm (GA115)	-0.081	-0.089	0.923	-0.104	-0.134	0.791	0.383	1				
Ba ppm (GX401)	-0.030	0.117	0.804	0.139	0.503	-0.136	-0.002	-0.143	1			
As ppm (HA140)	-0.147	-0.045	0.665	-0.134	-0.081	0.118	0.324	0.137	-0.077	1		
Ni ppm (GA140)	0.019	0.180	0.981	-0.028	-0.126	0.522	-0.108	0.396	-0.169	-0.064	1	
Co ppm (GA140)	0.345	0.140	0.694	0.361	0.065	0.369	-0.079	0.337	0.185	-0.110	0.332	1

Covariance	*Cu ppm (GA115)*	*Au ppm (GA334)*	*Au (R) (GA334)*	*Ag ppm (GA115)*	*Mo ppm (GA115)*	*Mn ppm (GA115)*	*Pb ppm (GA115)*	*Zn ppm (GA115)*	*Ba ppm (GX401)*	*As ppm (HA140)*	*Ni ppm (GA140)*	*Co ppm (GA140)*
Cu ppm (GA115)	676593.4											
Au ppm (GA334)	17.069	0.003										
Au (R) (GA334)	0.002	0.000	0.000									
Ag ppm (GA115)	922.017	0.027	0.000	1.456								
Mo ppm (GA115)	7768.131	0.339	0.006	15.274	4649.087							
Mn ppm (GA115)	-8854.045	-0.188	0.826	-18.007	-1467.367	24405.2						
Pb ppm (GA115)	614.303	0.135	0.049	10.195	262.791	469.354	4817.901					
Zn ppm (GA115)	-10210.8	-0.771	1.494	-19.304	-1395.897	18928.5	4070.349	23445.9				
Ba ppm (GX401)	-39881.2	10.801	1.175	272.295	55656.8	-34504.4	-252.636	-35587.4	2633214			
As ppm (HA140)	-1193.026	-0.025	0.016	-1.591	-54.435	182.600	222.141	206.525	-1234.331	97.353		
Ni ppm (GA140)	151.347	0.101	0.069	-0.331	-85.361	810.218	-74.529	602.147	-2718.133	-6.247	98.816	
Co ppm (GA140)	1935.612	0.054	0.033	2.966	30.032	393.062	-37.120	351.232	2046.225	-7.392	22.498	46.402

STATISTICS Line 8130N

Descriptive Statistics	*Cu ppm (GA115)*	*Au ppm (GA334)*	*Au (R) (GA334)*	*Ag ppm (GA115)*	*Mo ppm (GA115)*	*Mn ppm (GA115)*	*Pb ppm (GA115)*	*Zn ppm (GA115)*	*Ba ppm (GX401)*	*As ppm (HA140)*	*Ni ppm (GA140)*	*Co ppm (GA140)*
Mean	303.210	0.048	0.006	0.697	25.759	68.641	41.955	47.993	2028.207	12.572	7.017	8.983
Standard Error	197.863	0.013	0.004	0.294	15.458	15.430	10.267	8.880	383.136	1.355	1.627	1.225
Median	45.100	0.023	0.006	0.300	5.000	29.100	29.800	44.400	1405.000	9.800	1.500	7.000
Mode	-	0.011	-	0.050	1.000	-	-	2.400	-	9.800	1.500	7.000
Standard Deviation	1065.526	0.071	0.006	1.583	83.243	83.092	55.287	47.818	2063.253	7.299	8.763	6.597
Sample Variance	1135345.8	0.005	0.000	2.506	6929.315	6904.285	3056.668	2286.576	4257013.3	53.278	76.794	43.526
Kurtosis	27.774	13.090	-	20.400	26.242	1.106	19.863	-0.260	3.543	-0.474	1.376	1.846
Skewness	5.226	3.277	-	4.334	5.037	1.519	4.162	0.841	2.138	0.832	1.547	1.384
Range	5779.500	0.359	0.008	8.250	448.500	268.500	304.800	162.900	7517.000	23.400	30.500	27.500
Minimum	10.500	0.001	0.002	0.050	0.500	2.600	1.500	1.900	513.000	3.000	1.500	1.500
Maximum	5790.000	0.359	0.010	8.300	449.000	271.100	306.300	164.800	8030.000	26.400	32.000	29.000
Sum	8793.100	1.392	0.012	20.200	747.000	1990.600	1216.700	1391.800	58818.000	364.600	203.500	260.500
Count	29	29	2	29	29	29	29	29	29	29	29	29
Confidence Level (95.000%)	387.804	0.026	0.008	0.576	30.297	30.242	20.122	17.404	750.933	2.657	3.189	2.401

Correlation	*Cu ppm (GA115)*	*Au ppm (GA334)*	*Au (R) (GA334)*	*Ag ppm (GA115)*	*Mo ppm (GA115)*	*Mn ppm (GA115)*	*Pb ppm (GA115)*	*Zn ppm (GA115)*	*Ba ppm (GX401)*	*As ppm (HA140)*	*Ni ppm (GA140)*	*Co ppm (GA140)*
Cu ppm (GA115)	1											
Au ppm (GA334)	0.329	1										
Au (R) (GA334)	-1.000	1.000	1									
Ag ppm (GA115)	0.958	0.342	-	1								
Mo ppm (GA115)	0.151	0.079	-	0.175	1							
Mn ppm (GA115)	-0.021	0.288	-1.000	-0.053	-0.156	1						
Pb ppm (GA115)	0.061	0.105	1.000	0.188	0.021	-0.090	1					
Zn ppm (GA115)	-0.073	0.187	-1.000	-0.127	-0.208	0.837	-0.029	1				
Ba ppm (GX401)	-0.058	0.050	1.000	0.097	0.568	-0.104	0.057	-0.233	1			
As ppm (HA140)	-0.193	0.036	-1.000	-0.216	-0.101	-0.018	0.386	0.092	-0.025	1		
Ni ppm (GA140)	0.052	0.368	1.000	0.013	-0.127	0.199	-0.087	0.338	-0.188	-0.291	1	
Co ppm (GA140)	0.418	0.182	-1.000	0.503	0.090	0.104	-0.101	0.217	0.281	-0.109	0.165	1

Covariance	*Cu ppm (GA115)*	*Au ppm (GA334)*	*Au (R) (GA334)*	*Ag ppm (GA115)*	*Mo ppm (GA115)*	*Mn ppm (GA115)*	*Pb ppm (GA115)*	*Zn ppm (GA115)*	*Ba ppm (GX401)*	*As ppm (HA140)*	*Ni ppm (GA140)*	*Co ppm (GA140)*
Cu ppm (GA115)	1096195.9											
Au ppm (GA334)	24.116	0.005										
Au (R) (GA334)	-0.022	0.000	0.000									
Ag ppm (GA115)	1559.906	0.037	0.000	2.419								
Mo ppm (GA115)	12922.575	0.453	0.000	22.260	6690.373							
Mn ppm (GA115)	-1757.537	1.646	-0.005	-6.732	-1039.747	6666.206						
Pb ppm (GA115)	3485.620	0.400	0.080	15.926	92.543	-400.008	2951.265					
Zn ppm (GA115)	-3580.654	0.617	-0.007	-9.269	-801.112	3209.986	-74.201	2207.729				
Ba ppm (GX401)	-123157.7	7.128	0.706	307.065	94270.584	-17187.143	6287.561	-22212.137	4110219.8			
As ppm (HA140)	-1448.517	0.018	-0.006	-2.413	-59.303	-10.357	150.447	31.052	-364.305	51.441		
Ni ppm (GA140)	471.867	0.222	0.022	0.177	-89.668	140.223	-40.899	136.559	-3276.883	-17.984	74.146	
Co ppm (GA140)	2838.161	0.083	-0.011	5.067	47.935	54.851	-35.716	66.136	3692.279	-5.045	9.190	42.026

STATISTICS

Line 8010N

Descriptive Statistics	*Cu ppm (GA115)*	*Au ppm (GA334)*	*Au (R) (GA334)*	*Ag ppm (GA115)*	*Mo ppm (GA115)*	*Mn ppm (GA115)*	*Pb ppm (GA115)*	*Zn ppm (GA115)*	*Ba ppm (GX401)*	*As ppm (HA140)*	*Ni ppm (GA140)*	*Co ppm (GA140)*
Mean	146.286	0.012	0.023	0.166	15.591	177.568	51.736	167.691	1242.545	15.464	9.955	9.955
Standard Error	72.203	0.004	0.000	0.035	9.511	44.208	18.547	45.405	126.351	2.700	2.454	1.568
Median	28.850	0.006	0.023	0.075	3.500	84.950	28.350	70.600	1147.500	12.800	4.500	8.500
Mode	-	0.003	-	0.050	3.000	-	-	-	-	12.800	1.500	1.500
Standard Deviation	338.661	0.017	-	0.162	44.609	207.355	86.995	212.970	592.640	12.665	11.509	7.355
Sample Variance	114691.609	0.000	-	0.026	1989.968	42995.988	7568.068	45356.213	351222.355	160.413	132.450	54.093
Kurtosis	13.906	9.918	-	0.852	18.529	0.417	18.364	0.904	2.363	9.407	0.049	0.944
Skewness	3.601	2.916	-	1.318	4.230	1.186	4.166	1.340	1.020	2.643	1.285	0.908
Range	1510.000	0.075	0.000	0.550	207.000	646.200	415.900	696.800	2730.000	60.700	34.500	28.500
Minimum	10.000	0.001	0.023	0.050	1.000	7.100	10.500	2.900	30.000	2.300	1.500	1.500
Maximum	1520.000	0.076	0.023	0.600	208.000	653.300	426.400	699.700	2760.000	63.000	36.000	30.000
Sum	3218.300	0.270	0.023	3.650	343.000	3906.500	1138.200	3689.200	27336.000	340.200	219.000	219.000
Count	22	22	1	22	22	22	22	22	22	22	22	22
Confidence Level (95.000%)	141.515	0.007	-	0.068	18.641	86.646	36.352	88.993	247.644	5.292	4.809	3.073

Correlation	*Cu ppm (GA115)*	*Au ppm (GA334)*	*Au (R) (GA334)*	*Ag ppm (GA115)*	*Mo ppm (GA115)*	*Mn ppm (GA115)*	*Pb ppm (GA115)*	*Zn ppm (GA115)*	*Ba ppm (GX401)*	*As ppm (HA140)*	*Ni ppm (GA140)*	*Co ppm (GA140)*
Cu ppm (GA115)	1											
Au ppm (GA334)	0.845	1										
Au (R) (GA334)	-	-	1									
Ag ppm (GA115)	0.645	0.638	-	1								
Mo ppm (GA115)	0.005	-0.023	-	0.434	1							
Mn ppm (GA115)	-0.127	-0.118	-	0.000	-0.159	1						
Pb ppm (GA115)	-0.082	-0.012	-	0.415	0.147	0.059	1					
Zn ppm (GA115)	-0.120	-0.050	-	0.109	-0.164	0.765	0.501	1				
Ba ppm (GX401)	-0.001	-0.033	-	-0.116	0.008	-0.074	-0.092	0.002	1			
As ppm (HA140)	-0.146	-0.114	-	0.186	-0.058	0.103	0.286	0.094	-0.152	1		
Ni ppm (GA140)	-0.002	0.010	-	-0.063	-0.128	0.664	-0.141	0.434	-0.103	0.032	1	
Co ppm (GA140)	0.350	0.305	-	0.430	0.038	0.535	-0.073	0.442	0.075	-0.136	0.475	1

Covariance	*Cu ppm (GA115)*	*Au ppm (GA334)*	*Au (R) (GA334)*	*Ag ppm (GA115)*	*Mo ppm (GA115)*	*Mn ppm (GA115)*	*Pb ppm (GA115)*	*Zn ppm (GA115)*	*Ba ppm (GX401)*	*As ppm (HA140)*	*Ni ppm (GA140)*	*Co ppm (GA140)*
Cu ppm (GA115)	109478.354											
Au ppm (GA334)	4.595	0.000										
Au (R) (GA334)	0.000	0.000	0.000									
Ag ppm (GA115)	33.813	0.002	0.000	0.025								
Mo ppm (GA115)	66.358	-0.017	0.000	2.997	1899.514							
Mn ppm (GA115)	-8488.854	-0.395	0.000	-0.002	-1401.272	41041.625						
Pb ppm (GA115)	-2297.827	-0.017	0.000	5.592	543.760	1009.496	7224.065					
Zn ppm (GA115)	-8269.860	-0.169	0.000	3.584	-1487.881	32234.439	8867.878	43294.567				
Ba ppm (GX401)	-213.206	-0.310	0.000	-10.602	214.450	-8668.742	-4504.070	256.314	335257.702			
As ppm (HA140)	-598.254	-0.023	0.000	0.365	-31.301	257.874	300.567	241.043	-1089.535	153.121		
Ni ppm (GA140)	-9.057	0.002	0.000	-0.113	-62.700	1511.460	-135.196	1015.954	-669.362	4.396	126.430	
Co ppm (GA140)	832.602	0.036	0.000	0.489	12.050	778.694	-44.376	660.897	310.570	-12.083	38.418	51.634

ANALYTICAL METHODS

Element	Method	Laboratory	LDL (ppm)	UDL (ppm)	Pocedure
Cu	GA115/GA329	Analabs	0.05	1000	Digest with aqua regia followed by AAS determination, with MIBK (methyl iso-butyl ketone) extraction for gold (this latter for GA329)
Cu	GA104	Analabs	20	50,000	Total acid digestion (perchloric, aqua regia and hydrofluoric) followed by AAS determination
Au	GG334	Analabs	0.001	100	Aqua regia digest followed by carbon rod determination
Au	GG329	Analabs	0.02	20	Aqua regia digest followed by AAS determination
Ag	GA115/GA329	Analabs	0.1	20	Digest with aqua regia followed by AAS determination
Mo	GA115/GA329	Analabs	1	100	Digest with aqua regia followed by AAS determination
Mn	GA115/GA329	Analabs	0.5	1,000	Digest with aqua regia followed by AAS determination
Pb	GA115/GA329	Analabs	0.5	500	Digest with aqua regia followed by AAS determination
Zn	GA115/GA329	Analabs	0.5	1,000	Digest with aqua regia followed by AAS determination
Ba	GX401	Analabs	10	-	Pressed powder XRF
As	GA140 *	Analabs	50	5,000	Digest with aqua regia/perchloric acid followed by AAS determination
As	HA140/GA329	Analabs	0.5	50	Hydride generation followed by AAS determination
Ni	HA140/GA329	Analabs	3	10,000	Hydride generation followed by AAS determination
Co	HA140/GA329	Analabs	3	10,000	Hydride generation followed by AAS determination

* only one sample analysed by this method - all other samples below detection limit (for this method)

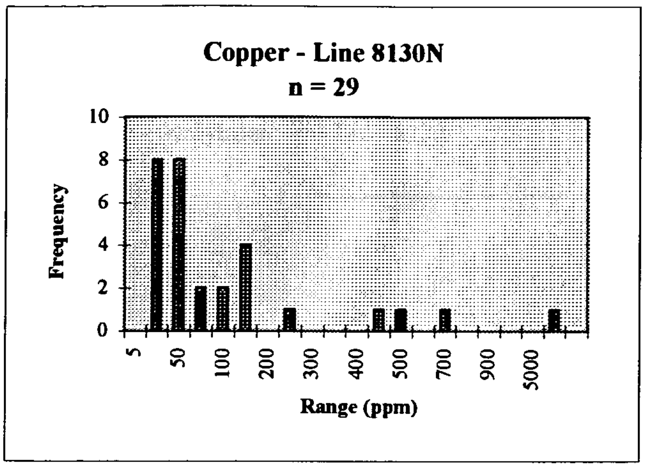
Copper - Line 8130N
n = 29
Frequency
0 2 4 6 8 10
5 50 100 200 300 400 500 700 900 5000
Range (ppm)

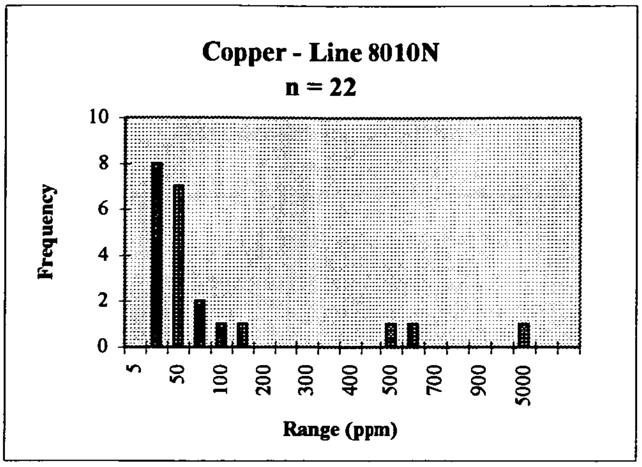
Copper - Line 8010N
n = 22
Frequency
0 2 4 6 8 10
5 50 100 200 300 400 500 700 900 5000
Range (ppm)

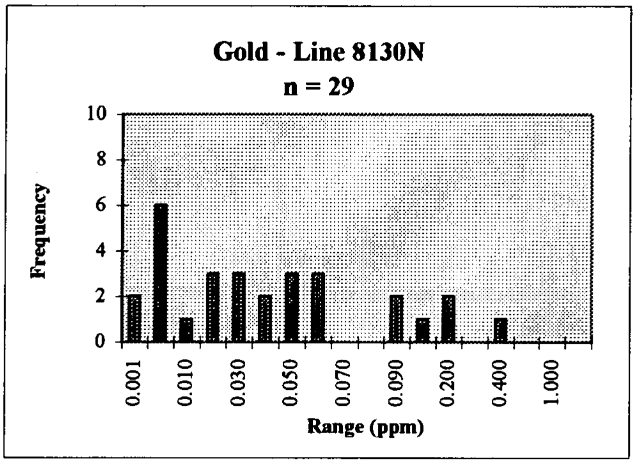
Gold - Line 8130N
n = 29
Frequency
0 2 4 6 8 10
0.001 0.010 0.030 0.050 0.070 0.090 0.200 0.400 1.000
Range (ppm)

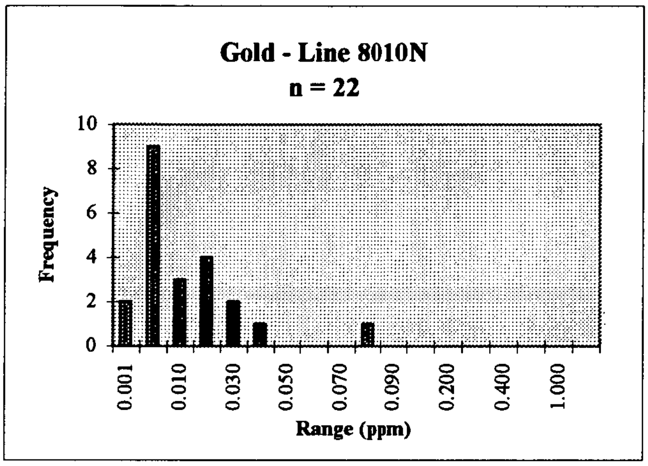
Gold - Line 8010N
n = 22
Frequency
0 2 4 6 8 10
0.001 0.010 0.030 0.050 0.070 0.090 0.200 0.400 1.000
Range (ppm)

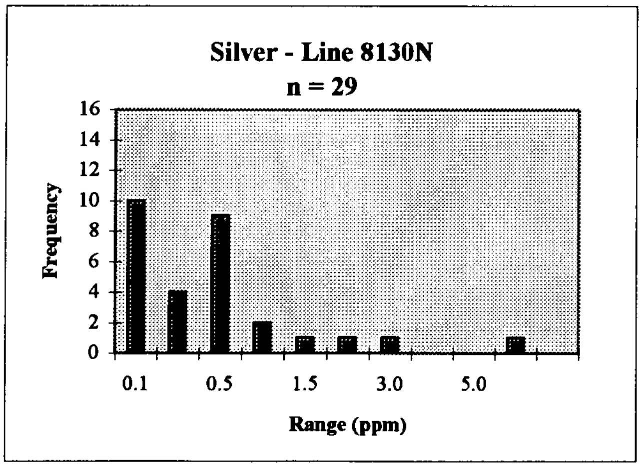
Silver - Line 8130N
n = 29
Frequency
0 2 4 6 8 10 12 14 16
0.1 0.5 1.5 3.0 5.0
Range (ppm)

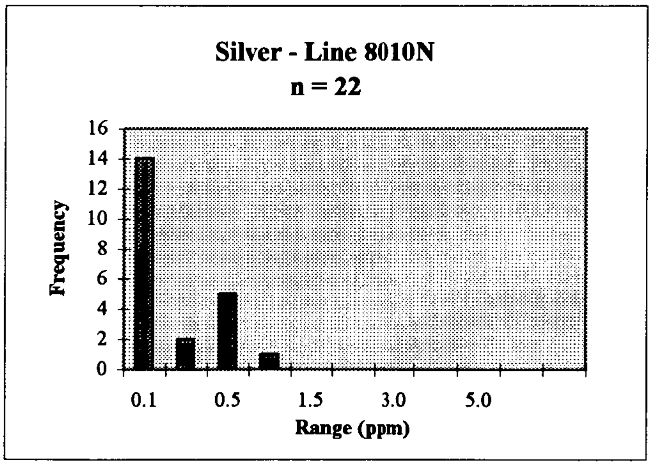
Silver - Line 8010N
n = 22
Frequency
0 2 4 6 8 10 12 14 16
0.1 0.5 1.5 3.0 5.0
Range (ppm)

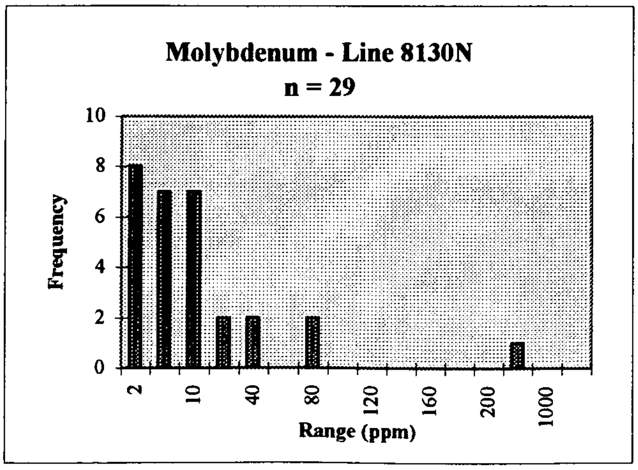
Molybdenum - Line 8130N
n = 29
Frequency
0 2 4 6 8 10
2 10 40 80 120 160 200 1000
Range (ppm)

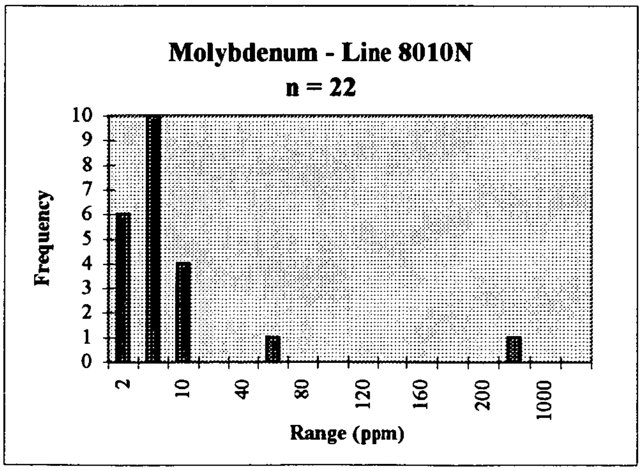
Molybdenum - Line 8010N
n = 22
Frequency
0 1 2 3 4 5 6 7 8 9 10
2 10 40 80 120 160 200 1000
Range (ppm)

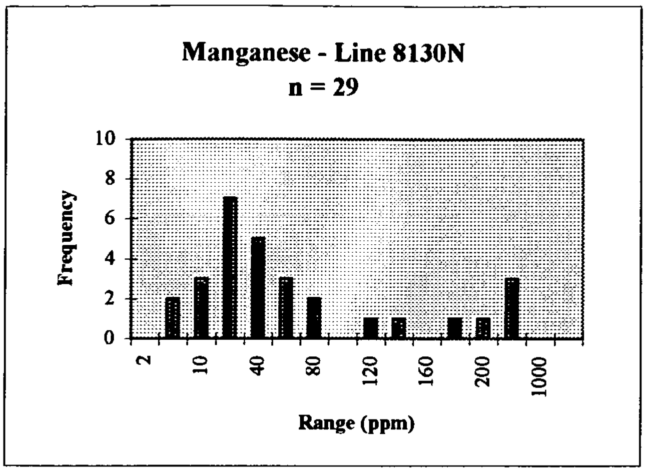
Manganese - Line 8130N
n = 29
Frequency
Range (ppm)
2
10
40
80
120
160
200
1000

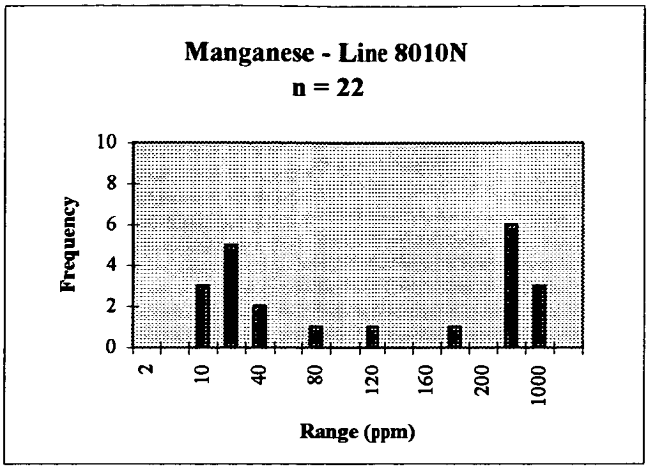
Manganese - Line 8010N
n = 22
Frequency
Range (ppm)
2
10
40
80
120
160
200
1000

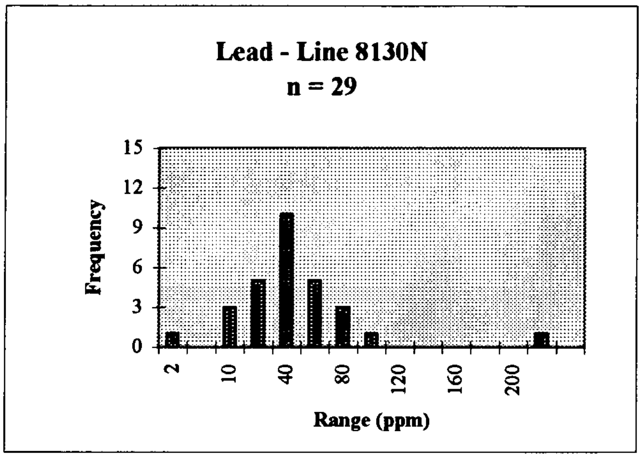
Lead - Line 8130N
n = 29
Frequency
Range (ppm)
2
10
40
80
120
160
200

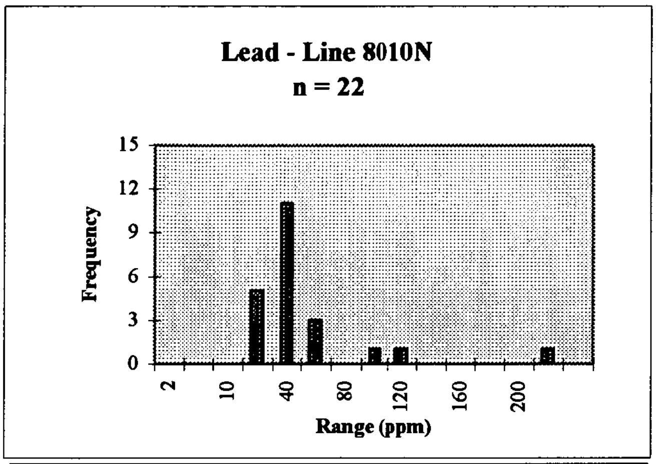
Lead - Line 8010N
n = 22
Frequency
Range (ppm)
2
10
40
80
120
160
200

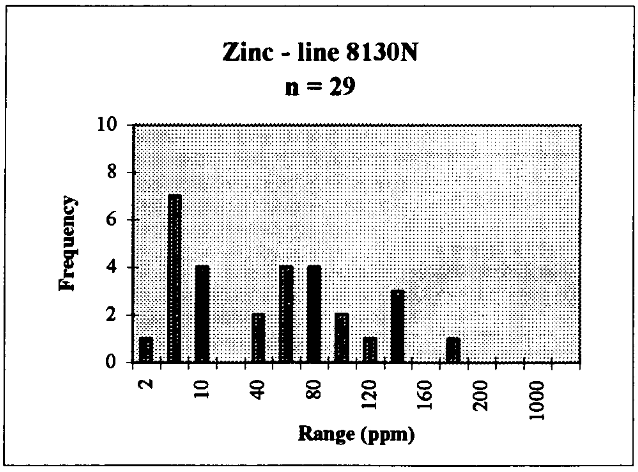
Zinc - line 8130N
n = 29
Frequency
Range (ppm)
2
10
40
80
120
160
200
1000

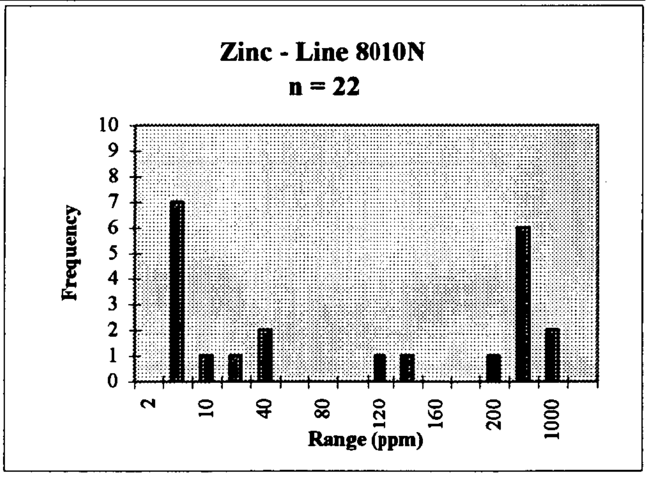
Zinc - Line 8010N
n = 22
Frequency
Range (ppm)
2
10
40
80
120
160
200
1000

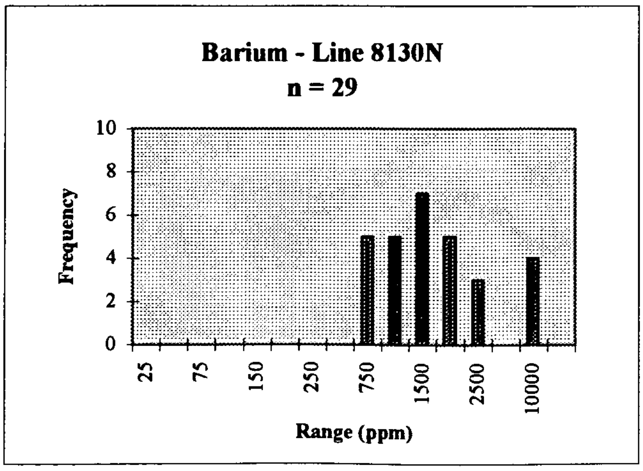
Barium - Line 8130N
n = 29
Frequency
Range (ppm)
25
75
150
250
750
1500
2500
10000

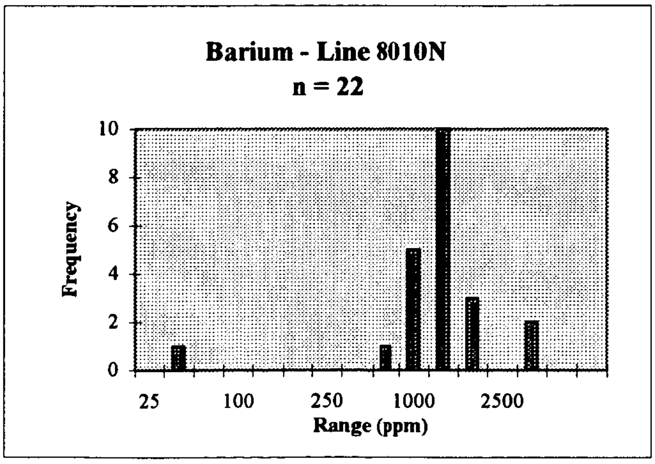
Barium - Line 8010N
n = 22
Frequency
Range (ppm)
25
100
250
1000
2500

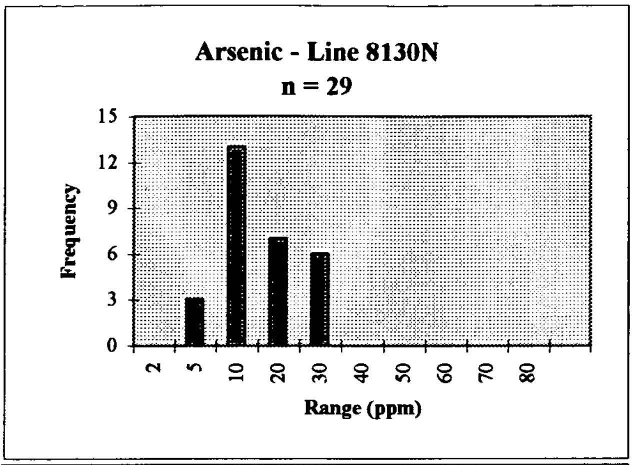
Arsenic - Line 8130N
n = 29
Frequency
Range (ppm)
2 5 10 20 30 40 50 60 70 80
0 3 6 9 12 15

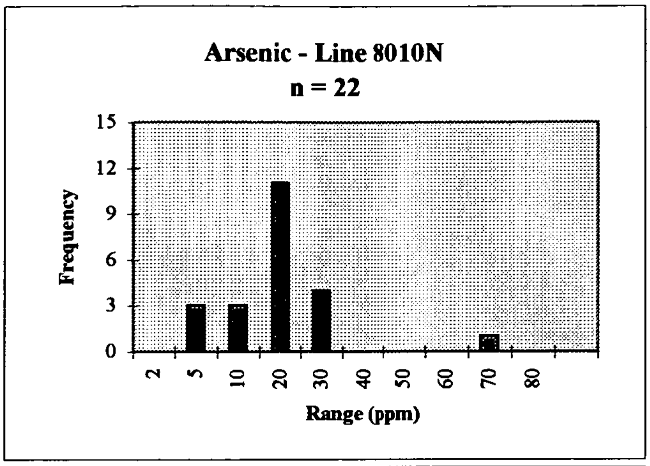
Arsenic - Line 8010N
n = 22
Frequency
Range (ppm)
2 5 10 20 30 40 50 60 70 80
0 3 6 9 12 15

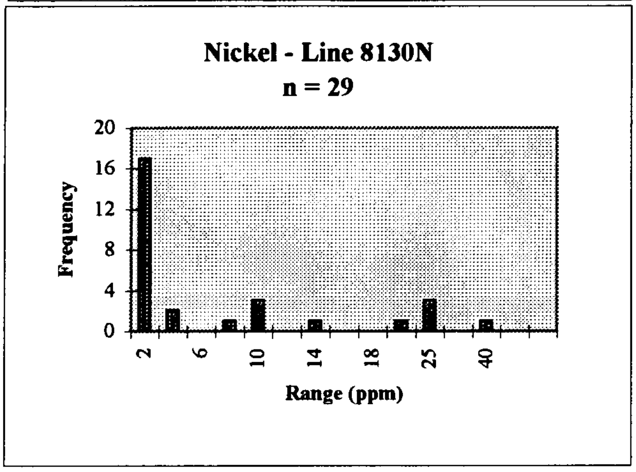
Nickel - Line 8130N
n = 29
Frequency
Range (ppm)
2 6 10 14 18 25 40
0 4 8 12 16 20

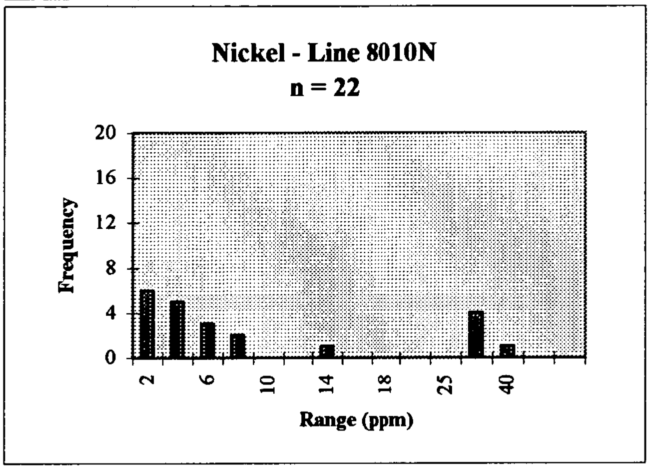
Nickel - Line 8010N
n = 22
Frequency
Range (ppm)
2 6 10 14 18 25 40
0 4 8 12 16 20

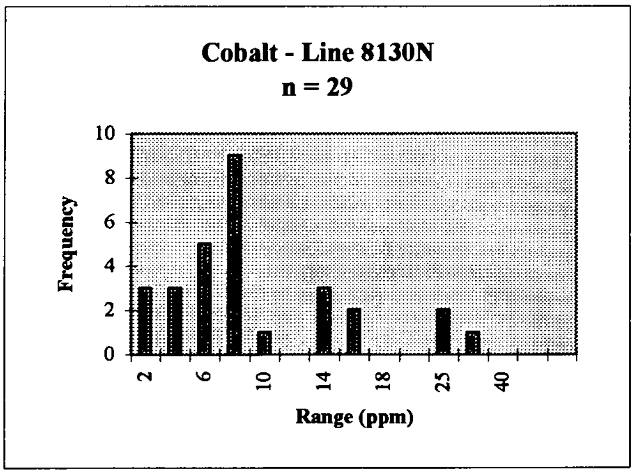
Cobalt - Line 8130N
n = 29
Frequency
Range (ppm)
2 6 10 14 18 25 40
0 2 4 6 8 10

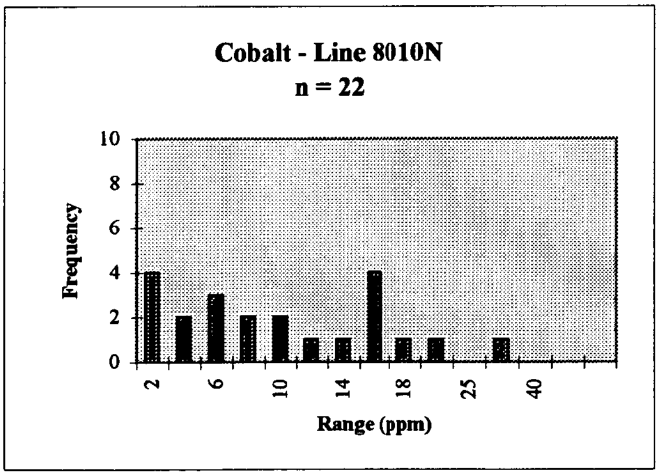
Cobalt - Line 8010N
n = 22
Frequency
Range (ppm)
2 6 10 14 18 25 40
0 2 4 6 8 10

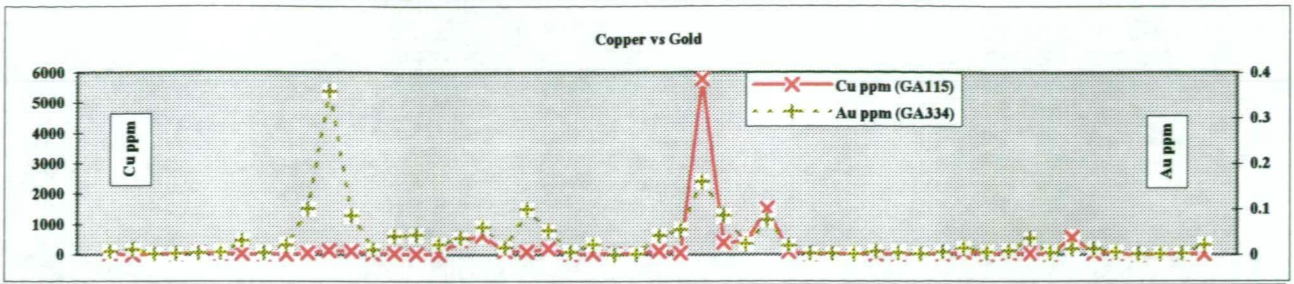
Copper vs Gold
Cu ppm (GA115)
Au ppm (GA334)
Cu ppm
Au ppm
6000
5000
4000
3000
2000
1000
0
0.4
0.3
0.2
0.1
0

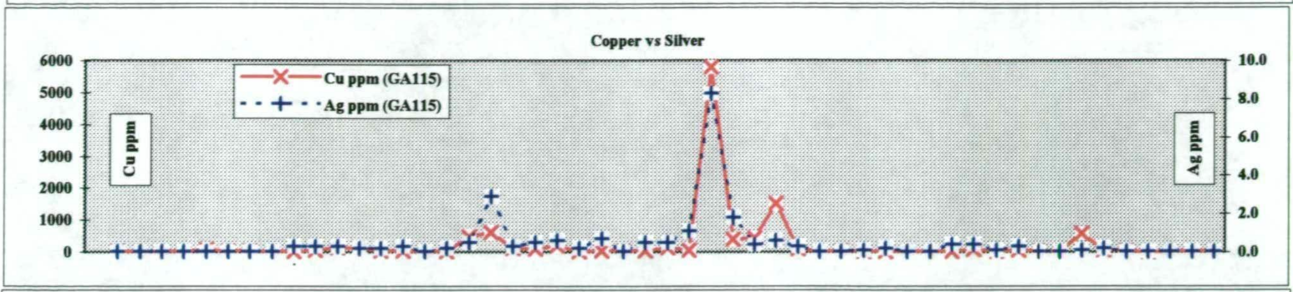
Copper vs Silver
Cu ppm (GA115)
Ag ppm (GA115)
Cu ppm
Ag ppm
6000
5000
4000
3000
2000
1000
0
10.0
8.0
6.0
4.0
2.0
0.0

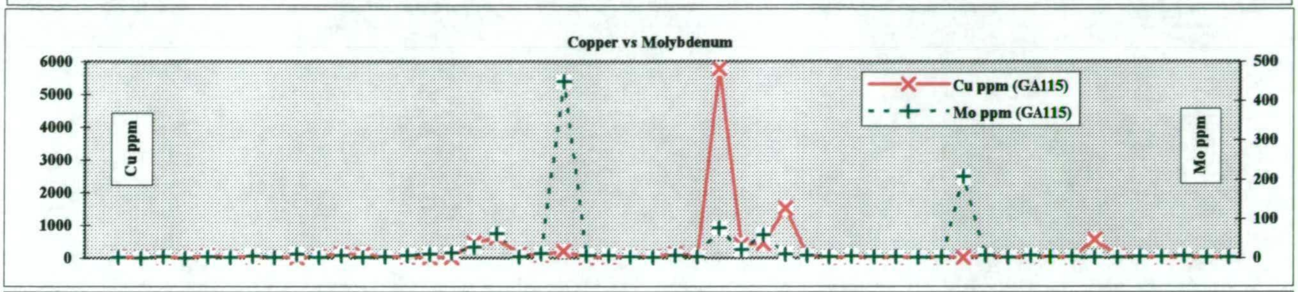
Copper vs Molybdenum
Cu ppm (GA115)
Mo ppm (GA115)
Cu ppm
Mo ppm
6000
5000
4000
3000
2000
1000
0
500
400
300
200
100
0

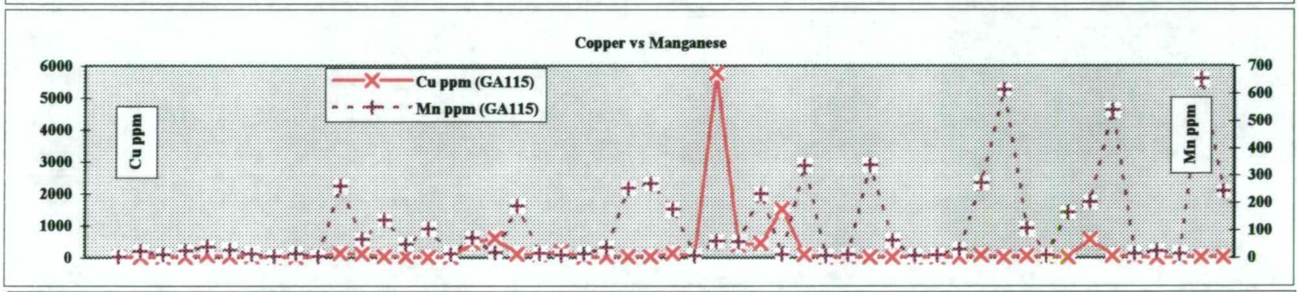
Copper vs Manganese
Cu ppm (GA115)
Mn ppm (GA115)
Cu ppm
Mn ppm
6000
5000
4000
3000
2000
1000
0
700
600
500
400
300
200
100
0

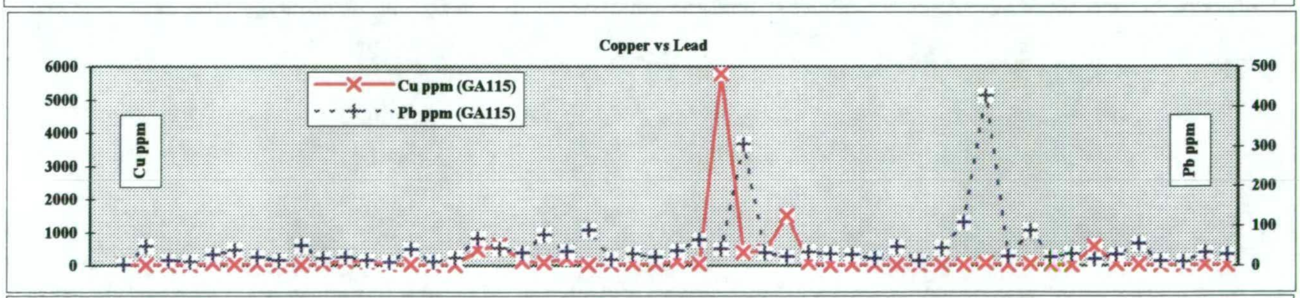
Copper vs Lead
Cu ppm (GA115)
Pb ppm (GA115)
Cu ppm
Pb ppm
6000
5000
4000
3000
2000
1000
0
500
400
300
200
100
0

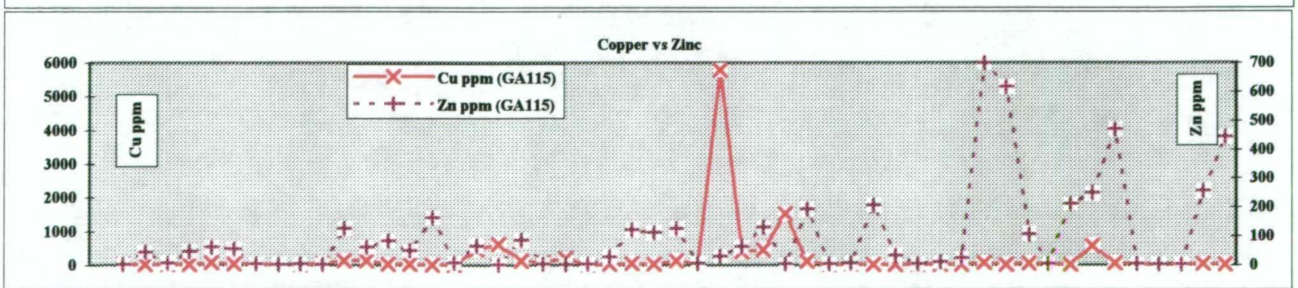
Copper vs Zinc
Cu ppm (GA115)
Zn ppm (GA115)
Cu ppm
Zn ppm
6000
5000
4000
3000
2000
1000
0
700
600
500
400
300
200
100
0

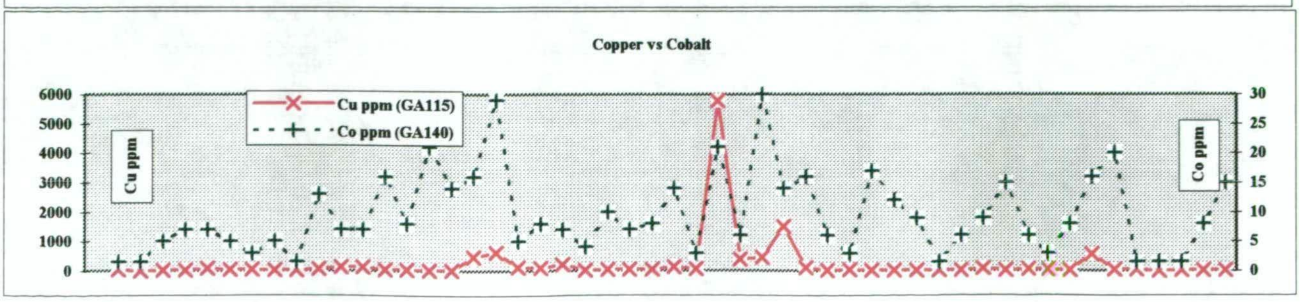
Copper vs Cobalt
Cu ppm (GA115)
Co ppm (GA140)
Cu ppm
Co ppm
6000
5000
4000
3000
2000
1000
0
30
25
20
15
10
5
0

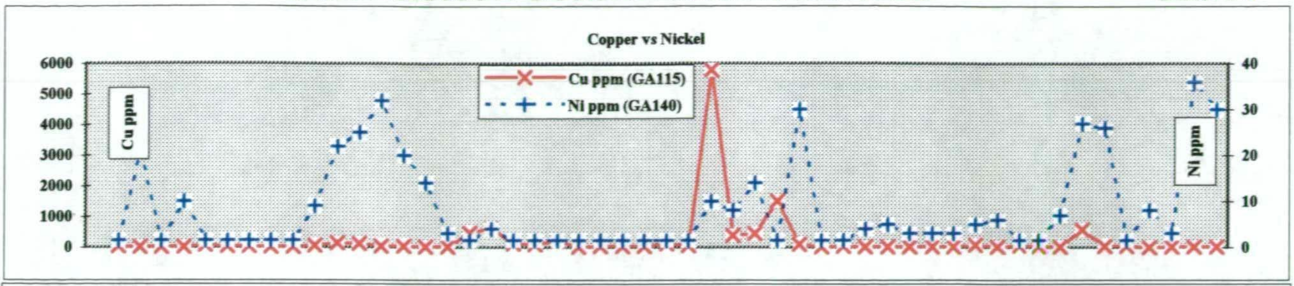

Copper vs Nickel
Cu ppm (GA115)
Ni ppm (GA140)
Cu ppm
Ni ppm

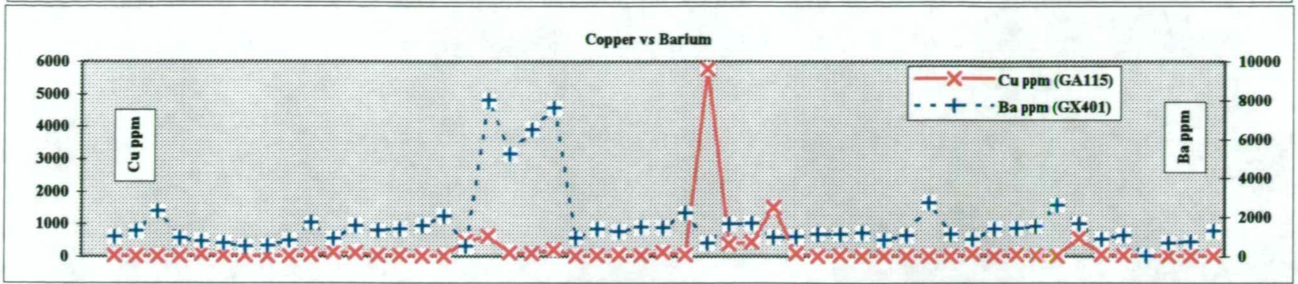

Copper vs Barium
Cu ppm (GA115)
Ba ppm (GX401)
Cu ppm
Ba ppm

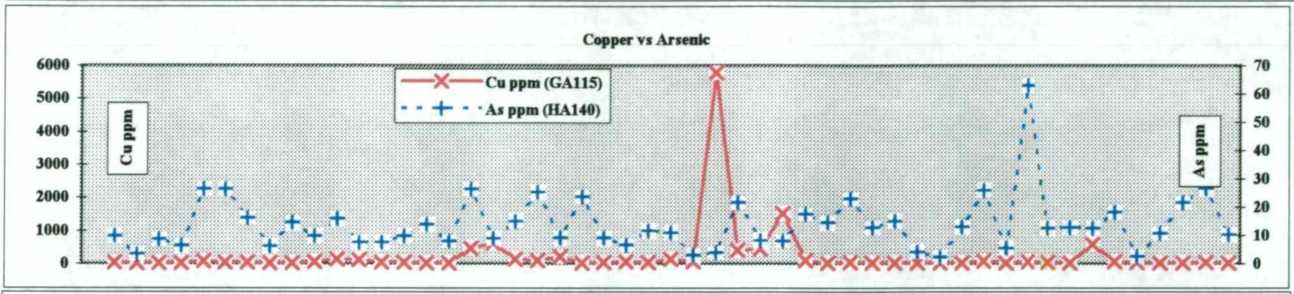

Copper vs Arsenic
Cu ppm (GA115)
As ppm (HA140)
Cu ppm
As ppm

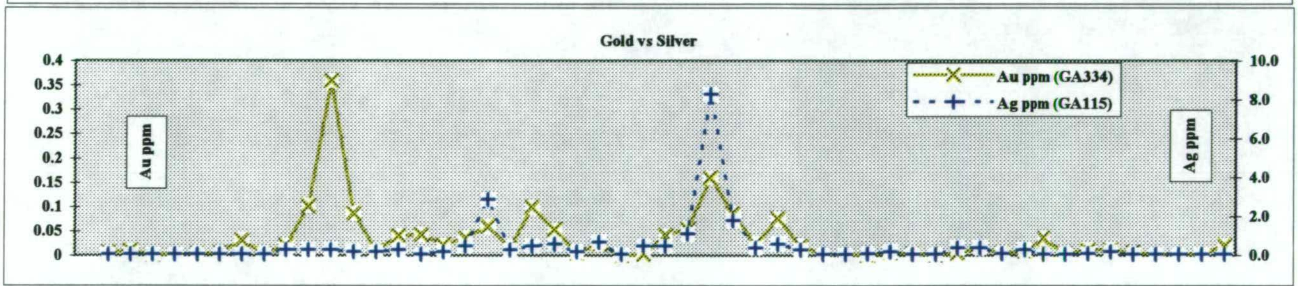

Gold vs Silver
Au ppm (GA334)
Ag ppm (GA115)
Au ppm
Ag ppm

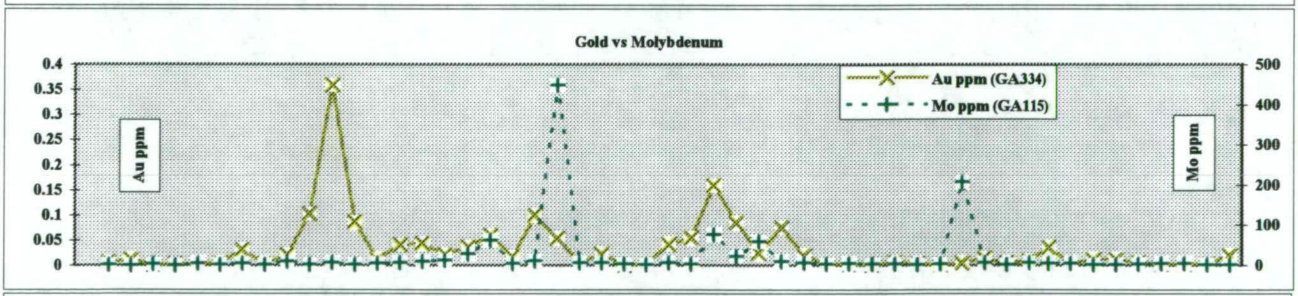

Gold vs Molybdenum
Au ppm (GA334)
Mo ppm (GA115)
Au ppm
Mo ppm

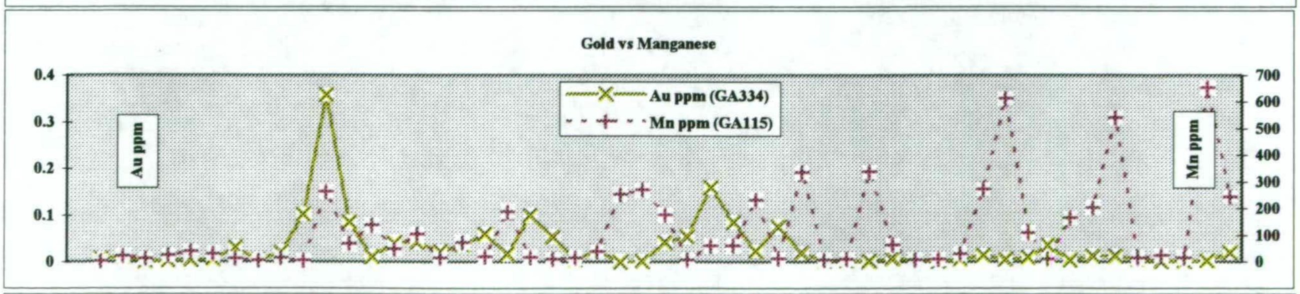

Gold vs Manganese
Au ppm (GA334)
Mn ppm (GA115)
Au ppm
Mn ppm

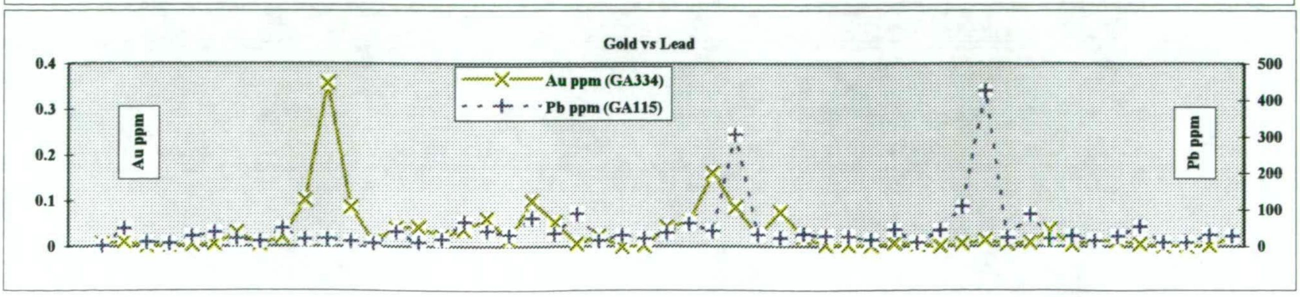

Gold vs Lead
Au ppm (GA334)
Pb ppm (GA115)
Au ppm
Pb ppm

ROYAL THARSIS - SURFACE GEOCHEMISTRY ORIENTATION CORRELATION PROFILES

Appendix I
Chart 2

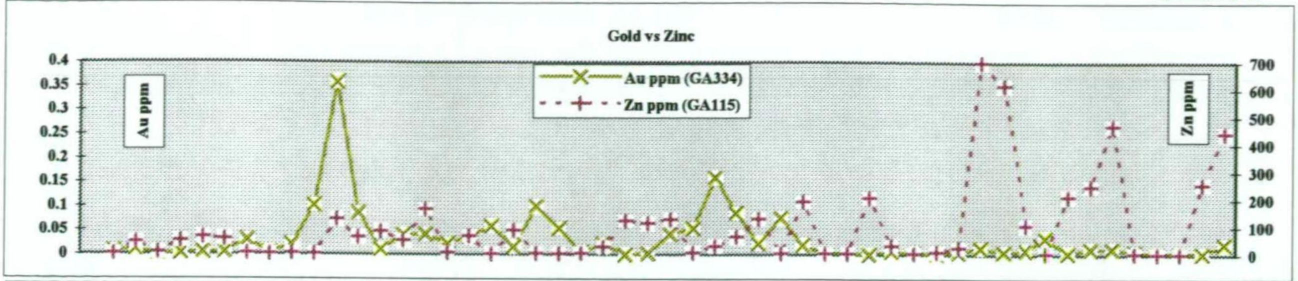

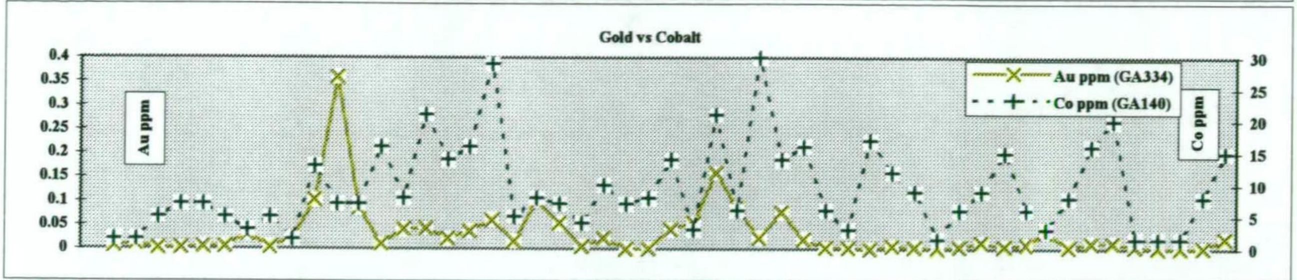

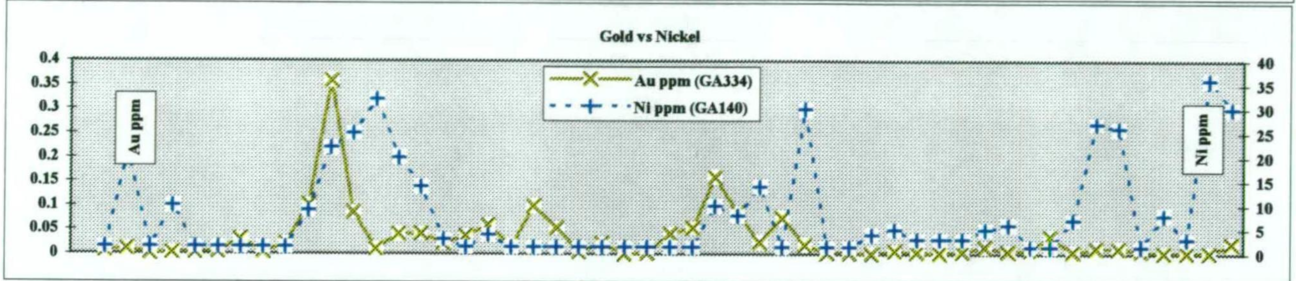

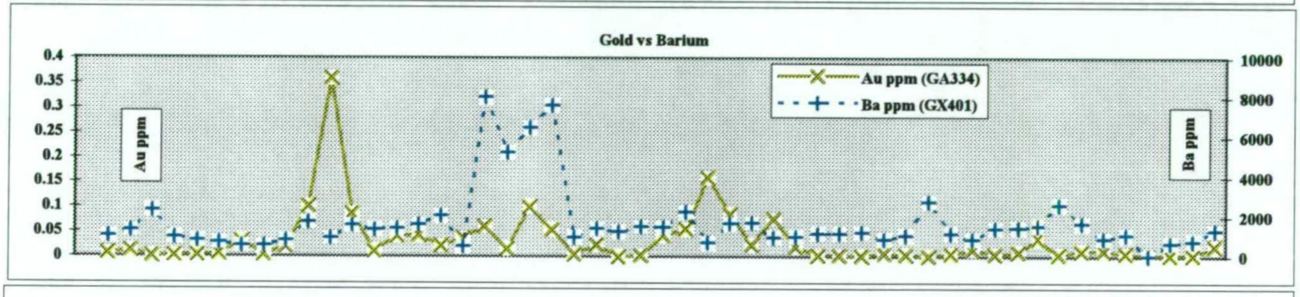

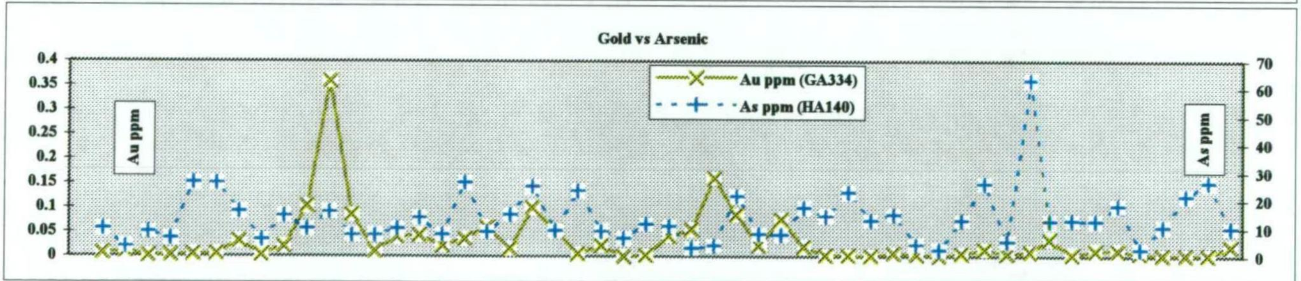

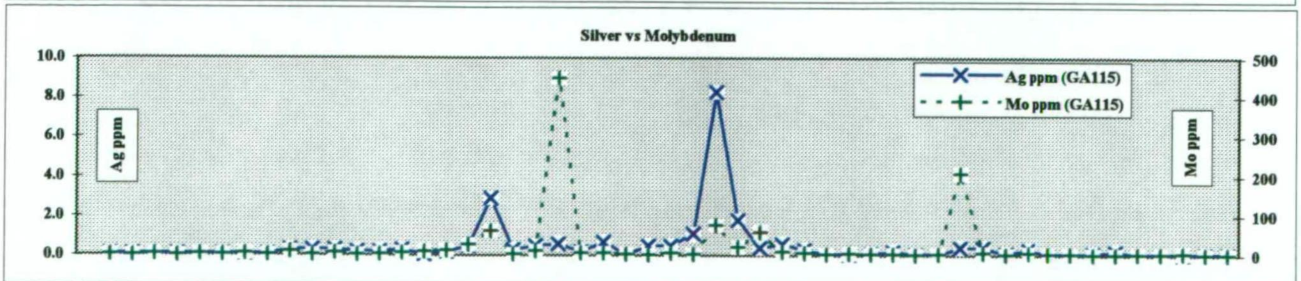

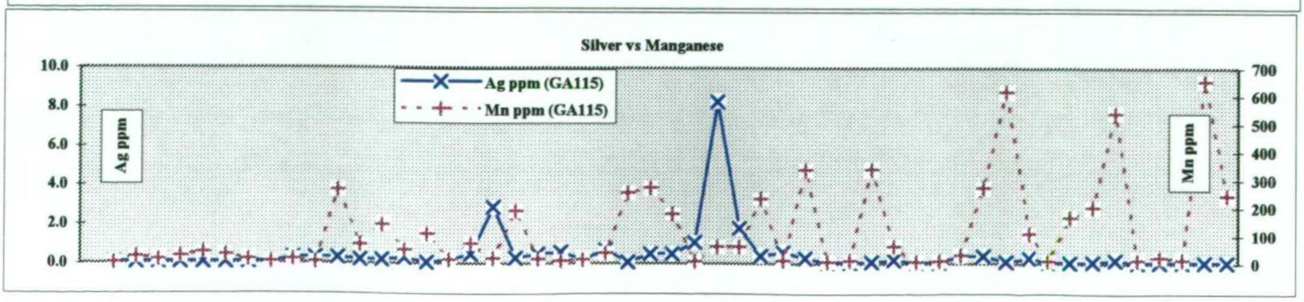

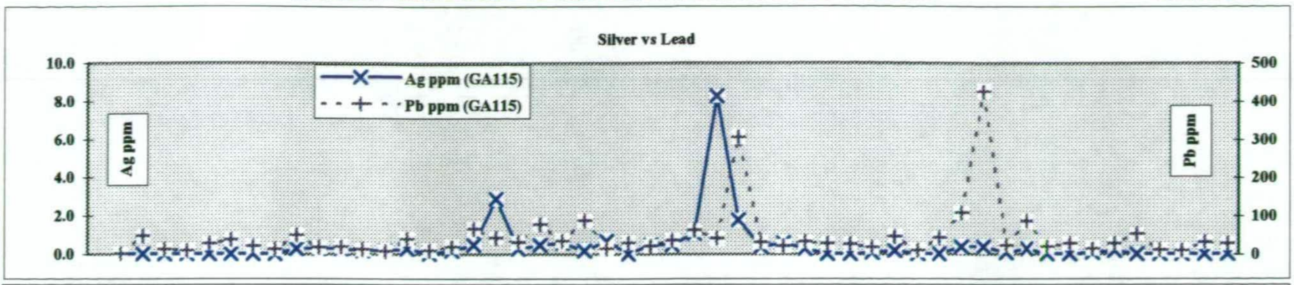
Silver vs Lead
Ag ppm (GA115)
Pb ppm (GA115)
Ag ppm
Pb ppm
10.0
8.0
6.0
4.0
2.0
0.0
500
400
300
200
100
0

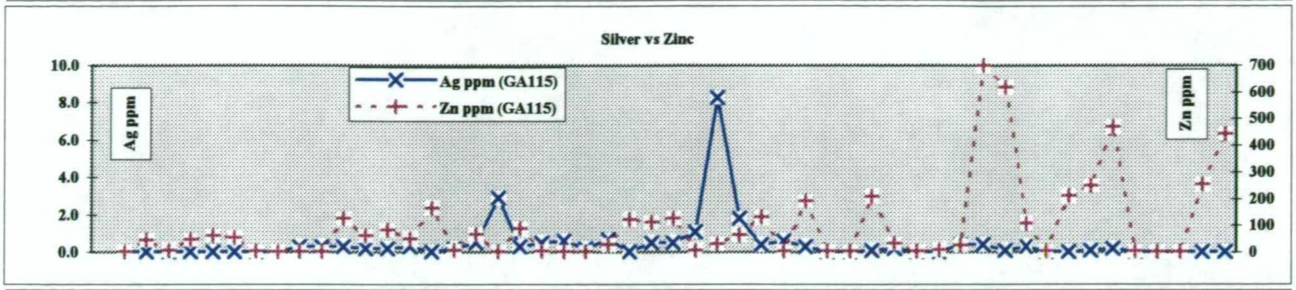
Silver vs Zinc
Ag ppm (GA115)
Zn ppm (GA115)
Ag ppm
Zn ppm
10.0
8.0
6.0
4.0
2.0
0.0
700
600
500
400
300
200
100
0

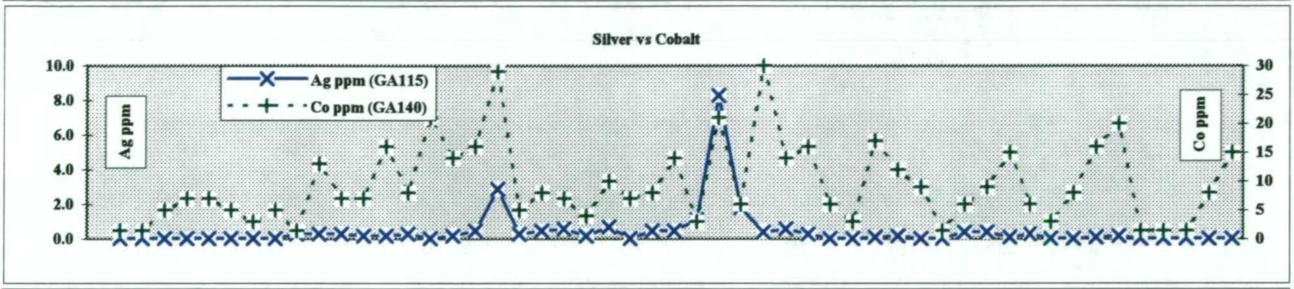
Silver vs Cobalt
Ag ppm (GA115)
Co ppm (GA140)
Ag ppm
Co ppm
10.0
8.0
6.0
4.0
2.0
0.0
30
25
20
15
10
5
0

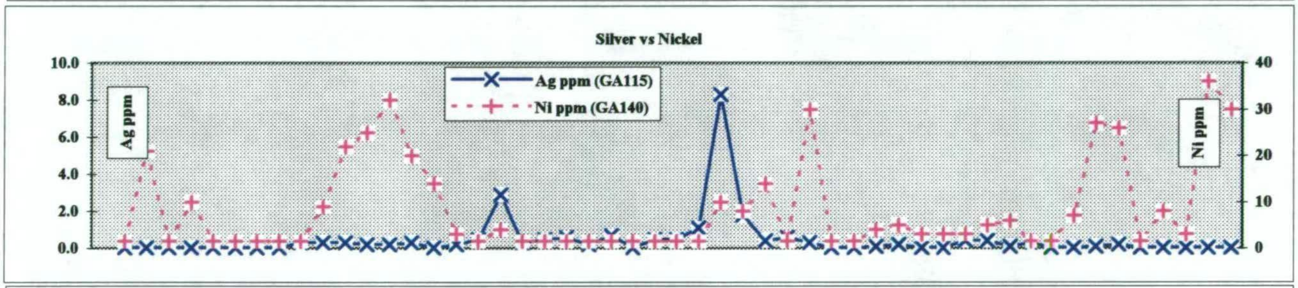
Silver vs Nickel
Ag ppm (GA115)
Ni ppm (GA140)
Ag ppm
Ni ppm
10.0
8.0
6.0
4.0
2.0
0.0
40
30
20
10
0

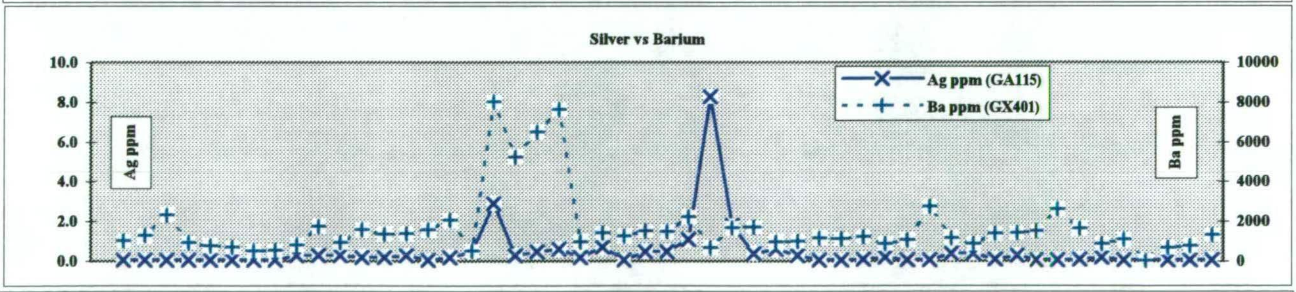
Silver vs Barium
Ag ppm (GA115)
Ba ppm (GX401)
Ag ppm
Ba ppm
10.0
8.0
6.0
4.0
2.0
0.0
10000
8000
6000
4000
2000
0

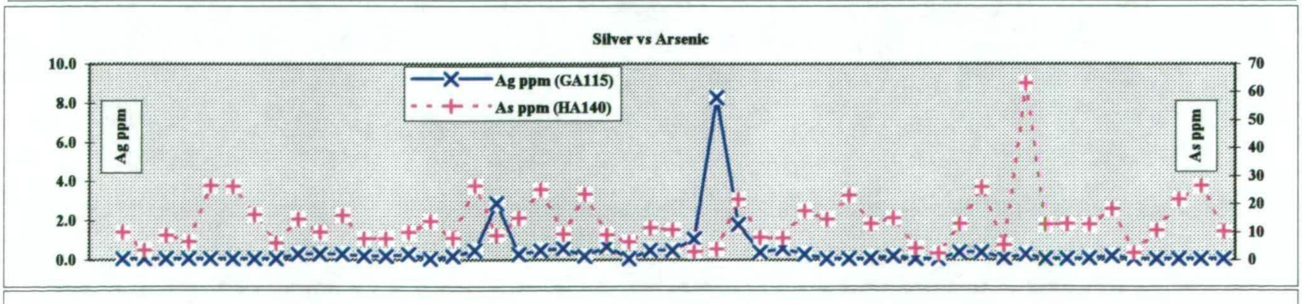
Silver vs Arsenic
Ag ppm (GA115)
As ppm (HA140)
Ag ppm
As ppm
10.0
8.0
6.0
4.0
2.0
0.0
70
60
50
40
30
20
10
0

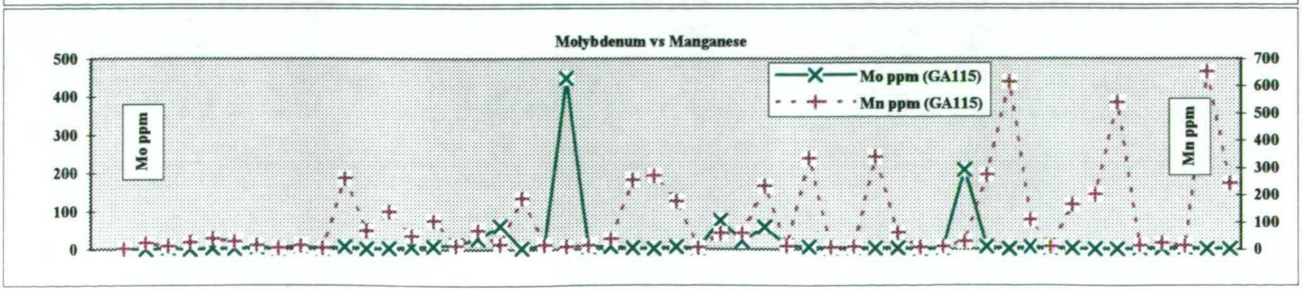
Molybdenum vs Manganese
Mo ppm (GA115)
Mn ppm (GA115)
Mo ppm
Mn ppm
500
400
300
200
100
0
700
600
500
400
300
200
100
0

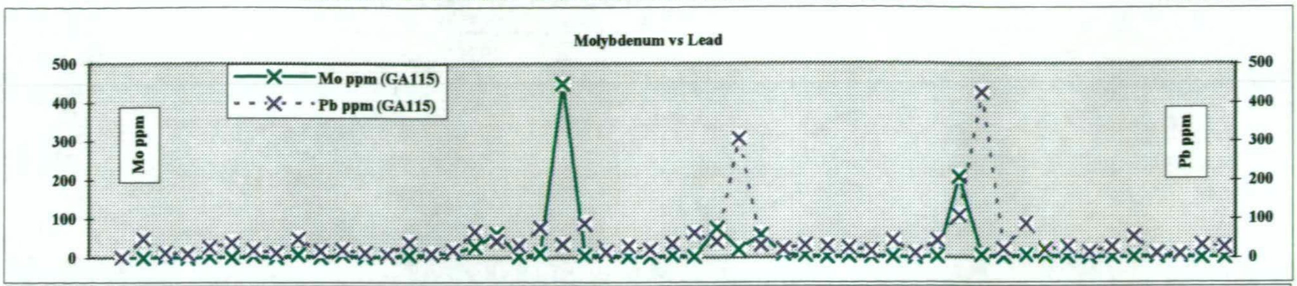
Molybdenum vs Lead
Mo ppm (GA115)
Pb ppm (GA115)
Mo ppm
Pb ppm
500
400
300
200
100
0

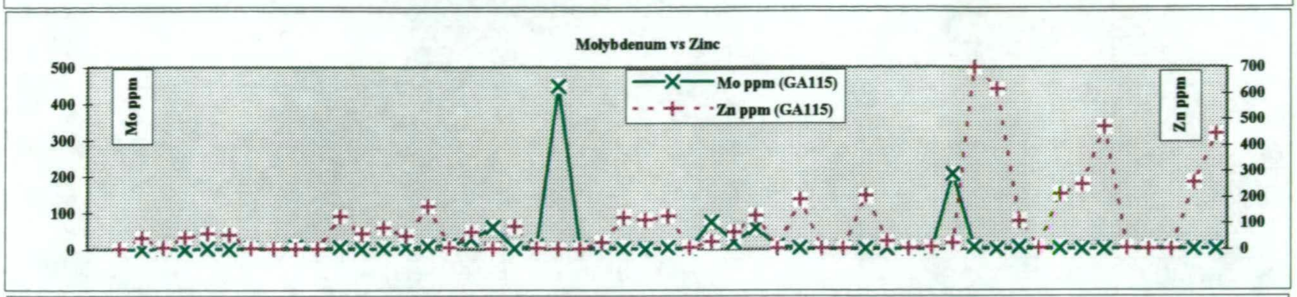
Molybdenum vs Zinc
Mo ppm (GA115)
Zn ppm (GA115)
Mo ppm
Zn ppm
500
400
300
200
100
0
700
600

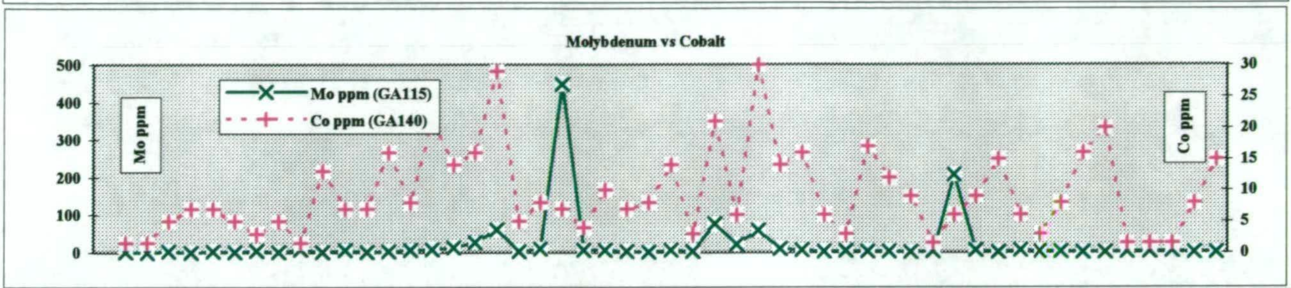
Molybdenum vs Cobalt
Mo ppm (GA115)
Co ppm (GA140)
Mo ppm
Co ppm
500
400
300
200
100
0
30
25
20
15
10
5

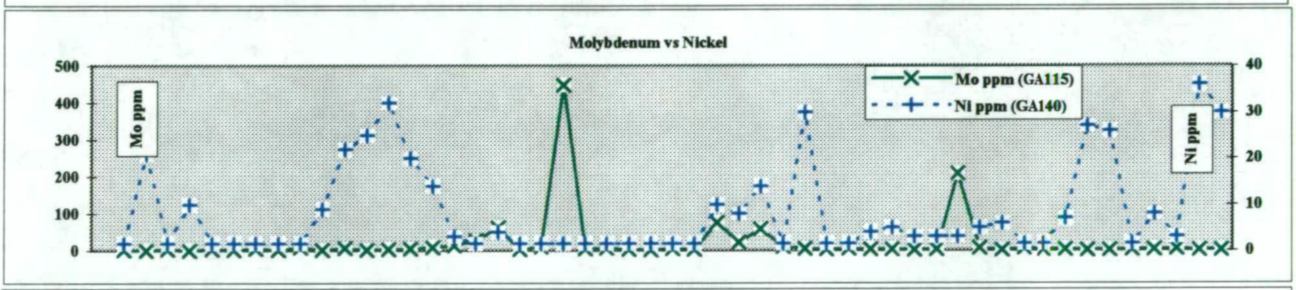
Molybdenum vs Nickel
Mo ppm (GA115)
Ni ppm (GA140)
Mo ppm
Ni ppm
500
400
300
200
100
0
40
30
20
10

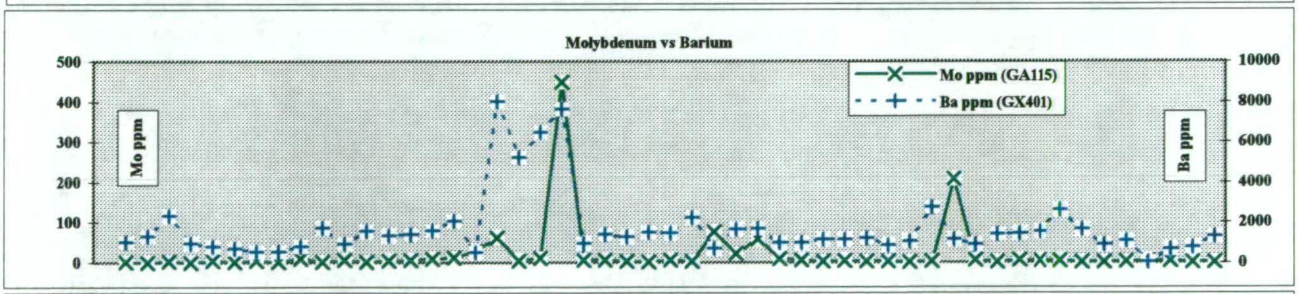
Molybdenum vs Barium
Mo ppm (GA115)
Ba ppm (GX401)
Mo ppm
Ba ppm
500
400
300
200
100
0
10000
8000
6000
4000
2000

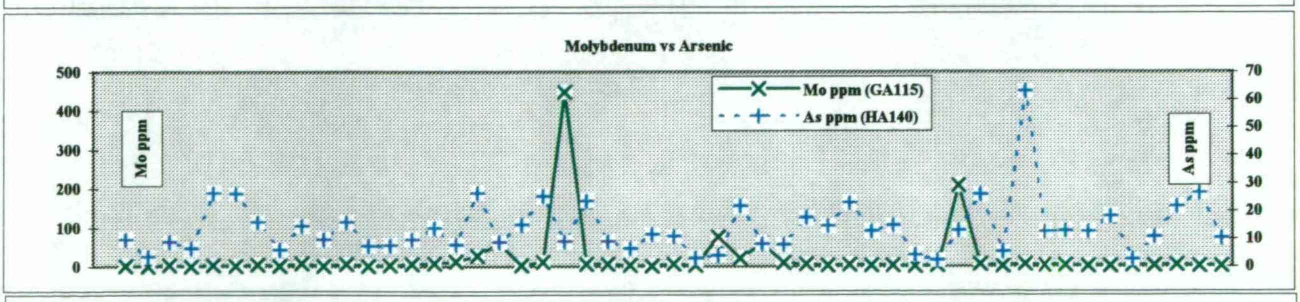
Molybdenum vs Arsenic
Mo ppm (GA115)
As ppm (HA140)
Mo ppm
As ppm
500
400
300
200
100
0
70
60
50
40
30
20
10

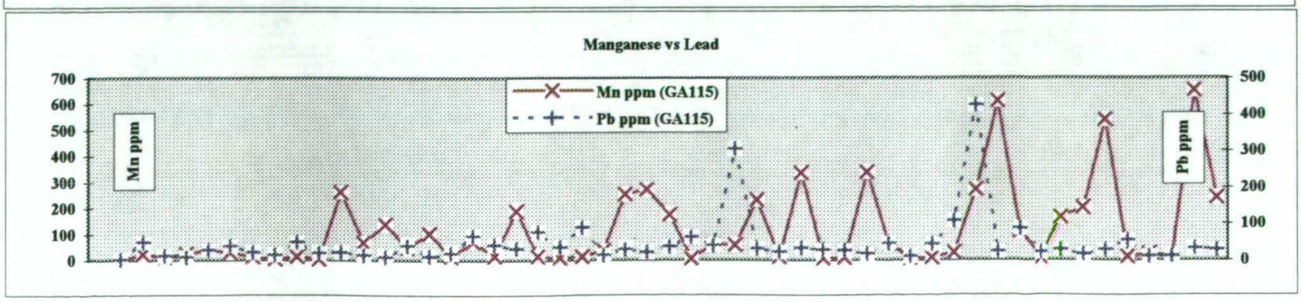
Manganese vs Lead
Mn ppm (GA115)
Pb ppm (GA115)
Mn ppm
Pb ppm
700
600
500
400
300
200
100
0

ROYAL THARSIS - SURFACE GEOCHEMISTRY ORIENTATION CORRELATION PROFILES

Appendix I
Chart 2

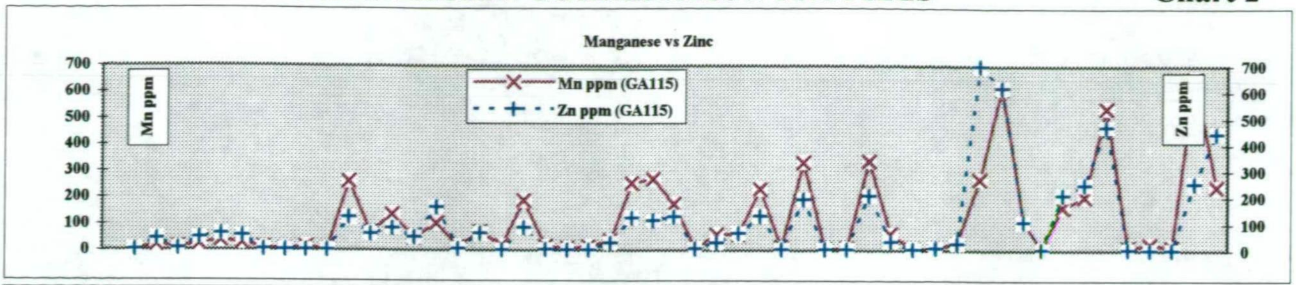

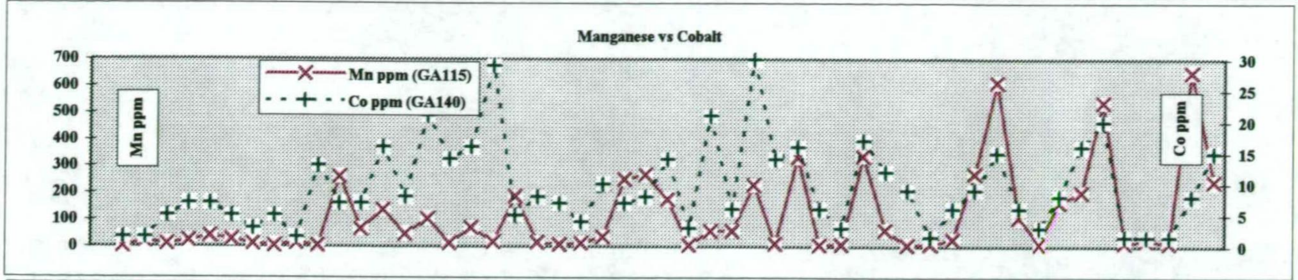

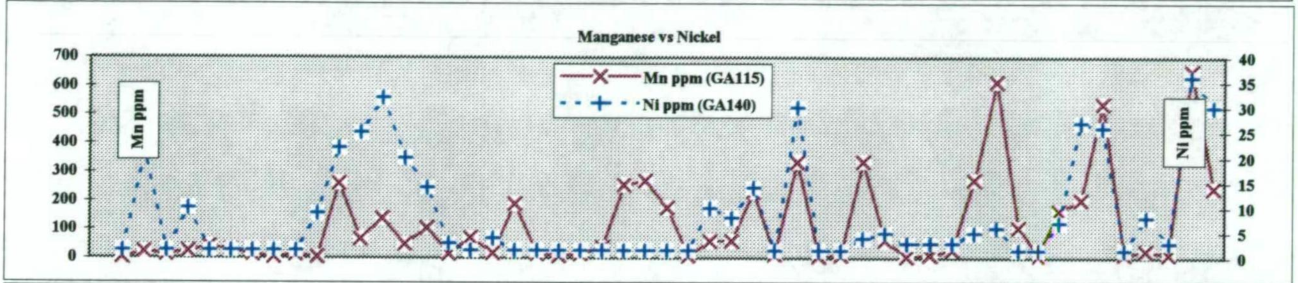

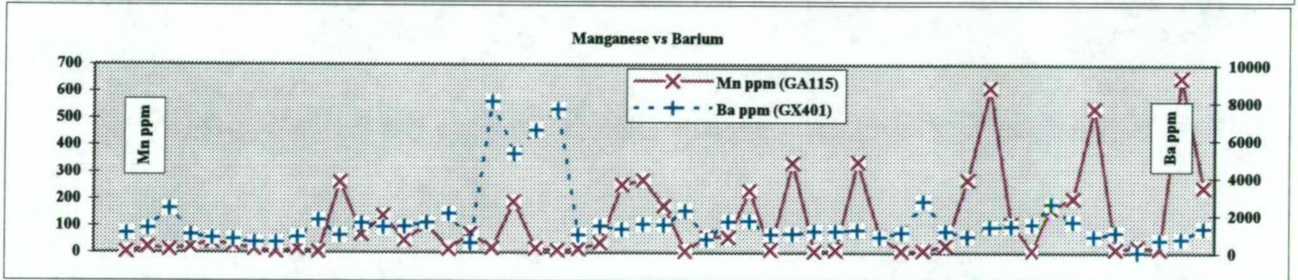

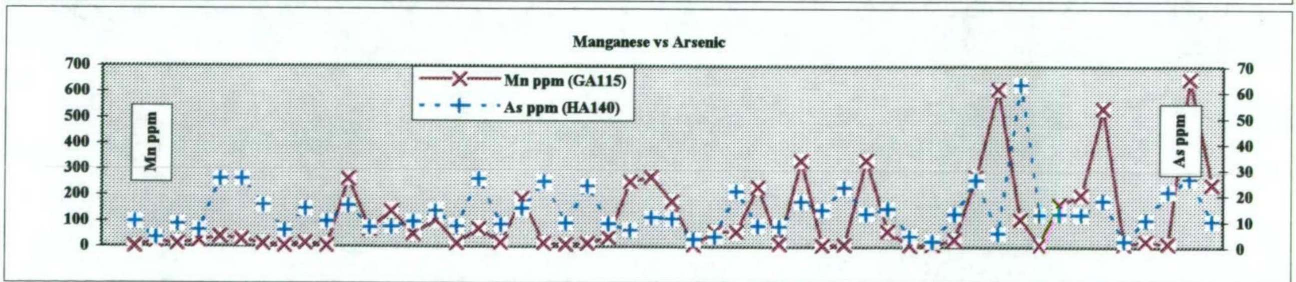

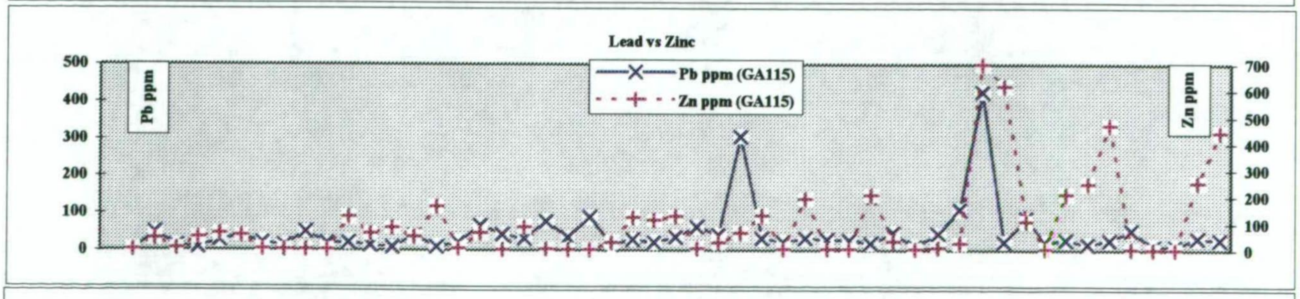

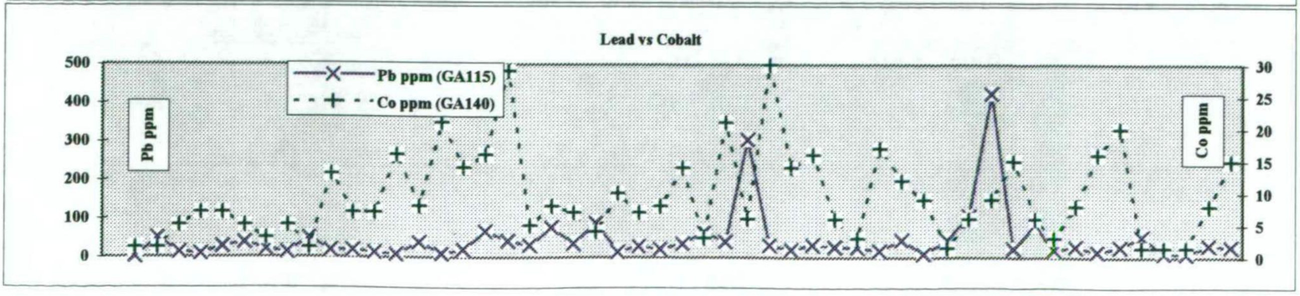

ROYAL THARSIS - SURFACE GEOCHEMISTRY ORIENTATION CORRELATION PROFILES

Appendix I
Chart 2

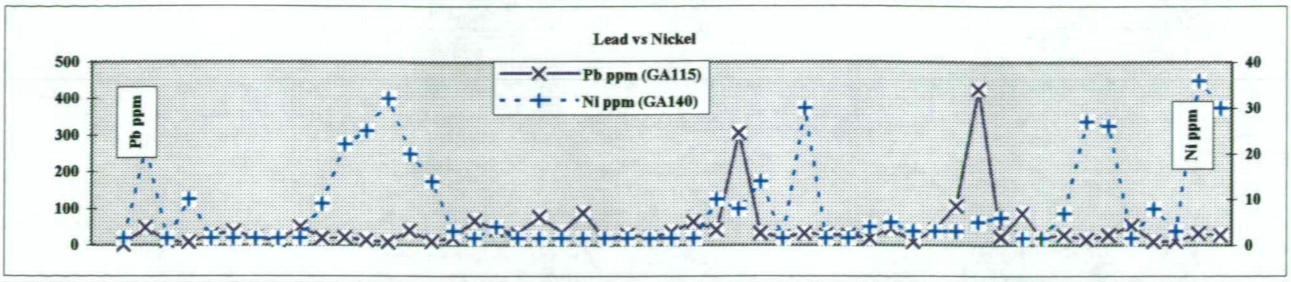

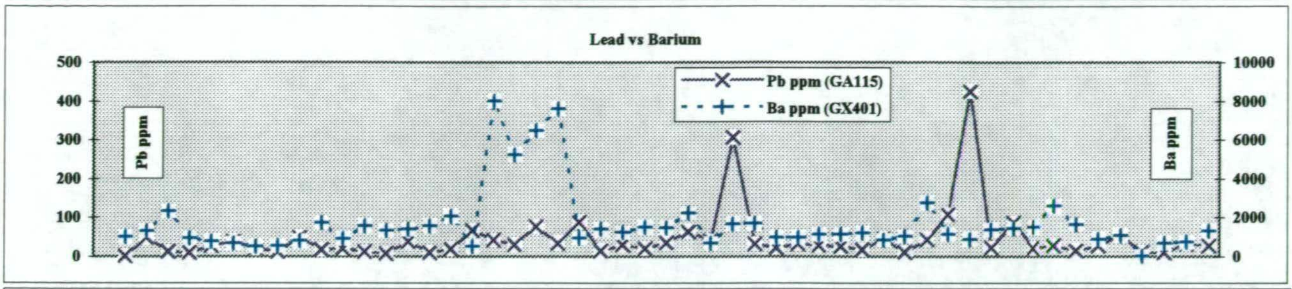

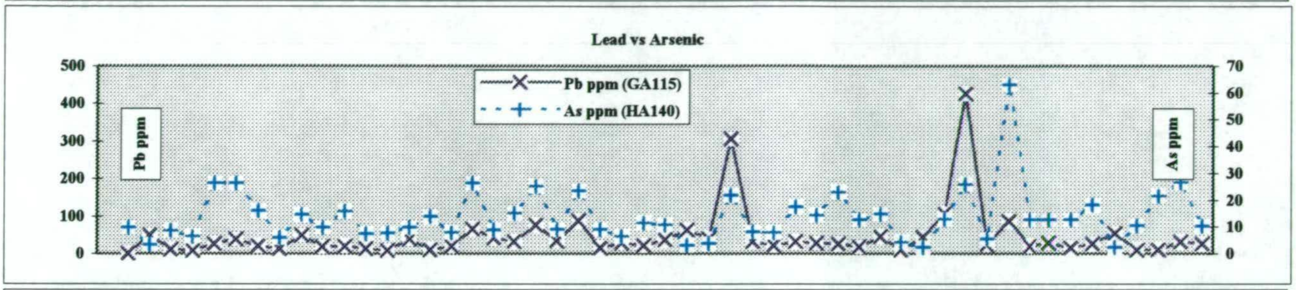

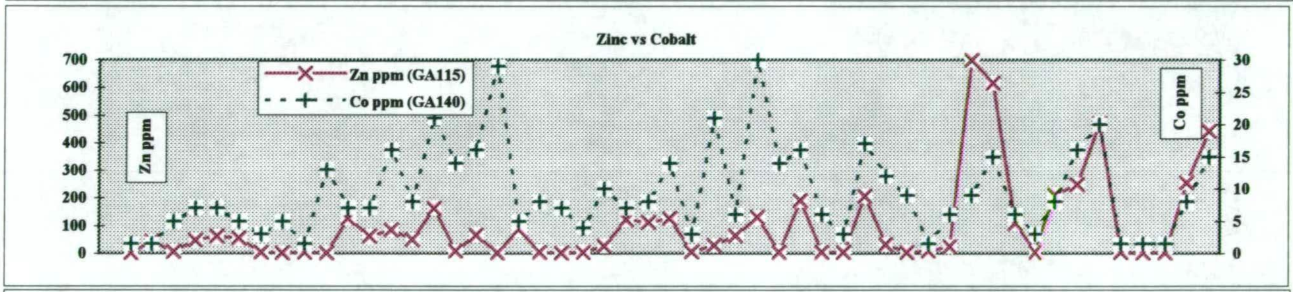

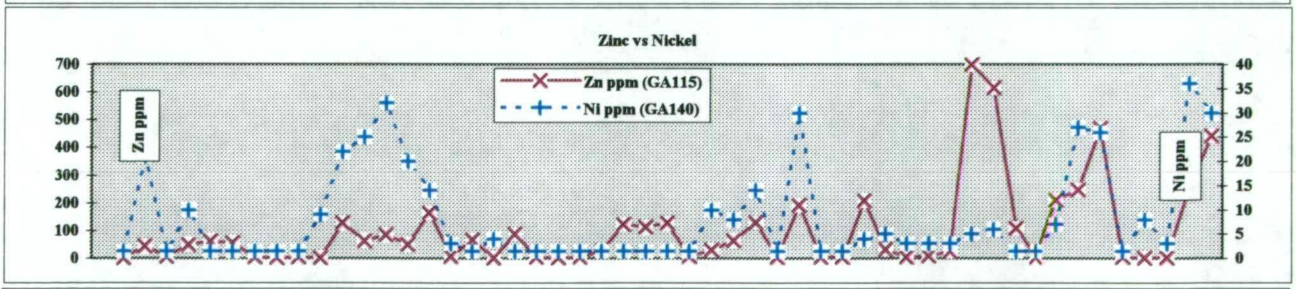

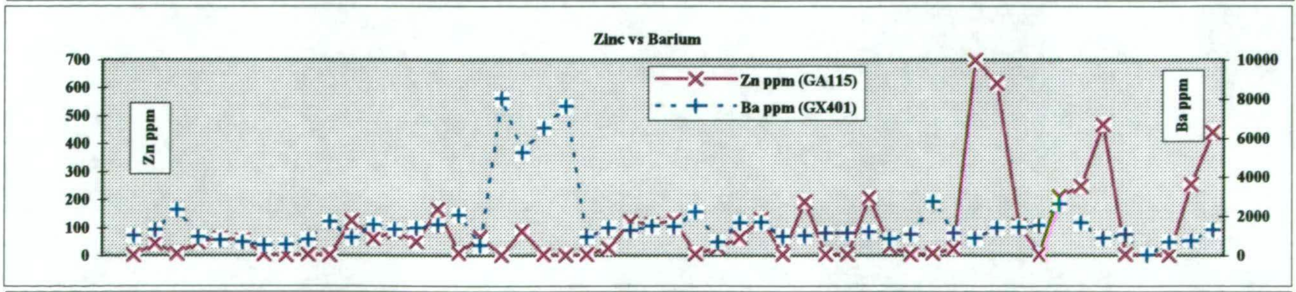

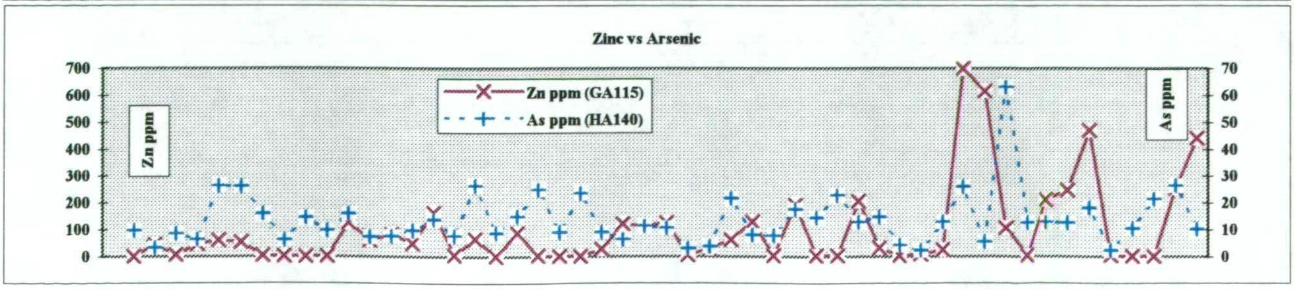

ROYAL THARSIS - SURFACE GEOCHEMISTRY
ORIENTATION CORRELATION PROFILES

Appendix I
Chart 2

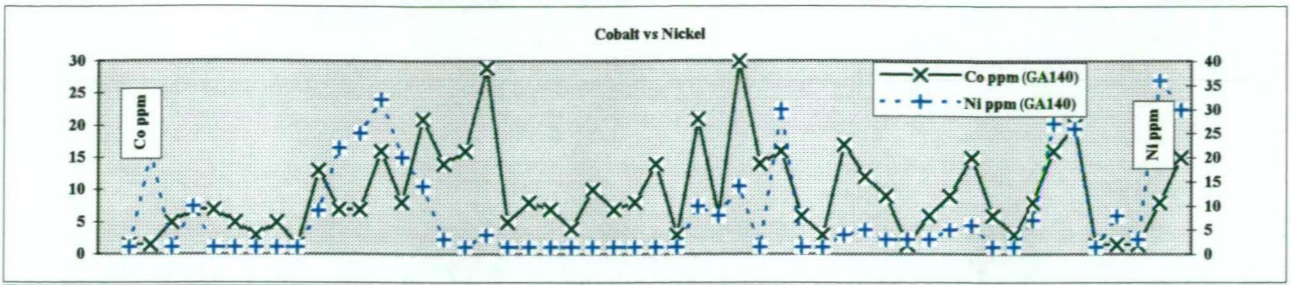

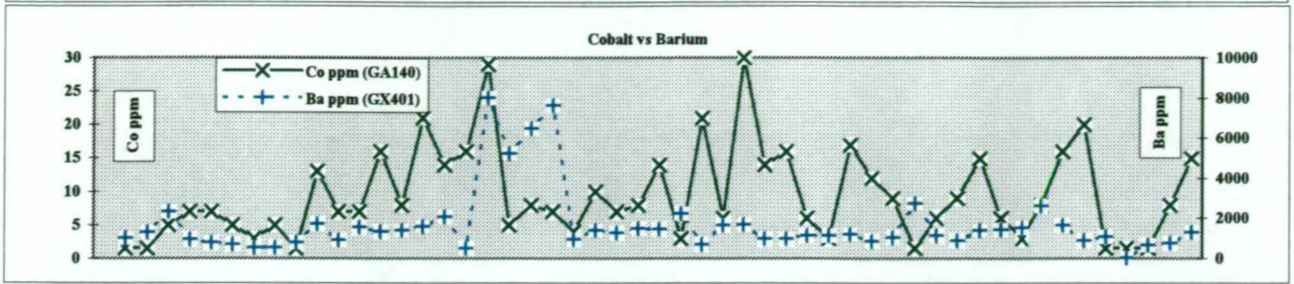

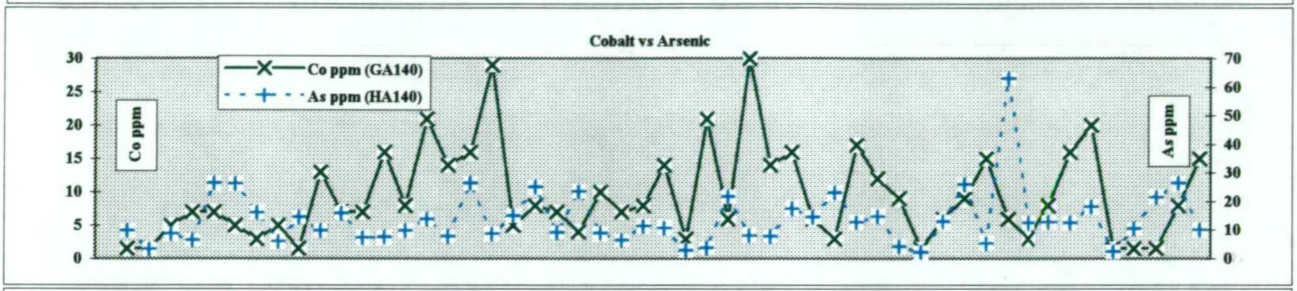

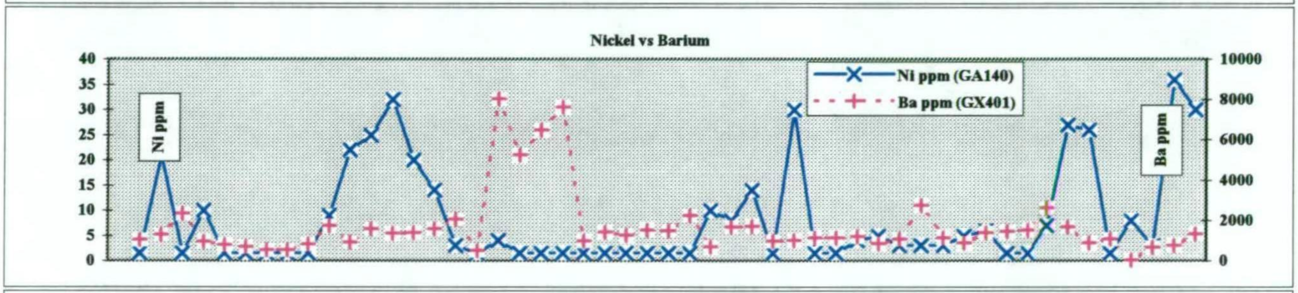

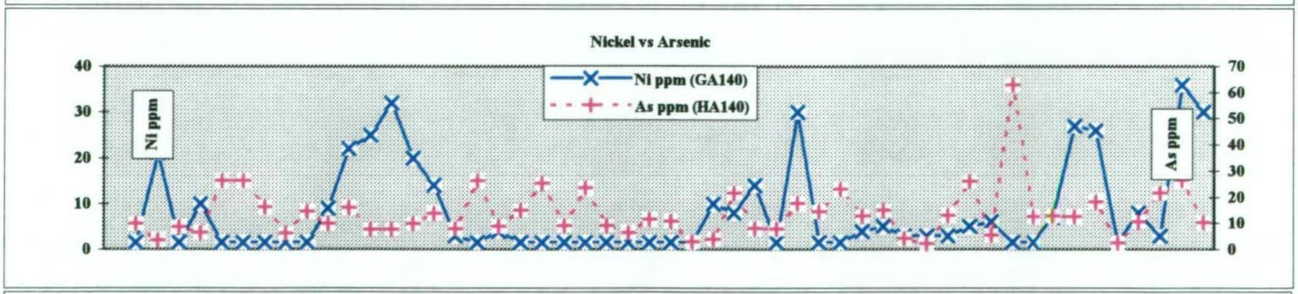

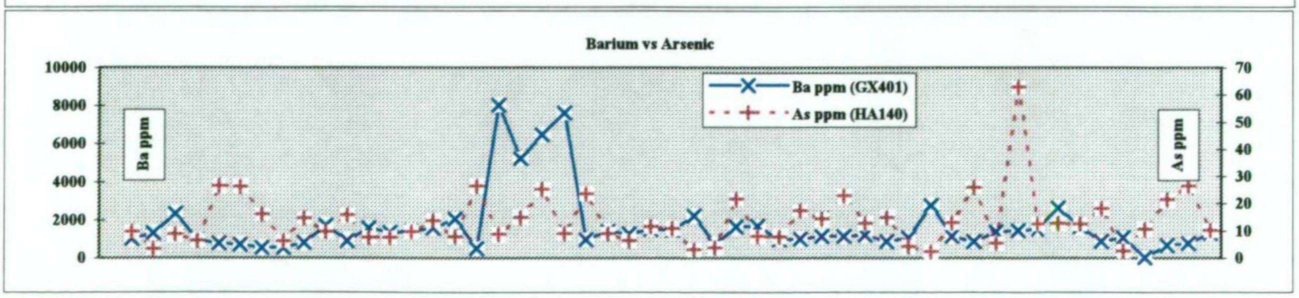

ROYAL THARSIS - SURFACE GEOCHEMISTRY ORIENTATION CORRELATION PLOTS

Appendix I
Chart 3

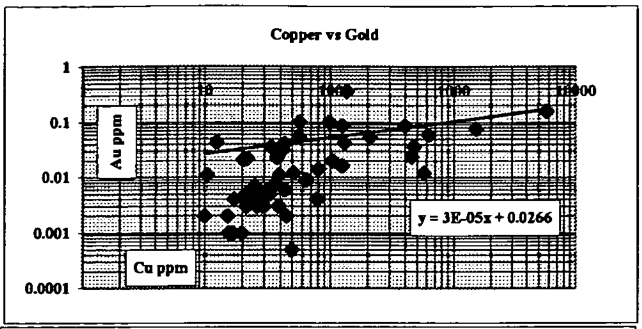

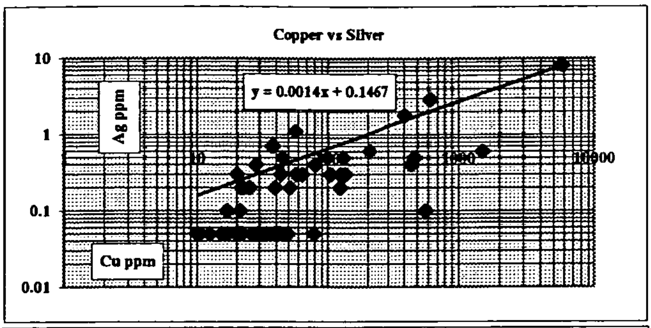

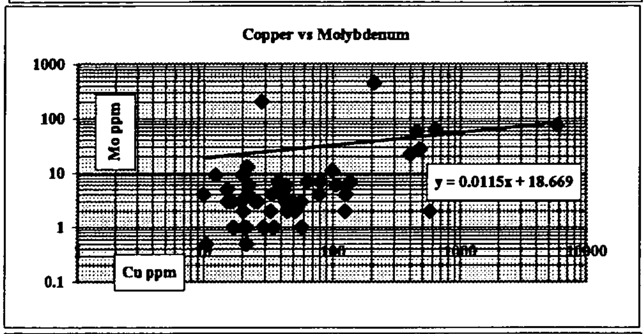

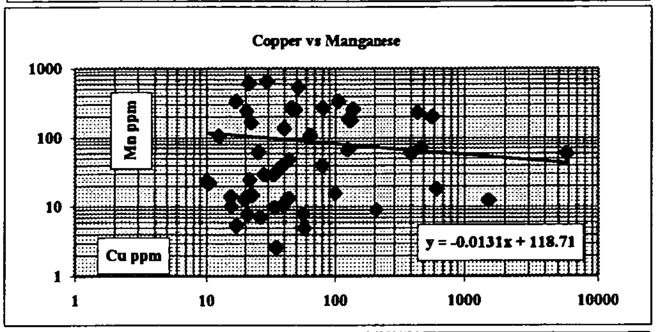

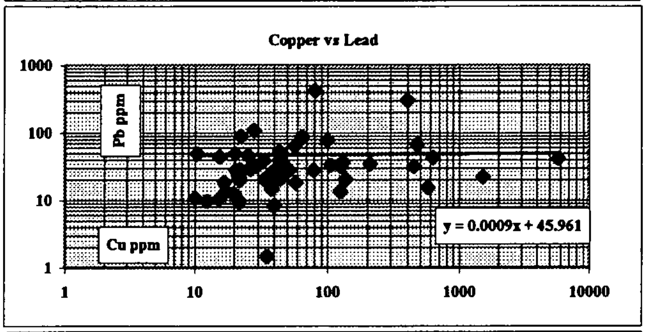

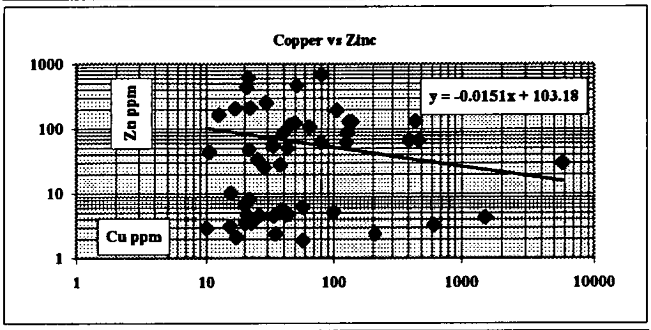

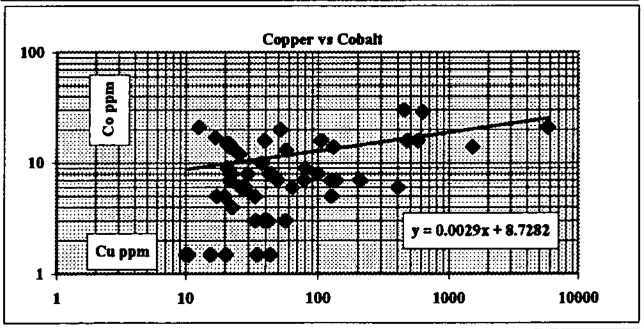

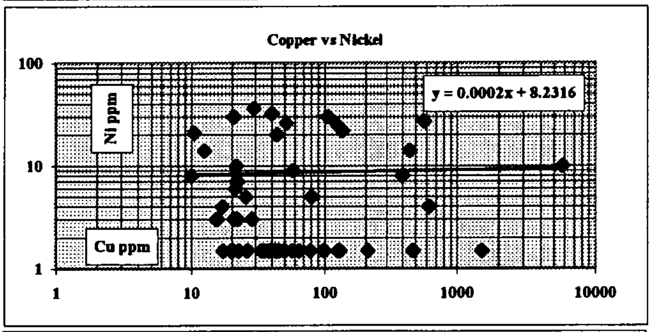

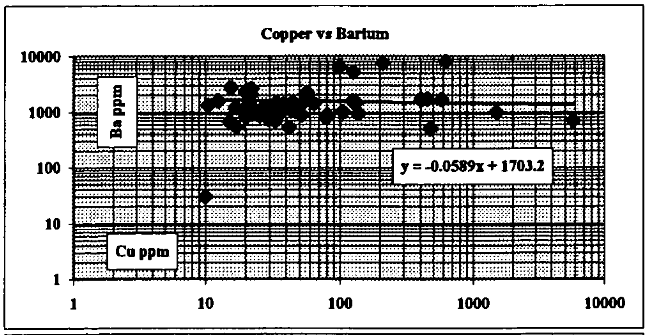

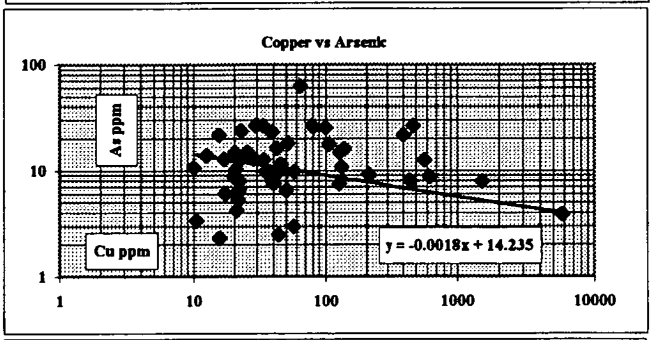

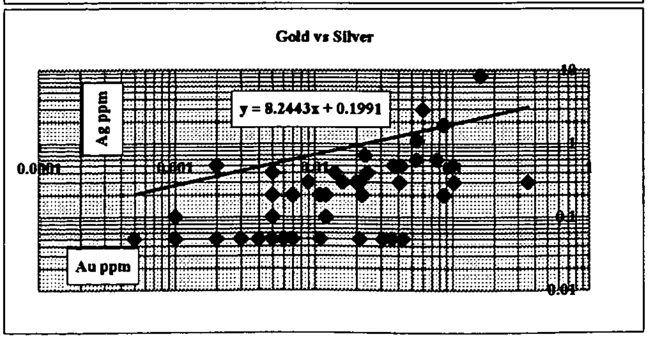

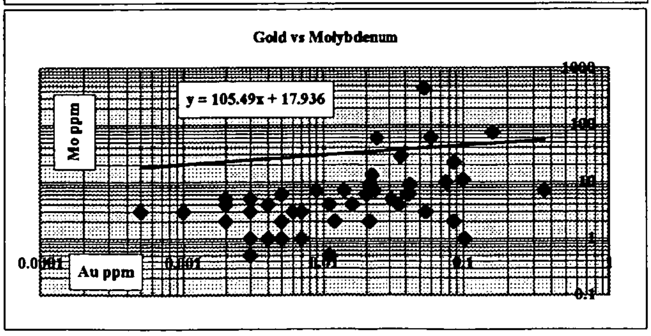

ROYAL THARSIS - SURFACE GEOCHEMISTRY Appendix I

ORIENTATION CORRELATION PLOTS Chart 3

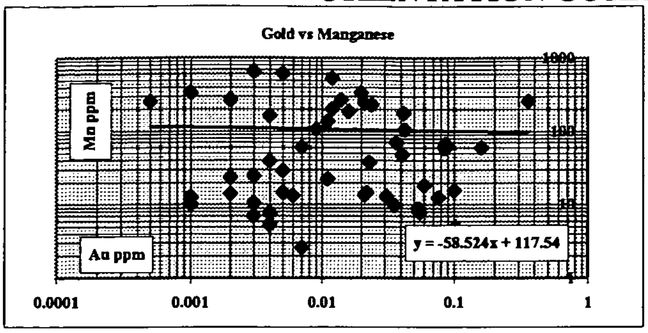

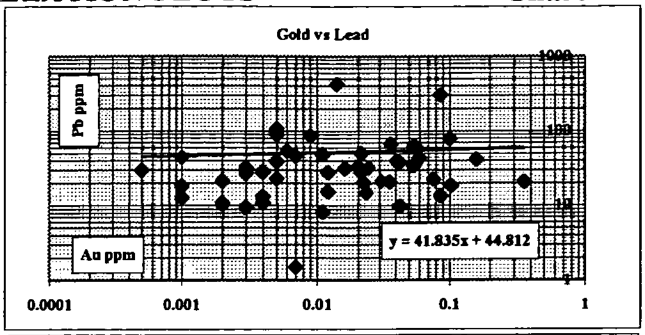

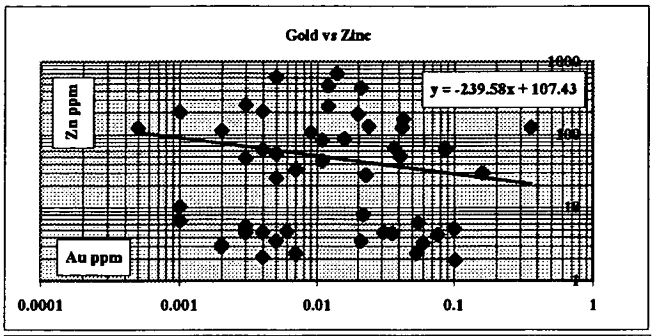

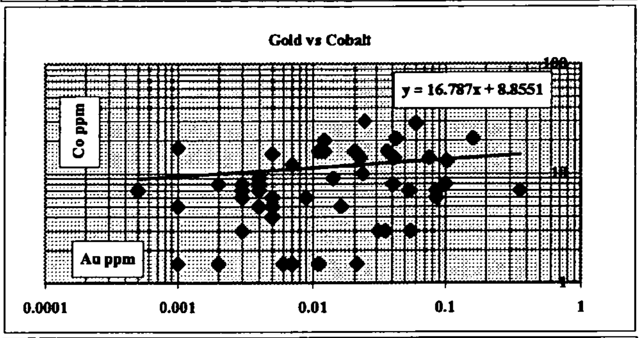

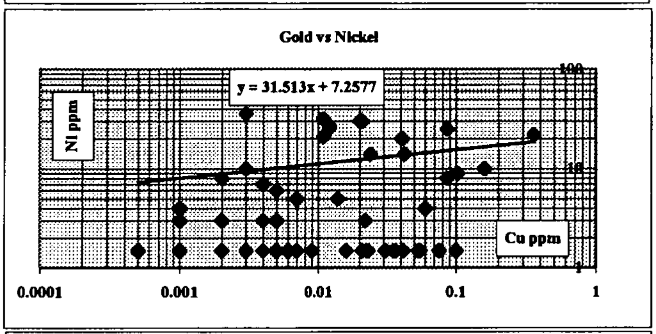

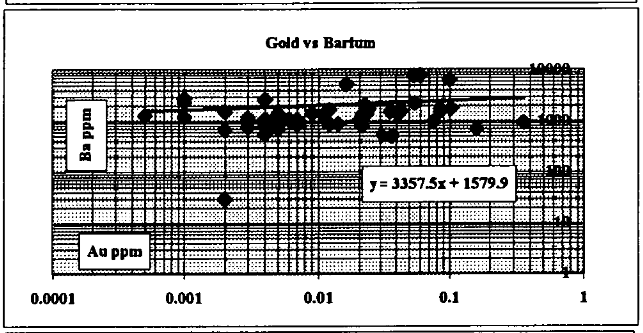

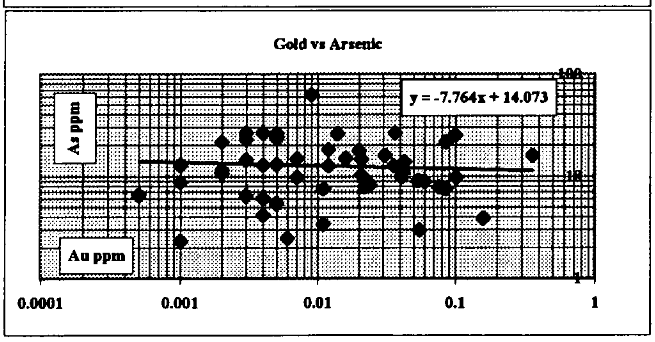

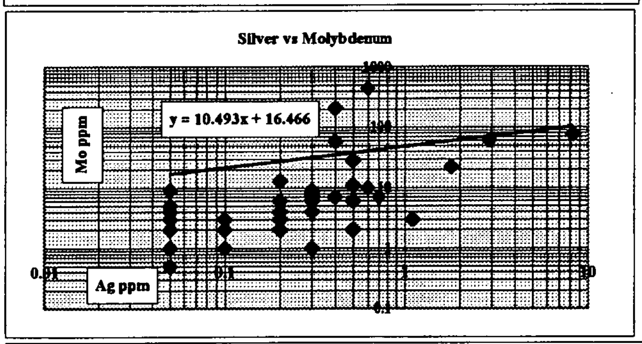

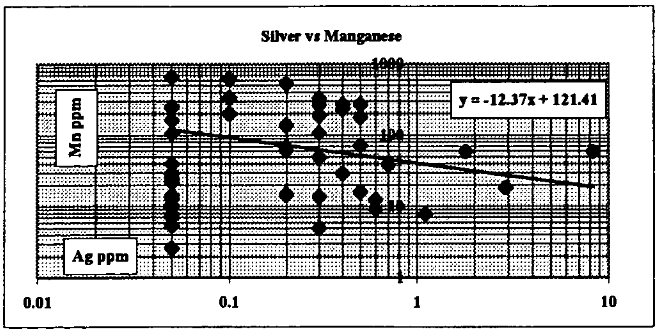

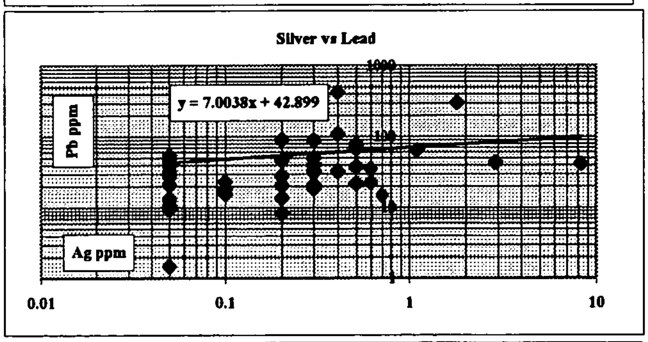

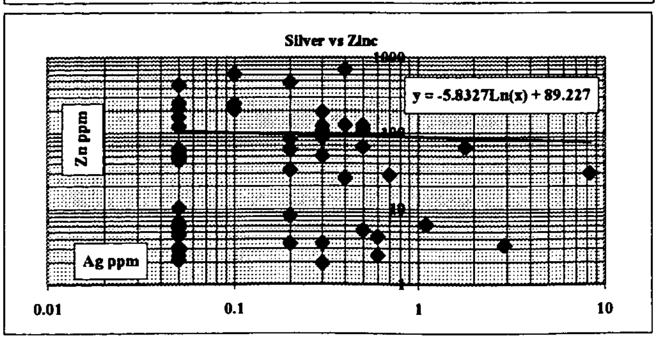

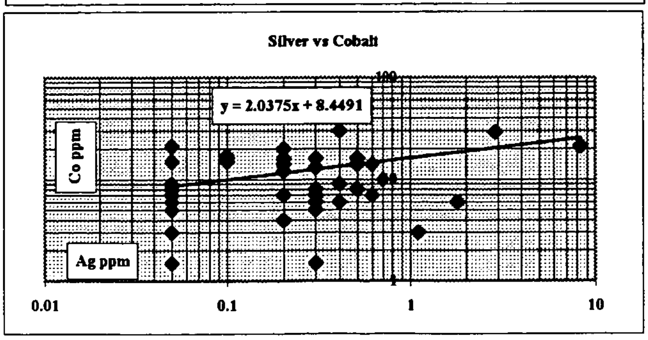

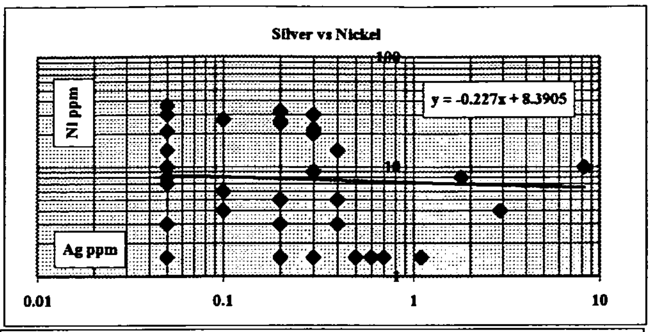
Silver vs Nickel
Ni ppm
y = -0.227x + 8.3905
Ag ppm
0.01
0.1
1
10

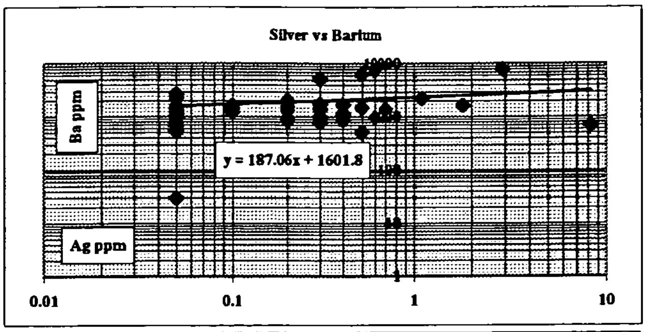
Silver vs Barium
Ba ppm
y = 187.06x + 1601.8
Ag ppm
0.01
0.1
1
10

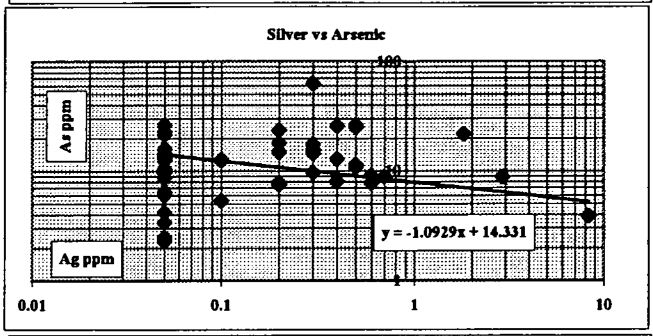
Silver vs Arsenic
As ppm
y = -1.0929x + 14.331
Ag ppm
0.01
0.1
1
10

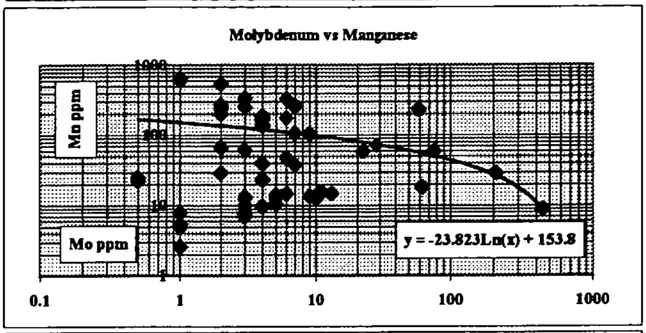
Molybdenum vs Manganese
Mn ppm
Mo ppm
y = -23.823Ln(x) + 153.8
0.1
1
10
100
1000

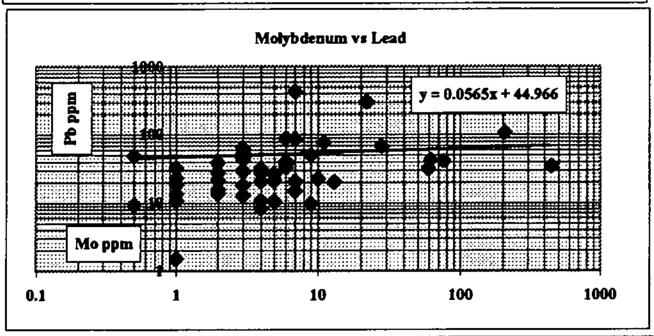
Molybdenum vs Lead
Pb ppm
y = 0.0565x + 44.966
Mo ppm
0.1
1
10
100
1000

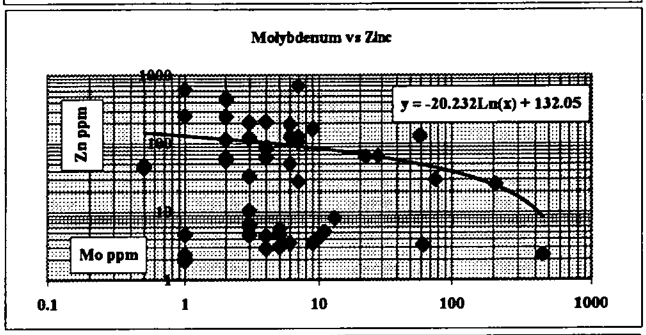
Molybdenum vs Zinc
Zn ppm
y = -20.232Ln(x) + 132.05
Mo ppm
0.1
1
10
100
1000

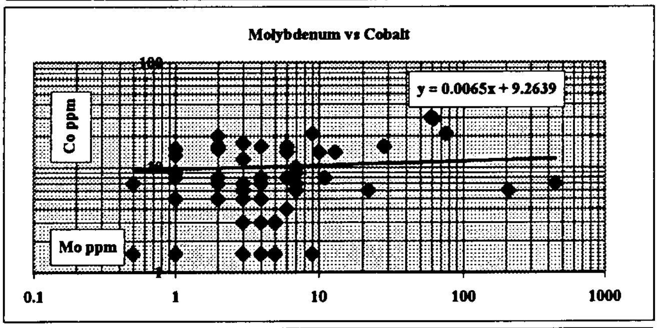
Molybdenum vs Cobalt
Co ppm
y = 0.0065x + 9.2639
Mo ppm
0.1
1
10
100
1000

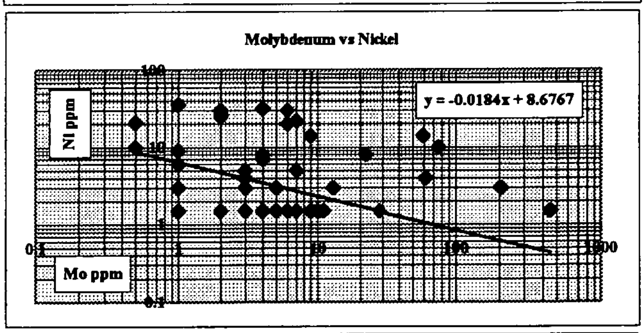
Molybdenum vs Nickel
Ni ppm
y = -0.0184x + 8.6767
Mo ppm

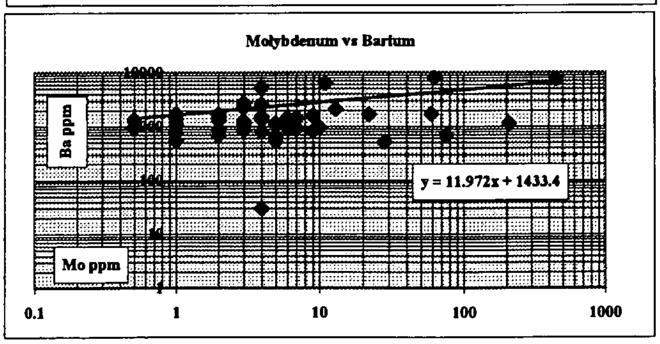
Molybdenum vs Barium
Ba ppm
y = 11.972x + 1433.4
Mo ppm
0.1
1
10
100
1000

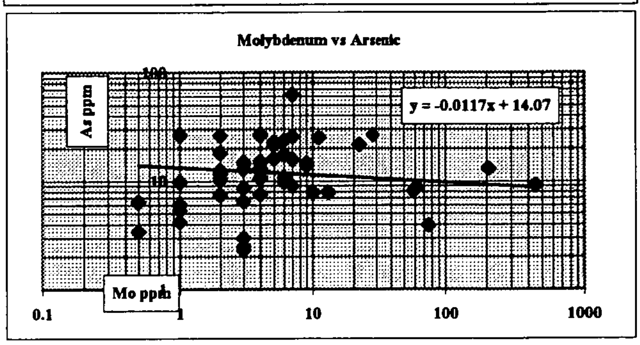
Molybdenum vs Arsenic
As ppm
y = -0.0117x + 14.07
Mo ppm
0.1
10
100
1000

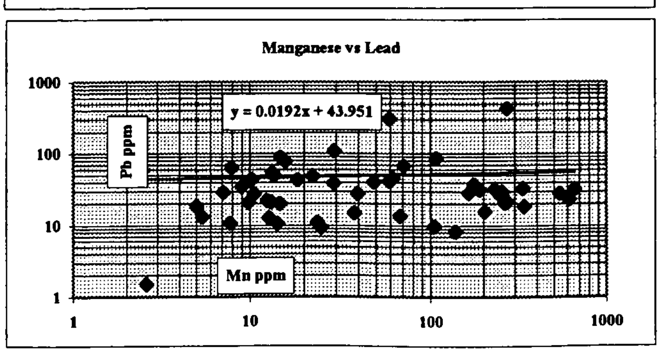
Manganese vs Lead
1000
100
10
1
Pb ppm
y = 0.0192x + 43.951
Mn ppm
1
10
100
1000

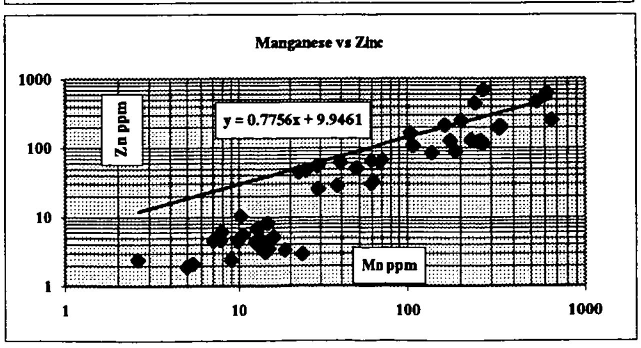
Manganese vs Zinc
1000
100
10
1
Zn ppm
y = 0.7756x + 9.9461
Mn ppm
1
10
100
1000

ROYAL THARSIS - SURFACE GEOCHEMISTRY
ORIENTATION CORRELATION PLOTS

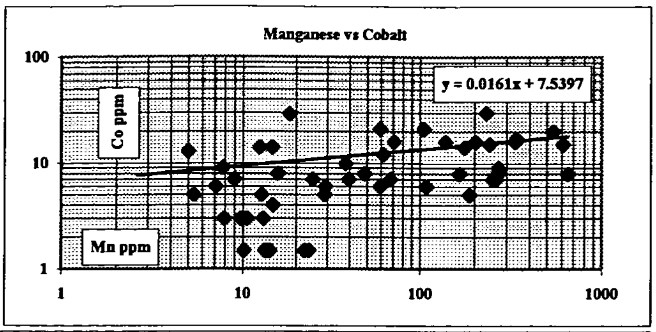

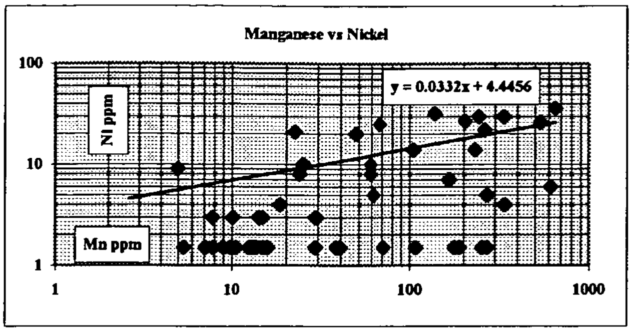

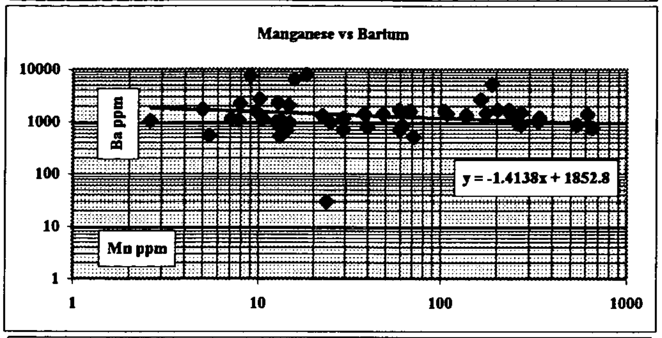

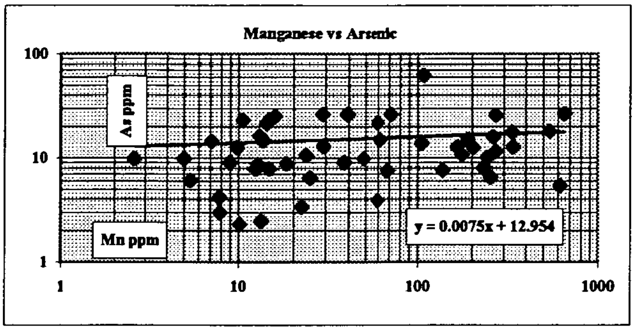

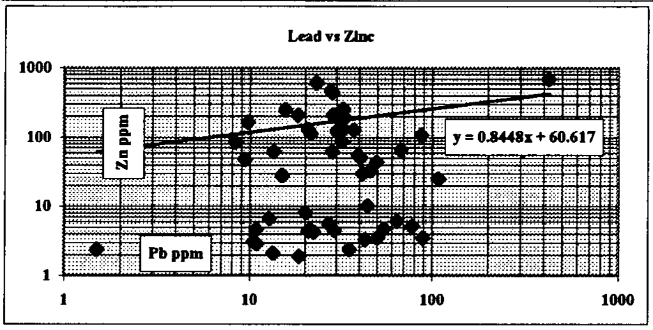

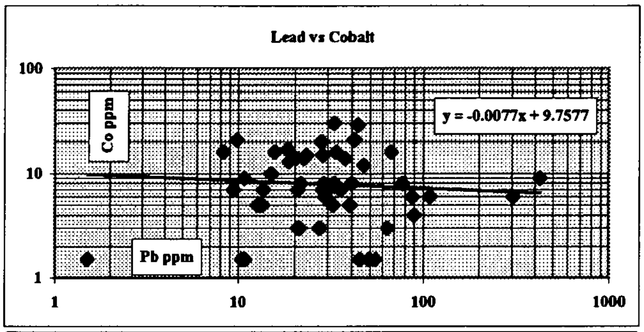

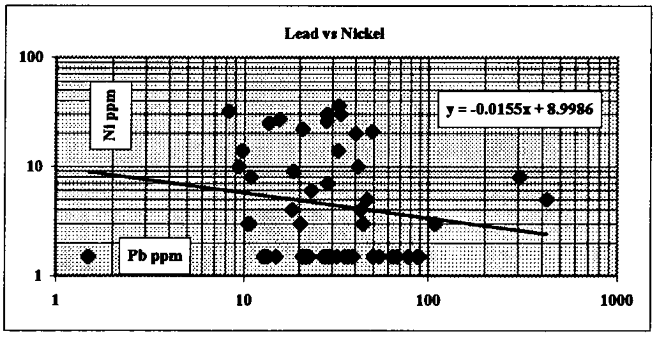

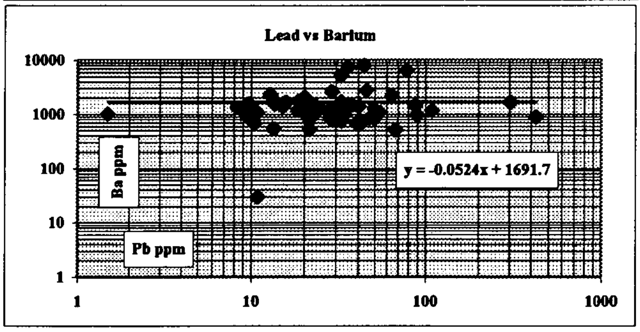

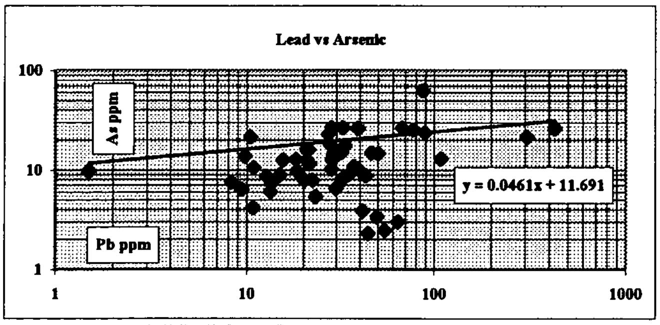

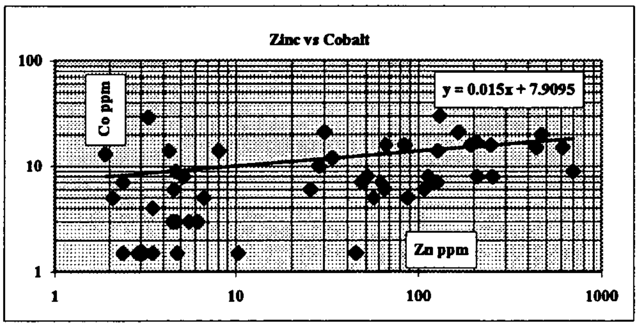

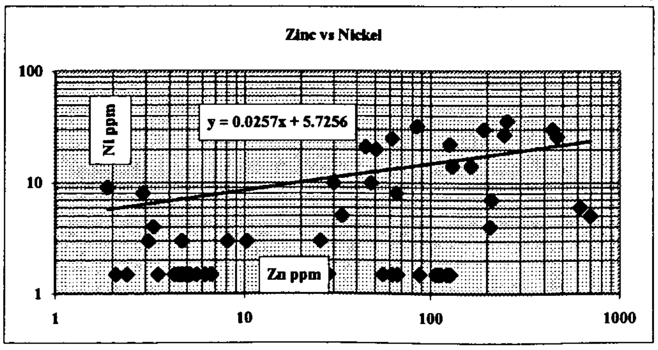

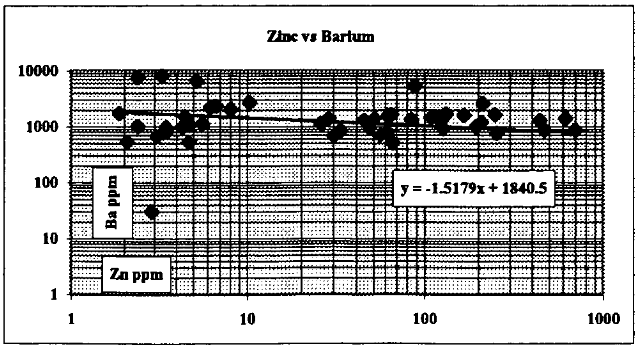

ROYAL THARSIS - SURFACE GEOCHEMISTRY
ORIENTATION CORRELATION PLOTS

Appendix I
Chart 3

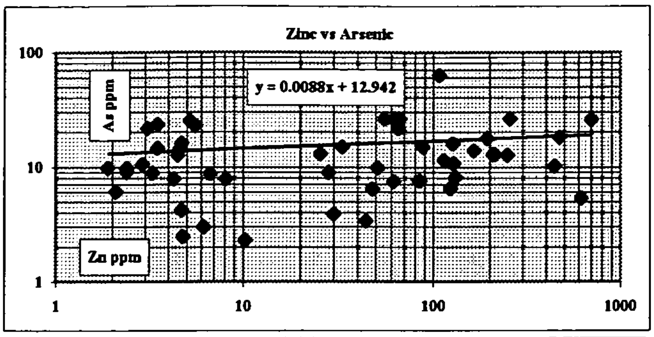

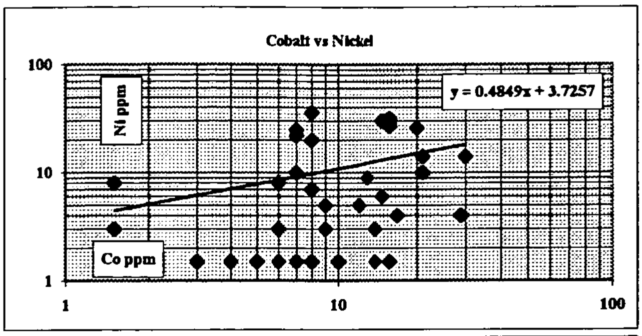

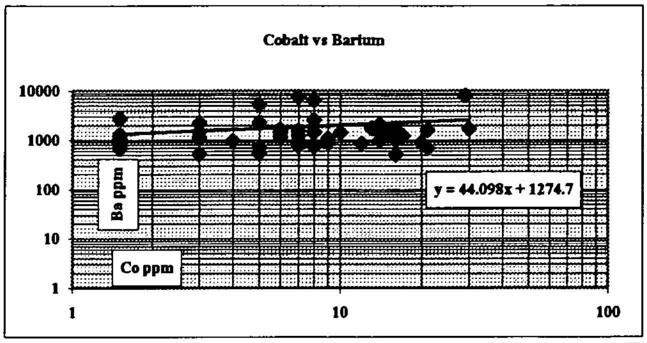

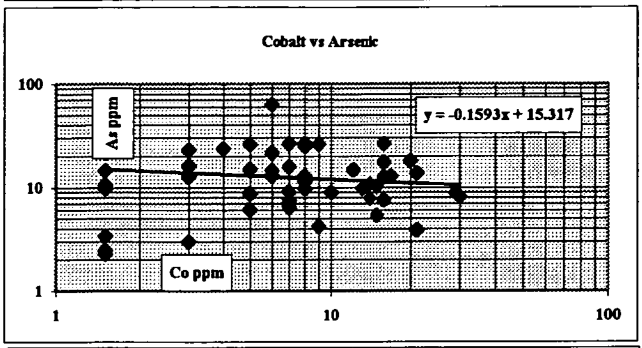

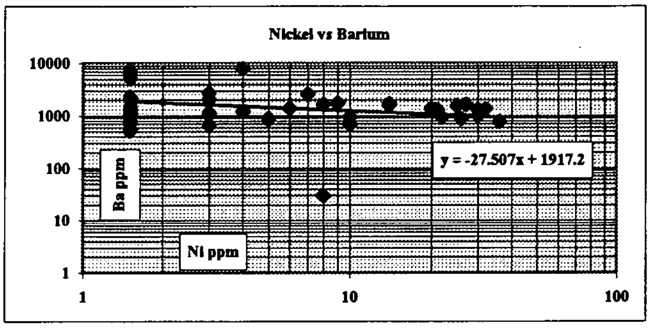

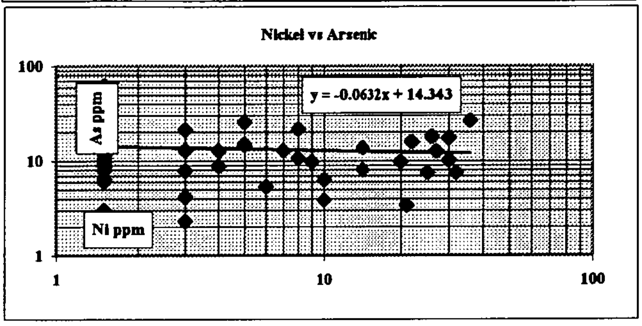

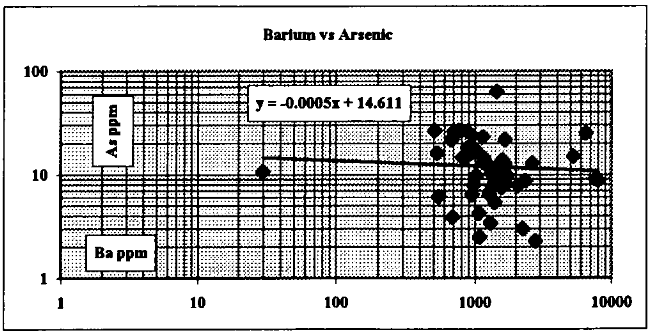

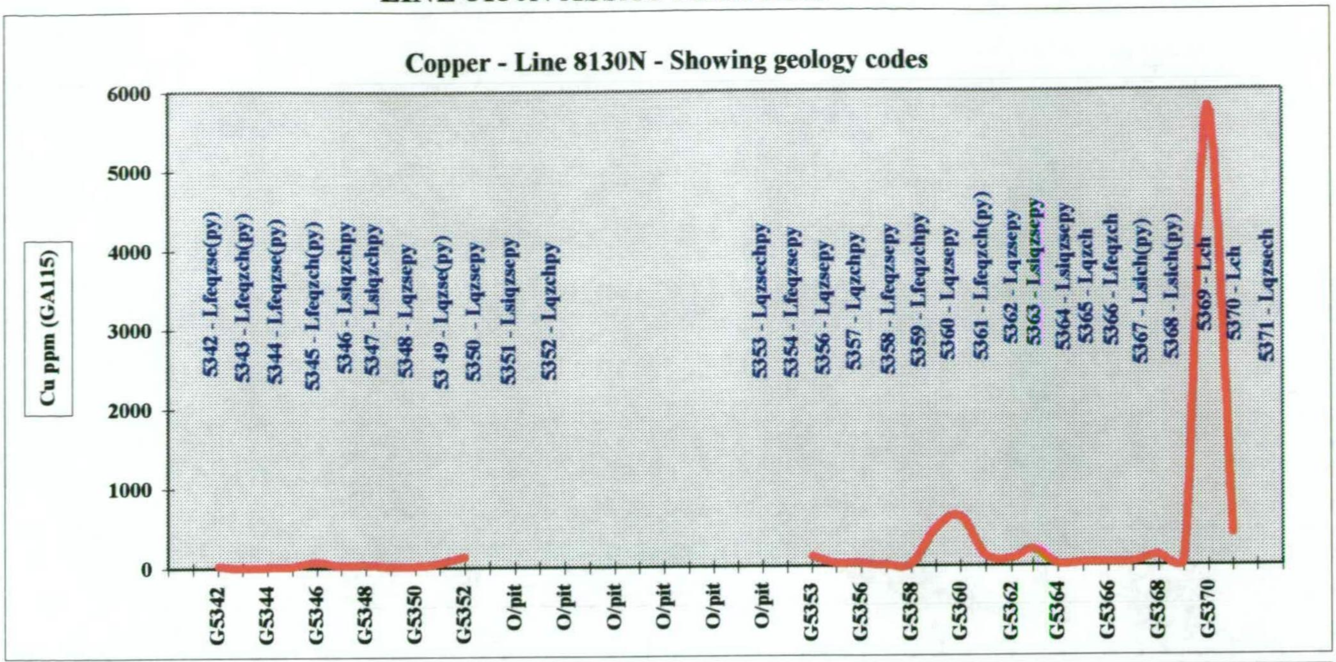
Copper - Line 8130N - Showing geology codes
Cu ppm (GA115)
6000
5000
4000
3000
2000
1000
0
5342 - Lfeqzse(py)
5343 - Lfeqzch(py)
5344 - Lfeqzse(py)
5345 - Lfeqzch(py)
5346 - Lsiqzchpy
5347 - Lsiqzchpy
5348 - Lqzsepy
53 49 - Lqzse(py)
5350 - Lqzsepy
5351 - Lsiqzsepy
5352 - Lqzchpy
5353 - Lqzsechpy
5354 - Lfeqzsepy
5356 - Lqzsepy
5357 - Lqzchpy
5358 - Lfeqzsepy
5359 - Lfeqzchpy
5360 - Lqzsepy
5361 - Lfeqzch(py)
5362 - Lqzsepy
5363 - Lsiqzsepy
5364 - Lsiqzsepy
5365 - Lqzch
5366 - Lfeqzch
5367 - Lsich(py)
5368 - Lsich(py)
5369 - Lch
5370 - Lch
5371 - Lqzsech
G5342
G5344
G5346
G5348
G5350
G5352
O/pit
O/pit
O/pit
O/pit
O/pit
O/pit
G5353
G5356
G5358
G5360
G5362
G5364
G5366
G5368
G5370

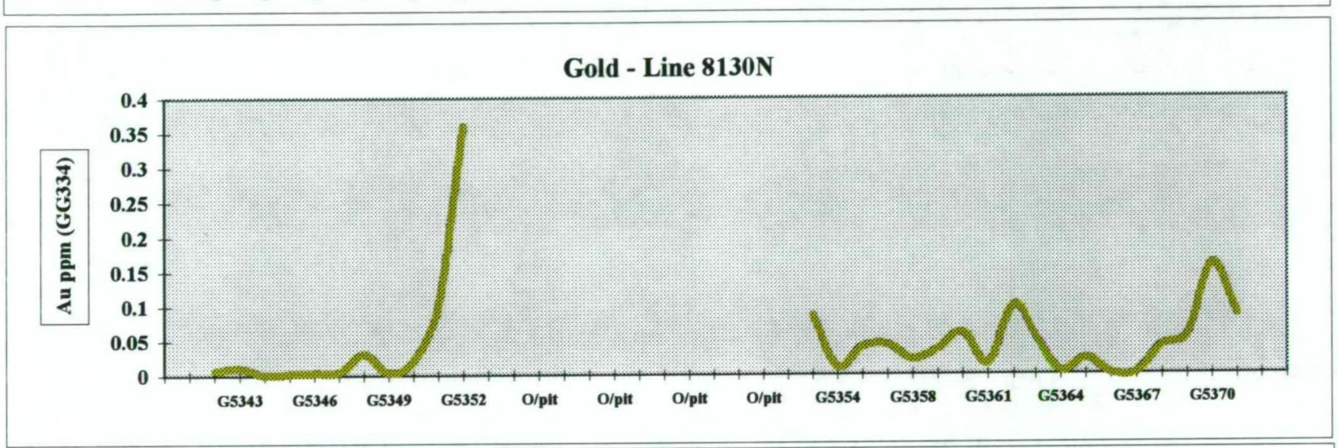
Gold - Line 8130N
Au ppm (GG334)
0.4
0.35
0.3
0.25
0.2
0.15
0.1
0.05
0
G5343
G5346
G5349
G5352
O/pit
O/pit
O/pit
O/pit
G5354
G5358
G5361
G5364
G5367
G5370

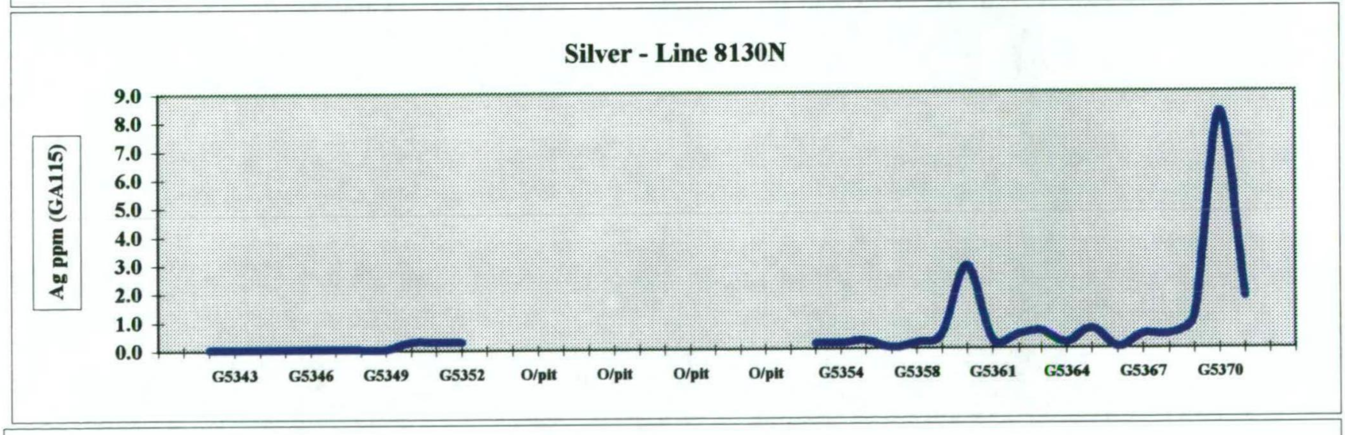
Silver - Line 8130N
Ag ppm (GA115)
9.0
8.0
7.0
6.0
5.0
4.0
3.0
2.0
1.0
0.0
G5343
G5346
G5349
G5352
O/pit
O/pit
O/pit
O/pit
G5354
G5358
G5361
G5364
G5367
G5370

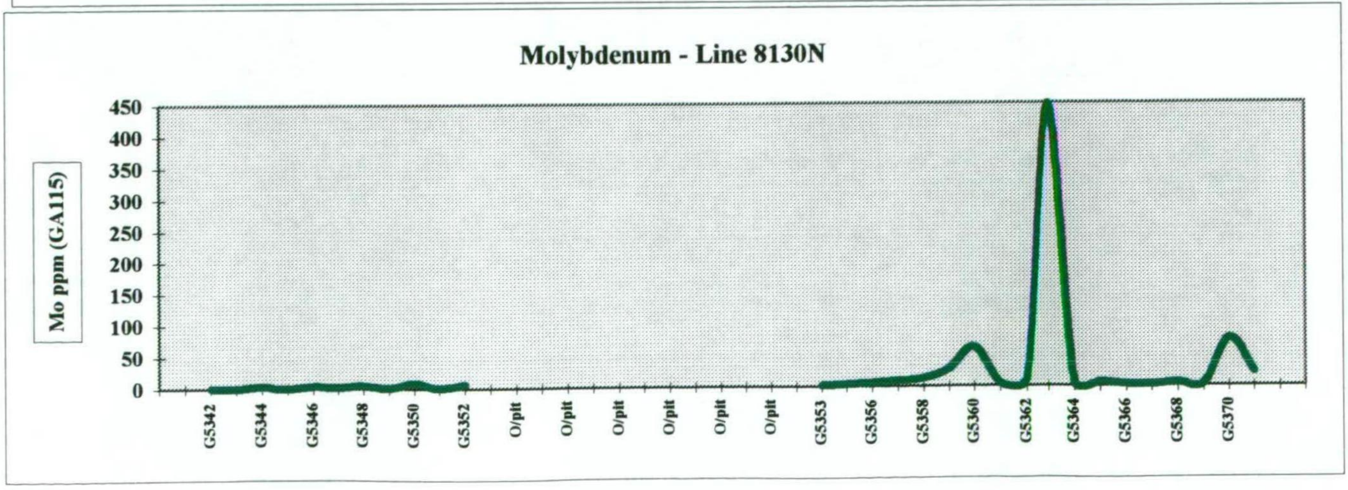
Molybdenum - Line 8130N
Mo ppm (GA115)
450
400
350
300
250
200
150
100
50
0
G5342
G5344
G5346
G5348
G5350
G5352
O/pit
O/pit
O/pit
O/pit
O/pit
O/pit
G5353
G5356
G5358
G5360
G5362
G5364
G5366
G5368
G5370

ROYAL THARSIS - SURFACE GEOCHEMISTRY
LINE 8130N ASSAY PROFILES

Appendix I
Chart 4

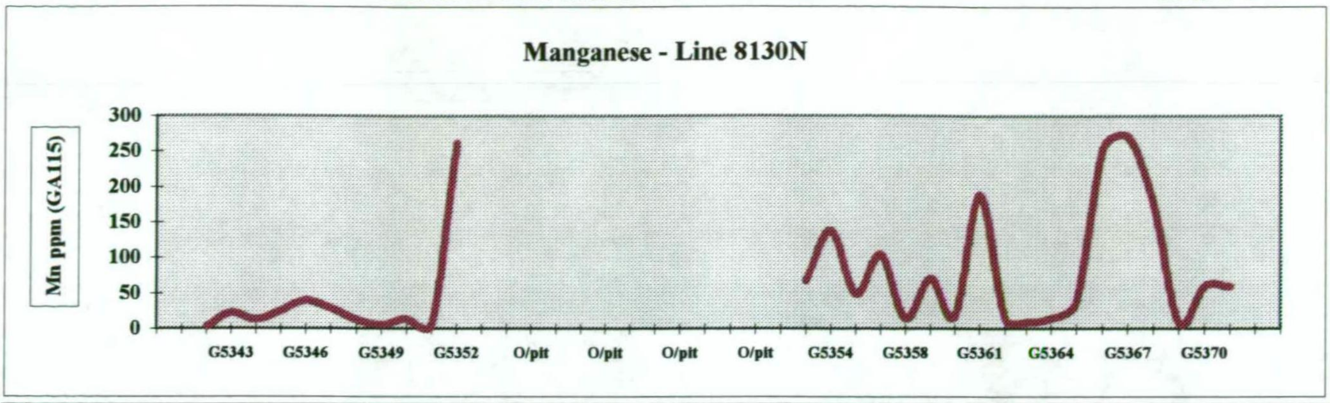

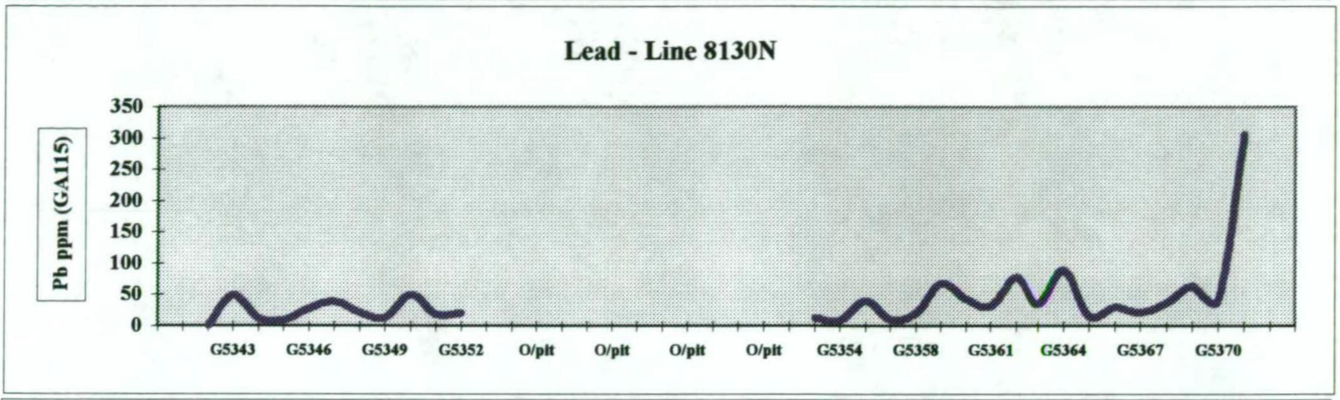

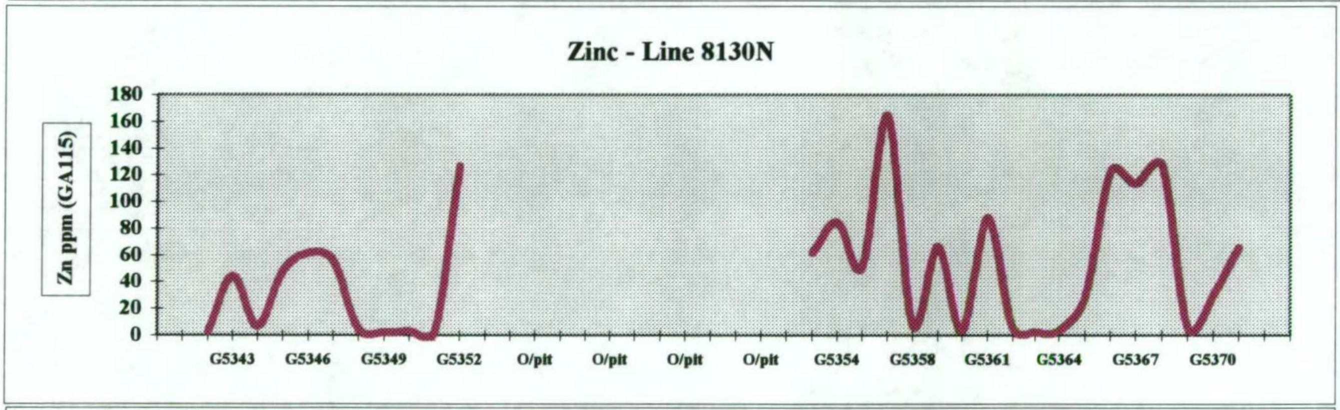

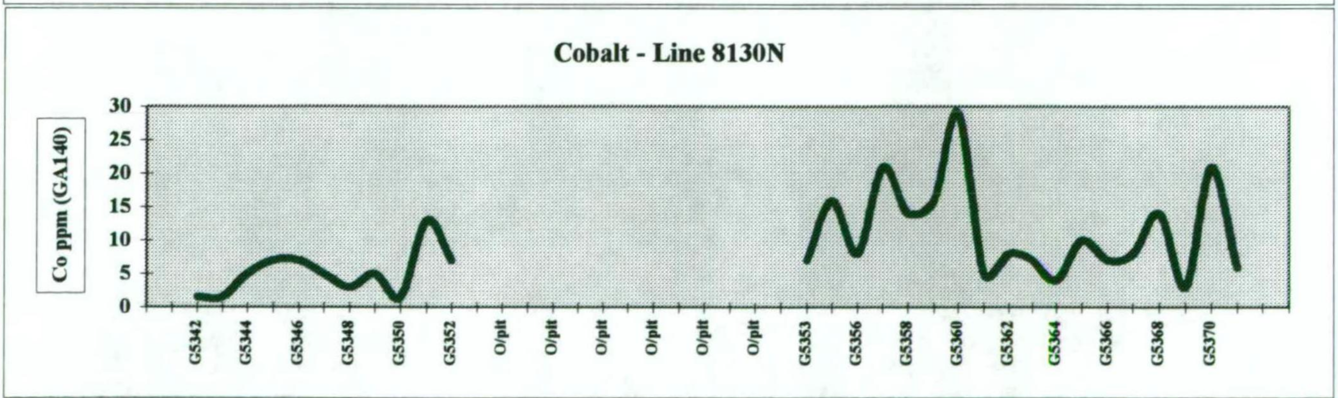

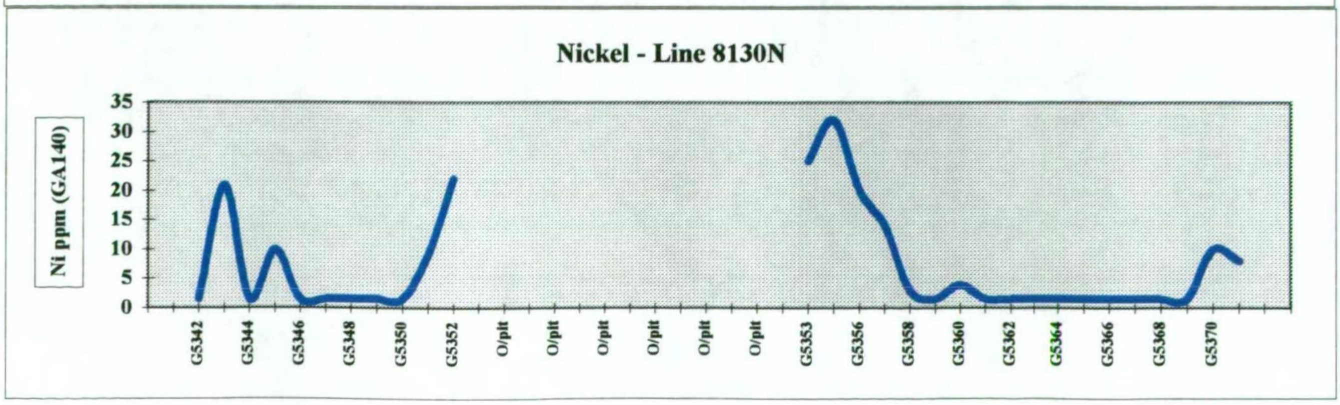

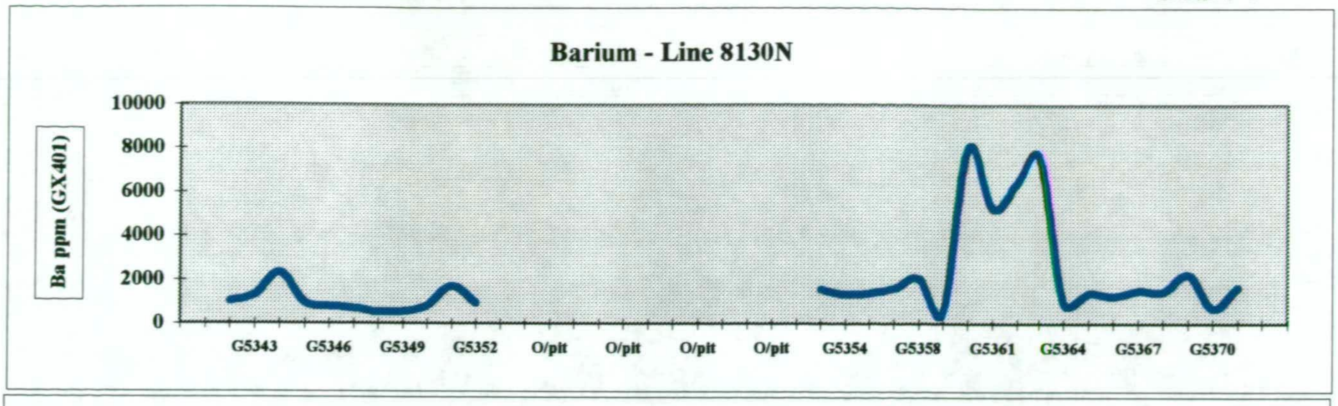

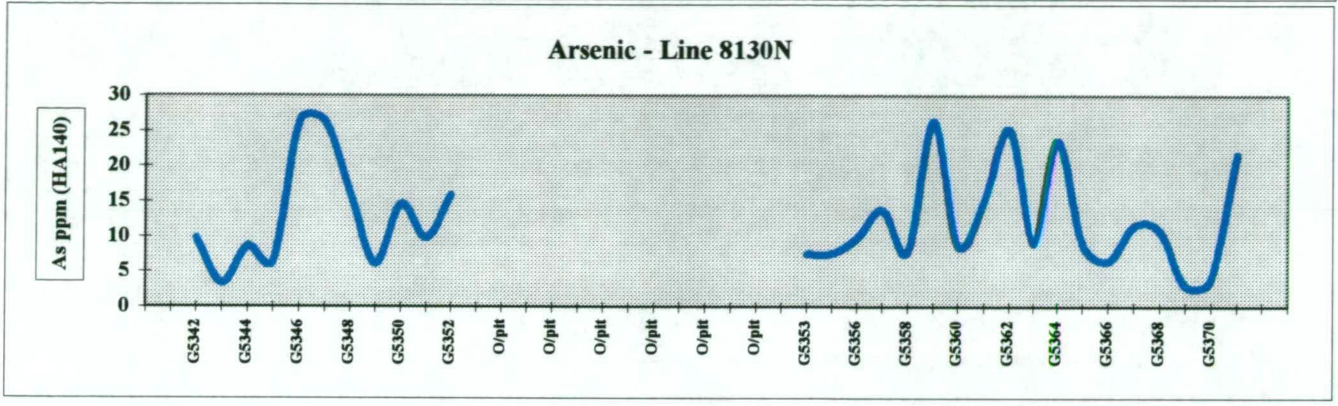

All profiles are facing north, with west to the left margin and east to the right margin.

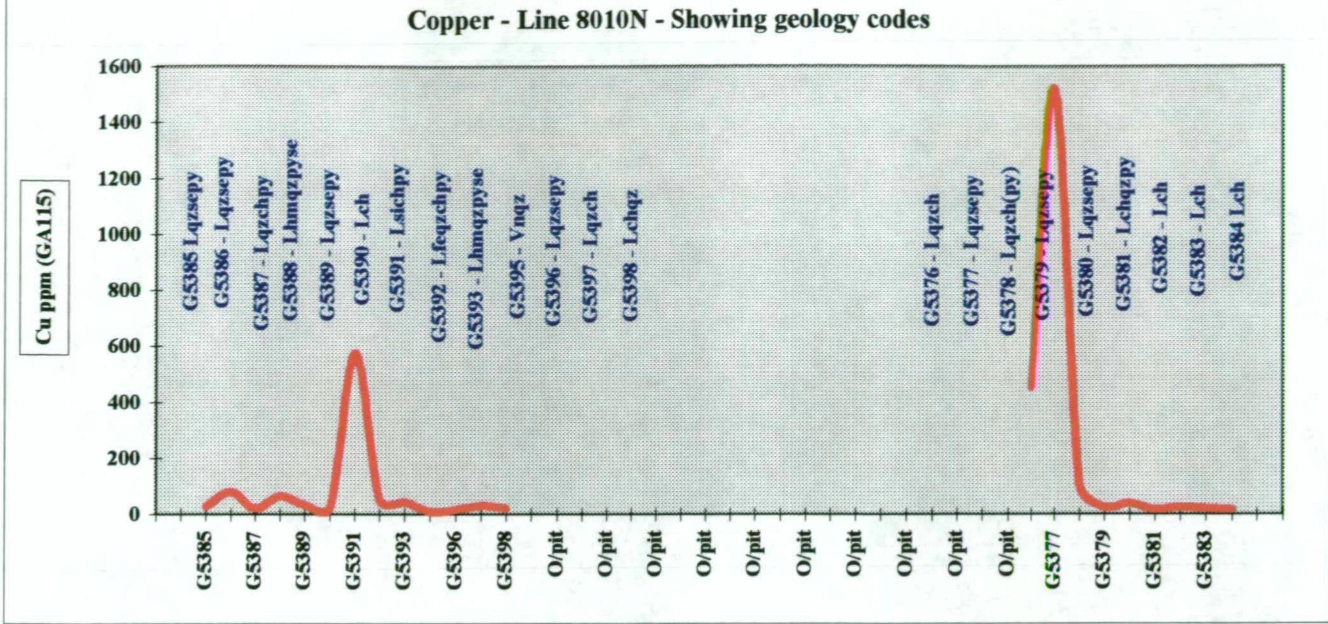
Copper - Line 8010N - Showing geology codes
Cu ppm (GA115)
1600
1400
1200
1000
800
600
400
200
0
G5385 Lqzsepy
G5386 - Lqzsepy
G5387 - Lqzchpy
G5388 - Lhmqzpyse
G5389 - Lqzsepy
G5390 - Lch
G5391 - Lsichpy
G5392 - Lfeqzchpy
G5393 - Lhmqzpyse
G5395 - Vnqz
G5396 - Lqzsepy
G5397 - Lqzch
G5398 - Lchqz
G5376 - Lqzch
G5377 - Lqzsepy
G5378 - Lqzch(py)
G5379 - Lqzsepy
G5380 - Lqzsepy
G5381 - Lchqzpy
G5382 - Lch
G5383 - Lch
G5384 Lch
G5385
G5387
G5389
G5391
G5393
G5396
G5398
O/pit
G5377
G5379
G5381
G5383

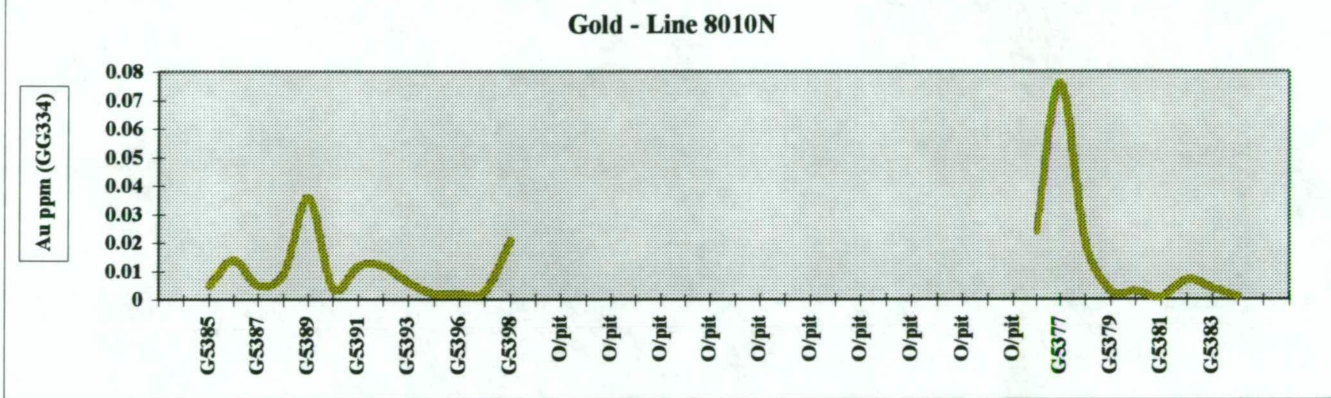
Gold - Line 8010N
Au ppm (GG334)
0.08
0.07
0.06
0.05
0.04
0.03
0.02
0.01
0
G5385
G5387
G5389
G5391
G5393
G5396
G5398
O/pit
G5377
G5379
G5381
G5383

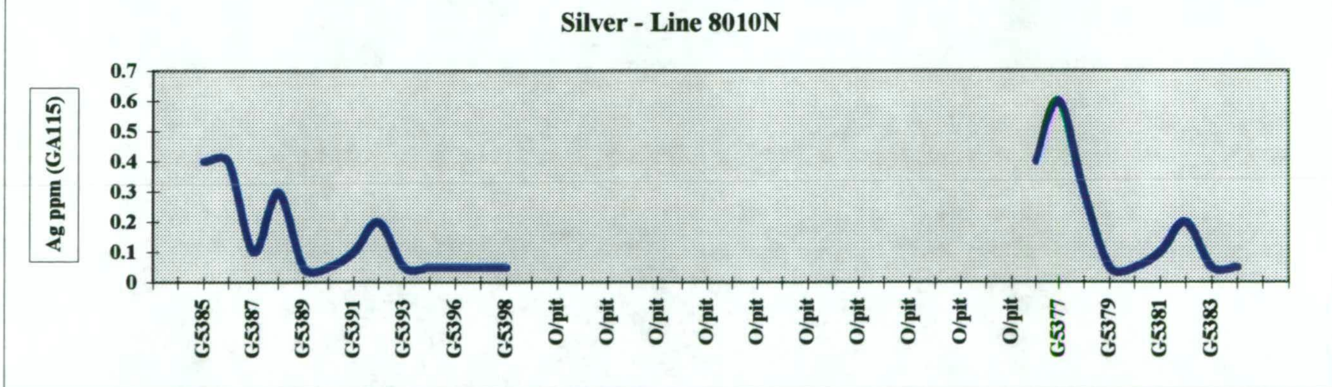
Silver - Line 8010N
Ag ppm (GA115)
0.7
0.6
0.5
0.4
0.3
0.2
0.1
0
G5385
G5387
G5389
G5391
G5393
G5396
G5398
O/pit
G5377
G5379
G5381
G5383

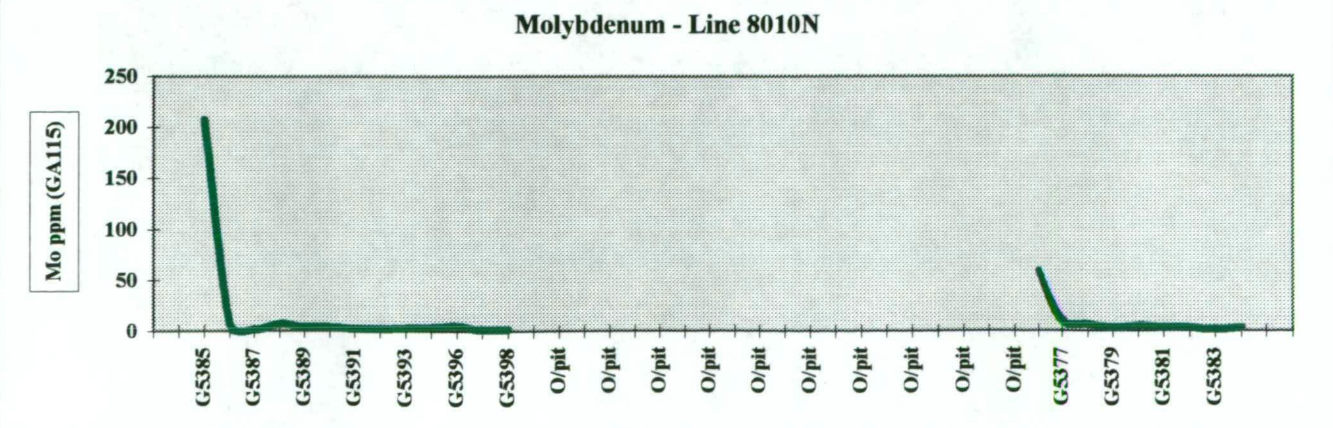
Molybdenum - Line 8010N
Mo ppm (GA115)
250
200
150
100
50
0
G5385
G5387
G5389
G5391
G5393
G5396
G5398
O/pit
G5377
G5379
G5381
G5383

Appendix I
Chart 5

ROYAL THARSIS - SURFACE GEOCHEMISTRY
LINE 8010N ASSAY PROFILES

Manganese - Line 8010N

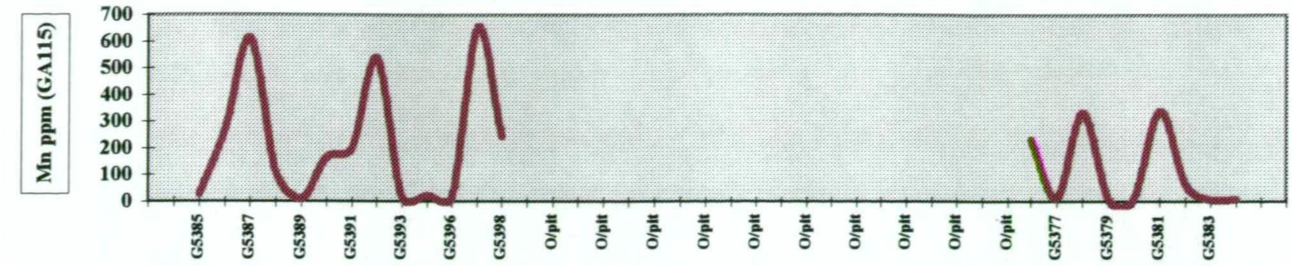

Lead - Line 8010N

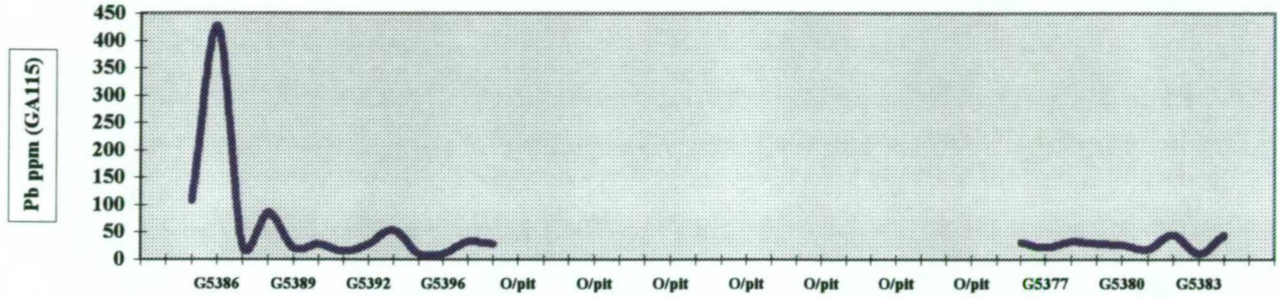

Zinc - Line 8010N

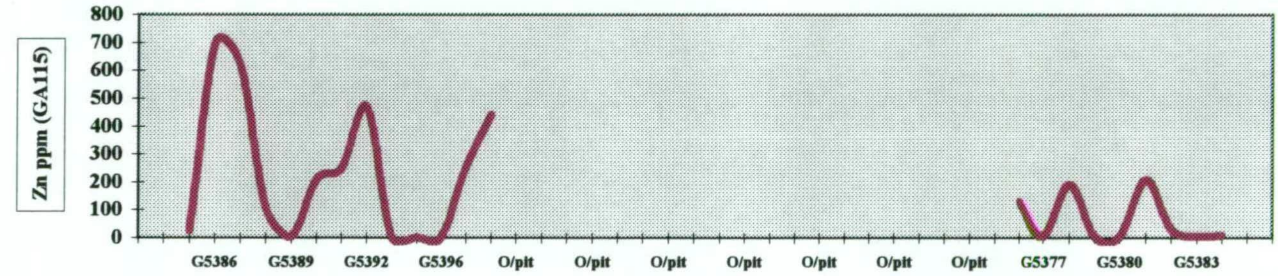

Cobalt - Line 8010N

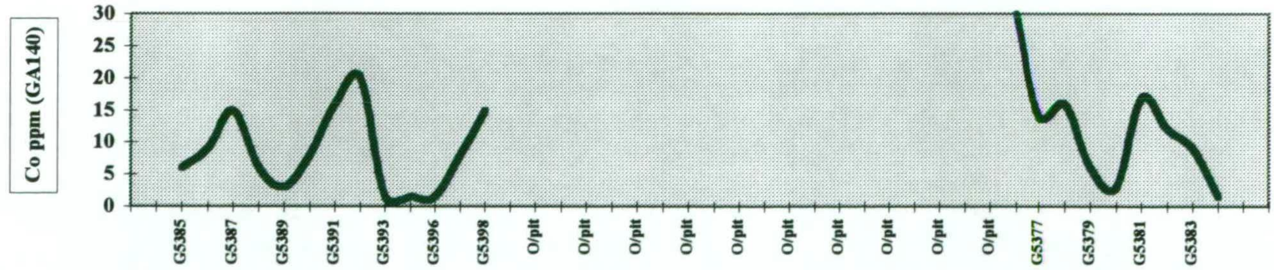

Nickel - Line 8010N

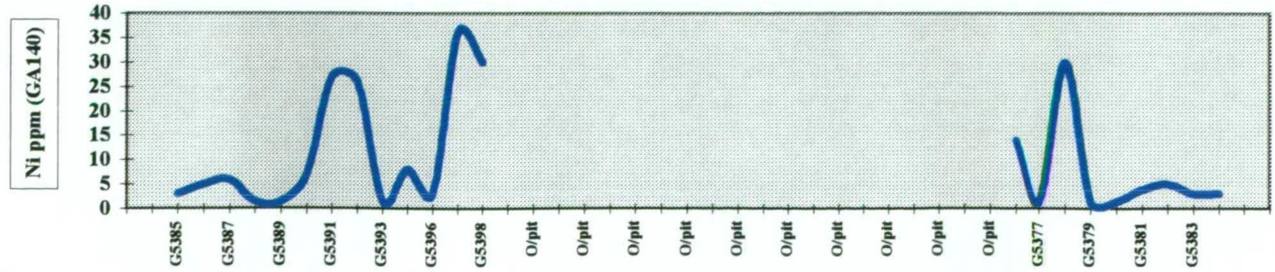

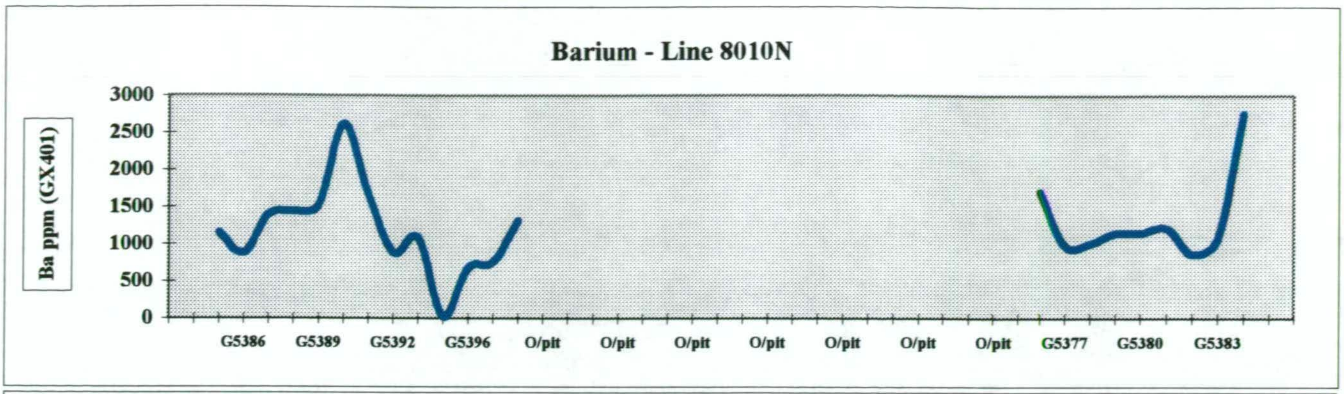

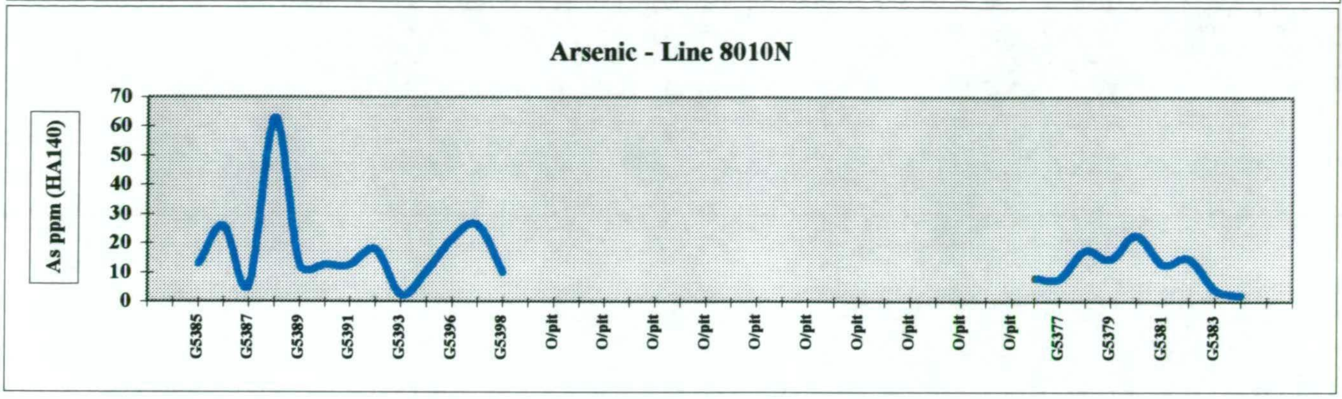

All profiles are facing north, with west to the left margin and east to the right margin.

Appendix II

Royal Tharsis

Surface Geochemistry

Rock Chip Sampling

APPENDIX II - CONTENTS

ROYAL THARSIS - SURFACE GEOCHEMISTRY
TRAVERSE ASSAY PROFILES

Appendix II
Chart 1
Traverse 7

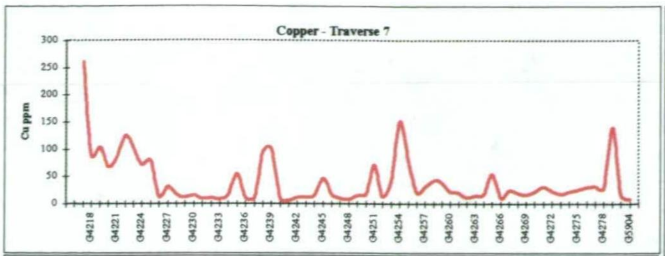

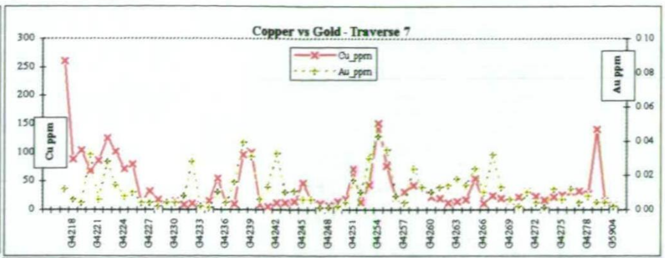

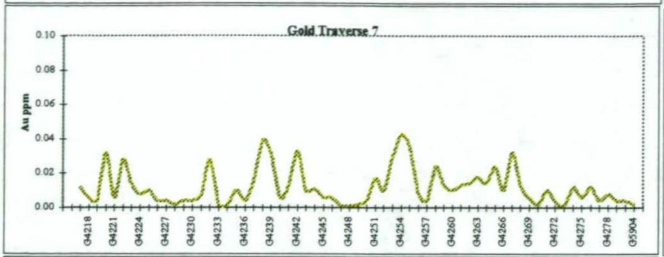

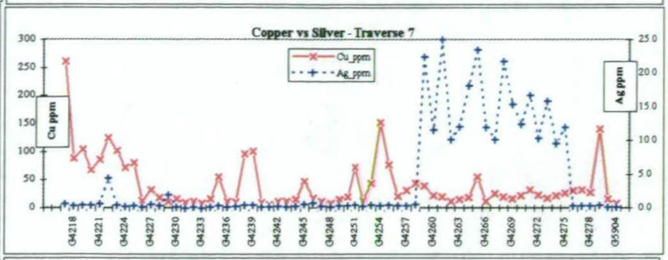

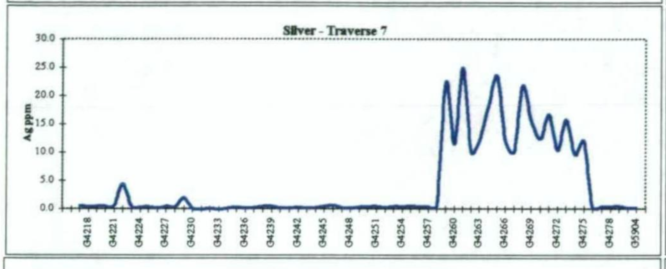

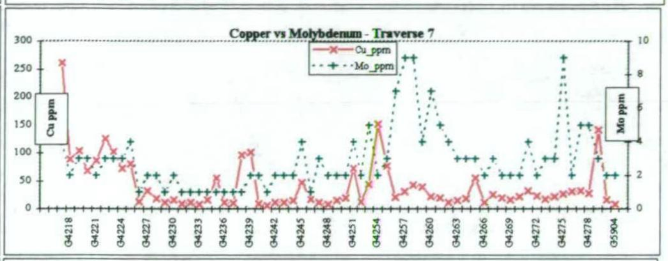

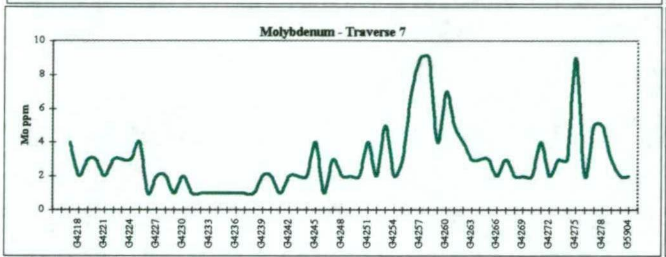

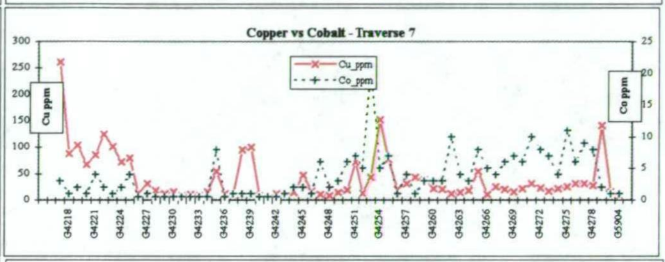

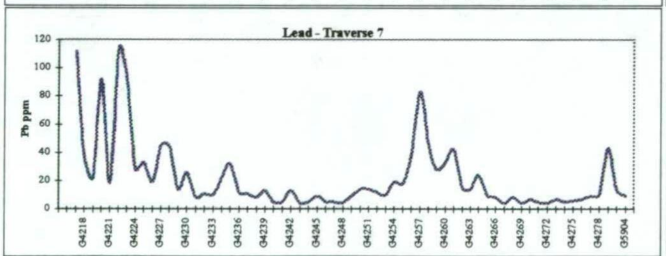

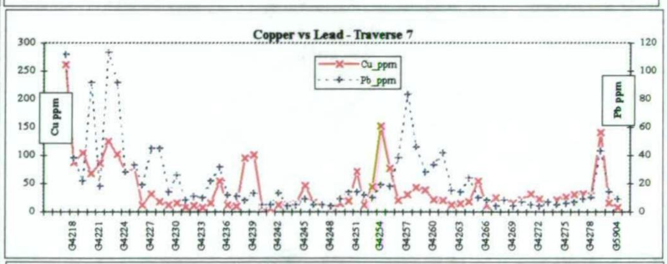

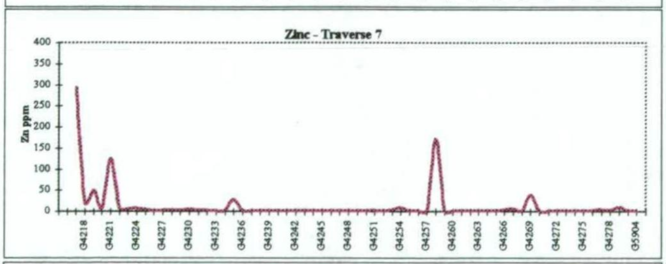

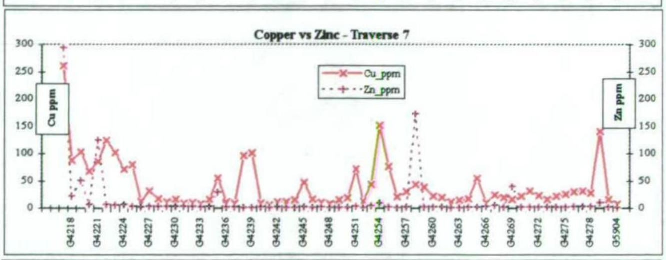

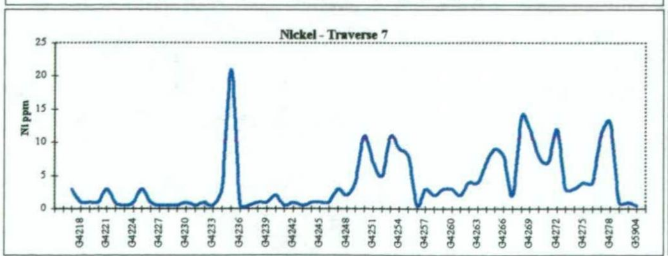

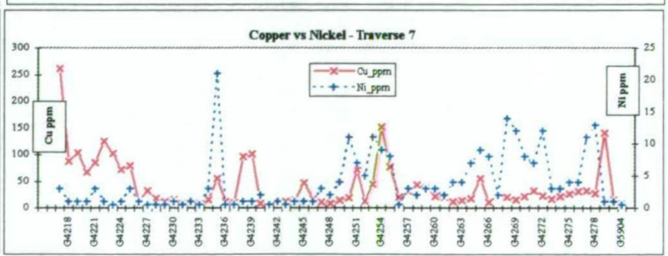

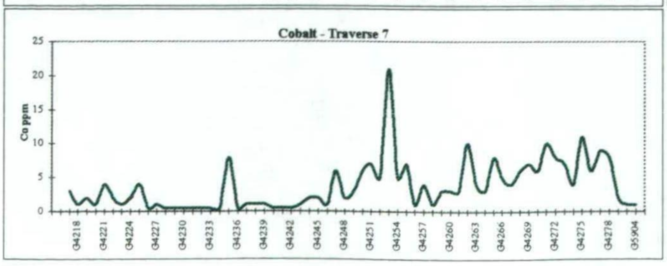

ROYAL THARSIS - SURFACE GEOCHEMISTRY
TRAVERSE ASSAY PROFILES

Appendix II
Chart 2
Traverse 8

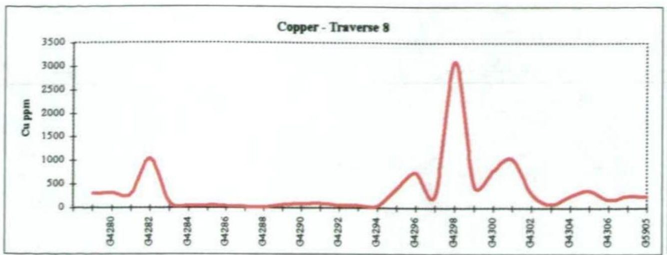

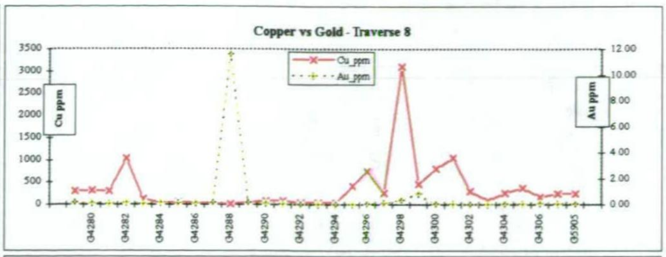

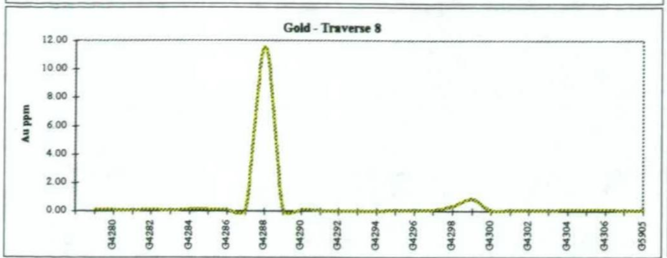

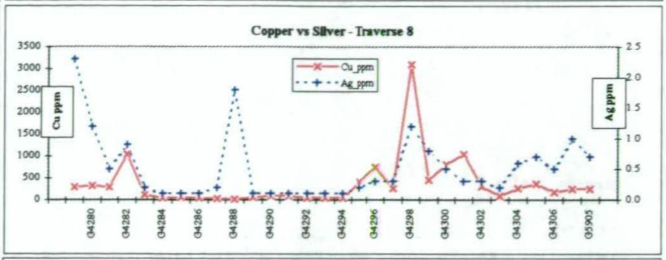

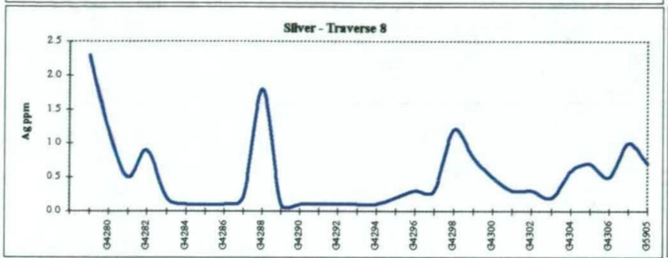

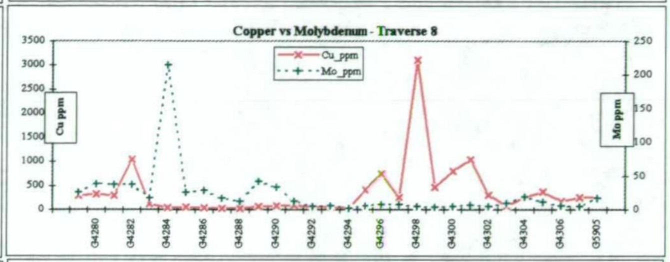

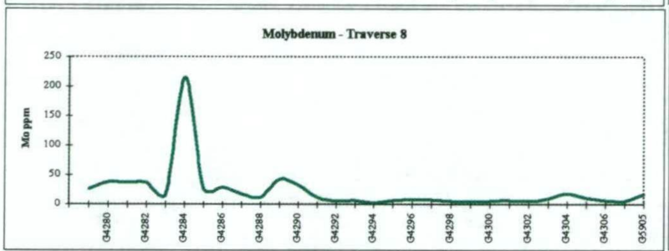

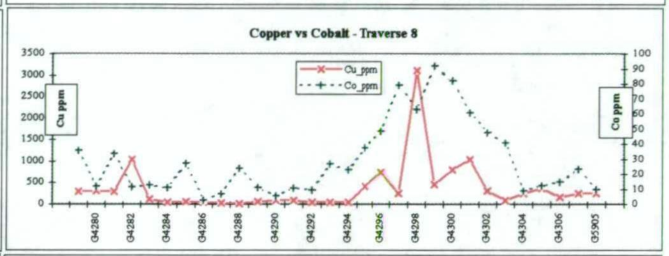

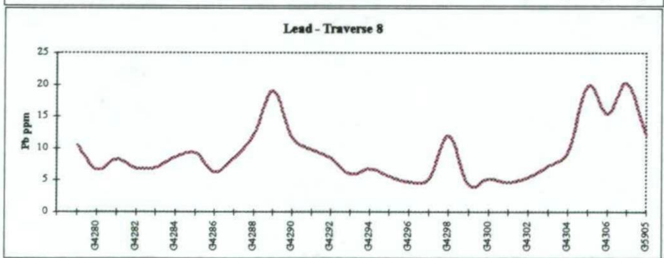

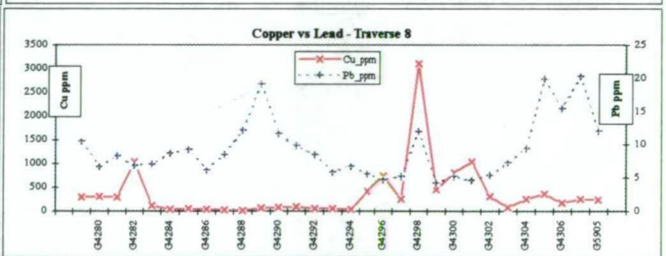

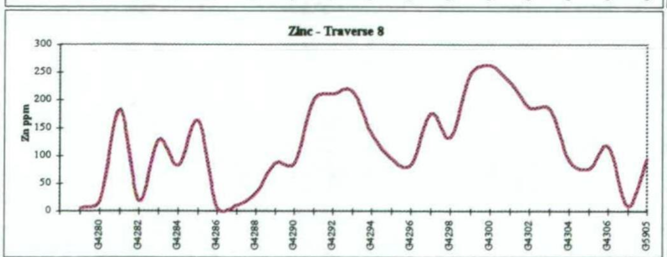

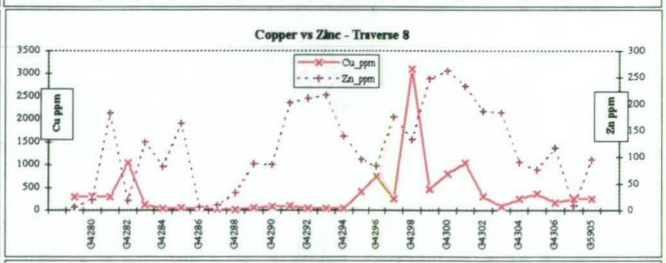

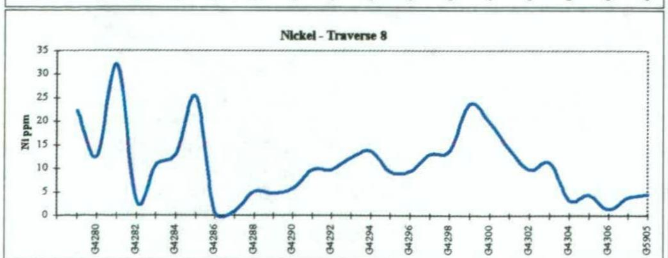

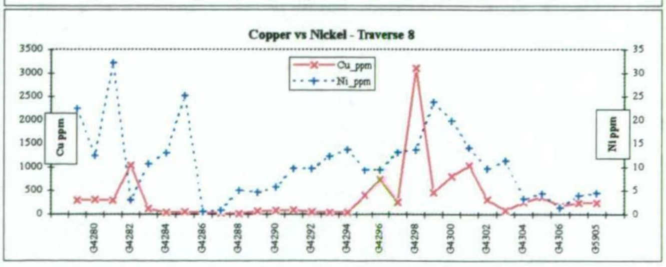

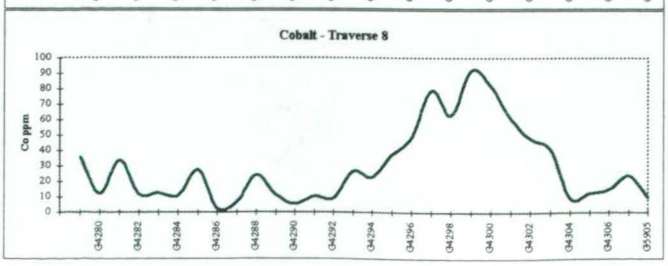

ROYAL THARSIS - SURFACE GEOCHEMISTRY
TRAVERSE ASSAY PROFILES

Appendix II
Chart 3
Traverse 9

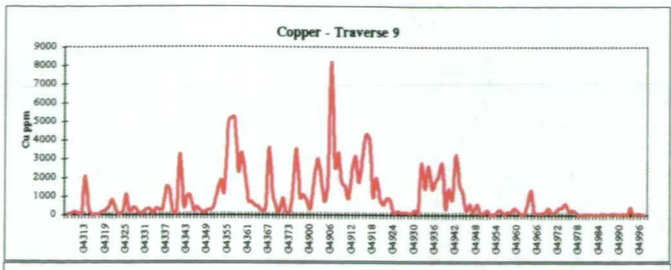

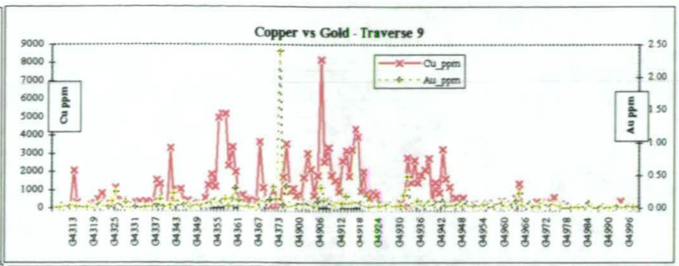

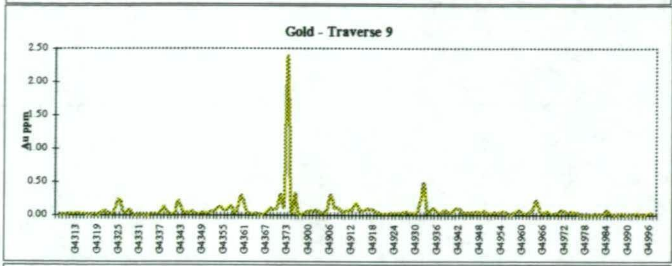

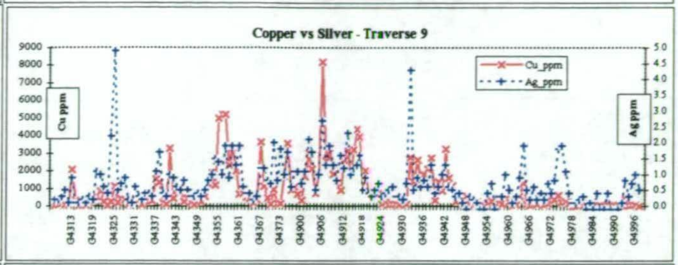

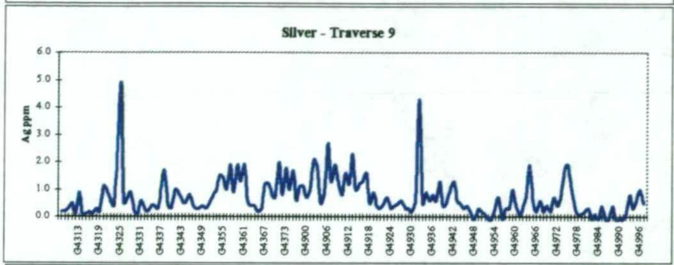

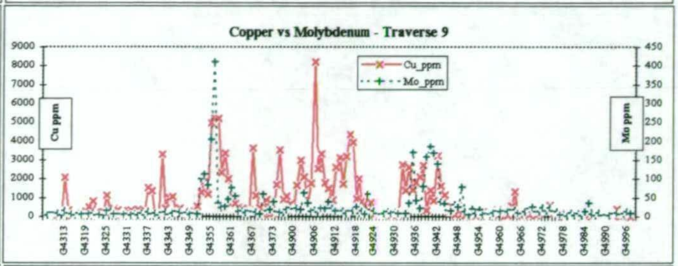

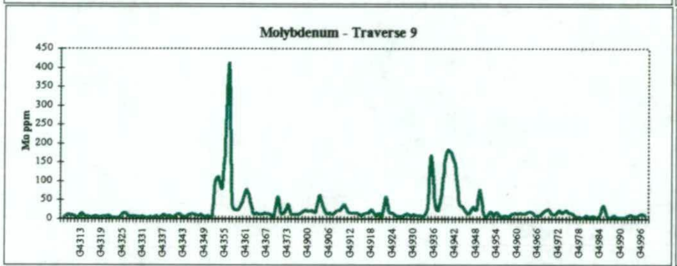

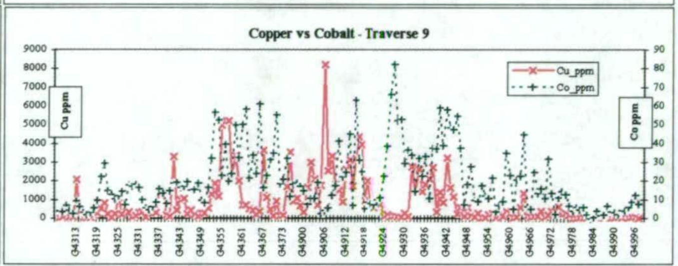

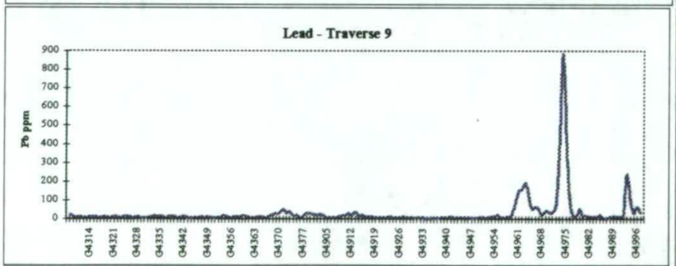

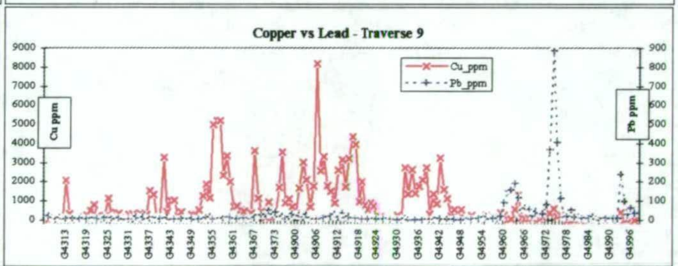

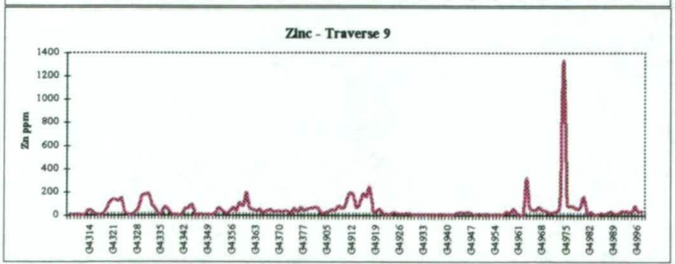

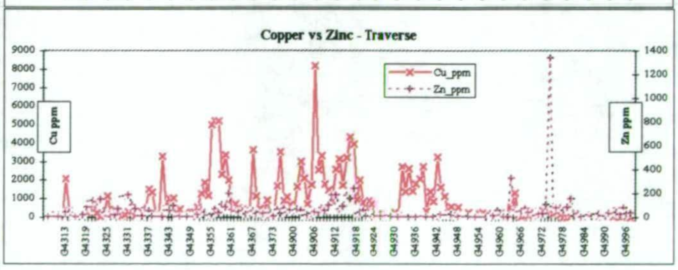

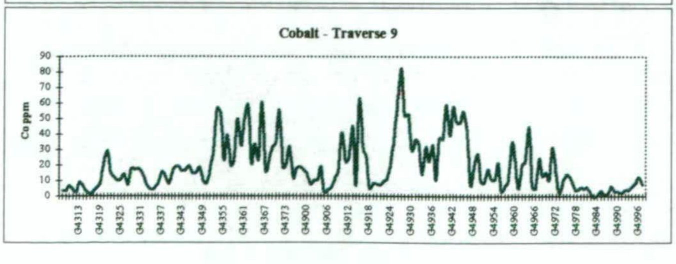

ROYAL THARSIS - SURFACE GEOCHEMISTRY
TRAVERSE ASSAY PROFILES

Appendix II
Chart 4
Traverse 10

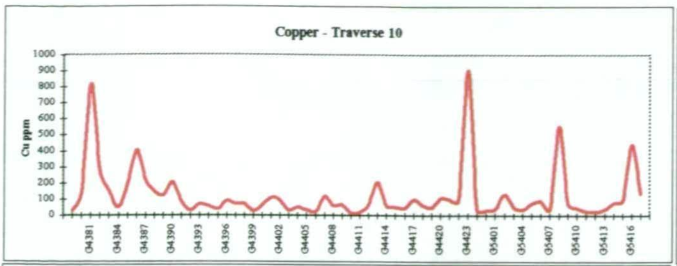

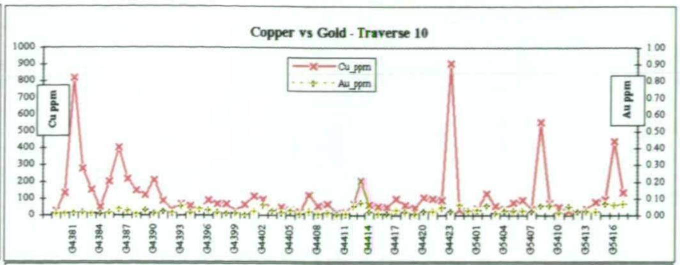

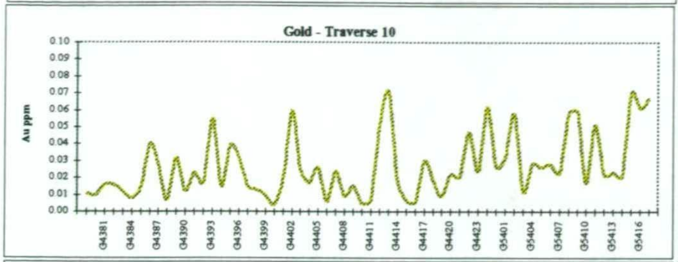

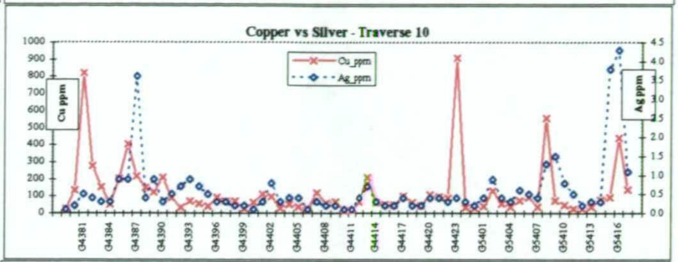

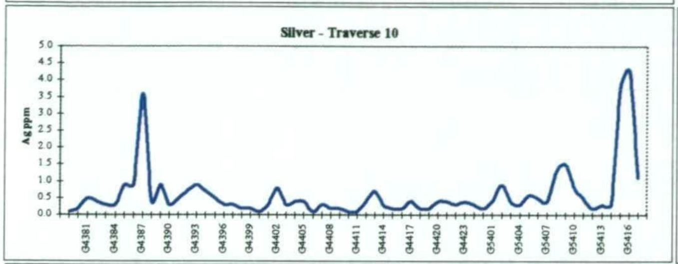

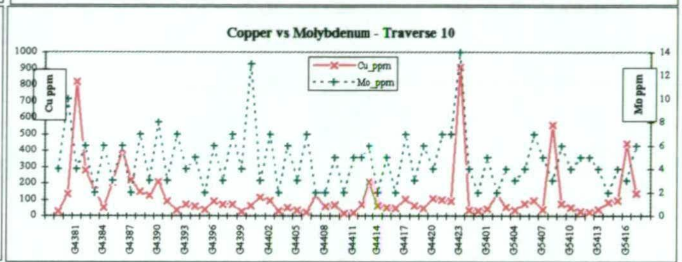

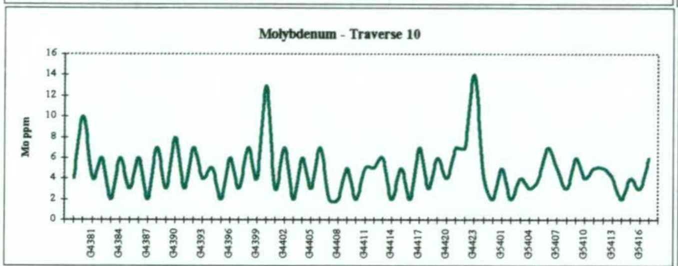

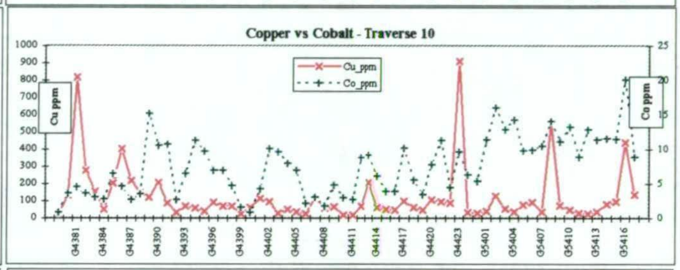

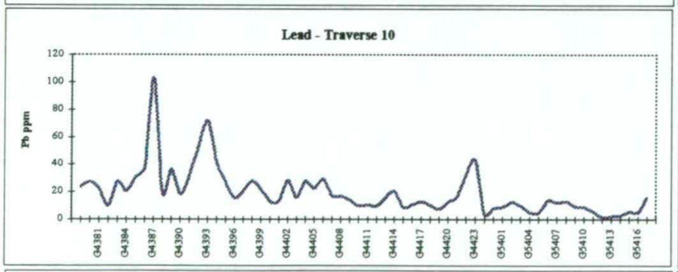

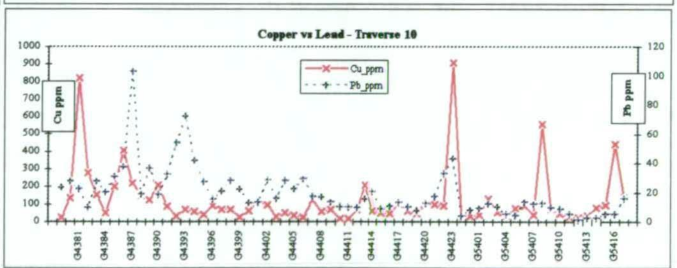

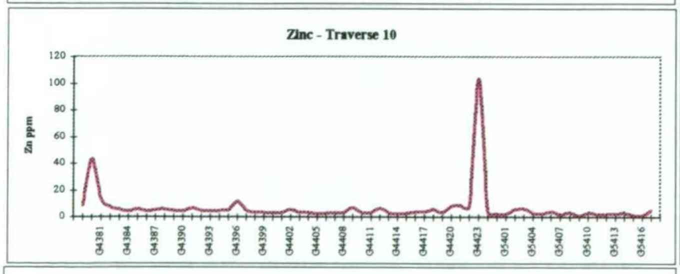

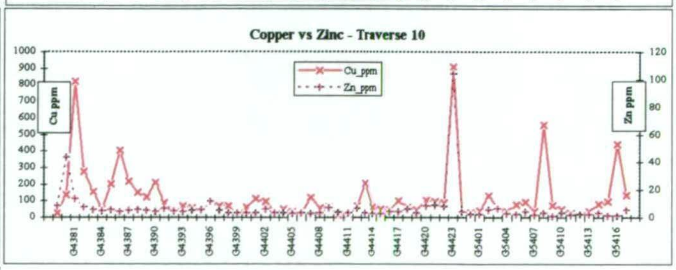

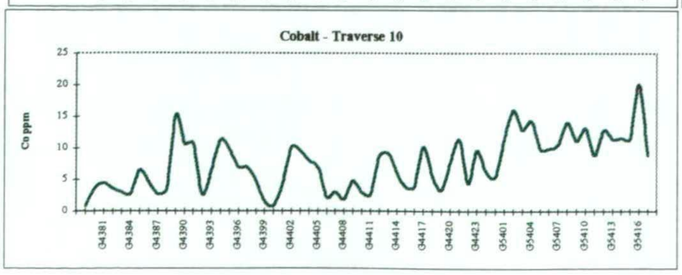

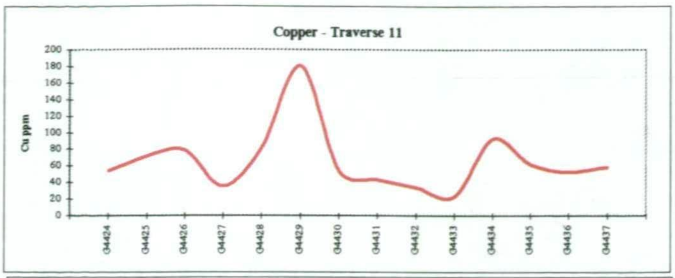
Copper - Traverse 11
Cu ppm

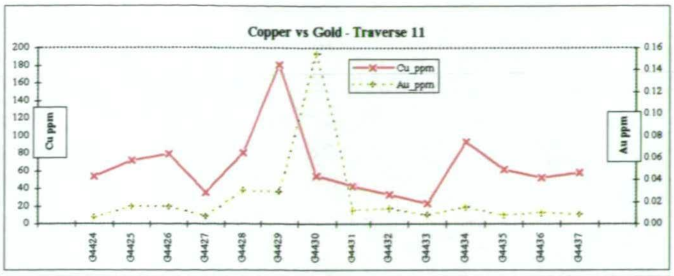
Copper vs Gold - Traverse 11
Cu ppm
Au ppm
Cu_ppm
Au_ppm

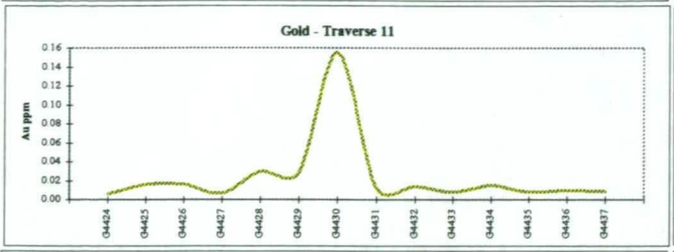
Gold - Traverse 11
Au ppm

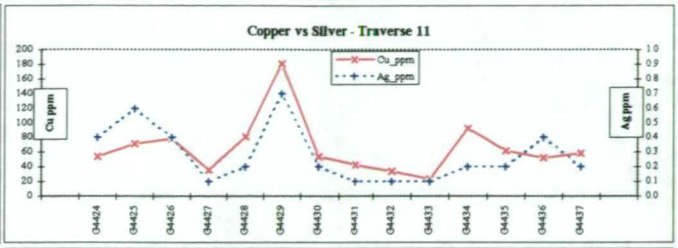
Copper vs Silver - Traverse 11
Cu ppm
Ag ppm
Cu_ppm
Ag_ppm

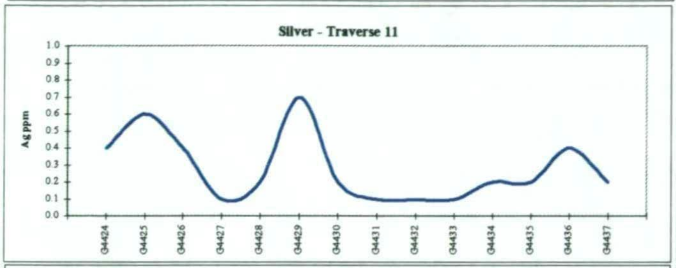
Silver - Traverse 11
Ag ppm

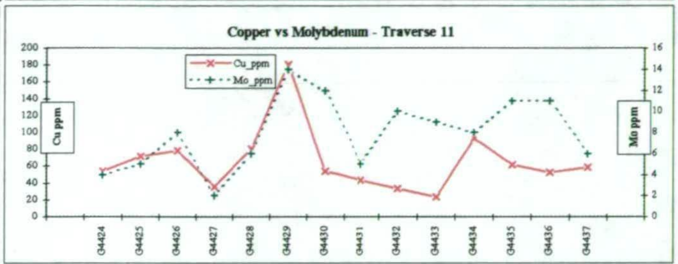
Copper vs Molybdenum - Traverse 11
Cu ppm
Mo ppm
Cu_ppm
Mo_ppm

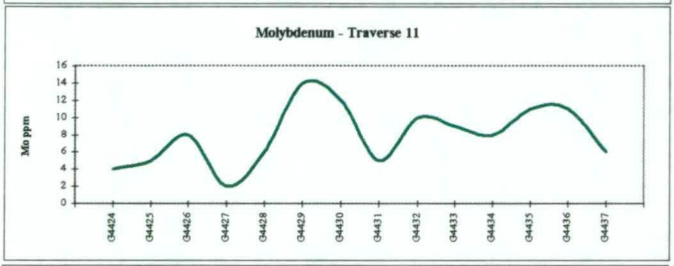
Molybdenum - Traverse 11
Mo ppm

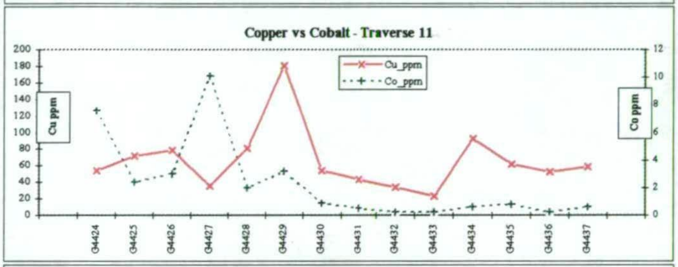
Copper vs Cobalt - Traverse 11
Cu ppm
Cu ppm
Cu_ppm
Co_ppm

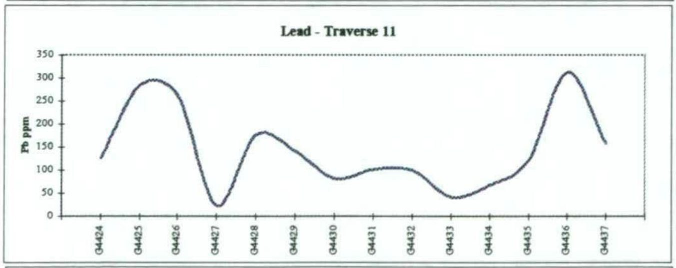
Lead - Traverse 11
Pb ppm

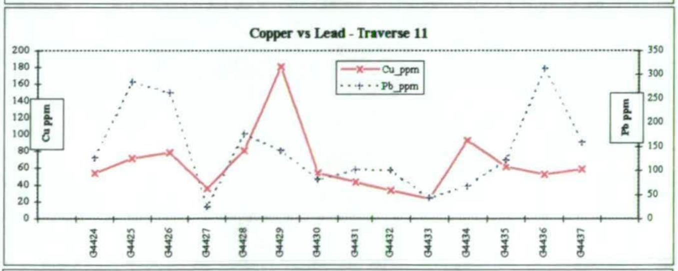
Copper vs Lead - Traverse 11
Cu ppm
Pb ppm
Cu_ppm
Pb_ppm

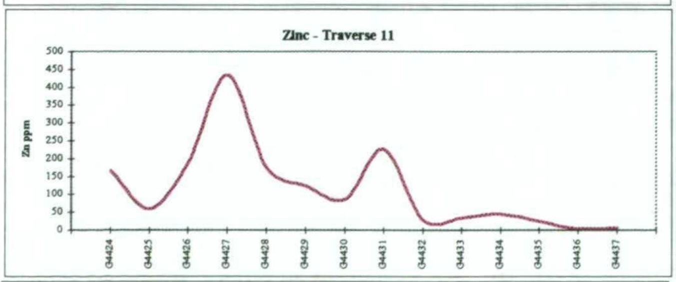
Zinc - Traverse 11
Zn ppm

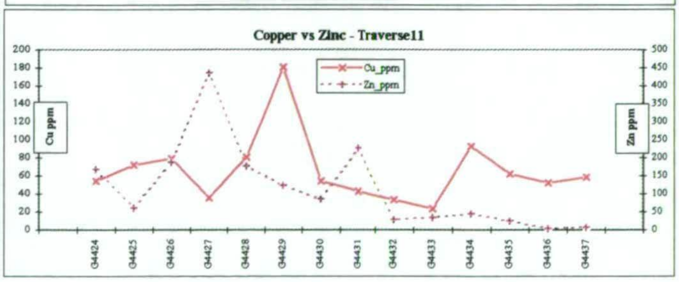
Copper vs Zinc - Traverse11
Cu ppm
Zn ppm
Cu_ppm
Zn_ppm

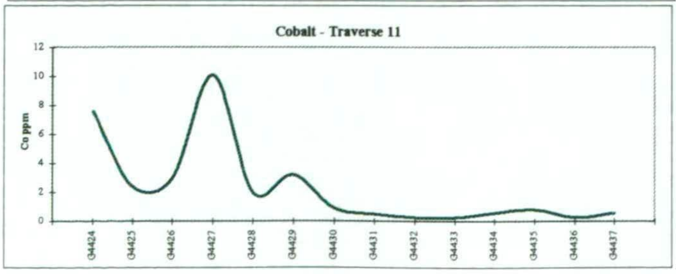
Cobalt - Traverse 11
Co ppm

ROYAL THARSIS - SURFACE GEOCHEMISTRY
TRAVERSE ASSAY PROFILES

Appendix II
Chart 6
Traverse 12

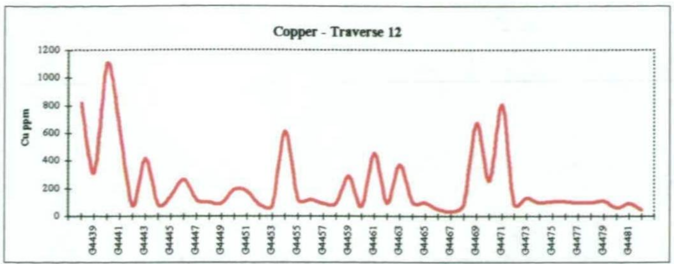

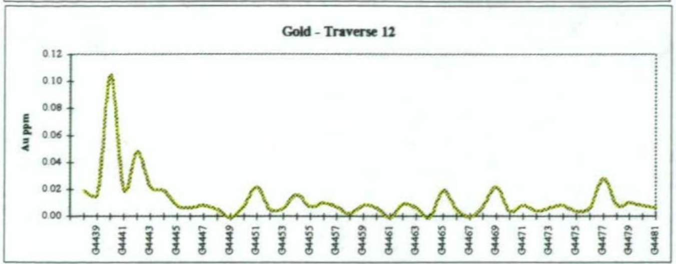

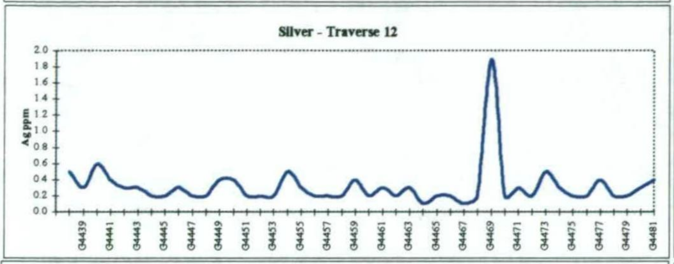

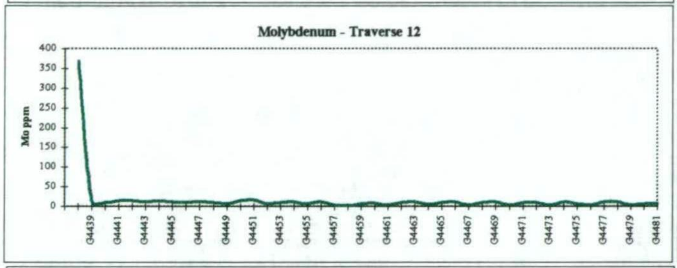

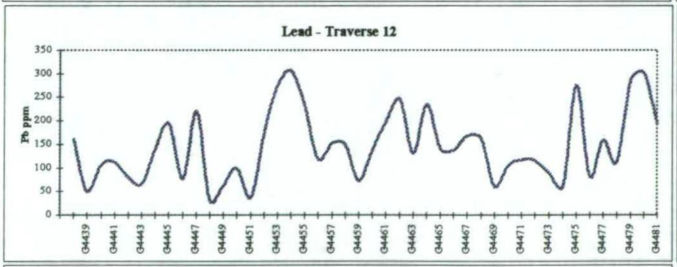

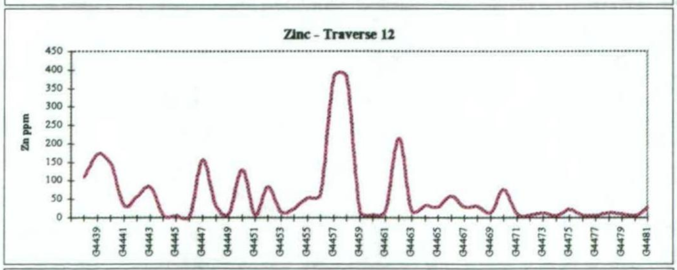

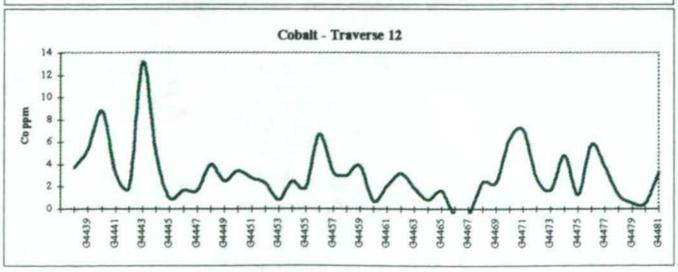

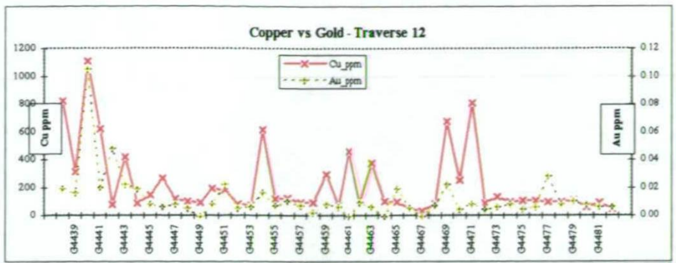

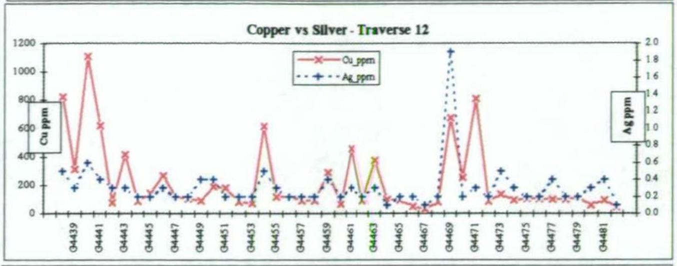

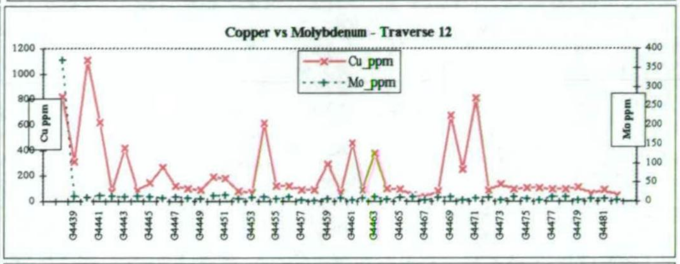

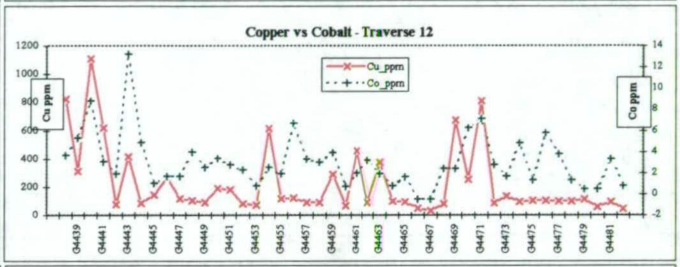

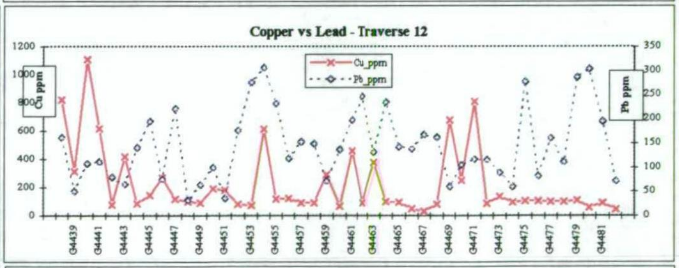

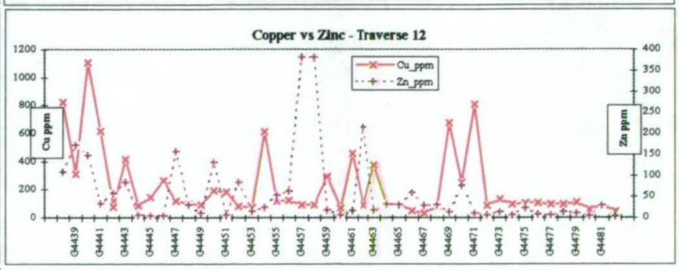

Appendix II
Chart 7
Traverse 13

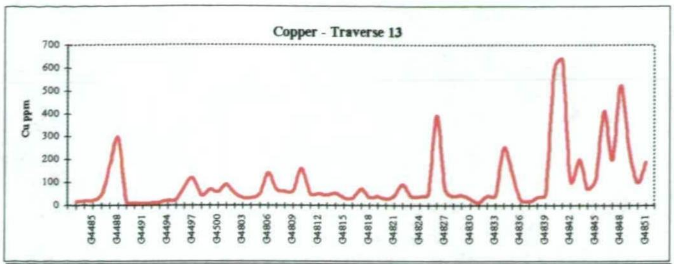

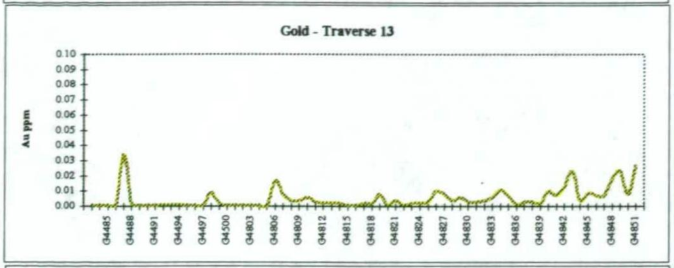

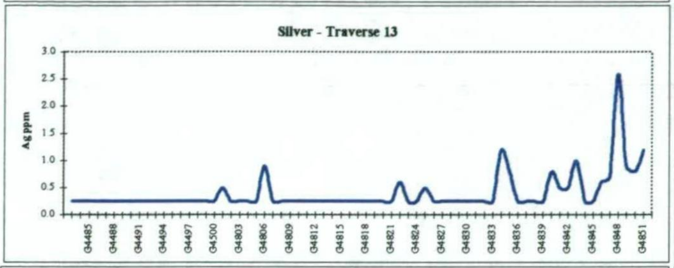

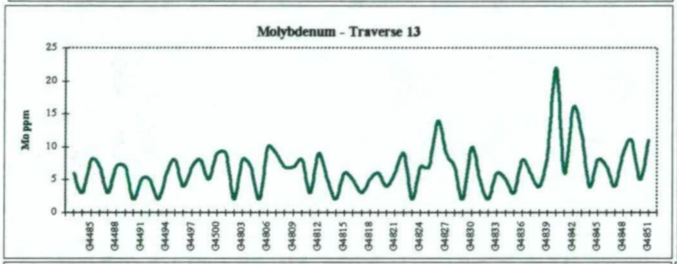

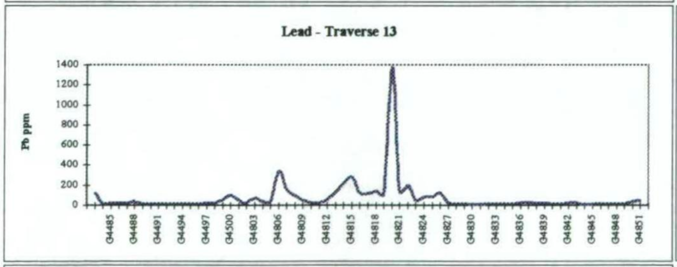

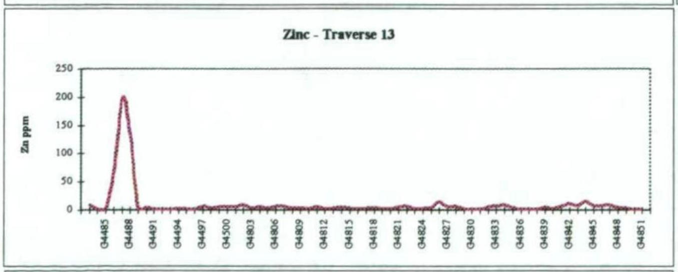

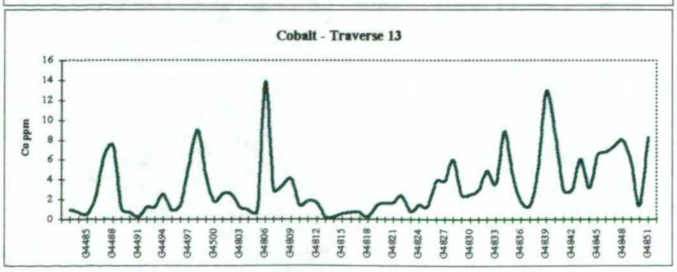

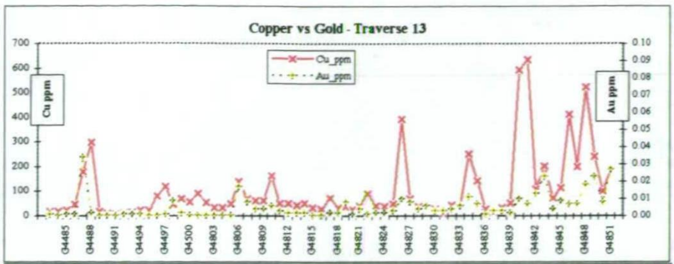

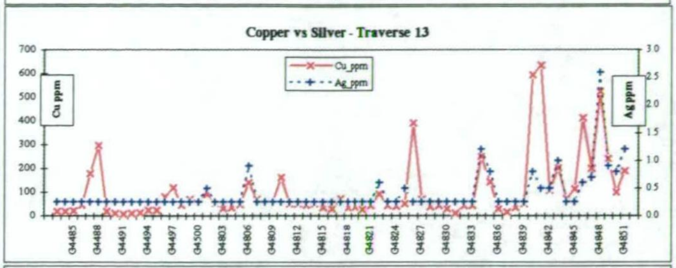

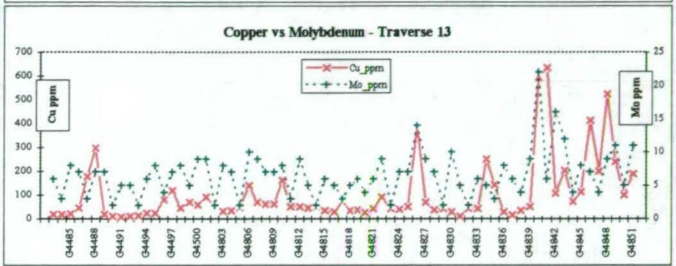

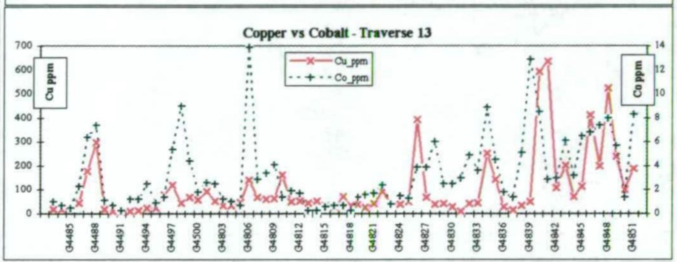

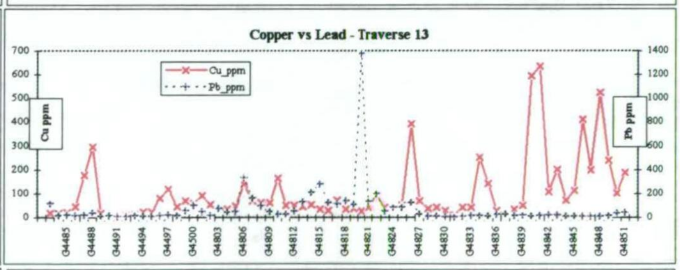

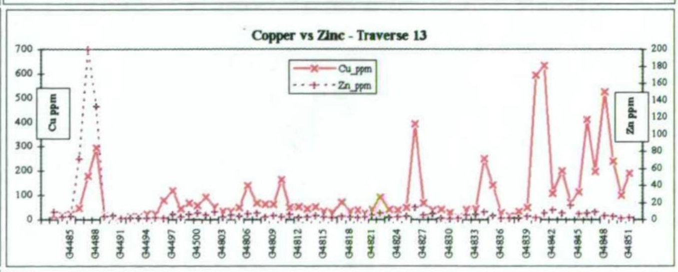

ROYAL THARSIS - SURFACE GEOCHEMISTRY
TRAVERSE ASSAY PROFILES

Appendix II
Chart 8
Traverse 14

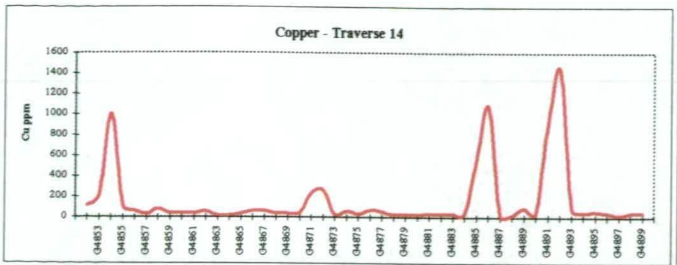

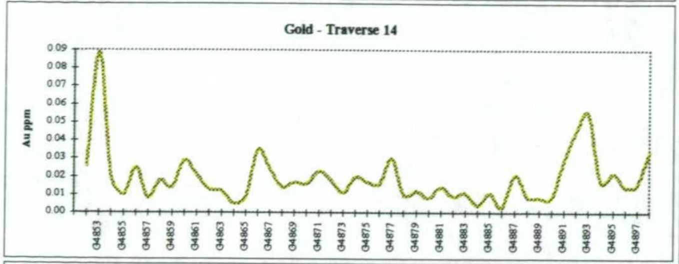

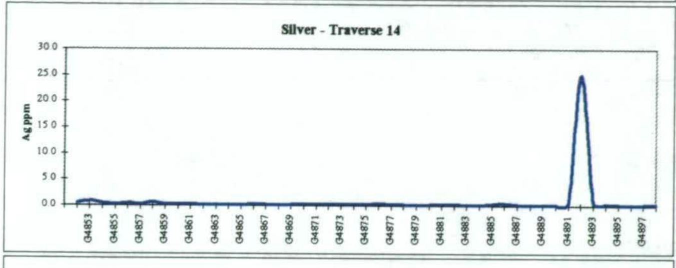

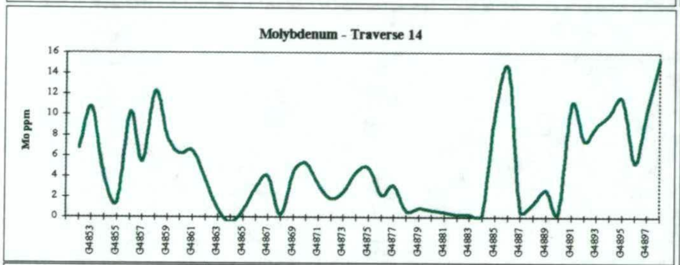

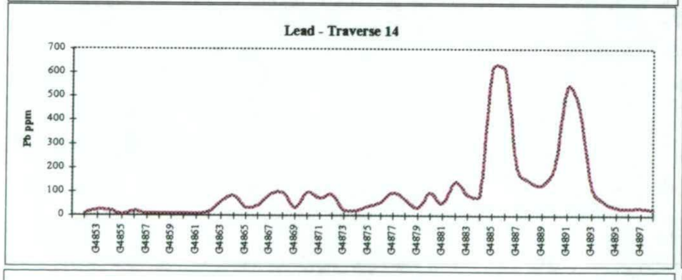

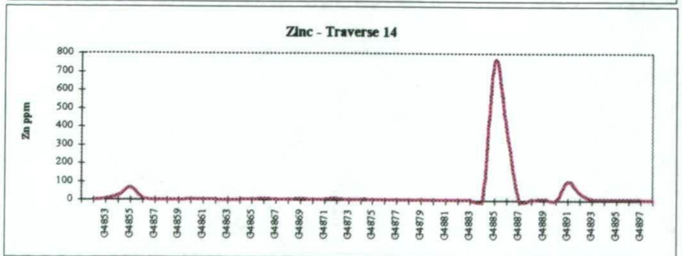

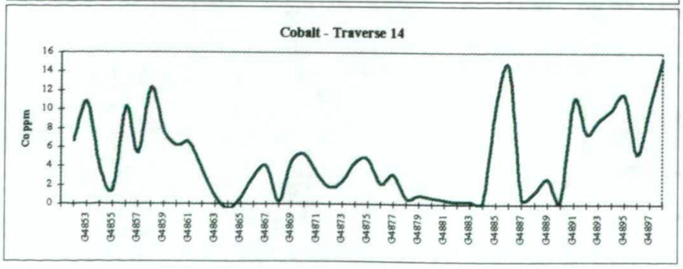

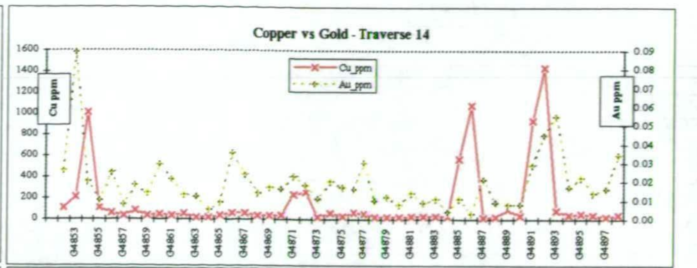

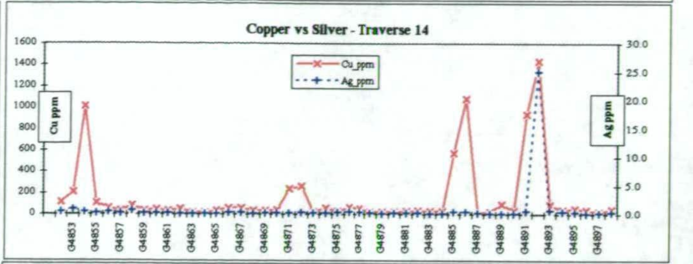

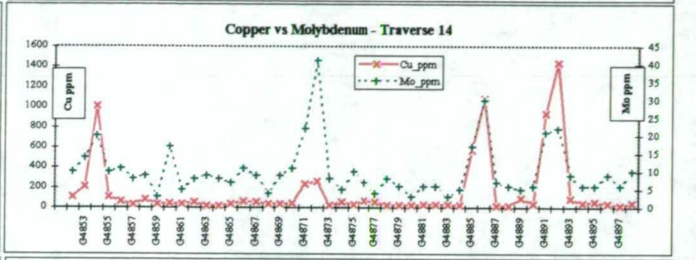

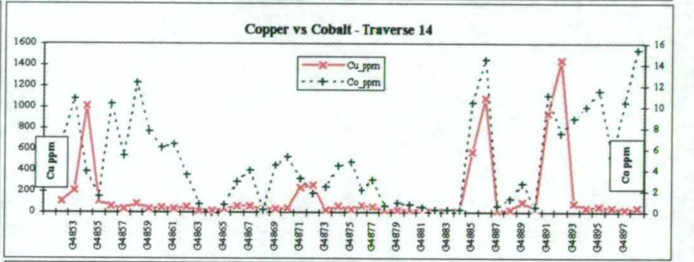

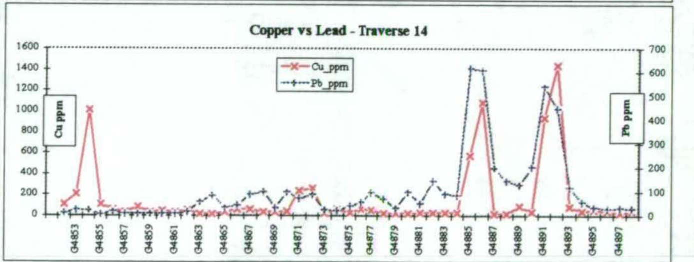

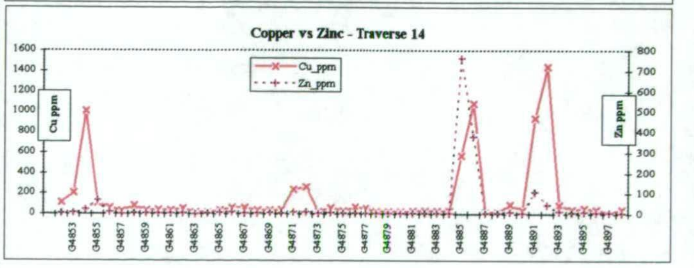

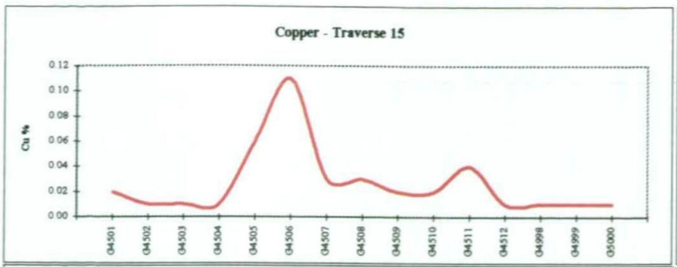
Copper - Traverse 15
Cu %
G4501
G4502
G4503
G4504
G4505
G4506
G4507
G4508
G4509
G4510
G4511
G4512
G4998
G4999
G5000

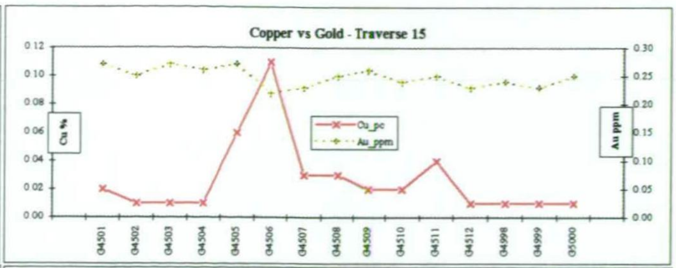
Copper vs Gold - Traverse 15
Cu %
Au ppm
Cu_pc
Au_ppm

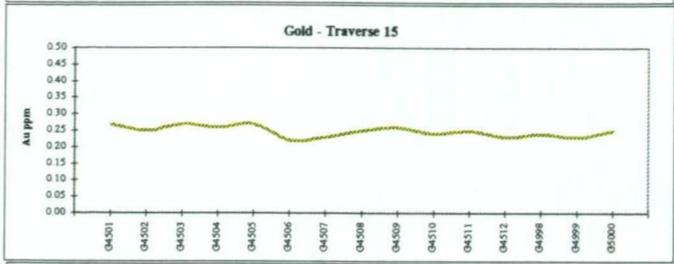
Gold - Traverse 15
Au ppm

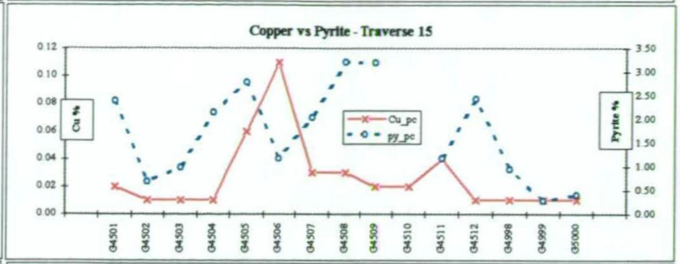
Copper vs Pyrite - Traverse 15
Cu %
Pyrite %
Cu_pc
py_pc

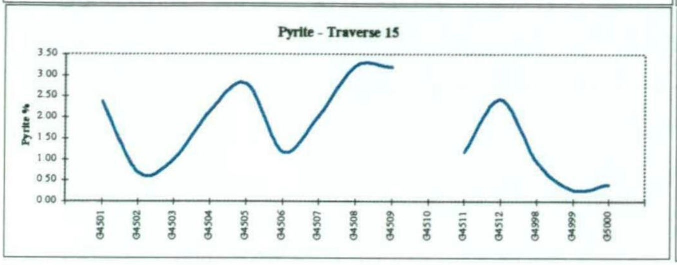
Pyrite - Traverse 15
Pyrite %

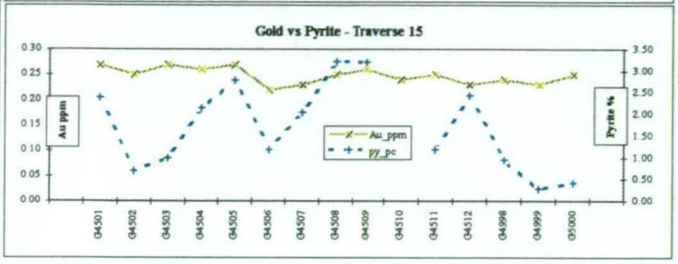
Gold vs Pyrite - Traverse 15
Au ppm
Pyrite %
Au_ppm
py_pc

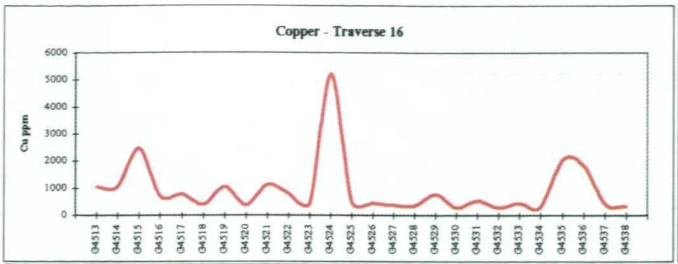

Copper - Traverse 16
Cu ppm

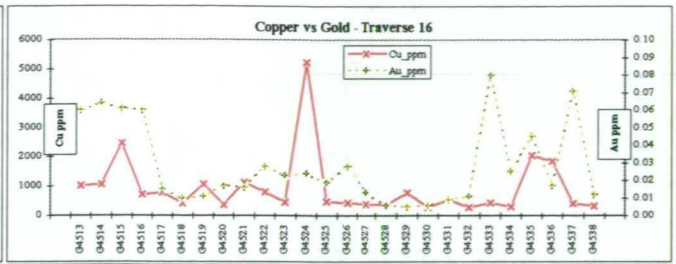

Copper vs Gold - Traverse 16
Cu_ppm
Au_ppm
Cu ppm
Au ppm

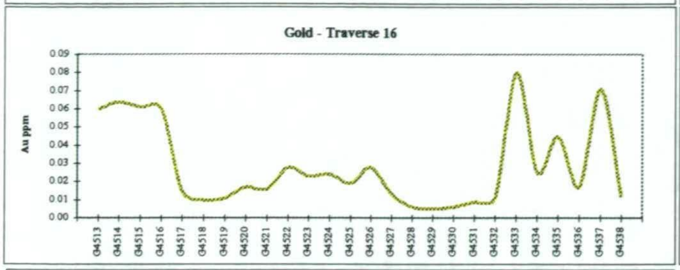

Gold - Traverse 16
Au ppm

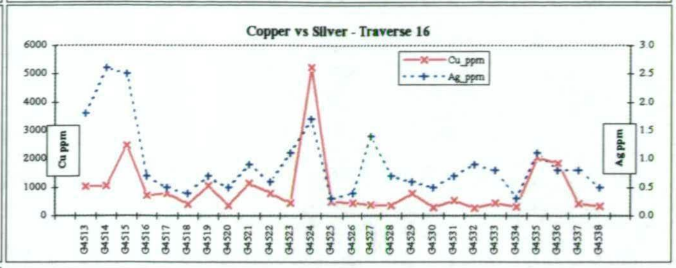

Copper vs Silver - Traverse 16
Cu_ppm
Ag_ppm
Cu ppm
Ag ppm

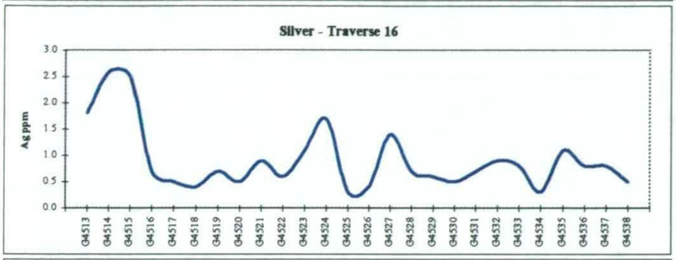

Silver - Traverse 16
Ag ppm

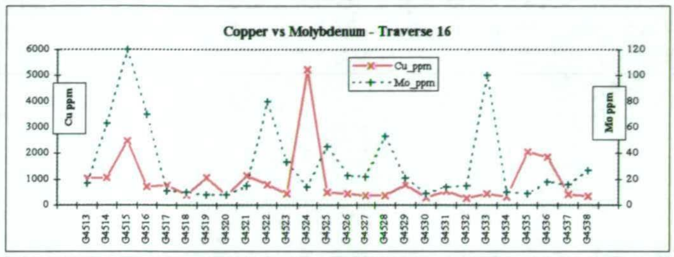

Copper vs Molybdenum - Traverse 16
Cu_ppm
Mo_ppm
Cu ppm
Mo ppm

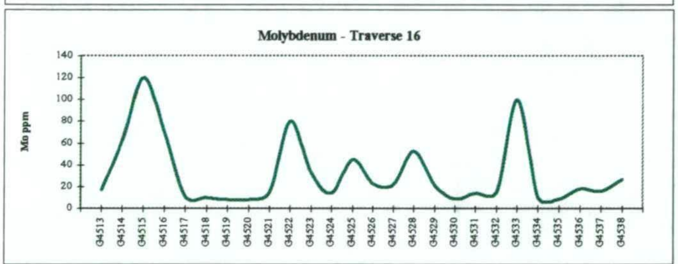

Molybdenum - Traverse 16
Mo ppm

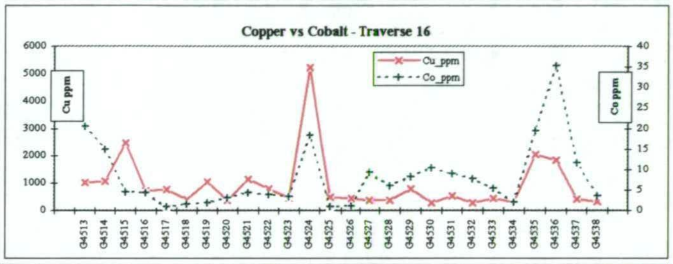

Copper vs Cobalt - Traverse 16
Cu_ppm
Co_ppm
Cu ppm
Co ppm

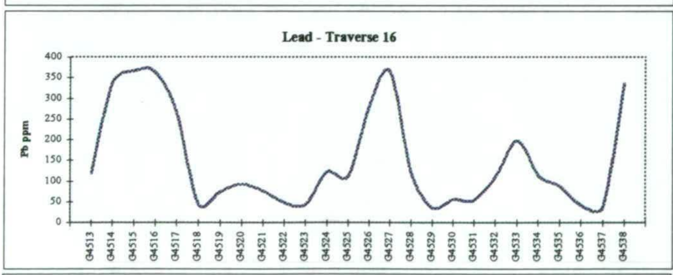

Lead - Traverse 16
Pb ppm

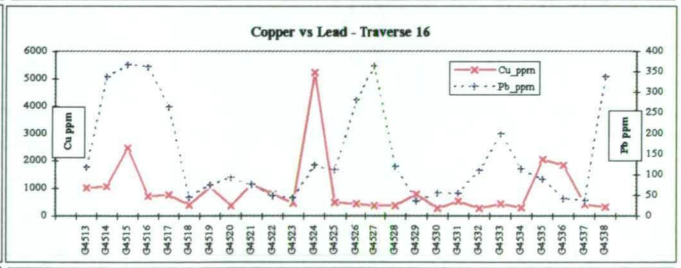

Copper vs Lead - Traverse 16
Cu_ppm
Pb_ppm
Cu ppm
Pb ppm

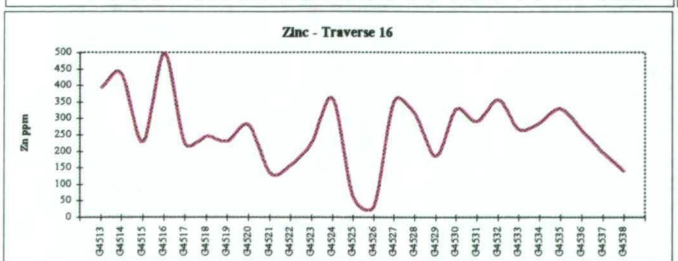

Zinc - Traverse 16
Zn ppm

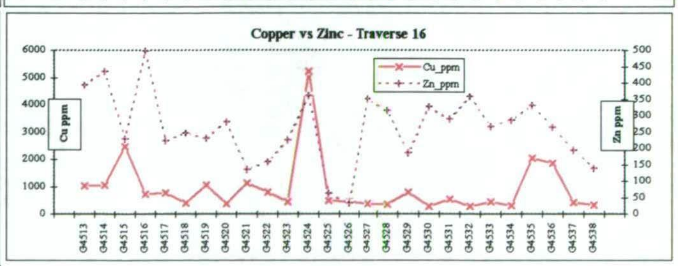

Copper vs Zinc - Traverse 16
Cu_ppm
Zn_ppm
Cu ppm
Zn ppm

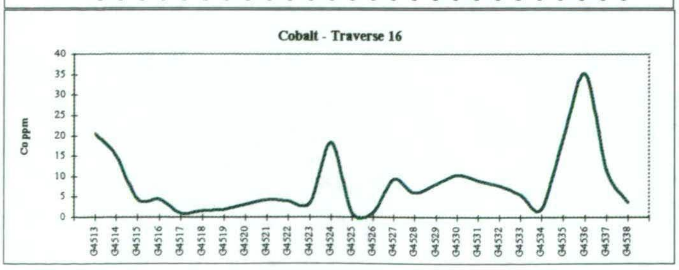

Cobalt - Traverse 16
Co ppm

ROYAL THARSIS - SURFACE GEOCHEMISTRY
TRAVERSE ASSAY PROFILES

Appendix II
Chart 11
Traverse 19

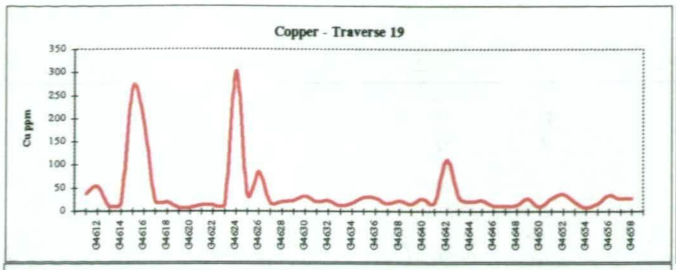

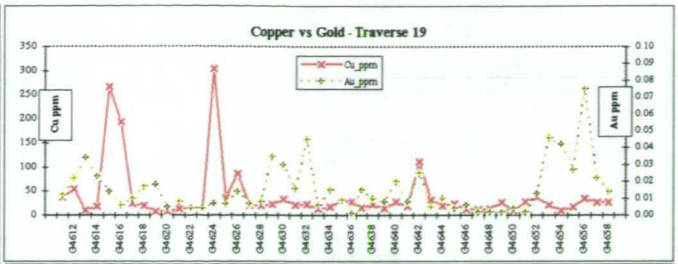

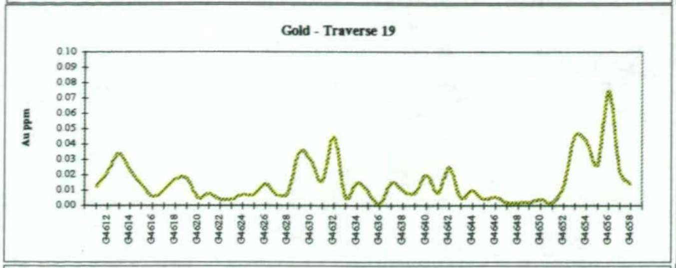

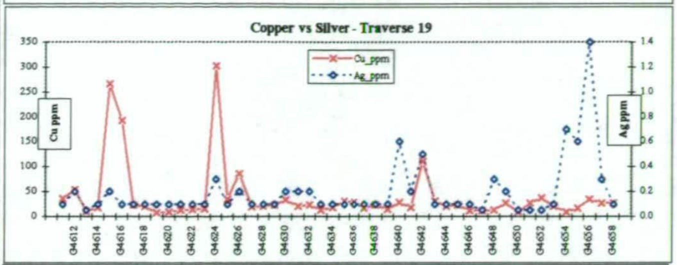

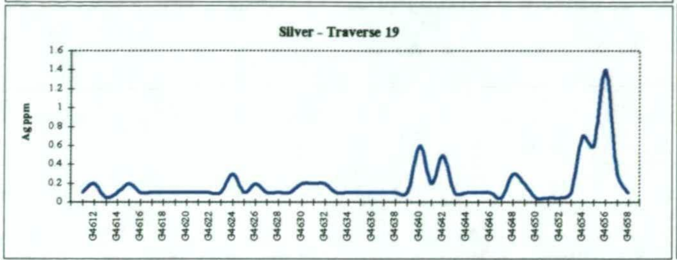

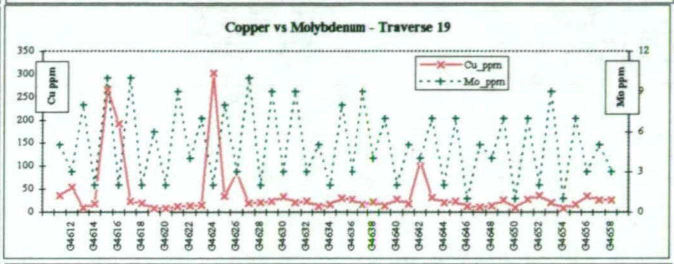

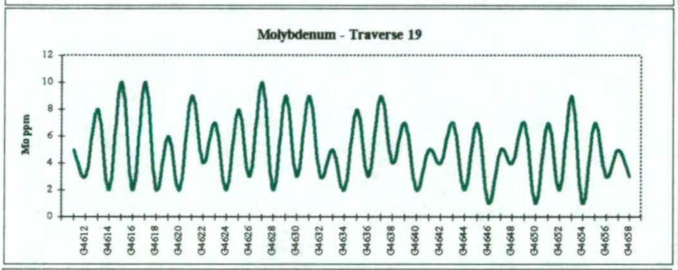

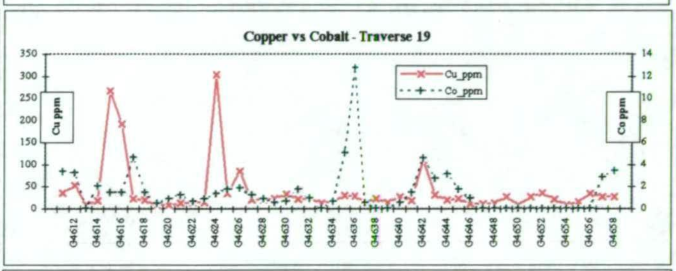

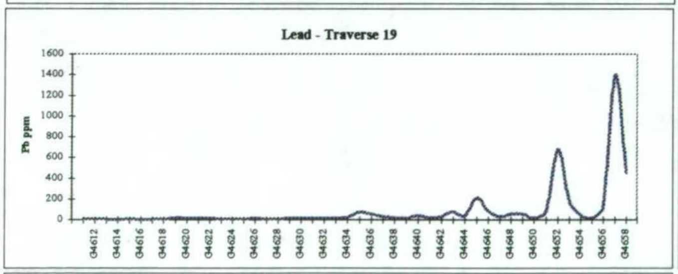

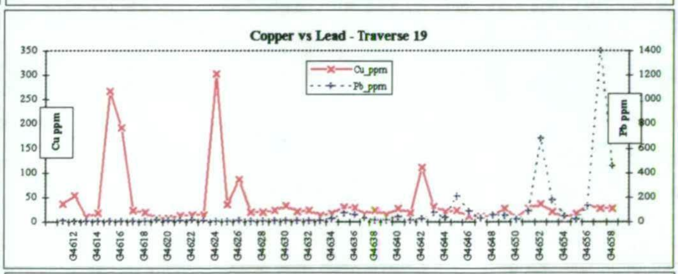

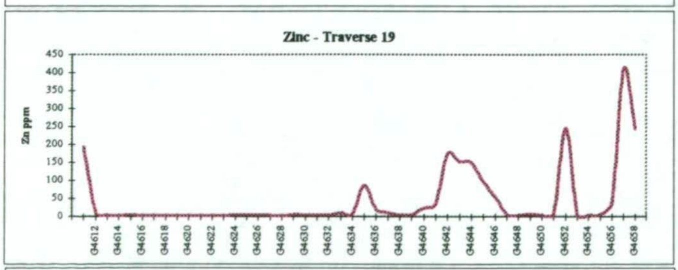

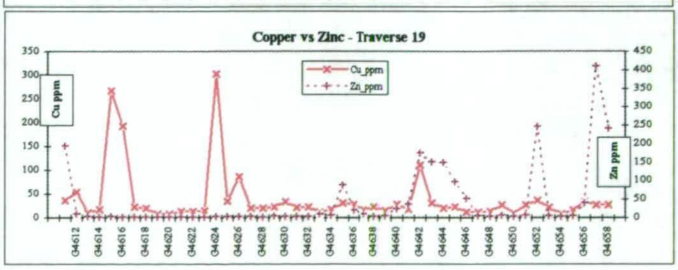

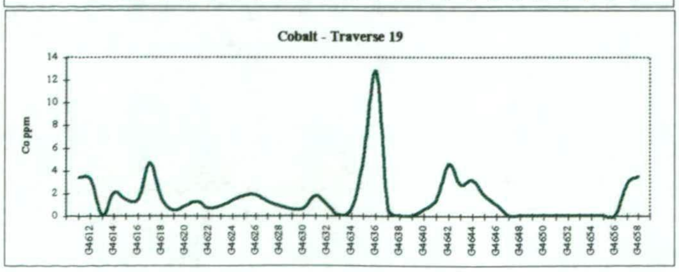

ROYAL THARSIS - SURFACE GEOCHEMISTRY
TRAVERSE ASSAY PROFILES

Appendix II
Chart 12
Traverse 20

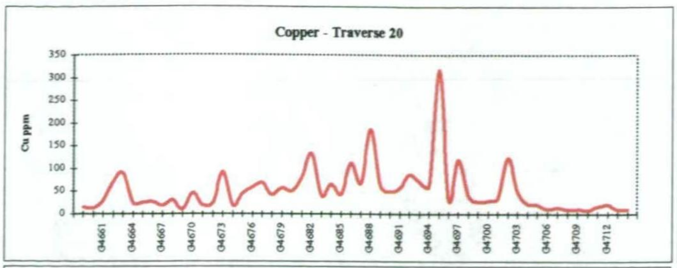

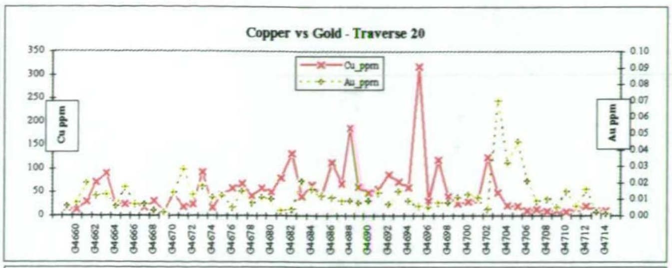

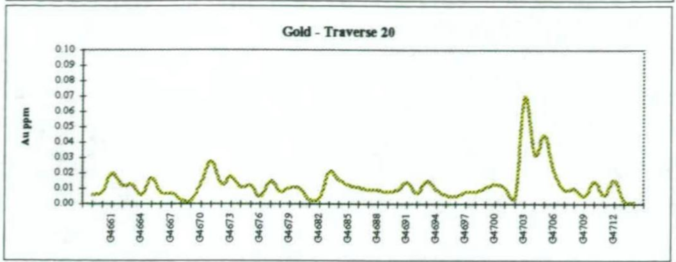

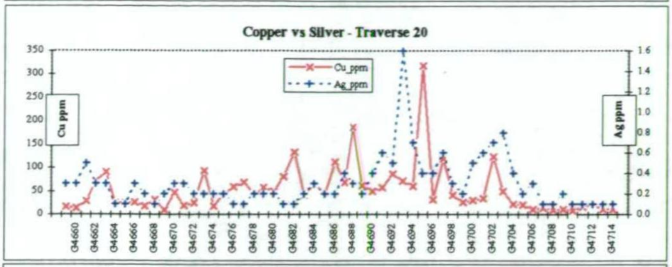

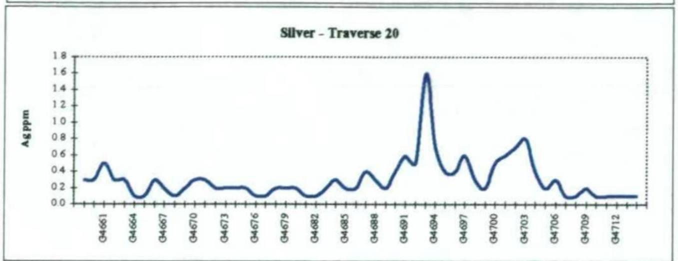

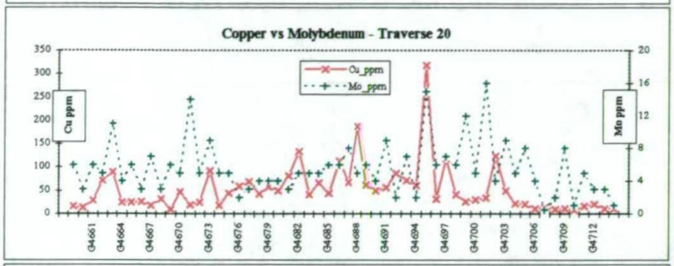

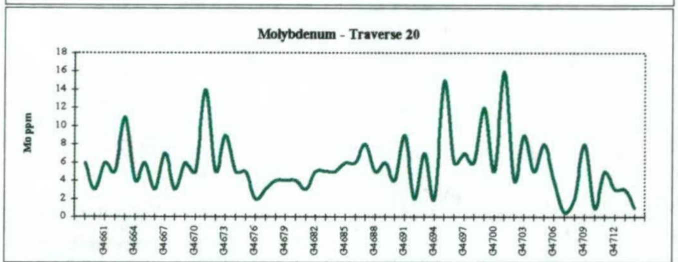

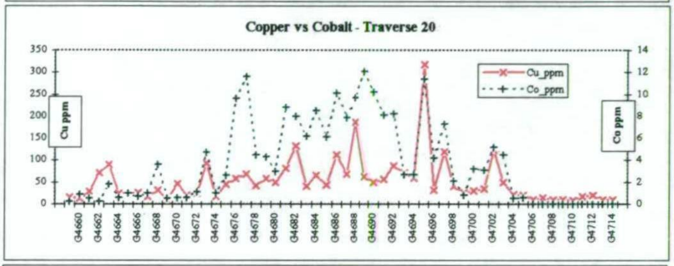

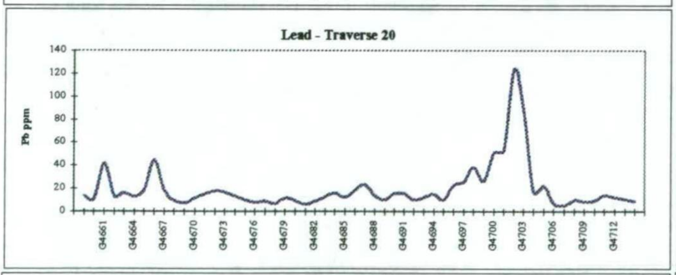

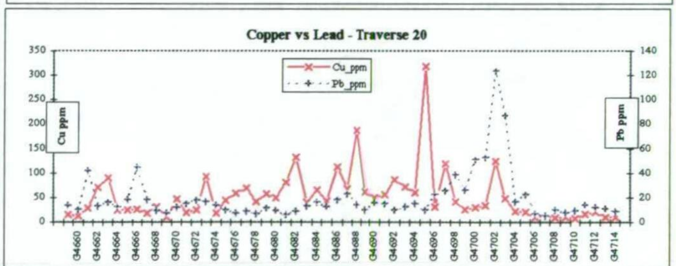

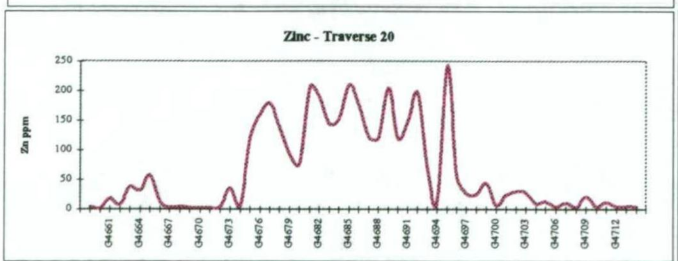

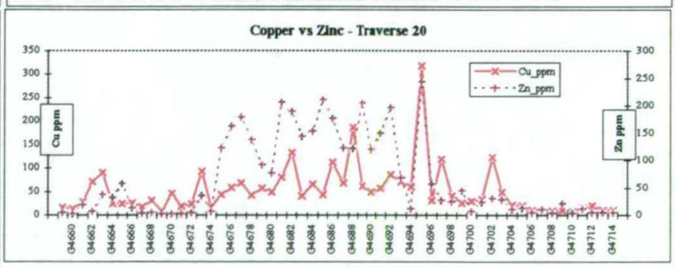

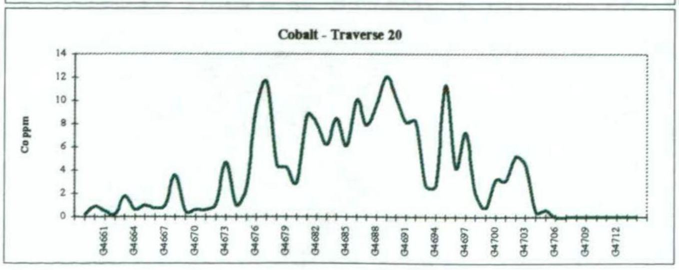

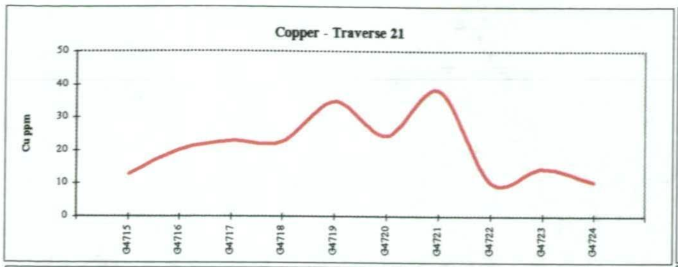
Copper - Traverse 21
Cu ppm
G4715 G4716 G4717 G4718 G4719 G4720 G4721 G4722 G4723 G4724

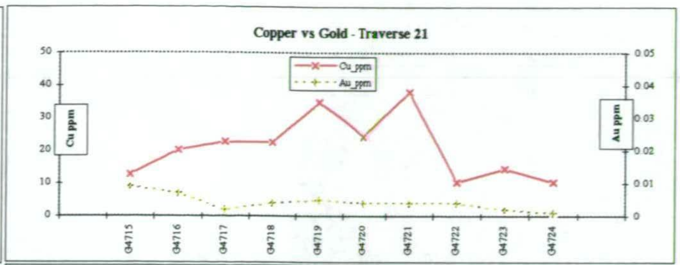
Copper vs Gold - Traverse 21
Cu_ppm
Au_ppm
Cu ppm
Au ppm
G4715 G4716 G4717 G4718 G4719 G4720 G4721 G4722 G4723 G4724

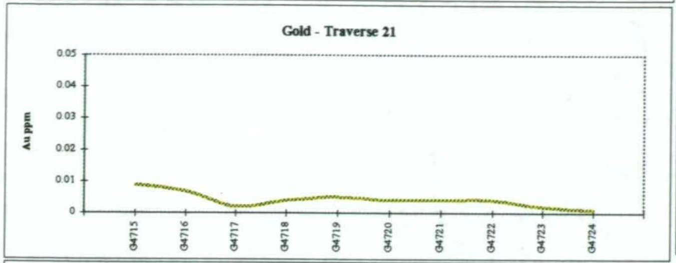
Gold - Traverse 21
Au ppm
G4715 G4716 G4717 G4718 G4719 G4720 G4721 G4722 G4723 G4724

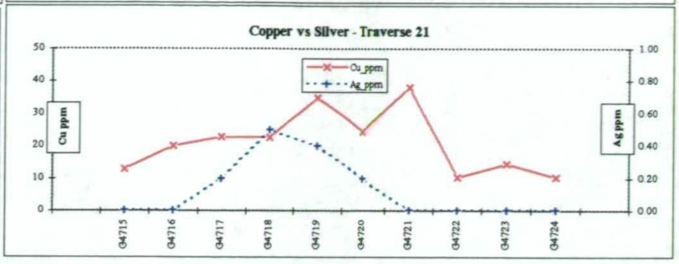
Copper vs Silver - Traverse 21
Cu_ppm
Ag_ppm
Cu ppm
Ag ppm
G4715 G4716 G4717 G4718 G4719 G4720 G4721 G4722 G4723 G4724

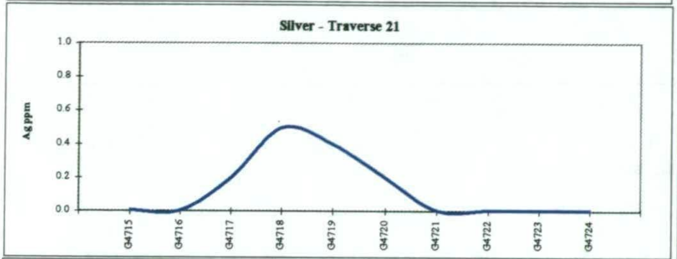
Silver - Traverse 21
Ag ppm
G4715 G4716 G4717 G4718 G4719 G4720 G4721 G4722 G4723 G4724

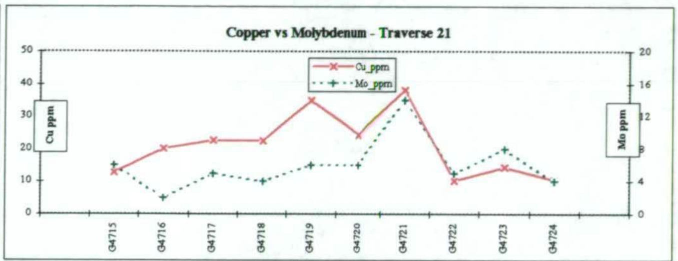
Copper vs Molybdenum - Traverse 21
Cu_ppm
Mo_ppm
Cu ppm
Mo ppm
G4715 G4716 G4717 G4718 G4719 G4720 G4721 G4722 G4723 G4724

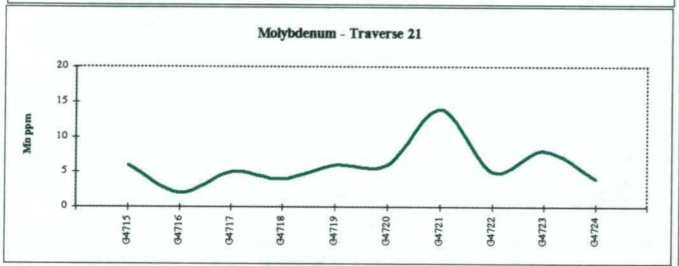
Molybdenum - Traverse 21
Mo ppm
G4715 G4716 G4717 G4718 G4719 G4720 G4721 G4722 G4723 G4724

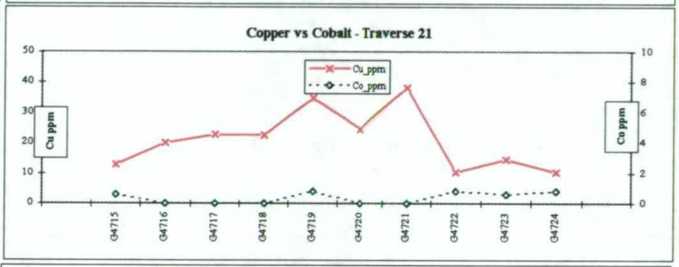
Copper vs Cobalt - Traverse 21
Cu_ppm
Co_ppm
Cu ppm
G4715 G4716 G4717 G4718 G4719 G4720 G4721 G4722 G4723 G4724

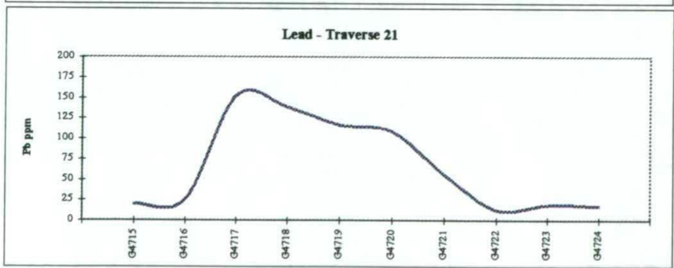
Lead - Traverse 21
Pb ppm
G4715 G4716 G4717 G4718 G4719 G4720 G4721 G4722 G4723 G4724

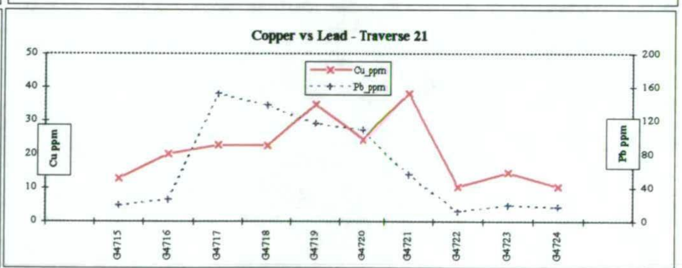
Copper vs Lead - Traverse 21
Cu_ppm
Pb_ppm
Cu ppm
Pb ppm
G4715 G4716 G4717 G4718 G4719 G4720 G4721 G4722 G4723 G4724

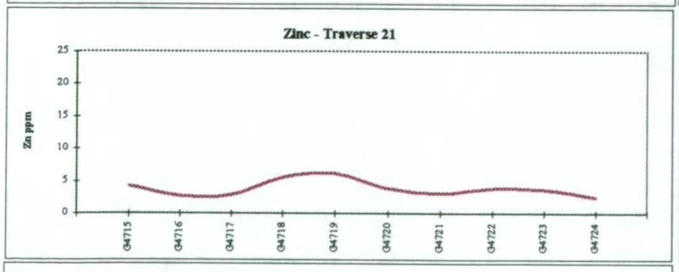
Zinc - Traverse 21
Zn ppm
G4715 G4716 G4717 G4718 G4719 G4720 G4721 G4722 G4723 G4724

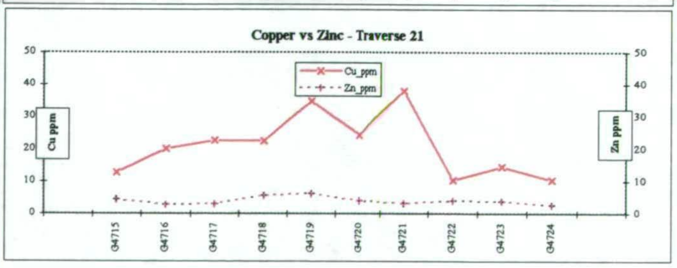
Copper vs Zinc - Traverse 21
Cu_ppm
Zn_ppm
Cu ppm
Zn ppm
G4715 G4716 G4717 G4718 G4719 G4720 G4721 G4722 G4723 G4724

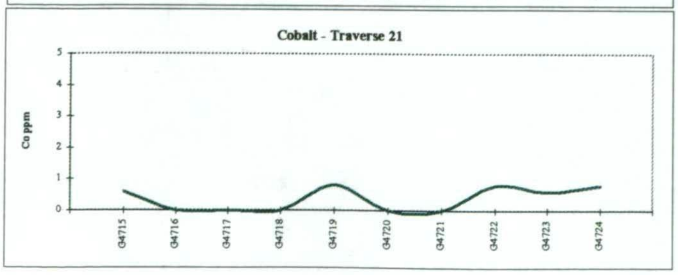
Cobalt - Traverse 21
Co ppm
G4715 G4716 G4717 G4718 G4719 G4720 G4721 G4722 G4723 G4724

Appendix II
Chart 14
Traverse 22

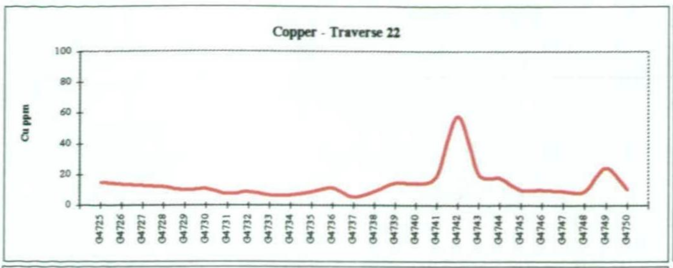

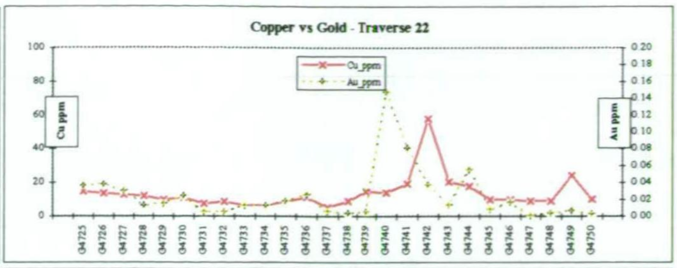

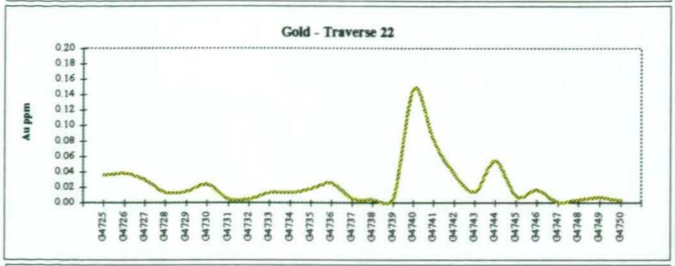

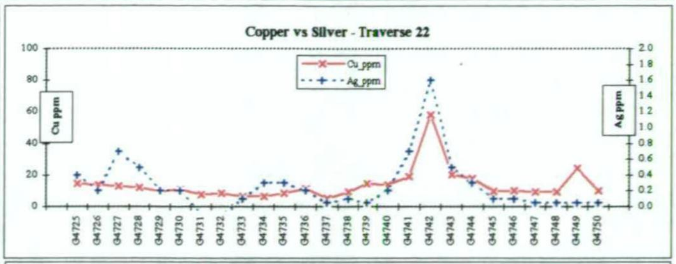

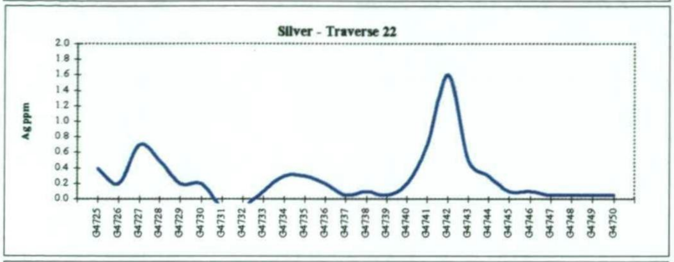

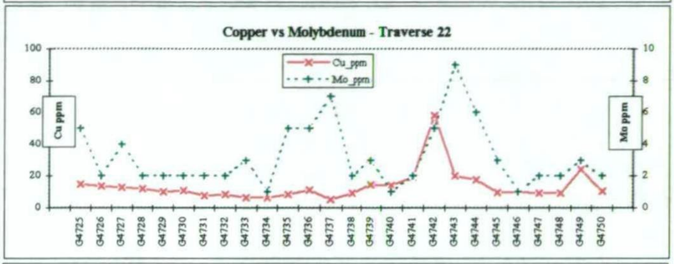

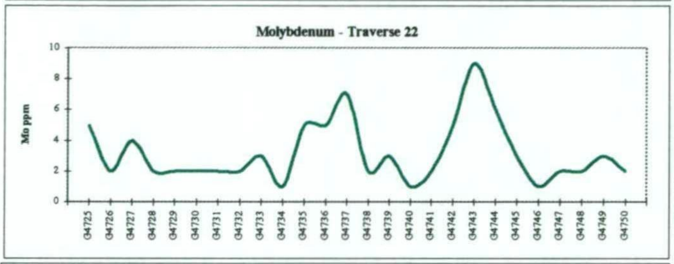

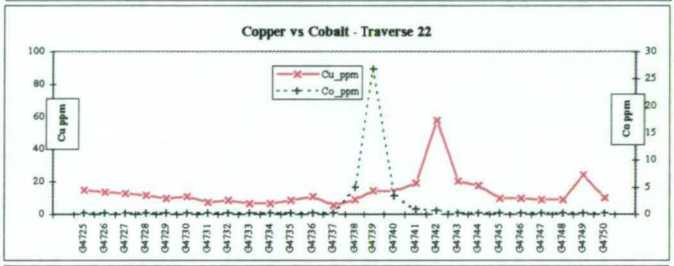

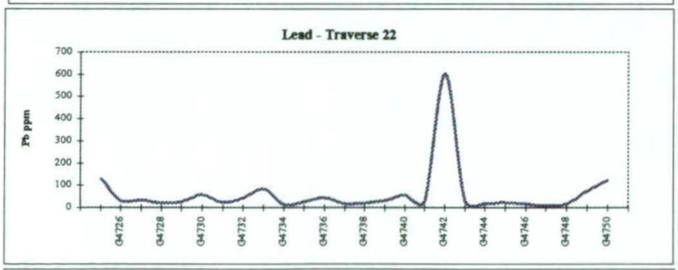

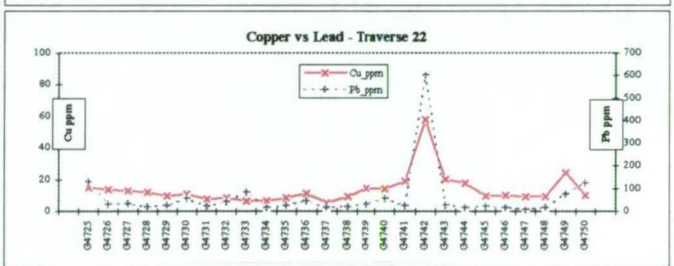

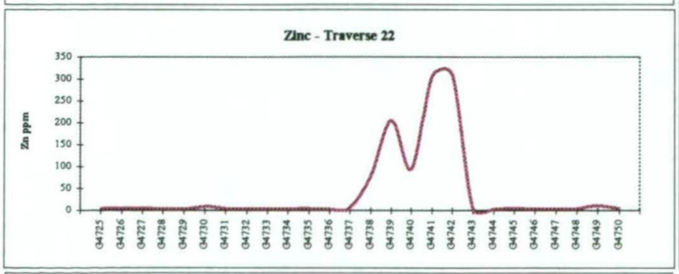

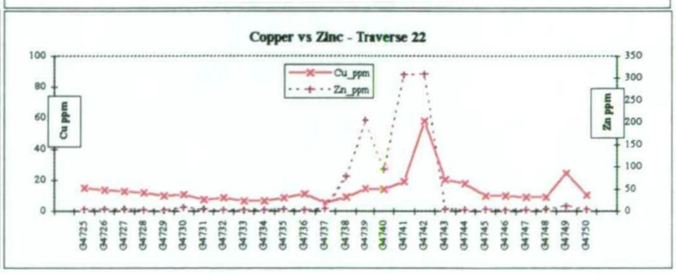

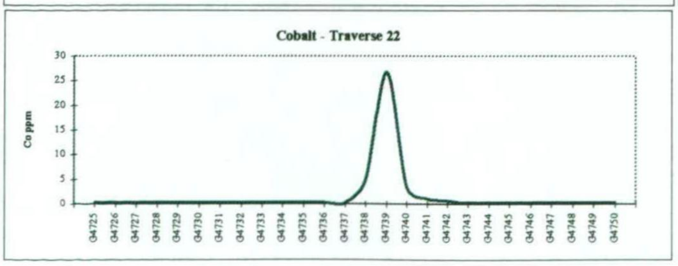

ROYAL THARSIS - SURFACE GEOCHEMISTRY
TRAVERSE ASSAY PROFILES

Appendix II
Chart 15
Traverse 23

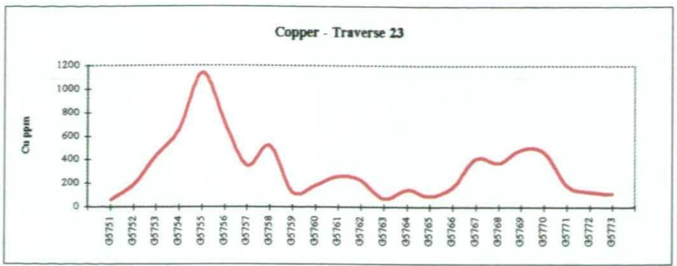

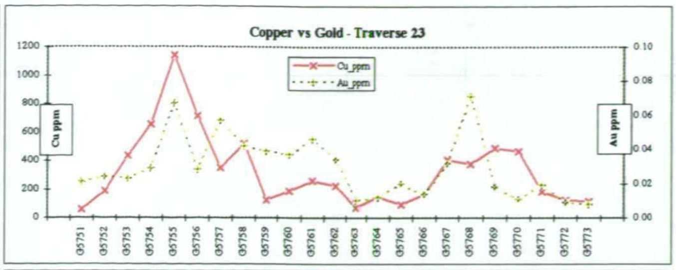

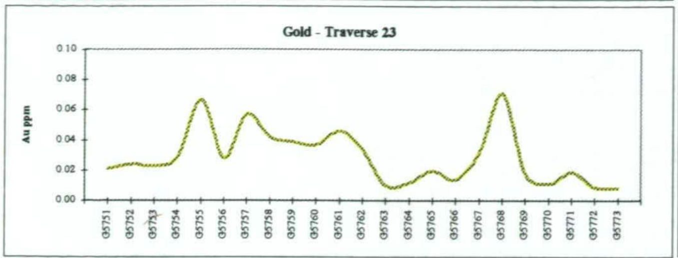

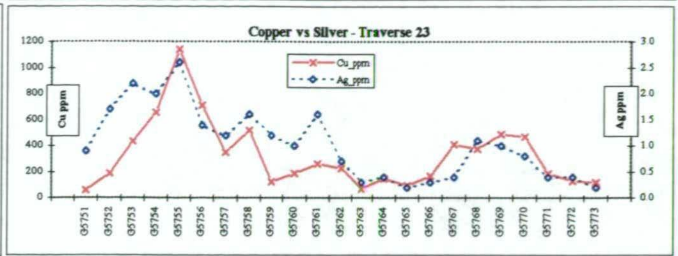

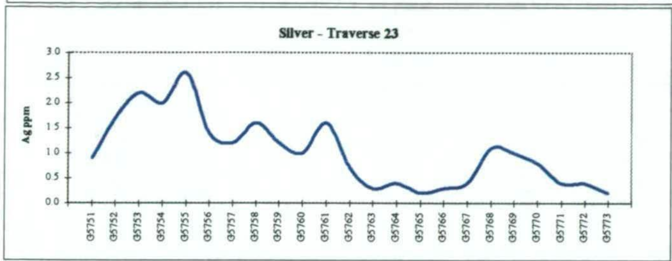

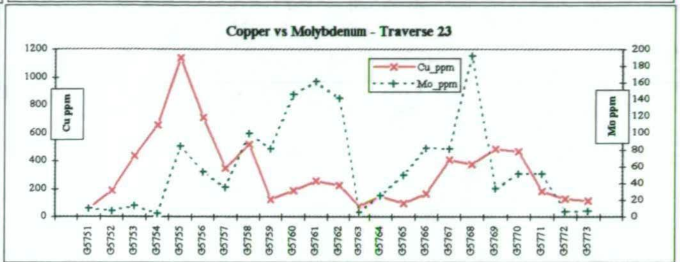

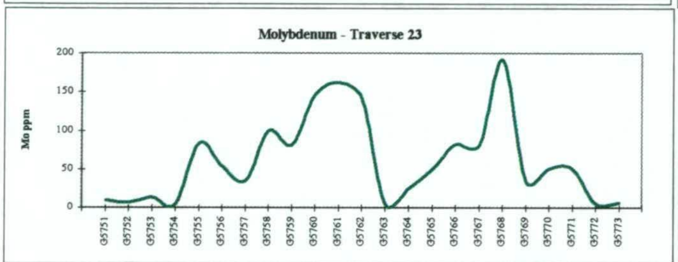

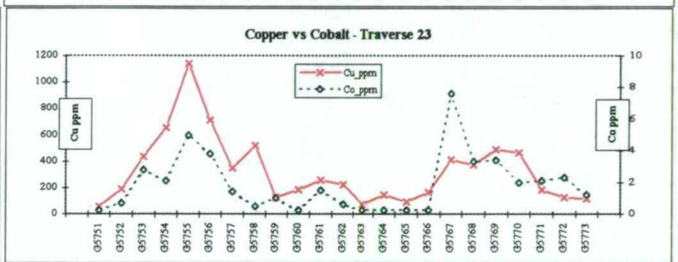

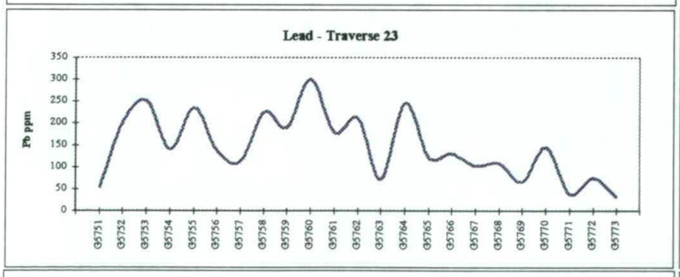

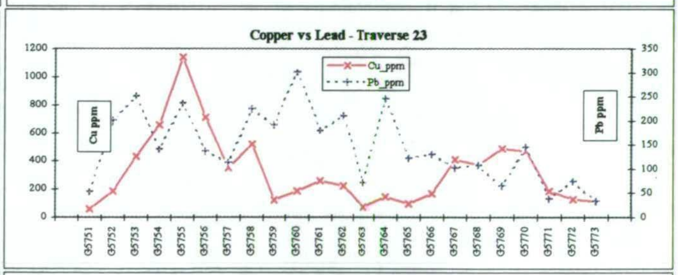

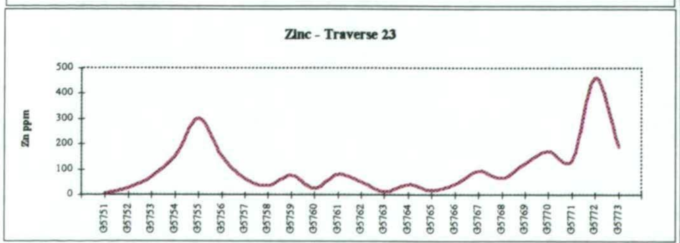

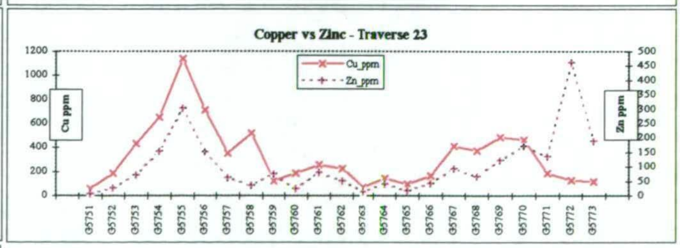

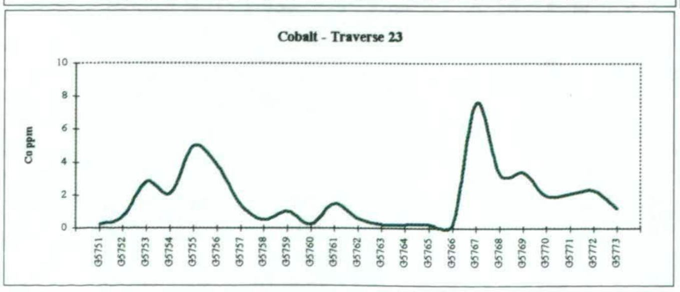

ROYAL THARSIS - SURFACE GEOCHEMISTRY
TRAVERSE ASSAY PROFILES

Appendix II
Chart 16
Traverse 24

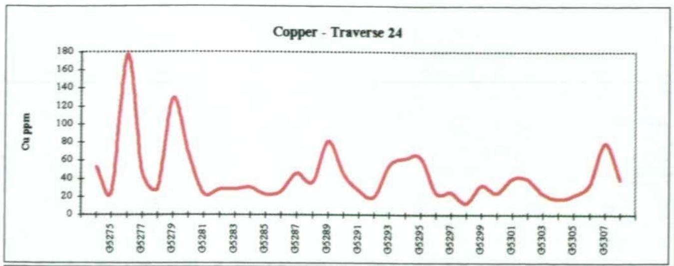

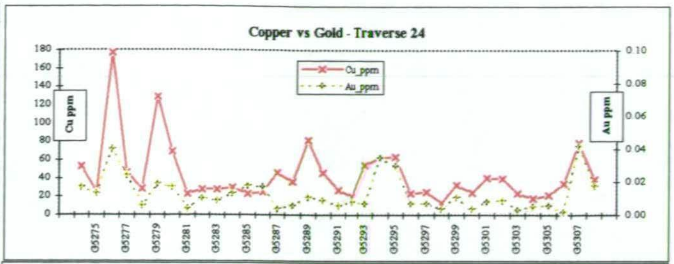

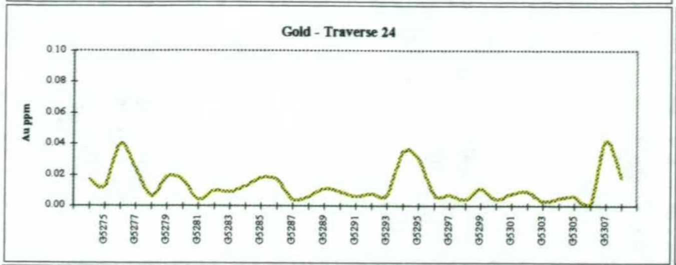

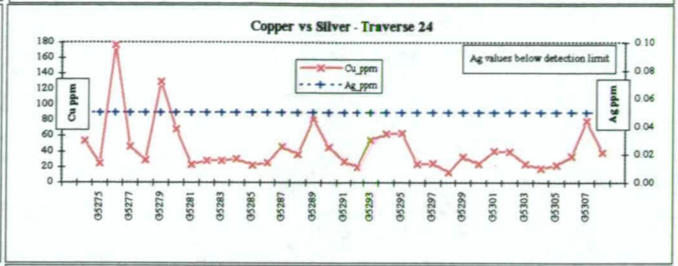

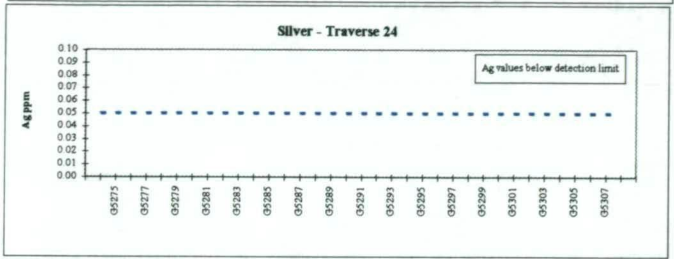

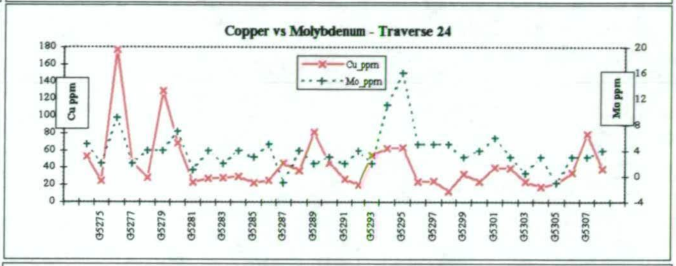

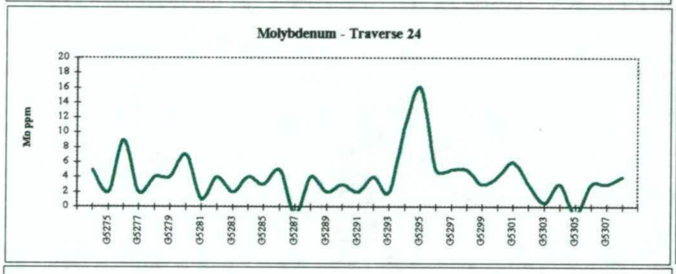

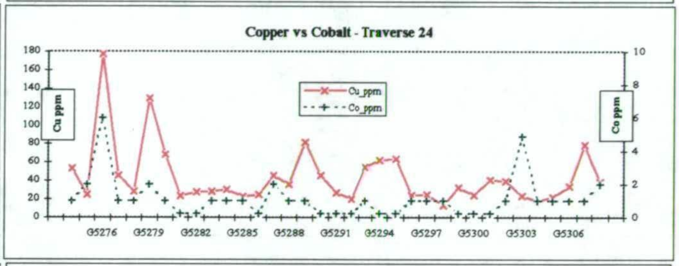

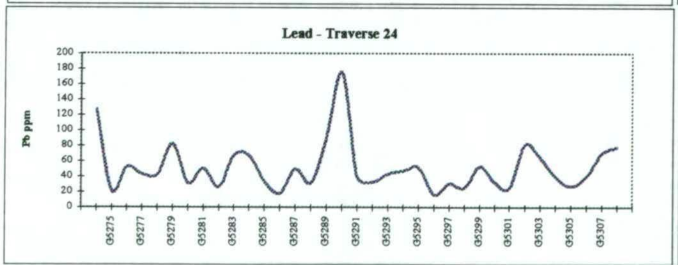

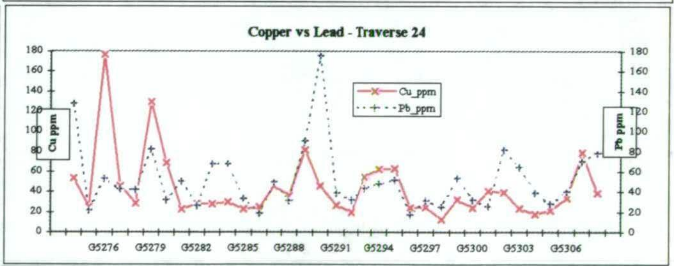

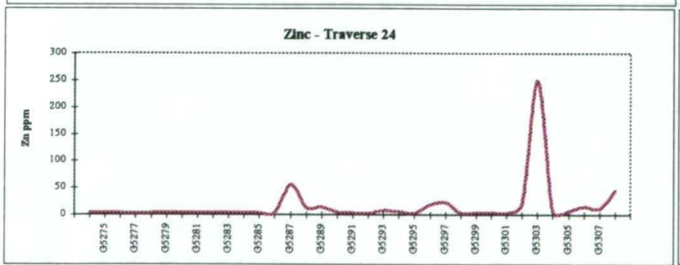

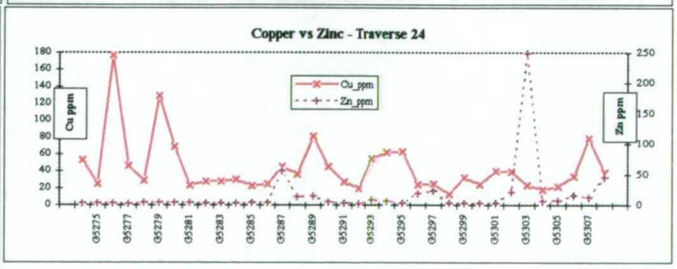

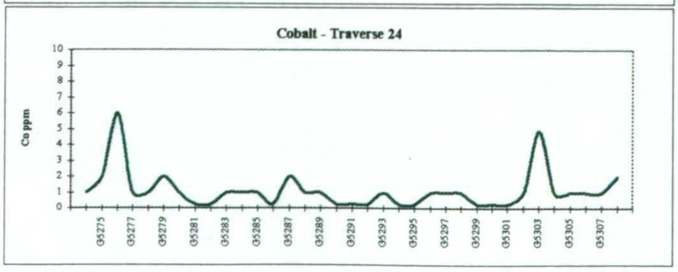

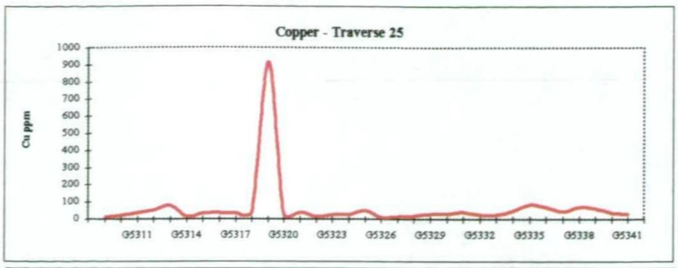

Copper - Traverse 25
Cu ppm

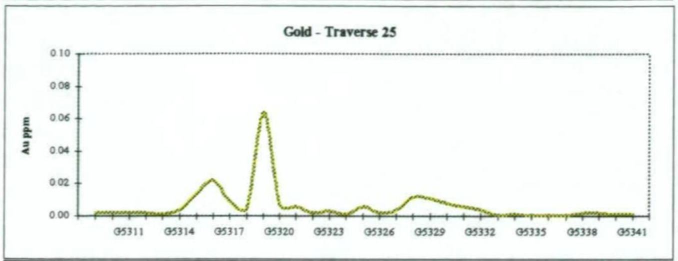

Gold - Traverse 25
Au ppm

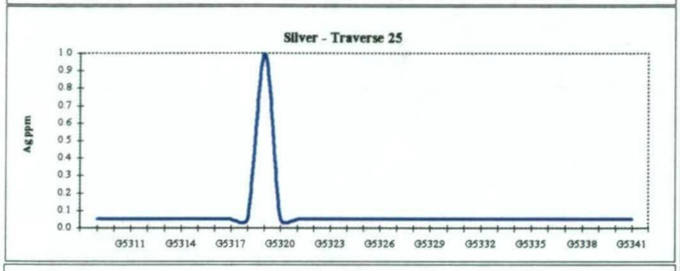

Silver - Traverse 25
Ag ppm

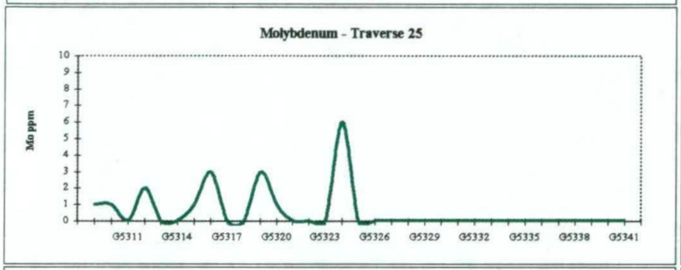

Molybdenum - Traverse 25
Mo ppm

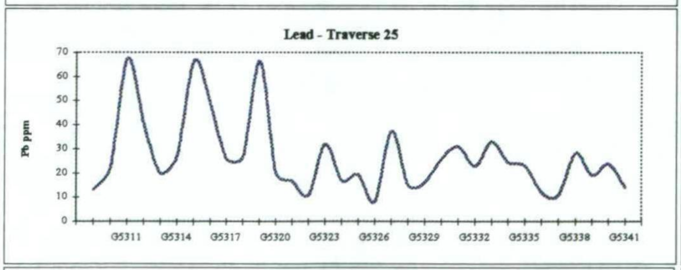

Lead - Traverse 25
Pb ppm

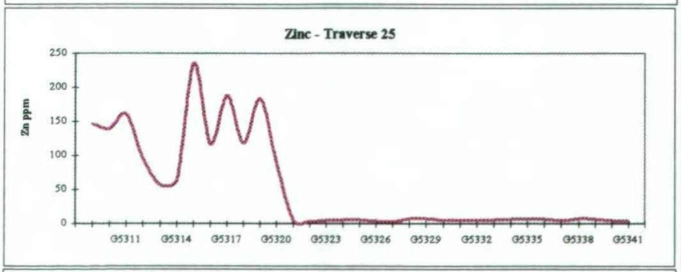

Zinc - Traverse 25
Zn ppm

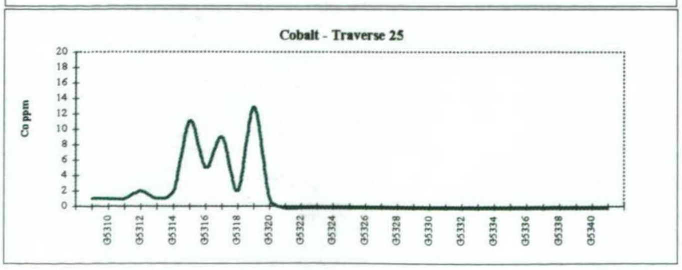

Cobalt - Traverse 25
Co ppm

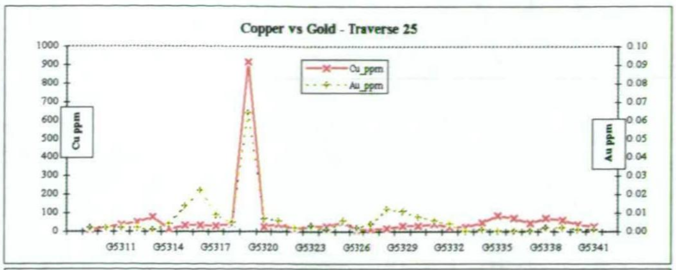

Copper vs Gold - Traverse 25
Cu ppm
Au ppm
Cu_ppm
Au_ppm

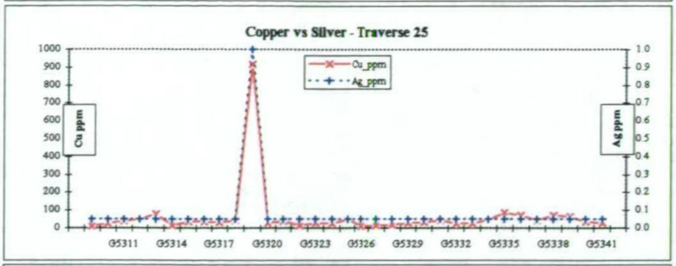

Copper vs Silver - Traverse 25
Cu ppm
Ag ppm
Cu_ppm
Ag_ppm

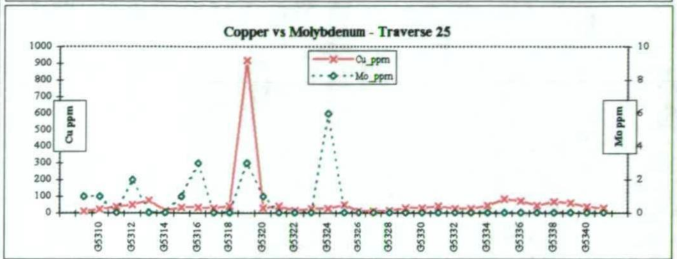

Copper vs Molybdenum - Traverse 25
Cu ppm
Mo ppm
Cu_ppm
Mo_ppm

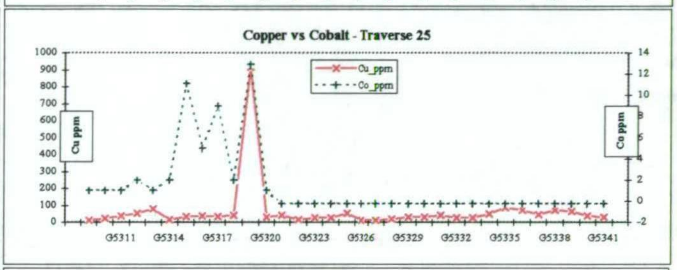

Copper vs Cobalt - Traverse 25
Cu ppm
Co ppm
Cu_ppm
Co_ppm

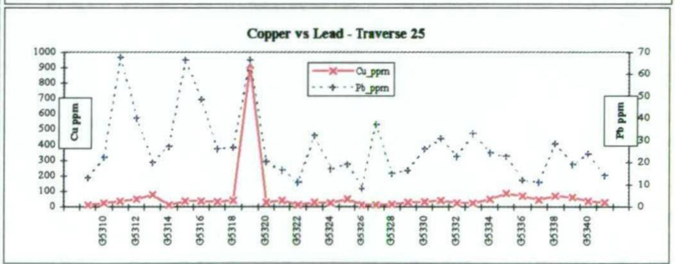

Copper vs Lead - Traverse 25
Cu ppm
Pb ppm
Cu_ppm
Pb_ppm

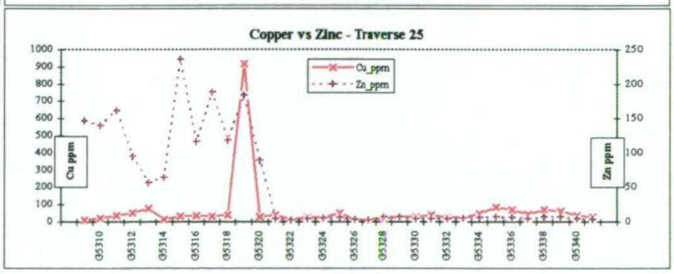

Copper vs Zinc - Traverse 25
Cu ppm
Zn ppm
Cu_ppm
Zn_ppm

ROYAL THARSIS - SURFACE GEOCHEMISTRY
TRAVERSE ASSAY PROFILES

Appendix II
Chart 18
Traverse 26

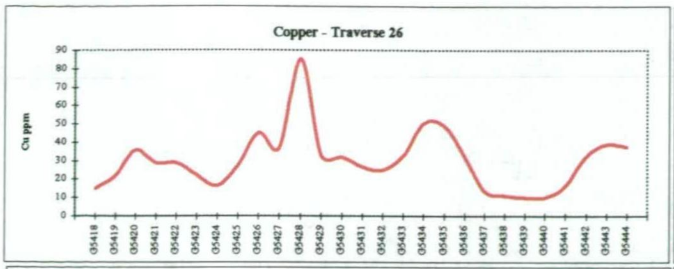

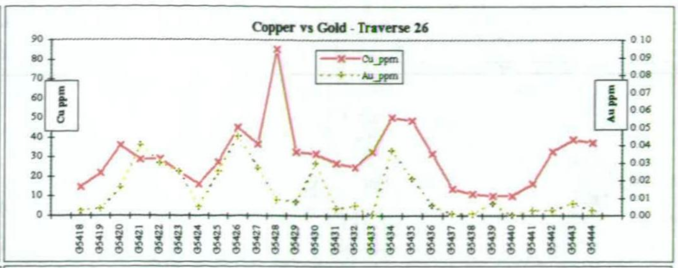

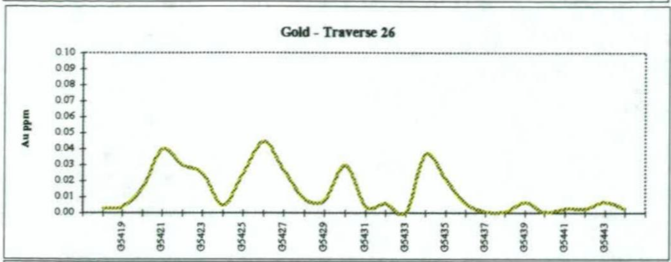

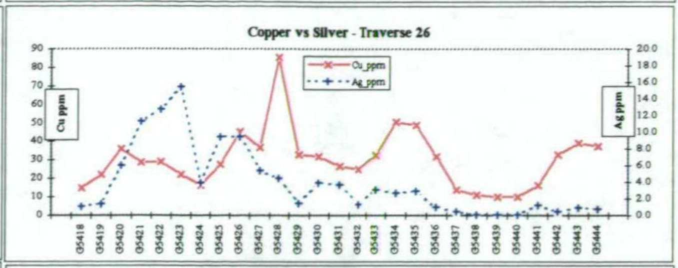

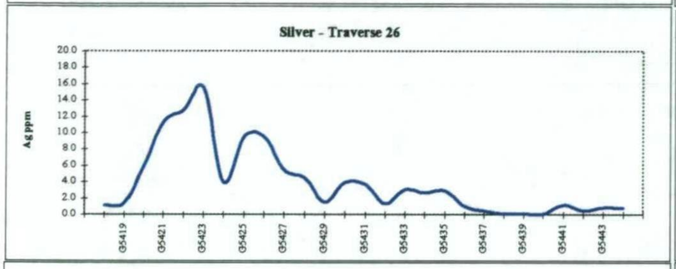

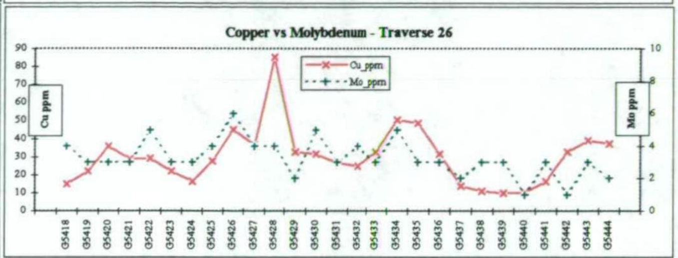

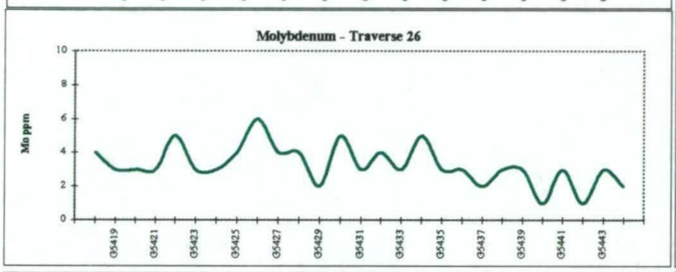

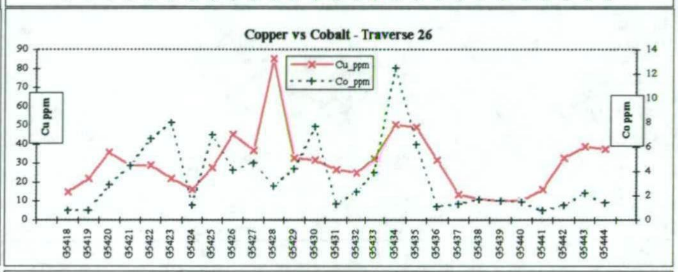

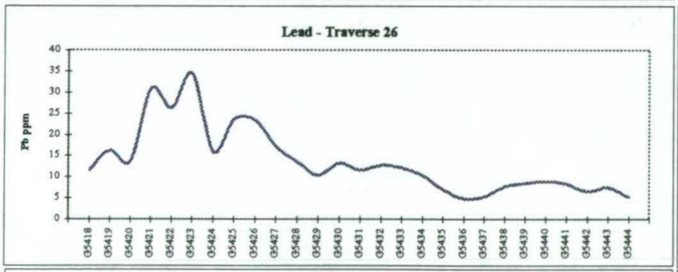

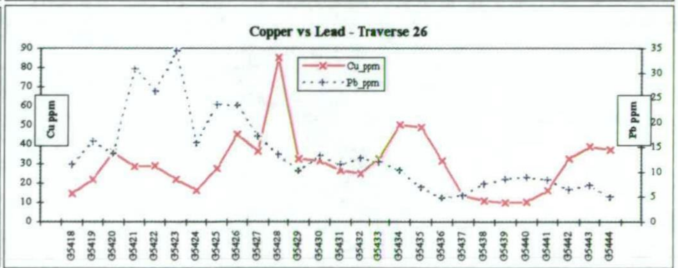

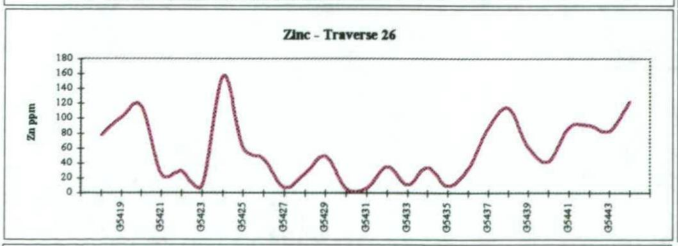

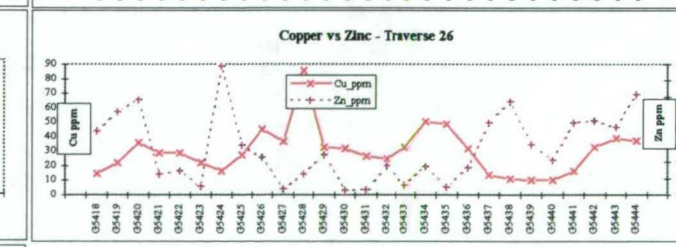

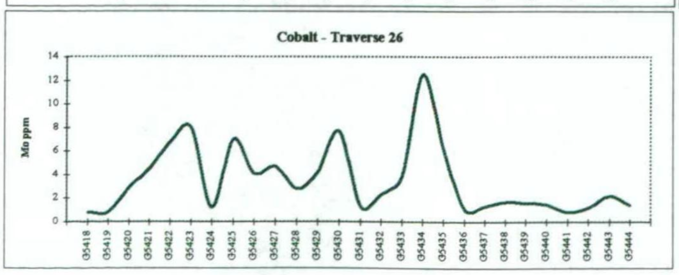

ROYAL THARSIS - SURFACE GEOCHEMISTRY
TRAVERSE ASSAY PROFILES

Appendix II
Chart 19
Traverse 27

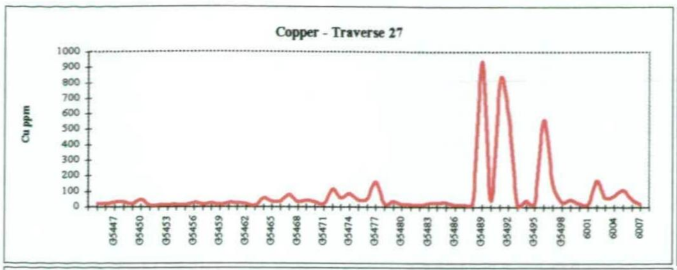

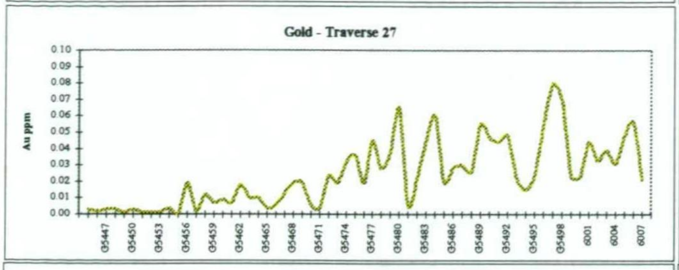

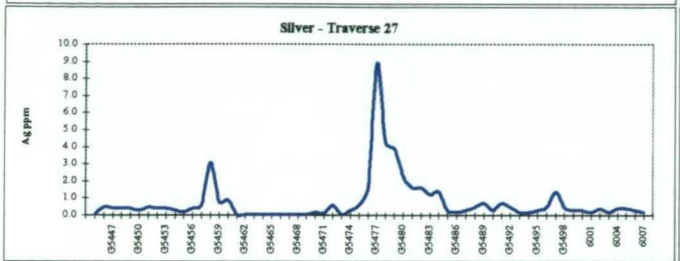

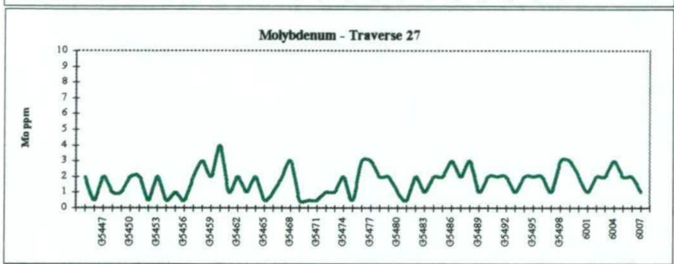

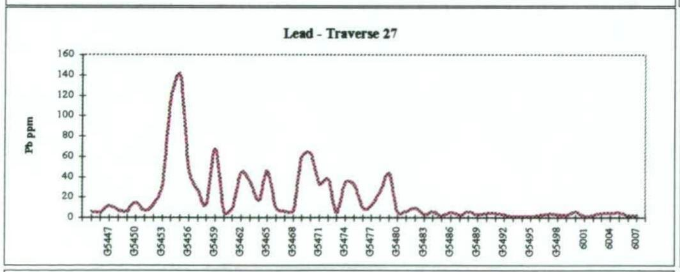

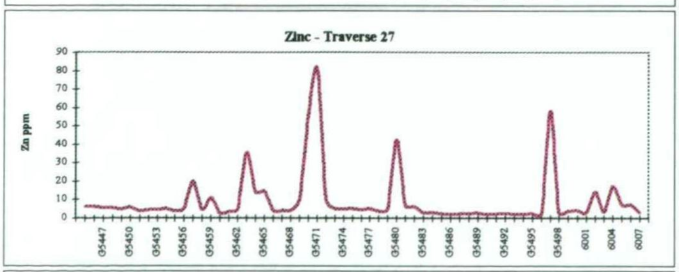

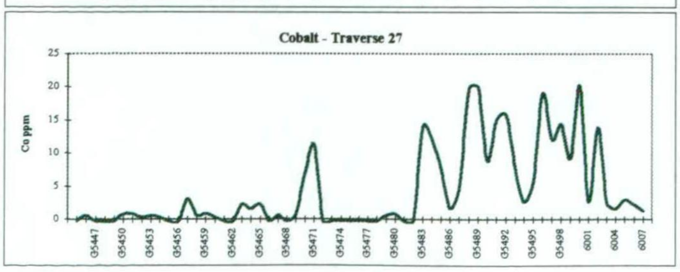

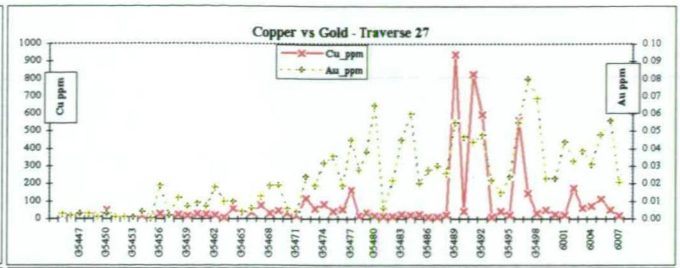

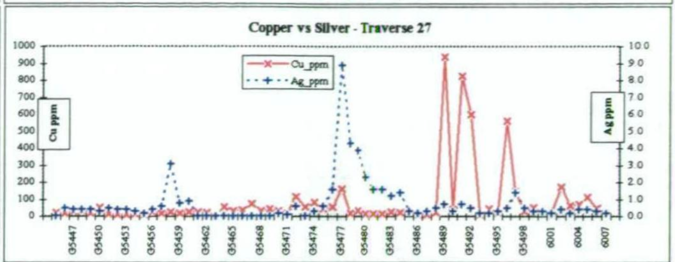

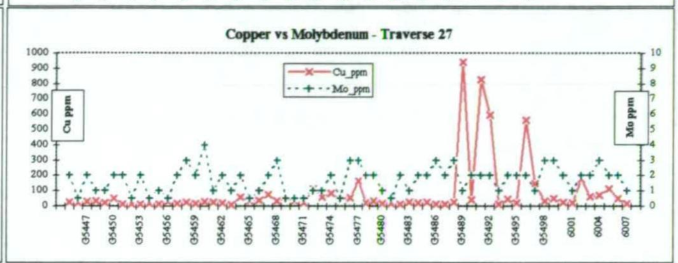

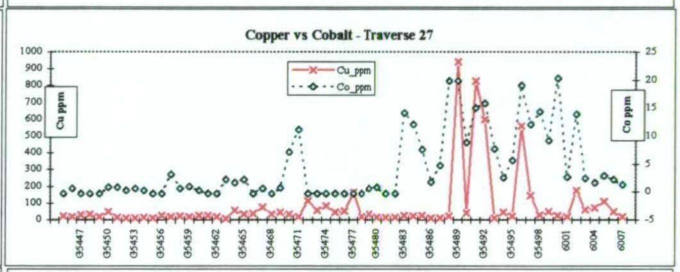

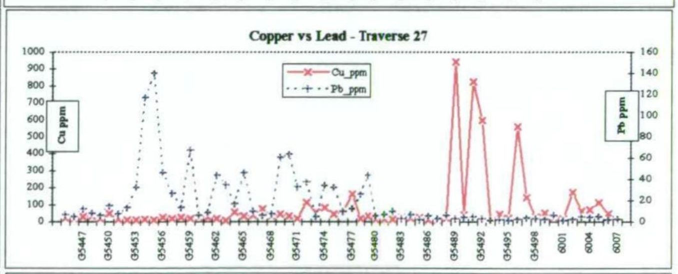

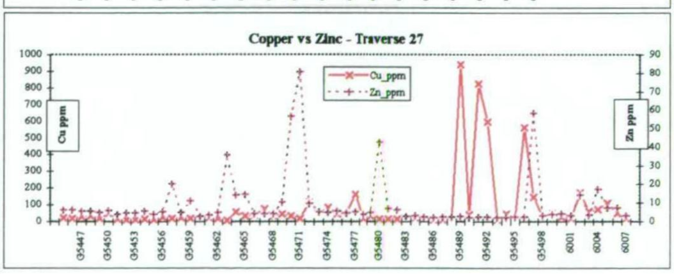

ROYAL THARSIS - SURFACE GEOCHEMISTRY
TRAVERSE ASSAY PROFILES

Appendix II
Chart 20
Traverse 28

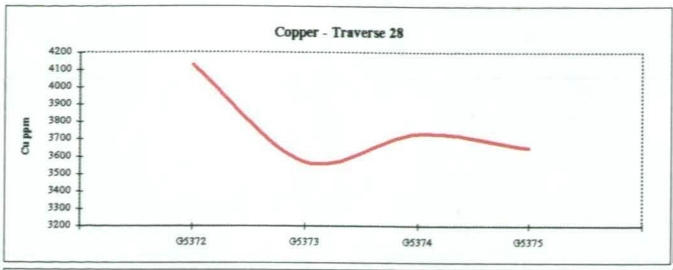

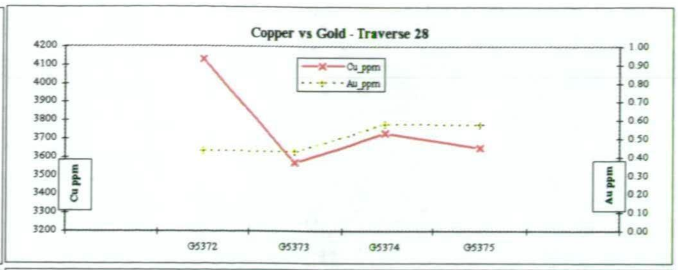

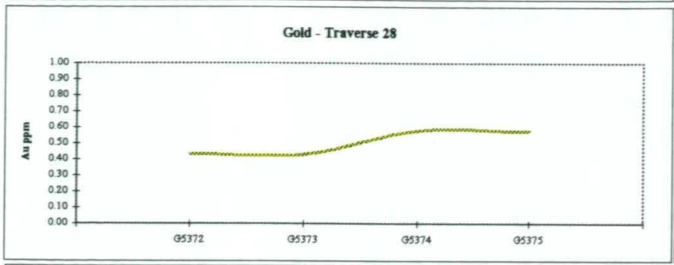

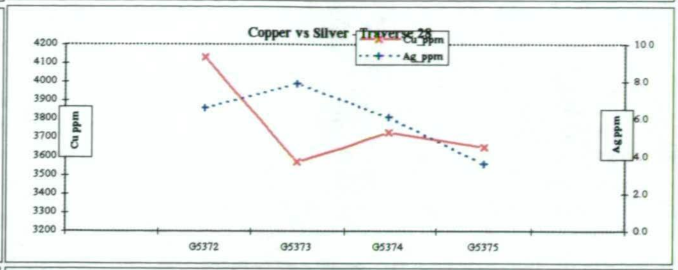

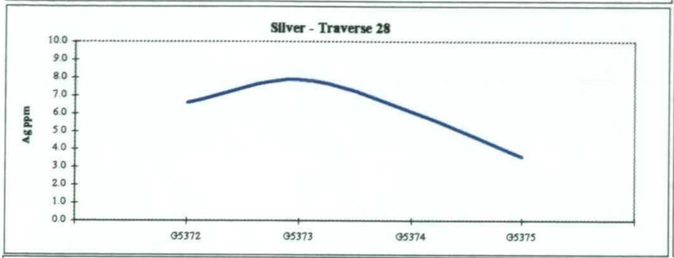

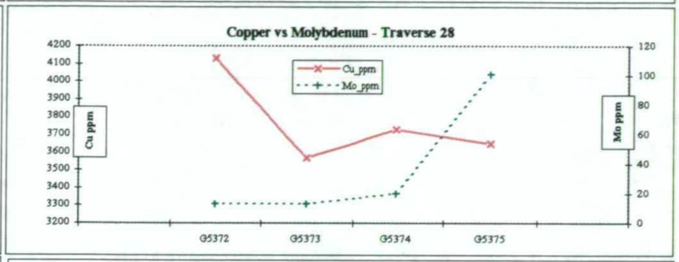

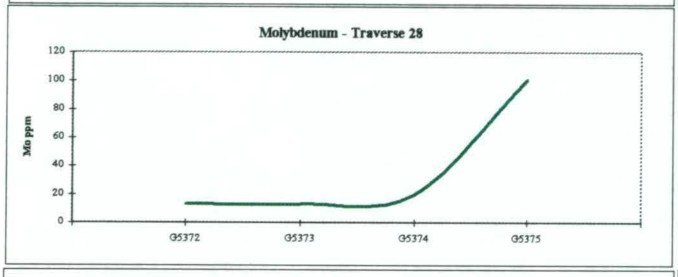

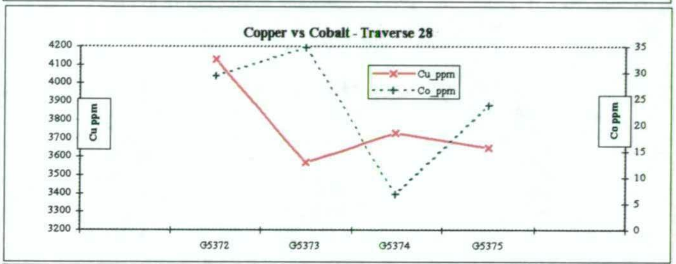

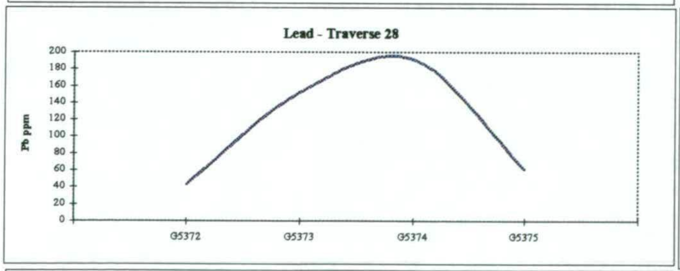

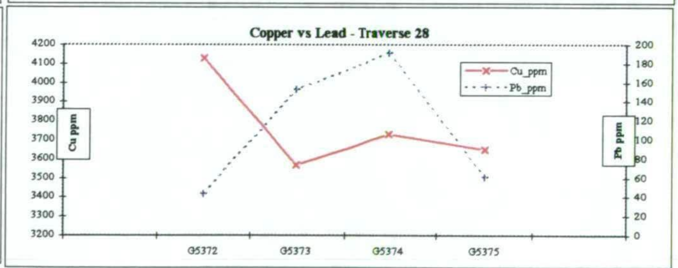

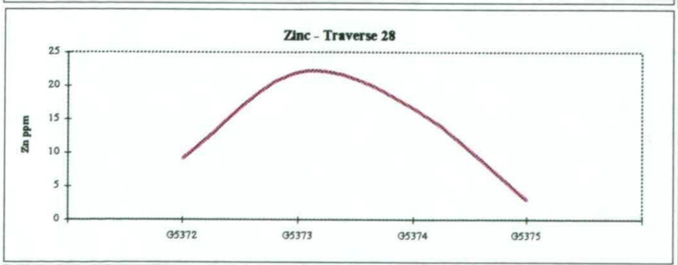

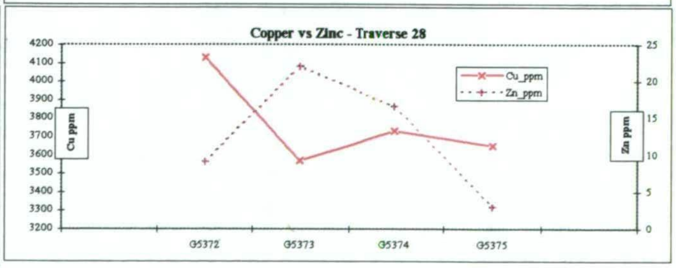

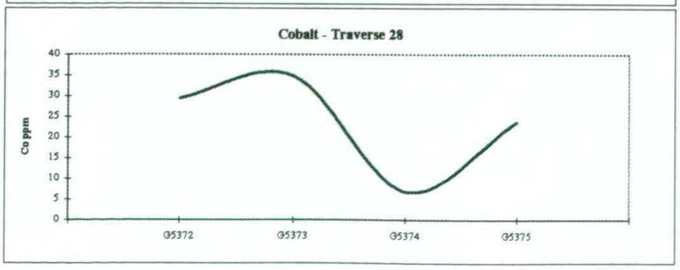

Appendix III

Royal Tharsis

Drill Hole Logs

APPENDIX III - LIST OF CONTENTS

Copper Mines of Tasmania - Lithological Codes

Project	Royal Tharsis Alteration	**Hole Number**	WL0479
Prospect	Royal Tharsis	**Section/s**	7770N
Tenement	1M/95	**COLLAR INFORMATION 315GRL GRID**	
Original Log By	J.Rowe	**North**	7788
		East	3542
Date	1979	**RL**	2035
		Azimuth	224
Summary Log By	W.J.D.Godsall	**Inclination**	-14
Method	Re-log	**Hole Length (m)**	226.15
		Hole Length (ft) (if applicable)	
Date	8/02/97		

Summary Log

From	To	Code	Description	Py%	Cp%	Depth	Code	Angle
0.00	70.00	Lqzse	Vein as minor unit.	8	tr	2	fo	60
70.00	74.45	Lqzch(se)-tf	Tuffaceous quartz chlorite, minor sericite	5		12	fo	60
74.45	84.30	Lqzsech-ittf	Intercalated and tuffaceus	12		42	fo	60
84.30	85.50	Ily	Disseminated haematite at base.	2		60	fo	65
85.50	89.45	Lqzch-tf	Tuffaceous quartz chlorite	8	tr	73	fo	65
89.45	111.85	Lqzse(ch)	Locally fragmental	6	tr	95	fo	70
111.85	125.50	Lqzch(se)	Sharp contact with distinct speckled texture. Local vnq	4	tr	105	fo	65
125.50	140.65	Lqzse-tf	Coarse tuffs and fragmentals	8	tr	137	fo	50
140.65	175.40	Lqzch(se)-fr	Weakly tuffaceous. Local vqzsd	5	tr	145	fo	60
175.40	182.30	Lqzch(se)-tf	Tuffaceous	3		205	fo	65
182.30	193.15	Lqzsesi	Local vqzsd. Chloritic basally.	5				
193.15	200.00	Ffz	No 2 fault					
200.00	207.00	Lqzse-fr	Very broken core.	7				
207.00	226.15	Lqzchse-fx	Tuffs and fragmentals. Local vqzsd.	3	tr			

Abbreviations: na - not available, ne- no entry, nd - not determined, no - not observed, fo - foliation, co - contact, S0 - bedding, Tr - trace

Significant Intersections

From	To	m	Description	Cu%	Au ppm	Ag ppm	Py%
			No significant copper intersection.				

Hole Purpose and Result

Drilled to test rock types and ground conditions for proposed decline extension to 40 Series.
Drilled away from known economic mineralisation.

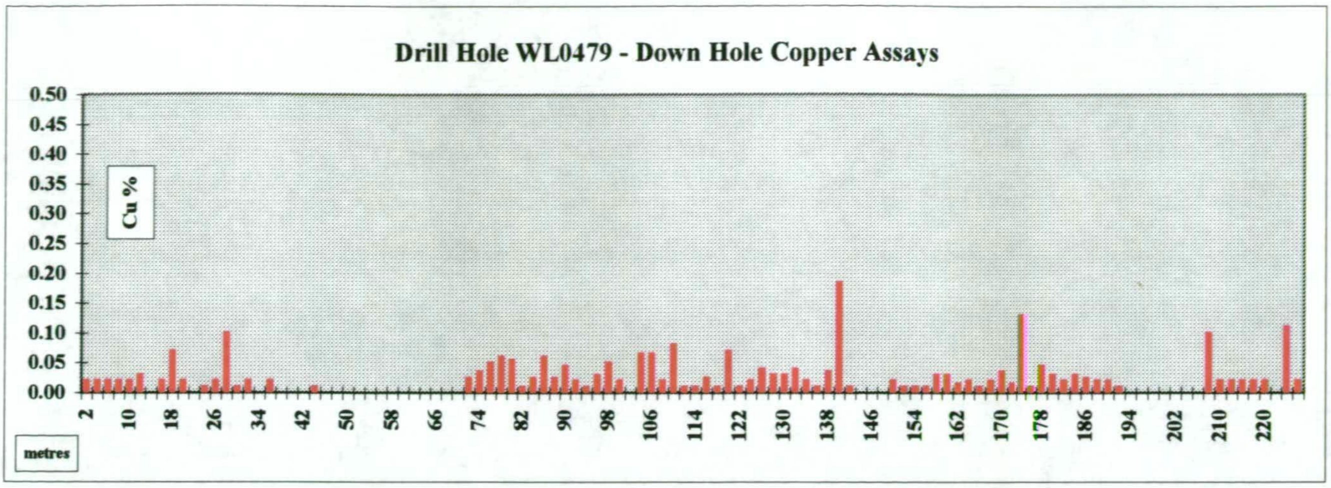
Drill Hole WL0479 - Down Hole Copper Assays
Cu %
0.50 0.45 0.40 0.35 0.30 0.25 0.20 0.15 0.10 0.05 0.00
2 10 18 26 34 42 50 58 66 74 82 90 98 106 114 122 130 138 146 154 162 170 178 186 194 202 210 220
metres

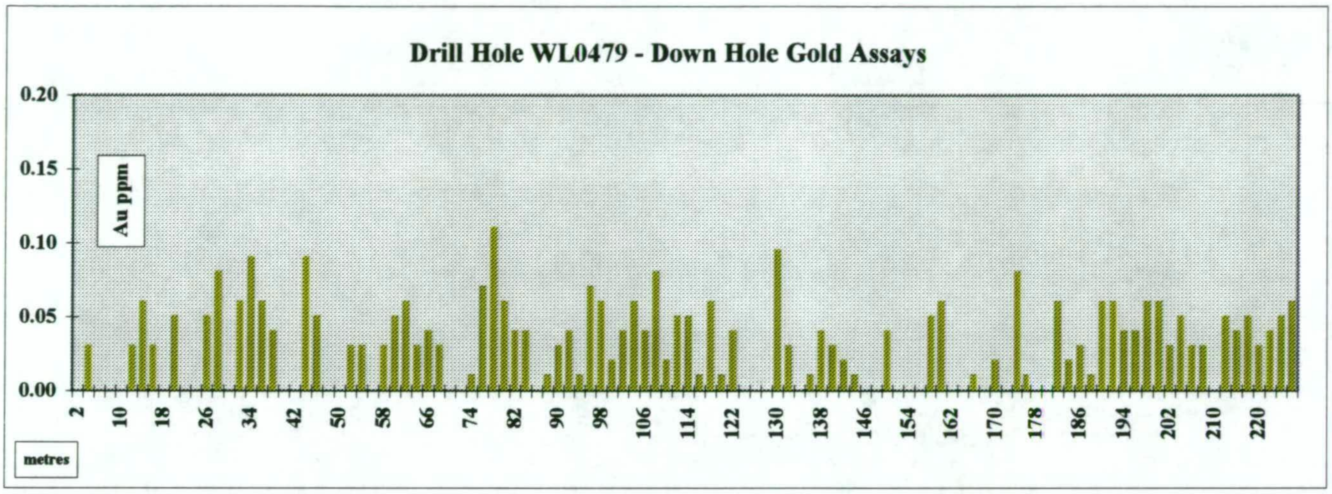
Drill Hole WL0479 - Down Hole Gold Assays
Au ppm
0.20 0.15 0.10 0.05 0.00
2 10 18 26 34 42 50 58 66 74 82 90 98 106 114 122 130 138 146 154 162 170 178 186 194 202 210 220
metres

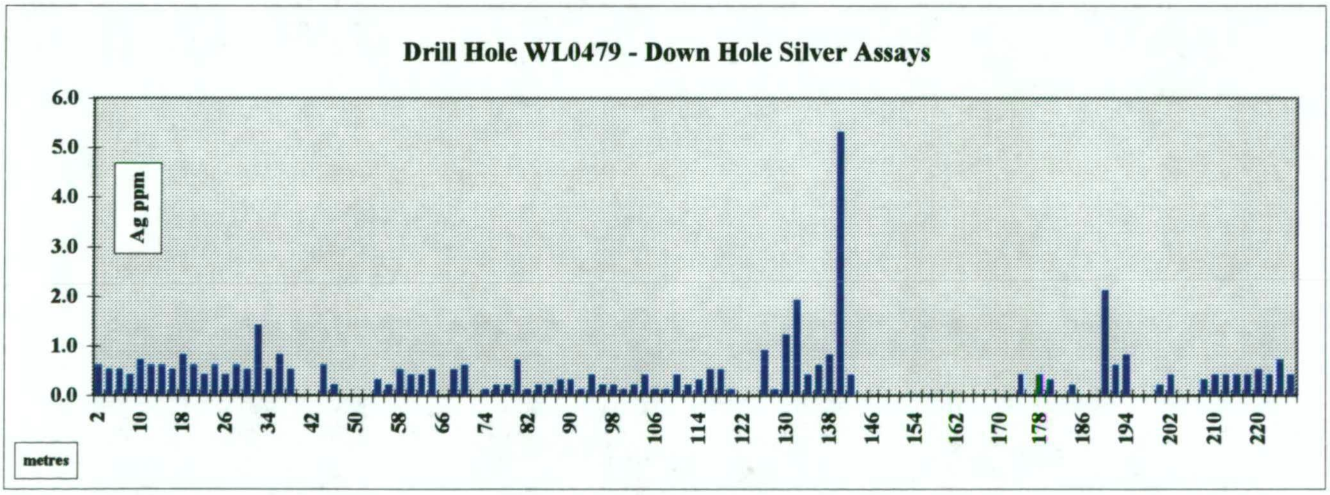
Drill Hole WL0479 - Down Hole Silver Assays
Ag ppm
6.0 5.0 4.0 3.0 2.0 1.0 0.0
2 10 18 26 34 42 50 58 66 74 82 90 98 106 114 122 130 138 146 154 162 170 178 186 194 202 210 220
metres

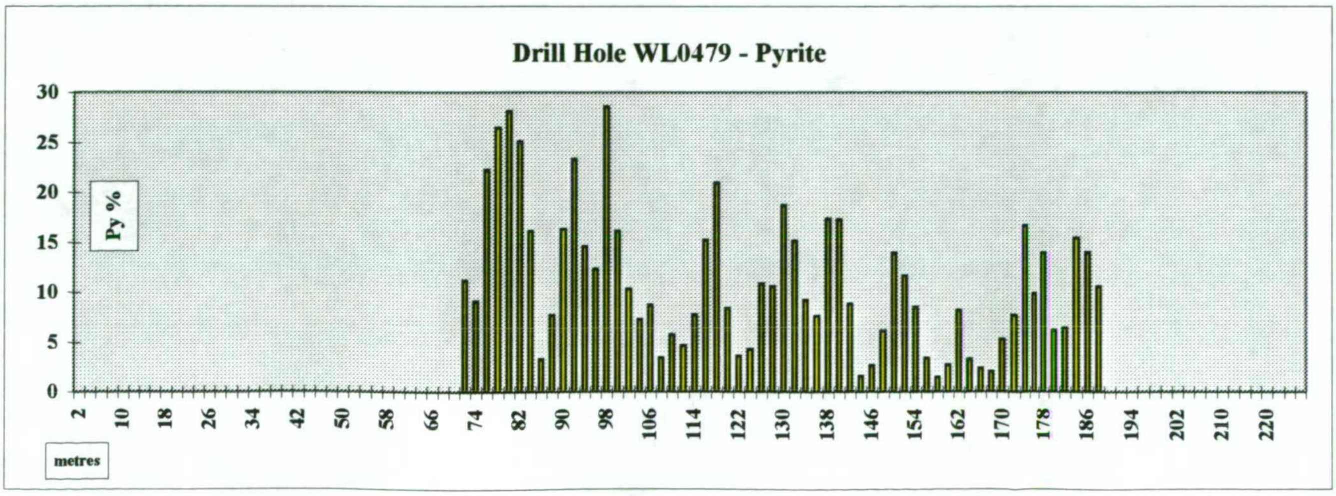
Drill Hole WL0479 - Pyrite
Py %
30 25 20 15 10 5 0
2 10 18 26 34 42 50 58 66 74 82 90 98 106 114 122 130 138 146 154 162 170 178 186 194 202 210 220
metres

Project: Royal Tharsis Alteration **Location:** hangingwall of Royal Tharsis **Hole Number:** WL0479

Major			Minor			Lithology				Alteration		Mineralisation						Structure & Veining			
From (m)	To (m)	Code	From (m)	To (m)	Code	Colour	Gr. Size	Texture	Description	Code	Description	Py %	Style	Cp %	Style	%	%	Depth (m)	Code	Angle	Description
0.00	70.00	Lqzse				gypi	mg	fr		qzsesi	Weakly siliceous	8	ds	tr				2	fo	60	
			0.00	31.20	Lqzsi	whpi	cg	wd	Pinkish white irregular fragmental texture. Weak foliation. Scattered and disseminated sulphides. Locally weathered. Siliceous and sericitic.	qzsise	Siliceous nature decreases down unit.	8	ds					12	fo	60	
			31.20	32.00	Vqz(sd)				Minor sericite and sulphides along fracture planes.									42	fo	60	
			32.00	70.00	Lqzse	gywh	cg	fr	Becoming less pink and with a poorly developed segregation associated with the weak fragmental texture. Locally massive sulphides as veins and interstitial masses.	qzsesi		12	in	tr				60	fo	65	
70.00	74.45	Lqzch				gngy	fg	it	Intercalated and tuffaceous with predominant chlorite content and subordinate sericite alteration.	qzch(se)	Pervasive	5	sr					73	fo	65	
74.45	84.30	Lqzse				gypi	mg	it	Intercalated and tuffaceous unit. Locally fragmental with milky (?detrital) quartz. Variable and alternating sercite and chlorite. Stringers and blebs of sulphides.	qzsech		12	ds								
			78.50	79.00	Vqz	wh		fx	Dark (near black) chlorite along fractures.												
84.30	85.50	Ily				bk	mg		Gradational basally becoming much more clearly defined down the hole. Locally fragmental and haematitic at the base. Scatttered sulphide specks/blebs.	hm		2									
85.50	89.45	Lqzch				gngy	fg	tf	Minor sericite intercalations basally. Distinctive sulphide veinlets with globular pyrite, veinlets being sub parallel to foliation and with generally sharp lower contacts. Locally cross cutting sulphide stringers.	qzch	Pervasive	8	vn	tr							
89.45	111.85	Lqzse								qzse(ch)	Pervasive with minor chlorite	6	ds	tr				95	fo	70	
			89.45	102.90	Lqzse	whgn	cg		Weakly foliated, faintly fragmental with disseminated almost banded sulphides sub parallel to foliation.	se	Pervasive	3	ds	tr				105	fo	65	
			102.90	107.50	Lqzse	gygn	fg		Green and foliated with locally pink fragmental texture. Disseminated sulphides, notably different to the preceeding minor unit.	qzse(ch)	Pervasive	5	ds	tr							
			107.50	108.00	Vqz	wh		mv	Tending to be massive.												
			108.00	111.85	Lqzch	gngy	fg	fo	Foliated with dominant chlorite and variable sericite. Sub parallel bands of sulphides as medium euhedral grains.	chse	Pervasive	6	ds	tr							
111.85	125.50	Lqzch							Chlorite content tends to decrease down the unit.	ch(se)		4	ds	tr							
			111.85	114.50	Lqzch	gngy	fg	fo	Sharp upper contact. Clots of chlorite. Disseminated sulphides frequently as bands sub parallel to foliation.	qzch(se)	Pervasive	6	bn	tr							
			114.50	121.60	Lqzch	gnwh	mg	fo	Gradational increase in sericite with sulphides more diffuse.	qzchse	Pervasive	5	ds	tr							
			121.60	125.50	Lqzmx	gnwh	fg	vn	Irregular quartz siderite veining, frequently containing dark green chlorite along fractures. Occasional Cp. Veins at: 121.6m-122.8m, 123.3m-123.7m, 124.0m-124.6m, 125.0m-125.5m.	sech		4	ds	tr							
125.50	140.65	Lqzse-tf				gypi	mg	fr	Mixture of medium to coarse tuffs and fragmentals, with fine grained sulphide disseminations and veinlets.	qzse	Pervasive with minor chlorite	8	ds	tr				137	fo	50	
140.65	175.40	Lqzch				gngy	fg	fr	Predominantly fragmental unit with minor interbedded tuffs.Fragmentals elongated along weak foliation. Disseminations and weak bands of sulphides.From 163m increasing content of quartz siderite veinlets generally sub parallel to foliation.	qzch(se)	Pervasive with minor sericite	5	ds	tr				145	fo	60	
			169.30	170.00	Lvqzsd	wh			Comb structured sideritic vein. Blebs of cp.												
175.40	182.30	Lqzch				gngy	mg	tf	Tuffacous unit with elongate clots of chlorite. Disseminated subhedral pyrite, geneally sub parallel to foliation.	qzch(se)	Minor sericite	3	ds								
			175.00	176.40	Lqzse	pi	fg		Pink foliated rock.	se	Pervasive	5	ds	tr							

Geologist: W.J.D.Godsall **Date:** 8/02/97 Page 1 of 2

Project: Royal Tharsis Alteration **Location:** hangingwall of Royal Tharsis **Hole Number:** WL0479

Major			Minor			Lithology				Alteration		Mineralisation						Structure & Veining			
From (m)	To (m)	Code	From (m)	To (m)	Code	Colour	Gr. Size	Texture	Description	Code	Description	Py %	Style	Cp %	Style	%	%	Depth (m)	Code	Angle	Description
182.30	193.15	Lqzse				whgn	fg	fx	Siliceous quartz sercite rock with chlorite basally. Generally disrupted and incompetent/broken ground with local/erratic quartz siderite veining.	qzsesi	Increasingly siliceous	5	ds								
193.15	200.00	Ffz				wh			Heavily broken Lqz. Locally fibrous/sericitic. scattered specks sulphides.	si	Siliceous	1									
200.00	207.00	Lqzse				gywh	mg	fx	In places heavily broken core, locally as incoherent rock fragments with some sandy pug infill. Blebs and disseminations of sulphides throughout.	sise		7	ds					205	fo	65	
207.00	226.15	Lqzch				gngy	mg		Mixed tuffs and fragmentals that appear dominantly as quartz chlorite with subordinate sericite. Locally veined with quartz carbonate as stringers and veinlets. Core heavily broken/faulted in places. Occasional speck cp.	qzch(se)	Pervasive	3	ds	tr							
			209.05	209.15	Ffl																
			211.10	211.60	Vqzsd																
			213.25	213.55	Ffl																
	EoH																				

Geologist: W.J.D.Godsall **Date:** 8/02/97 Page 2 of 2

Project	Royal Tharsis Alteration	**Hole Number**	WL0480
Prospect	Royal Tharsis	**Section/s**	7770N
Tenement	1M/95	**COLLAR INFORMATION 315GRL GRID**	
Original Log By	J.Rowe	**North**	7797
		East	3572
Date	1979	**RL**	2035
		Azimuth	75
Summary Log By	W.J.D.Godsall	**Inclination**	-09
Method	Re-log	**Hole Length (m)**	249.10
		Hole Length (ft)	
Date	9/02/97	**(if applicable)**	

Summary Log

From	To	Code	Description	Py%	Cp%	Depth	Code	Angle
0.00	63.00	Lqzsepy	Minor Lqzch	8		50.0	fo	75
63.00	69.80	Lqzchse	? fine tuff. Carbonate veining.	5		65.0	fo	80
69.80	124.00	Lqzsepy	Fragmental. Locally faulted.	8		80.0	fo	65
124.00	135.50	Lqzse	Tuff. Minor chlorite.	5				
135.50	142.40	Lqzse	Weakly brecciated.	10	tr			
142.40	202.00	Lqzsech	Chloritic fragments more homogeneous down hole	5	2			
202.00	227.40	Lqzse(py)	Massive	5	tr			
227.40	232.95	Lqzch	Minor haematite veinlets.	7	1			
232.95	246.65	Lqzse	Carbonate veinlets.	1				
246.65	249.10	Oct	Faulted contact.					

Abbreviations: na - not available, ne- no entry, nd - not determined, no - not observed, fo - foliation, co - contact, S0 - bedding, Tr - trace

Significant Intersections

From	To	m	Description	Cu%	Au ppm	Ag ppm	Py%
138.0	162.0	24.0	Sericitic and chloritic. Fragmental. Siderite veined	0.42	0.12	0.8	16.75
144.0	160.0	16.0	Sericitic and chloritic. Fragmental. Siderite veined	0.53	0.15	0.8	12.58

Hole Purpose and Result

Drilled to test rock types and ground conditions for proposed main decline extension and Royal Tharsis at 2000 RL.

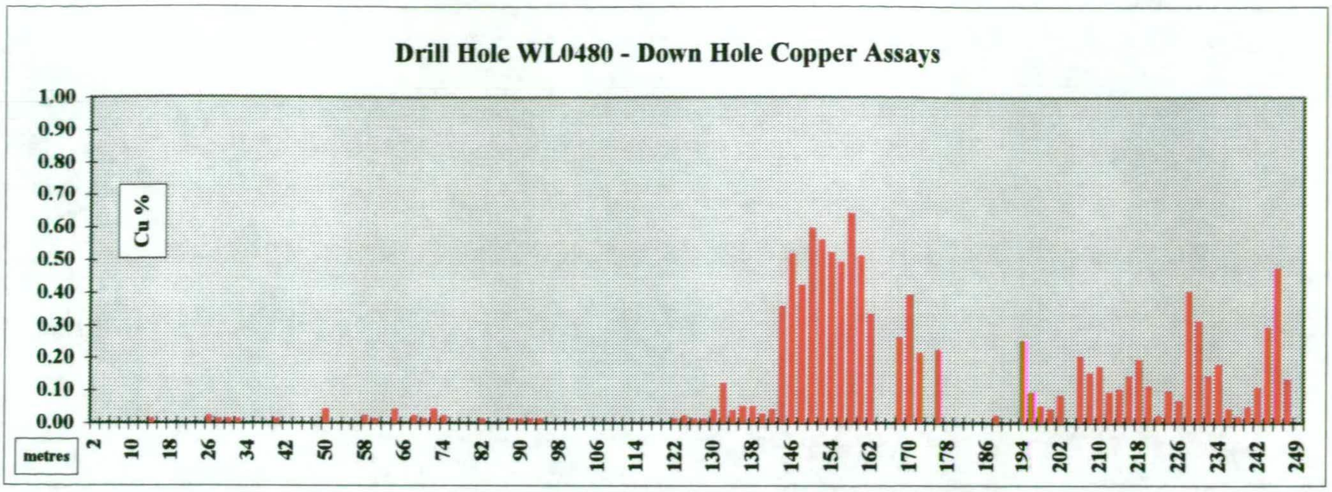
Drill Hole WL0480 - Down Hole Copper Assays
Cu %
metres

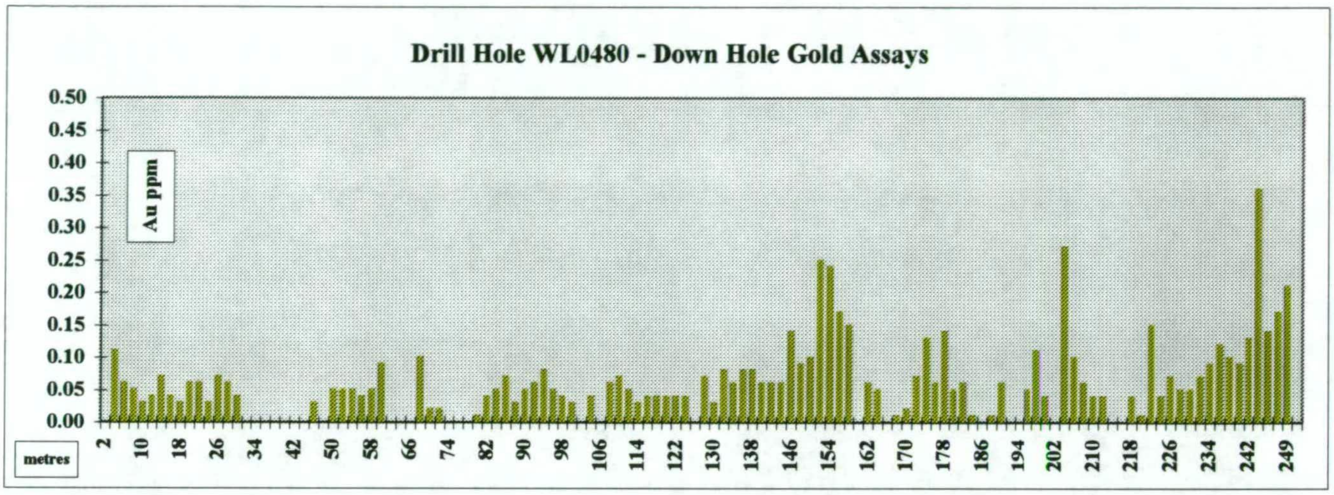
Drill Hole WL0480 - Down Hole Gold Assays
Au ppm
metres

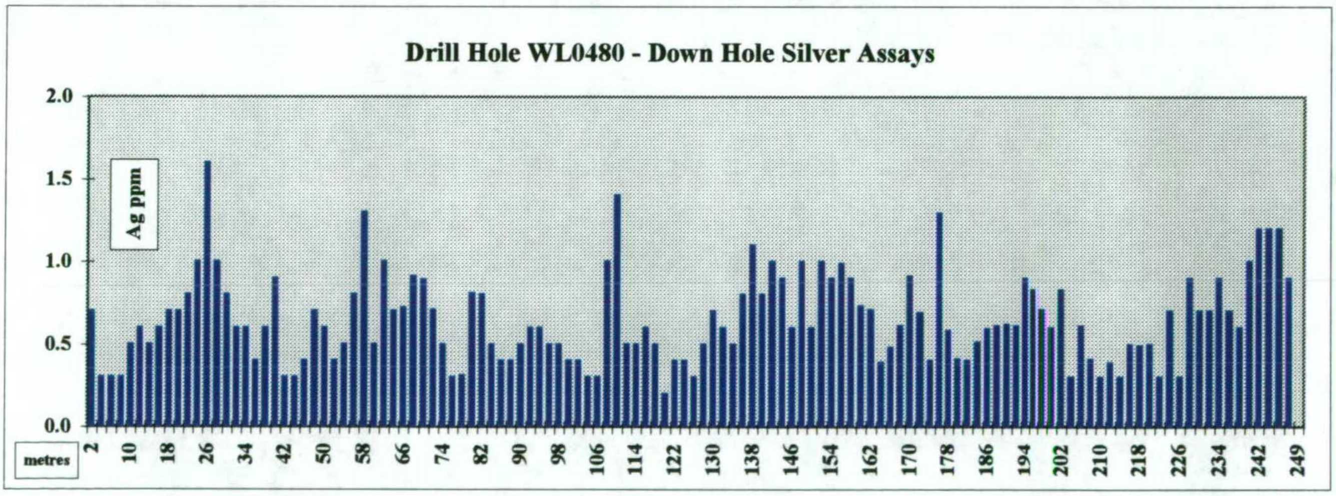
Drill Hole WL0480 - Down Hole Silver Assays
Ag ppm
metres

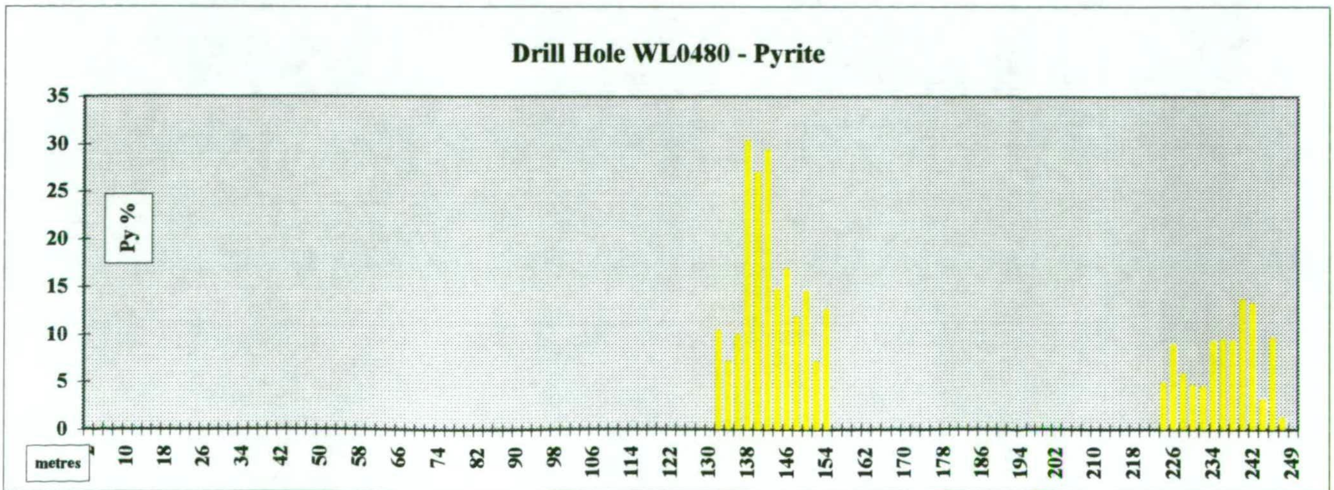
Drill Hole WL0480 - Pyrite
Py %
metres

Project: Royal Tharsis Alteration **Location:** hangingwall of Royal Tharsis **Hole Number:** WL0480

Major			Minor			Lithology				Alteration		Mineralisation						Structure & Veining			
From (m)	To (m)	Code	From (m)	To (m)	Code	Colour	Gr. Size	Texture	Description	Code	Description	Py %	Style	Cp %	Style	%	%	Depth (m)	Code	Angle	Description
0.00	63.00	Lqzse				gypk	mg		Quartz sericite rock with minor interbedded units of gyge qzchse rock. Siliceous appearance. Silicification masks original texture. Locally fragmental. Py occurs as semi-massive irregular veins and as medium grained subhedral disseminations.	qzse(ch)	Pervasive throughout.	8	ds					30	fo	70	
			3.45	6.65	Lqzch				Minor chlorite zone/band with subordinate sericite alteration.	qzchse	Pervasive							60	fo	80	
			11.00	13.30	Lqzch				Minor chlorite zone/band with subordinate sericite alteration.	qzchse	Pervasive										
			21.75	21.80	Ffl				Shear												
			34.30	34.70	Lqzch				Minor chlorite zone/band with subordinate sericite alteration.	qzchse	Pervasive										
			35.20	36.00	Lqzch				Minor chlorite zone/band with subordinate sericite alteration.	qzchse	Pervasive										
			43.80	46.10	Lqzch				Minor chlorite zone/band with subordinate sericite alteration.	qzchse	Pervasive										
			48.55	48.60	Ffl				Shear												
63.00	69.80	Lqzch				gngy	mg		Even textured - possibly a fine tuff. Occasional cross-cutting Py veins. Competent unit.Gradational btween Lqzchse and Lqzsech.	qzchse		5	sr					65	fo	80	
			63.00	63.50	Vqzsd				? fault contact?												
			64.20	64.70	Vqzsd				Broken veining												
			68.60	68.80	Vqzsd																
69.80	124.00	Lqzse				pkgy		fr	Quartz sericite fragmental rock that parts readily along sericite or hydromica joint and shear planes which are frequently sub parallel to foliation - locally conchoidal. Pyrite as erratic veinlets and disseminations. Prominent quartz siderite veinlets.	qzse	Pervasive	8	ds					70	fo	60	
			70.60	74.05	Lqzse				Minor chlorite zone/band.	qzchse								120	fo	70	
			78.00	81.10	Ffl				Heavily broken core.												
			86.95	89.40	Lqzse				Minor chlorite zone/band.	qzchse											
			92.25	95.40	Lqzse				Minor chlorite zone/band.	qzchse											
			97.40	100.00	Ffl				Heavily broken core.												
124.00	135.50	Lqzse				gn	fg		Fine to medium grained quartz sericite "tuff" with minor chlorite, Broken core associted with quartz and surrounding rock. Local quartz siderite veining.	se(ch)		5	ds								
135.50	142.40	Lqzse				pkgy	mg		Slight brecciated appearance. Textureless. Semi massive sulphides.	se	Pervasive	10	ds	1							
142.40	202.00	Lqzse							Chloritic fragments becoming more homogeneous down the hole.	qzsech											
			142.40	152.50	Lqzse	gygn	fg	fr	Fine to medium grained, tuffaceous with flecks of green chlorite. Local quartz siderite veining. Fragmental.	qzsech		9	ds	2	ds						
			152.50	202.00	Lqzse	gygn	fg	fr	Evenly textured monotonous unit. Visual variations in chlorite content. Finer and more homogeous than overlying unit. Generally competent with litle evidence of any significant structures. Fragmental.	qzsech		5	ds	<1							
202.00	227.40	Lqzse				pk	fg	mv	Massive featureless unit. Subordinate sericite.	se		6	ds	<1							
227.40	232.95	Lqzch				gn	fg		Quartz chlorite tuff with subordinate/trace sericite. Minor haematite veinlets.	ch(se)	Minor haematite	7	ds	2	bb						
232.95	246.65	Lqzse				pk	fg	mv	Sericite prominently subordinate to quartz. Faulted basal contact. Sulphides increase towards this contact which is characterised by quartz siderite veinlets.	qzse		3	ds								
246.65	249.10	Oct				pp			Purple Owen Conglomerate. Haematite dusting. Occasional ?sulphide? smears along fracture planes.	hm											
	EoH																				

Geologist: W.J.D.Godsall **Date:** 9/02/97 **Page** 1 **of** 1

Project	Royal Tharsis Alteration	**Hole Number**	WL0106
Prospect	Royal Tharsis	**Section/s**	7770N (-7830N)
Tenement	1M/95	**COLLAR INFORMATION 315GRL GRID**	
Original Log By	M.L.Wade	**North**	7779
		East	3659
Date	1957	**RL**	2423
		Azimuth	102
Summary Log By	W.J.D.Godsall	**Inclination**	-60
Method	Re-log	**Hole Length (m)**	308.46
		Hole Length (ft)	1012
Date	21/12/96	**(if applicable)**	

Summary Log

From	To	Code	Description	Py%	Cp%	Depth	Code	Angle
0.0	91.67	Lqzsepy	Patchy chlorite to 6.1m (20ft)	17	<1	0.2	fo	55
91.67	105.00	Lqzch	Siliceous. Limonitic	3		63.1	fo	60
105.00	110.26	Lqzsepy	Siliceous. Weakly chloritic	10		99.7	fo	75
110.26	112.01	Lchqz	Quartz porphyroblasts. Very sharp contacts.	7		106.7	fo	70
112.01	129.39	Lqzsepy	Green hydromicas	20		110.2	fo	80
129.39	156.97	Lqzch	Carbonate-haematite alteration	3		122.2	fo	55
156.97	180.44	Lqzsepy	Clots of chlorite	15		135.6	fo	65
180.44	193.62	Lqzch	Siliceous	7		178.6	fo	68
193.62	213.97	Lqzsepy	Haematite zones(s)	20	<1	191.7	fo	85
213.97	228.68	Lqzch	Minor sericite	3	2	199.3	fo	60
228.68	249.63	Lqzsech	Knobbly quartz texture.	3	1	217.9	fo	70
249.63	272.19	Lqzse	Carbonate alteration	2	<1	243.8	fo	65
272.19	308.46	Lqzsech	Intercalated sericitic and chlorite-sericite units.	4		260.6	fo	75
						273.4	fo	75

Abbreviations: na - not available, ne- no entry, nd - not determined, no - not observed, fo - foliation, co - contact, S0 - bedding, Tr - trace

Significant Intersections

From	To	m	Description	Cu%	Au ppm	Ag ppm	Py%
213.4	227.1	13.7	Lqzsepy	1.23	0.49	1.5	-
230.1	249.9	19.8	Lqzch	0.40	0.05	0.6	-
213.4	249.9	36.6	Lqzsech	0.70	0.24	1.0	-

Hole Purpose and Result

Hole abandoned at 308.46 m (1012 ft).

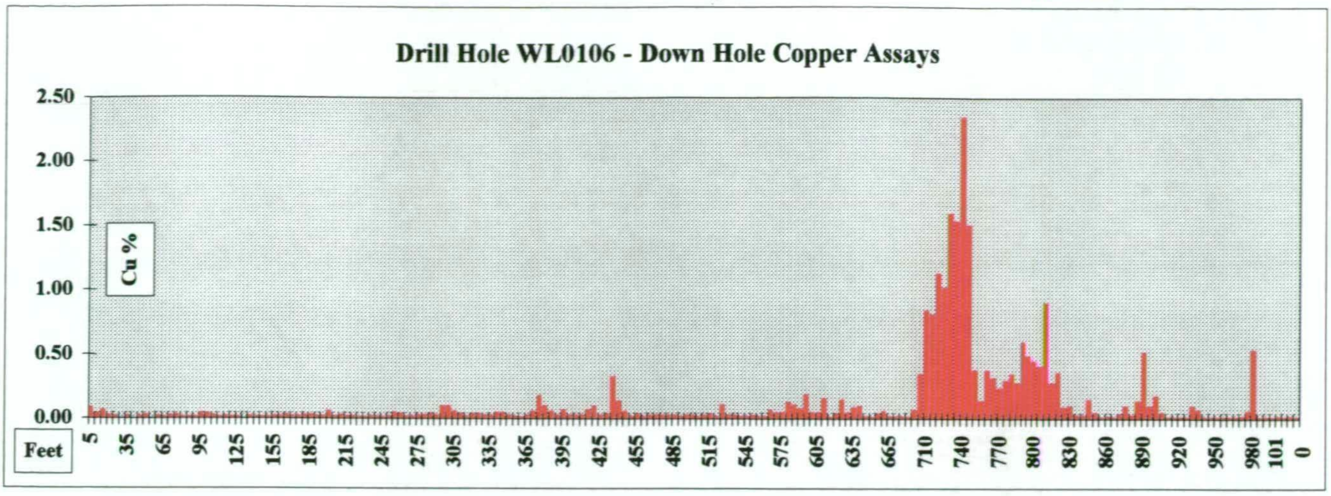
Drill Hole WL0106 - Down Hole Copper Assays
Cu %
Feet

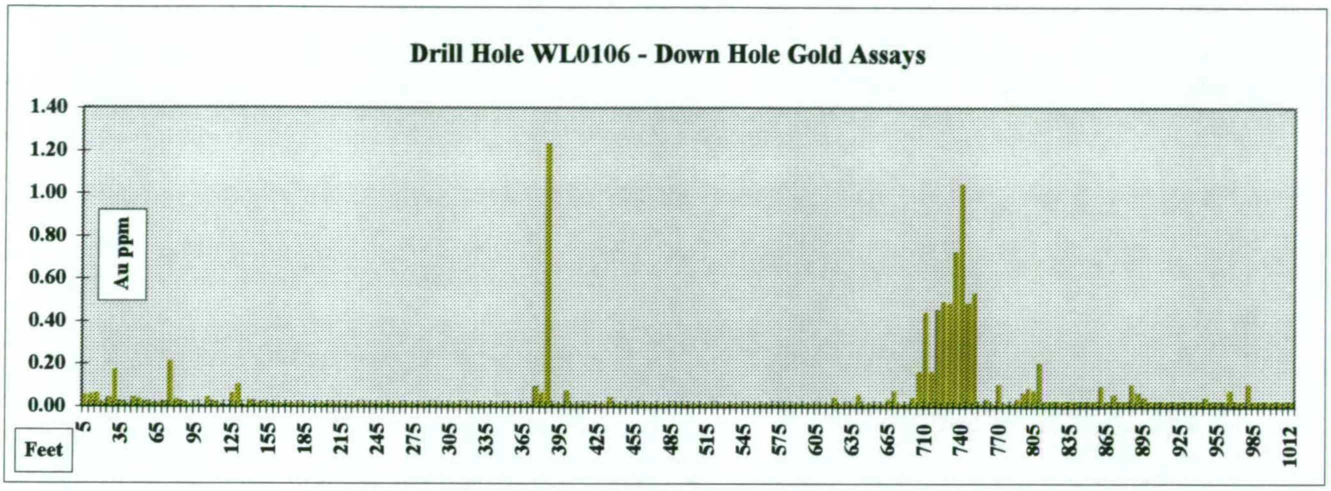
Drill Hole WL0106 - Down Hole Gold Assays
Au ppm
Feet

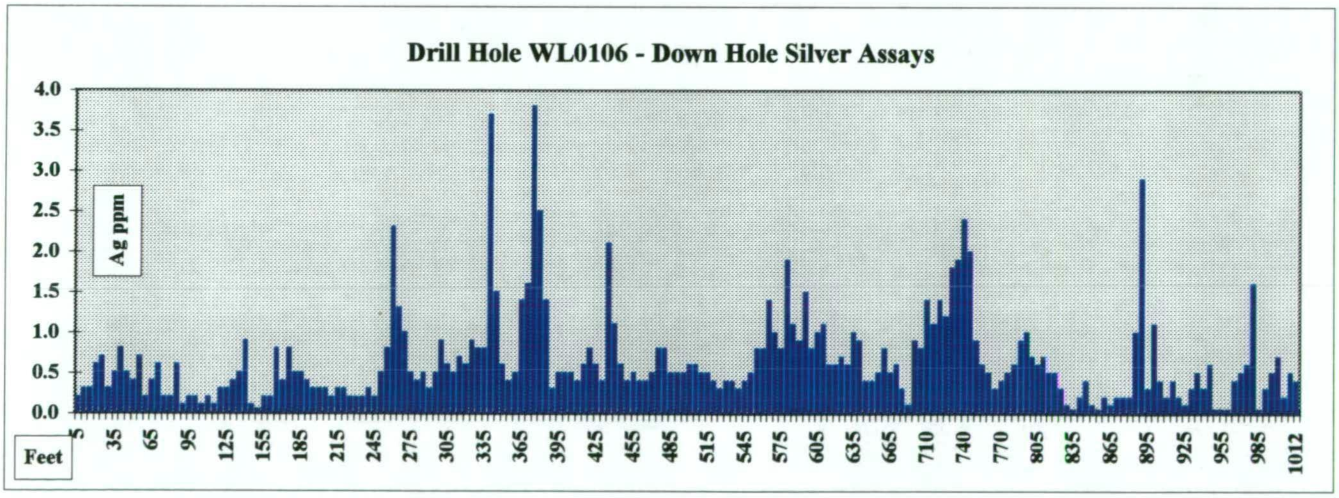
Drill Hole WL0106 - Down Hole Silver Assays
Ag ppm
Feet

Project: Royal Tharsis Alteration **Location:** periphery of Royal Tharsis orebody **Hole Number:** WL0106

Major			Minor			Lithology				Alteration		Mineralisation						Structure & Veining			
From	To	Code	From	To	Code	Colour	Gr. Size	Texture	Description	Code	Description	Py %	Style	Cp %	Style	%	%	Depth (m)	Code	Angle	Description
0.00	0.40	Lqzch				gyge	mg		Interlocking mosaic of qz-ch with cb/se altered ex feldspar?	cbhm	Haematite sparse	1						0.17	fo	55	
0.40	56.36	Lqzse				gypk	mg		Strongly segregated quartz-sericite domains/breccia texture?	hmcb	Pervasive	15						17.40	fo	35	
			0.40	6.10	Lqzse(ch)	gypk	mg		Very irregular & inconsistent, patchy ch alteration noted occasionally. Minor fl along joint planes.	hmcb	Pervasive	15						25.06	fo	25	
56.36	74.68	Lqzse				pk	fg		Highly siliceous rock with locally developed sericite.	hmcb	Pervasive	7		<1				33.93	fo	25	
74.68	91.67	Lqzse				gypk	mg		Silieous with variable pyrite content.	hmcb	Pervasive	15						37.58	fo	30	
			76.75	78.94	Lqzpy	gy	mg		Zone of very pervasive pyritic alteration - possible vein.			60						40.37	fo	50	
91.67	100.13	Lqzch				gyge	mg		Highly siliceous Lqz with ragged ch blebs & minor se. Limonitic cb/sd blebs throughout with scattered hm. Unit more chloritic down hole.	hmsd	Patchy	5						49.07	fo	55	
100.13	105.00	Lqzch				gyge	mg		Increasingly chloritic quartz-chlorite schist.	chsd	Patchy	2						61.60	fo	65	
105.00	110.26	Lqzse				pkgy	mg		Siliceous and weakly/locally chloritic.	hmcb	Pervasive	10						72.04	fo	60	
110.26	112.14	Lchqz				ge	fg	pp	Quartz porphyroblasts up to 0.5mm & finer sericitic flecks in chloritic groundmass. Contacts very sharp.	chsd	Patchy	7						74.82	fo	50	
112.14	129.39	Lqzse				pkgy	mg		Prominent greenish hydromicas.	sehm	Pervasive	20						82.13	fo	60	
129.39	156.97	Lqzch				gegy	cg		Highly siliceous with minor se. Sd-hm alteration locally strong. ch locally abundant enough to form segregated masses as well as irregular clots.	hmsd	Very strong, locally pervasive	3						88.74	fo	45	
			153.92	156.97	Lqzch	pkgy	cg		Down hole boundary zone gradational, clots of chlorite in haematitic qz-se schist, green & white micas in equal abundance.	sehmsd		5						90.83	fo	40	
156.97	180.44	Lqzse				pkgy	cg		Up hole boundary a little indefinite but ± 1 metre. Irregular clots of chlorite. Pale greenn sericite. Poor schistosity.	hm		15						104.40	fo	55	
180.44	193.62	Lqzch				ge	fgmg		Unit starts as highly siliceous & becomes progressively more chloritic & finer grained toward down hole boundary, 190.50 - 193.55 m (625-635ft.).	chsd	Moderate	7						113.80	fo	75	
193.62	213.97	Lqzse				gy	mg		Locally chloritic.	qzse		20						114.14	Vqzsd	120	Isolated veining
			193.62	199.57	Lqzse	pkgy	mg		Haematitic zone.	hm	Pervasive	7						117.97	fo	65	
			199.57	208.18	Lqzse	gy	mg		Pyritic quartz sericite schist.	qzse		25						121.80	fo	70	
			208.18	213.97	Lpyqz	yegy	mg		Massive pyrite zone.			80		<1				125.80	fo	80	Pyritic vein at contact
213.97	228.68	Lqzch				ge	fgmg		Uneven cleavage. Minor sericite.	chsd	Patchy	3	sr	2	ds			128.41	Vqzsd	80	0.3 m (1 ft) thick
228.68	249.63	Lqzse				pkge	cg		Variable ch alteration throughout. Unit develops knobbly texture in qz toward down hole boundary possibly after phenocrysts? - Tyndall Group? Down hole boundary gradational, ± 2m (5ft).	sechhm	Pervasive	3	sr	1	ds			139.55	fo	55	
249.63	272.19	Lqzse				pk	cg		Minor carbonate (sd) alteration	sehm	Pervasive	2	ds	<1				148.94	fo	75	
272.19	308.46	Lqzse				pk	cg		Sequence of intercalated pink quartz-sericite schists & quartz-chlorite schists up to 30cm (12") with magnetite stringers & disseminations mostly through chloritic horizons	chhmmt	Variable	4	ds					154.86	fo	65	
			286.51	294.74	Lqzse	ltpk	mg		Quartz schist minor sericite & pyrite	qzsehm	Pervasive	2	ds					163.56	fo	70	
			294.74	308.46	Lqzch	gepk	mg		Intercalated Lqzse & Lqzchse schists. Chlorite appears more pervasive but in general resembles up hole portion of unit. Sheared.	sehmmt	Variable	3	ds					175.39	fo	47	
																		186.18	fo	60	
																		191.72	fo	85	
																		199.34	fo	60	

Geologist: W.J.D.Godsall **Date:** 21/12/96 **Page** 1 **of** 2

Project: Royal Tharsis Alteration **Location:** periphery of Royal Tharsis orebody **Hole Number:** WL0106

Major			Minor			Lithology				Alteration		Mineralisation						Structure & Veining			
From	To	Code	From	To	Code	Colour	Gr. Size	Texture	Description	Code	Description	Py %	Style	Cp %	Style	%	%	Depth (m)	Code	Angle	Description
272.19	308.46	Lqzse								chhmmt	Variable							203.93	fo	68	
		(continued)																207.26	fo	70	
	EoH																	217.93	fo	70	
																		227.69	Vqzsd		20cm thick
																		228.60	fo	65	
																		228.90	Vqzsd		30 cm thick
																		243.84	fo	65	
																		260.60	fo	75	
																		273.41	fo	75	
																		288.65	fo	75	
																		300.23	fo	70	
																		303.28	fo	65	

Geologist: W.J.D.Godsall **Date:** 21/12/96 **Page** 1 **of** 2

Project	Royal Tharsis Alteration	**Hole Number**	WL0421
Prospect	Royal Tharsis	**Section/s**	7950N
Tenement	1M/95	**COLLAR INFORMATION 315GRL GRID**	
Original Log By	C.J.Webb	**North**	7947
		East	3849
Date	September 1976	**RL**	2196
		Azimuth	083
Summary Log By	W.J.D.Godsall	**Inclination**	-10
Method	Re-log	**Hole Length (m)**	65.20
		Hole Length (ft)	
Date	4/11/96	(if applicable)	

Summary Log

From	To	Code	Description	Py%	Cp%	Depth	Code	Angle
0.00	18.30	Lqzpych(mt)	Fragmental. Variable carbonate content	11	4	5.5	fo	80
18.30	44.30	Lqzse(py)(hm)	Pervasive haematite	9	7	19.7	fo	70
44.30	65.20	Lqzchsehm(py)	Fault zones may be Great Lyell fault.	4	4	30.4	fo	80
						37.8	fo	70
						41.3	fo	60
						57.9	fo	80

Abbreviations: na - not available, ne- no entry, nd - not determined, no - not observed, fo - foliation, co - contact, S0 - bedding, Tr - trace

Significant Intersections

From	To	m	Description	Cu%	Au ppm	Ag ppm	Py%
6.0	52.0	46.0		2.12	0.65	1.87	7.8
			Hole ends in mineralisation.				
			Average SG = 2.96 (10 * 6 metre composite samples)				

Hole Purpose and Result

Drilled from 11 level footwall drill drive.
Testing below Royal Tharsis mine stopes on section 51, 190 m RL
Extremely poor ground conditions predicted.
Core severly broken. Fault zones with clay and gravel, and low angle joints intersected.
Original assay data suspect (too high) due to low recovery.

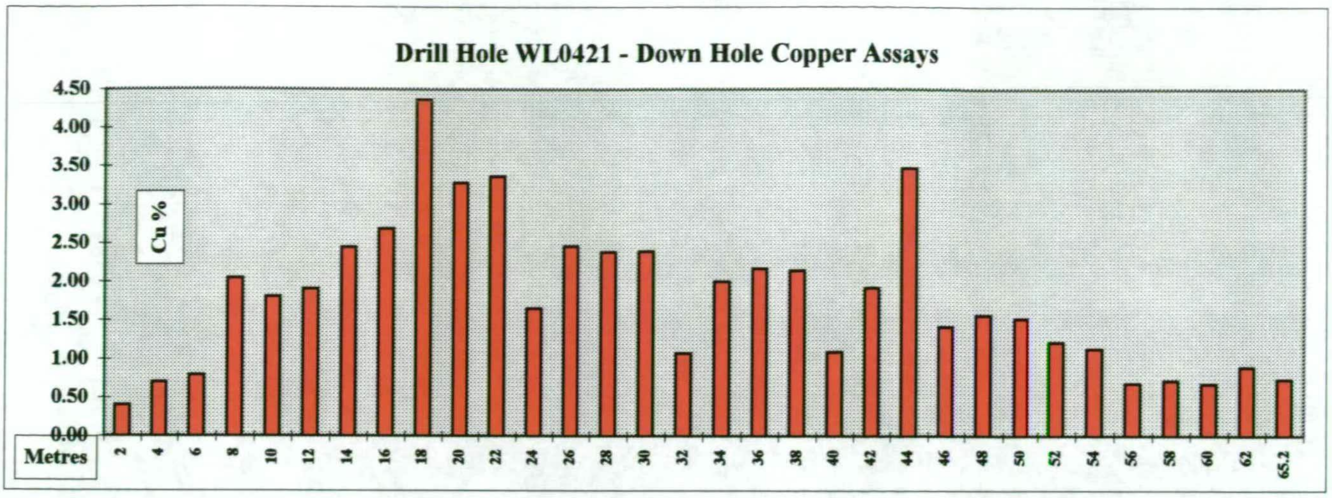
Drill Hole WL0421 - Down Hole Copper Assays
Cu %
Metres
4.50
4.00
3.50
3.00
2.50
2.00
1.50
1.00
0.50
0.00
2 4 6 8 10 12 14 16 18 20 22 24 26 28 30 32 34 36 38 40 42 44 46 48 50 52 54 56 58 60 62 65.2

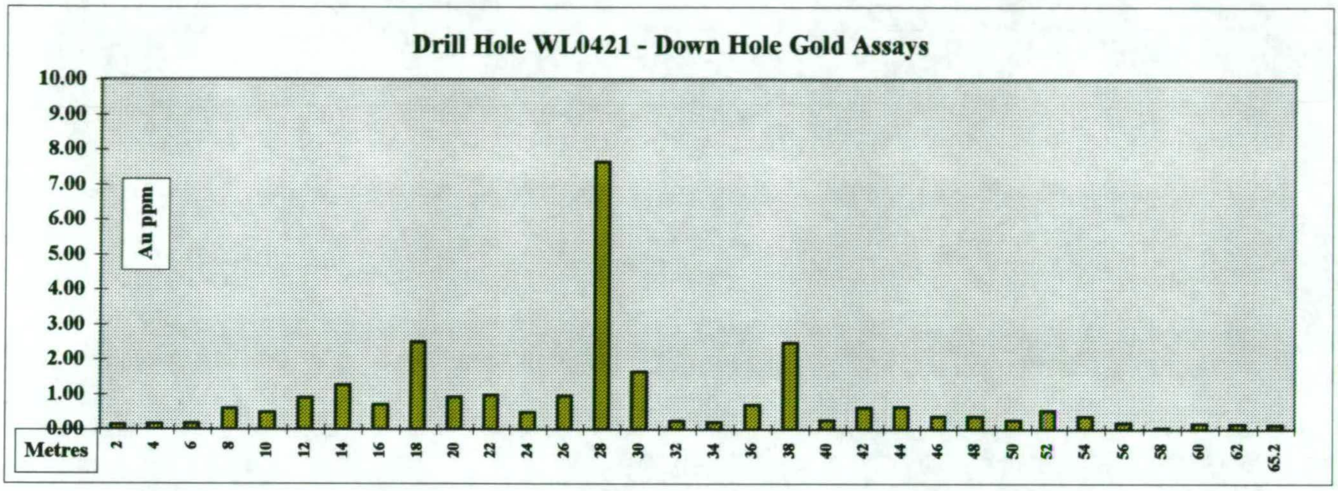
Drill Hole WL0421 - Down Hole Gold Assays
Au ppm
Metres
10.00
9.00
8.00
7.00
6.00
5.00
4.00
3.00
2.00
1.00
0.00
2 4 6 8 10 12 14 16 18 20 22 24 26 28 30 32 34 36 38 40 42 44 46 48 50 52 54 56 58 60 62 65.2

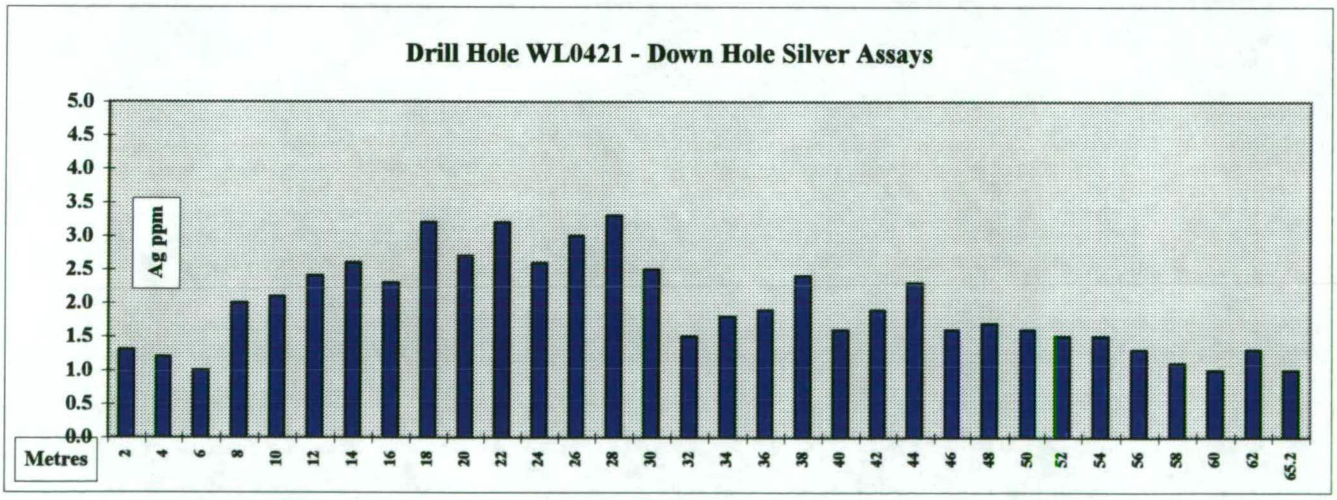
Drill Hole WL0421 - Down Hole Silver Assays
Ag ppm
Metres
5.0
4.5
4.0
3.5
3.0
2.5
2.0
1.5
1.0
0.5
0.0
2 4 6 8 10 12 14 16 18 20 22 24 26 28 30 32 34 36 38 40 42 44 46 48 50 52 54 56 58 60 62 65.2

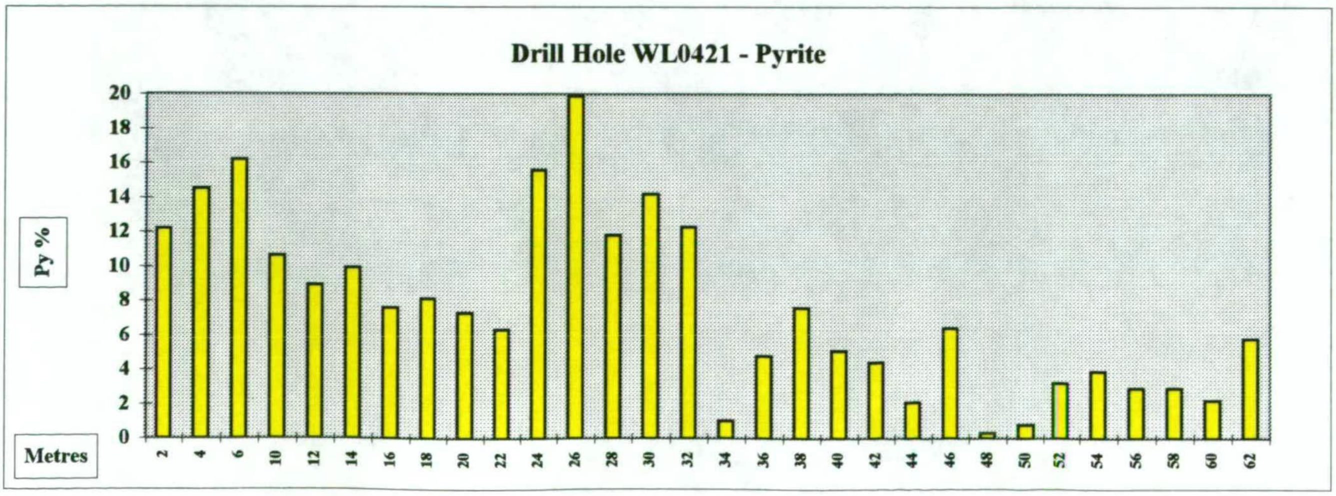
Drill Hole WL0421 - Pyrite
Py %
Metres
20
18
16
14
12
10
8
6
4
2
0
2 4 6 10 12 14 16 18 20 22 24 26 28 30 32 34 36 38 40 42 44 46 48 50 52 54 56 58 60 62

Project: Royal Tharsis Alteration **Location:** southern part of Royal Tharsis orebody **Hole Number:** WL0421

Major			Minor			Lithology				Alteration		Mineralisation						Structure & Veining			
From	To	Code	From	To	Code	Colour	Gr. Size	Texture	Description	Code	Description	Cp %	Style	Py %	Style	%	%	Depth (m)	Code	Angle	Description
0.00	18.30	Lqzych				gegy	mg	gn	Predominantly chloritic sequence, locally sericitic. Intermixed Lqzpych(mt) and Lqzpych(se)(mt). Fragmental. Variable carbonate (siderite) content. Siliceous.	sich(mt)	Pervasive chlorite.										
			0.00	2.30	Lqzch	gegy	mg		Sulphide veinlets and crack infill - locally along foliation. Mainly disseminated. Scatteredblebs mt and impregnated/disseminated py.	sich(mt)	Locally sericitic.	3	d	10	d			1.8	f1	70	
			2.30	9.80	Lqzse	pigy	mg	gn	Fragmental - irregular to elongate fragments with variable cream siderite veinlets. Disseminated sulphides, occasional veinlets, increasing down the hole. Lesser chlorite content increases with depth. Locally broken core.	sisecb		5	d	10	d			5.5	f1	80	
			9.80	18.30	Lqzch	gegy	mg	fx	Fragmental, becoming sericitic through the middle of the unit. Almost "massive" chlorite from 16.30m to 18.30m. Variable sulphide content in the form of disseminations and blebs, occasional stringers, locally massive.	chcbhm	Pervasive chlorite. Minor siderite.	3	d	9	d			13.8	f1	80	
18.30	44.30	Lqzse				pigy	mg	gn	Predominantly sericitic sequence with minor chlorite and pervasive micaceous haematite. In places core is heavily broken, Gradational contacts.	sise(hm)	Moderate to strong.										
			18.30	22.30	Lqzse	pigy	cg	fx	Lithic tuff. Weakly brecciated. Heavily broken core - locally faulted. Minor chlorite. Sulphides as disseminations and veinlets.	sehmcb	Moderate.	5	d	8	d			19.7	f1	70	
			22.30	24.90	Lqzch	gegy	mg	fr	Broken core. Minor pink haematite. Disseminated sulphides, localised granular blebs and veinlets. Occasional siderite stringers.	sich(hm)	Pervasive chlorite.	6	d	12	d			24.1	f2	80	
			24.90	35.20	Lqzse	pigy	cg	gn	Granular with minor chlorite. Pink micaceous haematite. Interstitial sulphides. Massive vein at 25.1m. Occasional siderite.	sehm	Moderate to strong.	3	d	8	d			30.4	f3	80	
			35.20	40.60	Ffz	pigy	cg	fx	Fragmental and locally faulted from 35.4m. Quartz sericite schist with carbonate and haematite. Siderite as veins, blebs and stringers, frequently as quartz-siderite veins that are brecciated/distorted. Quartz - magnetite vein at 36.6m.	hmcb	Moderate hematite. Weak carbonate.	3	d	8	d			37.8	f3	70	
			40.60	44.30	Lqzse	pigy	mg	fx	Granular and fragmental. Broken core, locally faulted as per original log. Molybdenite recorded in original log not identified - possibly haematite.	sisehm	Moderate to strong.	2	d	3	d			41.3	f2	60	
44.30	65.20	Lqzch				pigy	cg	fx	Core is heavily broken generally throughout the unit. (Faulting as per original log.) Micaceous - hydromica. Coarse breccia - lithic tuff. Fragmental and granular with minor siderite and ?trace? chlorite. Sulphides as disseminations. Some pug.	chsehm	Strongly pervasive.	2	d	6	d			57.9	f1	80	(Shallowing of SCA as in original log not observed.)
			54.05	57.48	Ffz				? Great Lyell fault?												
			62.40	65.20	Ffz				? Great Lyell fault?												
	EoH																				

Geologist: W.J.D.Godsall **Date:** 4/11/96 **Page** 1 **of** 1

Project	Royal Tharsis Alteration	**Hole Number**	WL0530A
Prospect	Royal Tharsis	**Section/s**	7950N
Tenement	1M/95	**COLLAR INFORMATION 315GRL GRID**	
Original Log By	M.Bird	**North**	7954
		East	3558
Date	1982	**RL**	1990
		Azimuth	212
Summary Log By	W.J.D.Godsall	**Inclination**	-39
Method	Re-log	**Hole Length (m)**	303.90
		Hole Length (ft) (if applicable)	
Date	18/01/97		

Summary Log

From	To	Code	Description	Py%	Cp%	Depth	Code	Angle
0.00	22.00	Lqzse(cb)(ch)	Variable carbonate content	1		0.0	fo	45
22.00	66.20	Lqzsecb	?carbonate zone as fringe to the pyritic zone	-		25.0	fo	50
66.20	72.50	Ffz		-		60.0	fo	55
72.50	91.40	Lqzse(cb)-fxvn	Locally faulted	-		85	fo	50
91.40	100.10	Lqzse(cb)	Veinlets sub parallel to S2	-		107	fo	65
100.10	100.90	Ily	Weakly magnetic lamprophyre	-		133	fo	70
100.90	124.50	Lqzsecb(ch)	Prominent carbonate	-		159	fo	75
124.50	138.20	Lqzsech(cb)	Clots of chlorite - ? fragmental	-		213	fo	80
138.20	147.60	Vqz	Transgressive to S2. Potential mica "barrier".	-		241	fo	75
147.60	173.10	Lqzse	Gradual drop off in cb veins to EoH	-		256	fo	80
173.10	176.70	Vqz	Cuts S2 - i.e. late	-		275	fo	75
176.70	212.85	Lqzch(se)	Gradational contacts	-		300	fo	85
212.85	233.25	Lqzse(ch)	Veined	-				
233.25	249.20	Lqzse	Veined	-				
249.20	261.3	Lqzchse	Intercalated chlorite clots	-				
261.3	278.2	Lqzse(ch)	Veinlets sub parallel to S2	-				
278.2	288.0	Lqzch	Prominent mixed micas.	-				
288.0	303.9	Lqzse	EoH in zone of lowest grade alteration.	-				

Abbreviations: na - not available, ne- no entry, nd - not determined, no - not observed, fo - foliation, co - contact, S0 - bedding, Tr - trace

Significant Intersections

From	To	m	Description	Cu%	Au ppm	Ag ppm	Py%
			No significant copper intersections				

Hole Purpose and Result

Drilled to test 40 series decline structures.
Drilled distal to the economic zone and towards the edge of the alteration zone

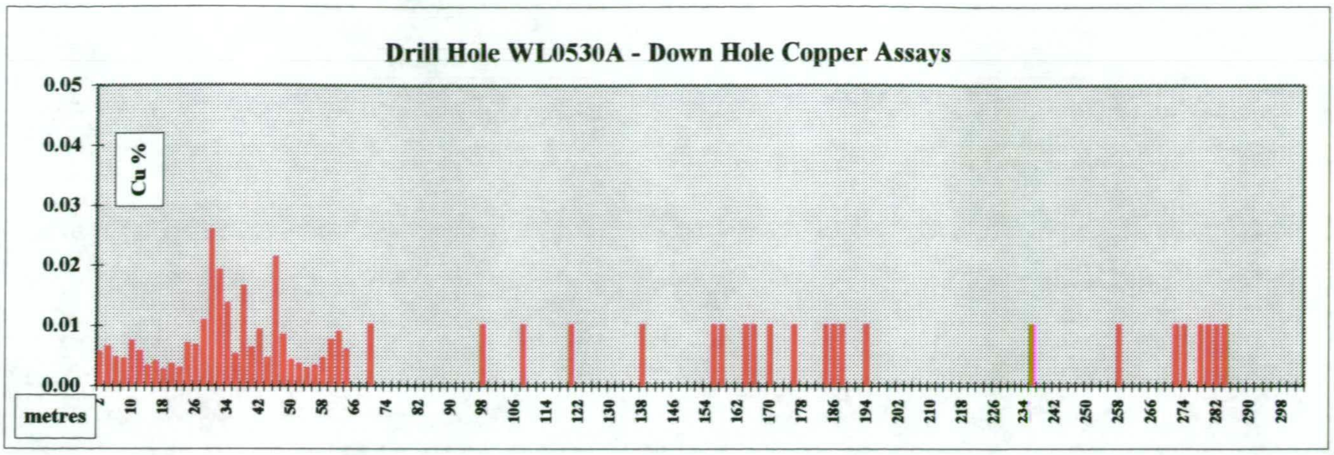
Drill Hole WL0530A - Down Hole Copper Assays
Cu %
metres

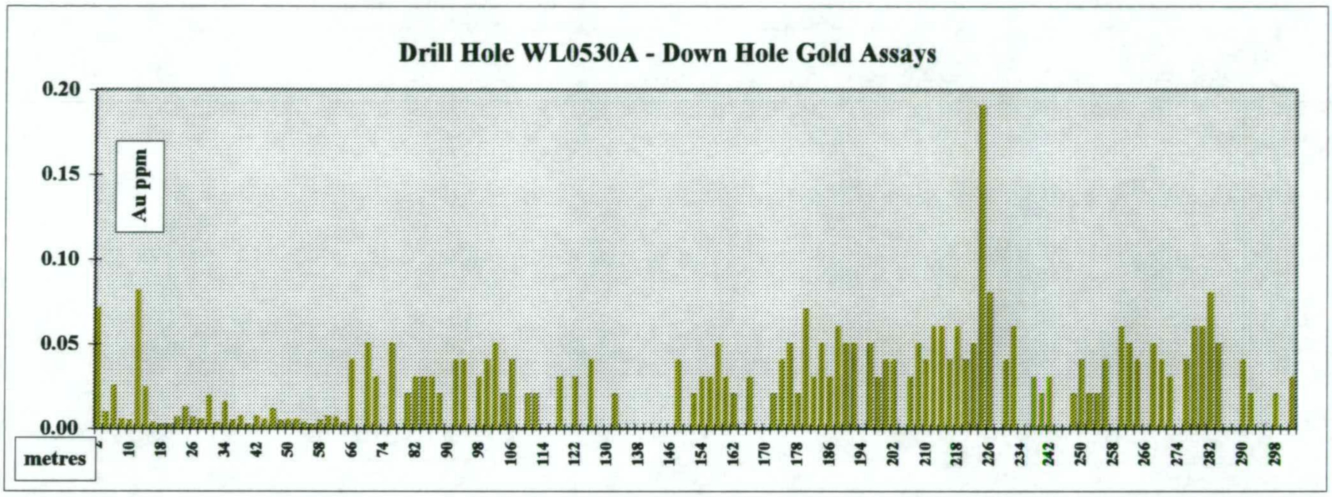
Drill Hole WL0530A - Down Hole Gold Assays
Au ppm
metres

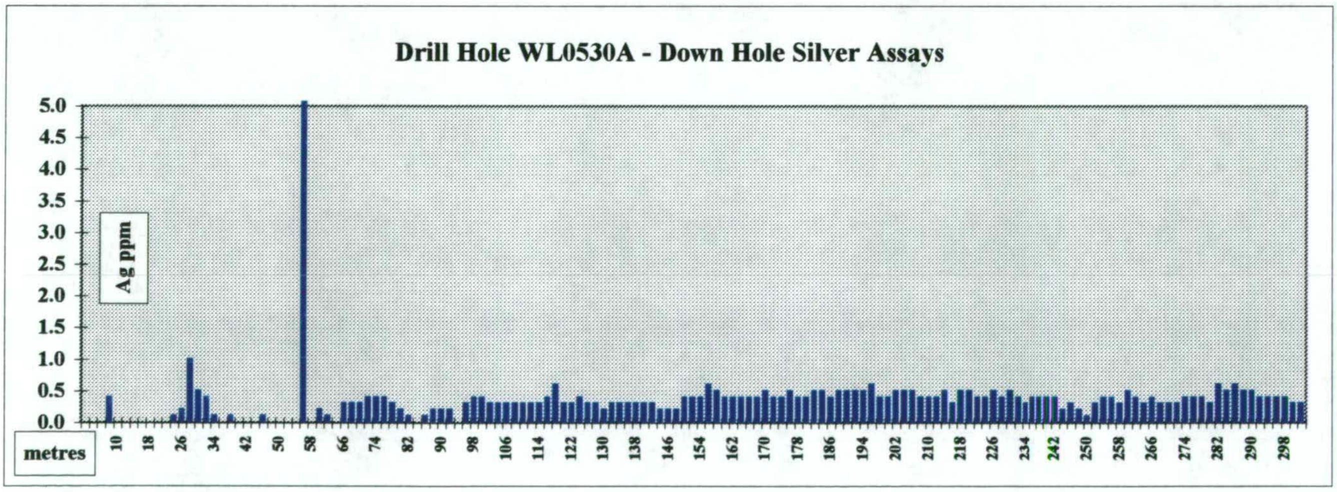
Drill Hole WL0530A - Down Hole Silver Assays
Ag ppm
metres

Project: Royal Tharsis Alteration **Location:** hangingwall of Royal Tharsis **Hole Number:** WL0530A

Major			Minor			Lithology				Alteration		Mineralisation						Structure & Veining			
From (m)	To (m)	Code	From (m)	To (m)	Code	Colour	Gr. Size	Texture	Description	Code	Description	Py %	Style	Cp %	Style	%	%	Depth (m)	Code	Angle	Description
0.00	22.00	Lqzse				gy	mg		Variable amounts of carbonate in form of siderite, frequently intermixed with white quartz. Disseminated sulphides as scattered specks.	secbch	Minor chlorite.	1	ds					0	fo	45	
22.00	66.20	Lqzse				gepi	mg		Prominent carbonate (?25%) content in the form of yellow to red siderite, occurring as veinlets, blebs and stringers.Generally concordant S2,occasionally cross-cutting. Slickensided. Localised slithers of light green ?chlorite/hydromica.	qzsecb	White micas and carbonate.							25	fo	50	
66.20	72.50	Ffz							Heavily broken core with som pug infill. Dominantly sericite carbonate schist with minor chlorite. No visible sulphide mineralistion.									60	fo	55	
72.50	91.40	Lqzse				whgy	mg	fx	Locally broken/faulted sericite schist. No visible mineralisation. Stringers/veinlets and blebs of quartz-siderite. Thin mud seams in the cleavage.	qzsecb	White micas and carbonate.							85	fo	50	
			76.45	76.70	Ffl																
			79.65	79.85	Ffl																
			89.31	89.90	Ffl																
91.40	100.10	Lqzse				gyge	mg		Becoming finer grained. Blebs and veinlets of siderite generally sub parallel to S2. No visible sulphide mineralisation. Locally contorted at base.	secb	White micas and carbonate.										
100.10	100.90	Ily				bl	cg		Black homogeneous lamprophyre dyke. Weakly/faintly magnetic. Red ?haematite through middle of unit.	hm	Haematitic and magnetitic.										
100.90	124.50	Lqzse				pigy	mg	vn	Quartz sericite schist with prominent carbonate (?15%) in the form of quartz-siderite veins and blebs, both sub parallel to S2 and discordant/cross-cutting. Minor chlorite. No visible sulphide mineralisation.	secbch	White micas and carbonate.							107	fo	65	
			103.25	103.50	Ffl																
124.50	138.20	Lqzse				gyge	fg	vn	Similar to 100.9m - 124.5m but with an increasing chlorite content and lesser carbonate. Localised clots of chlorite impart a faint fragmental appearance. No visible sulphide mineralisation.	qzse(ch)	Pervasive sericite and minor hydromicas.							133	fo	70	
138.20	147.60	Vqz				wh		mv	Brittle white quartz, tending to be massive, with a minor/local carbonate/siderite content and intermixed with sericite schist and dark green chlorite.												
147.20	173.10	Lqzse				pigy	fg	fx	Variable and gradational unit. Generally broken core. Locally chloritic, particularly through the middle of the unit. Minor quartz +/- carbonate veinlets and stringers. No visible mineralisation.	qzse								159	fo	75	
			164.20	167.80	Ffl			vn	Fractured core. Locally veined.												
			168.40	172.80	Ffl			vn	Fractured core. Locally veined.												
173.10	176.70	Vqz				wh			Heavily broken white quartz vein with dark green chlorite. ?not metamorphosed.												
176.70	212.85	Lqzch				gegy	fg	gn	Chloritic unit with a variable sericite content that locally becomes major, particularly through the lower part of the unit. Gradational contacts. Minor quartz +/- carbonate content in the form of blebs and stringers. ?copper carbonate stain at 190m.	qzchse	Pervasive										
			203.50	207.10	Ffl																
			207.50	210.50	Lqzse				Fragments of sericite chlorite schist.	qzsech	Pervasive										
212.85	232.75	Lqzse				pigy	fg		Dominantly sericitic becoming chloritic through the middle of the unit. Gradational contacts. Minor quartz +/- carbonate veinlets. No visible mineralisation.	qzsech	Pervasive							213	fo	80	
			222.50	227.35	Lqzch	gegy	fg		Gradational and relative increase in chlorite and decrease in sericite. No visible mineralisation.	qzchse	Pervasive										
232.75	233.25	Vqz				wh			Competent massive quartz vein with siderite staining and dark green chlorite.												

Geologist: W.J.D.Godsall **Date:** 18/01/97 **Page** 1 **of** 2

Project: Royal Tharsis Alteration **Location:** hangingwall of Royal Tharsis **Hole Number:** WL0530A

Major			Minor			Lithology				Alteration		Mineralisation						Structure & Veining			
From (m)	To (m)	Code	From (m)	To (m)	Code	Colour	Gr. Size	Texture	Description	Code	Description	Py %	Style	Cp %	Style	%	%	Depth (m)	Code	Angle	Description
233.25	248.70	Lqzse				pigy	fg		Minor chloritic content occurring as variable intercalations. Veinlets of quartz +/- carbonate generally sub parallel to S2. Possible relict albite. Faintly fragmental. No visible mineralisation.	qzse	Pervasive							241	fo	75	
248.70	249.20	Vqz				wh		mv	Massive white quartz vein with ochre brown siderite staining and dark green chlorite. Unit is actually two veins separated by fragmental Lqzse.												
249.20	261.30	Lqzch				gepi	fg		Variable chlorite - sericite unit, intercalated and with small almost elongate clots of chlorite. Gradational contacts. No visible mineralisation.	qzchse	Pervasive							256	fo	80	
261.30	278.20	Lqzse				gypi	fg	fr	Localsed bands/veinlets of quartz +/- carbonate, generally sub parallel to S2. No visible mineralisation.	qzsech	Pervasive							275	fo	75	
			267.30	270.40	Ffl																
278.20	288.00	Lqzch				gegy	fg	vn	Apparent and slight increase in vein content which drops off rapidly down the unit. Gradational contacts. No visible mineralisation.	qzch	Pervasive										
288.00	303.90	Lqzse				pige	mg	fr	Minor/irregular hydromica/chlorite, sometimes as clots. Ubiquitous fragmental texture that is generally small scale ?debris flow? Blebs/specks of siderite possibly after sulphides. Variable vein content as veinlets and specks. No visible mineralis'n.	qzse	Pervasive							300	fo	85	
	EoH																				

Geologist: W.J.D.Godsall **Date:** 18/01/97 **Page** 2 **of** 2

Project	Royal Tharsis Alteration	**Hole Number**	WL0531
Prospect	Royal Tharsis	**Section/s**	7950N
Tenement	1M/95	**COLLAR INFORMATION 315GRL GRID**	
Original Log By	M.Bird	**North**	7957
		East	3548
Date	1982	**RL**	1896
		Azimuth	067
Summary Log By	W.J.D.Godsall	**Inclination**	-39
Method	Re-log	**Hole Length (m)**	119.90
		Hole Length (ft) **(if applicable)**	
Date	1/12/97		

Summary Log

From	To	Code	Description	Py%	Cp%	Depth	Code	Angle
0.00	16.25	Lqzse	Haematitic	3	tr	5.0	fo	60
16.25	17.25	Ily	Lamprophyre	-	-	13.0	fo	50
17.25	44.30	Lqzse	Silica rich. Fragmental	15	tr	35.0	fo	45
44.30	62.60	Lqzse	Minor local chlorite	12	tr	54	fo	70
62.60	91.10	Lqzse	Locally faulted	12	tr	75	fo	65
91.10	119.90	Lqzse	Locally veined. Fault zone towards EoH.	10	tr	100	fo	75
						111	fo	45
						115	fo	75

Abbreviations: na - not available, ne- no entry, nd - not determined, no - not observed, fo - foliation, co - contact, S0 - bedding, Tr - trace

Significant Intersections

From	To	m	Description	Cu%	Au ppm	Ag ppm	Py%
			No significant copper mineralisation intersected				

Hole Purpose and Result

To test possible 15 level and 50 Series access and ground conditions.
Drill hole collar located in hangingwall. Owen Conglomerate not intersected. Ore zone not intersected.

Drill Hole WL0531 - Down Hole Copper Assays

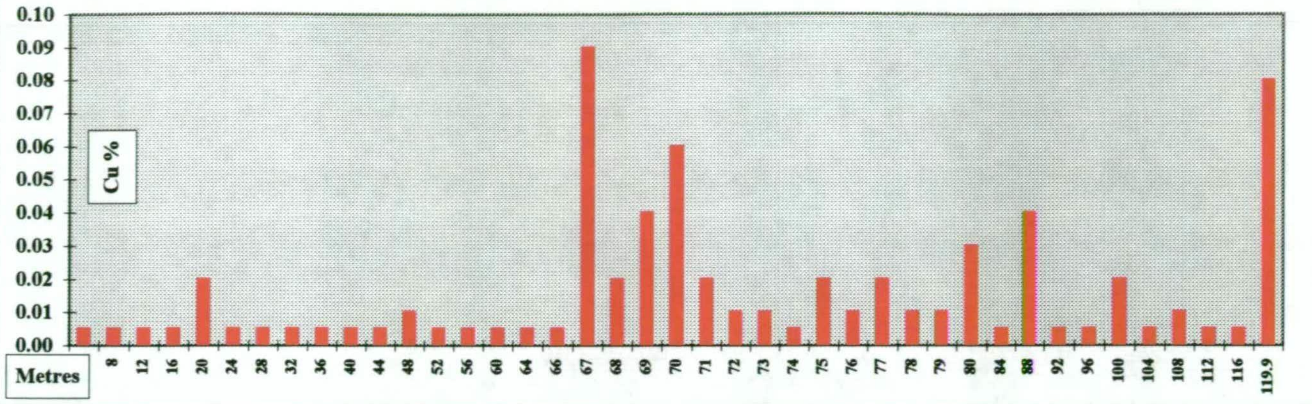

Drill Hole WL0531 - Down Hole Gold Assays

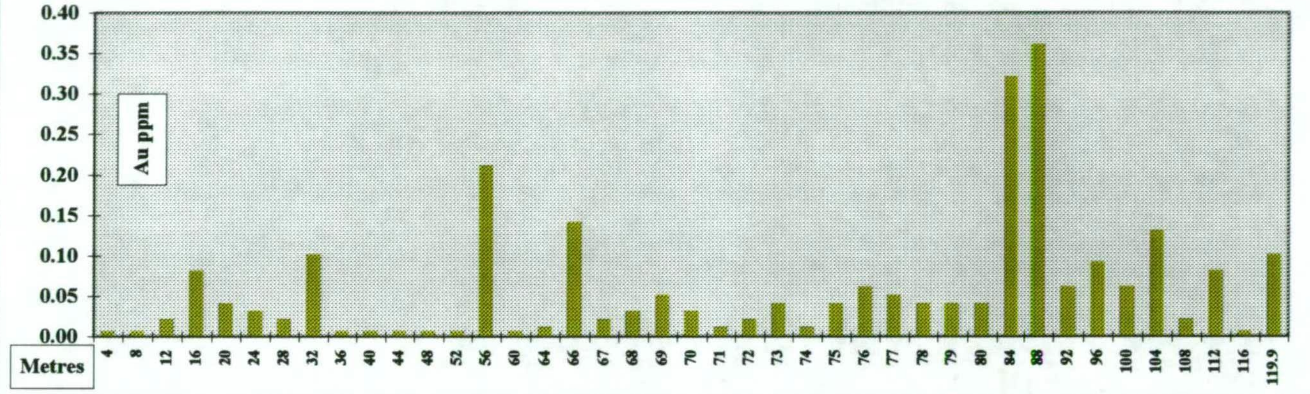

Drill Hole WL0531 - Down Hole Silver Assays

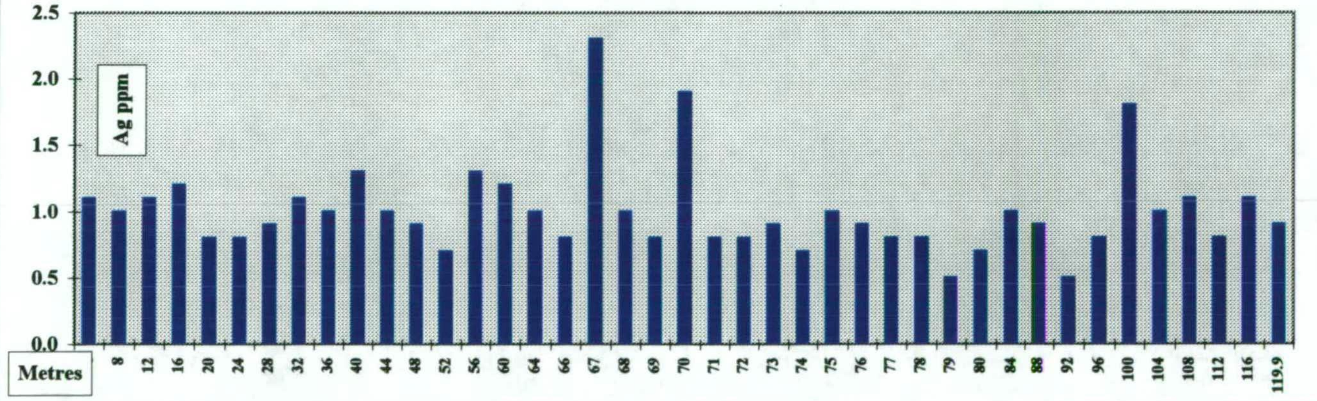

Drill Hole WL0531 - Pyrite

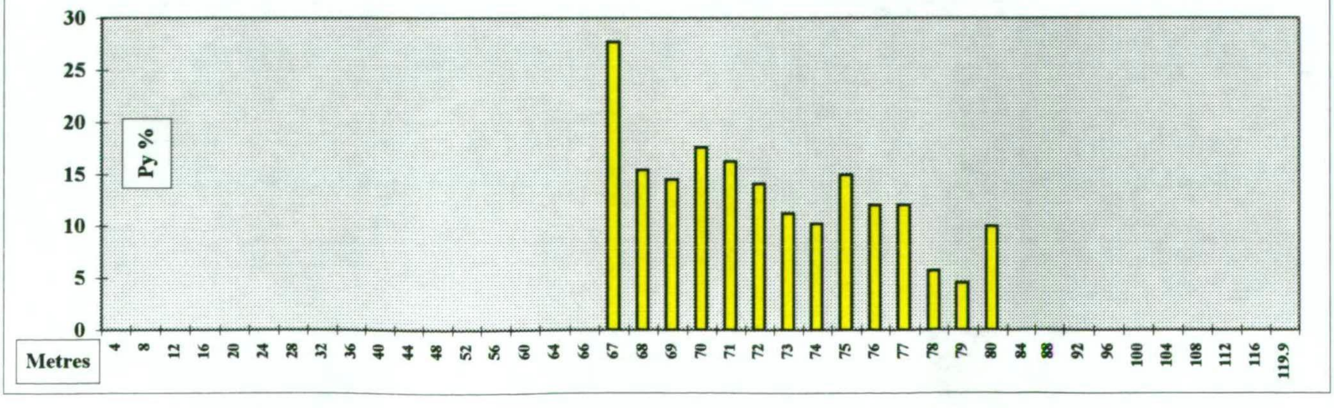

Project: Royal Tharsis Alteration **Location:** hangingwall of Royal Tharsis **Hole Number:** WL0531

Major			Minor			Lithology				Alteration		Mineralisation						Structure & Veining			
From (m)	To (m)	Code	From (m)	To (m)	Code	Colour	Gr. Size	Texture	Description	Code	Description	Py %	Style	Cp %	Style	%	%	Depth (m)	Code	Angle	Description
0.00	16.25	Lqzse	0.00	1.65	Lchsihm	gegy	fg	sc	Well developed schistosity in a dark greenish grey silica rock with irregular iron rich clasts. Minor iron staining after sulphides. Pyrite occurs as occasional/trace speck.	sechhm	Pervasive chlorite and haematite.	tr	ds					1.1	f3	60	
			1.65	14.90	Lqzse	wh	mg		White greyish silica rich rock with irregular quartz vein stringers, frequently showing iron staining after sulphides. Pyrite content increases down the hole. Siliceous. Upper part of the unit has a distinctive lime green colour.	sise	Pervasive silica, minor sericite.	3	ds					5	f2	60	
			14.90	15.20	Vqz	wh		vn	Broken quartz vein. Brittle. Minor schist along breaks.									10.5	f2	55	
			15.20	16.25	Lqzse	wh	mg		Similar to 1.65m -14.90m above.	sise	Pervasive silica.	3	ds					22	f2	50	
16.25	17.25	Ily				bk	fg		Black biotitic lamprophyre dyke.									28	f2	55	
17.25	44.30	Lqzse				whcr	mg	fr	White to cream grey silica rich rock. Variably and locally fragmental. Irregular quartz stringers/veinlets, limonitic and weakly sideritic. Locally broken/faulted core. Gradational contacts.	sise	Pervasive.	3	ds	tr	ds			32	f2	60	
			32.50	36.70	Lqzse	gyge	fg		Poorly developed chlorite clots in a greenish grey schistose unit. Occasional irregular iron stained quartz veinlet/stringer.	qzsech	Pervasive silica and lesser chlorite.	3	ds	tr	ds			33	f3	55	
			36.70	39.30	Vqzcb	wh		vn	Quartz carbonate veining, locally broken, and interbedded with sericitic schist.									36	f3	60	
			39.30	44.30	Lqzse(ch)	gyge	fg		Similar to 32.5m - 36.7m above.	sech	Pervasive.	3	ds	tr	ds			42	f2	55	
44.30	62.60	Lqzse				whgy	fg	fr	Light whitish becoming slightly greenish grey rock with a moderately well developed schistosity. Locally slickensided along schistosity planes. Broken core in places. Gradational contacts.	qzse	Pervasive.	4	ds	tr	ds			45	f3	58	
			56.80	62.60	Lqzse(ch)	gyge	fg		Similar to major unit but with slightly more chlorite. Competent ground - unbroken core.	qzsech	Pervasive.	4	ds	tr	ds			51.5	f2	62	
62.60	91.10	Lqzse				gy	fg	fr	Light grey and fragmental, with a poorly developed schistosity. A slight increase in sulphide mineralisation with occasional cp. Gradational contacts Locally segregated. Core broken in places.	qzse	Pervasive.	6	ds	2	ds			61	f2	55	
			75.60	75.70	Ffl				Broken core.									67	f1	64	
			84.30	84.70	Ffl				Broken core.									74	f1	72	
			89.80	90.50	Ffl				Broken core.									80	f1	55	
91.10	119.90	Lqzse				gy	mg	fr	Light grey quartz sericite schist. Disseminated sulphides decreasing down the unit. Localised minor chlorite content. From 110.95m to 119.3m core becomes broken and faulted. Local quartz ?siderite stringers.	qzse	Pervasive.	5	ds	tr	ds			87.9	f1	60	
			114.75	116.05	Vqz	wh		vn	Broken white quartz vein.									92	f1	62	
			116.40	119.30	Ffz				Very broken ground. Localised pug.									97	f1	56	
	EoH																	102	f1	58	
																		107	f1	62	
																		111	f1	45	
																		111.2	jo	15	
																		115	f1	75	

Geologist: W.J.D.Godsall **Date:** 1-Feb-97 **Page** 1 **of** 1

Project	Royal Tharsis Alteration	**Hole Number**	WL0348
Prospect	Royal Tharsis	**Section/s**	8010N
Tenement	1M/95	**COLLAR INFORMATION 315GRL GRID**	
Original Log By	N.W.Sheppard	**North**	7986
		East	3752
Date	1972	**RL**	2196
		Azimuth	089
Summary Log By	W.J.D.Godsall	**Inclination**	-24
Method	Re-log	**Hole Length (m)**	159.72
		Hole Length (ft)	524
Date	4/01/97	**(if applicable)**	

Summary Log

From	To	Code	Description	Py%	Cp%	Depth	Code	Angle
0.00	9.14	Lqzse(ch)	Fine grained	7		1.8	fo	70
9.14	13.72	Lqzse(ch)	Coarse grained	3		10.4	fo	70
13.72	18.29	Lqzsecb	Zone of intense carbonate alteration.	12		21.3	fo	65
18.29	26.82	Lqzse	Highly siliceous.	5		32.3	fo	70
26.82	29.87	Lqz(se)(ch)	Phyllic minerals in clots and segregations.	5		47.5	fo	70
29.87	40.92	Lqzse(py)	Fractured acid lava	8		57	fo	85
40.92	82.91	Lqzsech	intercalated Lqzsehm	4		68.6	fo	80
82.91	114.00	Lqzsepy-hm	Brecciated lavas. Intercalated lithic tuffs	7	<1	96	fo	85
114.00	134.42	Lqzchse-cd	Clots of chlorite more prevalent down hole.	4	2	109.1	fo	85
134.42	151.49	Lqzsecb	Becoming more siliceous down hole.	3	1	141.1	fo	75
151.49	158.12	Ost	Sandstone					
158.12	159.72	Oct	Conglomerate.					

Abbreviations: na - not available, ne- no entry, nd - not determined, no - not observed, fo - foliation, co - contact, S0 - bedding, Tr - trace

Significant Intersections

From	To	m	Description	Cu%	Au ppm	Ag ppm	Py%
114.3	125.0	10.7	Lqzchse-cd and Lqzsecb	1.03	0.46	1.6	4.4
128.0	141.7	13.7	Lqzchse-cd and Lqzsecb	0.48	0.09	1.2	2.6
114.3	141.7	27.4	Lqzchse-cd and Lqzsecb	0.66	0.23	1.3	3.7
			Average SG = 2.96 (10 * 6 metre composite samples)				

Hole Purpose and Result

Drilled from Royal Tharsis exploration drive.

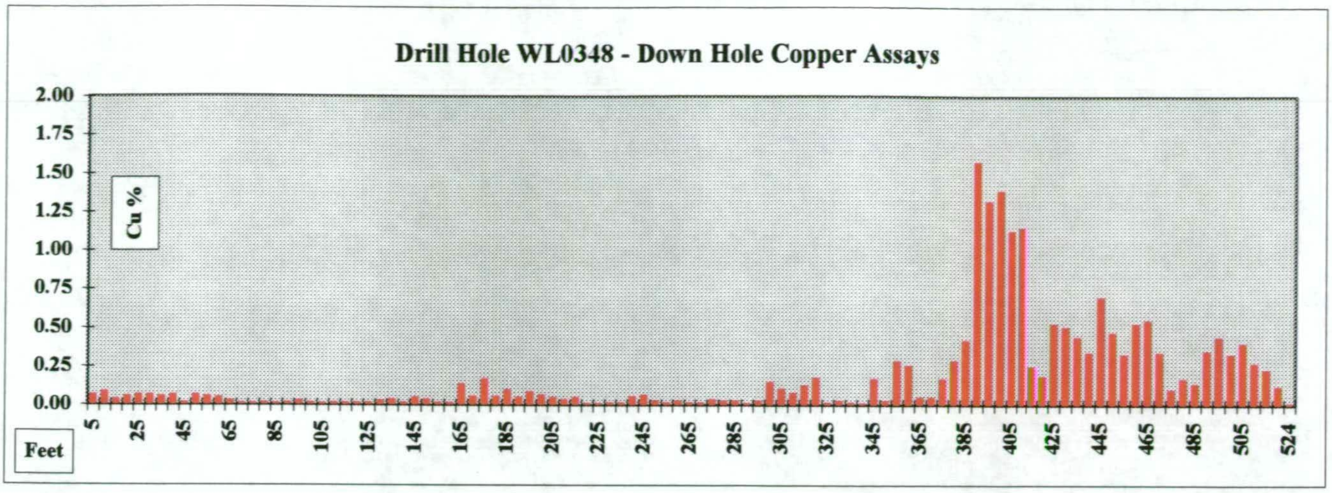
Drill Hole WL0348 - Down Hole Copper Assays
Cu %
Feet

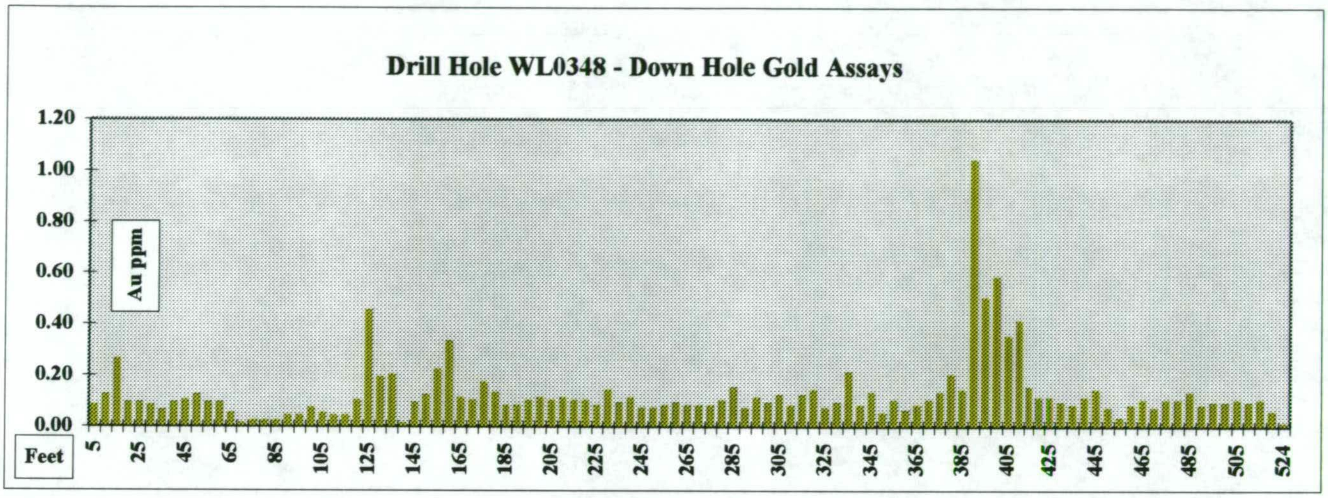
Drill Hole WL0348 - Down Hole Gold Assays
Au ppm
Feet

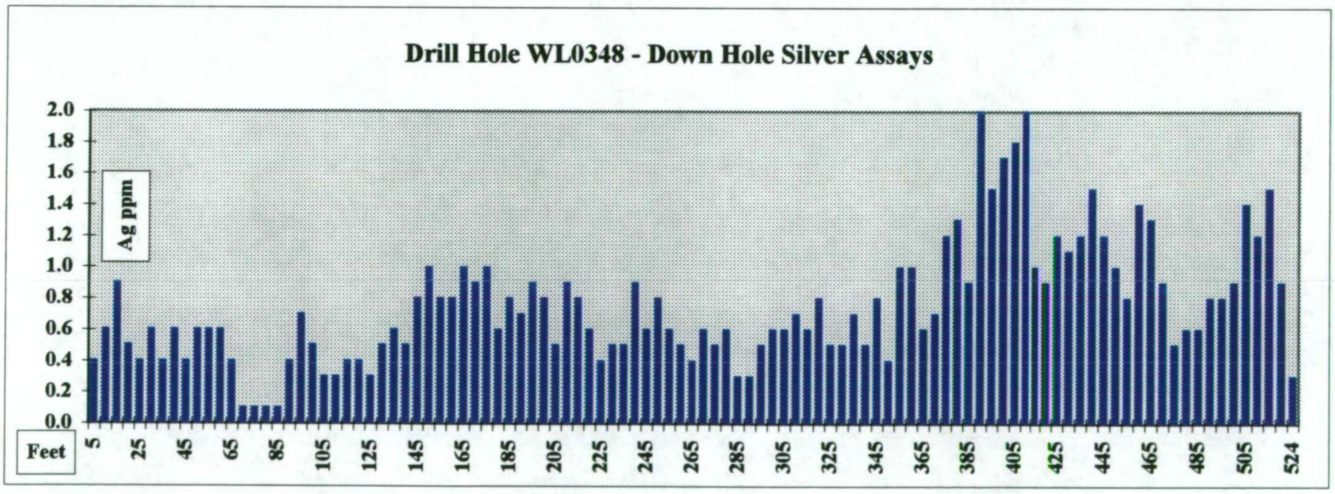
Drill Hole WL0348 - Down Hole Silver Assays
Ag ppm
Feet

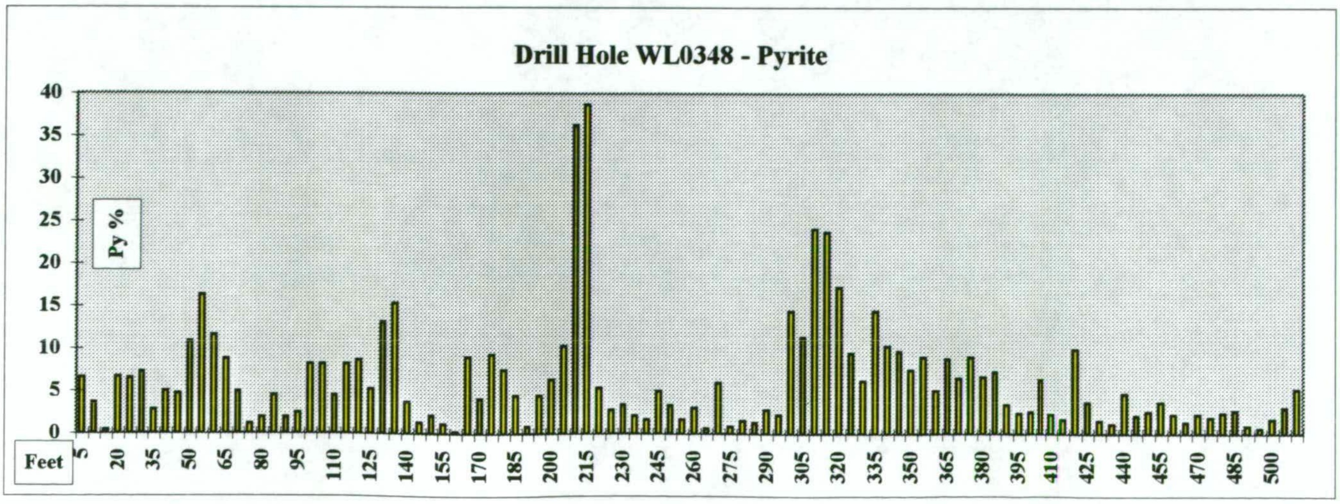
Drill Hole WL0348 - Pyrite
Py %
Feet

Project: Royal Tharsis Alteration **Location:** Royal Tharsis orebody **Hole Number:** WL0348

Major			Minor			Lithology				Alteration		Mineralisation						Structure & Veining			
From (m)	To (m)	Code	From	To	Code	Colour	Gr. Size	Texture	Description	Code	Description	Py %	Style	Cp %	Style	%	%	Depth (m)	Code	Angle	Description
0.00	9.14	Lqzse				gegy	fg		Strongly developed segregation texture gradational 0-10 m (30ft).	qzsech		7	ds					1.8	fo	70	
9.14	13.72	Lqzse				gy	cg		Moderately siliceous. Pseudo - fragmental. Minor hydromica. Occasional chalcedoric fragments.	qzsech		3	ds					10.4	fo	70	
13.72	18.29	Lqzse				gy	cg		Zone of intense carbonate alteration.	qzsecb		12	ds								
18.29	26.82	Lqz(se)				ltgy	fg		Strongly recrystallised and highly siliceous. Swirling layers of micas. Gradational basal contact.	qzse		5	ds					21.3	fo	65	
26.82	29.87	Lqz(se)				gegy	cg		Phyllic minerals in clots and segregations. Gradual merging to sericite - chlorite schist. Granular. Possible fine disseminated haematite.	qzsech		5	ds								
29.87	40.92	Lqzse				pkgy	mg		Sharp upper contact. Coarse fragmentals (fractured acid lava) - variable texture.	qzsehm	Weak-moderate	8	ds					32.3	fo	70	
40.92	82.91	Lqzse				gyge			Impersistent chlorite, with sharp intercalations of pkgy Lqzse-hm (chloritic tuffs). Tuffaceous from 46.3m (152ft) - ?lithic lapilli. Rock fragments stretched parallel to schistosity. Grades basally into lithic tuffs with intercalated acidic lavas.	qzsech		4	ds					47.5	fo	70	
			40.92	44.81	Vqzsd				Zone of veins up to 1m (2 - 3 ft) thick.			2	ds					57.0	fo	85	
82.91	114.00	Lqzse				gepk	fgmg		Variably brecciated (intense to moderate) lavas with intercalated lithic tuffs over the lower portion of the unit. Local siderite veinlets with stringers and patches of cp.	qzsehm	Moderate	7	ds	<1				68.6	fo	80	
114.00	134.42	Lqzch				gegy	mg	cd	Clots of chlorite developing amongst silica and becoming more pervasive down hole. Brecciated acidic lavas.	secbsd	Strong as concordant stringers and blebs	4	ds	2				96.0	fo	85	
134.42	151.49	Lqzse				gy	mg		Acid lava interfingering with crystal lithic tuff(s). Chlorite decreases markedly and variable/erratically, generally down the unit, texture similar. Becomes more siliceous down hole.	secbsd	Abundant concordant stringers and blebs	3	ds	1				109.1	fo	85	
			142.65	142.70	Vqz			fx	Massive light purple quartz, vein or lava? ?fault?									141.1	fo	75	
			147.85	147.90	Vqz			fx	Massive light purple quartz, vein or lava? ?fault?					1							
151.49	158.12	Ost							Coarse red sandstone (?Newton Creek Sandstone). Transitional upper contact, possibly from a lithic crystal tuff. Basally transitional into brecciated rhyolite with trace cp			1	ds	<1							
158.12	159.72	Oct							Purple pebble conglomerate (?Sedgwick Conglomerate?)												
	EoH																				

Geologist: W.J.D.Godsall **Date:** 4/01/97 **Page** 1 **of** 1

Project	Royal Tharsis Alteration	**Hole Number**	WL0609
Prospect	Royal Tharsis	**Section/s**	8010N
Tenement	1M/95	**COLLAR INFORMATION 315GRL GRID**	
Original Log By	P.B.Hills	**North**	7996
		East	3663
Date	1985	**RL**	2069
		Azimuth	113
Summary Log By	W.J.D.Godsall	**Inclination**	11
Method	Re-log	**Hole Length (m)**	207.00
		Hole Length (ft)	
Date	12/01/97	**(if applicable)**	

Summary Log

From	To	Code	Description	Py%	Cp%	Depth	Code	Angle
0.00	62.70	Lqzse(py)	Irregular quartz siderite veinlets	2		3.0	fo	70
62.70	71.30	Lqzsech	Gradational	4		27.0	fo	70
71.30	95.70	Lqzse(ch)	Veined	4	tr	40.0	fo	75
95.70	111.60	Lqzsese(hm)(si)-sh	Siliceous and haematitic	4	tr	43.5	fo	80
111.60	117.70	Lqzch(se)	Low sulphide content	1		59.0	fo	65
117.70	123.20	Lqzsesi	Fragmental and brecciated	12		66.0	fo	55
123.20	129.60	Lqzch(se)	Haematitic alteration	2		74.0	fo	60
129.60	162.00	Lqzsehm	Massive	10	2	88.5	fo	70
162.00	170.00	Lqzse(hm)-fl	Locally fragmental	6	3	101.8	fo	70
170.00	187.80	Lqzsechsd	Granular texture	4	6	117.5	fo	65
187.80	204.20	Lqzchse-Fgl	Possibly Great Lyell fault zone	4	4	123.0	fo	60
204.20	207.00	Oct	Sharp contact			127.0	fo	65
						155.0	fo	80
						164.0	fo	80
						168.0	fo	65
						204.0	S0	80

Abbreviations: na - not available, ne- no entry, nd - not determined, no - not observed, fo - foliation, co - contact, S0 - bedding, Tr - trace

Significant Intersections

From	To	m	Description	Cu%	Au ppm	Ag ppm	Py%
168.0	196.0	28.0	Lqzse(hm)(sd) - fl and Fgl	2.05	0.75	1.9	5.02
168.0	204.0	36.0	Lqzse(hm)(sd) - fl and Fgl	1.70	0.63	1.897	4.62

Hole Purpose and Result

Drilled to test Royal Tharsis mineralisation at 2100RL.

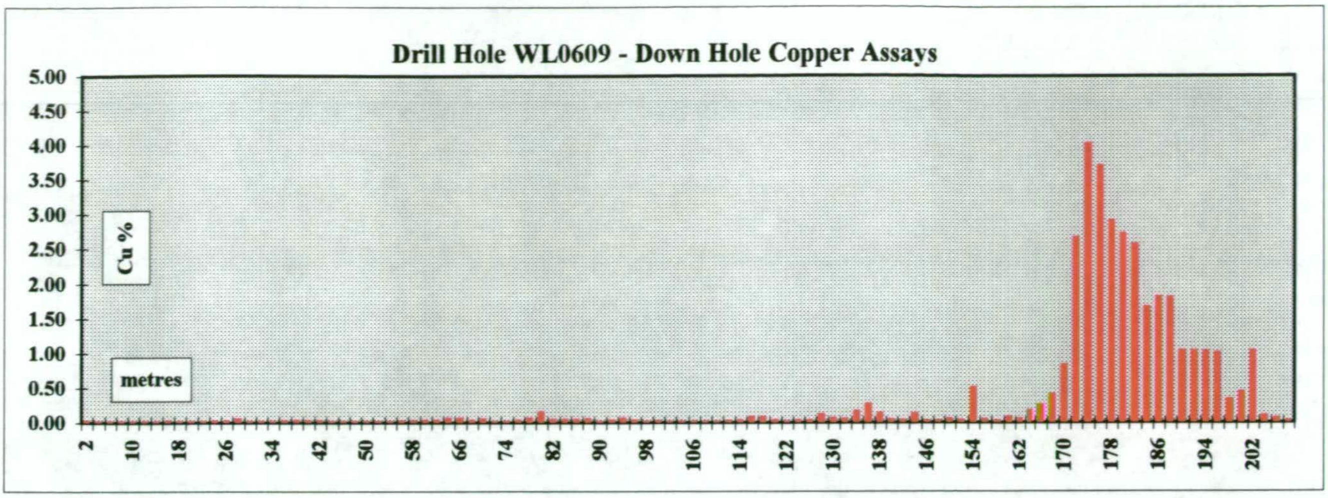
Drill Hole WL0609 - Down Hole Copper Assays
Cu %
metres
5.00
4.50
4.00
3.50
3.00
2.50
2.00
1.50
1.00
0.50
0.00
2
10
18
26
34
42
50
58
66
74
82
90
98
106
114
122
130
138
146
154
162
170
178
186
194
202

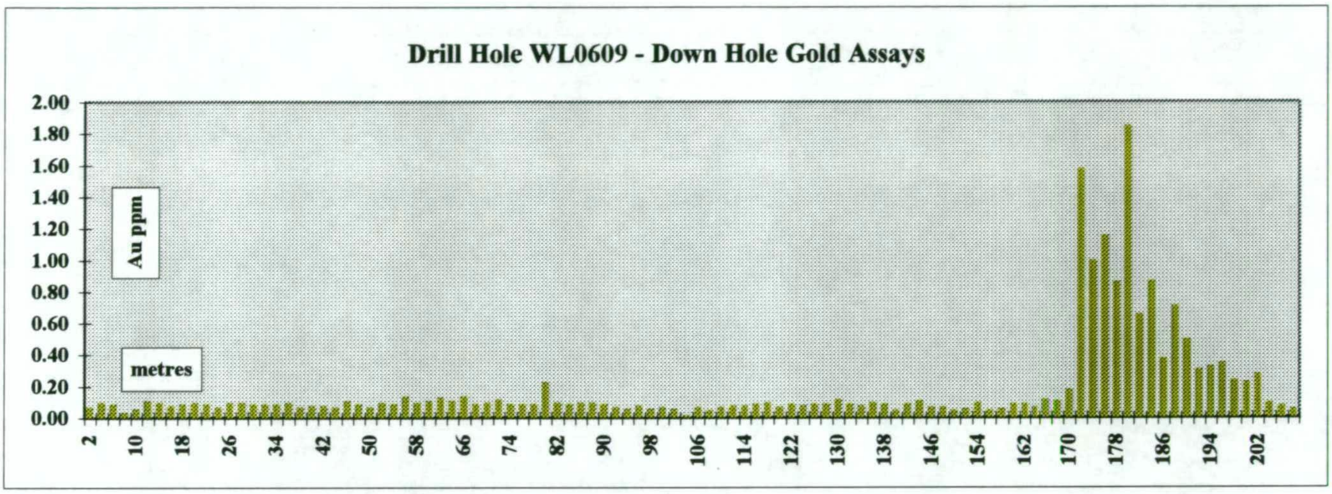
Drill Hole WL0609 - Down Hole Gold Assays
Au ppm
metres
2.00
1.80
1.60
1.40
1.20
1.00
0.80
0.60
0.40
0.20
0.00
2
10
18
26
34
42
50
58
66
74
82
90
98
106
114
122
130
138
146
154
162
170
178
186
194
202

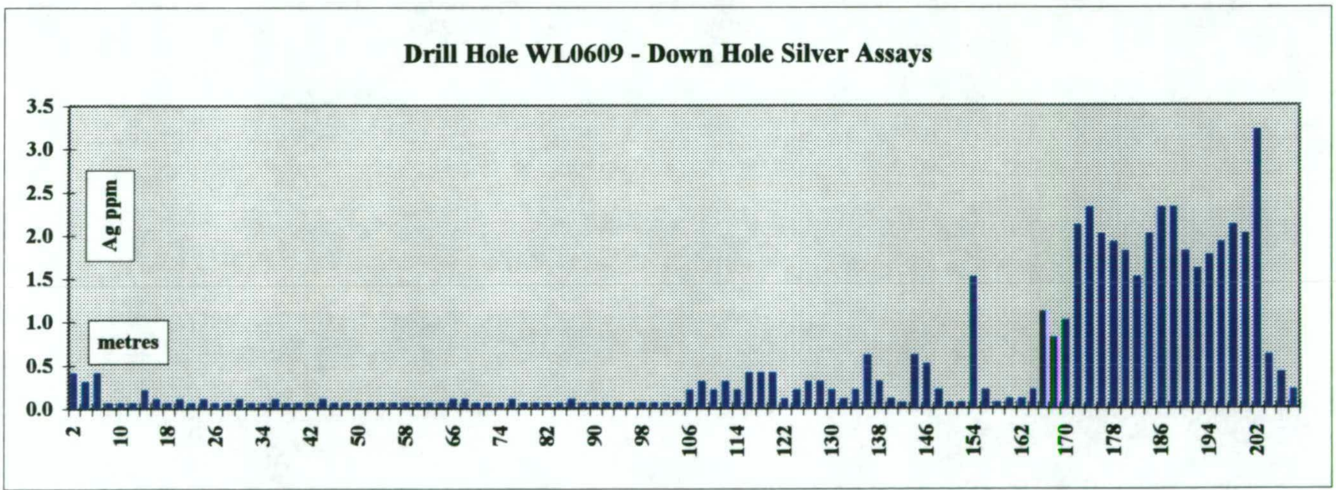
Drill Hole WL0609 - Down Hole Silver Assays
Ag ppm
metres
3.5
3.0
2.5
2.0
1.5
1.0
0.5
0.0
2
10
18
26
34
42
50
58
66
74
82
90
98
106
114
122
130
138
146
154
162
170
178
186
194
202

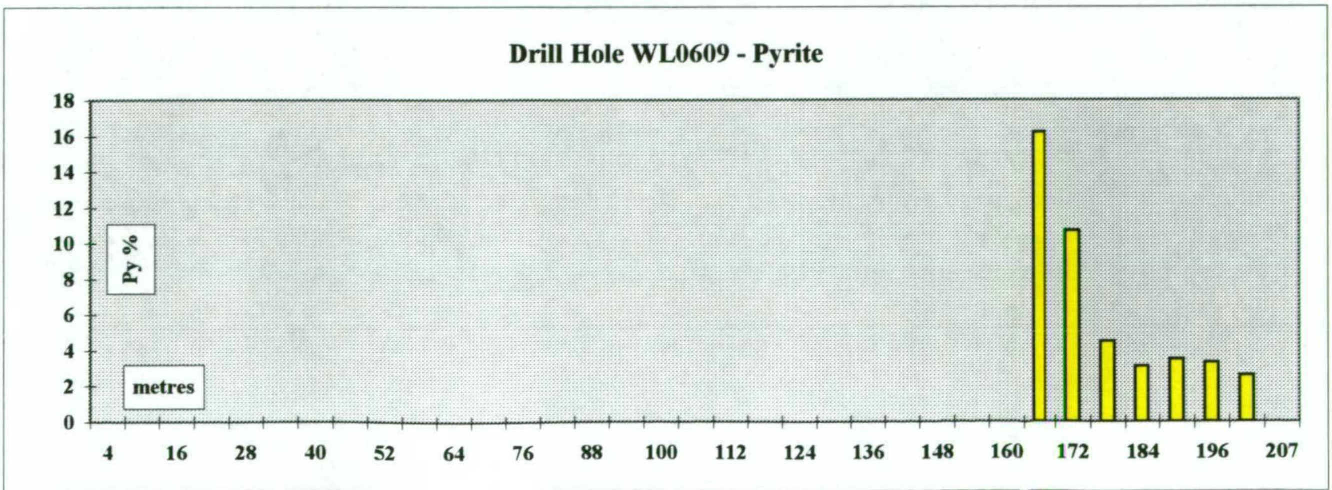
Drill Hole WL0609 - Pyrite
Py %
metres
18
16
14
12
10
8
6
4
2
0
4
16
28
40
52
64
76
88
100
112
124
136
148
160
172
184
196
207

Project: Royal Tharsis Alteration **Location:** Royal Tharsis orebody **Hole Number:** WL0609

Major			Minor			Lithology				Alteration		Mineralisation						Structure & Veining			
From (m)	To (m)	Code	From (m)	To (m)	Code	Colour	Gr. Size	Texture	Description	Code	Description	Py %	Style	Cp %	Style	%	%	Depth (m)	Code	Angle	Description
0.00	62.70	Lqzse				gy	mg		Generally uniform becoming slightly coarser down the unit. Locally chloritic. Most fracture faces somewhat puggy. Irregular veinlets of quartz and quartz siderite.	qzse	Pervasive	2	ds								
			0.00	1.20	Lqzse	gy	mg	sh	Broken core - possibly due to collar position.	qzse		2	ds								
			1.20	4.90	Lsech	gybr	mg	bn	Grey becoming locally brownish and weakly banded/foliated. Local vein stringers. Disseminated sulphides. Occasionally banded.	sese	Weakly chloritic and sideritic. Faint dusting hematite.	3	ds	<1	bb			3	fo	70	
			4.90	10.00	Vqz(sd)				Massive white quartz with blebs/stringers of brown siderite and with intermixed irregular chlorite. Ground generally incompetent.			3	mv								
			10.00	28.50	Lqzse	gywh	mg	bn	Locally chloritic. Irregular quartz and quartz siderite veinlets.	qzse		3	bb					27	fo	70	
			28.50	31.50	Lqzse	gy	fg	fl	Heavily broken core with prominent clay and pug.	qzse		2	ds								
			31.50	42.70	Lqzse	gy	mg	bn	As per major unit but more variable with a slightly more significant chlorite content occurring as clots and localised bands. Occasional vein, locally sideritic.	se(ch)	Locally chlorite.	1	ds					40	fo	75	
			42.70	44.20	Lqzch	gegy	fg		Dark greyish green, almost "argillaceous" in appearance, with possible faint/weak sigmoidal foliation. Irregular larger quartz clasts.	ch(se)	Pervasive	1	ds					43.5	fo	80	
			44.20	62.70	Lqzse	whgy	mg	mv	Massive greyish white with distinctive yellowish sericite. Pyrite as blebs, disseminations and coatings along schistosity planes. Minor local chlorite content.	qzse	Pervasive.	5	ds					59	fo	65	
62.70	71.30	Lqzse				gy	fg		Mixed Lqzse and Lqzch. Tending to be massive with lighter brown gradational units and occasional quartz vein, locally vuggy. Irregular siderite stringers. Fragmental and clastic at 68.7m.	sech	Pervasive	4	ds					66	fo	55	
			68.20	68.40	Ffg				Pug/clay												
71.30	95.70	Lqzse				gy	fg	mv	Minor Lqzch. Generally fine grained throughout with ubiquitous quartz siderite veinlets. Variable chlorite content which frequently imparts a darker colouration. Sulphide mineralisation tends to be banded rather than disseminated.	se(ch)	Pervasive	4	bn	<1	ds			74	fo	60	
			76.60	76.70	Ffg				Pug/clay									88.5	fo	70	
95.70	111.60	Lqzse				gypi	fg	sh	Pinkish gey fine grained siliceous with minor amounts of chlorite which impart a greenish colouration. From 106 metres ground becomes sheared and core heavily broken. Siliceous and sheared.	se(hm)	Pink colouration due to pervasive hm.	4	ds	<1	ds			101.8	fo	70	
111.60	117.70	Lqzch				gegy	fg		Minor Lqzse. Dominantly chloritic unit grading into sericitic units and with irregular veining. Sulphides generally low/absent in chloritic units.	ch(se)		1	ds								
			111.60	113.00	Lqzch	ge	mg		Uniform rock type with minor patches of siderite throughout.	qzch	Impregnated.	1	ds								
			113.00	113.40	Lqzse	gywh	mg	fl	Rapid transition/relatively sharp contact, minor Lqzse(ch).	se(ch)		5	ba								
			113.40	116.20	Vqz				Brittle and incompetent with intermixed chlorite.			3	mv								
			116.20	117.70	Lqzch				Similar to 111.6m - 113.0m but with a minor sericite content. Sulphides associated with sericitic phases.	ch(se)		8	ba					117.5	fo	65	
117.70	123.20	Lqzse				gy	mg	sh	Core moderately to heavily broken - pug in places. Locally fragmental and brecciated. Disseminations and bands of sulphide, locally massive/indurated and leached.	sise	Pervasive.	12	ds					123	fo	60	
123.20	129.60	Lqzch				gegy	mg		Pinkish through the middle of the unit. Stringers of siderite throughout. Heavily fractured towards the base of the unit. Locally pitted. Minor Lqzse(ch)	ch(se)	Local hm alteration.	2	ds					127	fo	65	
129.60	162.00	Lqzse				pi	cg	pr	Generally massive unit that is prominently pink due to ? haematite alteration. Localised sericite bands/veinlets and minor chlorite, usually as coatings along fractures. Locally fractured with minor fault/shear planes.	sehm	Weakly chloritic.	10	ds	2	ds			155	fo	80	

Geologist: W.J.D.Godsall **Date:** 12/01/97 **Page** 1 **of** 2

Project: Royal Tharsis Alteration **Location:** Royal Tharsis orebody **Hole Number:** WL0609

Major			Minor			Lithology				Alteration		Mineralisation						Structure & Veining			
From (m)	To (m)	Code	From (m)	To (m)	Code	Colour	Gr. Size	Texture	Description	Code	Description	Py %	Style	Cp %	Style	%	%	Depth (m)	Code	Angle	Description
162.00	170.00	Lqzse				pi	cg	pr	As for 129.6m - 162.0m but becoming more heavily sheared and faulted and with a less significant pink ? haematite content. Locally fragmental. Minor siderite content.	se(hm)		6	ds	3	ds			164	fo	80	
170.00	187.80	Lqzse					mg	pr	Grey to green to yellow to grey with a uniform granular texture. Occasional vein stringers. Prominent carbonate alteration.	sechsd		4	ds	6	ds			168	fo	65	
			183.50	184.80	Ffl				Gouge/pug.												
187.80	204.20	Lqzch						Fgl	Lithologically transitional with unit from 170.0m - 187.8m but with chlorite becoming dominant over sericite which becomes insignificant basally. Generally heavily broken core - fractured, sheared and faulted. Possibly GLF zone.	ch(se)		4	ds	4	ds			204	fo	80	
204.20	207.00	Oct							Typical Owen Conglomerate with subangular clasts and quartz fragments in a fine grained chloritic and haematitic matrix. Localised chloritic alteration rims/fronts. Generally competent. Sharp contact.												
	EoH																				

Geologist: W.Godsall **Date:** 12/01/97 Page 2 of 2

Project	Royal Tharsis Alteration	**Hole Number**	WL0290
Prospect	Royal Tharsis	**Section/s**	8070N
Tenement	1M/95	**COLLAR INFORMATION 315GRL GRID**	
Original Log By	M.J.McDonald	**North**	8046
		East	4096
Date	1968	**RL**	2482
		Azimuth	090
Summary Log By	W.J.D.Godsall	**Inclination**	-04
Method	Re-log	**Hole Length (m)**	30.78
		Hole Length (ft) (if applicable)	101
Date	15/02/97		

Summary Log

From	To	Code	Description	Py%	Cp%	Depth	Code	Angle
0.00	6.10	Lqzse(py)	Coarse grained	6		5.2	fo	70
6.10	15.24	Lqzchsepy	Fragmental. Haematitic	10	2	27.4	fo	70
15.24	30.78	Lqzse(py)	Felsic	7	1			

Abbreviations: na - not available, ne- no entry, nd - not determined, no - not observed, fo - foliation, co - contact, S0 - bedding, Tr - trace

Significant Intersections

From	To	m	Description	Cu%	Au ppm	Ag ppm	Py%
7.6	16.8	9.1	Lqzchse	0.58	-	-	10.2
9.1	15.2	6.1	Lqzchse	0.69	-	-	11.3
			Hole ends in mineralisation.				
			Average SG = 2.96 (10 * 6 metre composite samples)				

Hole Purpose and Result

Drilled to test for remnant ore in Royal Tharsis batter.
Hole stopped/completed in sulphide mineralisation.

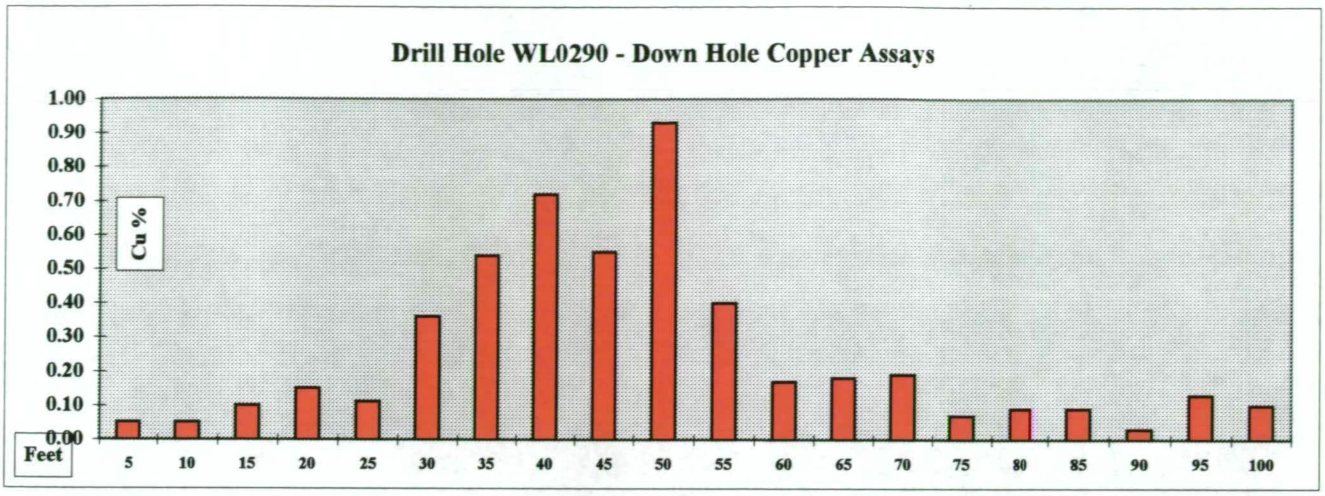
Drill Hole WL0290 - Down Hole Copper Assays
Cu %
1.00
0.90
0.80
0.70
0.60
0.50
0.40
0.30
0.20
0.10
0.00
Feet
5
10
15
20
25
30
35
40
45
50
55
60
65
70
75
80
85
90
95
100

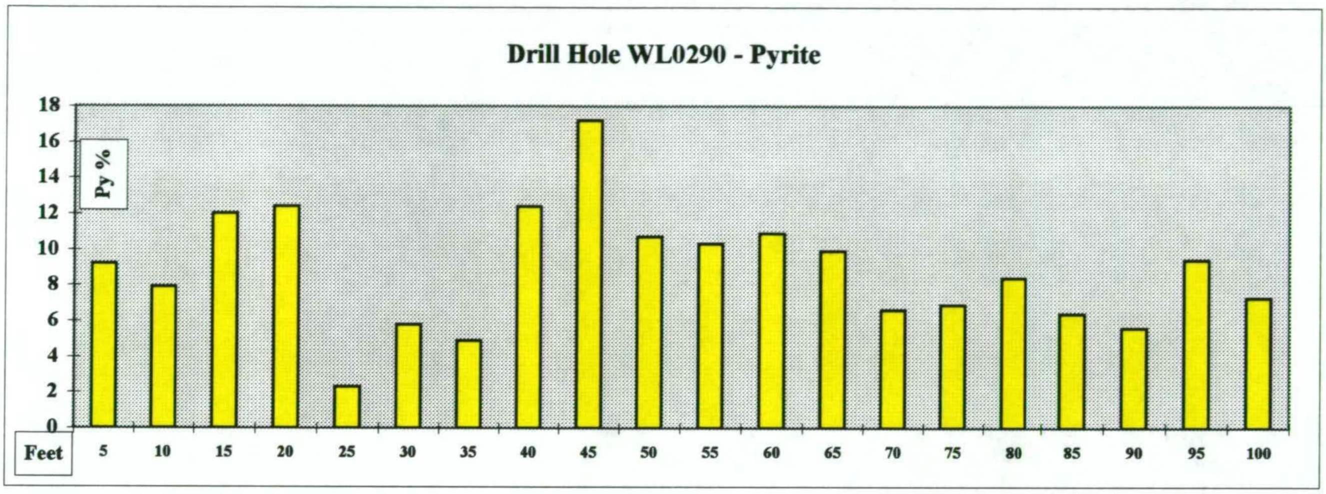
Drill Hole WL0290 - Pyrite
Py %
18
16
14
12
10
8
6
4
2
0
Feet
5
10
15
20
25
30
35
40
45
50
55
60
65
70
75
80
85
90
95
100

Project: Royal Tharsis Alteration **Location:** footwall of Royal Tharsis orebody **Hole Number:** WL0290

Major			Minor			Lithology				Alteration		Mineralisation						Structure & Veining			
From	To	Code	From	To	Code	Colour	Gr. Size	Texture	Description	Code	Description	Py %	Style	Cp %	Style	%	%	Depth (m)	Code	Angle	Description
0.00	6.10	Lqzse				gy	mg		Medium to coarse grained quartz sericite schist. Py as coarse blebs and disseminations. Negligible cp.	qzse	Pervasive	6	ds	<1				5.2	fo	70	
6.10	15.24	Lqzch	6.10	15.24	Lqzse	gygn	cg		Coarsely mottled. Chlorite occurs as clots/lathes as well as being pervasive. At 10.67m (35ft) sharp contact between schist and fragmental material. From 13.4 metres (44ft) significant fine haematite in the chlorite. Cp in comb-textured veining.	chsehm	Pervasive	10	ds	2							
15.24	30.78	Lqzse				pkgy	mg		Coarse grained quartz sericite schist with minor traces chlorite. Very uneven texture, becoming medium grained from 21.34 metres (70ft). Dominantly felsic.	qzse	Pervasive	7	ds	1	bb			27.4	fo	70	
	EoH																				

Geologist: W.J.D.Godsall **Date:** 15/02/97 **Page** 1 **of** 1

2.2 Lithological Descriptors

2.2.5 Sedimentary

Sak	arkose	Sdl	dolomite	Ssh	shale
Sif	bif	Sgw	greywacke	Ssl	siltstone
Sbx	breccia	Sij	jaspilite	Spg	spongolite
Scs	carbonaceous shale	Sls	limestone	Stl	tillite
Sch	chert	Sms	mudstone		
Scl	claystone	Sqt	quartzite		
Sct	conglomerate	Sst	sandstone		

2.2.6 Metamorphic

Mad	meta acid rock undifferentiated
Mis	meta intermediate rock undifferentiated
Mub	meta ultrabasic rock undifferentiated

Msa	slate	Mgl	granulite
Mls	marble	Mhb	homblendite
Mam	amphibolite	Mhf	hornfels
Mfd	freddite	Mme	migmatite
Mgn	gneiss	Mpi	phyllite
		Mqt	quartzite

When protolith is known M, may replace primary descriptor eg Mvt meta tholeite

2.2.6.1 Tectonites

Fbr	breccia
Fct	cataclasite
Ffl	fault
Ffz	fault zone
Ffg	fault gouge
Fmy	mylonite
Fpm	protomylonite
Fsn	shear zone
Ffx	Zone of strong fracturing (core)
Fgl	Great Lyell Fault Zone

2.2.6.2 Metamorphic Facies

zeolite
albite-epidote hornfels
hornblende hornfels
pyroxene hornfels
sanidinite

prehnite-pumpellyite
glaucophane
eclogite

greenschist ch-ab-ep-mu-ca-ac
amphibolite
granulite

2.2.6.3 Alteration Facies

pp	propylitic	cb-ch+/-se
ch	chloritic	ch dominant +/- se, sd <5%
se	sericitic	se dominant +/- se, sd <5%
pc	phyllic	qz-se-py +/-sd
si	silicified	si dominant +/- se, ch, sd
ar	argillic	ka / sk +/- se, ch, hm, ba
aa	advanced argillic	pz / ka / at +/- se, ch, hm, ba
kp	potassic	af / bt +/-se, ch, co

2.2 Lithological Descriptors (cont'd)

2.2.7 Secondary Lithological Descriptors - Minerals & Alteration

ac	actinolite	fl	fluorite	pl	plagioclase
ad	adularia	fu	fuchsite	pe	prehnite
ab	albite			py	pyrite
af	alkali feldspar	gh	gahnite	pz	pyrophyllite
at	altered	ga	galena	px	pyroxene
al	aluminous	gt	garnet	po	pyrrhotite
an	alunite	go	geothite		
am	amphibole	au	gold	qz	quartz
aa	andalusite	gf	graphite	qc	quartz-carbonate
nh	anhydrite	gu	grunerite	qf	quartzo-feldspathic
ak	ankerite	gp	gypsum	qn	quartz-tourmaline
ay	anthophyllite				
ai	apatite	hm	haematite	rh	rhodocrosite
as	arsenopyrite	hs	haematite, spec.	rb	riebeckite
ao	asbestos	hb	hornblende		
az	azurite				
		il	illite	sa	saussurite
ba	barite			sx	scheelite
be	beryl	ja	jarosite	se	sericite
bt	biotite			sp	serpentine
bi	bismuth	ka	kaolin	sd	siderite
bm	black mineral	ky	kyanite	si	silica
bo	bornite			sm	sillimanite
		pb	lead	ag	silver
ca	calcite	le	lepidolite	sk	smecktite
cb	carbonate	lx	leucoxene	zs	sphalerite
cs	cassiterite	li	limonite	sn	stannite
ce	cerussite			st	staurolite
cd	chalcedony	mf	mafic minerals	sb	stibnite
cc	chalcocite	ms	magnesite	sf	sulphide
cp	chalcopyrite	mt	magnetite		
ch	chlorite	ma	malachite	tl	talc, talcose
ct	chloritoid	me	metasomatic	tt	tetrahedrite-tennantite
cr	chromite	mi	mica	tz	topaz
co	chrysoprase	mw	mica - white	tn	tourmaline
cy	chrysotile	mg	mica - green	tm	tremolite
cl	clay	mx	mica - mixed		
cx	clinopyroxene	mn	minerals (gen)	ur	uraninite
cu	copper	mo	molybdenite	uo	uranium
cj	cordierite	mm	montmorillonite	up	uranophane
cv	covellite	mu	muscovite		
cm	cummingtonite			vl	violarite
		ol	olivine		
di	diopside	ox	orthopyroxene	zn	zinc
do	dolomite			zw	zinnwaldite
		pn	pentlandite		
ep	epidote	pu	phlogopite		
		ph	phosphate		
fd	feldspar	pc	phyllic		
fe	ferruginous	pi	pitchbiende		

3 Tertiary Descriptors - Texture, Structure & General Descriptors

ac	acicular
ag	agglomerate
am	amorphous
yg	amygdaliodal
ah	anhedral
ha	aphanitic
ap	apiltic
ar	arenose
ae	augen structure
ax	autoclastic
bn	banded
bd	bedded
s0	bedding, primary banding
bl	bladed
bh	bleached
bb	blebby
by	blocky
bo	botryoidal
bu	boudinaged
bx	breccia, brecciated
ch	chalcedonic
cs	clast supported
cl	clastic
s1	cleavage
cf	closed framework
cd	clotted
cg	coarse grained
cf	cobbles
xd	compact
cn	conchoidal
cv	concretionary
ct	conglomeratic
cw	contact - chilled
co	contact - general
cx	contact - imbricated
cy	contact - sheared
cz	contact - transitional
cb	core to bedding angle
ca	core to schistosity angle
xa	crenulated/folded
xb	cross bedded
xc	cumulate
de	deformed
ds	disseminated
dr	drusy
dp	damp
el	elongated
eg	equigranular
eu	euhedral
et	eutaxitic
fg	fine grained
fi	fissile
fy	flaggy
ff	flame structure
fb	flow banded
fl	fluidal
fo	foliated
f1	foliation - very weak, massive
f2	foliation - weak
f3	foliation - moderate
f4	foliation - strong
f5	foliation - very strong
fs	fossiliferous
fx	fractured
fr	fragmental
fh	fresh
gc	gneissic
go	gossanous
gb	graded bedding
gr	granitic
gb	granoblastic
gp	granophyric
gs	greasy
ht	heterogeneous
ho	homogeneous
hc	honeycomb
hy	hyaloclastite/ic
hz	hybridized
ig	ignimbrite
ic	inclusions
id	indurated
ib	interbedded
it	intercalated
in	interstitial
jp	jasperoidal
jo	jointed
ka	karsted/ic
kb	knobbly
kn	knotted
km	komatiitic
lm	laminated
le	leached
l0	lineation
l1	lineations (mineral)
l2	lineations (intersections)
ln	lenticular
lc	leucocratic
ll	lit par lit
lc	lithic
lp	lithophysae
lw	lower
mv	massive
mx	matrix
mp	matrix supported
mg	medium grained
ml	melanocratic
ms	mesocratic
mc	micro
mi	middle
me	migmatitic
mz	monomictic
mt	mottled
my	mylonitic
nb	nebulitic
nd	nodular
np	not preserved
oc	ocelli
oo	oolitic
oe	opaline
of	open framework
op	ophitic
ob	orbicular
ov	ovoid
pa	pallid
pv	partially preserved
pg	pegmatitic
pw	pillowed
ps	pisolitic
pt	pitted
pz	plasmic
pm	polymictic
pr	porphyritic
pp	porphyroblastic
qe	quartz eye
qg	quartz grains (in TOB etc)
qv	quartz veined
ra	radiating/stellate
re	recrystallized
rx	rock
rn	rounded

3 Tertiary Descriptors
(Texture, Structure & General Descriptors - cont'd)

r1	roundess - well rounded
r2	roundness - rounded
r3	roundess - subrounded
r4	roundess - subangular
r5	roundness - angular
r6	roundness - very angular
sc	schist, schistose
sz	schlieren
gn	segregated mineral texture
sh	shear/sheared
si	siliceous/silica flooded
sl	slatey
ss	slickensides
sf	soft
s1	sorting - very well
s2	sorting - well
s3	sorting - moderate
s4	sorting - poor
s5	sorting - very poor
sg	specific gravity
sx	spinifex texture
sv	spotted
sw	stockwork veined
sr	stringer
sf	strongly foliated
sl	stylolitic
es	subhedral
sa	sugary/sucrose
tb	tabular
th	tholeitic
ty	trachytic
tr	translucent
tf	tuffaceous
uf	uniform textured
va	variolitic
vv	varved
vn	veined
vm	vermiform
vi	vitric
vg	vuggy
wx	waxy
wd	weathered
w1	weathered - slight
w2	weathered - moderate
w3	weathered - strong
we	welded
wt	wet

4 Colour

bg	beige
bk	black
bl	blue
br	brown
bf	buff
cx	cream
fn	fawn
ge	green
gy	grey
kh	khaki
mv	mauve
oe	ochre
or	orange
pk	pink
pp	purple
rd	red
wh	white
ye	yellow

Value suffix (optional)

lt	light
md	medium
dk	dark

Appendix IV

Royal Tharsis

Petrological Samples

Summary of work commissioned by CMT and carried out by Consultant Petrologist, Dr J. Barron (Barron, 1997)

Appendix IV
Table 1

Petrology Samples

Sample Number	Drill hole	From (ft)	To (ft)	From (m)	To (m)	Coded Rock Description (for unit from which sample taken)
EXPA 3201	WL0290	14' 10"	15'			Lqzse(py)
EXPA 3202	WL0290	35'	35' 2"			Lqzchse(py)
EXPA 3203	WL0290	70' 6"	70' 8"			Lqzse(py)
EXPA 3204	WL0421			1.3	1.4	Lqzpych(mt) - specks hm
EXPA 3205	WL0421			27.2	27.3	Lqzse(py)(hm) - siliceous with carbonates
EXPA 3206	WL0421			36.4	36.5	Lqzse(py)(hm) - siliceous with carbonates
EXPA 3207	WL0421			59.7	59.8	Lqzchsehm(py)sicb - breccia'd lithic tuff
EXPA 3208	WL0106	69' 10"	70'			Lqzse siliceous
EXPA 3209	WL0106	312'	312' 2"			Lqzch - siliceous
EXPA 3210	WL0106	557' 9"	557' 11"			Lqzsepy - irregular clots ch
EXPA 3211	WL0106	640'	640' 2"			Lqzse - possible trace hm
EXPA 3212	WL0106	739' 6"	739' 9"			Lqzch - minor hm
EXPA 3213	WL0106	770'	770' 2"			Lqzsech
EXPA 3214	WL0106	919'	919' 3"			Lqzsech - se is minor, v.little (if any) ch
EXPA 3215	WL0106	951'	951' 2"			Lqzse - se is minor
EXPA 3216	WL0530A			49.9	50.0	Lqzsecb
EXPA 3217	WL0530A			75.0	75.1	Lqzse(cb) -fxvn
EXPA 3218	WL0530A			100.5	100.7	Ily - hm & py specks
EXPA 3219	WL0530A			134.4	134.5	Lqzsech(cb)
EXPA 3220	WL0530A			144.7	144.8	Vqz (chlorite-vein relationship)
EXPA 3221	WL0530A			179.7	179.8	Lqzch(se) - cb stringers
EXPA 3222	WL0530A			239.6	239.7	Lqzse - minor ch ?? albite ??
EXPA 3223	WL0530A			285.4	285.5	Lqzch
EXPA 3224	WL0530A			301.5	301.6	Lqzse (possible debris flow)
EXPA 3225	WL531			1.05	1.15	Lchsihm(cb)
EXPA 3226	WL531			9.9	10.0	Lqzsise
EXPA 3227	WL531			60.0	60.1	Lqzse(ch)(cb)
EXPA 3228	WL531			95.0	95.1	Lqzse(py)
EXPA 3229	WL480			145.0	145.1	Lqzsech (tuffaceous)
EXPA 3230	WL480			245.0	245.1	Lqzse

APPENDIX IV - CONTENTS

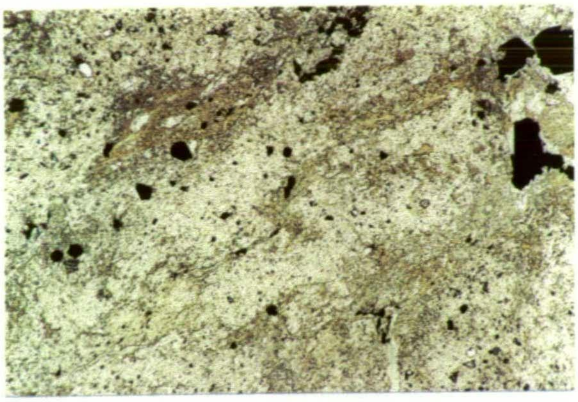

Figure 1
WL0290 EXPA3201 ppl, x 2.5
Altered fragmental (?brecciated) microporphyritic volcanic or shallow intrusive rock with some feldspathic fragments. Intensely altered to quartz-sericite assemblage and cut by quartz-(chlorite-barite) veins. Prismatic feldspar sites that define a "crowded" porphyritic texture.

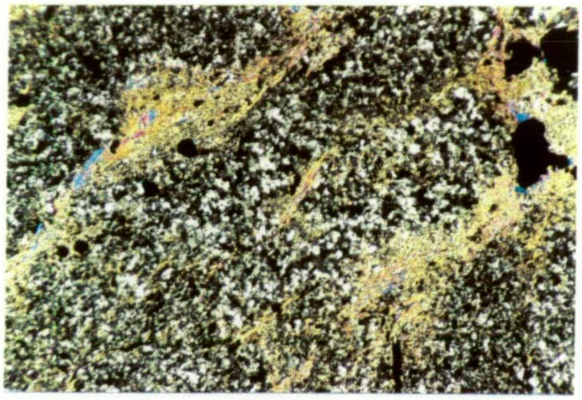

Figure 2
WL0290 EXPA3201 cpl, x 2.5
As for Figure 1 under crossed polarised light.

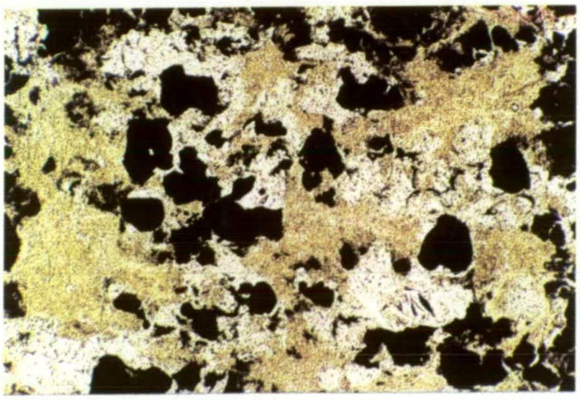

Figure 3
WL0290 EXPA3201 ppl, x 4
Possible prismatic feldspar crystal sites converted to pale brown smectite with colourless sericite in an altered (?brecciated) quartz microporphyritic volcanic or shallow intrusive rock that has been altered to a quartz-sericite assemblage.

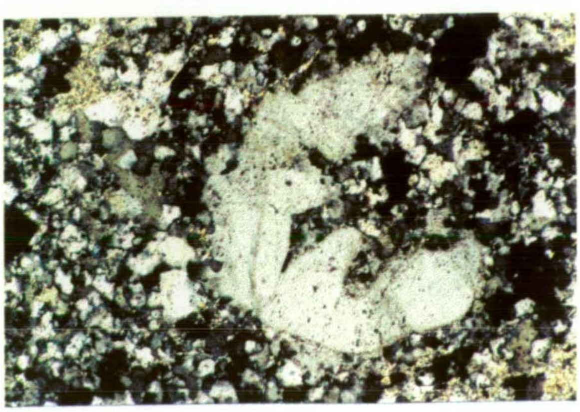

Figure 4
WL0290 EXPA3201 cpl, x 10
Strongly embayed subhedral quartz microphenocryst in an intensely altered quartz-sericite assemblage.

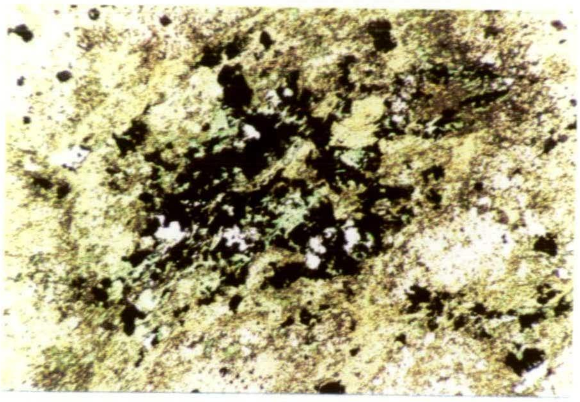

Figure 1
WL0290 EXPA3202 ppl, x 2.5
Poorly sorted lithic fragmental rock containing material from a quartz microporphyritic volcanic that is veined, deformed and altered to a quartz-sericite-chlorite-sulphide assemblage. Lithic fragment with poorly defined prismatic feldspar sites altered and converted largely to pyrite.

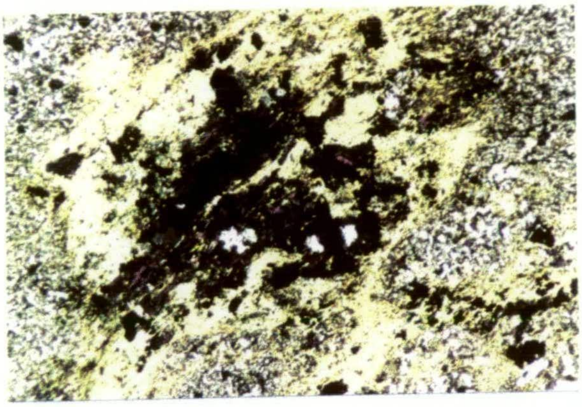

Figure 2
WL0290 EXPA3202 cpl, x 2.5
As for Figure 1 under crossed polarised light.

Figure 3
WL0290 EXPA3202 cpl, x 10
Embayed quartz microphenocryst partly resorbed in a granular quartz rich mosaic in an altered quartz-sericite-chlorite-sulphide assemblage, originating from a poorly sorted lithic fragmental rock.

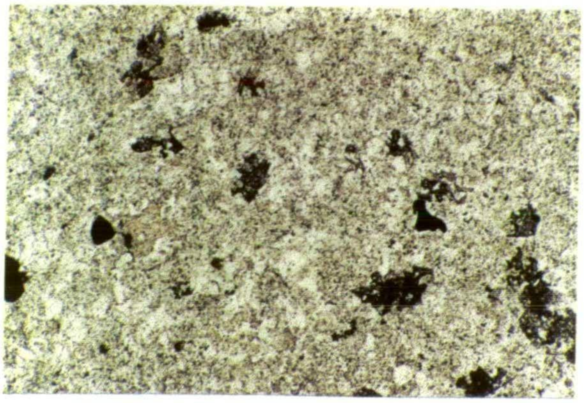

Figure 4
WL0290 EXPA3203 ppl, x 4
Finely recrystallised and foliated fragmental. Obliteration of primary textures to quartz-sericite-(carbonate) assemblage and containing abundant disseminated pyrite. Possible relict glass shard texture outlined by dusty haematite in granular quartz.

PLATE 3

Appendix IV

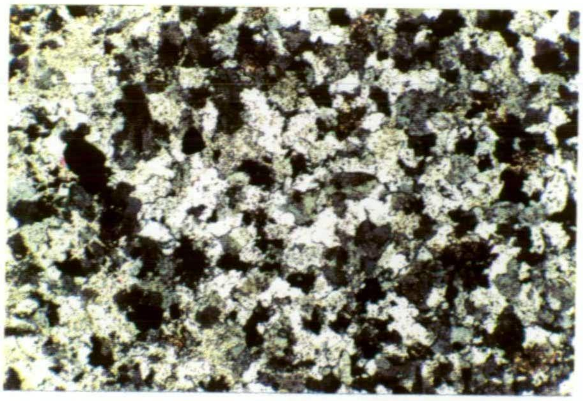

Figure 1
WL0290 EXPA3203 cpl, x 4
Finely recrystallised and foliated fragmental. Obliteration of primary textures, alteration to quartz-sericite-(carbonate) assemblage and containing abundant disseminated pyrite. Possible relict glass shard texture outlined by dusty haematite in granular quartz.

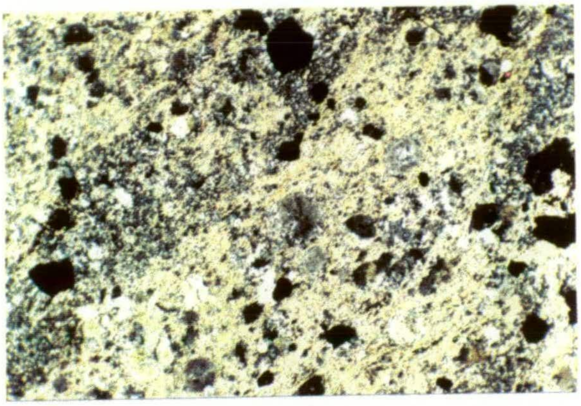

Figure 2
WL0290 EXPA3203 cpl, x 4
Possible glassy fragment with spherulitic quartz filled sites altered to quartz-sericite in a finely recrystallised and foliated fragmental. Abundant disseminated pyrite and alteration to quartz-sericite-(carbonate) assemblage has resulted in obliteration of primary textures.

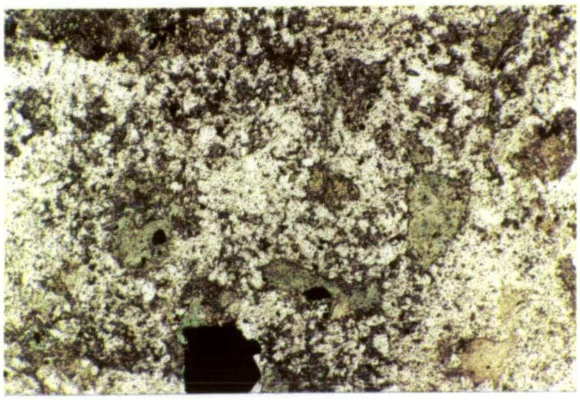

Figure 3
WL0421 EXPA3204 ppl, x 4
Partly fragmental porphyritic volcanic that has undergone intense and selective alteration to quartz-sericite-chlorite-carbonate-rutile assemblage with significant sulphide mineralisation. White feldspar and green mafic sites in a granular groundmass.

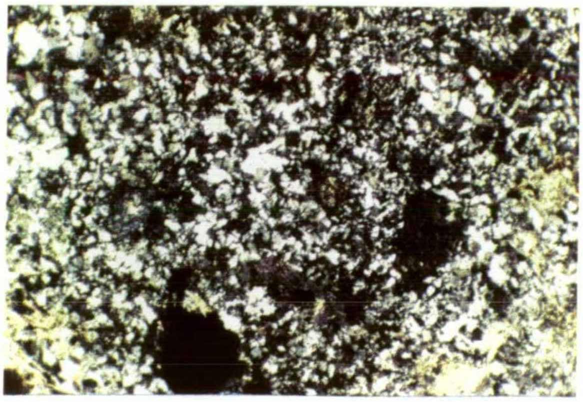

Figure 4
WL0421 EXPA3204 cpl, x 4
As for Figure 3 under crossed polarised light and showing some poor retention of textures.

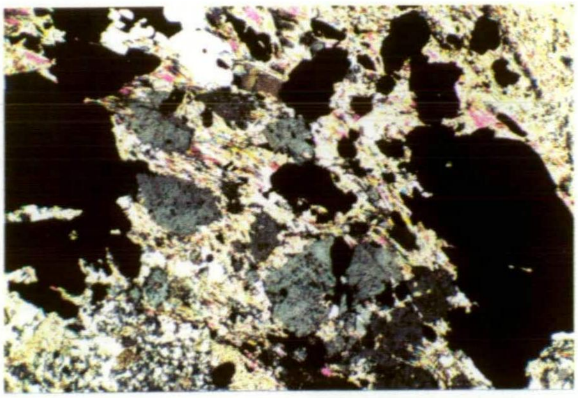

Figure 1
WL0421 EXPA3205 ppl, x 4
Intensely altered, well mineralised and strongly deformed volcaniclastic composed of a quartz-sericite-carbonate-apatite assemblage. Dark grey fractured apatite crystals set in a foliated sericite with pyrite and quartz.

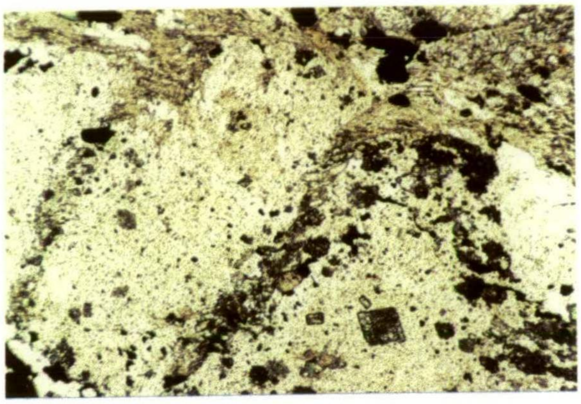

Figure 2
WL0421 EXPA3205 ppl, x 2.5
Granular quartz rich domains containing sparse carbonate rhombs in a strongly deformed volcaniclastic that is intensely altered.

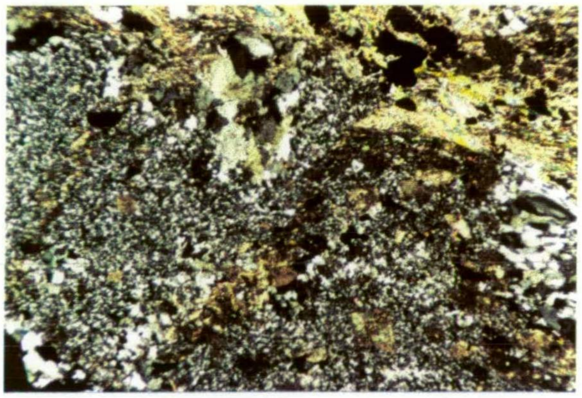

Figure 3
WL0421 EXPA3205 cpl, x 4
As for Figure 2 under crossed polarised light.

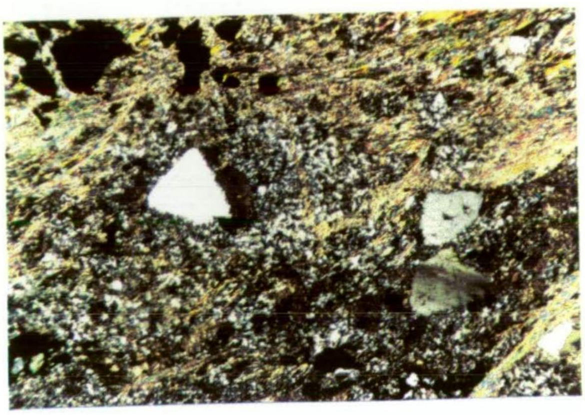

Figure 4
WL0421 EXPA3205 cpl, x 4
Crystals of once phenocrystic quartz in an intensely altered, well mineralised and strongly deformed volcaniclastic composed of a quartz-sericite-carbonate-apatite assemblage.

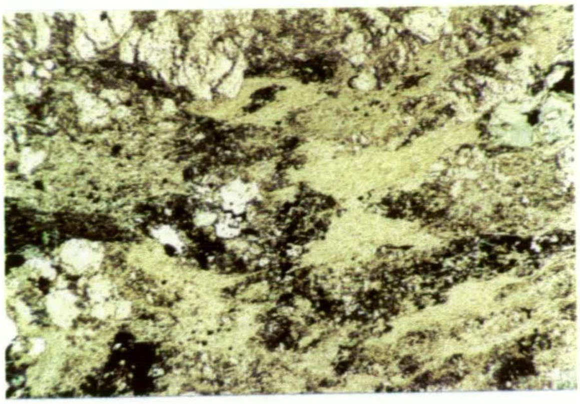

Figure 1
WL0421 EXPA3206 ppl, x 2.5
Finely recrystallised and foliated quartz-sericite-carbonate-chlorite schist that is well mineralised. Fragment containing deformed feldspar (sericite) and mafic (chlorite) sites with carbonate, chalcopyrite and pyrite.

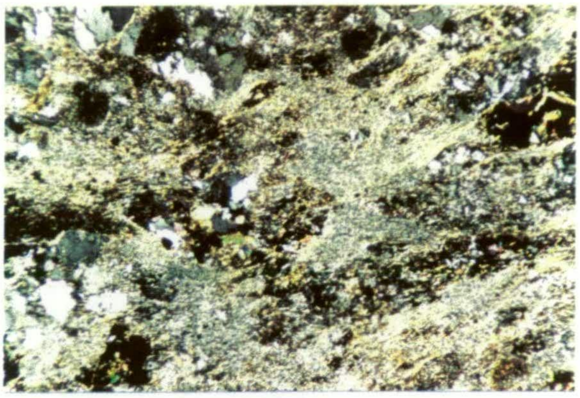

Figure 2
WL0421 EXPA3206 cpl, x 2.5
As for Figure 1 under crossed polarised light.

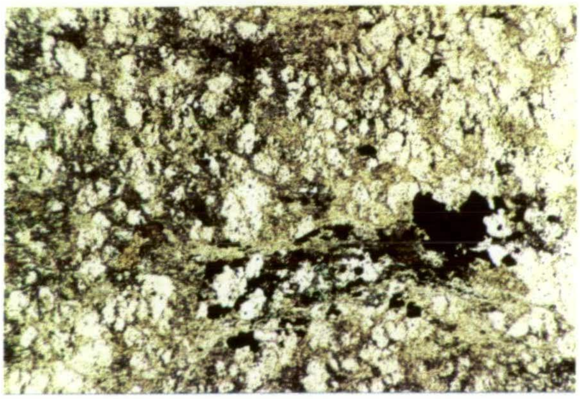

Figure 3
WL0421 EXPA3206 ppl, x 2.5
Tensional microfractures almost normal to the wavy foliation, in quartz rich domains in a finely recrystallised and foliated quartz-sericite-carbonate-chlorite schist that is well mineralised.

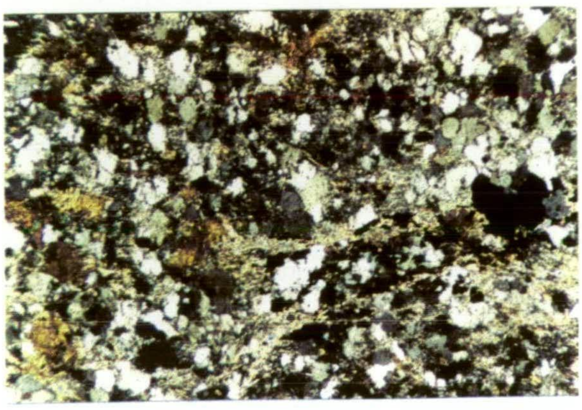

Figure 4
WL0421 EXPA3206 ppl, x 2.5
As for Figure 3 under crossed polarised light.

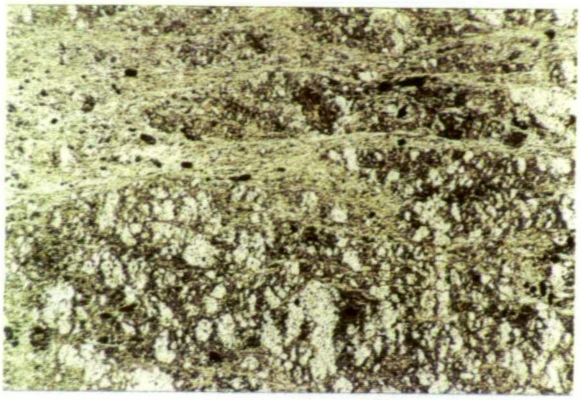

Figure 1
WL0421 EXPA3207 ppl, x 2.5
Finely recrystallised and well mineralised quartz-sericite-carbonate schist with no recognisable relict textures. Branching foliated domains and tensional microfractures in quartz rich domains.

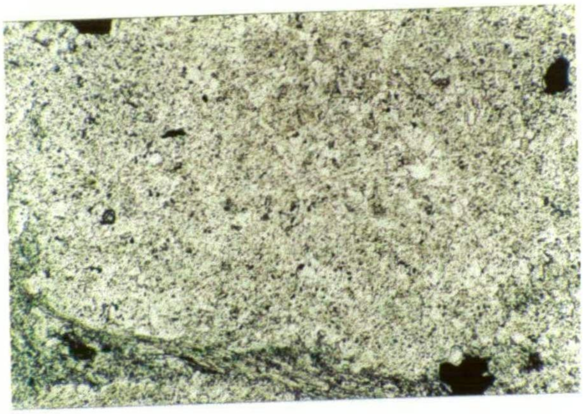

Figure 2
WL0421 EXPA3208 ppl, x 4
Lithic breccia that has been intensely and selectively altered to an assemblage of quartz-sericite and strongly pyrite mineralised. Possible glass shards in a granular quartz mosaic.

Figure 3
WL0421 EXPA3208 cpl, x 4
As for Figure 2 (different alignment) under crossed polarised light.

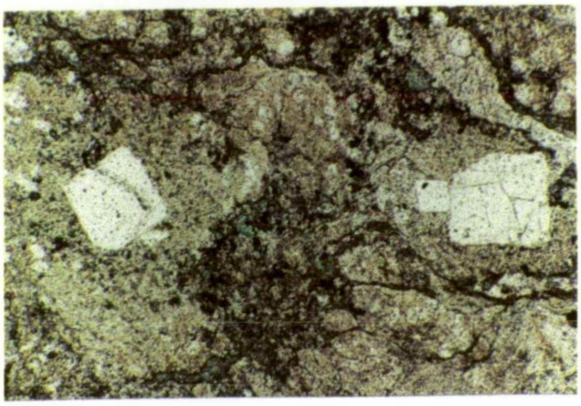

Figure 4
WL0106 EXPA3209 ppl, x 4
Autobrecciated volcanic flow strongly altered to quartz-sericite-(carbonate-chlorite) assemblage with sparsely disseminated pyrite. Acidic volcanic lithic fragments containing quartz microphenocrysts.

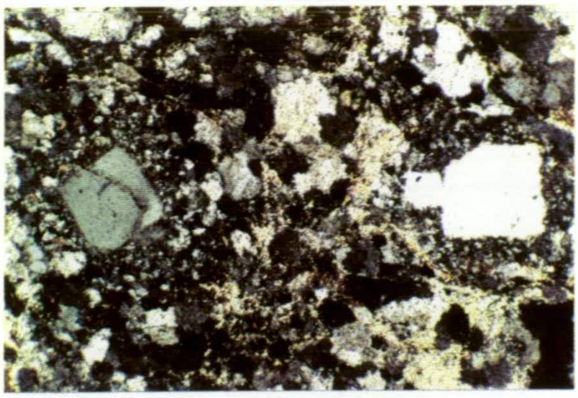

Figure 1
WL0106 EXPA3209 cpl, x 4
Autobrecciated volcanic flow strongly altered to quartz-sericite-(carbonate-chlorite) assemblage with sparsely disseminated pyrite. Acidic volcanic lithic fragments containing quartz microphenocrysts.

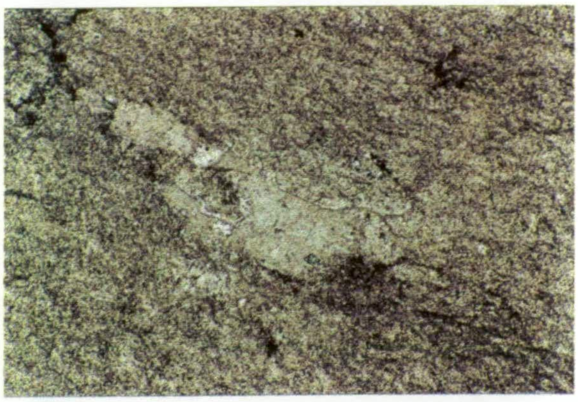

Figure 2
WL0106 EXPA3209 ppl, x 4
?tuffaceous fragment containing deformed felsic crystals altered to a sericitic assemblage in an autobrecciated volcanic flow that has been strongly altered to quartz-sericite-(carbonate-chlorite) assemblage.

Figure 3
WL0106 EXPA3209 cpl, x 4
As for Figure 2 under crossed polarised light.

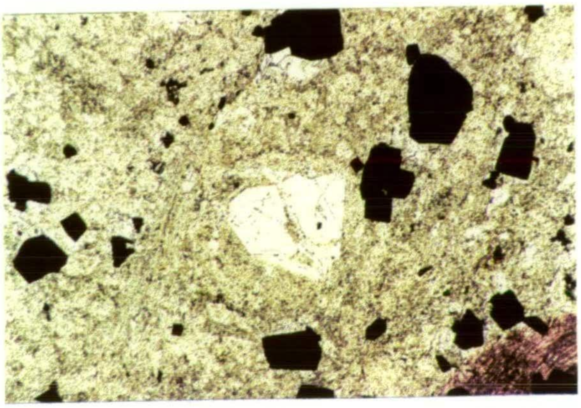

Figure 4
WL0106 EXPA3210 ppl, x 2.5
Unsorted fragmental, veined, foliated and altered to quartz-sericite-pyrite assemblage with traces of bornite-chalcocite-digenite and chalcopyrite. Fractured quartz phenocryst in silicified fragment.

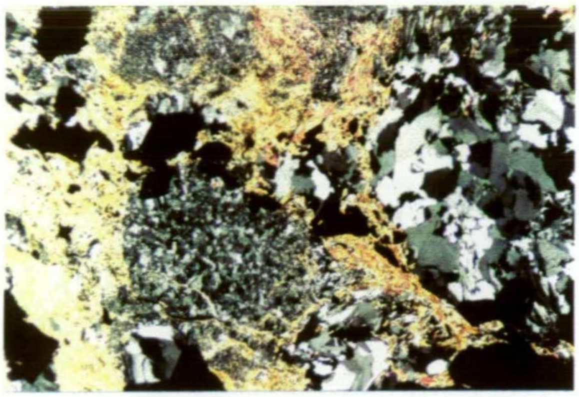

Figure 1
WL0106 EXPA3211 cpl, x 2.5
Tuffaceous rock that is intensely silicified, quartz-chlorite veined, hydrothermally brecciated, altered to quartz-sericite and strongly pyrite mineralised.

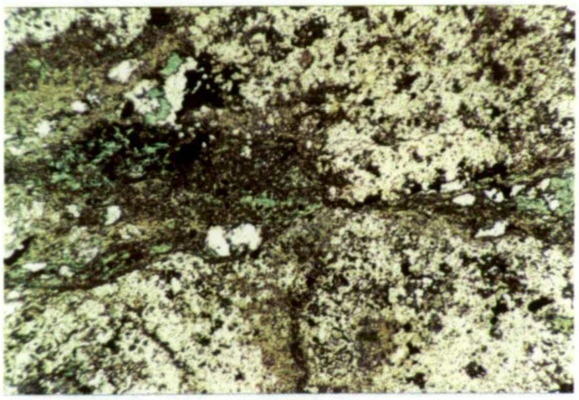

Figure 2
WL0106 EXPA3212 ppl, x 2.5
Deformed fine grained, granular quartz-carbonate fragmental with interstitial foliated chlorite-sericite. Possible altered boudins seperated by foliated mafic domains.

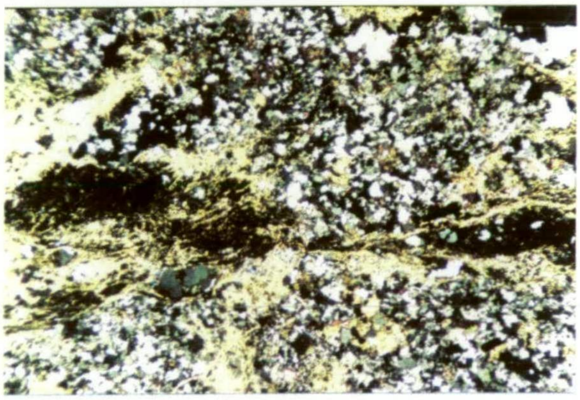

Figure 3
WL0106 EXPA3212 cpl, x 2.5
As for Figure 2 under crossed polarised light.

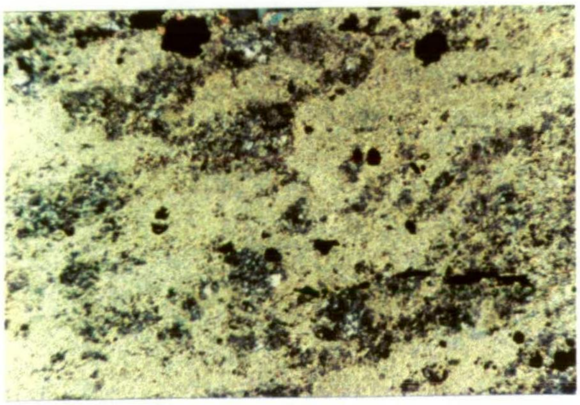

Figure 4
WL0106 EXPA3213 cpl, x 2.5
Fragmental or volcaniclastic that is weakly grain-layered and altered to an assemblage of sericite-chlorite-quartz with significant patchy vein-located sulphides. Once porphyritic texture in a lithic fragment with altered prismatic feldspars in a groundmass that is partly clouded granular quartz.

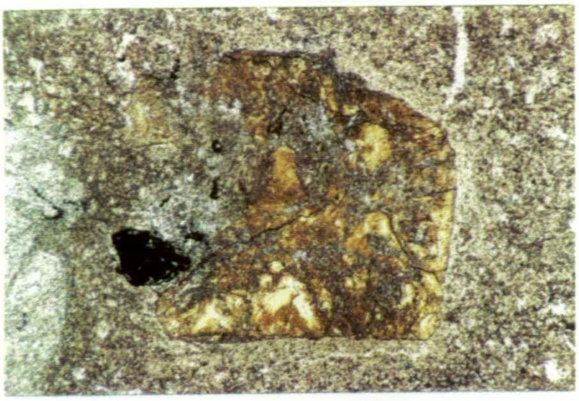

Figure 1
WL0106 EXPA3215 ppl, x 2.5
Very fine grained quartz-sericite rock that contains vague relict textures and with accessory rutile/titanian oxides, zircon and apatite. Large crystal site that could once have been ?cordierite and altered to pale brown smectite.

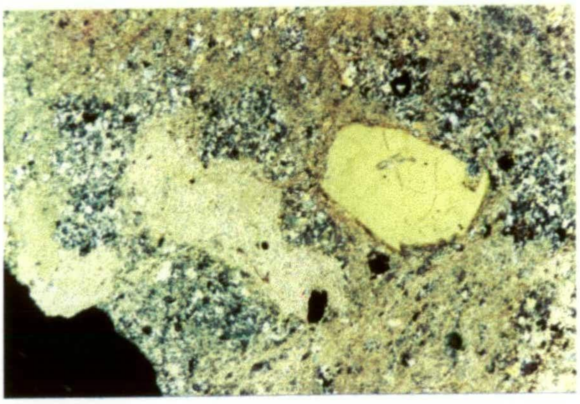

Figure 2
WL0106 EXPA3215 cpl, x 2.5
Quartz phenocryst and sites of altered ? feldspar.

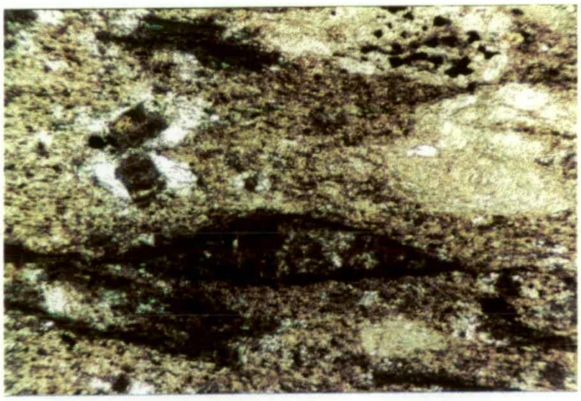

Figure 3
WL0530A EXPA3219 ppl, x 2.5
Porphyritic volcanic that is intensely altered to a quartz-sericite-carbonate assemblage and cut by deformed carbonate veins. Deformed and flattened sites of mafic (?amphibole) and felsic (?plagioclase) phenocrysts and set in a once microlitic feldspathic groundmass, with evenly distributed oxide granules.

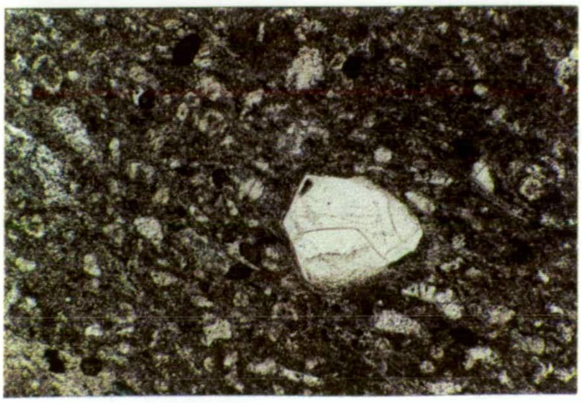

Figure 4
WL0530A EXPA3220 ppl, x 4
Vitric acidic volcanic that is intensely altered to a quartz-sericite assemblage and cut by irregular quartz-carbonate-(chlorite) veining. Quartz microphenocryst and sites of cuspate volcanic glass shards.

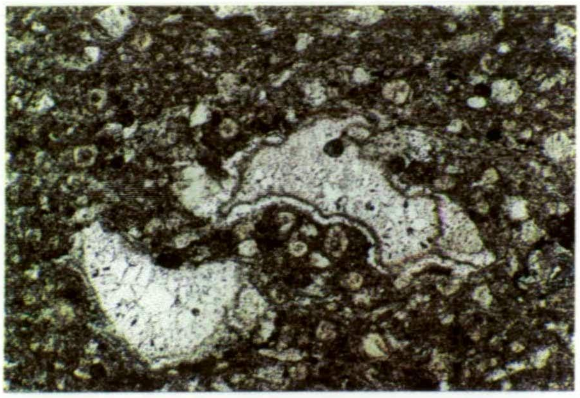

Figure 1
WL0530A EXPA3220 ppl, x 4
Vitric acidic volcanic, intensely altered to a quartz-sericite assemblage and cut by irregular quartz-carbonate-(chlorite) veining. Irregular vesicle sites and glass shards converted/filled to/with granular quartz, once containing colloform banded chalcedony.

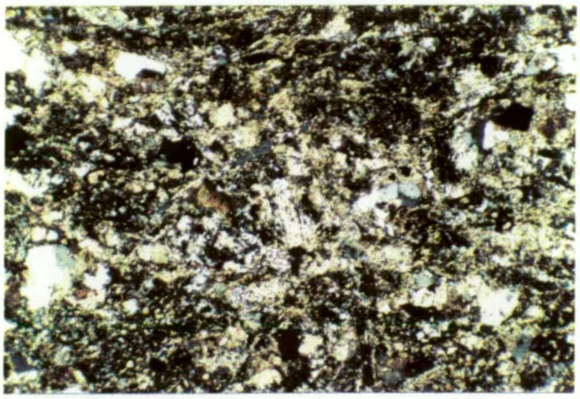

Figure 2
WL0530A EXPA3221 cpl, x 4
Mixed porphyritic and fragmental rock strongly deformed and altered to patchy sericite-carbonate-chlorite-quartz-(leucoxene) assemblage. Prisms of twinned albite and dark grey apatite.

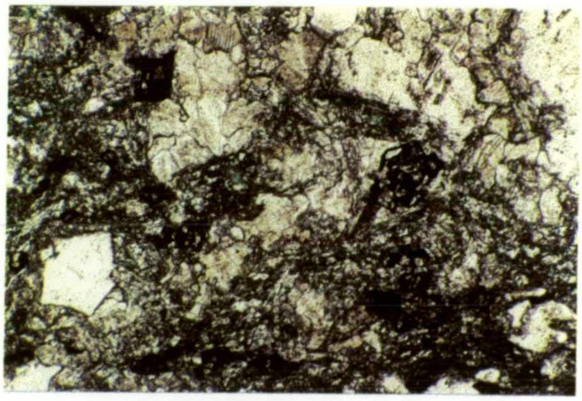

Figure 3
WL0530A EXPA3221 ppl, x 4
Feldpspar prisms and well preserved oxide crystal sites in a mixed porphyritic and fragmental rock that is strongly deformed and altered to a patchy sericite-carbonate-chlorite-quartz-(leucoxene) assemblage.

Figure 4
WL0530A EXPA3222 cpl, x 4
Strongly deformed and foliated volcaniclastic selectively altered to a fine grained quartz-sericite-carbonate-(chlorite) assemblage. Well preserved quartz microphenocryst in a fine grained recrystallised and foliated matrix.

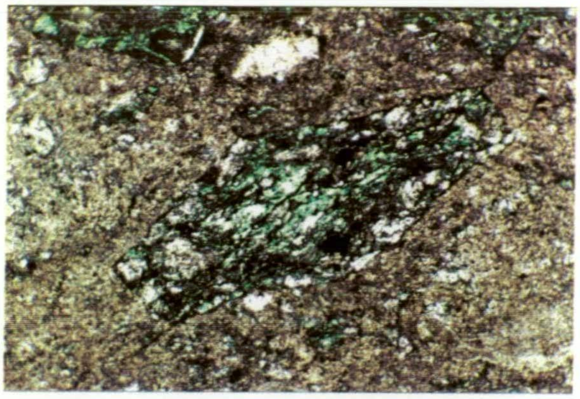

Figure 1
WL0530A EXPA3224 ppl, x 4
Foliated, intensely and selectively altered intermediate volcanic rock composed of a carbonate-chlorite-(sericite) assemblage with minor relict albite. Well preserved coarse grained amphibole phenocryst altered to (green) chlorite with dusty oxide markings and cleavage traces.

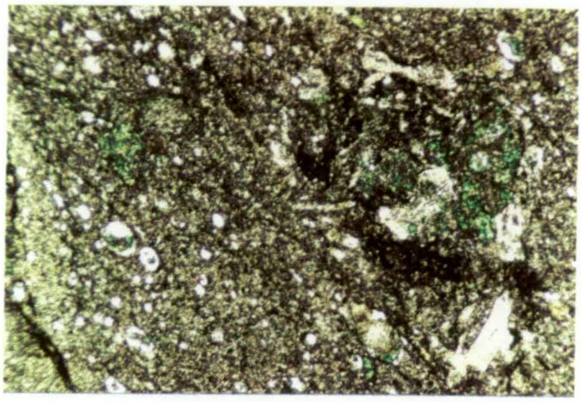

Figure 2
WL0530A EXPA3225 ppl, x 2.5
?pyroxene porphyritic and vesicular volcanic (?intermediate-mafic possibly trachyandesite type) altered to carbonate-chlorite-sericite in a groundmass that contains abundant dusty haematite. Glomeroporphyritic cluster in a groundmass containing abundant small rounded vesicle sites.

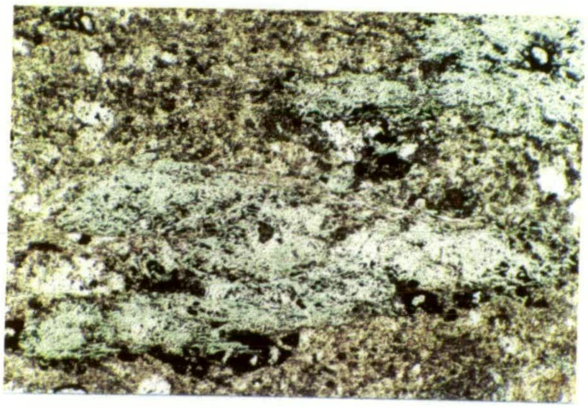

Figure 3
WL0530A EXPA3227 ppl, x 4
Unsorted lithic fragmental (?volcaniclastic) from an acid intermediate source. Strongly altered to a quartz-sericite-chlorite-carbonate assemblage that is selectively pyrite mineralised and cut by sparse deformed quartz carbonate veins. Chlorite altered mafic phenocryst sites.

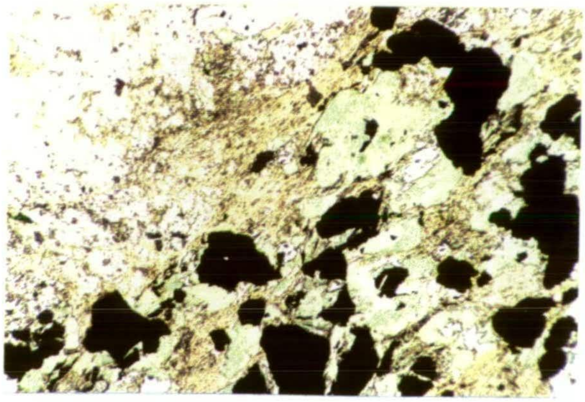

Figure 4
WL0480 EXPA3229 ppl, x 2.5
"Crowded" porphyritic possibly shallow intrusive igneous rock. Intensely altered to a quartz-sericite-chlorite-(carbonate) assemblage that hosts significant pyrite-chalcopyrite mineralisation. Poorly defined mafic (chlorite-altered) and felsic (quartz-sericite-altered) crystal sites. Sulphides are black.

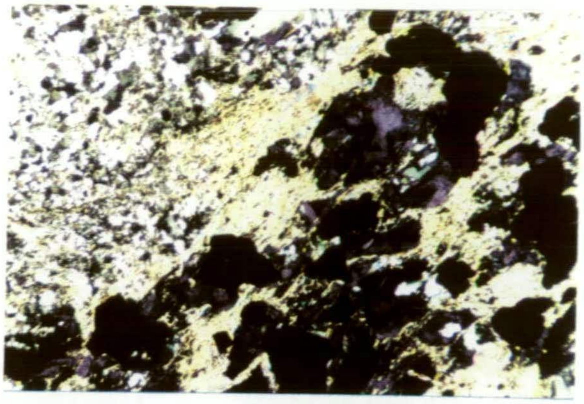

Figure 1
WL0480 EXPA3229 cpl, x 2.5
Poorly defined mafic (chlorite-altered) and felsic (quartz-sericite-altered) crystal sites under crossed polarised light.

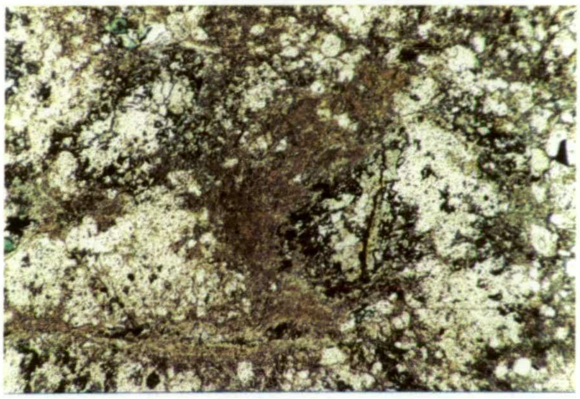

Figure 2
WL0480 EXPA3229 ppl, x 2.5
Granular quartz-carbonate altered prismatic sites that could represent previous feldspar prisms in a porphyritic possibly shallow intrusive igneous rock, intensely altered to a quartz-sericite-chlorite-(carbonate) assemblage and which hosts significant pyrite-chalcopyrite mineralisation.

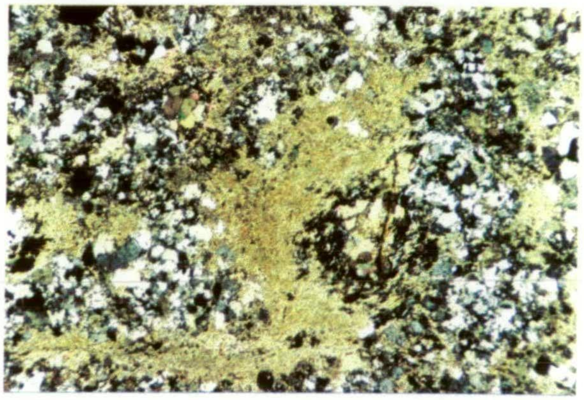

Figure 3
WL0480 EXPA3229 cpl, x 2.5
As for Figure 3 under crossed polarised light.

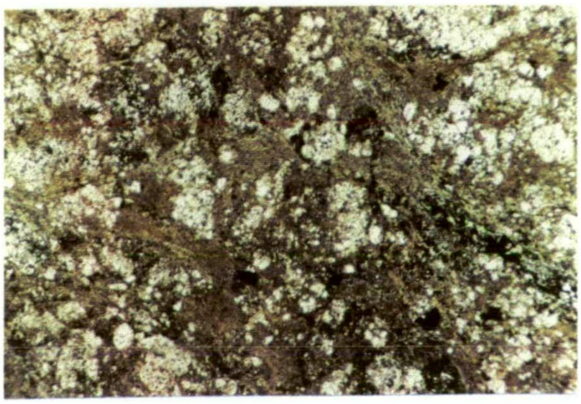

Figure 4
WL0480 EXPA3230 ppl, x 4
Feldspathic shallow ?intrusive porphyry that has been selectively altered to a quartz-sericite-(carbonate-chlorite) assemblage, cut by fine branching foliated sericitic zones. Poorly preserved unoriented prismatic shaped phenocryst sites (sericite altered) and elongate narrow green chlorite altered mafic crystal sites set in a quartz-sericite matrix.

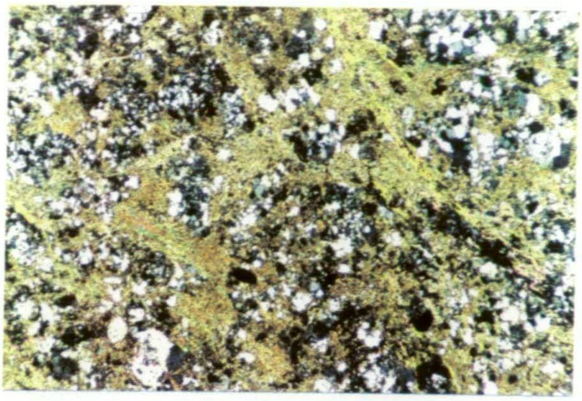

Figure 1
WL0480 EXPA3230 cpl, x 4
Poorly preserved unoriented prismatic shaped phenocryst sites (sericite altered) and elongate narrow green chlorite altered mafic sites set in a quartz-sericite matrix under crossed polarised light.

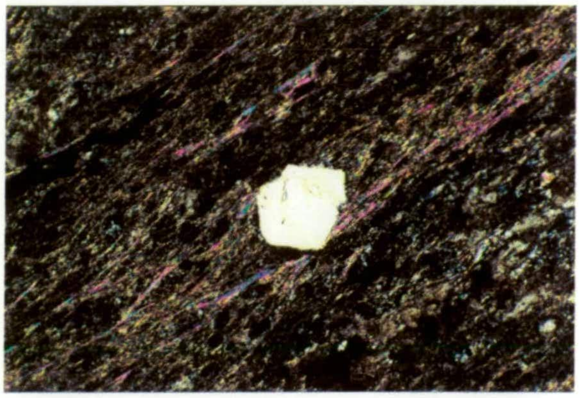

Figure 2
WL0106 EXPA3216 cpl, x 4
Volcaniclastic quartz sericite schist of variable primary composition. Carbonate veined and intensely deformed. Euhedral quartz phenocryst in a foliated sericite-quartz-carbonate host.

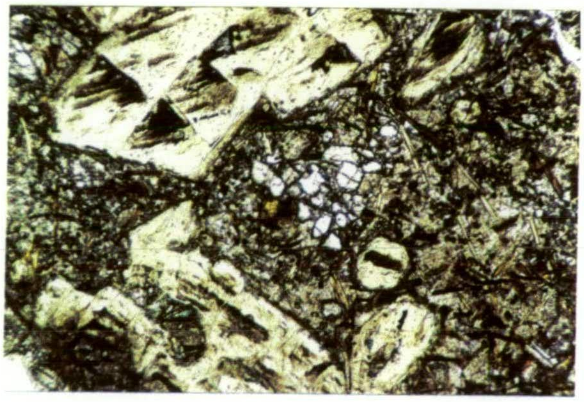

Figure 3
WL0530A EXPA3218 ppl, x 2.5
Fractionated lamprophyre dyke. Serpentine altered olivine phenocryst sites in colourless diopsidic pyroxene set in a groundmass with biotite flakes (brown), dusty K-feldspar and feldspathoids.

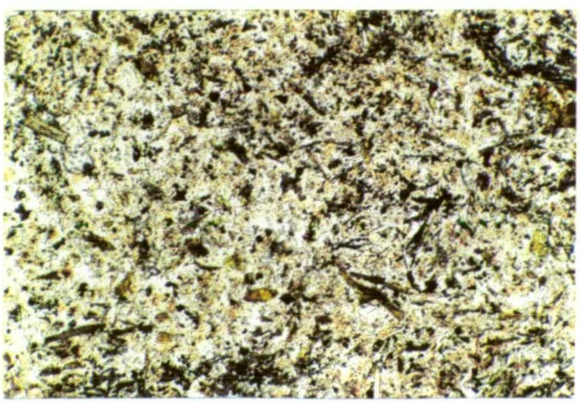

Figure 4
WL0530A EXPA3218 ppl, x 4
Fractionated lamprophyre dyke. Syenitic host rock. Alkali feldspars clouded with dusty haematite, biotite (brown) and oxide granules (black).

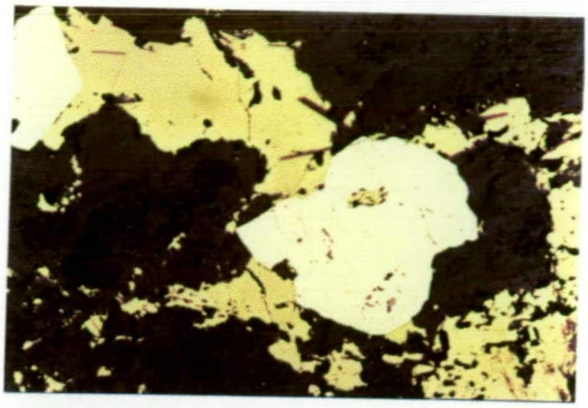

Figure 1
WL0290 EXPA3202
Reflected light x 10
Pyrite and interstitial anhedral chalcopyrite patches.

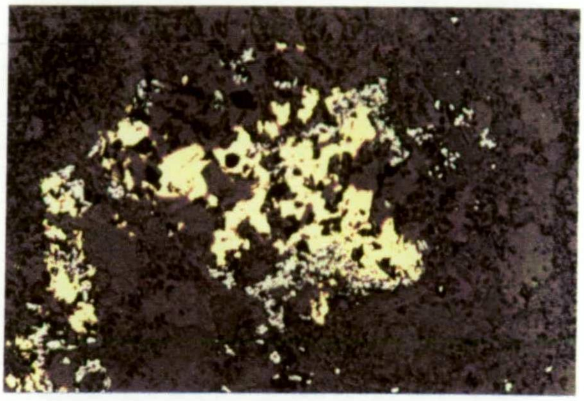

Figure 2
WL0290 EXPA3202
Reflected light x 10
Anhedral yellow chalcopyrite and grey haematite.

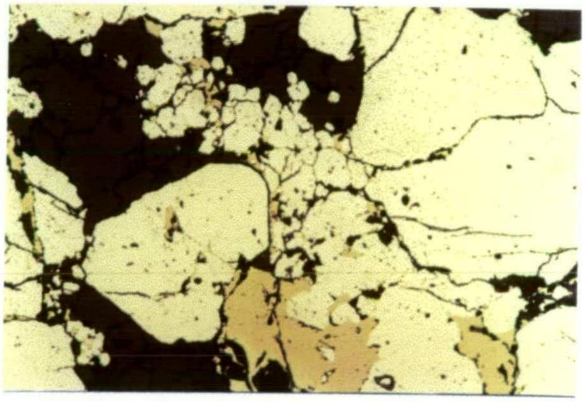

Figure 3
WL0290 EXPA3202
Reflected light x 10
Large pyrite crystals set in a finer grained granular pyrite with even later interstitial chalcopyrite.

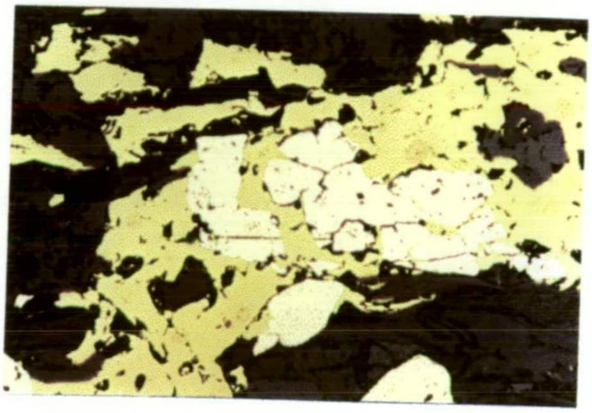

Figure 4
WL0290 EXPA3207
Reflected light x 10
Early subhedral and fractured pyrite set in later anhedral chalcopyrite.

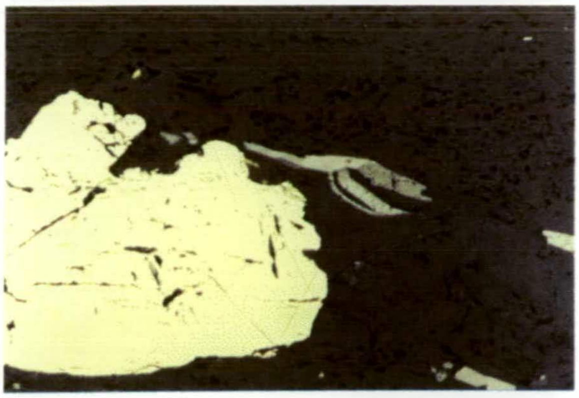

Figure 1
WL0421 EXPA3207
Reflected light x 20
Deformed molybdenite flakes (grey) and large anhedral pyrite clusters.

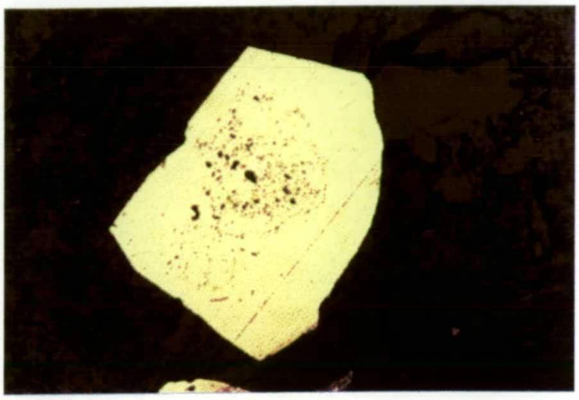

Figure 2
WL0106 EXPA3210
Reflected light x 10
Central zone of dusty inclusions in pyrite, including some chalcopyrite.

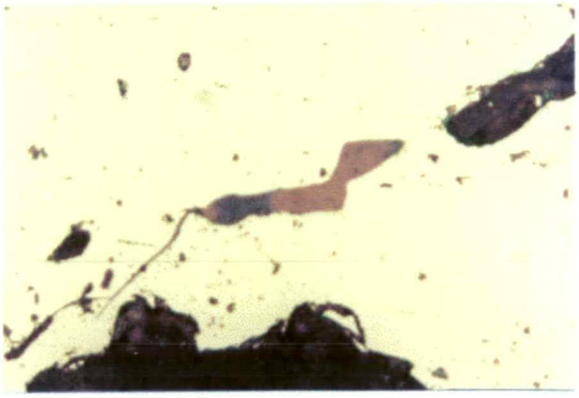

Figure 3
WL0106 EXPA3210
Reflected light x 40
Narrow veinlet of bornite partly intergrown with (or altered to) blue chalcocite-digenite. Enclosed in pyrite host.

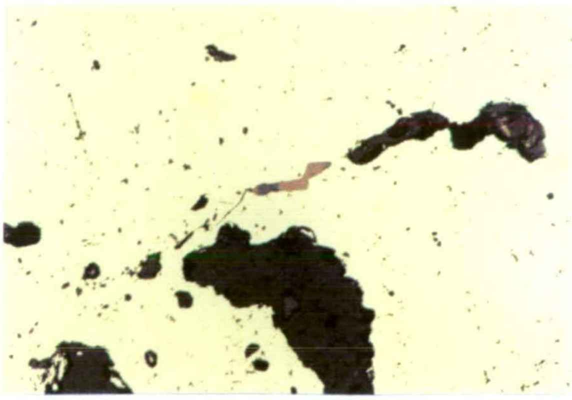

Figure 4
WL0106 EXPA3210
Reflected light x 20
As for Figure 4.

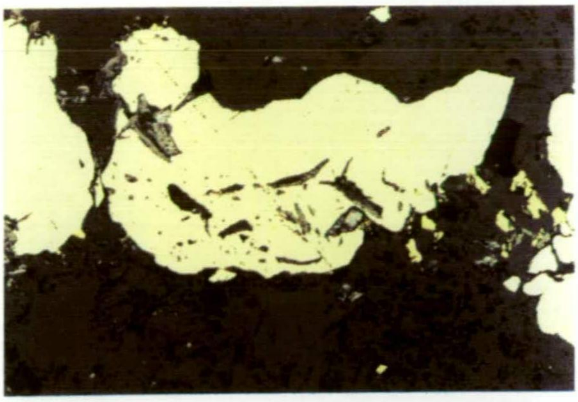

Figure 1
WL0106 EXPA3213
Reflected light x 20
Molybdenite flakes enclosed within pyrite.

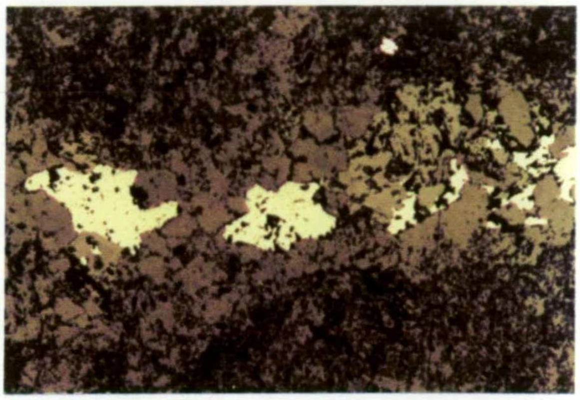

Figure 2
WL0531 EXPA3226
Reflected light x 10
Anhedral patches of monomineralic sphalerite in quartz veinlet.

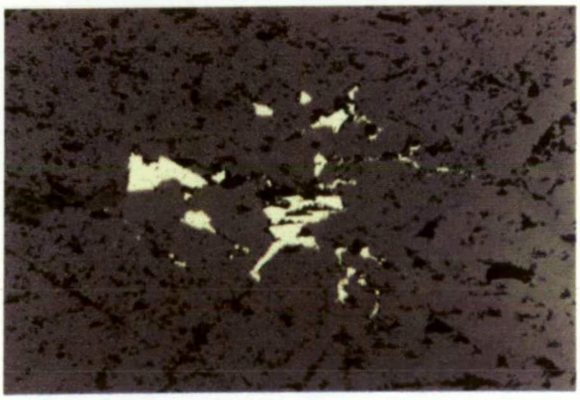

Figure 3
WL0531 EXPA3226
Reflected light x 20
Minor anhedral interstial galena in vein of coarse grained carbonate.

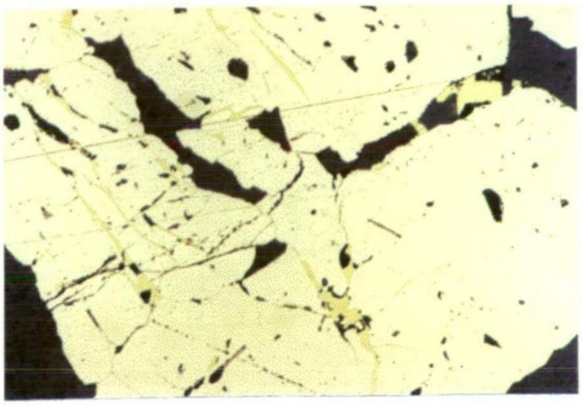

Figure 4
WL0480 EXPA3229
Reflected light x 20
Chalcopyrite occupying narrow microfractures and grain boundaries in early formed pyrite.

Appendix V

Royal Tharsis

Alteration Geochemistry: Whole Rock and Multi-Element Analyses

APPENDIX V - CONTENTS

APPENDIX V - CONTENTS

Royal Tharsis
WHOLE ROCK ANALYSES: 7950N-8070N

Appendix V
Chart 1

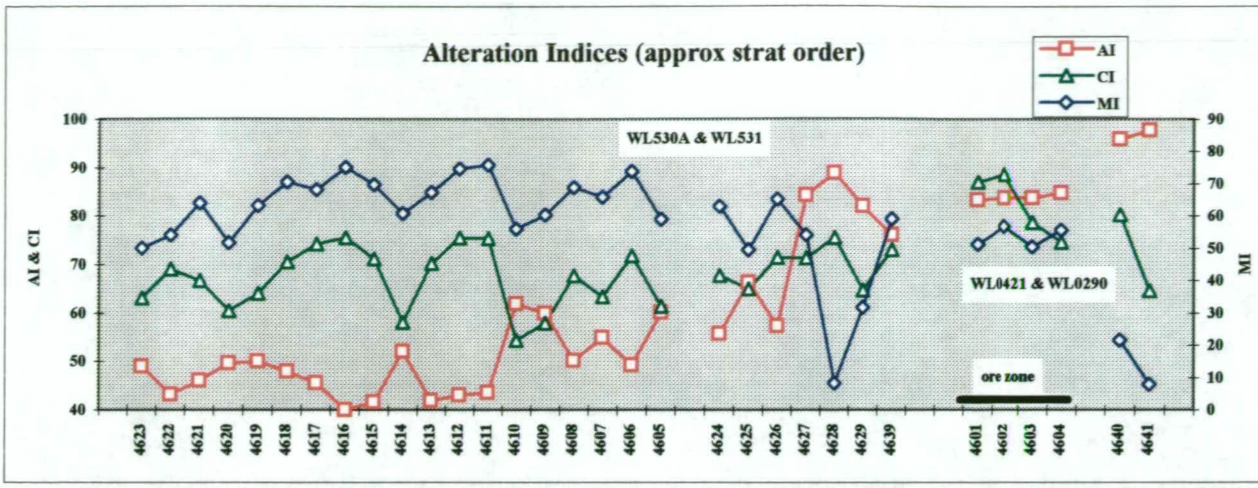

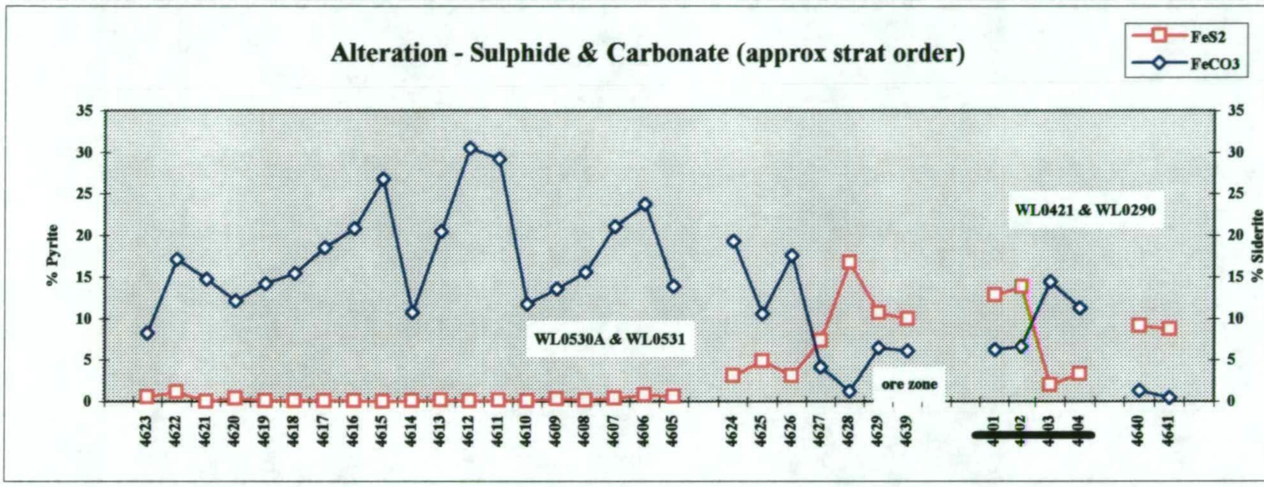

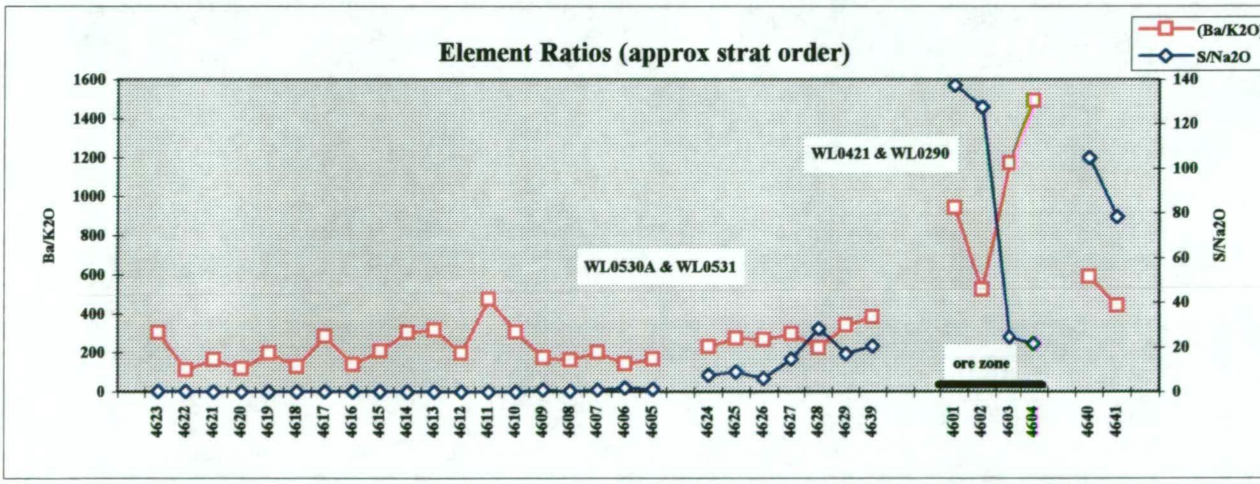

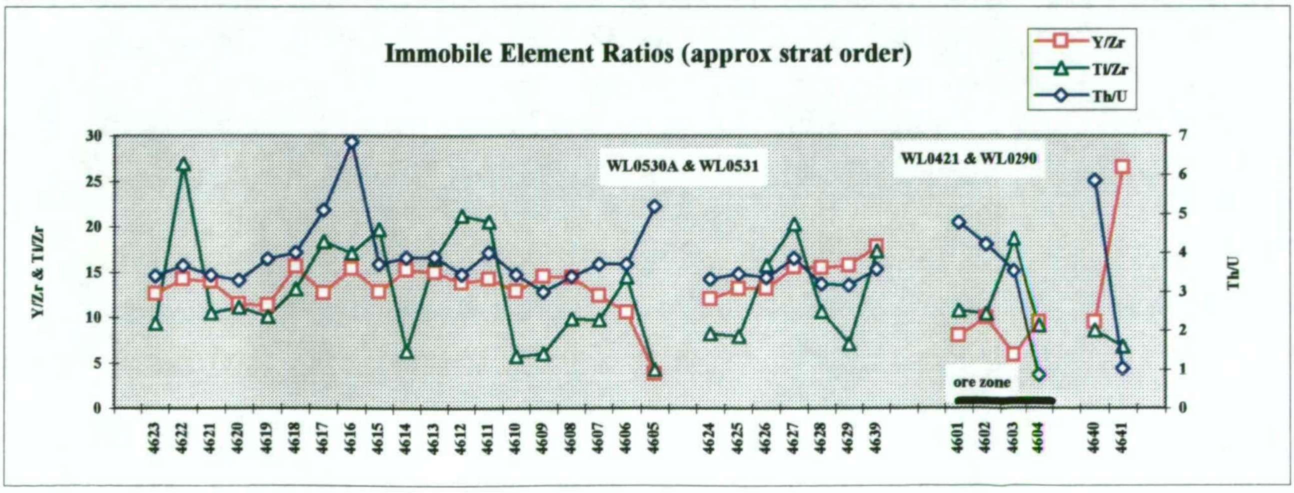

Royal Tharsis
WHOLE ROCK ANALYSES: 7950N-8070N

Appendix V
Chart 1

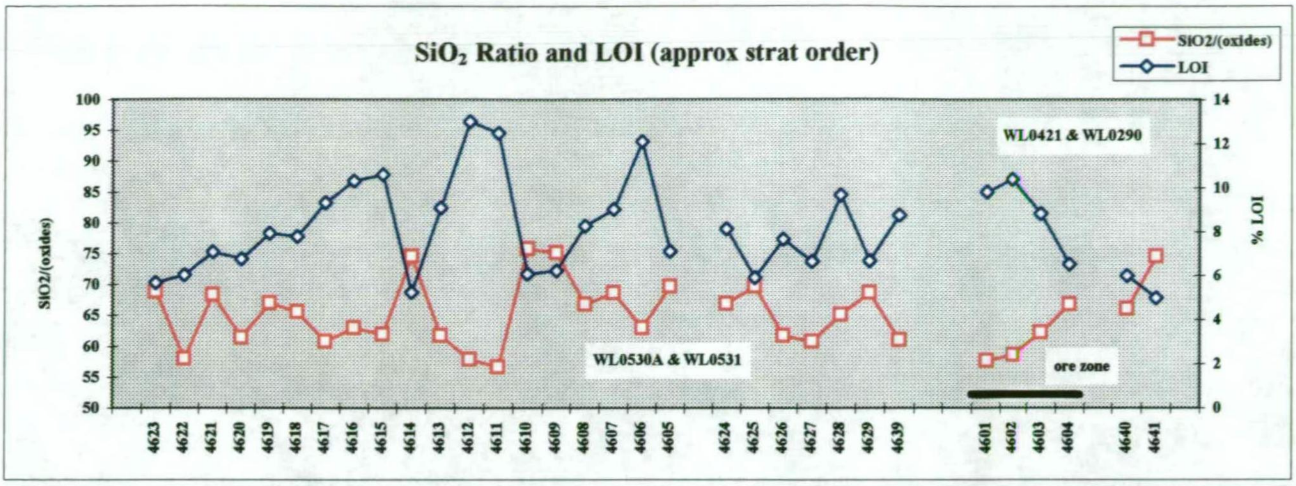

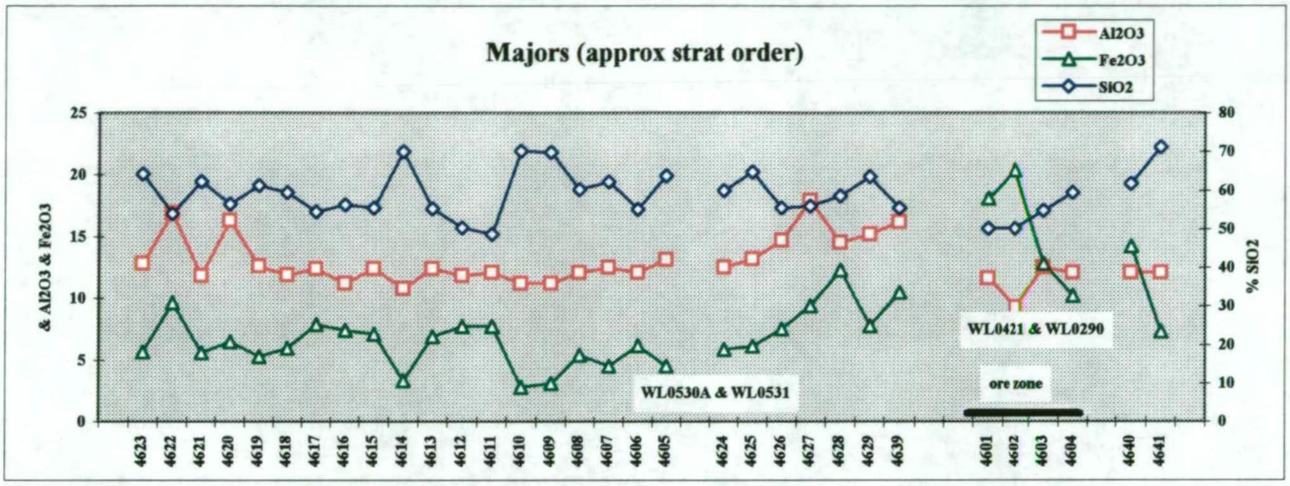

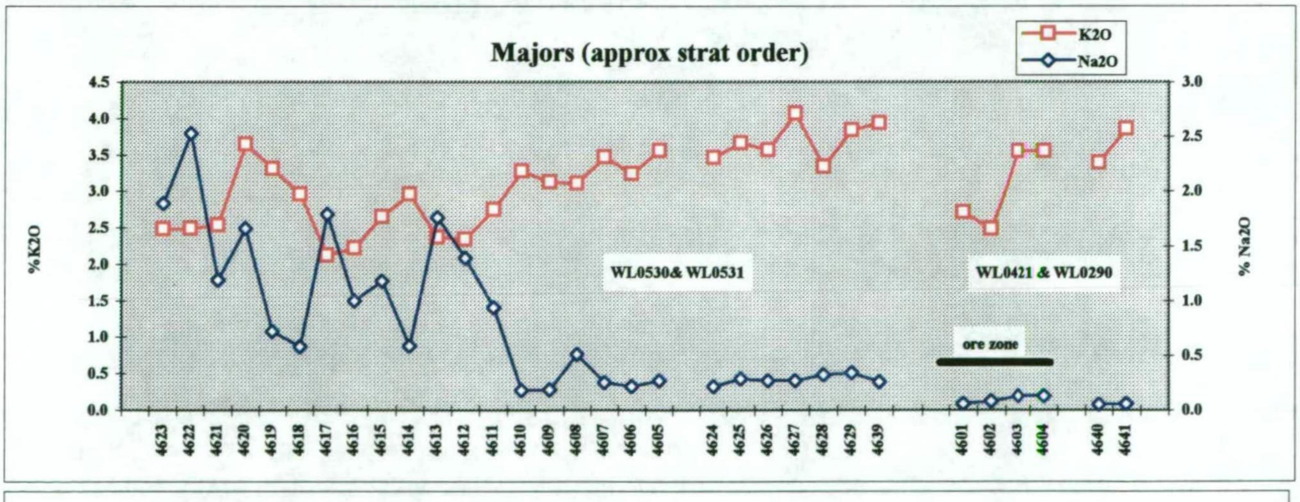

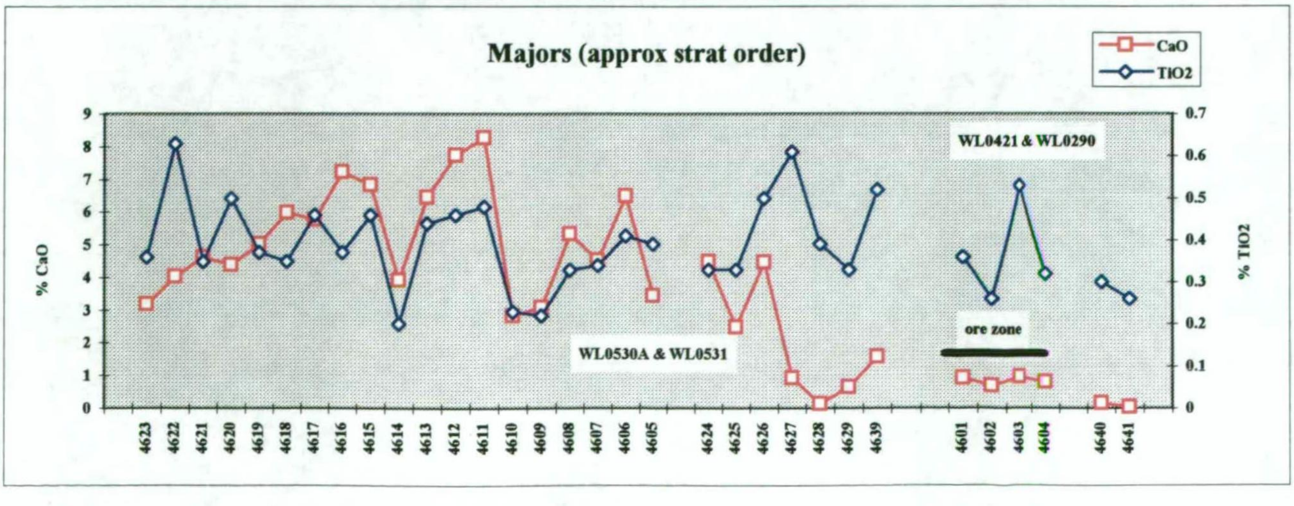

Royal Tharsis
WHOLE ROCK ANALYSES: 7950N-8070N

Appendix V
Chart 1

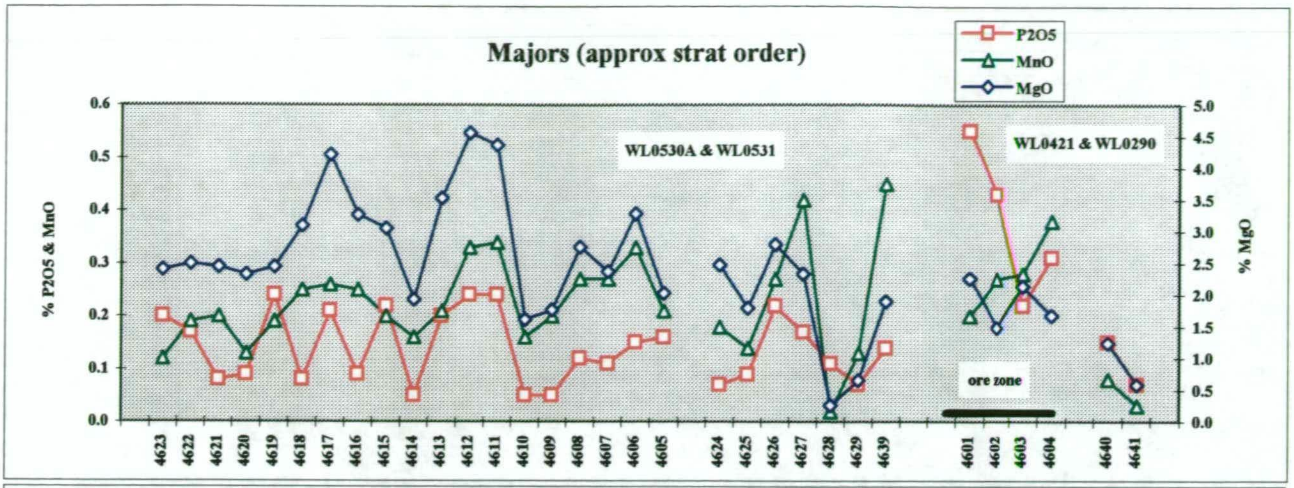

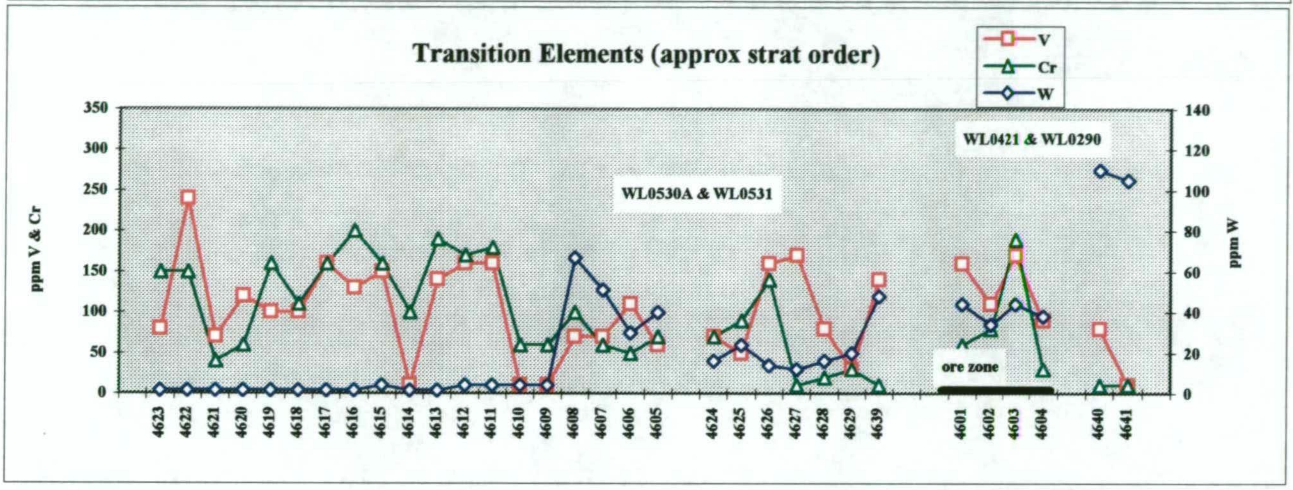

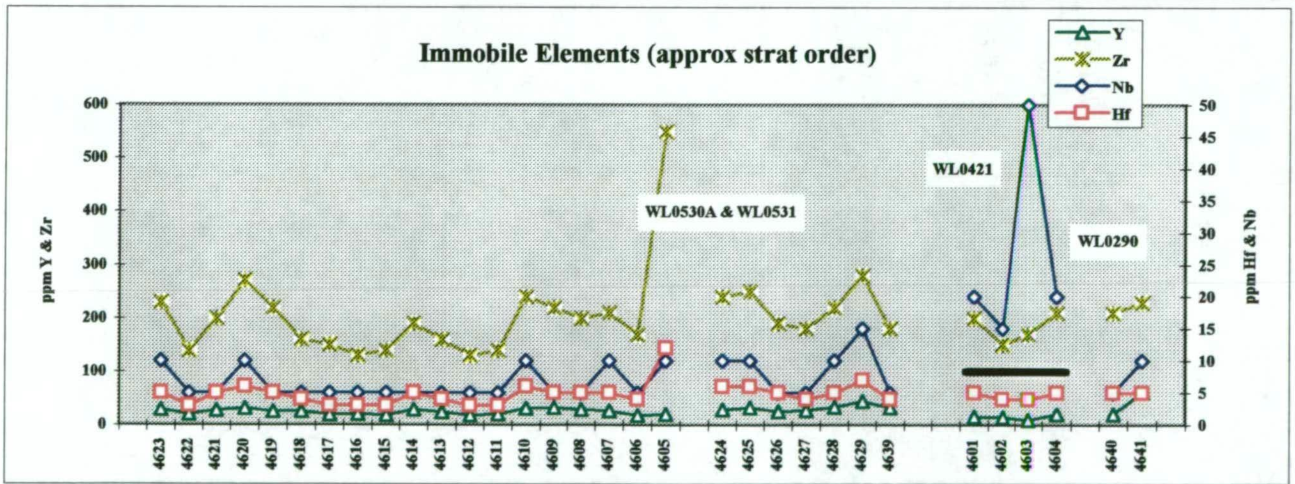

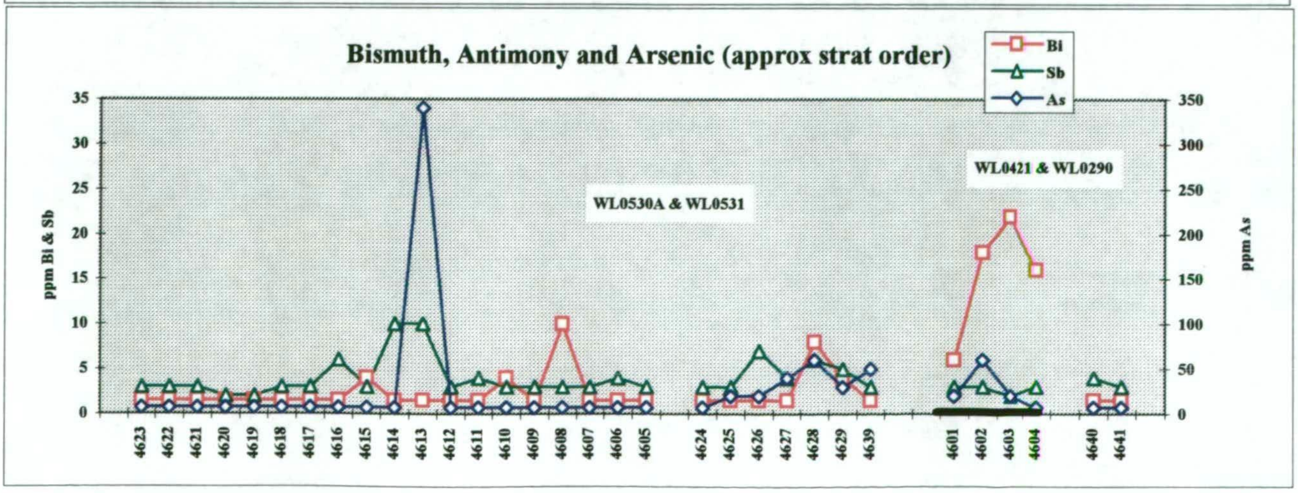

Royal Tharsis
WHOLE ROCK ANALYSES: 7950N-8070N

Appendix V
Chart 1

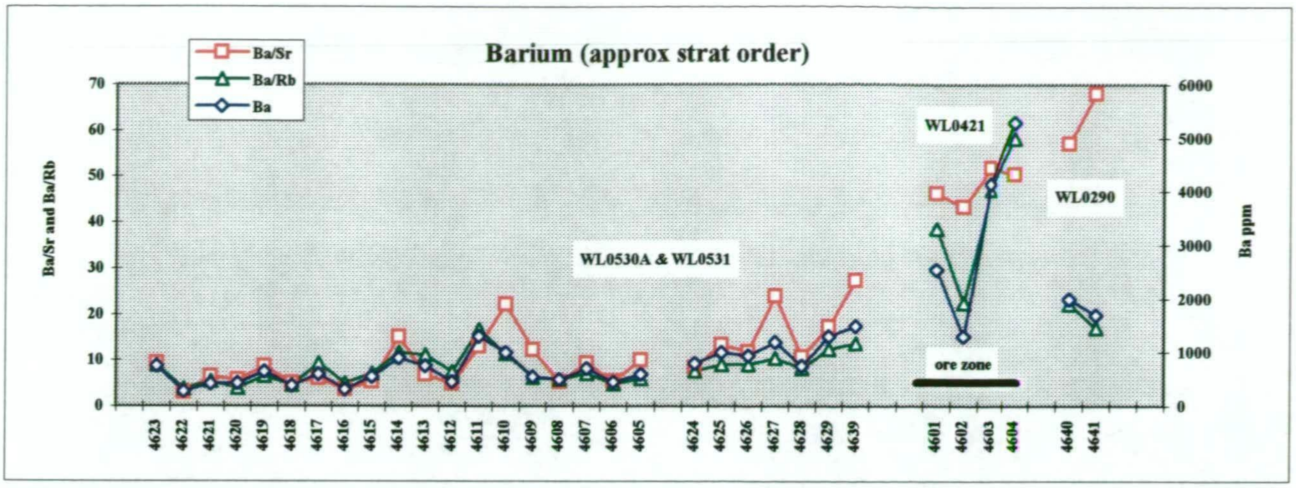

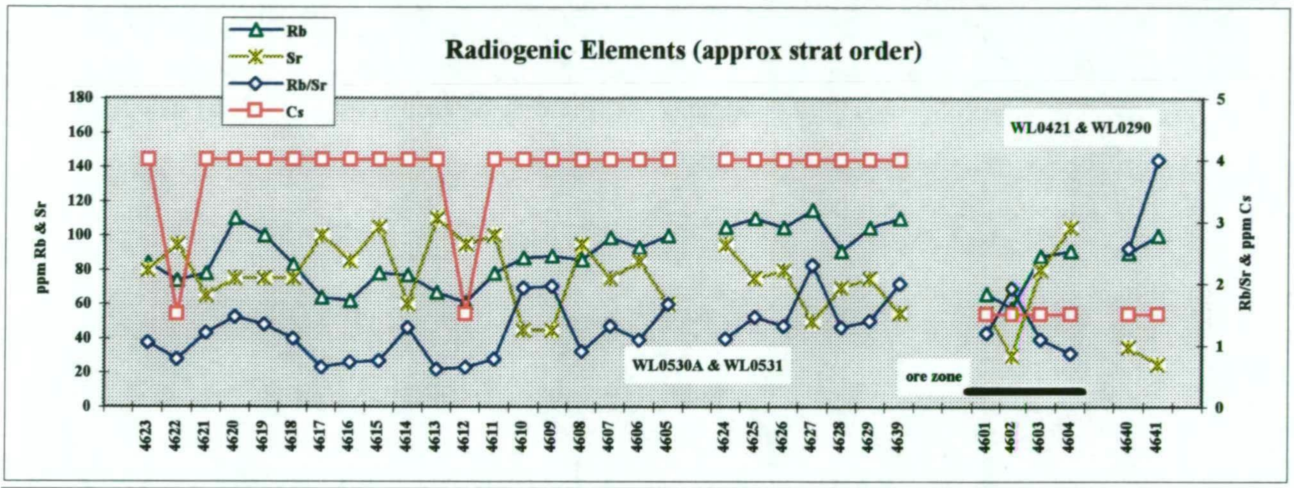

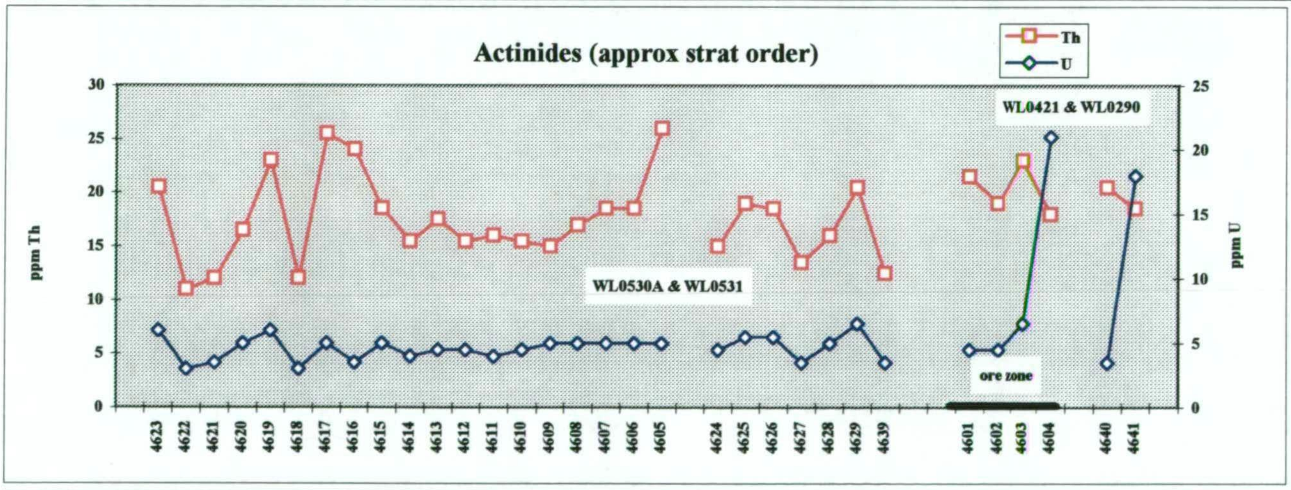

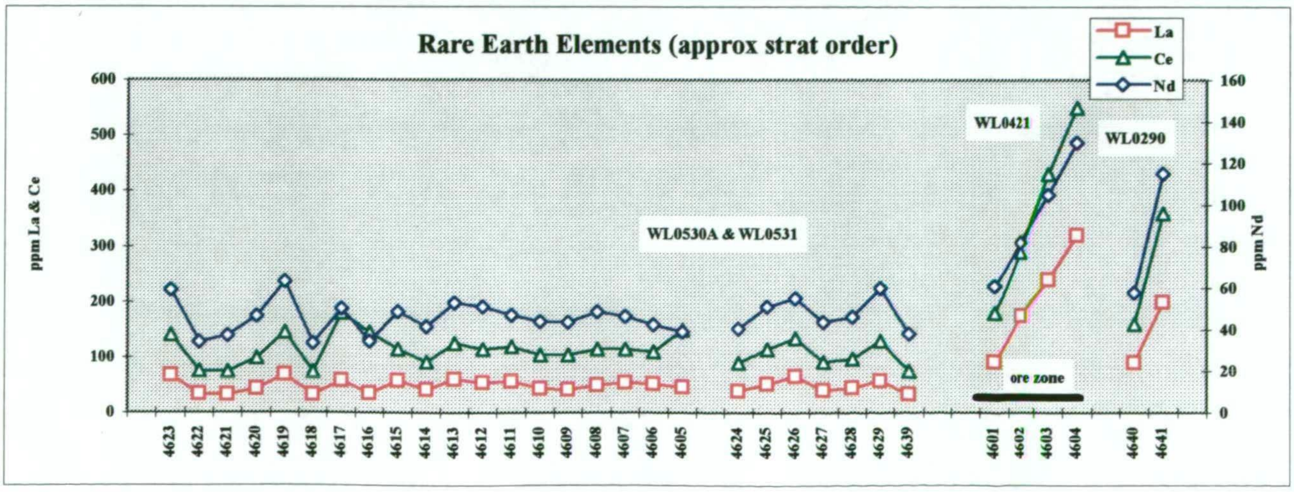

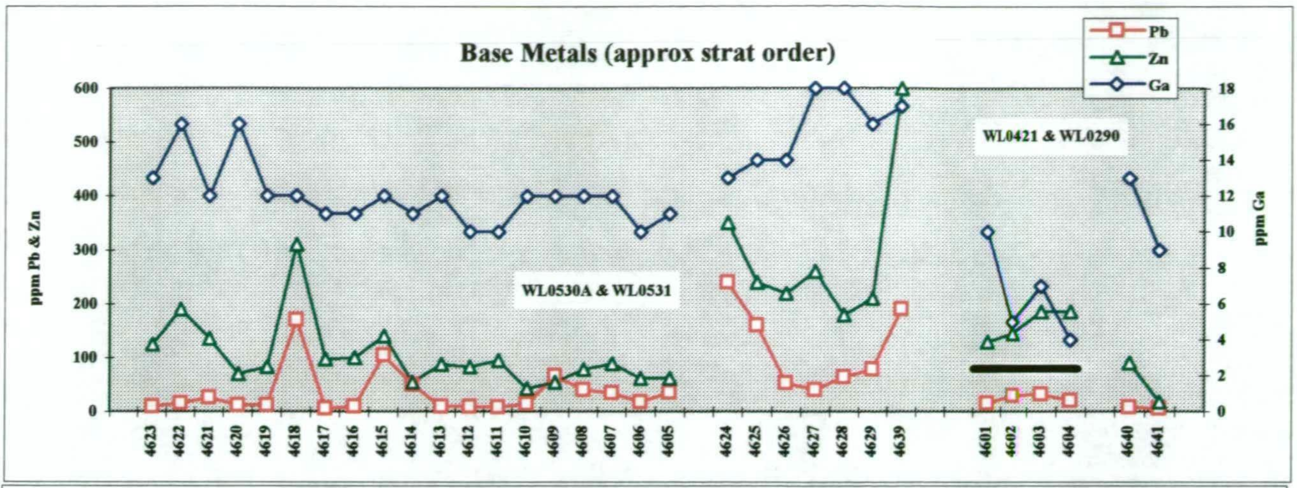
Base Metals (approx strat order)
Pb
Zn
Ga
ppm Pb & Zn
ppm Ga
WL0421 & WL0290
WL0530A & WL0531
4623 4622 4621 4620 4619 4618 4617 4616 4615 4614 4613 4612 4611 4610 4609 4608 4607 4606 4605 4624 4625 4626 4627 4628 4629 4639 4601 4602 4603 4604 4640 4641

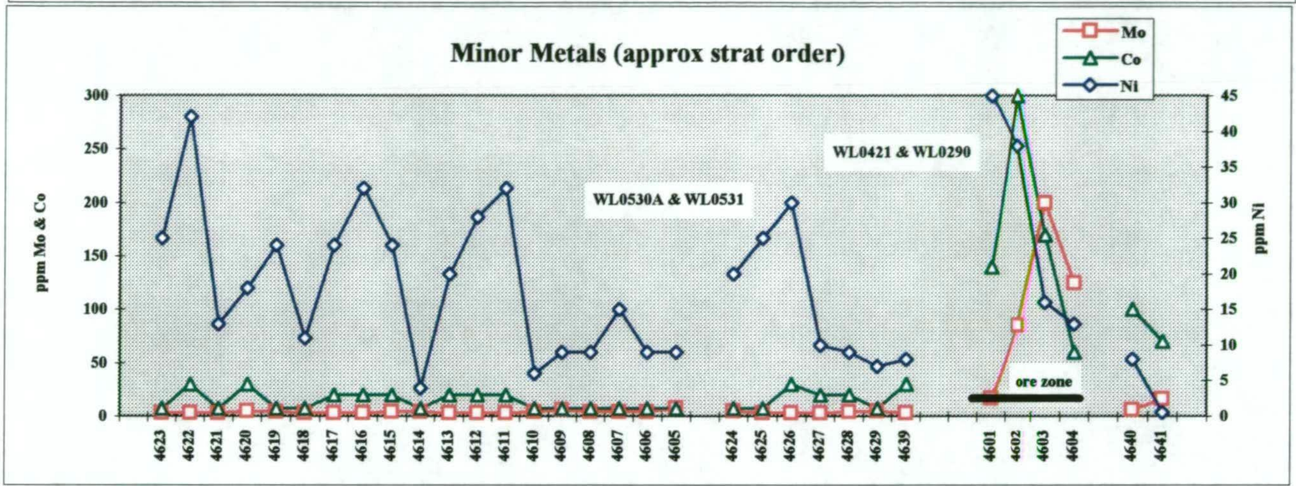
Minor Metals (approx strat order)
Mo
Co
Ni
ppm Mo & Co
ppm Ni
WL0421 & WL0290
WL0530A & WL0531
ore zone
4623 4622 4621 4620 4619 4618 4617 4616 4615 4614 4613 4612 4611 4610 4609 4608 4607 4606 4605 4624 4625 4626 4627 4628 4629 4639 4601 4602 4603 4604 4640 4641

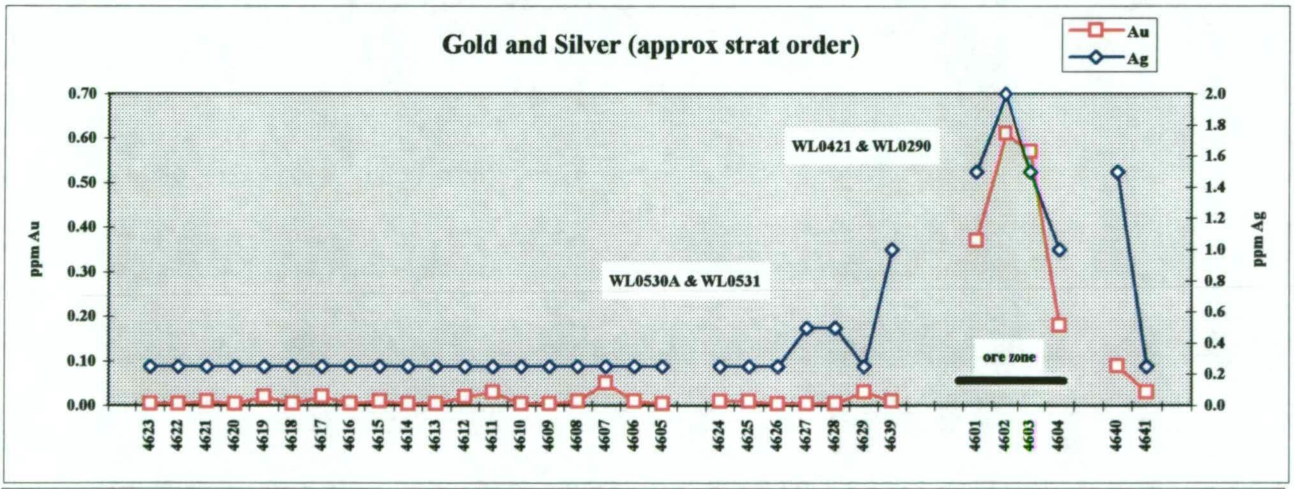
Gold and Silver (approx strat order)
Au
Ag
ppm Au
ppm Ag
WL0421 & WL0290
WL0530A & WL0531
ore zone
4623 4622 4621 4620 4619 4618 4617 4616 4615 4614 4613 4612 4611 4610 4609 4608 4607 4606 4605 4624 4625 4626 4627 4628 4629 4639 4601 4602 4603 4604 4640 4641

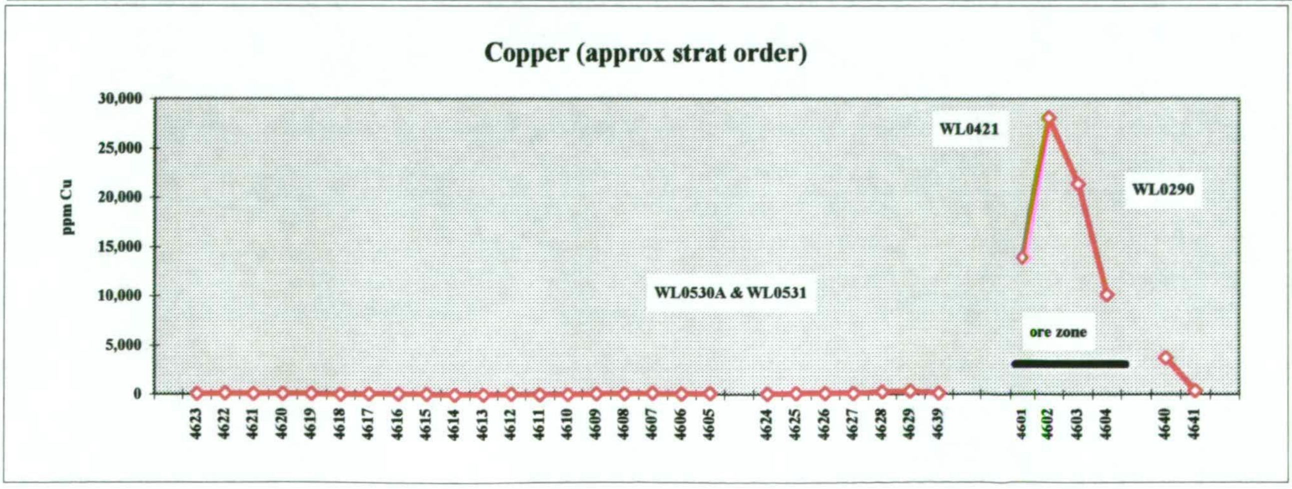
Copper (approx strat order)
ppm Cu
WL0421
WL0290
WL0530A & WL0531
ore zone
4623 4622 4621 4620 4619 4618 4617 4616 4615 4614 4613 4612 4611 4610 4609 4608 4607 4606 4605 4624 4625 4626 4627 4628 4629 4639 4601 4602 4603 4604 4640 4641

Royal Tharsis
WHOLE ROCK ANALYSES: 7770N-7830N

Appendix V
Chart 2

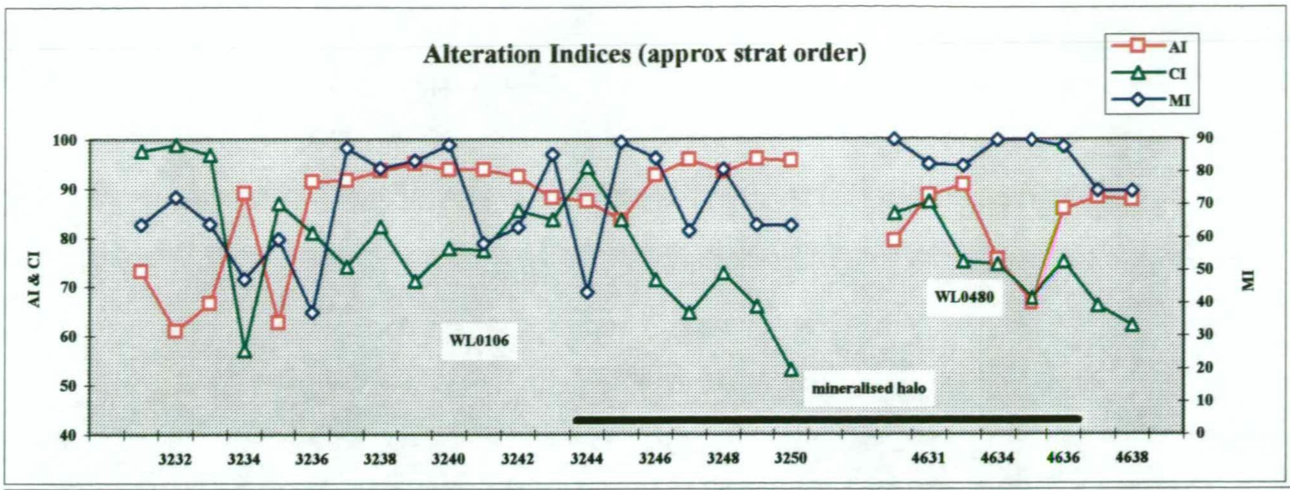

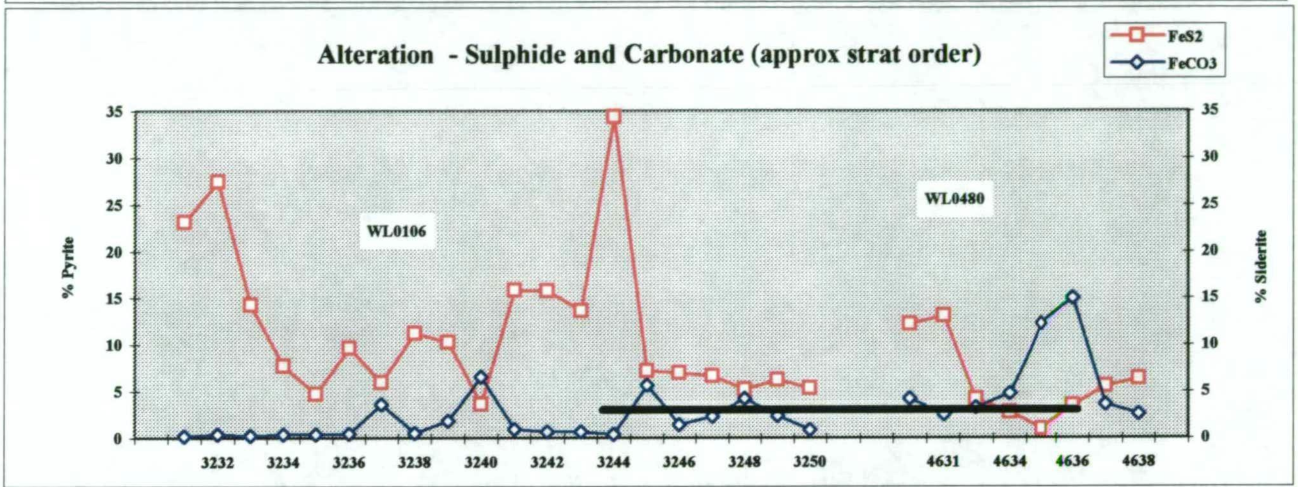

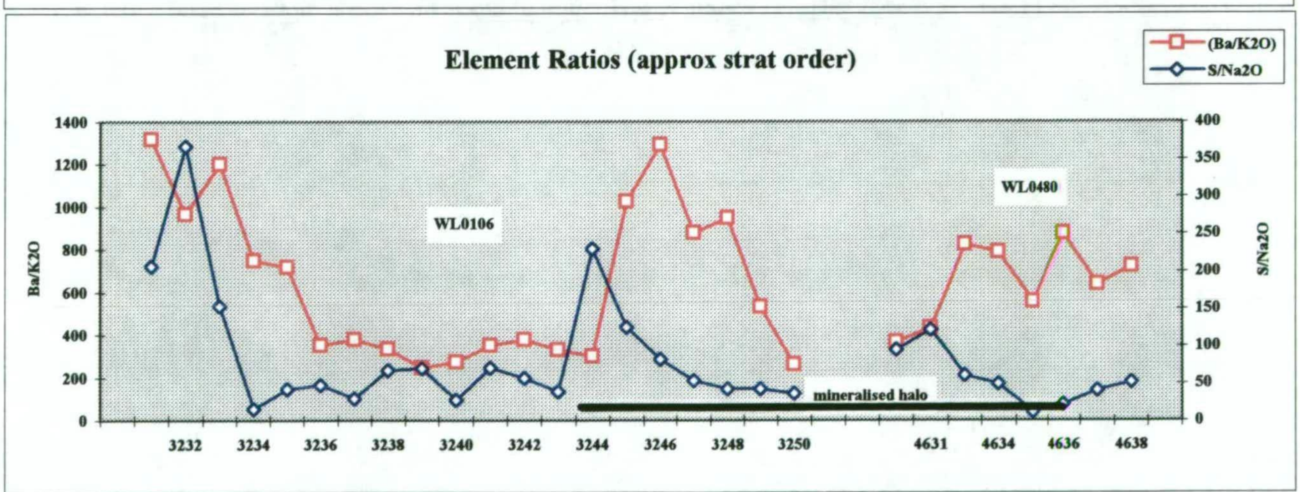

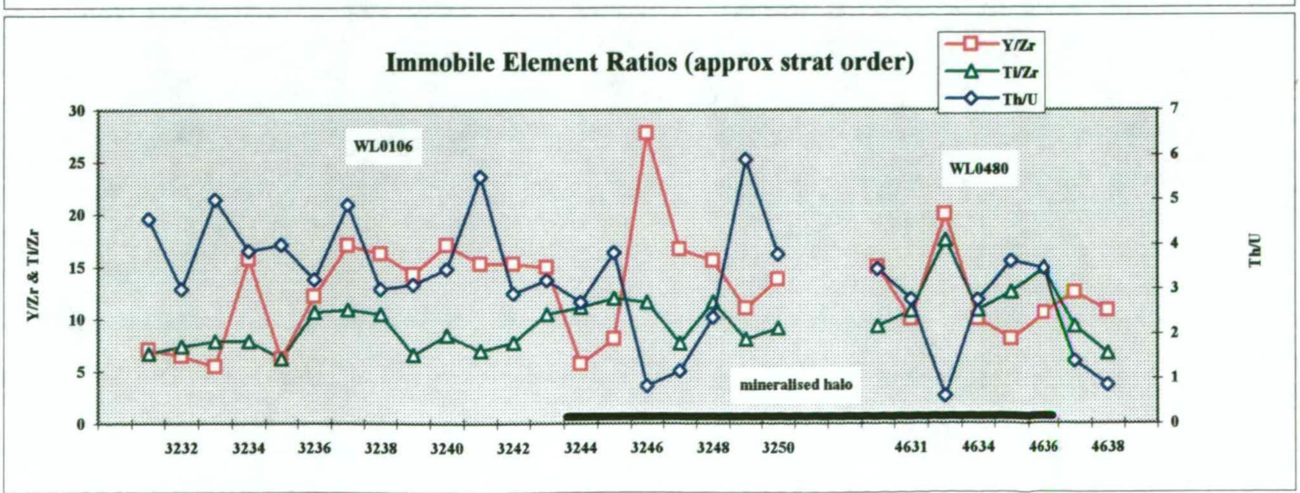

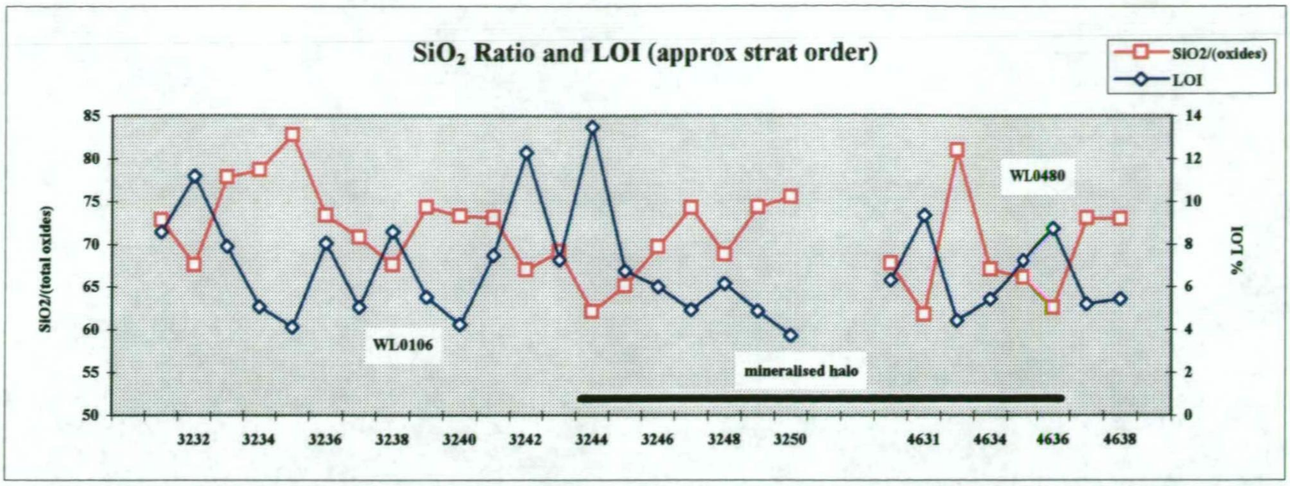
SiO₂ Ratio and LOI (approx strat order)
SiO2/(oxides)
LOI
SiO2/(total oxides)
% LOI
WL0106
WL0480
mineralised halo
3232
3234
3236
3238
3240
3242
3244
3246
3248
3250
4631
4634
4636
4638

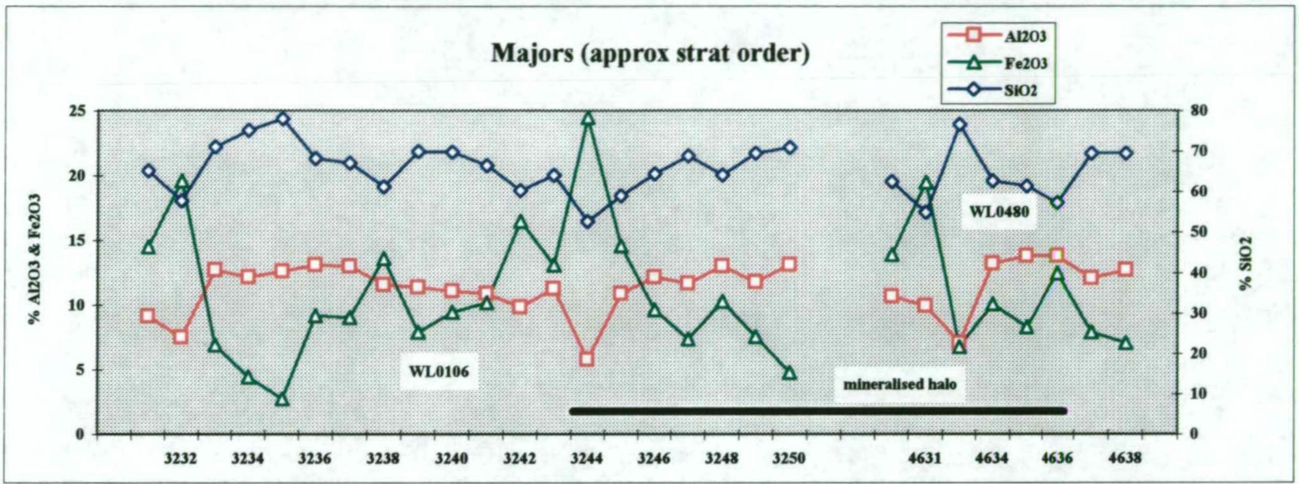
Majors (approx strat order)
Al2O3
Fe2O3
SiO2
% Al2O3 & Fe2O3
% SiO2
WL0106
WL0480
mineralised halo

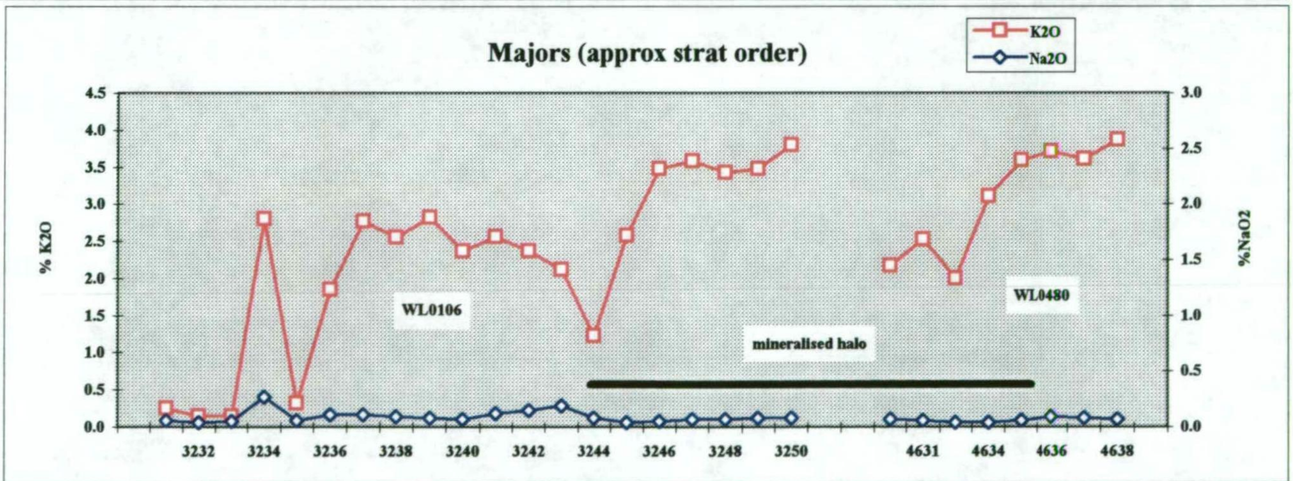
Majors (approx strat order)
K2O
Na2O
% K2O
%NaO2
WL0106
WL0480
mineralised halo

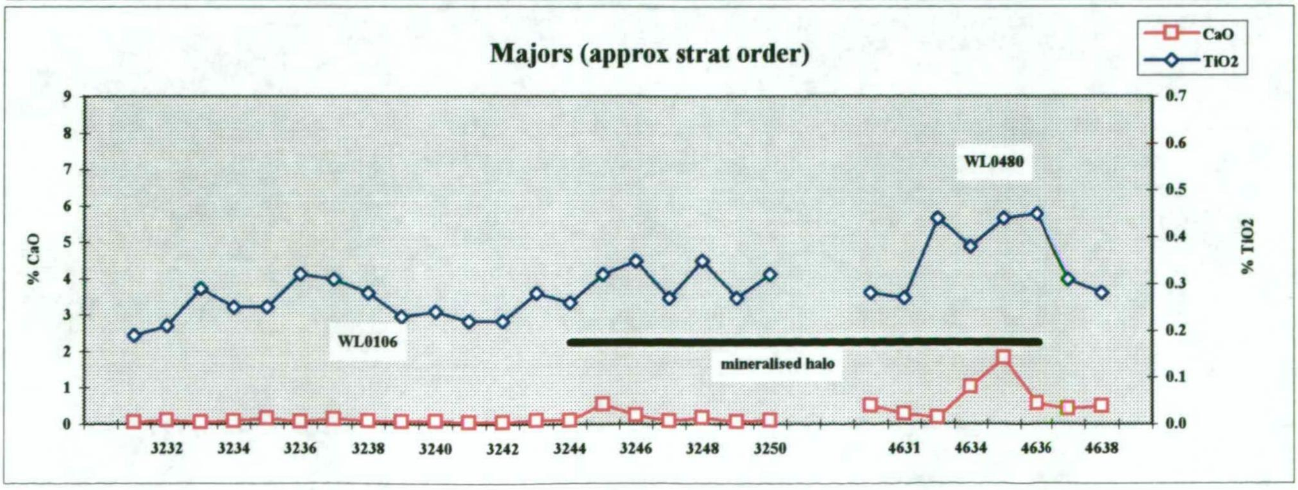
Majors (approx strat order)
CaO
TiO2
% CaO
% TiO2
WL0106
WL0480
mineralised halo

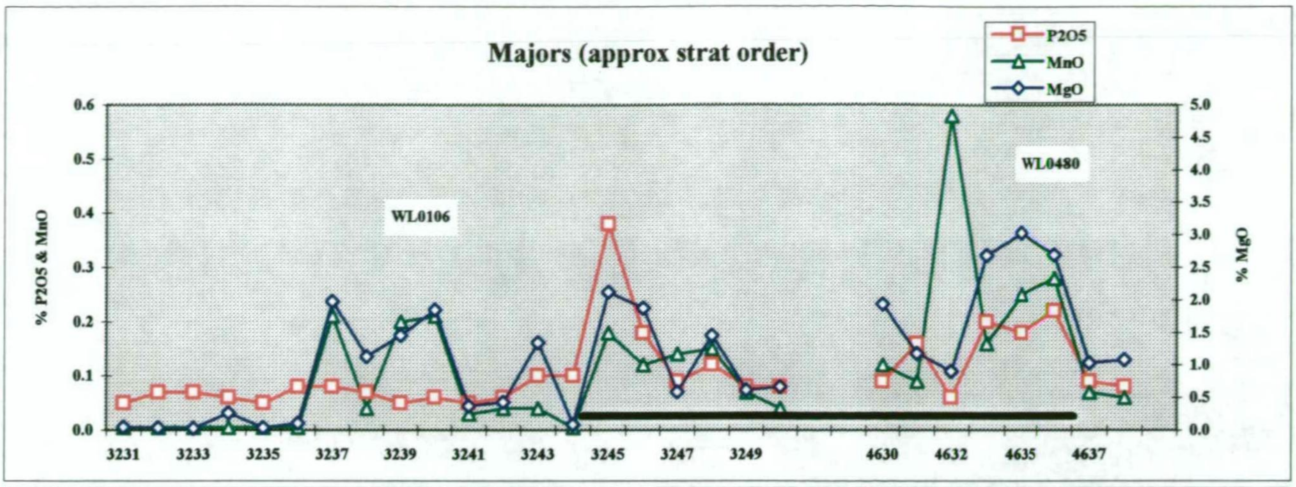
Majors (approx strat order)
P2O5
MnO
MgO
WL0106
WL0480
% P2O5 & MnO
% MgO
0.0
0.1
0.2
0.3
0.4
0.5
0.6
0.0
0.5
1.0
1.5
2.0
2.5
3.0
3.5
4.0
4.5
5.0
3231
3233
3235
3237
3239
3241
3243
3245
3247
3249
4630
4632
4635
4637

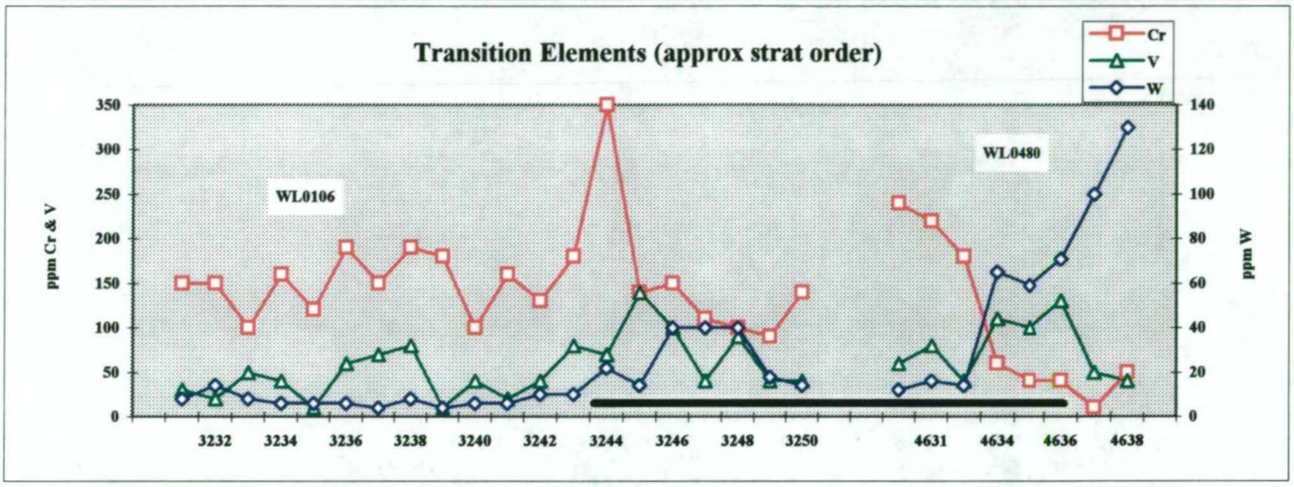
Transition Elements (approx strat order)
Cr
V
W
WL0106
WL0480
ppm Cr & V
ppm W
0
50
100
150
200
250
300
350
0
20
40
60
80
100
120
140
3232
3234
3236
3238
3240
3242
3244
3246
3248
3250
4631
4634
4636
4638

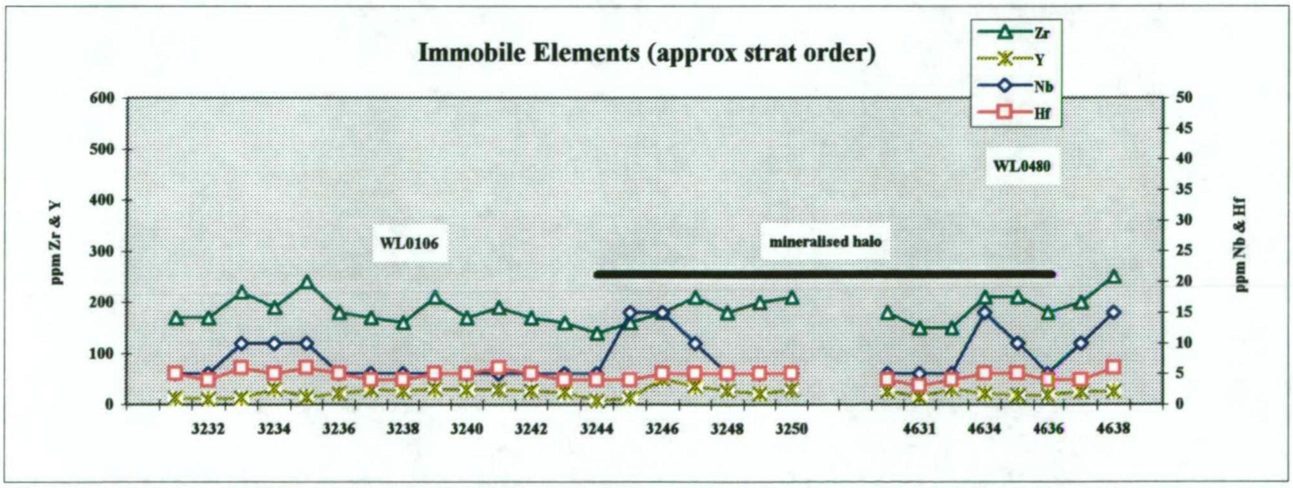
Immobile Elements (approx strat order)
Zr
Y
Nb
Hf
WL0106
WL0480
mineralised halo
ppm Zr & Y
ppm Nb & Hf
0
100
200
300
400
500
600
0
5
10
15
20
25
30
35
40
45
50
3232
3234
3236
3238
3240
3242
3244
3246
3248
3250
4631
4634
4636
4638

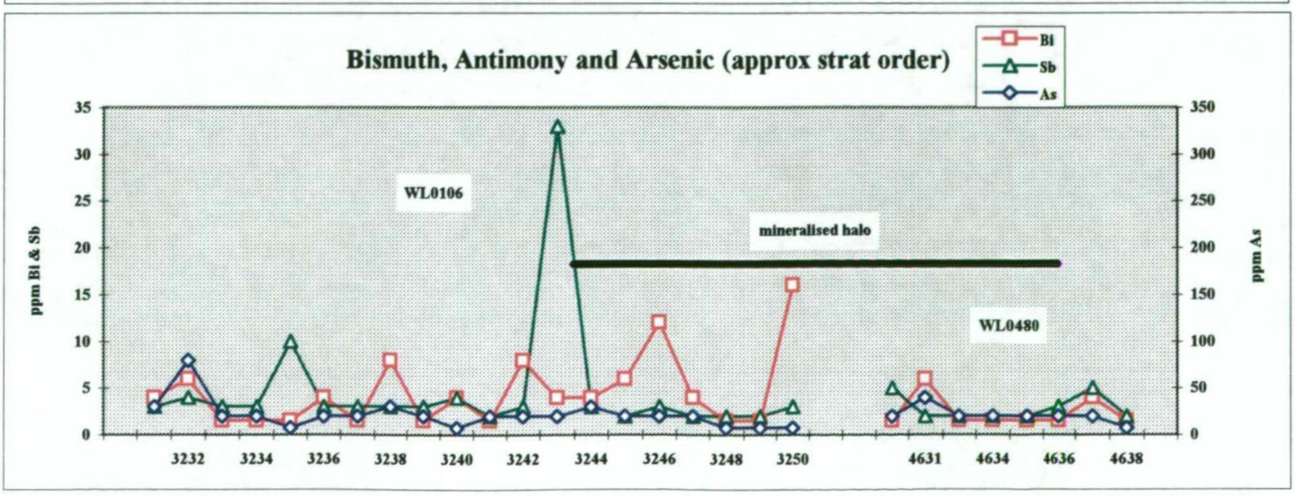
Bismuth, Antimony and Arsenic (approx strat order)
Bi
Sb
As
WL0106
WL0480
mineralised halo
ppm Bi & Sb
ppm As
0
5
10
15
20
25
30
35
0
50
100
150
200
250
300
350
3232
3234
3236
3238
3240
3242
3244
3246
3248
3250
4631
4634
4636
4638

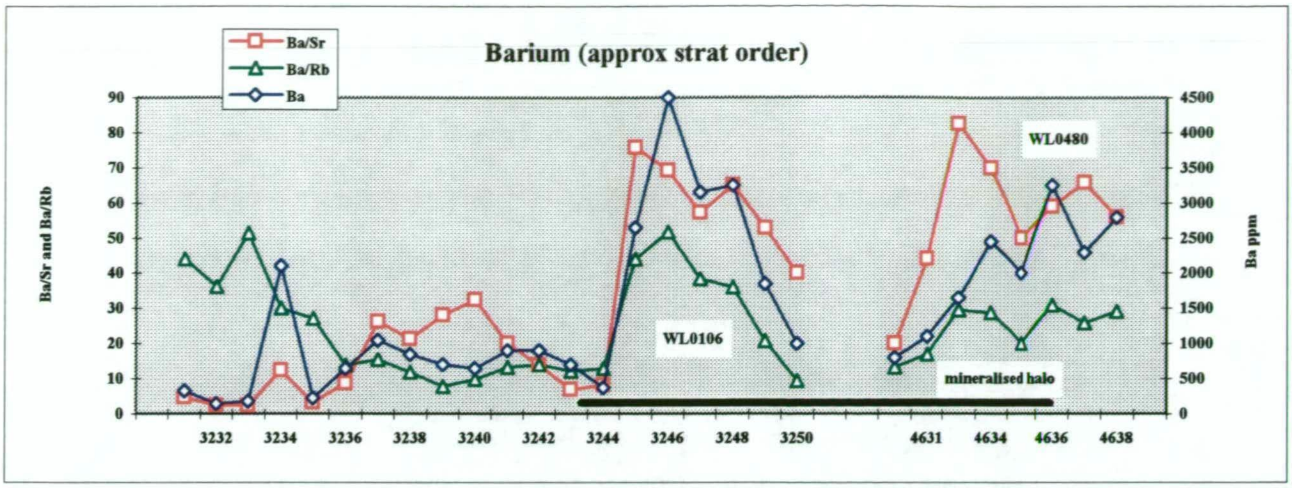
Barium (approx strat order)
Ba/Sr
Ba/Rb
Ba
Ba/Sr and Ba/Rb
Ba ppm
WL0106
WL0480
mineralised halo

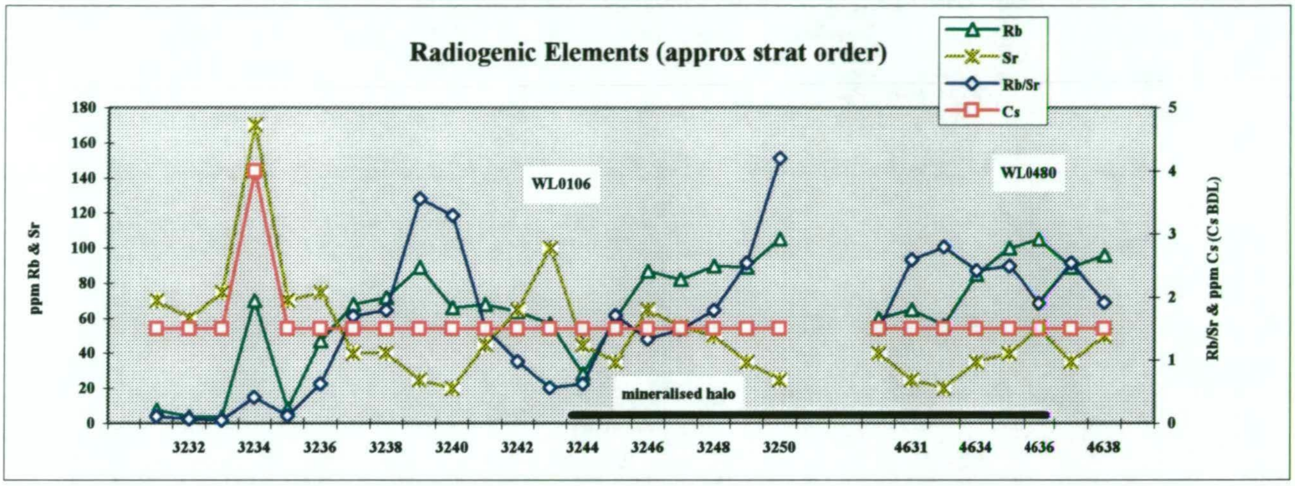
Radiogenic Elements (approx strat order)
Rb
Sr
Rb/Sr
Cs
ppm Rb & Sr
Rb/Sr & ppm Cs (Cs BDL)
WL0106
WL0480
mineralised halo

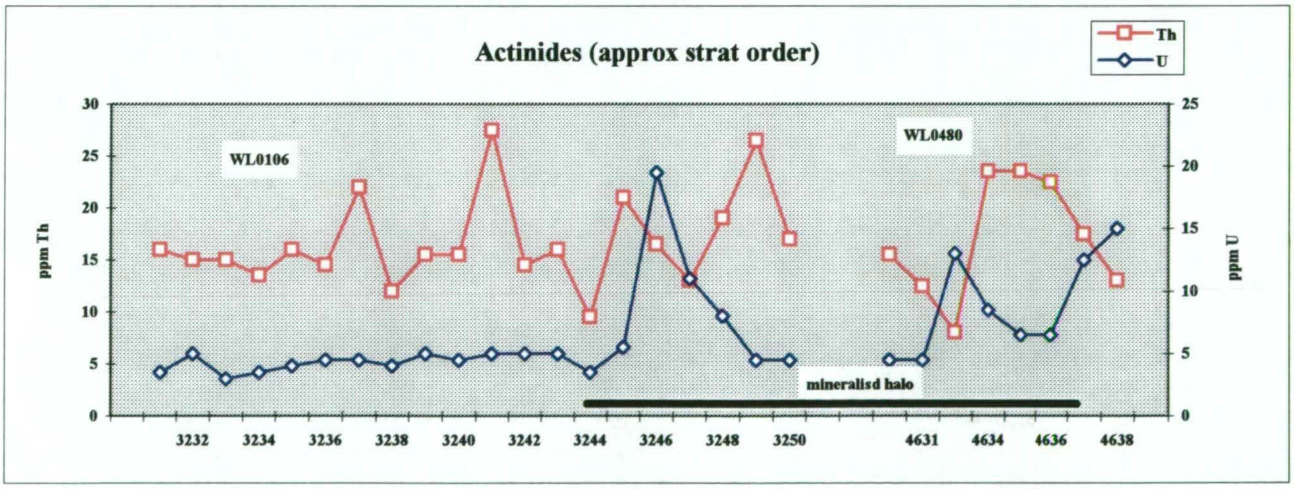
Actinides (approx strat order)
Th
U
ppm Th
ppm U
WL0106
WL0480
mineralisd halo

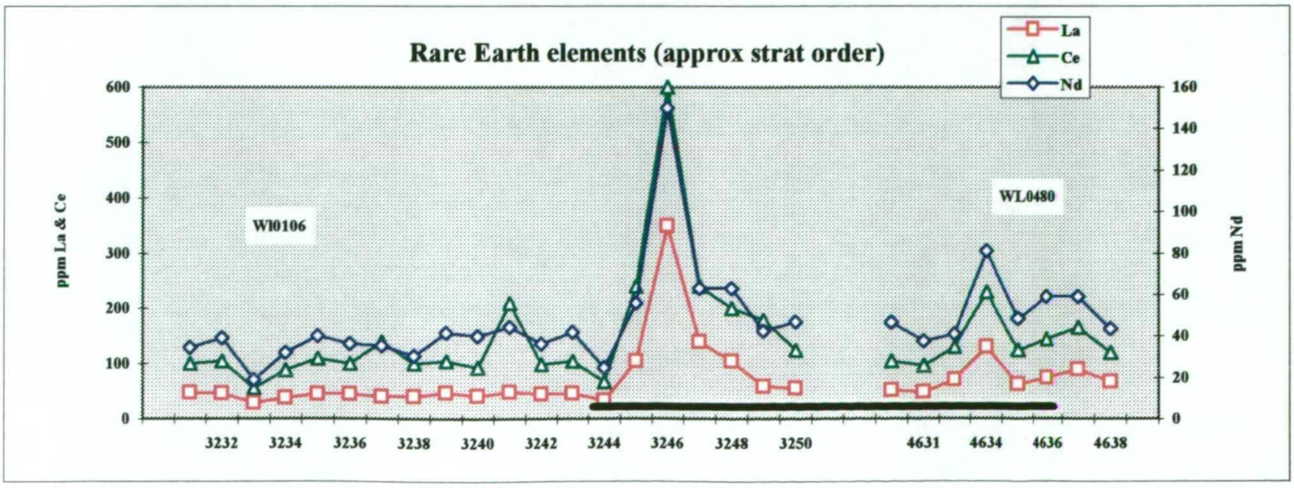
Rare Earth elements (approx strat order)
La
Ce
Nd
ppm La & Ce
ppm Nd
Wl0106
WL0480

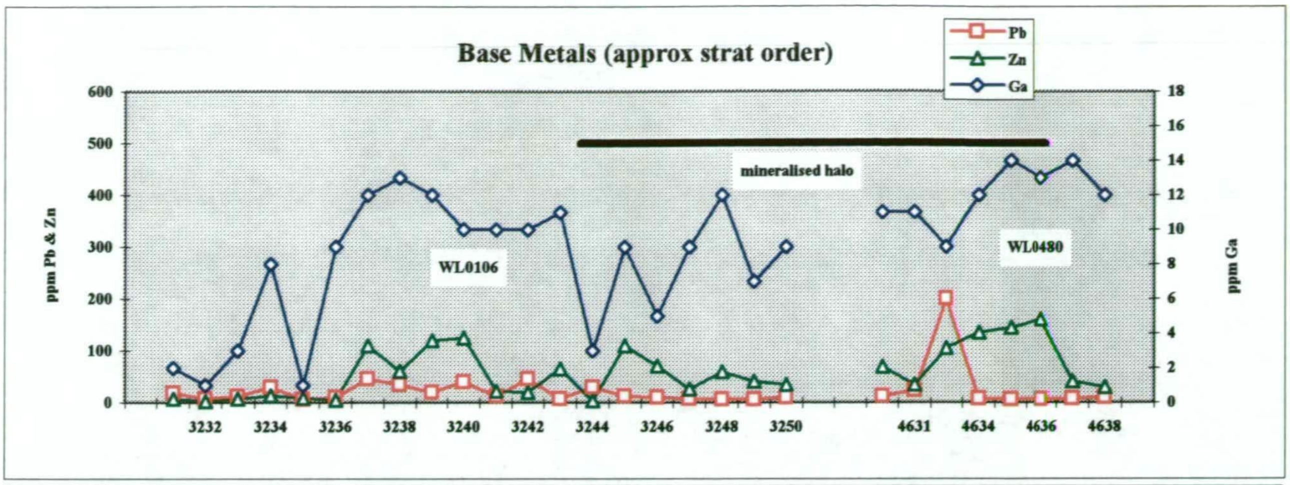

Base Metals (approx strat order)
Pb
Zn
Ga
ppm Pb & Zn
ppm Ga
mineralised halo
WL0106
WL0480
600
500
400
300
200
100
0
18
16
14
12
10
8
6
4
2
0
3232
3234
3236
3238
3240
3242
3244
3246
3248
3250
4631
4634
4636
4638

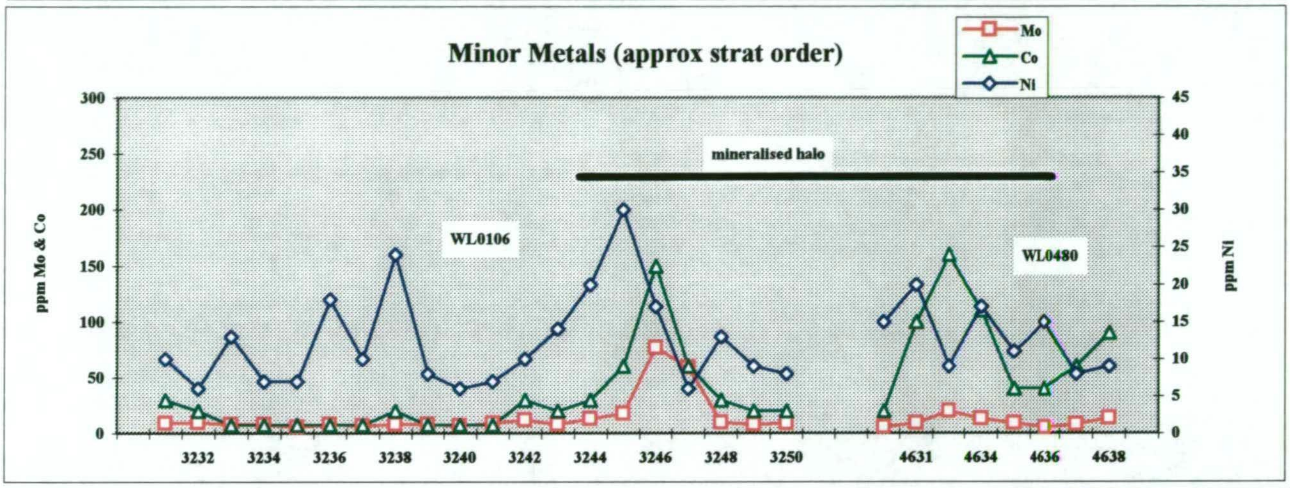

Minor Metals (approx strat order)
Mo
Co
Ni
ppm Mo & Co
ppm Ni
mineralised halo
WL0106
WL0480
300
250
200
150
100
50
0
45
40
35
30
25
20
15
10
5
0
3232
3234
3236
3238
3240
3242
3244
3246
3248
3250
4631
4634
4636
4638

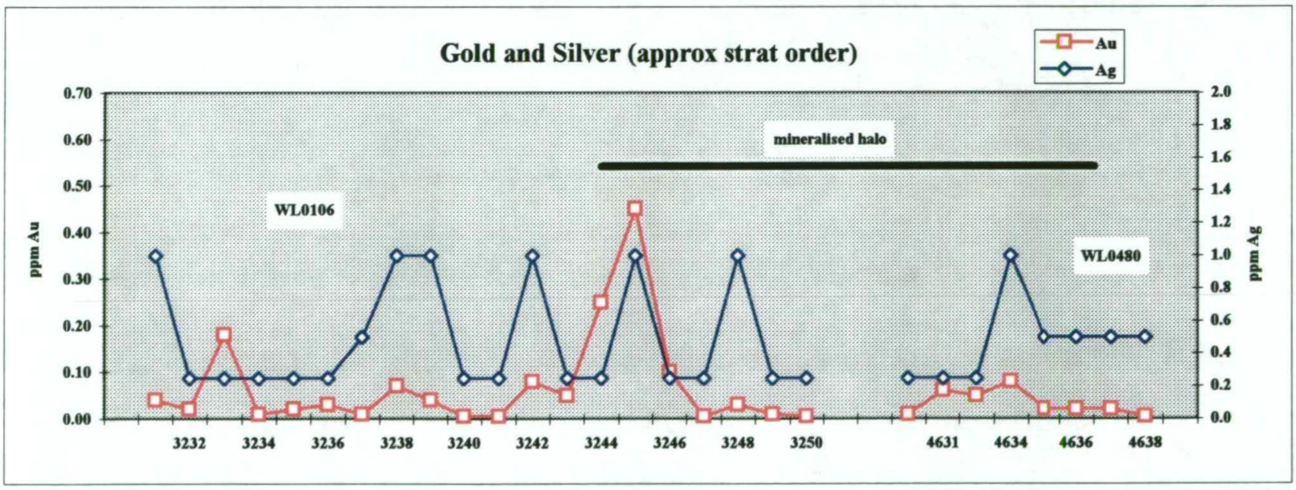

Gold and Silver (approx strat order)
Au
Ag
ppm Au
ppm Ag
mineralised halo
WL0106
WL0480
0.70
0.60
0.50
0.40
0.30
0.20
0.10
0.00
2.0
1.8
1.6
1.4
1.2
1.0
0.8
0.6
0.4
0.2
0.0
3232
3234
3236
3238
3240
3242
3244
3246
3248
3250
4631
4634
4636
4638

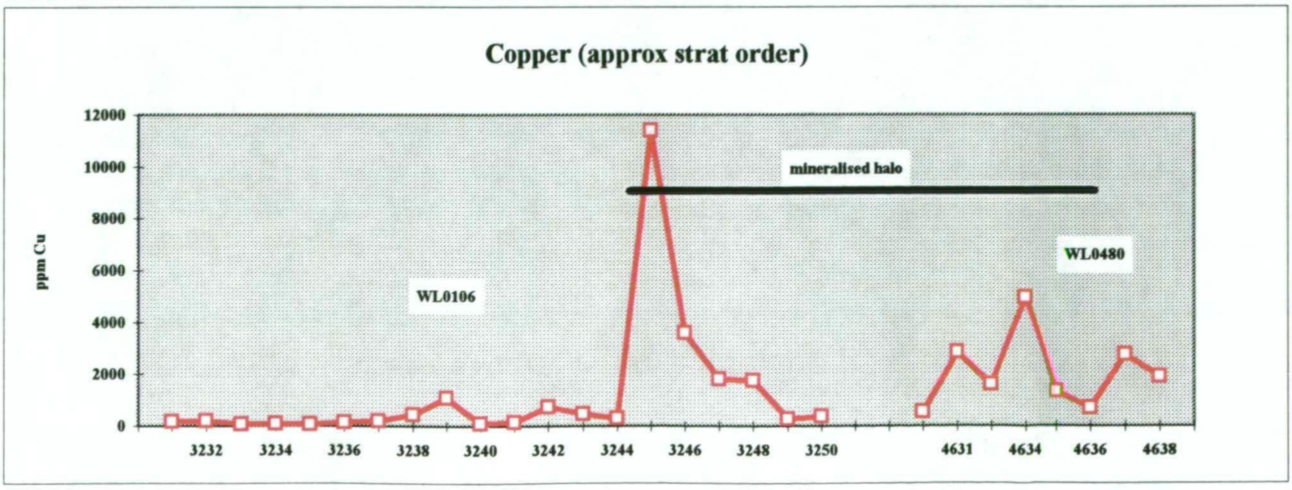

Copper (approx strat order)
ppm Cu
mineralised halo
WL0106
WL0480
12000
10000
8000
6000
4000
2000
0
3232
3234
3236
3238
3240
3242
3244
3246
3248
3250
4631
4634
4636
4638

Majors	Scheme	DL	Units	EXPA3231	EXPA3232	EXPA3233	EXPA3234	EXPA3235	EXPA3236
Al_2O_3	IC4E	0.01	%	9.15	7.54	12.7	12.2	12.6	13.1
CaO	IC4E	0.01	%	0.05	0.1	0.06	0.08	0.16	0.07
Fe_2O_3	IC4E	0.01	%	14.5	19.6	6.93	4.48	2.77	9.21
K2O	IC4E	0.01	%	0.25	0.15	0.15	2.8	0.32	1.85
MgO	IC4E	0.01	%	0.05	0.04	0.03	0.27	0.04	0.11
MnO	IC4E	0.01	%	<0.01	<0.01	<0.01	<0.01	<0.01	<0.01
Na_2O	IC4E	0.01	%	0.06	0.04	0.05	0.27	0.06	0.11
P_2O_5	IC4E	0.01	%	0.05	0.07	0.07	0.06	0.05	0.08
SiO_2	IC4E	0.01	%	65.2	57.8	71.1	75.2	78.1	68.3
TiO_2	IC4E	0.01	%	0.19	0.21	0.29	0.25	0.25	0.32
LOI	GRAV7	0.01	%	8.59	11.2	7.89	5.09	4.13	8.05
	Total			**98.09**	**96.75**	**99.27**	**100.7**	**98.48**	**101.2**
S	VOL2	0.05	%	12.4	14.7	7.65	4.15	2.55	5.2
C	GRAV4E	0.01	%	0.02	0.04	0.03	0.04	0.04	0.05
CO_2				0.07	0.15	0.11	0.15	0.15	0.18
Ishikawa Alteration Index				73.17	57.58	62.07	89.77	62.07	91.59
Chlorite Alteration Index				97.69	98.94	96.91	58.35	86.95	81.08
Manganese Alteration Index				24.39	44.12	35.48	4.06	35.59	5.77
Trace Elements									
V	IC4E	20	ppm	30	20	50	40	<20	60
Cr	IC4E	20	ppm	150	150	100	160	120	190
As	IC4M	15	ppm	30	80	20	20	<15	20
Ba	IC4M	10	ppm	330	145	180	2100	230	650
Bi	IC4M	3	ppm	4	6	<3	<3	<3	4
Cd	IC4M	3	ppm	<3	<3	<3	<3	<3	<3
Co	IC4M	15	ppm	30	20	<15	<15	<15	<15
Cs	IC4M	3	ppm	<3	<3	<3	4	<3	<3
Ga	IC4M	1	ppm	2	1	3	8	1	9
Hf	IC4M	1	ppm	5	4	6	5	6	5
In	IC4M	0.5	ppm	<0.5	<0.5	<0.5	<0.5	<0.5	<0.5
Mo	IC4M	2	ppm	9	10	8	8	6	8
Nb	IC4M	10	ppm	<10	<10	10	10	10	<10
Rb	IC4M	0.5	ppm	7.5	4	3.5	70	8.5	47
Sb	IC4M	1	ppm	3	4	3	3	10	3
Sr	IC4M	5	ppm	70	60	75	170	70	75
Ta	IC4M	2	ppm	<2	<2	<2	<2	<2	<2
Te	IC4M	5	ppm	<5	<5	<5	<5	<5	<5
Tl	IC4M	3	ppm	<3	<3	<3	<3	<3	<3
Th	IC4M	0.5	ppm	16	15	15	13.5	16	14.5
U	IC4M	0.5	ppm	3.5	5	3	3.5	4	4.5
W	IC4M	3	ppm	8	14	8	6	6	6
Y	IC4M	1	ppm	12	11	12	30	15	22
Zr	IC4M	15	ppm	170	170	220	190	240	180
La	IC4R	1	ppm	48	47	29	39	46	45
Ce	IC4R	1	ppm	100	105	56	88	110	100
Nd	IC4R	0.5	ppm	34.5	39	19	32	40	36.5
Cu	IC2E	1	ppm	180	190	79	95	70	150
Pb	IC2E	3	ppm	18	8	12	30	6	10
Zn	IC2E	1	ppm	7	3	7	14	9	5
Ni	IC2E	1	ppm	10	6	13	7	7	18
Ag	IC2E	0.5	ppm	1	<0.5	<0.5	<0.5	<0.5	<0.5
Au	FA1	0.01	ppm	0.04	0.02	0.18	0.01	0.02	0.03
Au Dp1	FA1	0.01	ppm				<0.01		

ROYAL THARSIS
WHOLE ROCK ANALYSES RESULTS

Appendix V
Table 1

Majors	Scheme	DL	Units	EXPA3237	EXPA3238	EXPA3239	EXPA3240	EXPA3241	EXPA3242
Al_2O_3	IC4E	0.01	%	13	11.6	11.4	11.1	10.9	9.87
CaO	IC4E	0.01	%	0.15	0.09	0.07	0.09	0.05	0.05
Fe_2O_3	IC4E	0.01	%	9.06	13.6	7.94	9.47	10.2	16.5
K2O	IC4E	0.01	%	2.77	2.55	2.82	2.37	2.56	2.37
MgO	IC4E	0.01	%	1.98	1.13	1.46	1.85	0.37	0.43
MnO	IC4E	0.01	%	0.21	0.04	0.2	0.21	0.03	0.04
Na_2O	IC4E	0.01	%	0.11	0.09	0.08	0.07	0.12	0.15
P_2O_5	IC4E	0.01	%	0.08	0.07	0.05	0.06	0.05	0.06
SiO_2	IC4E	0.01	%	67.1	61.3	70	69.8	66.6	60.3
TiO_2	IC4E	0.01	%	0.31	0.28	0.23	0.24	0.22	0.22
LOI	GRAV7	0.01	%	5.06	8.58	5.52	4.26	7.47	12.3
	Total			**99.83**	**99.33**	**99.77**	**99.52**	**98.57**	**102.29**
S	VOL2	0.05	%	3.2	6.05	5.6	1.95	8.5	8.5
C	GRAV4E	0.01	%	0.38	0.06	0.19	0.68	0.1	0.07
CO_2				1.39	0.22	0.70	2.49	0.37	0.26
Ishikawa Alteration Index				94.81	95.34	96.61	96.35	94.52	93.33
Chlorite Alteration Index				77.87	83.51	74.79	80.95	78.08	85.84
Manganese Alteration Index				43.86	15.65	41.65	47.30	11.55	15.15
Trace Elements									
V	IC4E	20	ppm	70	80	<20	40	20	40
Cr	IC4E	20	ppm	150	190	180	100	160	130
As	IC4M	15	ppm	20	30	20	<15	20	20
Ba	IC4M	10	ppm	1050	850	700	650	900	900
Bi	IC4M	3	ppm	<3	8	<3	4	<3	8
Cd	IC4M	3	ppm	<3	<3	<3	<3	<3	<3
Co	IC4M	15	ppm	<15	20	<15	<15	<15	30
Cs	IC4M	3	ppm	<3	<3	<3	<3	<3	<3
Ga	IC4M	1	ppm	12	13	12	10	10	10
Hf	IC4M	1	ppm	4	4	5	5	6	5
In	IC4M	0.5	ppm	<0.5	<0.5	<0.5	<0.5	<0.5	<0.5
Mo	IC4M	2	ppm	7	8	8	7	9	12
Nb	IC4M	10	ppm	<10	<10	<10	<10	<10	<10
Rb	IC4M	0.5	ppm	68	72	89	66	68	64
Sb	IC4M	1	ppm	3	3	3	4	2	3
Sr	IC4M	5	ppm	40	40	25	20	45	65
Ta	IC4M	2	ppm	<2	<2	<2	<2	<2	<2
Te	IC4M	5	ppm	<5	<5	<5	<5	<5	<5
Tl	IC4M	3	ppm	<3	<3	<3	<3	<3	<3
Th	IC4M	0.5	ppm	22	12	15.5	15.5	27.5	14.5
U	IC4M	0.5	ppm	4.5	4	5	4.5	5	5
W	IC4M	3	ppm	4	8	4	6	6	10
Y	IC4M	1	ppm	29	26	30	29	29	26
Zr	IC4M	15	ppm	170	160	210	170	190	170
La	IC4R	1	ppm	41	41	48	42	49	45
Ce	IC4R	1	ppm	140	100	105	93	210	99
Nd	IC4R	0.5	ppm	35.5	30.5	41.5	40	44.5	36.5
Cu	IC2E	1	ppm	190	450	1100	88	145	750
Pb	IC2E	3	ppm	46	34	20	40	12	46
Zn	IC2E	1	ppm	110	60	120	125	22	20
Ni	IC2E	1	ppm	10	24	8	6	7	10
Ag	IC2E	0.5	ppm	0.5	1	1	<0.5	<0.5	1
Au	FA1	0.01	ppm	0.01	0.07	0.04	<0.01	<0.01	0.08
Au Dp1	FA1	0.01	ppm						

ROYAL THARSIS
WHOLE ROCK ANALYSES RESULTS

Majors	Scheme	DL	Units	EXPA3243	EXPA3244	EXPA3245	EXPA3246	EXPA3247	EXPA3248
Al_2O_3	IC4E	0.01	%	11.3	5.8	10.9	12.2	11.7	13
CaO	IC4E	0.01	%	0.11	0.11	0.54	0.24	0.09	0.18
Fe_2O_3	IC4E	0.01	%	13.1	24.5	14.6	9.63	7.36	10.3
K2O	IC4E	0.01	%	2.12	1.23	2.58	3.48	3.58	3.43
MgO	IC4E	0.01	%	1.35	0.09	2.13	1.88	0.59	1.46
MnO	IC4E	0.01	%	0.04	<0.01	0.18	0.12	0.14	0.15
Na_2O	IC4E	0.01	%	0.19	0.08	0.04	0.05	0.07	0.07
P_2O_5	IC4E	0.01	%	0.1	0.1	0.38	0.18	0.09	0.12
SiO_2	IC4E	0.01	%	64.1	52.7	59.1	64.5	68.9	64.1
TiO_2	IC4E	0.01	%	0.28	0.26	0.32	0.35	0.27	0.35
LOI	GRAV7	0.01	%	7.28	13.5	6.76	6.01	4.94	6.15
	Total			**99.97**	**98.37**	**97.53**	**98.64**	**97.73**	**99.31**
S	VOL2	0.05	%	7.35	18.4	5	4.1	3.75	2.95
C	GRAV4E	0.01	%	0.07	0.04	0.59	0.15	0.24	0.44
CO_2				0.26	0.15	2.16	0.55	0.88	1.61
Ishikawa Alteration Index				92.04	87.42	89.04	94.87	96.30	95.14
Chlorite Alteration Index				85.05	94.41	85.35	74.92	66.40	75.40
Manganese Alteration Index				18.09	10.88	47.18	28.97	28.99	32.43
Trace Elements									
V	IC4E	20	ppm	80	70	140	100	40	90
Cr	IC4E	20	ppm	180	350	140	150	110	100
As	IC4M	15	ppm	20	30	20	20	20	<15
Ba	IC4M	10	ppm	700	370	2650	4500	3150	3250
Bi	IC4M	3	ppm	4	4	6	12	4	<3
Cd	IC4M	3	ppm	<3	<3	<3	<3	<3	<3
Co	IC4M	15	ppm	20	30	60	150	60	30
Cs	IC4M	3	ppm	<3	<3	<3	<3	<3	<3
Ga	IC4M	1	ppm	11	3	9	5	9	12
Hf	IC4M	1	ppm	4	4	4	5	5	5
In	IC4M	0.5	ppm	<0.5	<0.5	1	0.5	<0.5	<0.5
Mo	IC4M	2	ppm	8	13	18	77	59	10
Nb	IC4M	10	ppm	<10	<10	15	15	10	<10
Rb	IC4M	0.5	ppm	57	28.5	60	87	82	90
Sb	IC4M	1	ppm	33	3	2	3	2	2
Sr	IC4M	5	ppm	100	45	35	65	55	50
Ta	IC4M	2	ppm	<2	<2	<2	<2	<2	<2
Te	IC4M	5	ppm	<5	<5	<5	<5	<5	<5
Tl	IC4M	3	ppm	<3	<3	<3	<3	<3	<3
Th	IC4M	0.5	ppm	16	9.5	21	16.5	13	19
U	IC4M	0.5	ppm	5	3.5	5.5	19.5	11	8
W	IC4M	3	ppm	10	22	14	40	40	40
Y	IC4M	1	ppm	24	8	13	50	35	28
Zr	IC4M	15	ppm	160	140	160	180	210	180
La	IC4R	1	ppm	47	34	105	350	140	105
Ce	IC4R	1	ppm	105	67	240	600	240	200
Nd	IC4R	0.5	ppm	42	25	56	150	63	63
Cu	IC2E	1	ppm	480	300	11400	3600	1800	1750
Pb	IC2E	3	ppm	8	30	12	10	8	6
Zn	IC2E	1	ppm	65	4	110	70	26	59
Ni	IC2E	1	ppm	14	20	30	17	6	13
Ag	IC2E	0.5	ppm	<0.5	<0.5	1	<0.5	<0.5	1
Au	FA1	0.01	ppm	0.05	0.25	0.45	0.1	<0.01	0.03
Au Dp1	FA1	0.01	ppm			0.27			

ROYAL THARSIS
WHOLE ROCK ANALYSES RESULTS

Appendix V
Table 1

Majors	Scheme	DL	Units	EXPA3249	EXPA3250	EXPA4601	EXPA4602	EXPA4603	EXPA4604
Al_2O_3	IC4E	0.01	%	11.8	13.1	11.6	9.27	12.5	12.1
CaO	IC4E	0.01	%	0.07	0.1	0.93	0.69	0.97	0.81
Fe_2O_3	IC4E	0.01	%	7.58	4.8	18.1	20.4	12.8	10.2
K2O	IC4E	0.01	%	3.48	3.8	2.71	2.48	3.55	3.55
MgO	IC4E	0.01	%	0.62	0.67	2.26	1.48	2.14	1.68
MnO	IC4E	0.01	%	0.07	0.04	0.2	0.27	0.28	0.38
Na_2O	IC4E	0.01	%	0.08	0.08	0.06	0.08	0.13	0.13
P_2O_5	IC4E	0.01	%	0.08	0.08	0.55	0.43	0.22	0.31
SiO_2	IC4E	0.01	%	69.6	70.9	50.2	50.1	54.7	59.4
TiO_2	IC4E	0.01	%	0.27	0.32	0.36	0.26	0.53	0.32
LOI	GRAV7	0.01	%	4.89	3.74	9.82	10.4	8.83	6.54
	Total			**98.54**	**97.63**	**96.79**	**95.86**	**96.65**	**95.42**
S	VOL2	0.05	%	3.35	2.9	8.25	10.2	3.2	2.8
C	GRAV4E	0.01	%	0.25	0.09	0.65	0.69	1.5	1.17
CO_2				0.92	0.33	2.38	2.53	5.50	4.29
Ishikawa Alteration Index				96.47	96.13	83.39	83.72	83.80	84.76
Chlorite Alteration Index				67.64	56.25	87.01	88.57	78.77	74.69
Manganese Alteration Index				17.78	11.42	51.40	56.97	50.60	55.61
Trace Elements									
V	IC4E	20	ppm	40	40	160	110	170	90
Cr	IC4E	20	ppm	90	140	60	80	190	30
As	IC4M	15	ppm	<15	<15	20	60	20	<15
Ba	IC4M	10	ppm	1850	1000	2550	1300	4150	5300
Bi	IC4M	3	ppm	<3	16	6	18	22	16
Cd	IC4M	3	ppm	<3	<3	<3	<3	<3	<3
Co	IC4M	15	ppm	20	20	140	300	170	60
Cs	IC4M	3	ppm	<3	<3	<3	<3	<3	<3
Ga	IC4M	1	ppm	7	9	10	5	7	4
Hf	IC4M	1	ppm	5	5	5	4	4	5
In	IC4M	0.5	ppm	<0.5	<0.5	1	1	1	1
Mo	IC4M	2	ppm	8	9	17	85	200	125
Nb	IC4M	10	ppm	<10	<10	20	15	50	20
Rb	IC4M	0.5	ppm	89	105	66	58	88	91
Sb	IC4M	1	ppm	2	3	3	3	2	3
Sr	IC4M	5	ppm	35	25	55	30	80	105
Ta	IC4M	2	ppm	<2	<2	<2	<2	<2	<2
Te	IC4M	5	ppm	<5	<5	<5	<5	<5	<5
Tl	IC4M	3	ppm	<3	<3	<3	<3	<3	<3
Th	IC4M	0.5	ppm	26.5	17	21.5	19	23	18
U	IC4M	0.5	ppm	4.5	4.5	4.5	4.5	6.5	21
W	IC4M	3	ppm	18	14	44	34	44	38
Y	IC4M	1	ppm	22	29	16	15	10	20
Zr	IC4M	15	ppm	200	210	200	150	170	210
La	IC4R	1	ppm	60	56	92	175	240	320
Ce	IC4R	1	ppm	180	125	180	290	430	550
Nd	IC4R	0.5	ppm	42.5	47	61	82	105	130
Cu	IC2E	1	ppm	270	380	13900	28100	21400	10100
Pb	IC2E	3	ppm	6	10	16	30	32	20
Zn	IC2E	1	ppm	41	35	130	145	185	185
Ni	IC2E	1	ppm	9	8	45	38	16	13
Ag	IC2E	0.5	ppm	<0.5	<0.5	1.5	2	1.5	1
Au	FA1	0.01	ppm	0.01	<0.01	0.37	0.61	0.57	0.18
Au Dp1	FA1	0.01	ppm			0.45	0.71	0.47	

ROYAL THARSIS
WHOLE ROCK ANALYSES RESULTS

Appendix V
Table 1

Majors	Scheme	DL	Units	EXPA4605	EXPA4606	EXPA4607	EXPA4608	EXPA4609	EXPA4610
Al_2O_3	IC4E	0.01	%	13.1	12.1	12.5	12.1	11.2	11.2
CaO	IC4E	0.01	%	3.45	6.49	4.53	5.33	3.09	2.83
Fe_2O_3	IC4E	0.01	%	4.5	6.18	4.53	5.38	3.13	2.78
K2O	IC4E	0.01	%	3.56	3.24	3.47	3.11	3.13	3.28
MgO	IC4E	0.01	%	2.03	3.28	2.37	2.76	1.77	1.62
MnO	IC4E	0.01	%	0.21	0.33	0.27	0.27	0.2	0.16
Na_2O	IC4E	0.01	%	0.27	0.22	0.25	0.51	0.19	0.18
P_2O_5	IC4E	0.01	%	0.16	0.15	0.11	0.12	0.05	0.05
SiO_2	IC4E	0.01	%	63.7	55.1	62.2	60.2	69.9	70.2
TiO_2	IC4E	0.01	%	0.39	0.41	0.34	0.33	0.22	0.23
LOI	GRAV7	0.01	%	7.13	12.1	9.02	8.28	6.24	6.09
	Total			**98.5**	**99.6**	**99.59**	**98.39**	**99.12**	**98.62**
S	VOL2	0.05	%	0.35	0.4	0.2	0.1	0.15	<0.05
C	GRAV4E	0.01	%	1.44	2.47	2.19	1.62	1.41	1.22
CO_2				5.28	9.05	8.02	5.94	5.17	4.47
Ishikawa Alteration Index				60.04	49.28	54.99	50.13	59.90	61.95
Chlorite Alteration Index				61.35	71.87	63.41	67.74	58.01	54.36
Manganese Alteration Index				59.17	73.89	66.03	68.93	60.52	56.15
Trace Elements									
V	IC4E	20	ppm	60	110	70	70	<20	<20
Cr	IC4E	20	ppm	70	50	60	100	60	60
As	IC4M	15	ppm	<15	<15	<15	<15	<15	<15
Ba	IC4M	10	ppm	600	460	700	500	550	1000
Bi	IC4M	3	ppm	<3	<3	<3	10	<3	4
Cd	IC4M	3	ppm	<3	<3	<3	<3	<3	<3
Co	IC4M	15	ppm	<15	<15	<15	<15	<15	<15
Cs	IC4M	3	ppm	4	4	4	4	4	4
Ga	IC4M	1	ppm	11	10	12	12	12	12
Hf	IC4M	1	ppm	12	4	5	5	5	6
In	IC4M	0.5	ppm	<0.5	<0.5	<0.5	<0.5	<0.5	3
Mo	IC4M	2	ppm	8	4	4	4	6	4
Nb	IC4M	10	ppm	10	<10	10	<10	<10	10
Rb	IC4M	0.5	ppm	100	93	99	86	88	87
Sb	IC4M	1	ppm	3	4	3	3	3	3
Sr	IC4M	5	ppm	60	85	75	95	45	45
Ta	IC4M	2	ppm	<2	<2	<2	<2	<2	<2
Te	IC4M	5	ppm	<5	<5	<5	<5	<5	<5
Tl	IC4M	3	ppm	<3	<3	<3	<3	<3	<3
Th	IC4M	0.5	ppm	26	18.5	18.5	17	15	15.5
U	IC4M	0.5	ppm	5	5	5	5	5	4.5
W	IC4M	3	ppm	40	30	51	67	4	4
Y	IC4M	1	ppm	21	18	26	29	32	31
Zr	IC4M	15	ppm	550	170	210	200	220	240
La	IC4R	1	ppm	47	52	55	50	42	44
Ce	IC4R	1	ppm	150	110	115	115	105	105
Nd	IC4R	0.5	ppm	39	42.5	46.5	48.5	43.5	44
Cu	IC2E	1	ppm	140	55	135	54	52	15
Pb	IC2E	3	ppm	36	18	34	40	66	14
Zn	IC2E	1	ppm	62	62	89	79	55	43
Ni	IC2E	1	ppm	9	9	15	9	9	6
Ag	IC2E	0.5	ppm	<0.5	<0.5	<0.5	<0.5	<0.5	<0.5
Au	FA1	0.01	ppm	<0.01	0.01	0.05	0.01	<0.01	<0.01
Au Dp1	FA1	0.01	ppm						

Majors	Scheme	DL	Units	EXPA4611	EXPA4612	EXPA4613	EXPA4614	EXPA4615	EXPA4616
Al_2O_3	IC4E	0.01	%	12.1	11.8	12.4	10.8	12.4	11.2
CaO	IC4E	0.01	%	8.28	7.74	6.46	3.91	6.83	7.23
Fe_2O_3	IC4E	0.01	%	7.72	7.73	6.91	3.34	7.12	7.42
K2O	IC4E	0.01	%	2.75	2.34	2.37	2.96	2.65	2.22
MgO	IC4E	0.01	%	4.36	4.56	3.53	1.93	3.05	3.26
MnO	IC4E	0.01	%	0.34	0.33	0.21	0.16	0.2	0.25
Na_2O	IC4E	0.01	%	0.94	1.39	1.76	0.59	1.18	1
P_2O_5	IC4E	0.01	%	0.24	0.24	0.2	0.05	0.22	0.09
SiO_2	IC4E	0.01	%	48.6	50.3	55.3	70.1	55.4	56.2
TiO_2	IC4E	0.01	%	0.48	0.46	0.44	0.2	0.46	0.37
LOI	GRAV7	0.01	%	12.5	13	9.09	5.27	10.6	10.3
	Total			**98.31**	**99.89**	**98.67**	**99.31**	**100.11**	**99.54**
S	VOL2	0.05	%	0.1	0.05	0.1	0.05	<0.05	0.05
C	GRAV4E	0.01	%	3.03	3.16	2.12	1.11	2.78	2.16
CO_2				11.10	11.58	7.77	4.07	10.19	7.91
Ishikawa Alteration Index				43.54	43.04	41.78	52.08	41.58	39.97
Chlorite Alteration Index				75.39	75.53	70.24	58.16	71.17	75.53
Manganese Alteration Index				75.99	74.75	67.45	60.82	69.75	75.14
Trace Elements									
V	IC4E	20	ppm	160	160	140	<20	150	130
Cr	IC4E	20	ppm	180	170	190	100	160	200
As	IC4M	15	ppm	<15	<15	340	<15	<15	<15
Ba	IC4M	10	ppm	1300	460	750	900	550	310
Bi	IC4M	3	ppm	<3	<3	<3	<3	4	<3
Cd	IC4M	3	ppm	<3	<3	<3	<3	<3	<3
Co	IC4M	15	ppm	20	20	20	<15	20	20
Cs	IC4M	3	ppm	4	<3	4	4	4	4
Ga	IC4M	1	ppm	10	10	12	11	12	11
Hf	IC4M	1	ppm	3	3	4	5	3	3
In	IC4M	0.5	ppm	<0.5	<0.5	<0.5	<0.5	2.5	<0.5
Mo	IC4M	2	ppm	3	3	3	4	4	3
Nb	IC4M	10	ppm	<10	<10	<10	<10	<10	<10
Rb	IC4M	0.5	ppm	78	61	67	77	78	62
Sb	IC4M	1	ppm	4	3	10	10	3	6
Sr	IC4M	5	ppm	100	95	110	60	105	85
Ta	IC4M	2	ppm	<2	<2	<2	<2	<2	<2
Te	IC4M	5	ppm	<5	<5	<5	<5	<5	<5
Tl	IC4M	3	ppm	<3	<3	<3	<3	<3	<3
Th	IC4M	0.5	ppm	16	15.5	17.5	15.5	18.5	24
U	IC4M	0.5	ppm	4	4.5	4.5	4	5	3.5
W	IC4M	3	ppm	4	4	<3	<3	4	<3
Y	IC4M	1	ppm	20	18	24	29	18	20
Zr	IC4M	15	ppm	140	130	160	190	140	130
La	IC4R	1	ppm	57	54	60	42	58	35
Ce	IC4R	1	ppm	120	115	125	92	115	145
Nd	IC4R	0.5	ppm	47	51	53	41.5	48.5	34.5
Cu	IC2E	1	ppm	26	41	25	18	55	65
Pb	IC2E	3	ppm	8	10	10	50	105	10
Zn	IC2E	1	ppm	95	83	88	55	140	100
Ni	IC2E	1	ppm	32	28	20	4	24	32
Ag	IC2E	0.5	ppm	<0.5	<0.5	<0.5	<0.5	<0.5	<0.5
Au	FA1	0.01	ppm	0.03	0.02	<0.01	<0.01	0.01	<0.01
Au Dp1	FA1	0.01	ppm						

Majors	Scheme	DL	Units	EXPA4617	EXPA4618	EXPA4619	EXPA4620	EXPA4621	EXPA4622
Al_2O_3	IC4E	0.01	%	12.4	11.9	12.6	16.3	11.8	16.9
CaO	IC4E	0.01	%	5.77	5.98	5.02	4.39	4.63	4.03
Fe_2O_3	IC4E	0.01	%	7.87	5.98	5.29	6.47	5.59	9.65
K2O	IC4E	0.01	%	2.12	2.96	3.31	3.65	2.54	2.49
MgO	IC4E	0.01	%	4.21	3.09	2.44	2.32	2.44	2.5
MnO	IC4E	0.01	%	0.26	0.25	0.19	0.13	0.2	0.19
Na_2O	IC4E	0.01	%	1.79	0.58	0.72	1.66	1.19	2.53
P_2O_5	IC4E	0.01	%	0.21	0.08	0.24	0.09	0.08	0.17
SiO_2	IC4E	0.01	%	54.4	59.4	61.2	56.5	62.3	53.9
TiO_2	IC4E	0.01	%	0.46	0.35	0.37	0.5	0.35	0.63
LOI	GRAV7	0.01	%	9.32	7.77	7.92	6.76	7.09	6.03
	Total			**98.81**	**98.34**	**99.3**	**98.77**	**98.21**	**99.02**
S	VOL2	0.05	%	<0.05	0.05	<0.05	0.2	<0.05	0.65
C	GRAV4E	0.01	%	1.92	1.6	1.47	1.26	1.53	1.78
CO_2				7.03	5.86	5.39	4.62	5.61	6.52
Ishikawa Alteration Index				45.57	47.98	50.04	49.67	46.11	43.20
Chlorite Alteration Index				74.28	70.53	64.11	60.53	66.70	69.02
Manganese Alteration Index				68.16	70.55	63.20	51.73	64.00	54.16
Trace Elements									
V	IC4E	20	ppm	160	100	100	120	70	240
Cr	IC4E	20	ppm	160	110	160	60	40	150
As	IC4M	15	ppm	<15	<15	<15	<15	<15	<15
Ba	IC4M	10	ppm	600	380	650	430	420	280
Bi	IC4M	3	ppm	<3	<3	<3	<3	<3	<3
Cd	IC4M	3	ppm	<3	<3	<3	<3	<3	<3
Co	IC4M	15	ppm	20	<15	<15	30	<15	30
Cs	IC4M	3	ppm	4	4	4	4	4	<3
Ga	IC4M	1	ppm	11	12	12	16	12	16
Hf	IC4M	1	ppm	3	4	5	6	5	3
In	IC4M	0.5	ppm	<0.5	<0.5	<0.5	<0.5	<0.5	<0.5
Mo	IC4M	2	ppm	3	3	4	5	3	3
Nb	IC4M	10	ppm	<10	<10	<10	10	<10	<10
Rb	IC4M	0.5	ppm	64	83	100	110	78	74
Sb	IC4M	1	ppm	3	3	2	2	3	3
Sr	IC4M	5	ppm	100	75	75	75	65	95
Ta	IC4M	2	ppm	<2	<2	<2	<2	<2	<2
Te	IC4M	5	ppm	<5	<5	<5	<5	<5	<5
Tl	IC4M	3	ppm	<3	<3	<3	<3	<3	<3
Th	IC4M	0.5	ppm	25.5	12	23	16.5	12	11
U	IC4M	0.5	ppm	5	3	6	5	3.5	3
W	IC4M	3	ppm	<3	<3	<3	<3	<3	<3
Y	IC4M	1	ppm	19	25	25	31	28	20
Zr	IC4M	15	ppm	150	160	220	270	200	140
La	IC4R	1	ppm	58	32	69	43	32	34
Ce	IC4R	1	ppm	180	74	145	99	74	75
Nd	IC4R	0.5	ppm	50	33.5	63	46.5	37	34
Cu	IC2E	1	ppm	36	29	39	36	58	105
Pb	IC2E	3	ppm	6	170	12	12	26	16
Zn	IC2E	1	ppm	98	310	83	70	135	190
Ni	IC2E	1	ppm	24	11	24	18	13	42
Ag	IC2E	0.5	ppm	<0.5	<0.5	<0.5	<0.5	<0.5	<0.5
Au	FA1	0.01	ppm	0.02	<0.01	0.02	<0.01	0.01	<0.01
Au Dp1	FA1	0.01	ppm						

Majors	Scheme	DL	Units	EXPA4623	EXPA4624	EXPA4625	EXPA4626	EXPA4627	EXPA4628
Al_2O_3	IC4E	0.01	%	12.8	12.5	13.2	14.7	17.9	14.5
CaO	IC4E	0.01	%	3.2	4.5	2.48	4.47	0.93	0.13
Fe_2O_3	IC4E	0.01	%	5.67	5.87	6.13	7.54	9.37	12.3
K2O	IC4E	0.01	%	2.48	3.46	3.66	3.57	4.07	3.34
MgO	IC4E	0.01	%	2.4	2.47	1.8	2.8	2.33	0.26
MnO	IC4E	0.01	%	0.12	0.18	0.14	0.27	0.42	0.02
Na_2O	IC4E	0.01	%	1.89	0.22	0.29	0.27	0.27	0.32
P_2O_5	IC4E	0.01	%	0.2	0.07	0.09	0.22	0.17	0.11
SiO_2	IC4E	0.01	%	64.3	59.9	64.8	55.4	55.9	58.6
TiO_2	IC4E	0.01	%	0.36	0.33	0.33	0.5	0.61	0.39
LOI	GRAV7	0.01	%	5.69	8.13	5.92	7.68	6.66	9.68
	Total			**99.11**	**97.63**	**98.84**	**97.42**	**98.63**	**99.65**
S	VOL2	0.05	%	0.3	1.65	2.6	1.65	3.95	9
C	GRAV4E	0.01	%	0.86	2	1.1	1.83	0.43	0.13
CO_2				3.15	7.33	4.03	6.71	1.58	0.48
Ishikawa Alteration Index				48.95	55.68	66.34	57.34	84.21	88.89
Chlorite Alteration Index				63.19	67.81	64.94	71.40	71.26	75.58
Manganese Alteration Index				50.17	63.13	49.55	65.12	54.17	8.27
Trace Elements									
V	IC4E	20	ppm	80	70	50	160	170	80
Cr	IC4E	20	ppm	150	70	90	140	<20	20
As	IC4M	15	ppm	<15	<15	20	20	40	60
Ba	IC4M	10	ppm	750	800	1000	950	1200	750
Bi	IC4M	3	ppm	<3	<3	<3	<3	<3	8
Cd	IC4M	3	ppm	<3	<3	<3	<3	<3	<3
Co	IC4M	15	ppm	<15	<15	<15	30	20	20
Cs	IC4M	3	ppm	4	4	4	4	4	4
Ga	IC4M	1	ppm	13	13	14	14	18	18
Hf	IC4M	1	ppm	5	6	6	5	4	5
In	IC4M	0.5	ppm	<0.5	<0.5	<0.5	<0.5	<0.5	<0.5
Mo	IC4M	2	ppm	3	5	3	3	3	4
Nb	IC4M	10	ppm	10	10	10	<10	<10	10
Rb	IC4M	0.5	ppm	84	105	110	105	115	91
Sb	IC4M	1	ppm	3	3	3	7	4	6
Sr	IC4M	5	ppm	80	95	75	80	50	70
Ta	IC4M	2	ppm	<2	<2	<2	<2	<2	<2
Te	IC4M	5	ppm	<5	<5	<5	<5	<5	<5
Tl	IC4M	3	ppm	<3	<3	<3	<3	<3	<3
Th	IC4M	0.5	ppm	20.5	15	19	18.5	13.5	16
U	IC4M	0.5	ppm	6	4.5	5.5	5.5	3.5	5
W	IC4M	3	ppm	<3	16	24	14	12	16
Y	IC4M	1	ppm	29	29	33	25	28	34
Zr	IC4M	15	ppm	230	240	250	190	180	220
La	IC4R	1	ppm	67	40	52	66	41	45
Ce	IC4R	1	ppm	140	90	115	135	92	98
Nd	IC4R	0.5	ppm	59	40.5	51	55	43.5	46
Cu	IC2E	1	ppm	36	96	110	130	125	280
Pb	IC2E	3	ppm	10	240	160	53	40	64
Zn	IC2E	1	ppm	125	350	240	220	260	180
Ni	IC2E	1	ppm	25	20	25	30	10	9
Ag	IC2E	0.5	ppm	<0.5	<0.5	<0.5	<0.5	0.5	0.5
Au	FA1	0.01	ppm	<0.01	0.01	0.01	<0.01	<0.01	<0.01
Au Dp1	FA1	0.01	ppm						

ROYAL THARSIS
WHOLE ROCK ANALYSES RESULTS

Majors	Scheme	DL	Units	EXPA4629	EXPA4630	EXPA4631	EXPA4632	EXPA4634	EXPA4635
Al_2O_3	IC4E	0.01	%	15.2	10.7	9.95	7.09	13.2	13.8
CaO	IC4E	0.01	%	0.65	0.52	0.29	0.17	1.03	1.82
Fe_2O_3	IC4E	0.01	%	7.78	13.9	19.5	6.79	10.1	8.32
K2O	IC4E	0.01	%	3.84	2.17	2.53	2	3.11	3.59
MgO	IC4E	0.01	%	0.66	1.94	1.18	0.91	2.69	3.03
MnO	IC4E	0.01	%	0.13	0.12	0.09	0.58	0.16	0.25
Na_2O	IC4E	0.01	%	0.34	0.07	0.06	0.04	0.04	0.06
P_2O_5	IC4E	0.01	%	0.07	0.09	0.16	0.06	0.2	0.18
SiO_2	IC4E	0.01	%	63.5	62.6	54.9	76.7	62.8	61.4
TiO_2	IC4E	0.01	%	0.33	0.28	0.27	0.44	0.38	0.44
LOI	GRAV7	0.01	%	6.69	6.3	9.32	4.42	5.45	7.25
	Total			**99.19**	**98.69**	**98.25**	**99.2**	**99.16**	**100.14**
S	VOL2	0.05	%	5.75	6.6	7.3	2.4	1.95	0.65
C	GRAV4E	0.01	%	0.67	0.44	0.26	0.34	0.5	1.27
CO_2				2.45	1.61	0.95	1.25	1.83	4.65
Ishikawa Alteration Index				81.97	87.45	91.38	93.27	84.43	77.88
Chlorite Alteration Index				64.70	86.58	87.85	77.48	78.90	74.23
Manganese Alteration Index				31.81	43.43	31.48	74.53	45.50	54.20
Trace Elements									
V	IC4E	20	ppm	30	60	80	40	110	100
Cr	IC4E	20	ppm	30	240	220	180	60	40
As	IC4M	15	ppm	30	20	40	20	20	20
Ba	IC4M	10	ppm	1300	800	1100	1650	2450	2000
Bi	IC4M	3	ppm	4	<3	6	<3	<3	<3
Cd	IC4M	3	ppm	<3	<3	<3	<3	<3	<3
Co	IC4M	15	ppm	<15	20	100	160	110	40
Cs	IC4M	3	ppm	4	<3	<3	<3	<3	<3
Ga	IC4M	1	ppm	16	11	11	9	12	14
Hf	IC4M	1	ppm	7	4	3	4	5	5
In	IC4M	0.5	ppm	<0.5	<0.5	<0.5	<0.5	<0.5	<0.5
Mo	IC4M	2	ppm	5	6	9	20	13	9
Nb	IC4M	10	ppm	15	<10	<10	<10	15	10
Rb	IC4M	0.5	ppm	105	60	65	56	85	100
Sb	IC4M	1	ppm	5	5	2	2	2	2
Sr	IC4M	5	ppm	75	40	25	20	35	40
Ta	IC4M	2	ppm	<2	<2	<2	<2	<2	<2
Te	IC4M	5	ppm	<5	<5	<5	<5	<5	<5
Tl	IC4M	3	ppm	<3	<3	<3	<3	<3	<3
Th	IC4M	0.5	ppm	20.5	15.5	12.5	8	23.5	23.5
U	IC4M	0.5	ppm	6.5	4.5	4.5	13	8.5	6.5
W	IC4M	3	ppm	20	12	16	14	65	59
Y	IC4M	1	ppm	44	27	15	30	21	17
Zr	IC4M	15	ppm	280	180	150	150	210	210
La	IC4R	1	ppm	58	52	49	71	130	63
Ce	IC4R	1	ppm	130	105	97	130	230	125
Nd	IC4R	0.5	ppm	60	46.5	37.5	41	81	48.5
Cu	IC2E	1	ppm	300	550	2850	1600	4950	1350
Pb	IC2E	3	ppm	79	12	24	200	8	6
Zn	IC2E	1	ppm	210	69	34	105	135	145
Ni	IC2E	1	ppm	7	15	20	9	17	11
Ag	IC2E	0.5	ppm	<0.5	<0.5	<0.5	<0.5	1	0.5
Au	FA1	0.01	ppm	0.03	0.01	0.06	0.05	0.08	0.02
Au Dp1	FA1	0.01	ppm		0.01				

ROYAL THARSIS
WHOLE ROCK ANALYSES RESULTS

Appendix V
Table 1

Majors	Scheme	DL	Units	EXPA4636	EXPA4637	EXPA4638	EXPA4639	EXPA4640	EXPA4641
Al_2O_3	IC4E	0.01	%	13.8	12.1	12.7	16.2	12.1	12.1
CaO	IC4E	0.01	%	0.56	0.42	0.49	1.58	0.15	0.04
Fe_2O_3	IC4E	0.01	%	12.5	7.91	7.09	10.5	14.2	7.29
K2O	IC4E	0.01	%	3.71	3.61	3.87	3.94	3.39	3.86
MgO	IC4E	0.01	%	2.7	1.03	1.08	1.9	1.24	0.59
MnO	IC4E	0.01	%	0.28	0.07	0.06	0.45	0.08	0.03
Na_2O	IC4E	0.01	%	0.09	0.08	0.07	0.26	0.05	0.06
P_2O_5	IC4E	0.01	%	0.22	0.09	0.08	0.14	0.15	0.07
SiO_2	IC4E	0.01	%	57.4	69.5	69.5	55.5	61.7	71.2
TiO_2	IC4E	0.01	%	0.45	0.31	0.28	0.52	0.3	0.26
LOI	GRAV7	0.01	%	8.73	5.21	5.44	8.73	6.01	4.99
	Total			**100.44**	**100.33**	**100.66**	**99.72**	**99.37**	**100.49**
S	VOL2	0.05	%	1.95	3.25	3.6	5.35	5.25	4.7
C	GRAV4E	0.01	%	1.56	0.38	0.27	0.63	0.14	0.05
CO_2				5.72	1.39	0.99	2.31	0.51	0.18
Ishikawa Alteration Index				90.79	90.27	89.84	76.04	95.86	97.80
Chlorite Alteration Index				78.59	68.83	65.44	72.99	80.29	64.59
Manganese Alteration Index				46.93	23.28	21.67	59.14	21.64	7.98
Trace Elements									
V	IC4E	20	ppm	130	50	40	140	80	<20
Cr	IC4E	20	ppm	40	<20	50	<20	<20	<20
As	IC4M	15	ppm	20	20	<15	50	<15	<15
Ba	IC4M	10	ppm	3250	2300	2800	1500	2000	1700
Bi	IC4M	3	ppm	<3	4	<3	<3	<3	<3
Cd	IC4M	3	ppm	<3	<3	<3	<3	<3	<3
Co	IC4M	15	ppm	40	60	90	30	100	70
Cs	IC4M	3	ppm	<3	<3	<3	4	<3	<3
Ga	IC4M	1	ppm	13	14	12	17	13	9
Hf	IC4M	1	ppm	4	4	6	4	5	5
In	IC4M	0.5	ppm	<0.5	<0.5	<0.5	<0.5	<0.5	<0.5
Mo	IC4M	2	ppm	5	8	14	3	6	16
Nb	IC4M	10	ppm	<10	10	15	<10	<10	10
Rb	IC4M	0.5	ppm	105	89	96	110	90	100
Sb	IC4M	1	ppm	3	5	2	3	4	3
Sr	IC4M	5	ppm	55	35	50	55	35	25
Ta	IC4M	2	ppm	<2	<2	<2	<2	<2	<2
Te	IC4M	5	ppm	<5	<5	<5	<5	<5	<5
Tl	IC4M	3	ppm	<3	<3	<3	<3	<3	<3
Th	IC4M	0.5	ppm	22.5	17.5	13	12.5	20.5	18.5
U	IC4M	0.5	ppm	6.5	12.5	15	3.5	3.5	18
W	IC4M	3	ppm	71	100	130	48	110	105
Y	IC4M	1	ppm	19	25	27	32	20	61
Zr	IC4M	15	ppm	180	200	250	180	210	230
La	IC4R	1	ppm	74	90	67	34	90	200
Ce	IC4R	1	ppm	145	165	120	75	160	360
Nd	IC4R	0.5	ppm	59	59	43.5	38	58	115
Cu	IC2E	1	ppm	700	2750	1900	130	3750	370
Pb	IC2E	3	ppm	6	8	10	190	8	6
Zn	IC2E	1	ppm	160	41	30	600	90	18
Ni	IC2E	1	ppm	15	8	9	8	8	<1
Ag	IC2E	0.5	ppm	0.5	0.5	0.5	1	1.5	<0.5
Au	FA1	0.01	ppm	0.02	0.02	<0.01	0.01	0.09	0.03
Au Dp1	FA1	0.01	ppm			<0.01			

ROYAL THARSIS
WHOLE ROCK ANALYSES: SAMPLE LOCATIONS

Appendix V
Table 2

Sample No	Drill Hole	From	To	ft or m	315 GRL Grid (mid-pt) Northing	315 GRL Grid (mid-pt) Easting	315 GRL Grid (mid-pt) RL	AMG (mid-pt) Northing	AMG (mid-pt) Easting	AMG (mid-pt) RL
EXPA3231	WL0106	0	50	ft	7778.11	3662.44	2416.24	5,337,962.03	391,906.29	416.24
EXPA3232	WL0106	50	100	ft	7777.08	3670.46	2403.01	5,337,956.44	391,912.12	403.01
EXPA3233	WL0106	100	150	ft	7776.68	3678.60	2390.43	5,337,951.27	391,918.43	390.43
EXPA3234	WL0106	150	200	ft	7776.99	3687.07	2378.05	5,337,946.48	391,925.42	378.05
EXPA3235	WL0106	200	250	ft	7778.09	3696.09	2365.50	5,337,942.00	391,933.33	365.50
EXPA3236	WL0106	250	300	ft	7780.00	3705.32	2353.19	5,337,938.05	391,941.87	353.19
EXPA3237	WL0106	300	350	ft	7782.62	3714.38	2341.53	5,337,934.77	391,950.71	341.53
EXPA3238	WL0106	350	400	ft	7786.12	3723.44	2330.10	5,337,932.19	391,960.07	330.10
EXPA3239	WL0106	400	450	ft	7790.64	3732.74	2318.56	5,337,930.29	391,970.24	318.56
EXPA3240	WL0106	450	500	ft	7797.15	3743.55	2305.04	5,337,929.10	391,982.80	305.04
EXPA3241	WL0106	500	550	ft	7801.51	3750.52	2296.30	5,337,928.45	391,990.99	296.30
EXPA3242	WL0106	550	600	ft	7806.70	3759.31	2285.32	5,337,927.40	392,001.14	285.32
EXPA3243	WL0106	600	650	ft	7812.07	3768.39	2273.98	5,337,926.31	392,011.63	273.98
EXPA3244	WL0106	650	700	ft	7817.26	3777.17	2263.00	5,337,925.26	392,021.78	263.00
EXPA3245	WL0106	700	750	ft	7822.63	3786.26	2251.65	5,337,924.17	392,032.26	251.65
EXPA3246	WL0106	750	800/805	ft	7827.82	3795.04	2240.67	5,337,923.12	392,042.41	240.67
EXPA3247	WL0106	800	850	ft	7833.19	3804.12	2229.32	5,337,922.03	392,052.90	229.32
EXPA3248	WL0106	850	900	ft	7838.38	3812.91	2218.34	5,337,920.99	392,063.05	218.34
EXPA3249	WL0106	900	950	ft	7843.75	3821.99	2207.00	5,337,919.89	392,073.54	207.00
EXPA3250	WL0106	950	1012	ft	7849.63	3831.95	2194.55	5,337,918.70	392,085.05	194.55
EXPA4601	WL0421	0	16	m	7947.45	3856.41	2195.09	5,337,982.75	392,162.87	195.09
EXPA4602	WL0421	16	32	m	7949.12	3872.08	2192.31	5,337,974.78	392,176.46	192.31
EXPA4603	WL0421	32	48	m	7950.80	3887.75	2189.53	5,337,966.81	392,190.05	189.53
EXPA4604	WL0421	48	65.2	m	7952.52	3903.91	2186.67	5,337,958.59	392,204.06	186.67
EXPA4605	WL530A	0	16	m	7952.21	3551.90	1984.49	5,337,167.67	392,921.00	-15.51
EXPA4606	WL530A	16	32	m	7949.37	3539.61	1974.65	5,337,172.70	392,909.43	-25.35
EXPA4607	WL530A	32	48	m	7946.48	3527.09	1965.12	5,337,177.82	392,897.65	-34.88
EXPA4608	WL530A	48	64	m	7943.65	3514.17	1956.13	5,337,182.83	392,885.59	-43.87
EXPA4609	WL530A	64	80	m	7941.00	3500.57	1948.13	5,337,189.20	392,873.08	-51.87
EXPA4610	WL530A	80	96	m	7938.40	3486.39	1941.20	5,337,195.54	392,860.14	-58.80
EXPA4611	WL530A	96	112	m	7936.08	3471.59	1935.58	5,337,202.25	392,847.16	-64.42
EXPA4612	WL530A	112	128	m	7934.37	3456.42	1930.81	5,337,210.12	392,833.67	-69.19
EXPA4613	WL530A	128	144	m	7933.16	3441.00	1926.74	5,337,218.32	392,820.55	-73.26
EXPA4614	WL530A	144	160	m	7932.07	3425.47	1923.05	5,337,226.68	392,807.42	-76.95
EXPA4615	WL530A	160	176	m	7931.09	3409.82	1919.85	5,337,235.20	392,794.24	-80.15
EXPA4616	WL530A	176	192	m	7930.26	3394.07	1917.18	5,337,243.89	392,781.11	-82.82
EXPA4617	WL530A	192	208	m	7929.43	3378.29	1914.64	5,337,252.61	392,767.94	-85.36
EXPA4618	WL530A	208	224	m	7928.64	3362.50	1912.21	5,337,261.37	392,754.78	-87.79
EXPA4619	WL530A	224	240	m	7927.92	3346.68	1909.92	5,337,270.20	392,741.64	-90.08
EXPA4620	WL530A	240	256	m	7927.26	3330.84	1907.77	5,337,279.09	392,728.52	-92.23
EXPA4621	WL530A	256	272	m	7926.66	3314.98	1905.72	5,337,288.04	392,715.42	-94.28
EXPA4622	WL530A	272	288	m	7926.11	3299.11	1903.78	5,337,297.04	392,702.34	-96.22
EXPA4623	WL530A	288	303.9	m	7925.65	3283.72	1901.96	5,337,305.81	392,689.70	-98.04
EXPA4624	WL0531	0	16	m	7959.58	3553.45	1984.47	5,337,172.67	392,926.63	-15.53
EXPA4625	WL0531	16	32	m	7964.84	3565.12	1974.87	5,337,169.96	392,939.13	-25.13
EXPA4626	WL0531	32	48	m	7970.00	3577.37	1965.97	5,337,166.82	392,952.05	-34.03
EXPA4627	WL0531	48	64	m	7974.99	3590.03	1957.54	5,337,163.30	392,965.18	-42.46
EXPA4639	WL0531	64	80	m	7979.93	3602.85	1949.35	5,337,159.65	392,978.42	-50.66
EXPA4628	WL0531	80	96	m	7984.85	3615.68	1941.16	5,337,155.97	392,991.67	-58.84
EXPA4629	WL0531	96	119.9	m	7991.01	3631.73	1930.94	5,337,151.38	393,008.23	-69.06
EXPA4630	WL0480	120	136	m	7828.90	3694.36	2014.71	5,337,983.86	392,962.15	14.71
EXPA4631	WL0480	136	152	m	7832.94	3709.64	2012.20	5,337,978.02	392,976.83	12.20
EXPA4634	WL0480	152	168	m	7836.98	3724.92	2009.70	5,337,972.18	392,991.51	9.70
EXPA4635	WL0480	168	184	m	7841.01	3740.20	2007.20	5,337,966.34	393,006.19	7.20
EXPA4636	WL0480	184	200	m	7845.05	3755.48	2004.70	5,337,960.50	393,020.87	4.69
EXPA4637	WL0480	200	216	m	7849.09	3770.75	2002.19	5,337,954.66	393,035.55	2.19
EXPA4638	WL0480	216	232	m	7853.13	3786.03	1999.69	5,337,948.82	393,050.23	-0.31
EXPA4632	WL0531	232	249.1	m	7857.30	3801.79	1997.11	5,337,942.80	393,065.37	-2.89
EXPA4640	WL0290	0	50	ft	8046.41	4103.34	2481.78	5,337,915.44	392,420.15	481.78
EXPA4641	WL0290	50	101	ft	8046.56	4118.81	2480.89	5,337,906.35	392,432.68	480.89

ROYAL THARSIS
WHOLE ROCK ANALYSES
ANALYTICAL METHODS

Scheme	Detection Limit	Units	Elements	Method
IC4E	0.01	%	Majors: Al_2O_3, CaO, Fe_2O_3, K_2O, Na_2O, MgO,MnO, P_2O_5, SO_2, TiO_2,	Total fusion followed by XRF analysis
IC4E		ppm	Trace elements: V (20), Cr (20)	Whole rock fusion followed by ICP-OES
IC4M		ppm	Trace elements: As(15),Ba(10),Bi(3),Cd(3),Co(15), Cs(3),Ga(1),Hf(1),In(0.5),Mo(2), Nb(10),Rb(0.5),Sb(1),Sr(5),Ta(2), Te(5),Tl(3),Th(0.5),U(0.5),W(3), Y(1),Zr(15)	Whole rock fusion followed by ICP-MS measurements
IC4R		ppm	Rare earth elements: La (1), Ce (1), Nd (0.5)	Whole rock fusion followed by ICP-MS measurements
IC2E		ppm	Copper and base metals: Cu (1), Ag (0.5), Pb (3), Zn (1), Ni (1)	Aqua Regia digest followed by ICP-OES measurement
FA1	0.01	ppm	Gold	Fire assay: fusion with litharge and flux, cupellation, aqua regia digest, and AAS determination.
GRAV7	0.01	%	LOI	Gravimetric determination of loss on ignition
VOL2	0.05	%	Sulphur	Combustion with evolution and measurement of SO_2 by IR spectrophotemetry
GRAV4E	0.01	%	Carbon	Gravimetric. Absolute measurement of total carbon and calculation of CO_2

Note:
All samples analysed at Amdel Laboratories Limited, Adelaide, SA

ROYAL THARSIS
WHOLE ROCK ANALYSES - DATASET STATISTICS

Appendix V
Table 4

Descriptive Statistics	*Al2O3*	*CaO*	*Fe2O3*	*K2O*	*MgO*	*MnO*
Mean	12.163	2.088	9.300	2.822	1.777	0.171
Standard Error	0.267	0.321	0.601	0.120	0.147	0.016
Median	12.1	0.67	7.825	2.96	1.865	0.17
Mode	12.1	0.05	10.2	2.37	0.04	0.005
Standard Deviation	2.068	2.484	4.656	0.933	1.138	0.125
Sample Variance	4.276	6.168	21.680	0.871	1.295	0.016
Kurtosis	2.283	-0.371	1.341	1.965	-0.340	0.824
Skewness	-0.143	0.993	1.200	-1.374	0.296	0.746
Range	12.1	8.24	21.73	3.92	4.53	0.575
Minimum	5.8	0.04	2.77	0.15	0.03	0.005
Maximum	17.9	8.28	24.5	4.07	4.56	0.58
Sum	729.77	125.28	557.98	169.3	106.64	10.235
Count	60	60	60	60	60	60
% results BDL	0	0	0	0	0	12
Confidence Level (95.000%)	0.523	0.628	1.178	0.236	0.288	0.032

Descriptive Statistics	*Na2O*	*P2O5*	*SiO2*	*TiO2*	*V*	*Cr*
Mean	0.395	0.139	62.160	0.345	82.500	114.333
Standard Error	0.073	0.013	0.902	0.013	6.705	8.907
Median	0.13	0.095	61.95	0.33	75	110
Mode	0.06	0.05	64.1	0.32	40	150
Standard Deviation	0.566	0.099	6.990	0.101	51.933	68.997
Sample Variance	0.320	0.010	48.855	0.010	2697.034	4760.565
Kurtosis	3.786	5.094	-0.620	0.282	-0.005	0.750
Skewness	2.095	1.998	0.157	0.804	0.623	0.535
Range	2.49	0.5	29.5	0.44	230	340
Minimum	0.04	0.05	48.6	0.19	10	10
Maximum	2.53	0.55	78.1	0.63	240	350
Sum	23.7	8.31	3729.6	20.67	4950	6860
Count	60	60	60	60	60	60
% results BDL	0	0	0	0	10	8
Confidence Level (95.000%)	0.143	0.025	1.769	0.026	13.141	17.458

Descriptive Statistics	*As*	*Ba*	*Bi*	*Cd*	*Co*	*Cs*
Mean	23.667	1309.917	3.958	1.500	39.917	2.542
Standard Error	5.696	145.189	0.583	0.000	6.884	0.160
Median	20	900	1.5	1.5	20	1.5
Mode	7.5	650	1.5	1.5	7.5	1.5
Standard Deviation	44.124	1124.629	4.516	0.000	53.320	1.243
Sample Variance	1946.921	1264790	20.392	0.000	2843.001	1.545
Kurtosis	46.490	2.599	5.623	-	9.381	-1.946
Skewness	6.498	1.661	2.391	-	2.771	0.347
Range	332.5	5155	20.5	0	292.5	2.5
Minimum	7.5	145	1.5	1.5	7.5	1.5
Maximum	340	5300	22	1.5	300	4
Sum	1420	78595	237.5	90	2395	152.5
Count	60	60	60	60	60	60
% results BDL	47	0	62	100	37	58
Confidence Level (95.000%)	11.165	284.565	1.143	-	13.492	0.314

ROYAL THARSIS
WHOLE ROCK ANALYSES - DATASET STATISTICS

Descriptive Statistics	*Ga*	*Hf*	*In*	*Mo*	*Nb*	*Rb*
Mean	10.617	4.767	0.400	15.583	8.500	77.083
Standard Error	0.496	0.170	0.063	4.165	0.876	3.384
Median	11	5	0.25	7	5	83.5
Mode	12	5	0.25	3	5	105
Standard Deviation	3.845	1.320	0.490	32.261	6.784	26.215
Sample Variance	14.783	1.741	0.240	1040.756	46.017	687.213
Kurtosis	0.666	14.510	18.313	20.082	23.578	1.654
Skewness	-0.707	2.737	4.142	4.270	4.194	-1.249
Range	17	9	2.75	197	45	111.5
Minimum	1	3	0.25	3	5	3.5
Maximum	18	12	3	200	50	115
Sum	637	286	24	935	510	4625
Count	60	60	60	60	60	60
% results BDL	0	0	87	0	60	0
Confidence Level (95.000%)	0.973	0.334	0.124	8.163	1.716	6.633

Descriptive Statistics	*Sb*	*Sr*	*Ta*	*Te*	*Tl*	*Th*
Mean	4.000	63.667	1.000	2.500	1.500	17.417
Standard Error	0.545	3.651	0.000	0.000	0.000	0.556
Median	3	62.5	1	2.5	1.5	16.5
Mode	3	75	1	2.5	1.5	15.5
Standard Deviation	4.223	28.282	0.000	0.000	0.000	4.307
Sample Variance	17.831	799.887	0.000	0.000	0.000	18.552
Kurtosis	38.835	1.853	-	-	-	-0.209
Skewness	5.810	0.862	-	-	-	0.373
Range	31	150	0	0	0	19.5
Minimum	2	20	1	2.5	1.5	8
Maximum	33	170	1	2.5	1.5	27.5
Sum	240	3820	60	150	90	1045
Count	60	60	60	60	60	60
% results BDL	0	0	100	100	100	0
Confidence Level (95.000%)	1.068	7.156	-	-	-	1.090

Descriptive Statistics	*U*	*W*	*Y*	*Zr*	*La*	*Ce*
Mean	6.042	24.983	24.850	196.167	73.283	151.400
Standard Error	0.503	3.870	1.185	7.490	8.165	13.412
Median	5	14	25	190	52	115
Mode	5	1.5	29	210	47	105
Standard Deviation	3.898	29.976	9.178	58.021	63.242	103.892
Sample Variance	15.197	898.551	84.231	3366.412	3999.562	10793.57
Kurtosis	6.205	2.996	3.633	23.158	9.480	8.864
Skewness	2.560	1.809	1.181	3.944	3.009	2.857
Range	18	128.5	53	420	321	544
Minimum	3	1.5	8	130	29	56
Maximum	21	130	61	550	350	600
Sum	362.5	1499	1491	11770	4397	9084
Count	60	60	60	60	60	60
% results BDL	0	17	0	0	0	0
Confidence Level (95.000%)	0.986	7.585	2.322	14.681	16.002	26.288

ROYAL THARSIS
WHOLE ROCK ANALYSES - DATASET STATISTICS

Descriptive Statistics	*Nd*	*LOI*	*Cu*	*Pb*	*Zn*	*Ni*
Mean	51.358	7.564	1998.800	37.283	106.767	15.508
Standard Error	3.015	0.304	654.942	6.680	12.949	1.256
Median	45.25	7.19	165	16	85.5	13
Mode	63	6.76	36	10	7	9
Standard Deviation	23.354	2.357	5073.156	51.743	100.304	9.728
Sample Variance	545.408	5.555	25736917	2677.291	10061.0	94.640
Kurtosis	7.063	-0.082	14.931	6.045	9.224	0.949
Skewness	2.474	0.694	3.746	2.545	2.452	1.164
Range	131	9.76	28085	234	597	44.5
Minimum	19	3.74	15	6	3	0.5
Maximum	150	13.5	28100	240	600	45
Sum	3081.5	453.81	119928	2237	6406	930.5
Count	60	60	60	60	60	60
% results BDL	0	0	0	0	0	2
Confidence Level (95.000%)	5.909	0.596	1283.660	13.092	25.380	2.462

Descriptive Statistics	*Ag*	*S*	*Au*	*Au Dpl*	*C*
Mean	0.483	3.720	0.064	0.274	0.912
Standard Error	0.053	0.504	0.017	0.106	0.110
Median	0.25	2.925	0.02	0.27	0.64
Mode	0.25	0.025	0.005	0.005	0.04
Standard Deviation	0.411	3.901	0.129	0.281	0.855
Sample Variance	0.169	15.216	0.017	0.079	0.731
Kurtosis	2.907	2.893	9.635	-1.371	-0.154
Skewness	1.858	1.522	3.138	0.401	0.858
Range	1.75	18.375	0.605	0.705	3.14
Minimum	0.25	0.025	0.005	0.005	0.02
Maximum	2	18.4	0.61	0.71	3.16
Sum	29	223.175	3.83	1.92	54.71
Count	60	60	60	7	60
% results BDL	67	8	30	29	0
Confidence Level (95.000%)	0.104	0.987	0.033	0.208	0.216